PO Box 2345, Beijing 100023, China
Fax: +86-10-85381893
E-mail: wjg@wjgnet.com www.wjgnet.com

World J Gastroenterol 2004;10(22):3235-3239
World Journal of Gastroenterology
 ISSN 1007-9327

• ESOPHAGEAL CANCER •

Prognostic and clinicopathological features of E-cadherin, α-catenin, β-catenin, γ-catenin and cyclin D_1 expression in human esophageal squamous cell carcinoma

Ying-Cheng Lin, Ming-Yao Wu, De-Rui Li, Xian-Ying Wu, Rui-Ming Zheng

Ying-Cheng Lin, De-Rui Li, Department of Medical Oncology, Tumor Hospital, Shantou University Medical College, Shantou 515031, Guangdong Province, China
Ming-Yao Wu, Xian-Ying Wu, Rui-Ming Zheng, Department of Pathology, Shantou University Medical College, Shantou 515031, Guangdong Province, China
Supported by a grant of Shantou University Research & Development Fund, No. L03002
Correspondence to: Dr. Ying-Cheng Lin, Department of Medical Oncology, Tumor Hospital, Shantou University Medical College, Shantou 515031, Guangdong Province, China. linyingcheng@medmail.com.cn
Telephone: +86-754-8555844 Ext. 4042 **Fax:** +86-754-8560352
Received: 2004-01-20 **Accepted:** 2004-04-11

Abstract

AIM: To investigate the expression of E-cadherin, α-catenin, β-catenin, γ-catenin and cyclin D_1 in patients with esophageal squamous cell carcinoma (ESCC), and analyze their interrelationship with clinicopathological variables and their effects on prognosis.

METHODS: Expression of E-cadherin, α-catenin, β-catenin, γ-catenin and cyclin D_1 was determined by EnVision or SABC immunohistochemical technique in patients with ESCC consecutively, their correlation with clinical characteristics was evaluated and analyzed by univariate analysis.

RESULTS: The reduced expression rate of E-cadherin, α-catenin, β-catenin and γ-catenin was 88.7%, 69.4%, 35.5% and 53.2%, respectively. Cyclin D1 positive expression rate was 56.5%. Expression of γ-catenin was inversely correlated with the degree of tumor differentiation and lymph node metastasis (χ^2 = 4.183 and χ^2 = 5.035, respectively, P<0.05), whereas the expression of E-cadherin was correlated only with the degree of differentiation (χ^2 = 5.769, P<0.05). Reduced expression of E-cadherin and γ-catenin was associated with poor differentiation of tumor, reduced expression of γ-catenin was also associated with lymph node metastasis. There obviously existed an inverse correlation between level of E-cadherin and γ-catenin protein and survival. The 3-year survival rates were 100% and 56% in E-cadherin preserved expression group and in reduced expression one and were 78% and 48% in γ-catenin preserved expression group and in reduced expression one, respectively. The differences were both statistically significant. Correlation analysis showed the expression level of α-catenin correlated with that of E-cadherin and β-catenin (P<0.05).

CONCLUSION: The reduced expression of E-cadherin and γ-catenin, but not α-catenin, β-catenin and cyclin D1, implies more aggressive malignant behaviors of esophageal carcinoma cells and predicts the poor prognosis of patients.

Lin YC, Wu MY, Li DR, Wu XY, Zheng RM. Prognostic and clinicopathological features of E-cadherin, α-catenin, β-catenin, γ-catenin and cyclin D_1 expression in human esophageal squamous cell carcinoma. *World J Gastroenterol* 2004; 10 (22): 3235-3239
http://www.wjgnet.com/1007-9327/10/3235.asp

INTRODUCTION

Esophageal squamous cell carcinoma (ESCC) is one of the most common malignant tumors in China[1]. In recent years, the postoperative survival of patients with esophageal carcinoma has been improved. However, the overall prognosis for esophageal cancer patients remains poor, the 5-year survival rate of post operative advanced esophageal carcinoma patients was 20-35%. Although surgical techniques and preoperative management have progressed, early diagnosis and treatment are still important[2-5]. The prognostic clinical characterization of esophageal carcinoma remains inadequate using conventional histological grading and staging systems. Recently, various attempts have been made to investigate the relationship between certain molecular markers and the clinical course of squamous cell carcinoma of esophagus. In fact, the biological factors that determine a different individual outcome (recurrent, survival) at an analogous stage of disease are obscure[3-6].

E-cadherin and catenin are important adhesion molecules in normal epithelial tissue. Catenins, including α-catenin, β-catenin, γ-catenin, play an important role in the E-cadherin mediated intercellular signal transduction and cell adhesion. Loss of normal cellular adhesion plays a critical role in many aspects of tumor biology. For instance, alterations in cell-cell adhesion in cancer cells are reflected at the microscopic level in degree of cohesiveness and pattern of tumor growth. Detachment of cancer cells is an initial step in invasion of surrounding tissues and in spread to distant organs, and altered tumor cell adhesion is important in these processes. Several studies examined the role of the E-cadherin/catenin complex in growth mediation and maintenance of cell-cell adhesion in various tumors[7-19]. The expression of adhesion molecules may reflect biological behaviors and characteristics of tumors and are conducive to predict and evaluate the risk of relapse and metastasis in patients with postoperative esophageal carcinoma, thus having practical significance in guiding individualized treatment[3,18,20-23].

Cyclin D1 encodes a cell-regulatory protein that is expressed at high level during the G1 phase of the cell cycle. Cyclin D1 binds to cyclin-dependent kinases and proliferating cell nuclear antigens. The formation of these complexes has been implicated in the control of cell proliferation[24]. Cyclin D1 is the target gene of beta-catenin, overexpression of the latter in the cytoplasm may promote malignant transformation by triggering cyclin D1 expression in a number of cancers. It was regarded by several reports that cyclin D1 could predict the prognosis in some cancers, including esophageal cancer[25-28].

In this study, the expression of E-cadherin, α-catenin, β-catenin, γ-catenin and cyclin D1 in 62 ESCC patients was

analyzed, concerning the histopathological and survival data, effects on progression of cancer and their prognostic value in ESCC. The results may provide some suggestions for clinical treatments.

MATERIALS AND METHODS

Materials

Specimens of cancer tissues were taken from 62 consecutive patients with squamous cell carcinoma of the thoracic esophagus who had undergone esophagectomy with regional lymph node dissected from January to December of 1996 at the Department of Thoracic Surgery, Cancer Hospital of Shantou University Medical College. None of them received irradiation or chemotherapy preoperatively. The patients included 49 men and 13 women with a mean age of 54 (range 35-79) years. Three tumors were located in the upper thorax, 36 in the middle thorax and 23 in the lower thorax (Table 1). The removed specimens were examined histological with hematoxylin and eosin staining, and then the clinicopathologic stage was determined according to TNM classification. Survival time was calculated from the date of operation to death or the date of last follow-up. Follow-up time ranged from 6 to 54 mo with an average of 36 mo.

Table 1 Background data of patients

Term	No. of cases (%)
Total	62
Age (yr)	
<50	22 (35.5)
⩾50	40 (64.5)
Sex	
Male	49 (79.1)
Female	13 (20.9)
Location	
Upper thoracic	3 (4.8)
Middle thoracic	36 (56.5)
Lower thoracic	23 (37.1)
Histological grade	
I	16 (25.8)
II	35 (56.5)
III	11 (17.7)
Depth of invasion	
T1	2 (3.2)
T2	10 (16.1)
T3	32 (51.6)
T4	18 (29)
Lymph node metastasis	
Positive	35 (56.5)
Negative	27 (43.5)

Immunohistochemical staining

Immunohistochemical analysis was done retrospectively. Resected esophageal specimens, including both tumor and normal mucosae, were fixed in a 40 g/L formaldehyde solution and embedded in paraffin. The following antibodies were used in this study: mouse monoclonal anti-human cyclin D1 antibody (M-0024C, Antibody Company USA, diluted 1:50 in PBS), rabbit polyclonal anti-human E-cadherin antibody (BA0475, Antibody Company USA, diluted 1:100 in PBS), rabbit polyclonal anti-human α-catenin antibody (C-2081, Sigma Bioscience Company, USA, diluted 1:1 000 in PBS), rabbit polyclonal anti-human β-catenin antibody (C-2206, Sigma Chemical Company, USA, diluted 1:2 000 in PBS), goat polyclonal anti-human γ-catenin antibody (C-20 Santa Cruz Biot Co, USA, diluted 1:200 in PBS). Four μm thick sections of formalin-fixed paraffin-embedded tissue blocks of esophageal tumors were cut. The sections were deparaffinized, dehydrated and blocked to remove endogenous peroxidase activated by 3 mL/L H_2O_2 in methanol for 30 min. The sections were treated with microwave in 0.l mol/L citrate buffer pH 6.0 at 750 W for 12 min. After incubation with 100 mL/L normal goat serum to block non-specific binding, they were then incubated with the primary antibodies overnight at 4 ℃. After antibody was washed with PBS, the sections were incubated with the secondary antibody and immunostained by SABC method (γ-catenin, Boster Company, China) and EnVision method (E-cadherin, α-catenin, β-catenin and cyclin D1; EnVision, Cat. No. D-3001, 3002, Antibody Diagnostic Inc) according to the manufacturer's instructions, and finally DAB was visualized. Tissues were counterstained with hematoxylin. Negative control was designed by using PBS instead of primary antibody. Adjacent normal squamous epithelium served as an internal positive control of E-cadherin and catenin protein expression. Known immunostained-positive sections were used as positive control of cyclinD1 protein expression.

Positive criterion of immunohistochemical staining

Tumor sections were scored by light microscopy by 2 independent observers without knowledge of the stage and patient profiles. The percentage of positively stained cells was calculated after 100 cells were counted at more than 5 high-power (40×) fields. The following definitions were made: Cyclin D1: more than 10% positive staining in nuclei was defined as positive staining; E-cadherin and catenin: more than 10% positive staining in cell membrane was defined as positive staining; less than 50% positive staining in cell membrane was defined as reduced expression, more than 50% positive staining in cell membrane was defined as preserved expression.

Statistical analysis

χ^2 test or Fisher's exact probability test and Spearman rank correlation coefficient analysis were used to assess the association between immunohistochemical features and clinicopathological characteristics. The cumulative survival rate was calculated by the Kaplan-Meier method, and statistical significance was analyzed by the log-rank test. A P value less than 0.05 was considered statistically significant. All the statistical analyses were performed using the SPSS 10.0 V for Windows.

RESULTS

Expression of E-cadherin, α-catenin, β-catenin, γ-catenin and cyclin D1 in esophageal squamous cell carcinoma

The positive expression rate of E-cadherin, α-catenin, β-catenin, γ-catenin and cyclin D1 in 62 esophageal cancer patients was 62.9% (39/62), 79% (49/62), 95.2% (59/62), 75.8% (47/62) and 56.5% (35/62), respectively. The reduced expression rate of E-cadherin, α-catenin, β-catenin and γ-catenin was 88.7%, 69.4%, 35.5%, 53.2%, respectively. Cyclin D1 positive expression showed brown stained signals in the nuclei (Figure 1), only a small number of expressions in cytoplasm or membrane of cells. E-cadherin, α-catenin, β-catenin and γ-catenin positive expression showed brown stained signals in membrane of cells and the intercellular junctions (Figure 2A-C).

Relationship between expressions of E-cadherin, α-catenin, β-catenin , γ-catenin and cyclin D1 in esophageal squamous cell carcinoma

Significant positive correlation was found between the intensity of α-catenin and β-catenin (r = 0.274, P<0.05), E-cadherin and α-catenin (r = 0.279, P<0.05). No significant differences were seen in other protein expressions.

Table 2 The relationship between clinicopathology and the expression of cyclin D_1 E-cad and catenins

Type	Cases	CyclinD1		P	E-cad		P	α-cat		P	β-cat		P	γ-cat		P
		Positive	Negative		Preserved	Reduced		Preserved	Reduced		Preserved	Reduced		Preserved	Reduced	
Histological grade																
I	16	6	10		5	11		7	9		10	6		8	8	
II	35	15	20	>0.05	5	30	<0.05	11	24	>0.05	24	11	>0.05	19	16	<0.05
III	11	6	5		0	11		1	10		6	5		3	8	
Depth of invasion																
T_3	12	6	6	>0.05	4	8	>0.05	4	8	>0.05	6	6	>0.05	5	7	>0.05
T_4	50	31	19		6	44		15	35		34	16		25	25	
Lymph node metastases																
Positive	35	14	21	>0.05	6	29	>0.05	9	26	>0.05	23	12	>0.05	12	23	<0.05
Negative	27	13	14		4	23		10	17		17	10		18	9	

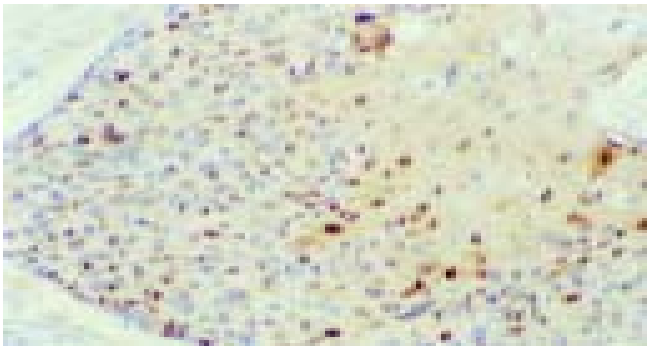

Figure 1 Positive expression of cyclinD1 protein in nuclei of esophageal squamous cell carcinoma. IHC×200.

Relationship between E-cadherin, α-catenin, β-catenin, γ-catenin and cyclin D1 expression and clinicopathologic variables in esophageal squamous cell carcinoma

Expression of E-cadherin correlated significantly only with histological grade. Poor differentiation was associated with reduced or loss of E-cadherin expression (P<0.05). Significant inverse correlation existed between the intensity of γ-catenin expression and histological grade, and lymph node metastasis (P<0.05). No significant correlation was found between abnormal expression of other proteins and histological grade, lymph node metastasis and depth of invasion (Table 2).

Relationship between E-cadherin, α-catenin, β-catenin, γ-catenin, and cyclin D1 expression and survival

Analysis of the 3-year survival after operation showed that the overall survival rate was 62% in 62 cases of esophageal cancer. Univariate analysis showed that the survival time was associated with the histological grade, depth of invasion, lymph node metastasis, expression of E-adherine and γ-catenin. Reduced E-cadherin or γ-catenin expression was correlated with poor prognosis. The mean survival time of grades I, II, III was 41, 45 and 12 mo (P<0.05), respectively. The 3-year survival rate was 67.1% and 49.4% in T3 and T4 patients (P<0.05), respectively, and was 47.8% and 80.3% in patients with positive and negative lymph node metastases (P<0.05), respectively. The median survival time was 54 mo and 37 mo in patients with preserved and reduced or loss of E-cadherin expression, the 3-year survival rate was 100% and 56% (P<0.05), respectively. The median survival time was 42 and 33 mo in patients with preserved and reduced or lost expression of γ-catenin, the 3-year survival rate was 78% and 48% (P<0.05), respectively. No difference in survival curves was seen between reduced expression of α- and β-catenins compared with preserved expression. Similar results were found in the positive and negative expressions of cyclin D1. The median survival time was 39 and 38 mo in the patients with preserved and reduced or lost expression of α-catenin, the 3-year survival rate was 65%. The median survival time was 36 and 39 mo in the patients with preserved and reduced or loss expression of β-catenin, the 3-year survival rate was 65%. The median survival time was 40 and 34 mo in the patients with positive and negative expressions of cyclin D1, the 3-year survival rate was 68% and 58% (P>0.05), respectively.

DISCUSSION

The main causes of treatment failure are recurrence and metastasis in resectable esophageal cancer. Modern molecular biology studies have demonstrated that invasion and metastasis of tumors as a continuous process, include three steps: a reduced cell-cell adhesion, alterations in the interaction of tumor cells with extracellular matrix, and invasion into surrounding

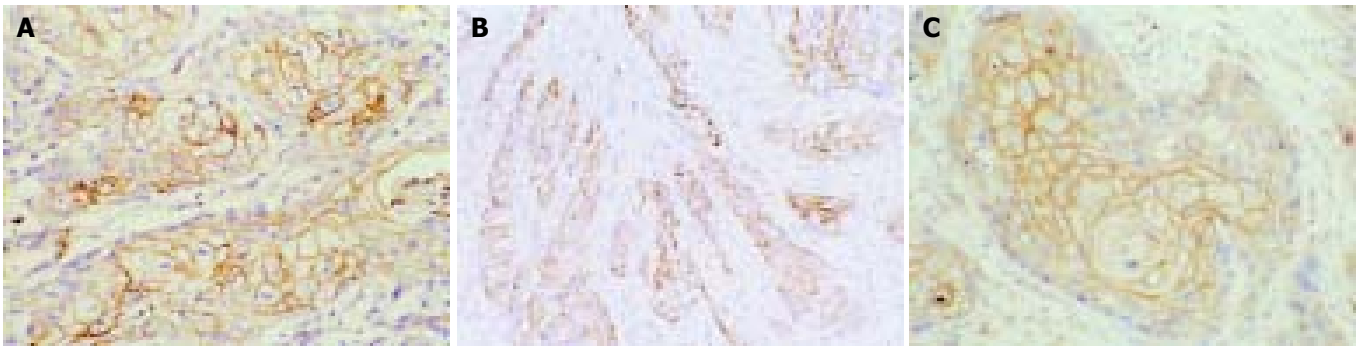

Figure 2 Positive expression of E-cadherin and γ-catenin proteins in membrane of esophageal squamous cell carcinoma. A: Positive expression of E-cadherin protein in membrane of esophageal well differentiated squamous cell carcinoma. IHC ×200; B: Positive expression of γ-catenin protein in membrane of esophageal squamous cell carcinoma. IHC×200; C: Positive expression of γ-catenin protein in membrane of esophageal squamous cell carcinoma. IHC×400.

tissues including blood vessels and lymph duct. Thus the first and critical step is that the tumor cells could detach from primary foci and re-adhere to metastatic position[12,29,30]. E-cadherin is a calcium-dependent cell-cell adhesion transmembrane glycoprotein, maintaining normal epithelial polarity, and intercellular adhesion, which are present in almost all normal epithelial cell surfaces. It is anchored to the cytoskeleton via cytoplasm proteins, including alpha and beta catenin[13,14,31]. E-cadherin, therefore, is one of the most important adhesion molecules expressed by epithelial cells and is regarded as an invasion suppressor molecule[13,14]. In this study, overall survival was inversely corrected with E-cadherin expression. Patients with preserved E-cadherin expressing tumor had a better prognosis than those with reduced expression of E-cadherin. This was in agreement with previous studies on a variety of cancers, such as cancer of head and neck[15,16], breast[17,18], stomach[19,32,33], bladder[27]. In all these studies, reduction or loss of E-cadherin expression was significantly associated with dedifferentiation, increased invasiveness, and high incidence of lymph node metastasis, hematogenous recurrence and poor prognosis in a number of human carcinomas, including esophageal cancer. But some other studies did not acquire the same results[3]. There were different results of reduced E-cadherin protein expression in specimens from patients with ESCC in various researches[21,23,32-35]. While in our investigation 88.7% of ESCC showed reduced expression of E-cadherin. It was postulated that selection of the patients entering into the study, immunohistochemical method, antibody origination, tumor heterogeneity and differences in staining evaluation might individually or in combination hold responsibility. As a marker associated with squamous cell differentiation[36], the level of E-cadherin expression had an inverse correlation with histological grade. Reduced or loss of E-cadherin expression was correlated with poor differentiation, but not with lymphatic metastases and depth of tumor invasion, suggesting that the reduction of E-cadherin expression is associated with loss of the ability of adhesion and facilitate to blood vessel metastases, as previously reported[21].

Catenins are a family of proteins including α-(102 ku), β-(88 ku), γ-(82 ku) catenins. The cytoplasmic domain of E-cadherin could bind directly to either β-catenin or γ-catenin, whereas α-catenin could link E-cadherin- (β, γ)-catenin complex to acting cytoskeleton. The integrity of the adhesion function of E-cadherin also depended on an intact catenin system[15]. β-catenin could also play a role in intracellular signaling and function as an oncogene when it bound to T-cell factor 4 (Tcf4)-binding site in the promotor region of cyclin D1 and transactivated genes after translocation to the nuclei[37-39]. Catenins had different clinicopathological roles in various cancers. In many epithelial carcinomas including carcinoma of the esophagus[3,6,20,22,23,33], head and neck[16], breast[17-19,25], stomach[19], colon[24] and bladder[27], catenins had a prognostic significance in survival. Some investigators reported that abnormal expression of α-catenin was associated with the prognosis of esophageal cancer. It also had predicative values for lymph node metastasis in esophageal carcinoma. Several reports suggested that abnormal expression of β-catenin could indicate poor prognosis in a number of tumors, including esophageal cancer[17,20,25,33]. γ-catenin was found to be more important in nodal metastasis in tongue cancer. It was also predictive of the presence of subclinical nodal metastasis in clinically node-negative neck[16]. The expression of α-catenin but not β- or γ-catenin was found to be correlated with the expression of E-cadherin in this study. The reduction or loss of γ-catenin expression was associated with more lymph node metastases than the preserved expression (P<0.05). There was a correlation between poor differentiation of tumor and reduction or loss of γ-catenin expression. The reduction or loss of γ-catenin expression was in association with shorter median survival time and lower 3-year survival rate. All these suggested that γ-catenin might be one of the prognostic factors in esophageal cancer. Howeres, the expression of α-catenin and β-catenin was not related to the histological grade, depth of invasion, lymph node metastases and survival time.

The clinical significance of cyclin D1 expression was different in various tumors. It has shown that cyclin D1 gene amplification or enhanced expression was correlated with higher histological grade of tumor, lymphatic or hematogenous metastasis and poor prognosis[40-43]. A controversial report, however, existed[6]. Some investigators thought cyclin D1 was the target gene of β-catenin. Although a positive correlation between β-catenin activation and cyclin D1 expression was reported, our study did not show such a result. Furthermore, cyclin D1 expression was not associated with the extent of tumor infiltration, grade of differentiation, lymphatic metastases and survival time. These inconsistencies with other authors may be associated with location of tumor, pathologic classification, biologic behaviors, examination methods and evaluating criteria.

Our study showed that the main prognostic factors of postoperative survival time were histological grade, depth of tumor invasion and lymph node metastasis. The reduced expression of E-cadherin or γ-catenin was associated with poor differentiation of tumor cells. Reduced or loss of γ-catenin expression also had predictive values for nodal metastasis. The reduction or loss of E-cadherin and γ-catenin expression could predict the shorter survival time. Therefore we suggest that adjuvant radiation or chemotherapy should be considered in esophageal carcinoma patients with reduced expression of E-cadherin and γ-catenin in T4 stage, poor-differentiation in histopathology, and lymph node metastases in order to improve the survival rate.

REFERENCES

1 **Su M,** Lu SM, Tina DP, Zhao H, Li XY, Li DR, Zheng ZC. Relationship between ABO blood groups and carcinoma of esophagus and cardia in Chaoshan inhabitants of China. *World J Gastroenterol* 2001; **7**: 657-661

2 **Hofstetter W,** Swisher SG, Correa AM, Hess K, Putnam JB Jr, Ajani JA, Dolormente M, Francisco R, Komaki RR, Lara A, Martin F, Rice DC, Sarabia AJ, Smythe WR, Vaporciyan AA, Walsh GL, Roth JA. Treatment outcomes of resected esophageal cancer. *Ann Surg* 2002; **236**: 376-384

3 **Shiozaki H,** Doki Y, Kawanishi K, Shamma A, Yano M, Inoue M, Monden M. Clinical application of malignancy potential grading as a prognostic factor of human esophageal cancers. *Surgery* 2000; **127**: 552-561

4 **Shimada Y,** Imamura M, Watanabe G, Uchida S, Harada H, Makino T, Kano M. Prognostic factors of oesophageal squamous cell carcinoma from the perspective of molecular biology. *Br J Cancer* 1999; **80**: 1281-1288

5 **Goldberg RM.** Gastrointestinal tract cancer in: Casciato DA, Lowitz BB, eds. Manual of clinical oncology.4th ed. *Lippincott Williams Wilkins Inc* 2000: 172-176

6 **Ikeda G,** Isaji S, Chandra B, Watanabe M, Kawarada Y. Prognostic significance of biologic factors in squamous cell carcinoma of the esophagus. *Cancer* 1999; **86**: 1396-1405

7 **Wijnhoven BP,** Dinjens WN, Pignatelli M. E-cadherin-catenin cell-cell adhesion complex and human cancer. *Br J Surg* 2000; **87**: 992-1005

8 **Yagi T,** Takeichi M. Cadherin superfamily genes: functions, genomic organization, and neurologic diversity. *Genes Dev* 2000; **14**: 1169-1180

9 **Ivanov DB,** Philippova MP, Tkachuk VA. Structure and Functions of classical cadherin. *Biochemistry* 2001; **66**: 1174-1186

10 **Van Aken E,** De Wever O, Correia da Rocha AS, Mareel M. Defective E-cadherin/catenin complexes in human cancer. *Virchows Arch* 2001; **439**: 725-751

11 **Behrens J.** Cadherins and catenins: role in signal transduction

and tumor progression. *Cancer Metastasis Rev* 1999; **18**: 15-30
12 **Beavon IR**. The E-cadherin-catenin complex in tumour metastasis: structure, function and regulation. *Eur J Cancer* 2000; **36**: 1607-1620
13 **Hirohashi S**. Inactivation of the E-cadherin-mediated cell adhesion system in human cancers. *Am J Pathol* 1998; **153**: 333-339
14 **Christofori G,** Semb H. The role of the cell-adhesion molecule E-cadherin as a tumour-suppressor gene. *Trends Biochem Sci* 1999; **24**: 73-76
15 **Chow V,** Yuen AP, Lam KY, Tsao GS, Ho WK, Wei WI. A comparative study of the clinicopathological significance of E-cadherin and catenins (α, β, γ) expression in the surgical management of oral tongue carcinoma. *J Cancer Res Clin Oncol* 2001; **127**: 59-63
16 **Andrews NA,** Jones AS, Helliwell TR, Kinsella AR. Expression of the E-cadherin-catenin cell adhesion complex in primary squamous cell carcinomas of the head and neck and their nodal metastases. *Br J Cancer* 1997; **75**: 1474-1480
17 **Bukholm IK,** Nesland JM, Borresen-Dale AL. Re-expression of E-cadherin, α-catenin and β-catenin, but not of γ-catenin, in metastatic tissue from breast cancer patients. *J Pathol* 2000; **190**: 15-19
18 **Lim SC,** Lee MS. Significance of E-cadherin / beta-catenin complex and cyclin D1 in breast cancer. *Oncol Rep* 2002; **9**: 915-928
19 **Jawhari A,** Jordan S, Poole S, Browne P, Pignatelli M, Farthing MJ. Abnormal immunoreactivity of the E-cadherin-catenin complex in gastric carcinoma: relationship with patient survival. *Gastroenterology* 1997; **112**: 46-55
20 **Kadowaki T,** Shiozaki H, Inoue M, Tamura S, Oka H, Doki Y, Iihara K, Matsui S, Iwazawa T, Nagafuchi A. E-cadherin and α-catenin expression in human esophageal cancer. *Cancer Res* 1994; **54**: 291-296
21 **Tamura S,** Shiozaki H, Miyata M, Kadowaki T, Inoue M, Matsui S, Iwazawa T, Takayama T, Takeichi M, Monden M. Decreased E-cadherin expression is associated with haematogenous recurrence and poor prognosis in patients with squamous cell carcinoma of the oesophagus. *Br J Surg* 1996; **83**: 1608-1614
22 **Sanders DS,** Bruton R, Darnton SJ, Casson AG, Hanson I, Williams HK, Jankowski J. Sequential changes in cadherin-catenin expression associated with the progression and heterogeneity of primary oesophageal squamous carcinoma. *Int J Cancer* 1998; **79**: 573-579
23 **Nakanishi Y,** Ochiai A, Akimoto S, Kato H, Watanabe H, Tachimori Y, Yamamoto S, Hirohashi S. Expression of E-cadherin, alpha-catenin, beta-catenin and plakoglobin in esophageal carcinomas and its prognostic significance: immunohistochemical analysis of 96 lesions. *Oncology* 1997; **54**: 158-165
24 **Utsunomiya T,** Doki Y, Takemoto H, Shiozaki H, Yano M, Sekimoto M, Tamura S, Yasuda T, Fujiwara Y, Monden M. Correlation of beta-catenin and cyclin D1 expression in colon cancers. *Oncology* 2001; **61**: 226-233
25 **Lin SY,** Xia W, Wang JC, Kwong KY, Spohn B, Wen Y, Pestell RG, Hung MC. Beta-catenin, a novel prognostic marker for breast cancer: its roles in cyclin D1 expression and cancer progression. *Proc Natl Acad Sci U S A* 2000; **97**: 4262-4266
26 **Itami A,** Shimada Y, Watanabe G, Imamura M. Prognostic value of p27 (Kip1) and CyclinD1 expression in esophageal cancer. *Oncology* 1999; **57**: 311-317
27 **Shiina H,** Igawa M, Shigeno K, Terashima M, Deguchi M, Yamanaka M, Ribeiro-Filho L, Kane CJ, Dahiya R. Beta-catenin mutations correlate with over expression of C-myc and cyclin D1 genes in bladder cancer. *J Urol* 2002; **168**: 2220-2226
28 **Ueta T,** Ikeguchi M, Hirooka Y, Kaibara N, Terada T. Beta-catenin and cyclin D1 expression in human hepatocellular carcinoma. *Oncol Rep* 2002; **9**: 1197-1203
29 **Korn WM.** Moving toward an understanding of the metastatic process in hepatocellular carcinoma. *World J Gastroenterol* 2001; **7**: 777-778
30 **Stamenkovic I.** Matrix metalloproteinases in tumor invasion and metastasis. *Semin Cancer Biol* 2000; **10**: 415-433
31 **Bair EL,** Massey CP, Tran NL, Borchers AH, Heimark RL, Cress AE, Bowden GT. Integrin- and cadherin-mediated induction of the matrix metalloprotease matrilysin in cocultures of malignant oral squamous cell carcinoma cells and dermal fibroblasts. *Exp Cell Res* 2001; **270**: 259-267
32 **Debruyne P,** Vermeulen S, Mareel M. The role of the E-cadherin / catenin complex in gastrointestinal cancer. *Acta Gastroenterol Belg* 1999; **62**: 393-402
33 **de Castro J,** Gamallo C, Palacios J, Moreno-Bueno G, Rodriguez N, Feliu J, Gonzatez-Baron M. Beta-catenin expression pattern in primary oesophageal squamous cell carcinoma. Relationship with clinicopathologic features and clinical outcome. *Virchows Arch* 2000; **437**: 599-604
34 **Jian WG,** Darnton SJ, Jenner K, Billingham LJ, Matthews HR. Expression of E-cadherin in oesophageal carcinomas from the UK and China: disparities in prognostic significance. *J Clin Pathol* 1997; **50**: 640-644
35 **Pomp J,** Blom J, van Krimpen C, Zwinderman AH, Immerzeel JJ. E-cadherin expression in oesophageal carcinoma treated with high-dose radiotherapy; correlation with pretreatment parameters and treatment outcome. *J Cancer Res Clin Oncol* 1999; **125**: 641-645
36 **Wu H,** Lotan R, Menter D, Lippmar SM, Xu XC. Expression of E-cadherin is associated with squamous differentiation in squamous cell carcinomas. *Anticancer Res* 2000; **20**: 1385-1390
37 **Peifer M.** β-catenin as oncogene: the smoking gun. *Science* 1997; **275**: 1752-1753
38 **Kolligs FT,** Bommer G, Goke B. Wnt / beta-catenin / tcf signaling: a critical pathway in gastrointestinal tumorigenesis. *Digestion* 2002; **66**: 131-144
39 **Gottardi CJ,** Wong E, Gumbiner BM. E-cadherin suppresses cellular transformation by inhibiting beta-catenin signaling in an adhesion-independent manner. *J Cell Biol* 2001; **153**: 1049-1060
40 **Kagawa Y,** Yoshida K, Hirai T, Toge T. Significance of the expression of p27Kip1 in esophageal squamous cell carcinomas. *Dis Esophagus* 2000; **13**: 179-184
41 **Matsumoto M,** Natsugoe S, Nakashima S, Sakamoto F, Okumura H, Sakita H, Baba M, Takao S, Aikou T. Clinical significance of lymph node micrometastasis of pN0 esophageal squamous cell carcinoma. *Cancer Lett* 2000; **153**: 189-197
42 **Itami A,** Shimada Y, Watanabe G, Imamura M. Prognostic value of p27 (Kip1) and CyclinD1 expression in esophageal cancer. *Oncology* 1999; **57**: 311-317
43 Prognostic significance of CyclinD1 and E-Cadherin in patients with esophageal squamous cell carcinoma: multiinstitutional retrospective analysis. Research Committee on Malignancy of Esophageal Cancer, Japanese Society for Esophageal Diseases. *J Am Coll Surg* 2001; **192**: 708-718

Edited by Wang XL and Zhu LH **Proofread by** Xu FM

PO Box 2345, Beijing 100023, China
Fax: +86-10-85381893
E-mail: wjg@wjgnet.com www.wjgnet.com

World J Gastroenterol 2004;10(22):3240-3244
World Journal of Gastroenterology
 ISSN 1007-9327

• GASTRIC CANCER •

Elevated level of spindle checkprotein MAD2 correlates with cellular mitotic arrest, but not with aneuploidy and clinicopathological characteristics in gastric cancer

Chew-Wun Wu, Chin-Wen Chi, Tze-Sing Huang

Chew-Wun Wu, Department of Surgery, Taipei-Veterans General Hospital, Taipei, Taiwan
Chin-Wen Chi, Department of Medical Research and Education, Taipei-Veterans General Hospital and Institute of Pharmacology, National Yang-Ming University, Taipei, Taiwan
Tze-Sing Huang, Division of Cancer Research, National Health Research Institutes, Taipei, Taiwan
Correspondence to: Dr. Tze-Sing Huang, Cooperative Laboratory at VGH-Taipei, No. 201, Shih-Pai Road Sec. 2, Taipei 112, Taiwan. tshuang@nhri.org.tw
Telephone: +886-2-28712121 Ext. 2641 **Fax:** +886-2-28748307
Received: 2004-02-11 **Accepted:** 2004-02-26

Abstract

AIM: To study the relevance of spindle assembly checkprotein MAD2 to cellular mitotic status, aneuploidy and other clinicopathological characteristics in gastric cancer.

METHODS: Western blot analyses were performed to analyze the protein levels of MAD2 and cyclin B1 in the tumorous and adjacent nontumorous tissues of 34 gastric cancer patients. Cell cycle distribution and DNA ploidy of cancer tissues were also determined by flow cytometry. Conventional statistical methods were adopted to determine the relevance of abnormal MAD2 level to mitotic status, aneuploidy and clinicopathological parameters.

RESULTS: Out of 34 gastric cancer patients 25 (74%) exhibited elevated MAD2 levels in their tumorous tissues compared with the corresponding nontumorous tissues. Elevation of MAD2 levels significantly correlated with the increased levels of cyclin B1 expression and G_2/M-phase distribution (P = 0.038 and P = 0.033, respectively), but was not relevant to aneuploidy. The gastric cancer patients with elevated MAD2 levels showed a tendency toward better disease-free and overall survival (P>0.05). However, no association was found between elevated MAD2 levels and patients' clinicopathological characteristics.

CONCLUSION: Elevation of MAD2 level is present in 74% of gastric cancer patients, and correlates with increased mitotic checkpoint activity. However, elevation of MAD2 level is not associated with patients' aneuploidy and any of the clinicopathological characteristics.

Wu CW, Chi CW, Huang TS. Elevated level of spindle checkprotein MAD2 correlates with cellular mitotic arrest, but not with aneuploidy and clinicopathological characteristics in gastric cancer. *World J Gastroenterol* 2004; 10(22): 3240-3244
http://www.wjgnet.com/1007-9327/10/3240.asp

INTRODUCTION

During the cell division cycle, the localization and segregation of chromosomes are under the surveillance of one group of proteins, called spindle assembly checkproteins[1-3]. Mitotic arrest-deficient proteins (MADs) and budding uninhibited by benzimidazole proteins (BUBs) are the major members of spindle assembly checkproteins[4-6]. Among them, MAD2 is a key component of MAD/BUB complex that can censor mis-segregation of chromosomes by monitoring the microtubule attachment and tension[4,7,8]. MAD2 is usually expressed at a high steady-state level and distributed at unattached kinetochores[9,10]. Re-localization of MAD2 along microtubules to the spindle poles is achieved by minus-end-directed dynein-dynactin complex only when all kinetochores properly attach to microtubules[10]. Once misaligned chromosomes or even a single unattached kinetochore is present, sufficient MAD2 molecules are kept in kinetochores to inhibit the onset of anaphase until all chromosomes exhibit proper bipolar attachment to the spindle. The kinetochore MAD2 can associate with and thus prevent the activation of anaphase-promoting complex (APC)[7,11-14]. APC is a kinetochore-localizing, CDC27-based ubiquitin ligase responsible for cyclin B1 degradation and in turn down-regulation of cyclin B1-associated CDC2 kinase activity, which is required for metaphase-anaphase transition and for exit from mitosis[7,11-14]. On the other hand, the microtubule-interfering agents, such as paclitaxel and nocodazole, can also elicit the spindle assembly checkpoint activity of MAD2[4,15,16]. In paclitaxel-treated cells, MAD2 mediates inhibition of APC's ability to ubiquitinate cyclin B1, which avoids the degradation of cyclin B1 and thus leads the cyclin B1/CDC2 activity to sustain longer[15]. This persistence of MAD2 and cyclin B1/CDC2 activation renders cells unable to exit from the metaphase and ultimately leads cells to apoptosis[15].

As described above, the role of MAD2 in spindle checkpoint machinery has been evidenced in many cell line studies. Clinically, it was reported that MAD2 was rarely the target for genetic alterations in digestive tract cancers[17,18]. Whatever from clinical investigation or animal models, the evidence demonstrating the relevance of MAD2 to cellular mitotic status or other histopathological characteristics is yet lacking. In this study, we investigated the level of MAD2 in 34 gastric cancer patients. The MAD2-related mitotic checkpoint activity was measured by cyclin B1 expression level and cell cycle G_2/M-phase fraction. Our data indicated that 25 out of 34 (74%) gastric cancer patients exhibited elevated MAD2 levels in their tumorous tissues rather than nontumorous tissues. Elevation of MAD2 level correlated with increased mitotic checkpoint activity but was not relevant to aneuploidy (chromosomal numerical alteration). Although the gastric cancer patients with elevated MAD2 levels exhibited a tendency toward better disease-free and overall survival, no correlation was found between abnormal MAD2 level and patients' clinicopathological characteristics.

MATERIALS AND METHODS

Patients and tumor specimens

Thirty-four primary gastric cancer tissues and their corresponding

normal mucosa were obtained from patients at Taipei Veterans General Hospital. The patients consisted of 25 men and 9 women (aged 43-80 years; mean: 63.8 years). Informed consent was obtained from each patient. All specimens were snap-frozen immediately after resection and stored at -80 ℃ until use. Parts of the specimens were taken for protein extraction and DNA content determination, and the remaining tissues were fixed in 40 g/L buffered formaldehyde for histologic examination. Hematoxylin and eosin staining of tissue sections was adopted to categorize the tumors according to the classification of Lauren[19].

Tissue lysate preparation and Western blot analysis

Tissue lysates were prepared by the method described previously[20]. Briefly, tumor and non-tumor specimens were ground down into powder in the presence of liquid nitrogen. Around 0.5 g of tissue powder was resuspended in 1.5 mL of 10 mmol/L Tris-Cl, pH 7.8, 140 mmol/L NaCl, 5 g/L deoxycholate, 10 mL/L NP-40, 1 mmol/L phenylmethylsulfonyl fluoride, 10 μg/mL aprotinin, 10 μg/mL pepstatin A, and 10 μg/mL leupeptin. The suspension was subjected to homogenization and further sonication on ice, and finally was ultracentrifuged at 100 000 *g* for 1 h at 4 ℃. The supernatant was saved and assayed for protein concentration (Bradford method). Aliquots (30 μg protein) of tissue lysates were separated on 100 g/L SDS-polyacrylamide gels, and electrotransferred onto polyvinylidene difluoride membranes. After blocked with PBST (phosphate-buffered saline plus 1 mL/L Tween-20) plus 50 g/L fat-free milk, the membranes were incubated with anti-MAD2, cyclin B1, and β-tubulin antibodies (Santa Cruz Biotechnology, Santa Cruz, CA, USA), respectively, in PBST plus 50 g/L milk at 4 ℃ for 12 h. The membranes were then washed three times with PBST buffer, and incubated with horseradish peroxidase-conjugated secondary antibodies for 1 h at room temperature. After washed three times with PBST buffer, the protein bands were detected by enhanced chemiluminescence (Amersham Biosciences, Piscataway, NJ, USA).

Flow cytometric analysis of DNA content

The DNA ploidy and cell-cycle phase distribution of tissue specimens were measured by flow cytometric analysis[21]. Frozen specimens were first minced into 2 to 5 mm^3 pieces and further digested into single cell suspensions[22]. Cell suspensions were fixed with 800 mL/L ethanol at -20 ℃ at least for 30 min before subsequent Triton X-100 permeabilization and propidium iodide staining[16]. The cellular DNA content was analyzed using a FACStar flow cytometer with an argon laser tuned to the 488-nm line for excitation (BD Biosciences, San Jose, CA, USA).

Statistical analyses

Data were analyzed by χ^2 or *t* test. Survival rate was calculated by the Kaplan-Meier method. Statistical comparisons were made with Logrank test. The difference was considered to be significant when *P* value was less than 0.05.

RESULTS

Elevated MAD2 level occurs in human gastric cancer

Western blot analysis was performed to analyze the MAD2 expression level of the tumorous and adjacent nontumorous tissues of 34 gastric cancer patients. As shown in Figure 1, the MAD2 protein was detected in both tumorous and nontumorous tissue lysates. In most patients, MAD2 seemed labile in the nontumorous tissues rather than the tumorous tissues. The differential MAD2 level was confirmed by comparison with the levels of β-tubulin in the same-paired tissue lysates. A patient with elevated MAD2 level was defined as one whose MAD2 level in the tumorous tissue was higher than that in the adjacent nontumorous tissue, and elevated MAD2 level could be found in 25 of 34 (74%) cases of human gastric cancer.

Elevated MAD2 level correlates with increased mitotic arrest but not aneuploidy

The MAD2-related mitotic arrest was measured by cyclin B1 level and cell cycle G_2/M-phase fraction. We found that 18 of 34 (53%) gastric cancer patients had elevated cyclin B1 expression level in their tumorous rather than nontumorous tissues (three examples shown in Figure 1). There was a statistically significant correlation between elevated MAD2 level and elevated cyclin B1 level ($P = 0.038$), as 16 of 25 (64%) gastric cancer patients who had elevated MAD2 levels also manifested higher levels of cyclin B1 in their tumorous tissues (Table 1). Moreover, the DNA contents of tumor specimens of 29 patients were successfully determined by flow cytometric analysis. The data presented by mean±SD (%) of phase fractions are shown in Table 2. We observed that the ratio of G_2/M-phase fraction in the tumor specimens exhibiting elevated MAD2 levels was statistically higher than that in the tumorous tissues with a normal MAD2 level (10.6 ± 4.9% *vs* 6.4 ± 4.0%, $P = 0.033$). No significant difference in the ratios of G_0/G_1 and S-phase fractions was found between the tumors with or without elevated MAD2 levels (Table 2). In addition, DNA ploidy was also determined from the tumor specimens of 32 patients. Although 18 of 32 (56%) patients were found to have aneuploid tumor cells, no correlation was observed between the occurrence of aneuploidy and elevated MAD2 level in cancer tissues ($P = 1.000$, Table 3).

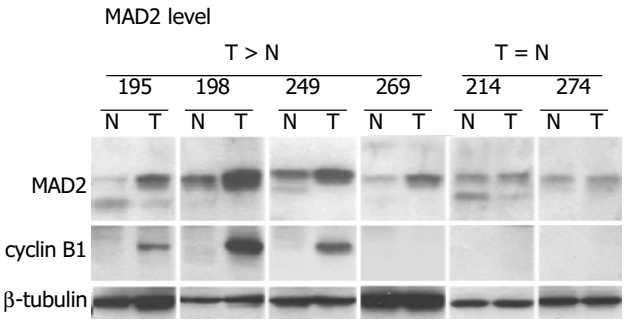

Figure 1 Examples of elevation of MAD2 and cyclin B1 levels in human gastric cancer. Western blot analyses were performed to analyze the protein levels of MAD2 and cyclin B1 in the lysates from non-tumorous tissues (N) and tumorous tissues (T) of gastric cancer patients, #195, #198, #249, #269, #214, and #274. The levels of β-tubulin in the same-paired tissue lysates were analyzed as internal control.

Table 1 Cyclin B1 expression status of 34 gastric cancer tissues with or without MAD2 overexpression

	Cyclin B1 level	
	T > N	T = N
MAD2 level		
T > N ($n = 25$)	16	9
T = N ($n = 9$)	2	7
	$P = 0.038$	

T: tumorous tissue; N: non-tumorous tissue.

Table 2 Cell cycle phase fractions of 29 gastric cancer tissues with or without MAD2 overexpression (mean±SD)

	Phase fraction (%)		
	G_0/G_1	S	G_2/M
MAD2 level			
T > N (n = 20)	80.8±5.9	8.6±7.0	10.6±4.9
T = N (n = 9)	83.5±7.4	9.9±7.7	6.4±4.0
	P = 0.301	P = 0.657	P = 0.033

T: tumorous tissue; N: non-tumorous tissue.

Table 3 DNA ploidy status of 32 gastric cancer tissues with or without MAD2 overexpression

	Diploidy	Aneuploidy
MAD2 level		
T > N (n = 23)	10	13
T = N (n = 9)	4	5
	P = 1.000	

T: tumorous tissue; N: non-tumorous tissue.

Elevated MAD2 level does not correlate with clinicopathological characteristics

The relationship of elevated MAD2 level with clinicopathological characteristics was also investigated and summarized (Table 4). The evaluated parameters included age at diagnosis, tumor site and size, cell differentiation grade, stromal reaction, invasive and metastatic status, *etc*. For the 34 studied patients, age and gender did not associate with higher levels of MAD2 in cancer tissues (P>0.05). There was no association between elevated MAD2 levels and different tumor sites (upper, middle, lower or whole stomach), tumor sizes, and other histopathological characteristics including grade of cell differentiation, Borrmann type, stromal reaction (medullary, intermediate or schirrhous type), infiltration type (α, β or γ), Lauren histological classification (intestinal or diffuse type), and TNM staging (I-IV), either. In addition, elevation of MAD2 level in cancer tissues was not correlated with the invasion parameters, including the lymphatic duct or vessel invasion and depth of cancer invasion (mucosa, submucosa, propria muscle, subserosa, serosa, serosa exposed), and metastatic status such as peritoneal dissemination and lymph node or liver metastasis (Table 4). Finally, the patients with elevated MAD2 levels in tumor tissues exhibited higher five-year overall and disease-free survival rates in comparison with those without elevated MAD2 levels (48.0% *vs* 20.8% and 46.3% *vs* 11.1%, respectively), but the difference did not reach a significant level (P = 0.478 and 0.229, respectively; Table 4).

Table 4 Relationships between elevated MAD2 levels and clinicopathological characteristics (mean±SD)

	MAD2 level		
	T>N (n = 25)	T=N (n = 9)	P
Age (yr)	62.8±10.3	66.4±5.0	0.325
Sex (male/female)	19/6	6/3	0.586
Site of tumor			0.828
Upper stomach	4	2	
Middle stomach	6	2	
Lower stomach	14	4	
Whole stomach	1	1	
Size of tumor (cm)	7.3±2.3	8.0±2.9	0.470
Grade of cell differentiation			0.146
Well differentiated	1	0	
Moderately differentiated	13	8	
Poorly differentiated	11	1	
Borrmann type			0.664
0	2	0	
1 + 2	6	2	
3 + 4	17	7	
Stromal reaction			0.739
Medullary type	6	3	
Intermediate type	12	3	
Schirrhous type	7	3	
Infiltration type			0.475
α	4	2	
β	8	1	
γ	13	6	
Lauren histological classification			0.448
Intestinal type	13	3	
Diffuse type	12	6	
Lymph node metastasis (Yes/No)	15/10	6/3	1.000
Lymphatic duct invasion (Yes/No)	18/7	7/2	1.000
Vascular invasion (Yes/No)	2/23	1/8	1.000
Liver metastasis (Yes/No)	1/24	0/9	1.000
Peritoneal dissemination (Yes/No)	2/23	1/8	1.000
Depth of cancer invasion			0.738
Mucosa, submucosa	1	0	
Propria muscle, subserosa	5	1	
Serosa	18	8	
Serosa (infiltration) exposed	1	0	
TNM stage			0.932
I	3	1	
II	8	2	
III	8	3	
IV	6	3	
Five-yr overall survival rate	48.0%	20.8%	0.478
Five-yr disease-free survival rate	46.3%	11.1%	0.229

DISCUSSION

Spindle assembly checkpoint is one of the mechanisms to guard the fidelity of cell division cycle[1-3]. MAD2 is a key component of spindle assembly checkprotein complex MAD/BUB that is responsible for monitoring the localization and segregation of chromosomes[4,7,8]. MAD2 could induce mitotic arrest by associating with and thus inhibiting APC when microtubule-interfering agents were present in cancer cell cultures[4,15]. However, the evidence demonstrating the clinical relevance of MAD2 to cancer cell mitotic status is yet lacking. In this study, we provided the clinical data to support the mitotic checkpoint role of MAD2 in cancer tissues. We found that 74% of our gastric cancer patients had elevated levels of MAD2 in their tumorous tissues. These patients also exhibited more cyclin B1 expression and G_2/M-phase distribution in their cancer cells. Because MAD2 can interfere with APC and APC is an ubiquitin ligase responsible for cyclin B1 degradation, elevation of both cyclin B1 expression and cellular G_2/M-phase ratio may be resulted from a higher mitotic checkpoint activity that is expected of elevated MAD2 level. Noteworthily, these patients had a tendency toward longer disease-free and overall survival. We speculate that the checkpoint activity of MAD2 exerted in these patients monitors the interaction of chromosomes with spindle fibers, which is finally linked with better disease-free and overall survival. Elevated level of MAD2 seems to be a possible target

for potential development of novel therapeutic or prognostic modalities in the future.

Our data indicate that elevated MAD2 levels did not prevent the occurrence of aneuploidy in gastric cancer. Aneuploidy is one of the hallmarks of cancer cells[23-25]. Considering spindle assembly checkproteins function as a monitor for the fidelity of chromosomal segregation, impairment of spindle assembly checkpoint is expected to associate with the development of cancer cell aneuploidy. However thus far, many aneuploid cancer cell lines did undergo mitotic arrest in response to spindle damage, indicating that not all cancer cells with aneuploidy had an impaired spindle checkpoint[26-28]. Moreover, accumulating studies have demonstrated that the BUBs (BUB1, BUBR1 and BUB3) and MADs (MAD1 and MAD2) were rarely the targets for genetic alterations in a variety of human cancer types including head-and-neck squamous cell carcinoma[29], non-small cell lung cancer[29,30], thyroid follicular neoplasms[28], hepatocellular carcinoma[27], and digestive tract cancers[17,18,30]. These data suggest that cancer cell aneuploidy may arise from the alternative defects yet to be discovered. Despite of the low frequency of gene mutation, a research of 43 gastric cancer patients concluded that overexpression of BUB1, BUBR1 or/and BUB3 was observed in >60% of cases[31]. There was no statistically positive correlation between overexpression of BUBs and cancer aneuploidy. Instead, the overexpression was significantly correlated with Ki-67 expression of tumor cells, suggesting that BUBs are proliferation-associated proteins other than spindle checkproteins in gastric cancer[31].

The gastric cancer patients with different molecular alterations were shown to have distinct histopathological features. For example, simultaneous overexpression of hepatocyte growth factor receptor (c-Met), autocrine motility factor receptor (AMFR) and urokinase-type plasminogen activator receptor (uPAR) was correlated with positive lymphatic vessel invasion and infiltration[32]. Estrogen receptor (ER) was more expressed in diffuse-type patients with regional lymph node metastasis[33]. Additionally, positive expression of nm23 was detected in as high as 74% of gastric cancer patients and was related to patients' age, tumor size, Borrmann type, Lauren classification, and TNM stage[34]. COX-2 overexpression significantly correlated with TNM staging; while abnormal expression of E-cadherin/β-catenin complex occurred more significantly in Borrmann types III/IV than in types I/II. In our present study, no histopathological parameter was found to be associated with elevated MAD2 level in gastric cancer patients. It was reported consistently that MAD2 was significantly overexpressed in colorectal adenocarcinoma, but was not related to differentiation or other clinical parameters.

In conclusion, an elevation of spindle checkprotein MAD2 level was observed in 74% of our gastric cancer patients, and was significantly correlated with the increased levels of cyclin B1 expression and G_2/M-phase distribution in cancer tissues. However, an elevated MAD2 level was not associated with aneuploidy and other clinical factors, including demographic features and histopathological characteristics.

REFERENCES

1 **Sorger PK,** Dobles M, Tournebize R, Hyman AA. Coupling cell division and cell death to microtubule dynamics**.** *Curr Opin Cell Biol* 1997; **9**: 807-814

2 **Cleveland DW**, Mao Y, Sullivan KF. Centromeres and kinetochores: from epigenetics to mitotic checkpoint signaling. *Cell* 2003; **112**: 407-421

3 **Mollinedo F**, Gajate C. Microtubules, microtubule-interfering agents and apoptosis. *Apoptosis* 2003; **8**: 413-450

4 **Li Y**, Benezra R. Identification of a human mitotic checkpoint gene: *hsMAD2*. *Science* 1996; **274**: 246-248

5 **Taylor SS**, Ha E, McKeon F. The human homologue of Bub3 is required for kinetochore localization of Bub1 and a Mad3/bub1-related protein kinase. *J Cell Biol* 1998; **142**: 1-11

6 **Skoufias DA**, Andreassen PR, Lacroix FB, Wilson L, Margolis RL. Mammalian mad2 and bub1/bubR1 recognize distinct spindle-attachment and kinetochore-tension checkpoints. *Proc Natl Acad Sci U S A* 2001; **98**: 4492-4497

7 **Li Y**, Gorbea C, Mahaffey D, Rechsteiner M, Benezra R. MAD2 associates with the cyclosome/anaphase-promoting complex and inhibits its activity. *Proc Natl Acad Sci U S A* 1997; **94**: 12431-12436

8 **Dobles M**, Liberal V, Scott ML, Benezra R, Sorger PK. Chromosomal missegregation and apoptosis in mice lacking the mitotic checkpoint protein Mad2. *Cell* 2000; **101**: 635-645

9 **Howell BJ**, Hoffman DB, Fang G, Murray AW, Salmon ED. Visualization of Mad2 dynamics at kinetochores, along spindle fibers, and at spindle poles in living cells. *J Cell Biol* 2000; **150**: 1233-1250

10 **Howell BJ**, McEwen BF, Canman JC, Hoffman DB, Farrar EM, Rieder CL, Salmon ED. Cytoplasmic dynein/dynactin drives kinetochore protein transport to the spindle poles and has a role in mitotic spindle checkpoint inactivation. *J Cell Biol* 2001; **155**: 1159-1172

11 **Fang G**, Yu H, Kirschner MW. The checkpoint protein MAD2 and the mitotic regulator CDC20 form a ternary complex with the anaphase-promoting complex to control anaphase initiation. *Genes Dev* 1998; **12**: 1871-1883

12 **Gorbsky GJ**, Chen RH, Murray AW. Microinjection of antibody to Mad2 protein into mammalian cells in mitosis induces premature anaphase. *J Cell Biol* 1998; **141**: 1193-1205

13 **Kallio M**, Weinstein J, Daum JR, Burke DJ, Gorbsky GJ. Mammalian p55CDC mediates association of the spindle checkpoint protein Mad2 with the cyclosome/anaphase-promoting complex, and is involved in regulating anaphase onset and late mitotic events. *J Cell Biol* 1998; **141**: 1393-1406

14 **Wassmann K**, Benezra R. Mad2 transiently associates with an APC/p55Cdc complex during mitosis. *Proc Natl Acad Sci U S A* 1998; **95**: 11193-11198

15 **Huang TS**, Shu CH, Chao Y, Chen SN, Chen LL. Activation of MAD 2 checkprotein and persistence of cyclin B1/CDC 2 activity associate with paclitaxel-induced apoptosis in human nasopharyngeal carcinoma cells. *Apoptosis* 2000; **5**: 235-241

16 **Huang TS**, Shu CH, Chao Y, Chen LT. Evaluation of GL331 in combination with paclitaxel: GL331's interference with paclitaxel-induced cell cycle perturbation and apoptosis. *Anti-Cancer Drug* 2001; **12**: 259-266

17 **Imai Y**, Shiratori Y, Kato N, Inoue T, Omata M. Mutational inactivation of mitotic checkpoint genes, hsMAD2 and hBUB1, is rare in sporadic digestive tract cancers. *Jpn J Cancer Res* 1999; **90**: 837-840

18 **Cahill DP**, da Costa LT, Carson-Walter EB, Kinzler KW, Vogelstein B, Lengauer C. Characterization of MAD2B and other mitotic spindle checkpoint genes. *Genomics* 1999; **58**: 181-187

19 **Lauren P**. The two histological main types of gastric carcinoma. Diffuse and so-called intestinal type carcinoma: an attempt at a histoclinical classification. *Acta Pathol Microbiol Scand* 1965; **64**: 31-49

20 **Chao Y**, Shih YL, Chiu JH, Chau GY, Lui WY, Yang WK, Lee SD, Huang TS. Overexpression of cyclin A but not Skp 2 correlates with the tumor relapse of human hepatocellular carcinoma. *Cancer Res* 1998; **58**: 985-990

21 **Chiu JH**, Kao HL, Wu LH, Chang HM, Lui WY. Prediction of relapse or survival after resection in human hepatomas by DNA flow cytometry. *J Clin Invest* 1992; **89**: 539-545

22 **Chen MH**, Yang WK, Whang-Peng J, Lee LS, Huang TS. Differential inducibilities of GFAP expression, cytostasis and apoptosis in primary cultures of human astrocytic tumors. *Apoptosis* 1998; **3**: 171-182

23 **Andreassen PR**, Martineau SN, Margolis RL. Chemical induction of mitotic checkpoint override in mammalian cells results in aneuploidy following a transient tetraploid state. *Mutation Res* 1996; **372**: 181-194

24 **Cahill DP**, Lengauer C, Yu J, Riggins GJ, Willson JK, Markowitz SD, Kinzler KW, Vogelstein B. Mutations of mitotic checkpoint genes in human cancers. *Nature* 1998; **392**: 300-303

25 **Masuda A**, Takahashi T. Chromosome instability in human lung cancers: possible underlying mechanisms and potential consequences in the pathogenesis. *Oncogene* 2002; **21**: 6884-6897
26 **Tighe A**, Johnson VL, Albertella M, Taylor SS. Aneuploid colon cancer cells have a robust spindle checkpoint. *EMBO Rep* 2001; **2**: 609-614
27 **Saeki A**, Tamura S, Ito N, Kiso S, Matsuda Y, Yabuuchi I, Kawata S, Matsuzawa Y. Frequent impairment of the spindle assembly checkpoint in hepatocellular carcinoma. *Cancer* 2002, **94**: 2047-2054
28 **Ouyang B**, Knauf JA, Ain K, Nacev B, Fagin JA. Mechanisms of aneuploidy in thyroid cancer cell lines and tissues: evidence for mitotic checkpoint dysfunction without mutations in BUB1 and BUBR1. *Clin Endocrinol* 2002; **56**: 341-350
29 **Yamaguchi K**, Okami K, Hibi K, Wehage SL, Jen J, Sidransky D. Mutation analysis of hBUB1 in aneuploid HNSCC and lung cancer cell lines. *Cancer Lett* 1999; **139**: 183-187
30 **Jaffrey RG**, Pritchard SC, Clark C, Murray GI, Cassidy J, Kerr KM, Nicolson MC, McLeod HL. Genomic instability at the BUB1 locus in colorectal cancer, but not in non-small cell lung cancer. *Cancer Res* 2000; **60**: 4349-4352
31 **Grabsch H**, Takeno S, Parsons WJ, Pomjanski N, Boecking A, Gabbert HE, Mueller W. Overexpression of the mitotic checkpoint genes BUB1, BUBR1, and BUB3 in gastric cancer-association with tumor cell proliferation. *J Pathol* 2003; **200**: 16-22
32 **Taniguchi K**, Yonemura Y, Nojima N, Hirono Y, Fushida S, Fujimura T, Miwa K, Endo Y, Yamamoto H, Watanabe H. The relation between the growth patterns of gastric carcinoma and the expression of hepatocyte growth factor receptor (c-met), autocrine motility factor receptor, and urokinase-type plasminogen activator receptor. *Cancer* 1998; **82**: 2112-2122
33 **Zhao XH**, Gu SZ, Liu SX, Pan BR. Expression of estrogen receptor and estrogen receptor messenger RNA in gastric carcinoma tissues. *World J Gastroenterol* 2003; **9**: 665-669
34 **Lee KE**, Lee HJ, Kim YH, Yu HJ, Yang HK, Kim WH, Lee KU, Choe KJ, Kim JP. Prognostic significance of p53, nm23, PCNA and c-erbB-2 in gastric cancer. *Jpn J Clin Oncol* 2003; **33**: 173-179

Edited by Zhu LH and Xu FM

PO Box 2345, Beijing 100023, China
Fax: +86-10-85381893
E-mail: wjg@wjgnet.com www.wjgnet.com

World J Gastroenterol 2004;10(22):3245-3250
World Journal of Gastroenterology
 ISSN 1007-9327

• GASTRIC CANCER •

Expression level of wild-type survivin in gastric cancer is an independent predictor of survival

Hua Meng, Cai-De Lu, Yu-Lei Sun, De-Jian Dai, Sang-Wong Lee, Nobuhiko Tanigawa

Hua Meng, Department of General Surgery, First Affiliated Hoppital of Dalian Medical University, Dalian 116011, Liaoning Province, China
De-Jian Dai, Department of Surgery, Second Affiliated Hospital of Zhejiang University School of Medicine, Hangzhou 310009, Zhejiang Province, China
Cai-De Lu, Department of Surgery, Lihuili Hospital of Ningbo University Medical School, Ningbo 315040, Zhejiang Province, China
Yu-Lei Sun, Department of Anaesthesiology, First Affiliated Hospital of Dalian Medical University, Dalian 116011, Liaoning Province, China
Sang-Wong Lee, Nobuhiko Tanigawa, Department of General and Gastroenterological Surgery, Osaka Medical College, 2-7 Daigaku-machi, Takatsuki, Osaka 569-8686, Japan
Supported by the National Natural Science Foundation of China, No. 30271483 and Grant-in-Aid from the Japanese Ministry of Education, Culture, Sports, Science, and Technology of Japan, No.13470262
Correspondence to: Cai-De Lu, M.D., Department of Surgery, Lihuili Hospital of Ningbo University Medical School, Ningbo 315040, Zhejiang Province, China. lucd71@hotmail.com
Telephone: +86-574-87392290 Ext.7707 **Fax:** +86-574-87392232
Received: 2003-10-30 **Accepted:** 2003-12-16

Abstract

AIM: *Survivin* is a novel antiapoptotic gene in which three splicing variants have been recently cloned and characterized. Survivin has been found to be abundantly expressed in a wide variety of human malignancies, whereas it is undetectable in normal adult tissues. We aimed to study the expression of three survivin splicing variants in gastric cancer, and to evaluate the prognostic significance of the expression of survivin variants in gastric cancer.

METHODS: Real time quantitative RT-PCR was performed to analyze the expression of survivin variants in 79 paired tumors and normal gastric mucosa samples at the mRNA level. Proliferative and apoptotic activity was measured using Ki-67 immunohistochemical analysis and the TUNEL method, respectively.

RESULTS: All the cases tested expressed wild-type survivin mRNA, which was not only the dominant transcript, but also a poor prognostic biomarker (P = 0.003). Non-antiapoptostic survivin-2B mRNA was correlated with tumor stage (P = 0.001), histological type (P = 0.004), and depth of tumor invasion (P = 0.041), while survivin-△Ex3 mRNA showed a significant association with apoptosis (P = 0.02).

CONCLUSION: Wild-type survivin mRNA expression levels are of important prognostic value and significant participation of survivin-2B and survivin-△Ex3 is suggested in gastric cancer development.

Meng H, Lu CD, Sun YL, Dai DJ, Lee SW, Tanigawa N. Expression level of wild-type survivin in gastric cancer is an independent predictor of survival. *World J Gastroenterol* 2004; 10(22): 3245-3250
http://www.wjgnet.com/1007-9327/10/3245.asp

INTRODUCTION

Apoptosis, also called programmed cell death, plays an important role in the development and homeostasis of tissues. Deregulation of apoptosis is involved in carcinogenesis by abnormally prolonged cell survival, facilitating the accumulation of transforming mutations and promoting resistance to immunosurveillance[1]. Several studies have consistently shown that survivin could mediate suppression of apoptosis. Surprisingly, in a single copy of *survivin* gene, three alternatively splicing transcripts have been identified. In addition to wild-type survivin, two novel survivin variants (survivin-2B, survivin-△Ex3), which have different antiapoptotic properties, have been generated. Survivin-2B has lost its anti-apoptotic potential, whereas its anti-apoptotic potential is preserved in survivin-△Ex3[2,3]. Their different functions in carcinogenesis are largely unknown.

Gastric carcinoma is one of the most frequent human malignancies[4]. As shown by our group[5], 34.5% of gastric cancers expressed survivin protein and a positive correlation between accumulated p53 and survivin expression in neoplasia was found. In this study, we investigated the distribution of survivin variants in paired tumors and normal gastric mucosa samples at the mRNA level and assessed the potential relationship between the expression of survivin variants and proliferative activity, apoptosis or prognostic significance.

MATERIALS AND METHODS

Patients and specimens

Matched pairs of tumors and normal gastric mucosa samples were obtained from 76 patients with gastric cancer and 1 patient with malignant lymphoma at the Department of General and Gastroenterological Surgery, Osaka Medical College Hospital during 2000-2002. The specimens resected at surgery were immediately frozen in liquid nitrogen and stored at -80 ℃ until total RNA extraction. Clinicopathological parameters were assigned according to the principles outlined by Japanese Classification of Gastric Carcinoma[6]. Samples included stage I cases (n = 22), stage II cases (n = 11), stages III cases (n = 20), stage IV cases (n = 26). There were 62 (78.5%) males and 17 (22.5%) females, and the mean age of the patients was 65.2 years (SD, 9.6 years; range, 40-87 years). No Patients received chemotherapy or radiation therapy either before or after surgery. The mean follow-up period was 19.7 mo (SD, 14.9 mo; range, 1.5-87 mo). Formalin-fixed paraffin-embedded blocks of primary tumors were taken from pathological archives. Two to four μm thick serial sections of 2-4 thicken were prepared from the cut surface of the blocks at the maximum cross-section of the tumors.

Total RNA extraction

Total RNA was extracted by an acid guanidinium-phenol-chloroform method using ISOGEN (Nippon Gene, Toyama, Japan) according to the manufacturer's instructions. Afterwards the total RNA was purified using DNase 1 (GIBCO-BRL, Gaithersburg, MD, USA). Extracted total RNA pellets were dissolved with RNase free diethyl pyrocarbonate (DEPC)-treated water.

Reverse transcription

Complementary DNA (cDNA) was synthesized with 5 μg of total RNA and 20 pmoL oligo $(dT)_{18}$ primer using an Advantage

RNA-for-PCR kit (CLONTECH, Inc., Palo Alto, USA), with the exception of 200 U SurperScript™ II RNase H- reverse transcriptase (Invitrogen, Inc., Carlsbad, USA) in a final 20 μL reaction volume. RT reactions were performed at 50 ℃ for 120 min. Finally, cDNA solution was diluted to a total volume 100 μL.

Quantitative real time RT-PCR

Quantitative real time RT-PCR was performed with a LightCycler (Roche Diagnostics, Mannheim, Germany). As an internal control, housekeeping gene G6PDH mRNA expression was measured at the same time. DEPC-treated H_2O was used as a negative control and MKN-74 was used as a positive control. Then, 1μL of cDNA mixture was subjected to amplification in 10 μL reaction mixture. The PCR conditions were initial denaturation at 95 ℃ for 10 min, followed by 40 cycles of denaturation at 95 ℃ for 10 s, annealing at 62 ℃ for 10 s for survivin, survivin-2B and survivin-△Ex3 (or at 63 ℃ for G6PDH), extension at 72 ℃ for 10 s, respectively. A standard curve using fluorescent data was generated from serial tenfold dilution of specific plasmids from 10^7 to 10^2 copies, respectively. The number of gene copies was calculated by the LightCycler Software Version3.5.3 according to the Fit Points Above Threshold method. Primer pairs and hybridization probes for survivin, survivin-2B, survivin-△Ex3 and G6PDH mRNA were as follows. The sequence of the common forward primer for survivin variants was 5'-CCACCGCATCTC TACATTCA-3'. To distinguish the 3 splice variants of survivin, the sequences of reverse primers for survivin variants were designed to correspond to exon/exon borders of the complementary strand (5'-TATGTTCCTCTATGGGGTCG-3' for survivin, 5'-AGTGCTGGTATTACAGGCGT-3' for survivin-2B, 5'-TTTCCT TTGCATGGGGTC-3' for survivin-△Ex3). The sequences of common hybridization probes for survivin variants were 5'-CAAGTCTGGCTCGTTCTCAGTGGG-3'-FITC and LCRed640-5'-CAGTGGATGAAGCCAGCCTCG-3'. The sequence of the forward primer for G6PDH was 5'-TGGACCTGACCTACGGCA ACAGATA-3'. The sequence of the reverse primer for G6PDH was 5'-GCCCTCATACTGGAAACCC-3'. The sequences of hybridization probes for G6PDH were 5'-TTTTCACCCCACTGC TGCACC-3'-FITC and LCRed640-5'-GATTGAGCTGGAGAAG CCCAAGC-3.

PCR products were additionally checked by electrophoresis on 30 g/L agarose gels (BIO-RAD, Inc., Hercules, USA) containing ethidium bromide and visualized under UV transillumination.

Sequence analysis

To confirm the identity of the PCR products, their bands were excised from agarose gels and isolated by a QIAquick gel extraction kit (Qiagen, Tokyo, Japan), ligated into a pGEM-T-cloning vector (Promega), and cloned according to standard protocols. Plasmid DNA was recovered using a Plasmid Mini kit (Qiagen, Tokyo, Japan). Cycle was sequenced and analyzed in an ABI-PRISM310 (Applied Biosystems) using T7 or SP6-site specific primers. The sequences of the PCR products were compared with those in GenBank, which were found to be identical (Data not shown).

Ki-67 immunohistochemical staining and assessment of proliferative index

Immunohistochemical staining was performed by the standard avidin-biotin-peroxidase complex technique using L.V. Dako LSAB kit (DAKO, Copenhagen, Denmark) as described previously[5,7,8]. The antibodies used were monoclonal mouse antibody Ki-67 (MIB-1, diluted 1:50; Immunotech, Marseilles, France). The labeling index (LI) of Ki-67 was determined in those tumor areas with positive stained nuclei. Five random areas within a section were chosen and counted under 200-fold magnification using a point counting technique. The average percentage of positivity was recorded as the Ki-67 LI for each case[7].

Histochemical detection of apoptosis and determination of AI

Apoptotic cells in tissue sections were detected by terminal deoxynucleotidyl transferase-mediated dUTP-biotin nick end labeling (TUNEL), using an Apop Tag *in situ* detection kit (Oncor, Gaithersburg, MD). The staining procedures were based on a method described previously[5,6,8]. The apoptotic index (AI) was expressed as the ratio of positively stained tumor cells and bodies to all tumor cells according to the criteria described elsewhere[5,7]. Five areas were randomly selected for counting under 400-fold magnification.

Statistical methods

All statistical analyses were performed by the SPSS11.0 software package for Windows (SPSS Inc., Chicago, IL). Differences in the numerical data between the two groups were evaluated using the Mann-Whitney U test. The χ^2 test was further used to compare the distribution of individual variables and any correlation between AI or Ki-67 index and expression of survivin variants. The correlation between AI and expression of survivin variants for each case was also analyzed by Spearman's rank correlation test. Survival curves were calculated using the Kaplan-Meier method and analyzed by the log rank test. A two-tailed *P* value less than 0.05 was considered statistically significant.

RESULTS

Expression of survivin variants in clinical materials and cell lines

Among the 79 tumor samples, survivin expression was detected in all tumor samples (79/79), survivin-2B expression was demonstrated in 78.5% (62/79) of the samples and survivin-△Ex3 expression was detected in 64.6% (51/79) of the samples (Figure 1). In contrast, survivin expression was detectable in 46 (58.2%) of the normal mucosa samples, while survivin2B expression and survivin-△Ex3 were detected in 23 (29.1%) and 12 (15.2%) of the mucosa samples respectively.

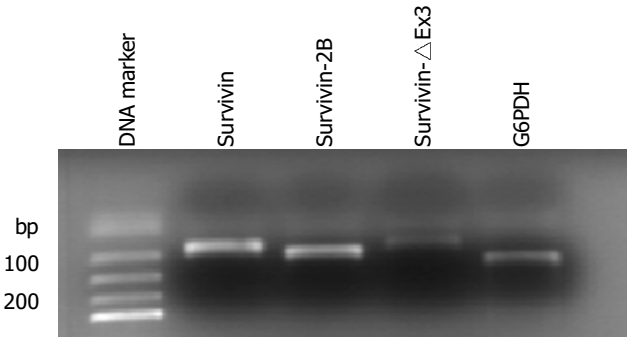

Figure 1 Amplification, separation and visualization of survivin (185 bp), survivin-2B (214 bp) survivin-△Ex3 (184 bp), and G6PDH (256 bp) mRNA (40 cycles) in a typical case.

The relative amounts of survivin variant mRNA were determined by dividing the amount of survivin variant mRNA by that of G6PDH mRNA for each sample. In tumor samples, the relative levels of survivin-2B and survivin-△Ex3 was further normalized by matched survivin. Because three alternatively spliced variants are derived from a common hnRNA precursor pool, these ratios seemed to be independent of any possible bias imposed by variations in housekeeping gene expression levels[9,10]. Although there was a significant difference in G6PDH expression between normal tissues and cancer samples at the same amount of total RNA used ($P<0.0001$, Mann-Whitney U test, Figure 2A), the survivin variant/G6PDH ratio in our cancer tissues were significantly higher than that in non-neoplastic tissues ($P<0.0001$, Mann-Whitney U test, Figure 2B).

Table 1 Relationship among expression levels of survivin variants and clinicopathologic parameters, proliferative activity or apoptosis

Parameters	No. of patients (%)	Sur/G6PDH	Sur-2B/G6PDH	Sur-△Ex3/G6PDH	Sur-2B/sur	Sur-△Ex3/sur
Gender (median)						
Male	62 (78.5)	P = 0.445	P = 0.598	P = 0.079	P = 0.125	P = 0.408
Female	17 (22.5)					
Age yr (median)						
<64	39	P = 0.462	P = 0.108	P = 0.177	P = 0.129	P = 0.262
>64	40					
Histological type						
Differentiated	47	P = 0.976	P = 0.004	P = 0.151	P = 0.053	P = 0.231
Undifferentiated	32					
Depth of invade						
Not invasion	27	P = 0.336	P = 0.042	P = 0.266	P = 0.354	P = 0.555
Invasion	40					
Clinical stage						
Stage I+II	(22+11)	P = 0.075	P = 0.001	P = 0.139	$\boldsymbol{P}$ = 0.018	P = 0.863
Stage III+IV	(20+26)					
Ki67 (median)						
Low	39	P = 0.791	P = 0.197	P = 0.567	P = 0.401	P = 0.512
High	40					
Apop Tag (median)						
Low	39	P = 0.421	P = 0.070	P = 0.0020	P = 0.408	P = 0.099
High	40					

Two-tailed P values were calculated by the Mann-Whitney U test. Differentiated type: Papillary type, Tubular type. Undifferentiated type: Poorly differentiated type, Signet ring cell type, Mucinous type. Not invasion: No invasion of the serosa. Invasion: invasion of the serosa.

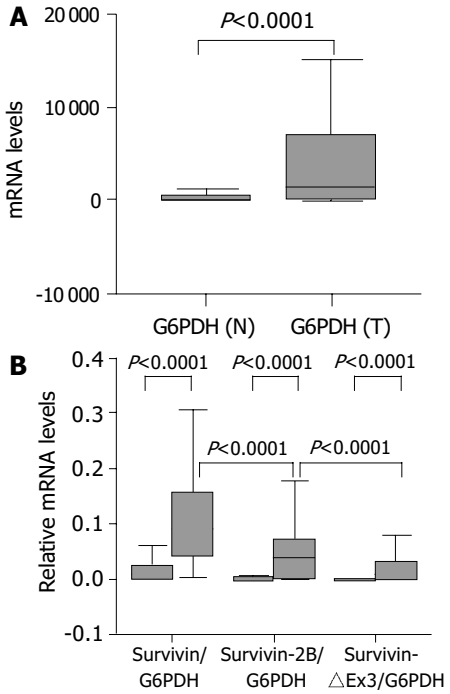

Figure 2 A: RT-PCR amplification of G6PDH in paired samples of normal gastric mucosa and gastric carcinoma. B: Relative (G6PDH-normalised) mRNA levels of survivin variants in paired samples of normal gastric mucosa and gastric carcinoma. Two-tailed P values were calculated by the Mann-Whitney U test.

Relationship between expression levels of survivin variants and clinicopathological parameters

The expression level of survivin-2B was significantly (P = 0.001, Table 1, P<0.0001, χ^2 test, Figure 3A) decreased in advanced (III+IV) stage compared with early (I+II) tumor stage. Furthermore, the level of survivin-2B was inversely correlated with the grade of tumor differentiation (P = 0.004, Table 1, P = 0.023, χ^2 test, Figure 3B) and depth of tumor invasion (P = 0.042, Table 1, P = 0.021, χ^2 test). A stage-dependent decrease of survivin-2B was also confirmed by the ratio of survivin-2B/survivin (P = 0.018, Table 1, P = 0.022, χ^2 test, Figure 3C).

None of the investigated clinicopathological parameters showed a statistically significant correlation with the expression of other types of survivin variants besides survivin-2B.

Correlation between expression levels of survivin variants and AI

Apoptotic cells and bodies were detected in all cases of gastric carcinoma tested (Table 1, Figure 4A). The mean AI was 1.07% (SD, 0.41%; range, 0.38-2.38%) with a median of 0.95%. The mean AI in survivin-△Ex3-low expression samples was significantly higher than that in survivin-△Ex3-high expression samples (P = 0.02, Table 1, P = 0.028, χ^2 test, Table 1). There was no correlation between apoptotic index and clinicopathological parameters described. Spearman's rank correlation test demonstrated a significant negative correlation between apoptotic index and expression level of survivin-△Ex3 (Γ = -0.257, P = 0.022).

Association of expression levels of survivin variants with PI

Proliferative cells were detected by intense nuclear immunoreactivity to the Ki-67 antigen, as illustrated in Figure 4B. The mean proliferative index (PI) in gastric tumors tested was 48.46% (SD, 9.54%; range, 28.49-82.98%) with a median of 46.87%. No significant relationship was identified between PI of tumor cells and clinicopathological parameters, as demonstrated in Table1. In addition, no significant association was found between PI and any type of survivin variants.

Prognostic value of survivin mRNA expression

Postoperative survival of the 79 gastric cancer patients was analyzed according to the expression level of survivin variants. Results are shown in Figure 5. Each survivin variant value was divided by the median value. The survival curve of patients with high-survivin expression was significantly lower than that of those with low-survivin expression (P = 0.003, log-rank test). No prognostic significance for either survivin-2B or survivin-△Ex3, however, was found in the current study.

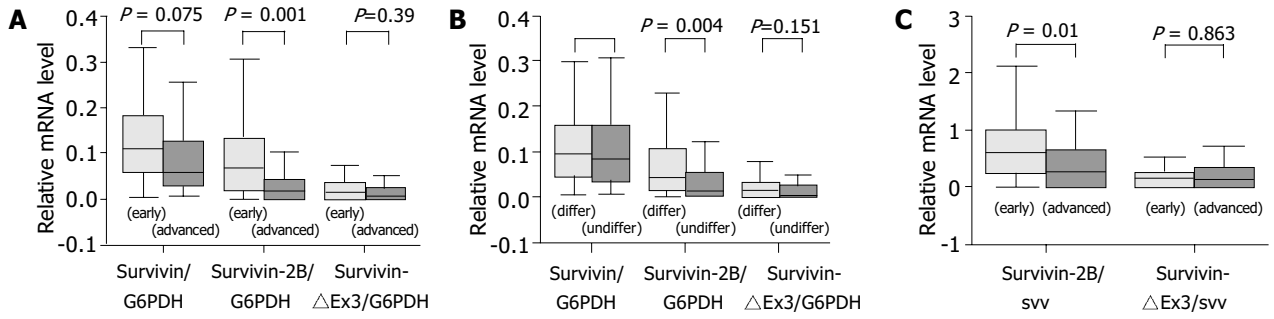

Figure 3 Relative mRNA levels of survivin variants. A: Significant decrease of relative (G6PDH-normalised) mRNA levels of survivin-2B in advanced stages (P = 0.001, Mann-Whitney U test). B: Significant decrease of relative (G6PDH-normalised) mRNA levels of survivin-2B in undifferentiated type (P = 0.004, Mann-Whitney U test). C: Significantly lower ratio of survivin-2B / survivin in advanced stages than that in early stages (P = 0.018, Mann-Whitney U test).

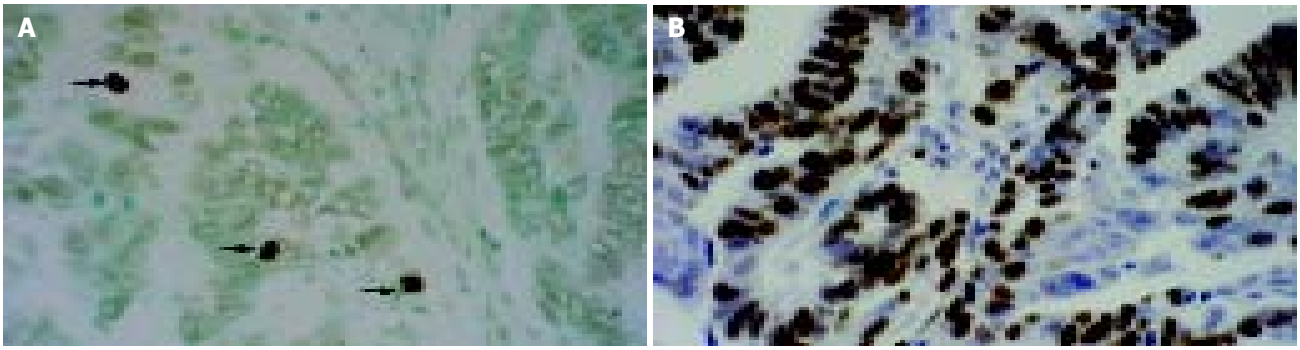

Figure 4 Histochemical staining for Ki-67 and apoptotic tumor cells. A: TUNEL *in situ* labeling for detecting apoptotic cells and bodies (arrows, magnification ×400) in adenocarcinoma. B: Ki-67 nuclear immunohistochemical staining revealing proliferating tumor cells in adenocarcinoma (magnification ×400).

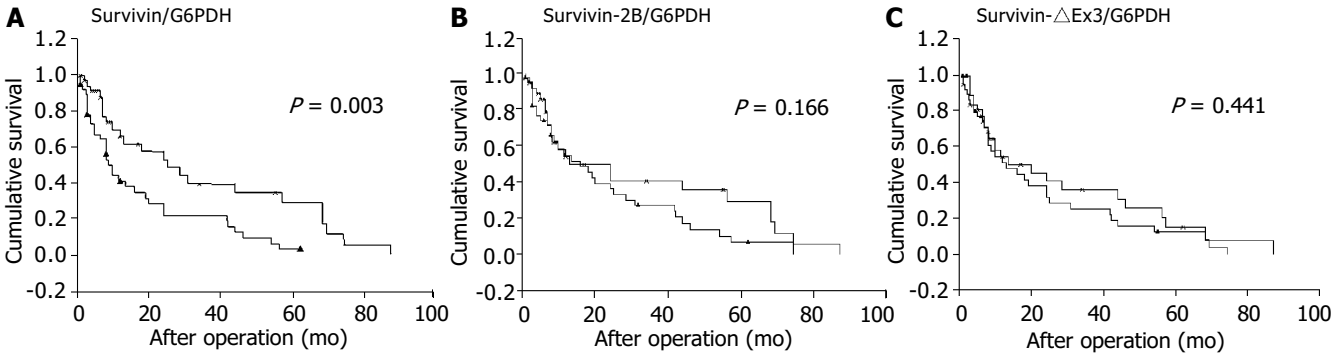

Figure 5 postoperative survivals of 79 gastric carcinoma patients. A: Shorter survival time of patients with high expression of wild-type survivin mRNA compared to patients with low expression of wild-type survivin expression (P = 0.003, log-rank test). B: No significance in expression of survivin-2B mRNA (P = 0.166, log-rank test). C: No significance in expression of survivin-△Ex3 mRNA (P = 0.441, log-rank test).

DISCUSSION

In this study, the prognostic significance of the expression of three survivin splicing variants in gastric carcinoma was examined for the first time. Interestingly, only increased wild-type survivin mRNA expression was prominently correlated with reduced survival time, whereas neither survivin-2B nor survivin-△Ex3 showed an association with prognosis. In accordance with recent studies, we did not find a correlation between mRNA expression levels of anti-apoptotic variants (survivin or survivin-△Ex3) and the investigated clinicopathological parameters[9,10]. There is no doubt, however, survivin plays a role in enhancing the malignant behavior of tumors. In cell culture systems, over-expression of survivin was consistently associated with inhibition of cell death[2]. Strong survivin mRNA expression showed chemo-radio resistance[11-13] and a correlation with recurrence in patients[14]. In retrospective trials, increased survivin mRNA or protein expression was reported to be a prognostic indicator of tumor progression in different types of human cancer[15-19]. Our observations further confirmed that survivin mRNA was a poor prognostic biomarker. This suggests that a relatively straightforward detection of survivin protein or mRNA in clinical patients may provide an initial marker of aggressive diseases, potentially requiring in-depth follow-up protocols or alternative treatment regimens in the future.

The notion that survivin inhibits apoptosis has been established, but the mechanism (s) by which this occurs has not been conclusively determined. The actual molecular interaction partners of survivin variants, however, have remained elusive[2]. Although there is a good agreement that deregulation of cell death/survival pathways contributes to malignant transformation, the potential predictive/prognostic impact of apoptosis regulatory molecules and AI has remained controversial[8]. This study failed to show the relationship between apoptotic index and survivin expression in gastric carcinoma although it was shown in previous[5,20] studies showed in gastric cancer that survivin expression was inversely correlated with apoptosis. These controversial findings were attributed in part to the dual function by which survivin regulates cell death and cell division. In recent studies, frameshift carboxyl terminus of survivin-△Ex3 was found to contain a bipartite localization signal, which mediates its strong nuclear accumulation and might interfere with degradation of survivin-△Ex3 protein by ubiquitin tagging. Survivin-△Ex3, therefore, could evade cell cycle-specific degradation by the ubiquitin-proteasome pathway, known for survivin. In contrast, cytoplasm has been found to be the most probable location of both survivin and survivin-2B[21,22]. Other unique features in survivin-△Ex3 were also identified, including a mitochondrial localization signal and a BH2 domain, which might inhibit apoptosis by association with bcl-2, and suppress Caspase-3 activity by BIR-dependent pathway[23]. Consequently, survivin-△Ex3 may play a more crucial role in the regulation of apoptosis.

Although mRNA levels of survivin-2B and survivin-△Ex3 have been found in different tumors[3,10,24,25], little is known about the protein levels of endogenous survivin-2B and survivin-△Ex3, due to the lack of survivin variant-specific antibodies. Our results showed that a low mRNA expression level of survivin-2B was inversely correlated to the advanced (III+IV) stage, undifferentiated tumor histology and deep tumor invasion. There are at least two reasonable explanations for this finding. After losing its antiapoptotic potential, survivin-2B was hypothesized to be a naturally occurring antagonist of survivin from competitive binding to heterologous interaction partners, or from the formation of inactive survivin: survivin-2B heterodimers with respect to recently observed dimer formation of survivin[21]. Downregulation of survivin-2B might weaken its functional antagonism, and moreover, could permit the generation of more survivin or survivin-△Ex3 because three survivin variants come from the same pool of a hnRNA precursor. Thus, the decrease in survivin-2B may result in the development, invasion and anaplasia of carcinomas.

In addition, our data showed that all gastric carcinoma samples expressed wild-type survivin at a significant level compared to the matched normal gastric mucosa samples. Similarly, the expression of survivin-2B or survivin-△Ex3 was significantly elevated in carcinoma tissue. Among three survivin variants, survivin was the dominant transcript. In this regard, our results were consistent with those of two recent TR-PCR studies[10,26] on gastric cancer in which a few gastric mucosa samples (17-23%) of the first-degree relatives also expressed survivin mRNA, but the normal control subjects did not. All these findings may help explain why survivin variants played important roles in the early stage of carcinogenesis of gastric cancer.

In summary, survivin mRNA is a poor prognostic biomarker and that non-antiapoptotic survivin-2B was correlated to tumor stage, histological type and depth of tumor invasion. Even more striking is the observation for the first time that neither survivin nor survivin-2B show a close association with the apoptosis index, as observed in survivin-△Ex3, although further experimental work is necessary to elucidate the functional properties of different splicing variants in more detail.

ACKNOWLEDGEMENTS

We thank Ms. Akiko Miyamoto and Drs. Takaharu Suga and Yoshiaki Tatsumi, Department of General and Gastroenterological Surgery, or Dr. Noda Naohiro, First Department of Pathology, Osaka Medical College for their excellent assistance throughout this investigation.

REFERENCES

1 **Rudin CM,** Thompson CB. Apoptosis and disease: regulation and clinical relevance of programmed cell death. *Annu Rev Med* 1997; **48**: 267-281

2 **Altieri DC.** Validating survivin as a cancer therapeutic target. *Nat Rev Cancer* 2003; **3**: 46-54

3 **Mahotka C,** Wenzel M, Springer E, Gabbert HE, Gerharz CD. Survivin-deltaEx3 and survivin-2B: two novel splice variants of the apoptosis inhibitor survivin with different antiapoptotic properties. *Cancer Res* 1999; **59**: 6097-6102

4 **Liu HF,** Liu WW, Fang DC, Men RP. Expression and significance of proapoptotic gene Bax in gastric carcinoma. *World J Gastroenterol* 1999; **5**: 15-17

5 **Lu CD,** Altieri DC, Tanigawa N. Expression of a novel antiapoptosis gene, survivin, correlated with tumor cell apoptosis and p53 accumulation in gastric carcinomas. *Cancer Res* 1998; **58**: 1808-1812

6 **Nishi M,** Omori Y, Miwa K. Japanese Classification of Gastric Carcinoma, First English edition. *TOKYO: KANEHARA & CO., LTD* 1995

7 **Kawasaki H,** Toyoda M, Shinohara H, Okuda J, Watanabe I, Yamamoto T, Tanaka K, Tenjo T, Tanigawa N. Expression of survivin correlates with apoptosis, proliferation, and angiogenesis during human colorectal tumorigenesis. *Cancer* 2001; **91**: 2026-2032

8 **Kawasaki H,** Altieri DC, Lu CD, Toyoda M, Tenjo T, Tanigawa N. Inhibition of apoptosis by survivin predicts shorter survival rates in colorectal cancer. *Cancer Res* 1998; **58**: 5071-5074

9 **Mahotka C,** Krieg T, Krieg A, Wenzel M, Suschek CV, Heydthausen M, Gabbert HE, Gerharz CD. Distinct *in vivo* expression patterns of survivin splice variants in renal cell carcinomas. *Int J Cancer* 2002; **100**: 30-36

10 **Krieg A,** Mahotka C, Krieg T, Grabsch H, Muller W, Takeno S, Suschek CV, Heydthausen M, Gabbert HE, Gerharz CD. Expression of different survivin variants in gastric carcinomas: first clues to a role of survivin-2B in tumour progression. *Br J Cancer* 2002; **86**: 737-743

11 **Asanuma K,** Moriai R, Yajima T, Yagihashi A, Yamada M, Kobayashi D, Watanabe N. Survivin as a radioresistance factor in pancreatic cancer. *Jpn J Cancer Res* 2000; **91**: 1204-1209

12 **Ikeguchi M,** Kaibara N. Changes in survivin messenger RNA level during cisplatin treatment in gastric cancer. *Int J Mol Med* 2001; **8**: 661-666

13 **Kato J,** Kuwabara Y, Mitani M, Shinoda N, Sato A, Toyama T, Mitsui A, Nishiwaki T, Moriyama S, Kudo J, Fujii Y. Expression of survivin in esophageal cancer: correlation with the prognosis and response to chemotherapy. *Int J Cancer* 2001; **95**: 92-95

14 **Azuhata T,** Scott D, Takamizawa S, Wen J, Davidoff A, Fukuzawa M, Sandler A. The inhibitor of apoptosis protein survivin is associated with high-risk behavior of neuroblastoma. *J Pediatr Surg* 2001; **36**: 1785-1791

15 **Ikeguchi M,** Kaibara N. Survivin messenger RNA expression is a good prognostic biomarker for oesophageal carcinoma. *Br J Cancer* 2002; **87**: 883-887

16 **Adida C,** Berrebi D, Peuchmaur M, Reyes-Mugica M, Altieri DC. Anti-apoptosis gene, survivin, and prognosis of neuroblastoma. *Lancet* 1998; **351**: 882-883

17 **Adida C,** Haioun C, Gaulard P, Lepage E, Morel P, Briere J, Dombret H, Reyes F, Diebold J, Gisselbrecht C, Salles G, Altieri DC, Molina TJ. Prognostic significance of survivin

expression in diffuse large B-cell lymphomas. *Blood* 2000; **96**: 1921-1925

18 **Chakravarti A,** Noll E, Black PM, Finkelstein DF, Finkelstein DM, Dyson NJ, Loeffler JS. Quantitatively determined survivin expression levels are of prognostic value in human gliomas. *J Clin Oncol* 2002; **20**: 1063-1068

19 **Kamihira S,** Yamada Y, Hirakata Y, Tomonaga M, Sugahara K, Hayashi T, Dateki N, Harasawa H, Nakayama K. Aberrant expression of caspase cascade regulatory genes in adult T-cell leukaemia: survivin is an important determinant for prognosis. *Br J Haematol* 2001; **114**: 63-69

20 **Wakana Y,** Kasuya K, Katayanagi S, Tsuchida A, Aoki T, Koyanagi Y, Ishii H, Ebihara Y. Effect of survivin on cell proliferation and apoptosis in gastric cancer. *Oncol Rep* 2002; **9**: 1213-1218

21 **Mahotka C,** Liebmann J, Wenzel M, Suschek CV, Schmitt M, Gabbert HE, Gerharz CD. Differential subcellular localization of functionally divergent survivin splice variants. *Cell Death Differ* 2002; **9**: 1334-1342

22 **Rodriguez JA,** Span SW, Ferreira CG, Kruyt FA, Giaccone G. CRM1-mediated nuclear export determines the cytoplasmic localization of the antiapoptotic protein Survivin. *Exp Cell Res* 2002; **275**: 44-53

23 **Wang HW,** Sharp TV, Koumi A, Koentges G, Boshoff C. Characterization of an anti-apoptotic glycoprotein encoded by Kaposi's sarcoma-associated herpesvirus which resembles a spliced variant of human survivin. *EMBO J* 2002; **21**: 2602-2615

24 **Hirohashi Y,** Torigoe T, Maeda A, Nabeta Y, Kamiguchi K, Sato T, Yoda J, Ikeda H, Hirata K, Yamanaka N, Sato N. An HLA-A24-restricted cytotoxic T lymphocyte epitope of a tumor-associated protein, survivin. *Clin Cancer Res* 2002; **8**: 1731-1739

25 **Kappler M,** Kohler T, Kampf C, Diestelkotter P, Wurl P, Schmitz M, Bartel F, Lautenschlager C, Rieber EP, Schmidt H, Bache M, Taubert H, Meye A. Increased survivin transcript levels: an independent negative predictor of survival in soft tissue sarcoma patients. *Int J Cancer* 2001; **95**: 360-363

26 **Yu J,** Leung WK, Ebert MP, Ng EK, Go MY, Wang HB, Chung SC, Malfertheiner P, Sung JJ. Increased expression of survivin in gastric cancer patients and in first degree relatives. *Br J Cancer* 2002; **87**: 91-97

Edited by Wang XL **Proofread by** Xu FM

PO Box 2345, Beijing 100023, China
Fax: +86-10-85381893
E-mail: wjg@wjgnet.com www.wjgnet.com

World J Gastroenterol 2004;10(22):3251-3254
World Journal of Gastroenterology
 ISSN 1007-9327

• LIVER CANCER •

Detection of bcl-2 and bax expression and bcl-2/JH fusion gene in intrahepatic cholangiocarcinoma

Lin-Lang Guo, Sha Xiao, Ying Guo

Lin-Lang Guo, Sha Xiao, Ying Guo, Department of Pathology, Zhujiang Hospital, Guangzhou 510282, Guangdong Province, China
Correspondence to: Dr. Lin-Lang Guo, Department of Pathology, Zhujiang Hospital, Guangzhou 510282, Guangdong Province, China. linlangg@yahoo.com
Telephone: +86-20-61643495 **Fax:** +86-20-84311872
Received: 2003-05-10 **Accepted:** 2003-06-04

Abstract

AIM: To investigate the relationship between bcl-2 gene and its related protein bax and intrahepatic cholangiocellular carcinoma (CCC).

METHODS: Semi-nested *in situ* PCR (SNISPCR) and immunohistochemistry were performed to detect bcl-2/JH fusion gene and bcl-2, bax protein expression in 29 cases of CCC.

RESULTS: No bcl-2/JH fusion gene was found in all cases of CCC, 72.4% of 29 cases expressed bcl-2 protein. Bcl-2 protein expression was related to histopathological grades ($P<0.05$). There was no corresponding relationship between bcl-2/JH fusion gene formation and bcl-2 protein expression in CCC ($P<0.05$). Bax was expressed in 10.3% of 29 cases. The ratio of bcl-2 to bax in normal liver tissues (3.5 to 1) was different from that in tumor tissues (7.0 to 1).

CONCLUSION: It is suggested that bcl-2/JH fusion gene formation is not a frequent event and may not play an important role in the pathogenesis of CCC. However, aberrant ratio of bcl-2 to bax protein expression may be involved in the course of tumorigenesis of CCC. Abnormal bcl-2 protein expression may not be solely resulted from bcl-2/JH fusion gene.

Guo LL, Xiao S, Guo Y. Detection of bcl-2 and bax expression and bcl-2/JH fusion gene in intrahepatic cholangiocarcinoma. *World J Gastroenterol* 2004; 10(22): 3251-3254
http://www.wjgnet.com/1007-9327/10/3251.asp

INTRODUCTION

Bcl-2 gene was first identified in B-cell leukemia and follicular lymphoma which confered a survival advantage on B-cells by inhibiting apoptosis. Bcl-2 gene at chromosome 18 is juxtaposed with the immunoglobulin heavy chain gene (JH) on chromosome 14[1]. The t (14; 18) chromosome translocation was present in 70% to 85% of follicular lymphoma and in 20% to 30% of diffuse large-cell lymphomas[1-4]. While aberrant expression of bcl-2 protein was also found in follicular lymphoma. In the early study, bcl-2 gene was mainly investigated in lymphoid tissues. Recently, bcl-2 gene aberrant expression has been observed in a variety of tumors, such as adenocarcinoma of the prostate, bladder carcinoma, squamous cell carcinoma of the lung, nasopharyngeal carcinoma, breast carcinoma and cholangiocarcinoma[5-17]. However, bcl-2/JH fusion gene and its relationship with bcl-2 protein expression have not been detected in cholangiocellular carcinoma (CCC).

Bax, an important homologue of bcl-2, is a promoter of apoptosis. It has been proposed that the sensitivity of cells to apoptosis stimuli be closely related to the ratio of bcl-2/bax and other bcl-2 homology. When bcl-2 is in excess, cells are protected. However, when bax is in excess and bax homodimers dominate, cells are susceptible to apoptosis[18]. Whether bcl-2/bax expression ratio is involved in the course of tumorigenesis of CCC remains unknown.

In this study, we demonstrated that bcl-2/JH fusion gene, bcl-2 and its related protein bax expression with semi-nested *in situ* PCR (SNISPCR) and immunohistochemistry in 29 cases of CCC to understand the relationship between bcl-2 gene and its related protein bax in CCC.

MATERIALS AND METHODS

Tissue preparation

A total of 29 samples were obtained by surgical resection in our department from 1995-06-01 to 1998-02-28. All samples were independently reviewed by two pathologists and graded as recommended by WHO. The cases of CCC were classified as follows: 6 cases of well differentiated, 14 cases of moderately differentiated and 9 cases of poorly differentiated carcinomas. Undamaged liver tissues from surgical resection specimens of young adults with minor liver injury who underwent partial hepatectomy were used as normal controls. All tissues were fixed in 40 g/L formaldehyde (pH 7.0) for 12-24 h and embedded in paraffin and then 4 μm thick serial sections were cut and mounted on poly-l-lysine coated slides.

Immunohistochemical staining

The sections were deparaffinized and rehydrated routinely. Antigens were retrieved by heating the sections in a microwave oven at 700 W in 10 mmol/L citrate buffer (pH 6.0) for 10 min. After blocked with 3 mL/L H_2O_2 and swine serum, specimens were then incubated with the primary antibodies, directed against bcl-2 (Maxim Biotech Co., China) and bax (Senta Cruz). The staining was performed by streptavidin peroxidase enzyme conjugate method using a S-P kit (Zymed). Reaction products were visualized by DAB. Brown-yellow granules in cytoplasm were recognized as positive staining.

Semi-nested in situ PCR

Pretreatment: Sections were deparaffinized and dehydrated routinely, then washed in 0.1 mol/L HCI and PBS, digested with proteinase K (10 mg/L), and placed on the platform in a DNA thermal cycler at 98 ℃ for 2 min.

Amplification *in situ*: The final volume of 20 μL (200 μmol/L each of dATP, dCTP, dGTP and dTTP, 1.5 U Taq polymerase,10× buffer). Two and half sets of primers specific for the two hot breakpoint regions on bcl-2 gene were synthesized according to the DNA sequences published by Gribben[19]. The following oligonucleotides were used as primer pairs: A, 5'-CAGCCTTGA AACATTGATGG-3' for the mbr (in major breakpoint region); B, 5'-CGTGCTGGTACCACTCCTG-3' for the mcr (in minor breakpoint region); C, 5'-TATGGTGGTTTGACCTTTAG-3' for the mbr (in major breakpoint region); D, 5'-GGACCTTCCTTGG

TGTGTTG-3' for mcr (in minor breakpoint region); Immunoglobulin heavy chain (JH), 5'-ACCTGAGGAGACGGTGACC-3'. At first, mbr-JH fusion gene was amplified by primer A and JH, and mcr-JH fusion gene was amplified by primer B and JH. The slides were covered after adding reaction mixture. The samples were subjected to 25 amplification cycles, each cycle consisiting of denaturation at 94 ℃ for 1 min, annealing at 55 ℃ for 1 min and extension at 72 ℃ for 1 min. The final extension period was extended to 10 min. Reamplification was performed for 30 cycles using primer C, JH for mbr-JH fusion gene and D, JH for mcr-JH fusion gene. The conditions were the same as stated above.

In situ hybridization

The covers were removed and dehydrated routinely. The slides were incubated in 40 g/L poly formeldehyde for 10 min. Forty μL hybridization solution (probe concentration 50 pmol/L) was added on slides overnight at 37 ℃ in a wet box. The oligonucleotide probe was labeled with biotin. Sequences of the probes were 5'-CCCTCCTGCCCTCCTTCCG-3' for mbr and 5'-GGACCTTC CTTGGTGTGTTG-3' for mcr.

Non-specific antigen was blocked with 20 mL/L bovine serum and 3 g/L Triton X-100, followed by incubation with anti-biotin antibody alkaline phosphates mixture for 1 h. Slides were then visualized with BCIP/NBT. Purple-blue granules in nuclei were regarded as positive.

Controls

Follicular lymphoma was used as positive control. Negative controls included blank control with no primers, dNTP or Taq polymerase omission in PCR reaction solution, and probe omission in hybridization solution. To exclude false positive or negative results, each sample was analyzed at least twice. Non-corresponding tissues such as normal skin tissue were also treated to exclude the false positive possibility.

Statistical analysis

Statistical significance was calculated by χ^2 test, which was used to analyze the relation between bcl-2 and bax protein staining and positive bcl-2/JH fusion gene and histopathological grades. $P<0.05$ was considered as statistically significant.

RESULTS

Expression of bcl-2 protein in CCC

Twenty-one of 29 cases expressed bcl-2 protein, induding 5 well differentiated, 13 moderately differentiated and 3 poorly differentiated carcinomas. There was a statistically significant difference between moderately differentiated and poorly differentiated carcinomas in Bcl-2 expression ($P<0.05$, $\chi^2 = 5.58$). Bcl-2 was also expressed in 87.5% (14/16) in normal liver tissues of small bile ducts (Figures 1, 3).

Detection of bcl-2/JH fusion gene in CCC

Bcl-2/JH fusion gene was not detected in any case of CCC and normal liver tissues.

Relationship between bcl-2 protein expression and bcl-2/JH fusion gene

No bcl-2/JH fusion gene was detected in bcl-2 protein positive and negative groups. There was no correlation between bcl-2 protein expression and bcl-2/JH fusion gene.

Expression of bax protein in CCC

Bax was expressed in 3 (10.3%) of 29 cases , in which 1/6 was well differentiated carcinoma, 2/14 were moderately differentiated carcinomas and none was poorly differentiated carcinoma. There was no statistically significant difference between bax expression and histological grades. Four (25%) of 16 normal liver tissue samples expressed bax protein (Figures 2, 4).

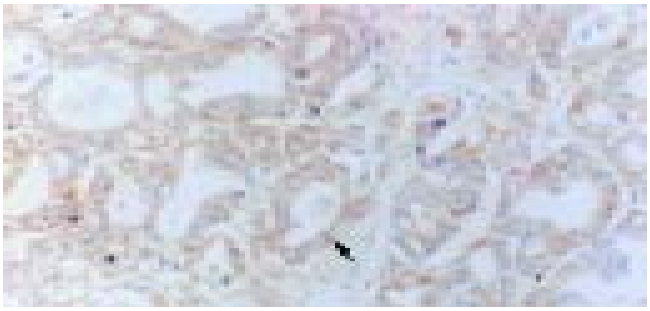

Figure 1 Primary hepatic cholangiocarcinoma. Brown-yellow staining in cytoplasm of carcinoma cells for bcl-2 protein (arrowhead) Immunohistochemistry staining ×200.

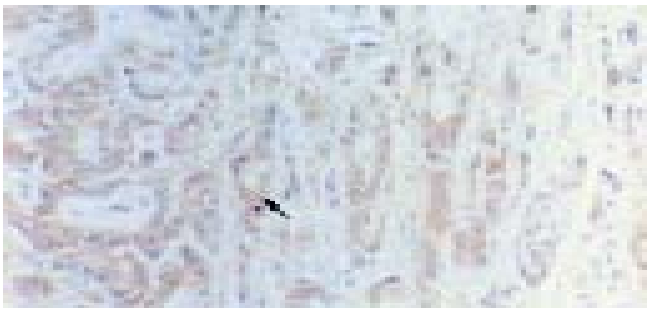

Figure 2 Primary hepatic cholangiocarcinoma. Brown-yellow staining in cytoplasm of carcinoma cells for bax protein (arrowhead) Immunohistochemistry staining ×200.

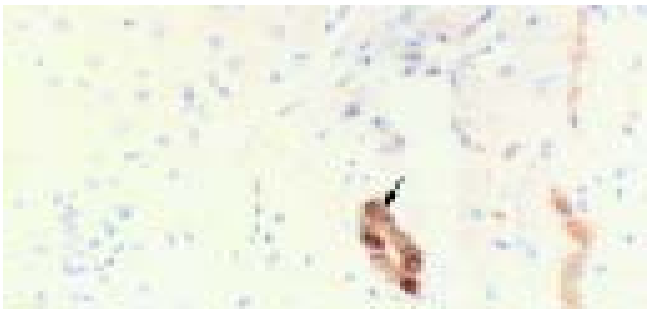

Figure 3 Normal liver. Brown-yellow staining in cytoplasm of small bile duct epithelial cells for bcl-2 protein (arrowhead) Immunohistochemistry staining ×200.

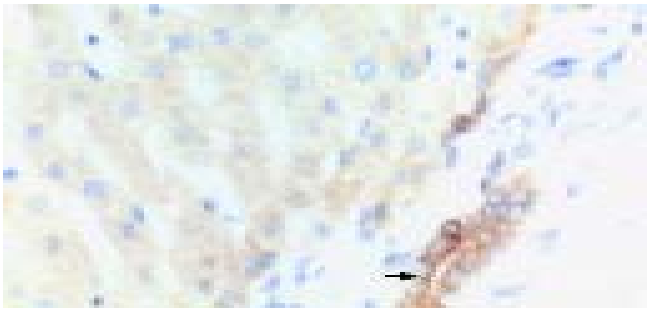

Figure 4 Normal liver. Brown-yellow staining in cytoplasm of small bile duct epithelial cells for bax protein (arrowhead) Immunohistochemistry staining ×200.

Ratio of bcl-2 to bax in normal liver and CCC

In normal liver tissues, the expression rates of bcl-2 and bax

were 87.5% and 25%, while positive rates of bcl-2 and bax were 72.4% and 10.3% in CCC respectively. The ratio of bcl-2 to bax was 3.5 to 1 in normal liver tissues and 7.0 to 1 in CCC (Figure 5).

Figure 5 Non-Hodgkin's lymphoma. Purple-blue deposition in nuclear of lympoma cells (positive for mbr, arrowhead). In situ PCR ×400.

DISCUSSION

Varying results of bcl-2 protein expression in CCC were reported. Bcl-2 protein expression in normal and pathological human liver has been reported by Charlotte *et al*.[11]. In the report, Charlotte *et al.* described that bcl-2 protein was expressed by small bile duct epithelia in normal liver, but not by hepatocytes or large bile duct epithelia. Eight of 11 CCCs were stained positively for bcl-2, whereas all 15 hepatocellular carcinomas were bcl-2 negative. So the authors suggested that bcl-2 protein appeared to be a diagnostic marker in distinguishing CCC from hepatocellular carcinoma[11]. Skopelitou *et al.* found all ten samples of CCC were positive for bcl-2 protein staining[12]. Ito *et al.* reported 31.7% (13/41) of CCCs were positive for bcl-2 protein[13]. However, Terada *et al.* showed low or negative expression of bcl-2 protein in bile duct epithelia and CCC[14-17]. In our report, 21 of 29 CCCs expressed bcl-2 protein (72.4%), which was similar to that reported by Charlotte *et al*. Significant differences of bcl-2 expression in CCC have not been known yet, probably because of the different methods used, and the difference of intrahepatic cholangiocarcinoma specimens from the liver[13,16].

To clarify the role of bcl-2/JH in the pathogenesis of CCC, mbr-JH and mcr-JH which have been shown to be the important molecular event in the genesis of follicular lymphoma, were also studied in 29 cases of CCC. This is the first study to examine bcl-2/JH fusion gene in CCC by *in situ* PCR. Mbr-JH or mcr-JH was negative in all cases of CCC. It is suggested that bcl-2/JH fusion gene formation was not a common event and might not play an important role in the pathogenesis of CCC.

In the present study, bcl-2 protein expression did not correlate with bcl-2/JH in CCC. Similar results were also found in mucosa-associated lymphoma, large cell lymphoma, Hodgkin's disease and nasopharyngeal carcinoma[20-25]. These findings suggested that abnormal bcl-2 protein expression might not be solely resulted from bcl-2/JH fusion sequences. Whether other types of bcl-2 gene aberrance such as mutation or methylation corresponding to bcl-2 protein expression are existed in CCC requires further investigation.

Compared to a high expression rate of bcl-2 in CCC (72.4%), only 10.3% (3/29) samples expressed bax. To understand the significance of the ratio of bcl-2 to bax in the regulation of apoptosis, Oltvai *et al*.[18] found that over-expressed bcl-2 in two cell lines with high levels of bax and in cells with the lowest bcl-2 to bax ratio (0.55) was 73% viable at 24 h, but lost viability by d 7. When cells with high bcl-2 to bax ratios (2.04 and 1.65), they possessed viable cells over 2 wk following IL-3 deprivation. These data suggested a model in which the ratio of bcl-2 to bax could determine survival or death following an apoptotic stimulus. Similar results were also found by Lilling *et al.* and others[26-29]. The alteration of Bcl-2 and Bax might be an important mechanism in the pathogenesis and progression of some tumors[30-32]. Yue *et al*.[30] showed that Bcl-2/Bax in acute myelogenous leukemia was significantly higher than that in normal control ($P<0.001$). Madewell *et al*.[31] found that the bax:bcl-2 ratio was lower in skin tumors than that in normal skin. But a lowered bcl-2/bax ratio and increased apoptosis were observed in oral squamous cell carcinomas, compared with normal oral epithelium[32]. In this study, the ratio of bcl-2 to bax (7.0 to 1) in CCC was different from that in normal small bile ducts (3.5 to 1). We suppose that the changes of the ratio between bcl-2 and bax protein may influence the susceptibility of bile duct cells to apoptosis and would be involved in the tumorigenesis of CCC. Further evidence would be obtained from further investigations.

REFERENCES

1 **Tsujimoto Y,** Finger LR, Yunis J, Nowell PC, Croce CM. Cloning of the chromosome breakpoint of neoplastic B cells with the t (14; 18) chromosome translocation. *Science* 1984; **226**: 1097-1099

2 **Weiss LM,** Warnke RA, Sklar J, Cleary ML. Molecular analysis of the t (14; 18) chromosomal translocation in malignant lymphomas. *N Engl J Med* 1987; **317**: 1185-1189

3 **Bskhshi A,** Jensen JP, Goldman P, Wright JJ, McBride OW, Epstein AL, Korsmeyer SJ. Cloning the chromosomal breakpoint of t (14; 18) human lymphomas: clustering around JH on chromosome 14 and near a transcriptional unit on 18. *Cell* 1985; **41**: 899-906

4 **Aisenberg AC,** Wilkes BM, Jacobson JO. The bcl-2 gene is rearranged in many diffuse B-cell lymphomas. *Blood* 1988; **71**: 969-972

5 **Mcdonnell TJ,** Troncoso P, Brisbay SM, Logothetis C, Chung LW, Hsieh JT, Tu SM, Campbell ML. Expression of the protooncogene bcl-2 in the prostate and its association with emergence of androgen-independent prostate cancer. *Cancer Res* 1992; **52**: 6940-6944

6 **Nakopoulou L,** Vourlakou C, Zervas A, Tzonou A, Gakiopoulou H, Dimopoulos MA. The prevalence of bcl-2, p53, and Ki-67 immunoreactivity in transitional cell bladder carcinomas and their clinicopathologic correlates. *Hum Pathol* 1998; **29**: 146-154

7 **Lu QL,** Elia G, Lucas S, Thomas JA. Bcl-2 proto-oncogene expression in Epstein-Barr-virus-associated nasopharyngeal carcinoma. *Int J Cancer* 1993; **53**: 29-35

8 **Pezzella F,** Turley H, Kuzu I, Tungekar MF, Dunnill MS, Pierce CB, Harris A, Gatter KC, Mason DY. Bcl-2 protein in non-small-cell lung carcinoma. *N Engl J Med* 1993; **329**: 690–694

9 **Papadimitriou CS,** Costopoulos JS, Christoforidou BP, Kotsianti AJ, Karkavelas GS, Hytiroglou PM, Koufogiannis DJ, Nenopoulou HE. Expression of Bcl-2 protein in human primary breast carcinomas and its correlation with multifocality, histopathological types and prognosis. *Eur J Cancer* 1997; **33**: 1275-1280

10 **Tjalma W,** De Cuyper E, Weyler J, Van Marck E, De Pooter C, Albertyn G, van Dam P. Expression of bcl-2 in invasive and in situ carcinoma of the uterine cervix. *Am J Obstet Gynecol* 1998; **178**(1 Pt 1): 113-117

11 **Charlotte F,** L'Hermine A, Martin N, Geleyn Y, Nollet M, Gaulard P, Zafrani ES. Immunohistochemical detection of bcl-2 and protein in normal and pathological human liver. *Am J Pathol* 1994; **144**: 460-465

12 **Skopelitou A,** Hadjiyannakis M, Alexopoulou V, Krikoni O, Kamina S, Agnantis N. Topographical immunohistochemical expression of bcl-2 protein in human liver lesions. *Anticancer Res* 1996; **16**: 975-978

13 **Ito Y,** Takeda T, Sasaki Y, Sakon M, Monden M, Yamada T, Ishiguro S, Imaoka S, Tsujimoto M, Matsuura N. Bcl-2 expression in cholangiocellular carcinoma is inversely correlated with biologically aggressive phenotypes. *Oncology* 2000; **59**: 63-67

14 **Terada T,** Nakanuma Y. Utility of pancreatic digestive enzyme immunohistochemistry in the differential diagnosis of hepatocellular carcinoma, cholangiocarcinoma and metastatic adenocarcinoma of the liver. *Pathol Int* 1996; **46**: 183-188

15 **Okaro AC,** Deery AR, Hutchins RR, Davidson BR. The expres-

sion of antiapoptotic proteins Bcl-2, Bcl-X(L), and Mcl-1 in benign, dysplastic, and malignant biliary epithelium. *J Clin Pathol* 2001;**54**: 927-932

16 **Arora DS,** Ramsdale J, Lodge JP, Wyatt JI. p53 but not bcl-2 is expressed by most cholangiocarcinomas: a study of 28 cases. *Histopathology* 1999; **34**: 497-501

17 **Fiorentino M,** D'Errico A, Altimari A, Barozzi C, Grigioni WF. High levels of BCL-2 messenger RNA detected by *in situ* hybridization in human hepatocellular and cholangiocellular carcinomas. *Diagn Mol Pathol* 1999; **8**: 189-194

18 **Oltvai ZN,** Milliman CL, Korsmeyer SJ. Bcl-2 heterodimerizes *in vivo* with a conserved homolog, Bax, that accelerates programmed cell death. *Cell* 1993; **74**: 609-619

19 **Gribben JG,** Freedman A, Woo SD, Blake K, Shu RS, Freeman G, Longtine JA, Pinkus GS, Nadler LM. All advanced stage non-Hodgkin's lymphomas with a polymerase chain reaction amplifiable breakpoint of bcl-2 have residual cells containing the bcl-2 rearrangement at evaluation and after treatment. *Blood* 1991; **78**: 3275-3280

20 **Tang SC,** Visser L, Hepperle B, Hanson J, Poppema S. Clinical significance of bcl-2-MBR gene rearrangement and protein expression in diffuse large-cell non-Hodgkin's lymphoma: an analysis of 83 cases. *J Clin Oncol* 1994; **12**: 149-154

21 **Isaacson PG,** Wotherspoon AC, Diss TC, Pan LX. Bcl-2 expression in lymphomas. *Lancet* 1991; **337**: 175-176

22 **Huebner-Chan D,** Fernandes B, Yang G, Lim MS. An immunophenotypic and molecular study of primary large B-cell lymphoma of bone. *Mod Pathol* 2001; **14**: 1000-1007

23 **Kneba M,** Eick S, Herbst H, Pott C, Bolz I, Dallenbach F, Hiddemann W, Stein H. Low incidence of mbr bcl-2/JH fusion genes in Hodgkin's disease. *J Pathol* 1995; **175**: 381-389

24 **Nolte M,** Werner M, Spann W, Schnabel B, von Wasielewski R, Wilkens L, Hubner K, Fischer R, Georgii A. The bcl-2/JH gene rearrangement is undetectable in Hodgkin's lymphomas: results from the German Hodgkin trial. *Virchows Arch* 1995; **426**: 37-41

25 **Harn HJ,** HO LI, Liu CA, Liu GC, Lin FG, Lin JJ, Chang JY, Lee WH. Down regulation of bcl-2 by p53 in nasopharyngeal carcinoma and lack of detection of its specific t(14; 18) chromosomal translocation in fixed tissues. *Histopathology* 1996; **28**: 317-323

26 **Lilling G,** Hacohen H, Nordenberg J, Livnat T, Rotter V, Sidi Y. Differential sensitivity of MCF-7 and LCC2 cells, to multiple growth inhibitory agents: possible relation to high bcl-2/bax ratio? *Cancer Lett* 2000; **161**: 27-34

27 **Chresta CM,** Masters JR, Hickman JA. Hypersensitivity of human testicular tumors to etoposide-induced apoptosis is associated with functional p53 and a high Bax: Bcl-2 ratio. *Cancer Res* 1996; **56**: 1834-1841

28 **Perlman H,** Zhang X, Chen MW, Walsh K, Buttyan R. An elevated bax/bcl-2 ratio corresponds with the onset of prostate epithelial cell apoptosis. *Cell Death Differ* 1999; **6**: 48-54

29 **Raisova M,** Hossini AM, Eberle J, Riebeling C, Wieder T, Sturm I, Daniel PT, Orfanos CE, Geilen CC. The Bax/Bcl-2 ratio determines the susceptibility of human melanoma cells to CD95/fas-mediated apoptosis. *J Invest Dermatol* 2001; **117**: 333-340

30 **Yue B,** Chen Y, Yu D, Xiang Z. Study on the relationship between the Bcl-2/Bax ratio and the growth types of leukemic cells and drug resistance in acute myelogenous leukemia. *J Tongji Med Univ* 1998; **18**: 101-104

31 **Madewell BR,** Gandour-Edwards R, Edwards BF, Matthews KR, Griffey SM. Bax/bcl-2: cellular modulator of apoptosis in feline skin and basal cell tumours. *J Comp Pathol* 2001; **124**: 115-121

32 **Loro LL,** Vintermyr OK, Liavaag PG, Jonsson R, Johannessen AC. Oral squamous cell carcinoma is associated with decreased bcl-2/bax expression ratio and increased apoptosis. *Hum Pathol* 1999; **30**: 1097-1105

Edited by Zhang JZ and Wang XL **Proofread by** Xu FM

PO Box 2345, Beijing 100023, China
Fax: +86-10-85381893
E-mail: wjg@wjgnet.com www.wjgnet.com

World J Gastroenterol 2004;10(22):3255-3260
World Journal of Gastroenterology
 ISSN 1007-9327

• COLORECTAL CANCER •

Nuclear factor-κB p65 (RelA) transcription factor is constitutively activated in human colorectal carcinoma tissue

Liang-Liang Yu, Hong-Gang Yu, Jie-Ping Yu, He-Sheng Luo, Xi-Ming Xu, Jun-Hua Li

Liang-Liang Yu, Jie-Ping Yu, He-Sheng Luo, Xi-Ming Xu, Jun-Hua Li, Department of Gastroenterology, Renmin Hospital, Wuhan University, Wuhan 430060, Hubei Province, China
Hong-Gang Yu, Laboratory for Experimental Gastroenterology, Department of Medicine I, St. Joseph Hospital, Ruhr-University Bochum, Bochum, Germany
Supported by Grants Grom National Natural Science Foundation of China No.39470330, and Natural Science Foundation of Hubei Province, China (SJ-97J083)
Correspondence to: Dr. Liang-Liang Yu, Department of Gastroenterology, Renmin Hospital, Wuhan University, Wuhan 430060, Hubei Province, China. yuliangliang@sina.com
Telephone: +86-27-88077184
Received: 2003-11-12 **Accepted:** 2003-12-16

Abstract

AIM: Activation of transcription factor nuclear factor-κB (NF-κB) has been shown to play a role in cell proliferation, apoptosis, cytokine production, and oncogenesis. The purpose of this study was to determine whether NF-κB was constitutively activated in human colorectal tumor tissues and, if so, to determine the role of NF-κB in colorectal tumorigenesis, and furthermore, to determine the association of RelA expression with tumor cell apoptosis and the expression of Bcl-2 and Bcl-x_L.

METHODS: Paraffin sections of normal epithelial, adenomatous and adenocarcinoma tissues were analysed immunohistochemically for expression of RelA, Bcl-2 and Bcl-x_L proteins. Electrophoretic mobility shift assay (EMSA) was used to confirm the increased nuclear translocation of RelA in colorectal tumor tissues. The mRNA expressions of Bcl-2 and Bcl-x_L were determined by reverse transcription polymerase chain reaction (RT-PCR) analysis. Apoptotic cells were detected by terminal deoxynucleotidyl transferase-mediated deoxyuridine triphosphate fluorescence nick end labeling (TUNEL) method.

RESULTS: The activity of NF-κB was significantly higher in adenocarcinoma tissue in comparison with that in adenomatous and normal epithelial tissues. The apoptotic index (AI) significantly decreased in the transition from adenoma to adenocarcinoma. Meanwhile, the expressions of Bcl-2 and Bcl-x_L protein and their mRNAs were significantly higher in adenocarcinoma tissues than that in adenomatous and normal epithelial tissues.

CONCLUSION: NF-κB may inhibit apoptosis via enhancing the expression of the apoptosis genes Bcl-2 and Bcl-x_L. And the increased expression of RelA/nuclear factor-κB plays an important role in the pathogenesis of colorectal carcinoma.

Yu LL, Yu HG, Yu JP, Luo HS, Xu XM, Li JH. Nuclear factor-κB p65 (RelA) transcription factor is constitutively activated in human colorectal carcinoma tissue. *World J Gastroenterol* 2004; 10(22): 3255-3260
http://www.wjgnet.com/1007-9327/10/3255.asp

INTRODUCTION

Rel/NF-κB is a family of dimeric transcription factors that control the expression of numerous genes involved in cell growth, differentiation, regulation of apoptosis, cytokine production, and neoplastic transformation[1,2]. The Rel/NF-κB family comprises NF-κB1 (p50), NF-κB2 (p52), and the Rel proteins, RelA (p65), RelB, and c-Rel, which have a high level of sequence homology within their NH2-terminal 300 amino acids, the Rel homology domain[3]. The p50 and p52 can interact with the RelA proteins to form all possible homo- and heterodimer combinations. The most common dimer is the RelA (p65) /NF-κB1 (p50) heterodimer, i.e., NF-κB. In most unstimulated cells, Rel/NF-κB proteins are sequestered in the cytoplasm and are complexed with specific inhibitor proteins called IκB that render the Rel/NF-κB proteins inactive[3]. Stimulation of cells leads to phosphorylation and degradation of IκB and allows translocation of Rel/NF-κB to the nucleus, resulting in expression of target genes[4]. A surprising variety of inducers have been found to activate Rel/NF-κB[3]. These pathways are involved in innate immune responses that involve cytokines such as tumor necrosis factor (TNF) -α and IL-1, responses to physical stresses such as UV light and ionizing radiation (χ and γ), and responses to oxidative stresses such as hydrogen peroxide and butyl peroxide[5].

Several investigators have reported constitutive activation of NF-κB in various types of human tumor cell lines, including those of lymphoid origin such as Hodgkin/Reed Sternberg cells[6], T-cell lymphoma Hut 78 cells[7], and multiple myeloma cells[8]. In addition, nonlymphoid cell lines including ovarian cancer cells[9], lung carcinoma cells[10], breast cancer cells[11], thyroid carcinoma cells[12], melanomas[13], and bladder cancer cells[14] exhibited enhanced NF-κB activity.

Recent studies also indicated that NF-κB was constitutively activated in tumors such as pancreatic cancer and breast cancer[15,16]. However, little information is available concerning NF-κB activation in colorectal carcinoma, which is one of the most aggressive forms of cancer. The major objective of this study was to determine whether NF-κB was constitutively activated in colorectal carcinoma tissues, to examine whether the expression of Bcl-2 and Bcl-x_L was regulated by NF-κB activation, and to evaluate the correlation between NF-κB activity and apoptosis in colorectal carcinoma.

MATERIALS AND METHODS

Materials

Ten normal colorectal mucosa, thirty colorectal adenoma (average age of the patients: 56.8 years), and thirty colorectal carcinoma (average age of the patients: 58 years) patients who gave informed consent before surgical treatment were entered into the present study. Specimens were obtained from the Department of Pathology, Renmin Hospital, Wuhan University (Wuhan, China). The patients had received neither chemotherapy nor radiation therapy before tumor resection. To justify comparisons, we excluded lesions from patients with familial colon carcinoma syndrome and suspected de novo cancers. Tissues were fixed with 40 g/L formaldehyde and embedded in paraffin for H & E staining and

immunohistochemistry. Tissue specimens were snap-frozen immediately in liquid N_2 and stored at -80 ℃ for EMSA assays and RT-PCR analysis. The study was approved by the Institutional Board of the Ethics Committee of Wuhan University under full consideration of the declaration on human rights of Helsinki.

Immunohistochemistry

Formalin-fixed, paraffin-embedded tissue blocks were cut into 5 μm thick and mounted onto glass slides. After that, they were kept in an oven at 4 ℃ overnight. Immunostaining was performed as previously described with a slight modification[17]. Sections were deparaffinized in xylene and rehydrated. Endogenous peroxidase activity was blocked with 1% hydrogen peroxide for 20 min. To improve the quality of staining, microwave oven-based antigen retrieval was performed. Slides were probed with either anti-RelA (1:50, mouse monoclonal, Santa Cruz Biotechnology), anti-Bcl-2 (1:100, mouse monoclonal, Santa Cruz Biotechnology) or anti-Bcl-x_L (1:100, mouse monoclonal, Santa Cruz Biotechnology). Sections were washed three times with PBS for 10 min each and incubated with biotin-labeled anti-mouse IgG for 1 h at room temperature. After three washes with PBS for 10 min each, sections were stained with a streptavidin-peroxidase detection system. Incubation with PBS instead of the primary antibody served as a negative control. In specimens containing positive cells, the positive cells were counted in ten randomly selected fields under high power microscope (200-fold or 400-fold magnification) for each sample, and the average was expressed as the density of positive cells.

Determination of apoptosis

The TUNEL assay, originally described by Gavrieli *et al*.[18], was used with minor modifications. Briefly, tissue sections of 5 μm were mounted onto glass slides, deparaffinized, hydrated, and treated for 15-30 min at 37 ℃ with proteinase-K (Roche Co.; 20 μg/mL in 10 mmol/L Tris-HCl buffer, pH 7.4). Slides were rinsed twice with PBS. Then, 50 μL of TUNEL reaction mixture (450 μL nucleotide mixture containing fluoresceinated dUTP in reaction buffer plus 50 μL enzyme TdT from calf thymus, Roche Co.) were added to the samples. To ensure homogeneous distribution of the TUNEL reaction mixture on tissue sections and to avoid evaporative loss, slides were covered with coverslips during incubation. Slides were incubated in a humidified chamber for 60 min at 37 ℃. After rinsed, slides were incubated with anti-fluorescein antibody, with Fab fragment from sheep, conjugated with horse-radish peroxidase for 30 min at 37 ℃. Slides were rinsed twice with PBS. Then, 50-100 μL of DAB substrate was added and incubated for 10 min at room temperature. Samples can be counterstained prior to analysis by light microscope. Positive signals were defined as presence of a distinct brown color nuclear staining of the neoplastic cells or morphologically defined apoptotic bodies. The apoptotic index (AI) was determined by counting a total of at least 1 000 neoplastic nuclei in 10 randomly chosen fields at 400-fold magnification. Apoptotic cells were identified using a TUNEL assay in conjunction with characteristic morphological changes such as cell shrinkage, membrane blebbing, and chromatin condensation, to distinguish apoptotic cells and apoptotic bodies from necrotic cells.

EMSA

Nuclear extracts were harvested according to protocols described previously.[19] In brief, fresh samples were minced and homogenized in 400 μL of hypotonic lysis buffer A (10 mmol/L HEPES pH 7.9, 10 mmol/L KCl, 0.1 mmol/L EDTA, 0.1 mmol/L EGTA,1 mmol/L DTT, and 1 mmol/L PMSF). Homogenized tissues were incubated on ice for 5 min, NP-40 was added to a final concentration of 5 g/L, and samples were vigorously mixed and centrifuged. The cytoplasmic proteins were removed and the pellet nuclei were resuspended in 50 μL buffer C (20 mmol/L HEPES pH 7.9, 0.4 mol/L NaCl, 1 mmol/L EDTA, 1 mmol/L EGTA, 1 mmol/L DTT, and 1 mmol/L PMSF). After 30 min agitation at 4 ℃, the samples were centrifuged and supernatants, containing nuclear proteins, were transferred to a fresh vial. The protein concentrations of nuclear extracts were determined by Bio-Rad protein assay. The nuclear extracts were stored at -80 ℃ until use. Nuclear protein extracts of carcinomas, adenomas, and normal tissues were analyzed by EMSA for NF-κB nuclear translocation as previously described[20-22]. EMSA binding reaction mixture contained 8 μg protein of nuclear extracts, 2 μg of poly (deoxyinosinic- deoxycytidylic acid) (Sigma Co.), and [^{32}P]-labeled double-stranded oligonucleotide containing the binding motif of NF-κB probe (4 000 cpm) in binding buffer (10 mmol/L HEPES pH 7.9, 50 mmol/L NaCl, 1 mmol/L EDTA, 1 mmol/L DTT, 100 mL/L glycerol, and 0.2 g/L albumin). The sequence of the double-stranded oligomer used for EMSA was 5'-AGTTGAGGGGACTTTCCCAGGC-3'. The reaction was incubated for 30 min at room temperature before separation on a 50 g/L acrylamide gel, followed by autoradiography. For supershift experiments, 2 μg of mouse monoclonal antibodies against the p65 subunit (Santa Cruz Biotechnology) of NF-κB was incubated with the nuclear extracts 10 min before the addition of the [^{32}P]-labeled probe and then analyzed as described.

RT-PCR

The mRNA expressions of Bcl-2 and Bcl-x_L were assessed using RT-PCR standardized by coamplifying housekeeping gene β-actin, which served as an internal control. Total RNA was isolated from the normal epithelial, adenomatous and adenocarcinoma tissues by the single-step method[23]. Total RNA was reversely transcribed into cDNA and used for PCR with human specific primers for Bcl-2, Bcl-x_L and β-actin. Sequences of Bcl-2 primers were 5'-CAGCTGCACCTGACGCCCTT-3' (forward primer) and 5'-GCCTCCGTTATCCTGGATCC-3' (reverse primer), generating a 199 bp PCR product; for Bcl-x_L, the forward primer was 5'-AAGGATACAGCTGGAGTCAG-3' and the reverse primer was 5'-ATCAATGGCAACCCATCCTG-3', generating a 316 bp PCR product; for β-actin, the forward primer was 5'-AGCGGGAAATCGTGCGTGAC-3' and the reverse primer was 5'-ACTCCTGCTTGCTGATCCACATC-3', producing a 471 bp PCR product[24,25]. Briefly, the PCR was amplified by 32 repeat denaturation cycles at 95 ℃ for 30 s, annealing at 60 ℃ for 30 s, and extension at 72 ℃ for 30 s. During the first cycle, the denaturation was extended to 2 min, and in the final cycle the extension step was extended to 5 min. PCR products were separated on 15 g/L agarose gels containing 0.5 g/L of ethidium bromide and visualized by UV transillumination.

Statistical analysis

All statistical analyses were performed with SPSS10.0 statistical package for Microsoft Windows. Student's *t* test and one-way analysis of variance (ANOVA) were used to compare continuous variables among groups. Correlation coefficients between continuous variables were calculated by the method of Pearson's correlation coefficient. The χ^2 test was used to compare binomial proportions. A P value of <0.05 was considered significant.

RESULTS

RelA/NF-κB expression in colorectal carcinoma tissues

To investigate whether RelA/NF-κB-DNA binding activities were altered in human colorectal carcinoma tissues, we first carried out immunohistochemical analyses. The monoclonal antibodies used in this study detected only activated RelA

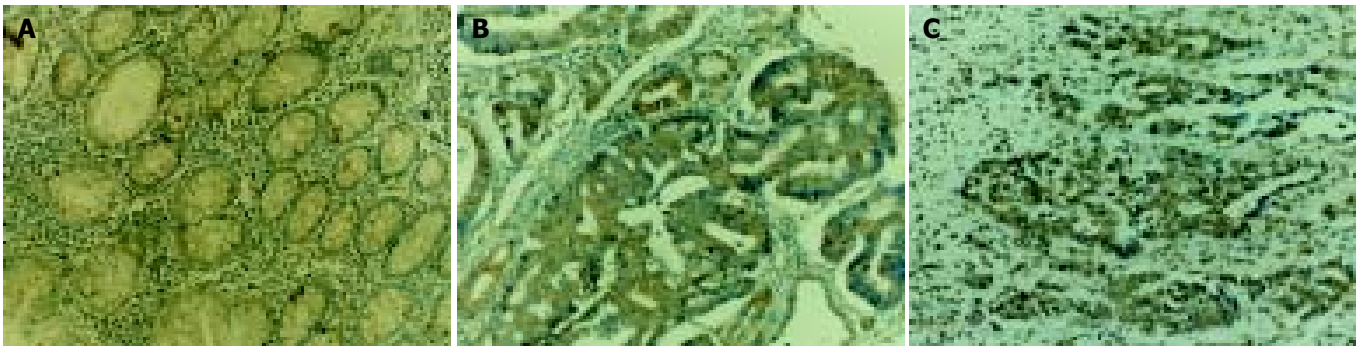

Figure 1 Immunohistochemical staining of RelA in tissue sections of colorectal adenoma (A) and adenocarcinoma (B, C). RelA protein is mainly expressed in the cytoplasm of tumor cells and nuclear accumulation of RelA is also detected. ×200.

proteins[17]. RelA staining was shown as brown color and detected in normal colorectal mucosa, colorectal adenoma and colorectal adenocarcinoma specimens. In colorectal adenoma and adenocarcinoma, positive staining of RelA was mainly observed in the cytoplasm, and nuclear staining for RelA was also detected (Figure 1). Tissues of colorectal adenocarcinoma showed more cells with nuclear staining for RelA than those in colorectal adenoma tissues. No nuclear staining for RelA was found in normal colorectal mucosa. As shown in Table 1, the density of RelA-positive cells was significantly increased (P<0.01) in the transition from normal mucosa to adenoma and adenocarcinoma.

EMSA

To confirm the finding that RelA/NF-κB-DNA binding activities were activated in human colorectal carcinoma tissues, we carried out EMSA analyses. Figure 2 shows increased NF-κB DNA binding activity in adenocarcinoma tissues compared with that in adenoma and normal tissues. HPIAS-1000 SOFTWARE ANALYSIS took the image of electrophoresis. The absorbance of EMSA brands showed that the RelA/NF-κB complexes were not presented in normal colorectal epithelium, 0.6587±0.0021 in adenocarcinoma, and 0.2153±0.0013 in adenoma. The RelA expressions were significantly increased (P<0.05) in the transition from normal colorectal epithelium to colon tumor tissues. To confirm the specificity of NF-κB DNA binding, we performed supershift analysis with antibodies specific for RelA (p65) and a competitive study with a 50-fold excess of unlabeled oligonucleotide. An antibody specific for RelA which recognizes RelA/NF-κB heterodimer, unlabeled oligonucleotide diminished the intensity of RelA/NF-κB complexes, indicating that complex was the NF-κB binding-specific band. Our results showed that RelA was frequently activated in human colorectal tumor tissues but not in normal colon tissue.

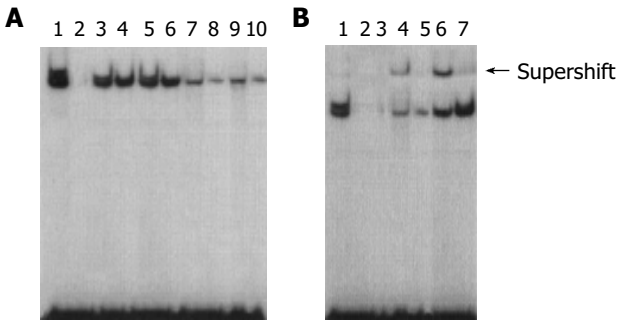

Figure 2 Electrophoretic mobility shift assay demonstrating increased nuclear translocation and DNA binding of NF-κB. A: lane 1, positive control (using Hela nuclear extract); lane 2, normal; lanes 3-6, adenocarcinoma; lanes 7-10, adenoma. B: lane 1, positive control (using Hela nuclear extract); lanes 2-3, specific competitor (using excess of unlabeled oligonucleotide); lanes 4-5, adenoma; lanes 6-7, adenocarcinoma; lane 4 and 6, supershift (addition of p65 antibodies to the nuclear extracts).

Bcl-2 and Bcl-x_L protein expression in colorectal carcinoma tissues

In the present study, the expressions of Bcl-2 and Bcl-x_L were also investigated using immunohistochemistry. Immunostaining specific for Bcl-2 and Bcl-x_L was cytoplasmic and shown as brown color (Figures 3, 4). The expressions of Bcl-2 and Bcl-x_L were significantly increased (P<0.01) from normal mucosa to tumor tissue (Table 1). Expressions of Bcl-2 and Bcl-x_L were both significantly associated (r = 0.95,0.88; P<0.05) with RelA expression in adenoma and adenocarcinoma.

Table 1 Changes in expression of RelA, Bcl-2, Bcl-x_L and AI in transition from normal mucosa to tumor tissues

Group	*n*	RelA	Bcl-2	Bcl-x_L	AI
Normal	10	9.31±0.56	15.62±0.75	11.35±0.71	13.09±0.78
Adenoma	30	54.01±4.53	55.64±6.51	56.43±6.14	105.91±6.11
Adenocarcinoma	30	70.92±7.23	78.23±8.33	77.32±6.51	31.53±3.71

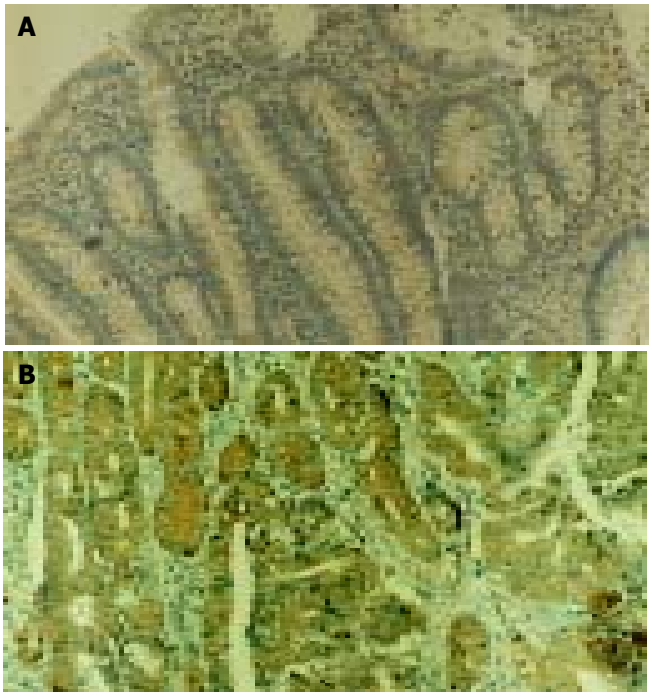

Figure 3 Immunohistochemical staining of Bcl-2 in tissue sections of colorectal adenoma (A) and adenocarcinoma (B). Bcl-2 expression is restricted to the cytoplasm of cancer cells. ×200.

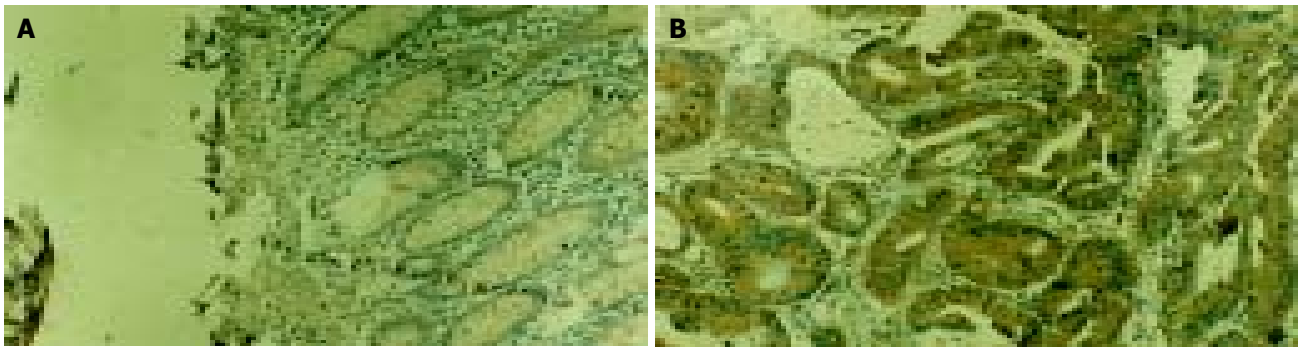

Figure 4 Immunohistochemical staining of Bcl-x_L in tissue sections of colorectal adenoma (A) and adenocarcinoma (B). Bcl-x_L expression is restricted to the cytoplasm of cancer cells.×200.

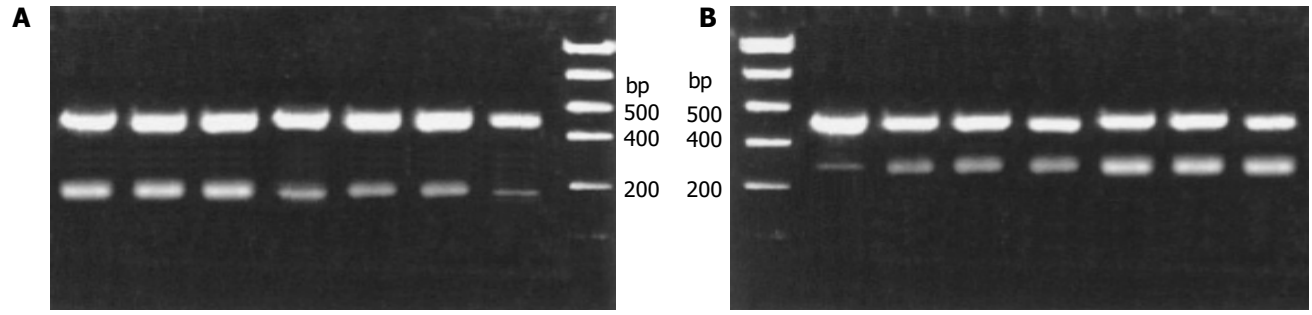

Figure 5 The mRNA expressions of Bcl-2 and Bcl-x_L were assessed using RT-PCR standardized by coamplifying the housekeeping gene β-actin. A: the mRNA expression of Bcl-2. lanes 1-3, adenocarcinoma; lanes 4-6, adenoma; lane 7, normal; lane 8, marker. B: the mRNA expression of Bcl-2. lane 1, marker; lane 2, normal; lanes 3-5, adenoma; lanes 6-8, adenocarcinoma.

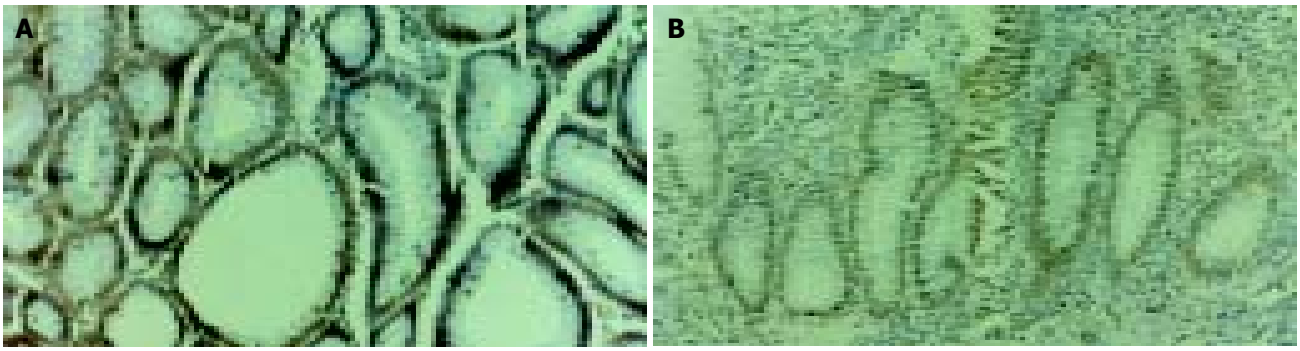

Figure 6 TUNEL staining in tissue sections of colorectal adenoma (A) and adenocarcinoma (B). TUNEL staining is restricted to the nucleus of apoptotic cells.×200.

Bcl-2 and Bcl-x_L mRNA expression in colorectal carcinoma tissues

RT-PCR analysis of mRNA expressions of Bcl-2 and Bcl-x_L was standardized by co-amplifying these genes with the housekeeping gene β-actin. HPIAS-1000 SOFTWARE ANALYSIS took the image of electrophoresis with β-action as internal standard. The relative absorbance of mRNA expression for Bcl-2: 2.43±0.27% in normal tissues, 17.96±1.51% in adenoma, and 36.71±2.17% in adenocarcinoma; for Bcl-x_L: 3.54±0.33% in normal tissues, 23.02±2.11% in adenoma, and 39.71±2.49% in adenocarcinoma (Figure 5). Our results showed that colon tumor tissue constitutively expressed Bcl-2 and Bcl-x_L. The mRNA expressions of Bcl-2 and Bcl-x_L were significantly increased (P<0.05) in the transition from normal colorectal epithelium to colon tumor tissue.

Cell apoptosis

In this study, TUNEL staining was restricted to the nucleus of apoptotic cells. TUNEL-positive staining cells were detected in normal colorectal mucosa, adenoma, and adenocarcinoma. The AI was significantly increased (P<0.01) in the transition from normal colorectal mucosa to adenoma, but decreased from adenoma to adenocarcinoma (Figure 6). There was no association between the AI and the histological classification of adenoma and adenocarcinoma. The density of RelA-positive cells inversely correlated with the AI in the transition from adenoma to adenocarcinoma (r = -0.89; P<0.001).

DISCUSSION

We have demonstrated that RelA-DNA binding activity was constitutively activated in the majority of human colorectal carcinomas. Whereas the role for RelA/NF-κB in tumorigenesis has not firmly established, recent work has suggested that it may play a role in this process. RelA/NF-κB activation has been shown to be necessary for tumor formation in Hodgkin lymphoma cells[26,27]. More recently, the inhibition of RelA/NF-κB activity through the use of specific NF-κB inhibitors (gliotoxin and MG132) resulted in spontaneous caspase-independent apoptosis in Hodgkin and Reed-Sternberg cells[28]. Also, an increase in RelA/NF-κB levels was identified in breast cancer

cell lines, primary human breast cancer, hepatocellular carcinoma, pancreatic adenocarcinoma, and gastric carcinoma when compared with nontransformed controls or normal tissues[29-32]. In addition, NF-κB transcriptional activity was required for oncogenic Ras-induced cellular transformation[33], which likely occurred through the inhibition of transformation-associated apoptosis[34]. However, the role of NF-κB in colorectal tumorigenesis is unknown and currently under investigation.

We primarily used immunohistochemistry to detect NF-κB activation in human colorectal carcinoma tissues. Its expression was significantly increased in the transition from normal colorectal mucosa to adenoma and adenocarcinoma. In our immunohistochemical analyses, we used monoclonal antibodies to detect RelA/NF-κB-DNA binding activities, and their sensitivity and specificity have been characterized previously. They were useful in differentiating between activated and inactivated forms of RelA and facilitated the detection of the activated RelA proteins. In the current investigation, only 10-20% of RelA/NF-κB protein was detectable in the nucleus, which was consistent with previous reports[32]. And 80-90% of RelA still remained in the cytoplasm when RelA proteins were activated. It is unclear why the majority of RelA/ NF-κB proteins that were freed from IκB remained in the cytoplasm. Possible explanations for this[32] are: (1) IκB was mutated and therefore could not bind to RelA and masked the nuclear translocation signal in RelA; (2) mutations in RelA prohibited IκB binding to RelA, and (3) the RelA upstream signal transduction cascades were constitutively activated.

The Bcl-2 proto-oncogene is an apoptosis inhibitor originally described in association with the t (14; 18) (q32; q21) translocation in follicular B cell lymphoma, which places the Bcl-2 gene under the stimulatory control of the IgH promoter-enhancer at 14q32, resulting in increased Bcl-2 mRNA and protein[35] and inhibition of apoptosis. The Bcl-x_L proto-oncogene, a member of Bcl-2 family, is a homologue of Bcl-2 and is an apoptosis inhibitor. The Bcl-2 and Bcl-x_L oncoproteins have been described in normal colonic mucosa[35], where these were restricted to the epithelial regenerative compartment and the intestinal crypt bases. In our study, the expression of Bcl-2 and Bcl-x_L was increased in the transition from normal mucosa to adenoma and adenocarcinoma. These results also show that the increased RelA/NF-κB expression occurred concomitantly with an increased expression of Bcl-2 and Bcl-x_L. To date, a number of gene products that inhibit apoptosis have been identified. These include Bcl-2 and Bcl-x_L genes. Indeed, Bcl-2 and Bcl-x_L have been identified as NF-κB target gene[36], but the exact role NF-κB plays in its regulation remains controversial.

In recent years, increasing evidence indicates that activation of NF-κB plays an important role in coordinating the control of apoptotic cell death. NF-κB has been shown to prevent Fas-induced death in B cells through the upregulation of Bcl-2 and Bcl-x_L expression[36], but has also been demonstrated to promote apoptosis in thymocytes by downregulating Bcl-2 and Bcl-x_L gene expression[37]. However, the exact mechanism of NF-κB in the regulation of apoptosis is not entirely clear. There are at least two distinct mechanisms by which NF-κB blocks apoptosis[38]: (1) induction of antiapoptosis factors including IEX-1L, TRAF1, TRAF2, c-IAP-1, c-IAP-2 *etc*; (2) interference of apoptotic pathway by protein-protein interaction. However, these two distinct mechanisms are not mutually exclusive since either mechanism alone cannot fully explain the antiapoptotic action of NF-κB. In our study, apoptosis was significantly decreased in the transition from adenoma to adenocarcinoma, which was in contrast to the expressions of RelA, Bcl-2, and Bcl-x_L. We also observed an inverse relation between AI and the expression of RelA in the transition from adenoma to adenocarcinoma, implying that increased RelA protein expression to a certain level might be anti-apoptotic and thus promote tumorigenic cell behavior. The anti-apoptotic role of NF-κB has been well characterized and various down-stream targets of NF-κB, including Bcl-2 and Bcl-x_L have been identified. In the present study, the statistical correlation between the increased expression of RelA, elevated Bcl-2 and Bcl-x_L expression implies that in colorectal tissue, activation of RelA might exhibit anti-apoptotic effects at least in part through upregulation of Bcl-2 and Bcl-x_L expression. This has been shown to decrease mitochondrial permeability changes and cytochrome C release and thus to block apoptosis[39].

To date, NF-κB has been believed to play an important role in coordinating the control of apoptotic cell death. However, the mechanism by which NF-κB blocks apoptosis is still controversial. Some laboratories have reported that activation of NF-κB is able to either promote or prevent apoptosis, depending on different stimuli and different cell types[40-42]. For example, Grimm *et al*.[43] reported that serum starvation activated NF-κB and induced human embryonic kidney cells into apoptosis. Qin *et al*.[44] found that NF-κB activation contributed to the excitotoxin-induced death of striatal neurons. However, somewhat inconsistent results have also been presented by Beg and Baltimore[45] that NF-κB activation generally inhibited apoptosis in embryonic fibroblasts. A question arises: who is right on earth? We think the answer is expected by further studies.

In conclusion, our results demonstrate that the RelA/NF-κB pathway is activated constitutively in colorectal carcinoma tissues, suggesting that activation of RelA/NF-κB might play an important role in colorectal tumorigenesis. Further studies are required to elucidate the mechanisms of NF-κB activation and to determine whether NF-κB might serve as a therapeutic target in the anti-neoplastic treatment of colorectal cancer.

REFERENCES

1 **Zhu JW,** Yu BM, Ji YB, Zheng MH, Li DH. Upregulation of vascular endothelial growth factor by hydrogen peroxide in human colon cancer. *World J Gastroenterol* 2002; **8**: 153-157

2 **Loncar MB,** Al-Azzeh ED, Sommer PS, Marinovic M, Schmehl K, Kruschewski M, Blin N, Stohwasser R, Gott P, Kayademir T. Tumour necrosis factor alpha and nuclear factor kappaB inhibit transcription of human TFF3 encoding a gastrointestinal healing peptide. *Gut* 2003; **52**: 1297-1303

3 **Ghosh S,** May MJ, Kopp EB. NF-κB and Rel proteins: evolutionarily conserved mediators of immune responses. *Annu Rev Immunol* 1998; **16**: 225-260

4 **Micheau O,** Tschopp J. Induction of TNF receptor I-mediated apoptosis via two sequential signaling complexes. *Cell* 2003; **114**: 181-190

5 **Siebenlist U,** Franzoso G, Brown K. Structure, regulation and function of NF-κB. *Annu Rev Cell Biol* 1994; **10**: 405-455

6 **Bargou RC,** Leng C, Krappmann D, Emmerich F, Mapara MY, Bommert K, Royer HD, Scheidereit C, Dorken B. High-level nuclear NF-κB and Oct-2 is a common feature of cultured Hodgkin/Reed-Sternberg cells. *Blood* 1996; **87**: 4340-4347

7 **Giri D K,** Aggarwal BB. Constitutive activation of NF-κB causes resistance to apoptosis in human cutaneous T cell lymphoma HuT-78 cells. Autocrine role of tumor necrosis factor and reactive oxygen intermediates. *J Biol Chem* 1998; **273**: 14008-14014

8 **Feinman R,** Koury J, Thames M, Barlogie B, Epstein J, Siegel DS. Role of NF-κB in the rescue of multiple myeloma cells from glucocorticoid-induced apoptosis by bcl-2. *Blood* 1999; **93**: 3044–3052

9 **Xiao CW,** Yan X, Li Y, Reddy SA, Tsang BK. Resistance of human ovarian cancer cells to tumor necrosis factor alpha is a consequence of nuclear factor kappaB-mediated induction of Fas-associated death domain-like interleukin-1beta-converting enzyme-like inhibitory protein. *Endocrinology* 2003; **144**: 623-630

10 **Mukhopadhyay T,** Roth JA, Maxwell SA. Altered expression of the p50 subunit of the NF-κB transcription factor complex in non-small cell lung carcinoma. *Oncogene* 1995; **11**: 999-1003

11 **Nakshatri H,** Bhat-Nakshatri P, Martin DA, Goulet RJ Jr,

Sledge GW Jr. Constitutive activation of NF-κB during progression of breast cancer to hormone-independent growth. *Mol Cell Biol* 1997; **17**: 3629–3639

12 **Visconti R**, Cerutti J, Battista S, Fedele M, Trapasso F, Zeki K, Miano MP, de Nigris F, Casalino L, Curcio F, Santoro M, Fusco A. Expression of the neoplastic phenotype by human thyroid carcinoma cell lines requires NF-κB p65 protein expression. *Oncogene* 1997; **15**: 1987-1994

13 **Ivanov VN**, Bhoumik A, Ronai Z. Death receptors and melanoma resistance to apoptosis. *Oncogene* 2003; **22**: 3152-3161

14 **Sumitomo M,** Tachibana M, Ozu C, Asakura H, Murai M, Hayakawa M, Nakamura H, Takayanagi A, Shimizu N. Induction of apoptosis of cytokine-producing bladder cancer cells by adenovirus-mediated IκB overexpression. *Hum Gene Ther* 1999; **10**: 37-47

15 **Zelvyte I,** Ohlsson B, Axelson J, Janciauskiene S. Diverse responses between human pancreatic cancer cell lines to native alpha 1-antitrypsin and its C-terminal fragment. *Anticancer Res* 2003; **23**: 2267-2273

16 **Sovak MA,** Arsura M, Zanieski G, Kavanagh KT, Sonenshein GE. The inhibitory effects of transforming growth factor beta1 on breast cancer cell proliferation are mediated through regulation of aberrant nuclear factor-kappaB/Rel expression. *Cell Growth Differ* 1999; **10**: 537-544

17 **Zabel U,** Henkel T, Silva MS, Baeuerle PA. Nuclear uptake control of NF-κB by MAD-3, an IkB protein present in the nucleus. *EMBO J* 1993; **12**: 201–211

18 **Gavrieli Y,** Sherman Y, Ben-Sasson SA. Identification of programmed cell death in situ via specific labeling of nuclear DNA fragmentation. *J Cell Biol* 1992; **119**: 493–501

19 **Huang Y,** Johnson KR, Norris JS, Fan W. Nuclear factor-κB/IκB signaling pathway may contribute to the mediation of paclitaxel induced apoptosis in solid tumor cells. *Cancer Res* 2000; **60**: 4426-4432

20 **Wong BC,** Jiang X, Fan XM, Lin MC, Jiang SH, Lam SK, Kung HF. Suppression of RelA/p65 nuclear translocation independent of IκBa degradation by cyclooxygenase-2 inhibitor in gastric cancer. *Oncogene* 2003; **22**: 1189-1197

21 **Li-Weber M,** Laur O, Dern K, Krammer PH. T cell activation-induced and HIV tat-enhanced CD95(APO-1/Fas) ligand transcription involves NF-κB. *Eur J Immunol* 2000; **30**: 661-670

22 **Sosic D,** Richardson JA, Yu K, Ornitz DM, Olson EN. Twist regulates cytokine gene expression through a negative feedback loop that represses NF-κB activity. *Cell* 2003; **112**: 169-180

23 **Chomczynski P,** Sacchi N. Single-step method of RNA isolation by acid guanidine isothiocyanate-phenolchloroform extraction. *Anal Biochem* 1987; **162**: 156-159

24 **Kitamura S,** Kondo S, Shinomura Y, Kanayama S, Miyazaki Y, Kiyohara T, Hiraoka S, Matsuzawa Y. Met/HGF receptor modulates bcl-w expression and inhibits apoptosis in human colorectal cancers. *Br J Cancer* 2000; **83**: 668-673

25 **Nakajima-Iijima S,** Hamada H, Reddy P, Kakunaga T. Molecular structure of the human cytoplasmic β-actin gene: Interspecies homology of sequences in the introns. *Proc Natl Acad Sci U S A* 1985; **82**: 6133-6137

26 **Bargou RC,** Emmerich F, Krappmann D, Bommert K, Mapara MY, Arnold W, Royer HD, Grinstein E, Greiner A, Scheidereit C, Dorken B. Constitutive nuclear factor-kappaB-RelA activation is required for proliferation and survival of Hodgkin's disease tumor cells. *J Clin Invest* 1997; **100**: 2961-2969

27 **Schenkein D.** Proteasome inhibitors in the treatment of B-cell malignancies. *Clin Lymphoma* 2002; **3**: 49-55

28 **Izban KF,** Ergin M, Huang Q, Qin JZ, Martinez RL, Schnitzer B, Ni H, Nickoloff BJ, Alkan S. Characterization of NF-kappaB expression in Hodgkin's disease: Inhibition of constitutively expressed NF-kappaB results in spontaneous caspase-independent apoptosis in Hodgkin and Reed-Sternberg cells. *Mod Pathol* 2001; **14**: 297-310

29 **Sovak MA,** Bellas RE, Kin DW, Zanieski DJ, Rogers AE, Traish AM, Sonenshein GE. Aberrant nuclear factor-kappa B/Rel expression and the pathogenesis of breast cancer. *J Clin Invest* 1997; **100**: 2952–2960

30 **Tai DI,** Tsai SL, Chang YH, Huang SN, Chen TC, Chang KS, Liaw YF. Constitutive activation of nuclear factor kappaB in hepatocellular carcinoma. *Cancer* 2000; **89**: 2274-2281

31 **Sasaki N,** Morisaki T, Hashizume K, Yao T, Tsuneyoshi M, Noshiro H, Nakamura K, Yamanaka T, Uchiyama A, Tanaka M, Katano M. Nuclear factor-kappaB p65 (RelA) transcription factor is constitutively activated in human gastric carcinoma tissue. *Clin Cancer Res* 2001; **7**: 4136-4142

32 **Wang WX,** Abbruzzese JL, Evans DB, Larry L, Cleary KR, Chiao PJ. The nuclear factor-κB relA transcription factor is constitutively activated in human pancreatic adenocarcinoma cells. *Clin Cancer Res* 1999; **5**: 119–127

33 **Finco TS,** Westwick JK, Norris JL, Beg AA, Der CJ, Baldwin AS Jr. Oncogenic Ha-Rasinduced signaling activates NF-κB transcriptional activity, which is required for cellular transformation. *J Biol Chem* 1997; **272**: 24113-24116

34 **Mayo MW,** Wang CY, Cogswell PC, Rogers-Graham KS, Lowe SW, Der CJ, Baldwin AS Jr. Requirement for NF-κB activation to suppress p53-independent apoptosis induced by oncogenic ras. *Science* 1997; **278**: 1812-1815

35 **Popescu RA,** Lohri A, de Kant E, Thiede C, Reuter J, Herrmann R, Rochlitz CF. Bcl-2 expression is reciprocal to p53 and c-myc expression in metastatic human colorectal cancer. *Eur J Cancer* 1998; **34**: 1268-1273

36 **Lee HH,** Dadgostar H, Cheng Q, Shu J, Cheng G. NF-κB mediated up-regulation of Bcl-x and Bfl-1/A1 is required for CD40 survival signaling in B lymphocytes. *Proc Natl Acad Sci U S A* 1999; **96**: 9136-9141

37 **Hettmann T,** DiDonato J, Karin M, Leiden JM. An essential role for nuclear factor κB in promoting double positive thymocyte apoptosis. *J Exp Med* 1999; **189**: 145-158

38 **Kajino S,** Suganuma M, Teranishi F, Takahashi N, Tetsuka T, Ohara H, Itoh M, Okamoto T. Evidence that *de novo* protein synthesis is dispensable for anti-apoptotic effects of NF-κB. *Oncogene* 2000; **19**: 2233-2239

39 **Aams J,** Cory S. The Bcl-2 protein family arbiters of cell survival. *Science* 1998; **281**: 1322-1326

40 **Glasgow JN,** Wood T, Perez-Polo JR. Identification and characterization of nuclear factor-κB binding sites in the murine Bcl-x promoter. *J Neurochem* 2000; **75**: 1377-1389

41 **O'Connor L,** Huang DC, O'Reilly LA, Strasser A. Apoptosis and cell division. *Currt Opin Cell Biol* 2000; **12**: 257-263

42 **Yoneda T,** Imaizumi K, Maeda M, Yui D, Manabe T, Katayama T, Sato N, Gomi F, Morihara T, Mori Y, Miyoshi K, Hitomi J, Ugawa S, Yamada S, Okabe M, Tohyama M. Regulatory mechanisms of TRAF2-mediated signal transduction by Bcl-10, a MALT lymphoma-associated protein. *J Biol Chem* 2000; **275**: 11114-11120

43 **Grimm S,** Bauer MK, Baeuerle PA, Schulze-Osthoff K. Bcl-2 down-regulates the activity of transcription factor NF-κB induced upon apoptosis. *J Cell Biol* 1996; **134**: 13-23

44 **Qin ZH,** Wang Y, Nakai M, Chase TN. Nuclear Factor-κB contributes to excitotoxin-induced apoptosis in rat striatum. *Mol Pharmacol* 1998; **53**: 33-42

45 **Beg AA,** Baltimore D. An essential role for NF-κB in preventing TNF-α-induced cell death. *Science* 1996; **274**: 782-784

Edited by Zhang JZ and Zhu LH **Proofread by** Xu FM

PO Box 2345, Beijing 100023, China
Fax: +86-10-85381893
E-mail: wjg@wjgnet.com www.wjgnet.com

World J Gastroenterol 2004;10(22):3261-3263
World Journal of Gastroenterology
 ISSN 1007-9327

• COLORECTAL CANCER •

Expression of vascular endothelial growth factor-C and the relationship between lymphangiogenesis and lymphatic metastasis in colorectal cancer

Yi-Tao Jia, Zhong-Xin Li, Yu-Tong He, Wei Liang, Hui-Chai Yang, Hong-Jun Ma

Yi-Tao Jia, Wei Liang, Department of Oncology, the People's Hospital of Hebei Province, Shijiazhuang 050051, Hebei Province, China
Zhong-Xin Li, Yu-Tong He, Hui-Chai Yang, Department of Surgery, the Forth Hospital of Hebei Medical University, Shijiazhuang 050011,Hebei Province, China
Hong-Jun Ma, Experimental Centre of Electron Microscopy of Hebei Medical University, Shijiazhuang 050011, Hebei Province, China
Correspondence to: Dr. Zhong-Xin Li, Department of Surgery, the Forth Hospital of Hebei Medical University, Shijiazhuang 050011, Hebei Province, China
Telephone: +311-6033941-347
Received: 2003-12-23 **Accepted:** 2004-03-02

Abstract

AIM: To investigate the expression of vascular endothelial growth factor-C (VEGF-C) and the relationship between VEGF-C and lymphangiogenesis, lymph node metastasis in colorectal cancer.

METHODS: Fifty six cases of colorectal cancer were selected randomly. Expression of VEGF-C was detected by immunohistochemistry, and lymphatic vessels were stained by enzyme histochemical method.

RESULTS: VEGF-C expression was found in 66.7% (37/56) patients. In VEGF-C positive and negative patients, the lymphatic vessel density was 25.16±7.52 and 17.14±7.22, respectively ($P<0.05$). The rate of lymph node metastasis in VEGF-C positive patients (81.1%) was significantly higher than that in the negative group (42.1%).

CONCLUSION: VEGF-C expression may induce lymphangiogenesis in colorectal cancer, as a result, tumor cells can entry the lymphatic vessels easily. VEGF-C may serve as a useful prognotic factor in colorectal carcinoma.

Jia YT, Li ZX, He YT, Liang W, Yang HC, Ma HJ. Expression of vascular endothelial growth factor-C and the relationship between lymphangiogenesis and lymphatic metastasis in colorectal cancer. *World J Gastroenterol* 2004; 10(22): 3261-3263
http://www.wjgnet.com/1007-9327/10/3261.asp

INTRODUCTION

Colorectal cancer is a common cause of death throughout the world including China. The lymphatic system is the primary pathway of metastasis for gastrointestinal tract malignancies, and the extent of lymph node involvement is a key prognostic factor for the outcome of patients. However, the mechanism of lymphatic metastasis remains unclear.

Lymphangiogenesis, the development of new lymph vessels, is a relatively new area of clinical investigations. Recently, vascular endothelial growth factor C (VEGF-C) has been identified as a new member of the VEGF family[1,2], and is belived to be the only lymphangiogenic factor in the VEGF family. It activates both vascular endothelial growth factor receptor 2 (VEGFR-2) and VEGFR-3[3,4]. VEGF-C induces the proliferation of lymphatic vessels in the stroma of gastric carcinoma by activating VEGFR-3 in lymphatic endothelial cells[5]. But the precise role of VEGF-C in colorectal cancer has not been clearly understood. Therefore, in the current study, we used an enzyme-histochemical method for 5'-nucleotidase (5'-Nase) to distinguish lymph vessels in colorectal carcinoma, and immunohistochemistry to examine the correlation between the expression of VEGF-C, lymphangiogenesis and the clinicopathologic features.

MATERIALS AND METHODS

Patients

Fifty-six Chinese colorectal carcinoma patients were surgically treated in the Department of Surgery, the Forth Hospital of Hebei Medical University, China from 2001 to 2002. The patients included 34 males and 22 females, and ranged in age from 33 to 75 years (average age 58.5 years). The lesions included 13 colon cancers and 43 rectal cancers, two patients with stage I, 17 patients with stage II, 34 patients with stage III and three patients with stage IV.

Immunohistochemistry

Immunohistochemical staining for VEGF-C was performed using the streptavidin-peroxidase technique. Formalin fixed and paraffin embeded tissues were cut into 4 μm thick sections and placed on saline coated slides. After deparaffinization in xylene and rehydration, endogeneous peroxidase activity was blocked after incubated with 30 mL/L hydrogen peroxidase for 20 min. Tissue sections were then autoclaved at 121 ℃ in 10 mmol/L citrate buffer (pH 6.0) for 10 min for antigen retrieval and cooled at room temperature for 30 min, them incubated for 3 h with a 1:40 dilution of anti-VEGF-C rabbit polyclonal antibody (Santa Cruz Biotech, USA). Bound peroxidase was visualized using a solution of diaminobezidine as chromogen, and nuclei were counterstained with hematoxylin. Scoring was carried out by two independent observers who were blinded to the patient's status. Positive staining was defined as the presence of VEGF-C immunoreactivity in at least 10% of tumor cells.

Enzyme-histochemistry

Cryosections (7 μm thick) of tissue were processed for 5'-nucleotide-alkaline phosphatase (5'-Nase-ALPase) double staining according to Ji *et al.*'s report[6]. After rinsed in 0.1 mol/L cacodylate buffer (pH 7.2), specimens were incubated in the reaction medium for 5'-Nase for 50 min at 37 ℃ with 5'-adenosine monophosphate (AMP) (Sigma chemical, St. Louis, MO, USA) as a substrate, lead nitrate (Sigma, USA) as a capture agent, and 2 mmol/L L-tetramisole (Sigma, USA) as an inhibitor of nonspecific alkaline phosphatase. After washed with distilled water, the tissues were treated with 10 mg/L ammonium sulfide solution for 1 min at room temperature. Then, the sections were incubated in the reaction medium for ALPase for 30 min at 4 ℃ with fast blue BB, N,N-

dimethylformamide, naphtol AS-MX phosphate (Sigma, USA).

Lymphatic vessel density (LVD) counting

The stained sections were screened at ×40 magnification to identify the regions of the highest vascular density within the tumor. Lymphatic vessels were counted in 3 regions of the highest vascular density at ×100 magification. The number of lymphatic vessels was the mean of vessels in these areas.

Statistical analysis

The data were analysed by t test and χ^2 test. All reported P values were two-sided, and P <0.05 was considered statistically significant.

RESULTS

Immunohistochemistry

In specimens of normal colorectal mucosa, no VEGF-C protein was stained. Among the 56 examined tumors, 37 (66.7%) showed VEGF-C protein expression in the cytoplasm (Figure 1).

Figure 1 VEGF-C in cytoplasm of colorectal adenocarcinoma (SP ×200).

Enzyme-histochemistry

Lymphatic vessels were 5'-Nase positive (brown) and blood vessels were ALPase positive (blue). The most lymphatic vessels were enlarged and dilated especially in peritumor areas. The walls of lymphatic vessels were thinner than that of blood vessels, and their profiles of lumens were more irregular. While the intratumoral lymphtic vessels were strip-like (Figure 2). The LVD of VEGF-C positive tumors (25.16±7.52) was significantly higher than that of VEGF-C negative tumors (17.14±7.22) (P = 0.04). No significant lymphangiogenesis was observed in normal and adenoma tissues.

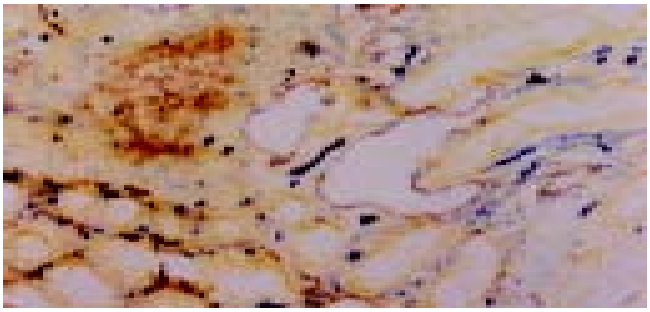

Figure 2 Positive 5'-Nase (brown) and ALPase (blue) in lymphatic and blood vessels (×100).

Correlation between VEGF-C and clinicopathologic factors

VEGF-C expression was observed frequently in patients with colorectal carcinoma. A positive association between VEGF-C expression and lymphatic metastasis was observed (P<0.05, Table 1). However, no significant correlations with gender, histologic differentiation, invasive depth, TNM stage were observed.

Table 1 Relationship between expression of VEGF-C and clinicopathologic features in colorectal carcinoma

Characteristic		n	VEGF-C (+)	VEGF-C (–)	P
Gender	Male	34	25	9	0.143
	Female	22	12	10	
Lymph node metastasis	(+)	37	30	8	0.007
	(–)	9	8	11	
Differentiation	Well	40	25	15	0.372
	Poorly	16	12	4	
Invasion depth	Muscularis	17	10	7	0.499
	Adventitia	39	27	12	
Stage	I-II	19	13	6	0.790
	III-IV	37	24	13	

DISCUSSION

Clinical and pathological data pointed to the metastasis of solid tumors via the lymphatics as an important early event in metastatic diseases[7]. However, little has been achieved in lymphangiogenesis and the role of lymphangiogenesis in promoting the metastasis of tumor cells via the lymphatic vessels. This might, in part, be due to difficulty in studing lymphatic vessels because of their morphology and lack of lymphatic-specific markers[6,7]. Approximatly 10 years ago, Kato *et al.*[8] developed an enzyme-histochemical method for 5'-Nase-ALPase to distinguish lymphatic vessels from blood vessels. Many other markers such as LYVE1 and podoplanin were found later[9,10]. Now, lymphangiogenesis or new lymphatic vessel growth has become an exciting area of reaserch in cancer biology[11]. So far, the occurrence and involvment of lymphangiogenesis have been demonstrated in some experimental mouse tumors , human head and neck cancers, oral squamous cell cancer by using these markers[12-16]. Similarly, in our study, lymphangiogenesis was observed in primary colorectal carcinomas, and the vicinity of tumor was the dominant region. Most of lymphatic vessels were dilated, as a result, tumor cells could invade the lymphatics easily. On the other hand, most of the intratumor lymphatic capillaries were strip-like. It is believed that tumor cells could utilize peritumoral lymphatics to spread, while intratumoral lymphatics should be regarded as an additional pathway rather than a necessity for metastasis[17].

Vascular endothelial growth factor-C (VEGF-C) is the first lymphangiogenic factor identified. Moreover, there is ample evidence for the expression of VEGF-C in human tumors. But the precise role of VEGF-C in colorectal cancer is less well understood. With respect to VEGF-C expression, several authors have demonstrated associations between this growth factor expression and poor clinicopathological outcome[18-25]. Immunohistochemical detection of VEGF-C expression at the deepest invasive site of colorectal carcinoma was found in about 50% advanced tumors. Furudoi *et al.*[26] suggested that the expression of VEGF-C was correlated with lymphatic and venous invasion, lymph node status, Dukes stage, liver metastasis, depth of invasion, poorer histological grade and microvessel density.

It is widely known that VEGF-C can bind to both VEGFR-2

and VEGFR-3. Activation of VEGFR-2 results in the mitogenesis of vascular endothelial cells. In contrast, VEGFR-3 activation by VEGF-C is considered to induce proliferation of lymphatic endothelial cells. Thus, angiogenic versus lymphangiogenic responses to VEGF-C have been found to depend on the expression of its receptors in blood versus lymphatic endothelial cells of the target tissue[27]. In addition, the activation of lymphatics by VEGF-C is considered to induce secretion of chemokines and similar factors by the lymphatic endothelium, thus attracting tumor cells and facilitating their entry into lymphatics[28]. Besides VEGF-C, another new member of VEGF family, VEGF-D, could also stimulate lymphangiogenesis by activating VEGFR-3 in human tumors[29-32]. But the relationship between VEGF-C and VEGF-D expressions, as well as the role of VEGF-D in human tumors is still unclear.

In summary, our findings demonstrate a causal role of lymphangiogenesis in tumor metastasis, suggesting VEGF-C expression is related to the high incidence of metastasis in colorectal carcinoma. However, the mechanism of lymphangiogenesis is extremely complex, which is a subject of ongoing investigation.

REFERENCES

1 **Pepper MS**. Lymphangiogenesis and tumor metastasis: myth or reality? *Clin Cancer Res* 2001; **7**: 462-468

2 **Stacker SA,** Achen MG, Jussila L, Baldwin ME, Alitalo K. Lymphangiogenesis and cancer metastasis. *Nat Rev Cancer* 2002; **2**: 573-583

3 **Jussila L,** Alitalo K. Vascular growth factors and lymphangiogenesis. *Physiol Rev* 2002; **82**: 673-700

4 **Baldwin ME,** Stacker SA, Achen MG. Molecular control of lymphangiogenesis. *Bioessays* 2002; **24**: 1030-1040

5 **Yonemura Y,** Fushido S, Bando E, Kinoshita K, Miwa K, Endo Y, Sugiyama K, Partanen T, Yamamoto H, Sasaki T. Lymphangiogenesis and the vascular endothelial growth factor receptor (VEGFR)-3 in gastric cancer. *Eur J Cancer* 2001; **37**: 918-923

6 **Ji RC,** Kato S. Lymphatic network and lymphangiogenesis in the gastric wall. *J Histochem Cytochem* 2003; **51**: 331-338

7 **Stacker SA,** Baldwin ME, Achen MG. The role of tumor lymphangiogenesis in metastatic spread. *FASEB J* 2002; **16**: 922-934

8 **Kato S.** Introlobular lymphatic vessels and their relationship to blood vessels in the mouse thymus. Light- and electron-mircroscopic study. *Cell Tissue Res* 1988; **253**: 181-187

9 **Jackson DG.** The lymphatics Revisited New perspectives from the Hyaluronan Receptor LYVE-1. *Trends Cardiovasc Med* 2003; **13**: 1-7

10 **Reis-Filho JS,** Schmitt FC. Lymphangiogenesis in tumors: what do we know? *Microsc Res Tech* 2003; **60**: 171-180

11 **Duff SE,** Li C, Jeziorska M, Kumar S, Saunders MP, Sherlock D, O'Dwyer ST, Jayson GC. Vascular endothelial growth factors C and D and lymphangiogenesis in gastrointestinal tract malignancy. *Br J Cancer* 2003; **89**: 426-430

12 **Mattila MM,** Ruohola JK, Karpanen T, Jackson DG, Alitalo K, Harkonen PL.VEGF-C induced lymphangiogenesis is associated with lymph node metastasis in orthotopic MCF-7 tumors. *Int J Cancer* 2002; **98**: 946-951

13 **Krishnan J,** Kirkin V, Steffen A, Hegen M, Weih D, Tomarev S, Wilting J, Sleeman JP. Differential *in vivo* and *in vitro* expression of vascular endothelial growth factor (VEGF) -C and VEGF-D in tumors and its relationship to lymphatic metastasis in immunocompetent rats. *Cancer Res* 2003; **63**: 713-722

14 **He Y,** Kozaki K, Karpanen T, Koshikawa K, Yla-Herttuala S, Takahashi T, Alitalo K. Suppression of tumor lymphangiogenesis and lymph node metastasis by blocking vascular endothelial growth factor receptor 3 signaling. *J Natl Cancer Inst* 2002; **94**: 819-825

15 **Beasley NJ,** Prevo R, Banerji S, Leek RD, Moore J, van Trappen P, Cox G, Harris AL, Jackson DG. Intratumoral lymphangiogenesis and lymph node metastasis in head and neck cancer. *Cancer Res* 2002; **62**: 1315-1320

16 **Sedivy R,** Beck-Mannagetta J, Haverkampf C, Battistutti W, Honigschnabl S. Expression of vascular endothelial growth factor-C correlates with the lymphatic microvessel density and the nodal status in oral squamous cell cancer. *J Oral Pathol Med* 2003; **32**: 455-460

17 **Cassella M,** Skobe M. Lymphatic vessel activation in cancer. *Ann N Y Acad Sci* 2002; **979**: 120-130

18 **Tanaka K,** Sonoo H, Kurebayashi J, Nomura T, Ohkubo S, Yamamoto Y, Yamamoto S. Inhibition of infiltration and angiogenesis by thrombospondin-1 in papillary thyroid carcinoma. *Clin Cancer Res* 2002; **8**: 1125-1131

19 **Takahashi A,** Kono K, Itakura J, Amemiya H, Feng Tang R, Iizuka H, Fujii H, Matsumoto Y. Correlation of vascular endothelial growth factor-C expression with tumor-infiltrating dendritic cells in gastric cancer. *Oncology* 2002; **62**: 121-127

20 **Ichikura T,** Tomimatsu S, Ohkura E, Mochizuki H. Prognostic significance of the expression of vascular endothelial growth factor (VEGF) and VEGF-C in gastric carcinoma. *J Surg Oncol* 2001; **78**: 132-137

21 **Masood R,** Kundra A, Zhu S, Xia G, Scalia P, Smith DL, Gill PS. Malignant mesothelioma growth inhibition by agents that target the VEGF and VEGF-C autocrine loops. *Int J Cancer* 2003; **104**: 603-610

22 **Arinaga M,** Noguchi T, Takeno S, Chujo M, Miura T, Uchida Y. Clinical significance of vascular endothelial growth factor C and vascular endothelial growth factor receptor 3 in patients with non small cell lung carcinoma. *Cancer* 2003; **97**: 457-464

23 **Kaio E,** Tanaka S, Kitadai Y, Sumii M, Yoshihara M, Haruma K, Chayama K. Clinical significance of angiogenic factor expression at the deepest invasive site of advanced colorectal carcinoma. *Oncology* 2003; **64**: 61-73

24 **Tang RF,** Itakura J, Aikawa T, Matsuda K, Fuji H, Korc M, Matsumoto Y. Overexpression of lymphangiogenic growth factor VEGF-C in human pancreatic cancer. *Pancreas* 2001; **22**: 285-292

25 **Liu XE,** Sun XD, Wu JM. Expression and significance of VEGF-C and FLT-4 in gastric cancer. *World J Gastroenterol* 2004; **10**: 352-355

26 **Furudoi A,** Tanaka S, Haruma K, Kitadai Y, Yoshihara M, Chayama K, Shimamoto F. Clinical significance of vascular endothelial growth factor C expression and angiogenesis at the deepest invasive site of advanced colorectal carcinoma. *Oncology* 2002; **62**: 157-166

27 **Nisato RE,** Tille JC, Pepper MS. Lymphangiogenesis and tumor metastasis. *Thromb Haemost* 2003; **90**: 591-597

28 **Mandriota SJ,** Jussila L, Jeltsch M, Compagni A, Baetens D, Prevo R, Banerji S, Huarte J, Montesano R, Jackson DG, Orci L, Alitalo K, Christofori G, Pepper MS. Vascular endothelial growth factor-C-mediated lymphangiogenesis promotes tumour metastasis. *EMBO J* 2002; **20**: 672-682

29 **Nakamura Y,** Yasuoka H, Tsujimoto M, Yang Q, Imabun S, Nakahara M, Nakao K, Nakamura M, Mori I, Kakudo K. Flt-4-positive vessel density correlates with vascular endothelial growth factor-d expression, nodal status, and prognosis in breast cancer. *Clin Cancer Res* 2003; **9**: 5313-5317

30 **Stacker SA,** Hughes RA, Achen MG. Molecular targeting of lymphatics for therapy. *Curr Pharm Des* 2004; **10**: 65-74

31 **Onogawa S,** Kitadai Y, Tanaka S, Kuwai T, Kimura S, Chayama K. Expression of VEGF-C and VEGF-D at the invasive edge correlates with lymph node metastasis and prognosis of patients with colorectal carcinoma. *Cancer Sci* 2004; **95**: 32-39

32 **Koyama Y,** Kaneko K, Akazawa K, Kanbayashi C, Kanda T, Hatakeyama K. Vascular endothelial growth factor-C and vascular endothelial growth factor-d messenger RNA expression in breast cancer: association with lymph node metastasis. *Clin Breast Cancer* 2003; **4**: 354-360

Edited by Kumar M and Wang XL **Proofread by** Xu FM

PO Box 2345, Beijing 100023, China
Fax: +86-10-85381893
E-mail: wjg@wjgnet.com www.wjgnet.com

World J Gastroenterol 2004;10(22):3264-3268
World Journal of Gastroenterology
 ISSN 1007-9327

• VIRAL HEPATITIS •

Hepatitis B virus genotypes, phylogeny and occult infection in a region with a high incidence of hepatocellular carcinoma in China

Zhong-Liao Fang, Hui Zhuang, Xue-Yan Wang, Xian-Min Ge, Tim J Harrison

Zhong-Liao Fang, Hui Zhuang, Department of Microbiology, School of Basic Medicine, Peking University Health Science Center, Beijing 100083, China
Xue-Yan Wang, Center for Disease Prevention and Control of Guangxi Zhuang Autonomous Region, Nanning 530021, Guangxi Zhuang Autonomous Region, China
Xian-Min Ge, Guangxi Worker Hospital, Nanning 530021, Guangxi Zhuang Autonomous Region, China
Tim J Harrison, Centre for Hepatology, Royal Free and University College Medical School, University College London, London, United Kingdom
Supported by Beijing Municipal Committee of Science and Technology, No. H020920020190
Correspondence to: Professor Hui Zhuang, Department of Microbiology, School of Basic Medicine, Peking University Health Science Center, Beijing 100083, China. zhuanghu@publica.chinfo.net
Telephone: +86-10-82802221 **Fax:** +86-10-82801617
Received: 2003-12-19 **Accepted:** 2004-03-02

Abstract

AIM: To determine the genotypes and phylogeny of hepatitis B viruses (HBVs) in asymptomatic HBV carriers, and the prevalence of occult HBV infection in Long An County, Guangxi Zhuang Autonomous Region, an area with a high incidence of hepatocellular carcinoma.

METHODS: A nested polymerase chain reaction (nPCR) was used for detection of HBV DNA in serum samples from 36 blood donors with asympmatic HBV infection, and in serum samples from 52 HBsAg negative family members of the children who did not receive hepatitis B vaccination in Long An County. PCR products were sequenced, and the genotype of each HBV sequence was determined by comparison with sequences of known genotypes in the GenBank and EMBL nucleotide databases using the BLAST programme. Phylogenetic trees were constructed by the quartet maximum likelihood analysis using the TreePuzzle software.

RESULTS: Twenty (55.56%) of 36 HBV asymptomatic carriers were positive for HBV DNA. They were all genotype C by comparison with sequences of known genotypes in the GenBank and EMBL nucleotide databases. The full-length HBV DNA sequence isolated from the sample No. 624 contained 3 215 bases. No interesting mutations were found in this isolate. The homology analysis showed that this strain was closer to the Vietnamese HBV genotype C strain, with a homology of 97%, compared its relation to the same genotype of HBV isolated in Shanghai. Six (11.5%) of the 52 HBsAg negative family members were positive for HBV DNA. A point mutation was found in the sample No. 37, resulting in the substitution of amino acid glycine to arginine in the "a" determinant. Other samples with positive HBV DNA did not have any unusual amino acid substitutions in or around the "a" determinant, and were attributed to the wild-type HBV.

CONCLUSION: The HBVs isolated from asymptomatic carriers of Long An County were all identified as genotype C, and the prevalence of occult HBV infection in the population of the county is as high as 11.5%. It is suggested that genotype C and persistent occult HBV infection may play an important role in the development of HCC in the county.

Fang ZL, Zhuang H, Wang XY, Ge XM, Harrison TJ. Hepatitis B virus genotypes, phylogeny and occult infection in a region with a high incidence of hepatocellular carcinoma in China. *World J Gastroenterol* 2004; 10(22): 3264-3268
http://www.wjgnet.com/1007-9327/10/3264.asp

INTRODUCTION

Infection with hepatitis B virus (HBV) may lead to a wide spectrum of liver diseases ranging from mild, self-limited to fulminant hepatitis in acute infection, and from an asymptomatic carrier state to severe chronic hepatitis, cirrhosis, and hepatocellular carcinoma (HCC) in chronic infection. Human HBV, a prototype member of the family hepadnaviridae, is a circular, partially double-stranded DNA virus of approximately 3200 nt[1]. Traditionally, HBV was classified into 4 subtypes or serotypes (adr, adw, ayr, and ayw) based on antigenic determinants of hepatitis B surface antigen (HBsAg)[2]. Epidemiological studies found that the prevalence of these serotypes varied in different parts of the world. In addition, antibody to the common determinant "a" confers protection against all serotypes. Advances in molecular biology techniques revealed significant diversities in sequences of HBV isolates, accounting for allelic differences among the 4 major HBV serotypes. Based on an intergroup divergence of 8% or more in the complete nucleotide sequence, HBV has been classified into eight genotypes, designated as A to H[3-5]. Recent reports suggested that infections with HBV genotype C were associated with more severe liver diseases, including HCC, than infections with genotype B[6-8]. However, HBV genotype B was suggested to be associated with the development of HCC in Taiwanese below the age of 50 years[9].

Occult HBV infection is characterized by the presence of HBV infection with undetectable HBsAg. Undoubtedly, carriers of occult HBV may transmit the virus through blood transfusion or organ transplantation. Epidemiological and molecular studies performed since the 1980s indicate that persistent HBV infection might play a critical role in the development of HCC and in HBsAg-negative patients[10,11].

The incidence rate of HCC in Long An County, southern Guangxi, China, is about 49.9/100 000, the highest in the world, and over 90% of HCC cases in the county are individuals with positive HBsAg in serum[12,13]. In this study, HBV preC and basic core promoter from 36 HBV asymptomatic carriers in Long An County were amplified and sequenced. The whole genome of a strain from one of the carriers, and genotypes and phylogeny of all the isolates were also analyzed to clarify the difference among HBV strains from different areas. In addition, 52 serum samples from family members of children without hepatitis B vaccination, with negative HBsAg, from the county were

detected for HBV DNA to determine the prevalence of occult HBV infection in the population.

MATERIALS AND METHODS

Serum samples

A total of 36 sera were obtained from asymptomatic blood donors who were infected persistently with HBV in Long An County, southern Guangxi, China. Another 52 serum samples were collected from family members of children failed to have hepatitis B vaccination from the county. Sera were tested for HBsAg, anti-HBc, anti-HBs, HBeAg, and anti-HBe using HBV Marker ELISA kits (produced by Xiamen Xinchuang Scientific Technology Company, Limited, Fujian, China) (Tables 1, 2).

Table 1 Serological markers of 20 asymptomatic carriers with positive HBV DNA

No.	Age (yr)	Sex	HBsAg	Anti-HBs	Anti-HBc	HBeAg	Anti-HBe
601	18	Male	+	-	+	+	-
602	18	Male	+	-	+	+	-
603	28	Female	+	-	+	+	-
604	20	Male	+	-	+	+	-
605	27	Male	+	-	+	+	-
606	18	Male	+	-	+	+	-
607	31	Female	+	-	+	+	-
609	22	Female	+	-	+	+	-
610	19	Male	+	-	+	+	-
615	38	Male	+	-	+	+	-
618	22	Male	+	-	+	-	-
619	20	Male	+	-	+	+	-
621	24	Male	+	-	+	+	-
622	28	Male	+	-	+	+	-
623	30	Male	+	-	+	+	-
624	25	Male	+	-	+	+	-
629	28	Female	+	-	+	+	-
630	28	Female	+	-	+	+	-
633	18	Male	+	-	+	+	-
634	19	Male	+	-	+	+	-

Table 2 Serological markers of HBsAg-negative asymptomatic carriers with positive HBV DNA

Sample No.	HBsAg	Anti-HBs	Anti-HBs Titre (mIU/mL)	HBeAg	Anti-HBe	Anti-HBc
1	-	+	5.1	-	+	+
14	-	+	108.0	-	+	-
16	-	+	18.2	-	+	+
23	-	+	13.9	-	-	-
25	-	-	-	-	+	+
37	-	-	-	-	-	+

PCR amplification and sequence analysis

DNA was extracted from 85 μL serum by phenol/chloroform extraction following digestion by pronase. For preC and basic core promoter amplification: the first round of PCR 35 cycles was carried out using primers B935 (nt 1240-1260, 5' GCGCTGCAG AAGGTTTGTGGCTCCTCTG-3') and MDC1 (nt 2 304-2 324, 5'-TTGATAAGA TAGGGGCATTTG-3'). For each cycle, the samples was amplified at 94 ℃ for 30 s, at 50 ℃ for 30 s, and at 72 ℃ for 90 s in a 50 μL reaction. The second round of 30 PCR cycles was carried out on 5 μL of the first round product using primers CPRF1 (nt 1 678-1 695, 5'-CAATGTCAACGACCG ACC-3') and CPRR1 (nt 1 928-1 948, 5'-GAGTAACTCCACAG TAGCTCC-3') and the same reaction conditions of the first round.

For the surface gene amplification: the first round of 35 ycles PCR was carried out using primers MD14(5'-GCGCT GCAGCTATGCCTCATCTTC-3', nt 418-433) and HCO2 (5'-GCGAAGCTTGCTGTACAGACTTGG-3', nt 761-776). For each cycle, the samples was amplified at 94 ℃ for s, at 45 ℃ for 45 s, and at 72 ℃ for 2 min in a 50 μL reaction. The second round of 30 PCR cycles was carried out on 5 μL of the first round product using primers ME15 (5'-GCGCTGCAGCAAGGTATGTTG CCCG-3', nt 455-470) and HDO3 (5'-GCGAAGCTTCATCAT CCATATAGC-3', nt 734-748) and the same reaction conditions of the first round. PCR products from the second round were confirmed by 15 g/L agarose gels electrophoresis and then purified using the Wizard (PCR Preps DNA purification system (Promega, Madison, WI) according to the manufacturer's instructions. Cycle sequencing was carried out directly on 2 mL purified DNA using primers CPRF1 and 33P-dATP by the thermo sequenase radiolabeled terminator cycle sequencing kit (USB Corporation, Cleveland, OH) according to the manufacturer's instructions.

Sample NO. 624 was selected for whole genome sequencing. Its DNA was extracted from 170 μL serum by phenol/chloroform extraction following digestion by pronase. The whole HBV genome was amplified in three fragments. Primers for fragment 1 for the first and second round PCR were LSOB1, BPOLEO1 and LSBI1, and POLSEQ2. Primers for fragment 2 for the first and second round PCR were MDN5, BPOLEO1, BPOLBO2 and PSISEQ2. Primers for fragment 3 for the first and second round PCR were POLSEQ1, MDD2, POLSEQ6 and MDC1. The conditions of 30 PCR cycles were at 94 ℃ for 30 s, at 50 ℃ for 30 s, and at 72 ℃ for 90 s in a 50 μL reaction. PCR products from the second round PCR for each fragment were cloned into the vector pCR2.1 (Invitrogen, Leek, The Netherlands) and mini preparations of DNA made from 1.5 mL of 15 mL cultures of individual colonies by phenol extraction and ethanol precipitation of the cell pellet. Plasmids with inserts were identified by digestion with *Eco*RI and remainder of the cultures used for extraction of DNA using a QIAprep spin kit (Qiagen, Crawley, UK). The purified DNA was sequenced as above. Sequencing primers for fragment 1 were LSB1, PSISEQ2, ds 2, ds, ADELN, MD14, ADELP, POLSEQ8, POLSEQ9, POLSEQ6, POLSEQ2. Primers for fragment 2 were BPOLBO2, POLSEQ4, LSOB1, POLSEQ5 and PSISEQ2. Primers for fragment 3 were POLSEQ6, B935, BPOLEO1, MDN5, B936 and MDC1 (Tables 3, 4).

Table 3 PCR Primers

Primers	Sequence	Position (nt)
LSOB1	5'-GGCATTATTTGCATACCCTTTGG-3'	2739-2762
BPOLEO1	5'-CTGAGAGTCCAAGAGTCCTCT-3'	1657-1677
LSBI1	5'-TTGTGGGTCACCATATTCTT-3'	2809-2829
POLSEQ2	5'-AGCAAACACTTGGCATAGGC-3'	1168-1188
MDN5	5'-AGGAGGCTGTAGGCATAAAT-3'	1774-1794
BPOLEO1	5'-CTGAGAGTCCAAGAGTCCTCT-3'	1657-1677
BPOLBO2	5'-TCTTGTCTTACTTTTGGAAGA-3'	2216-2236
PSISEQ2	5'-GCTGTTCCGGAATTGGAGCC-3'	65-84
POLSEQ1	5'-ACCAAGCGTTGGGGCTACTC-3'	847-866
MDD2	5'-GAAGAATAAAGCCCAGTAAA-3'	2481-2500
POLSEQ6	5'-TTTCACTTTCTCGCCAACTTA-3'	1089-1109
MDC1	5'-TTGATAAGATAGGGGCATTTG-3'	2304-2324

Table 4 Sequencing primers

Primers	Sequence	Position (nt)
LSB1	5'-TTGTGGGTCACCATATTCTT-3'	2809-2829
PSISEQ2	5'-GCTGTTCCGGAATTGGAGCC-3'	65-84
ds2	5'-AGTCCGGTACGTCACCTTG-3'	3198-1
ds	5'-TACCGAAAATGGAGAACACA-3'	147-166
ADELN	5'-TAGTCCAGAAGAACCAACAAG-3'	432-453
MD14	5'-GCGCTGCAGCTATGCCTCATCTTC-3'	418-433
ADELP	5'-CCTGTATTCCCATCCCATCATC-3'	597-618
POLSEQ8	5'-TGTTTTCGAAAACTTCCTGT-3'	943-962
POLSEQ9	5'-ACAGGAAGTTTTCGAAAACA-3'	943-962
POLSEQ6	5'-TTTCACTTTCTCGCCAACTTA-3'	1089-1109
POLSEQ2	5'-AGCAAACACTTGGCATAGGC-3'	1168-1188
BPOLBO2	5'-TCTTGTCTTACTTTTGGAAGA-3'	2216-2236
POLSEQ4	5'-AAATGCCCCTATCTTATCAA-3'	2305-2323
LSOB1	5'-GGCATTATTTGCATACCCTTTGG-3'	2739-2762
POLSEQ5	5'-GGGTCCTTGTTGGGGTTGAAG-3'	2979-2999
B935	5'-GAAGGTTTGTGGCTCCTCTG-3'	1240-1260
BPOLEO1	5'-CTGAGAGTCCAAGAGTCCTCT-3'	1657-1677
MDN5	5'-AGGAGGCTGTAGGCATAAAT-3'	1774-1794
B936	5'-TGGAGGCTTGAACAGTAGGACAT-3'	1851-1874
MDC1	5'-TTGATAAGATAGGGGCATTTG-3'	2304-2324

Database sequences

The following complete genomes (represented by their accession number) were used in phylogenetic tree analyses: genotype A: AJ344115; genotype B: AF282917, D00331; genotype C: AY040627, AF461357, M38454, AY057948, AF241410, AF241411, AF330110, AB048705, AB026812, D00329, AB014398, X75665, X14193, X52939, X59795; genotype D: AF280817, AJ344116; genotype E: X75664; genotype F: AB036908; genotype G: AF405706.

Genotype and phylogeny analysis

The genotype of each HBV sequence was determined by comparison with sequences of known genotypes in the GenBank and EMBL nucleotide databases using the programme BLAST[14]. Phylogenetic trees were constructed by maximum likelihood analysis by quartet puzzling[15]. TreePuzzle is available at http://www.tree-puzzle.de.

RESULTS

HBV genotypes

Compared with sequences of known genotypes in the GenBank and EMBL nucleotide databases using the programme BLAST, all genotypes of each HBV sequence from the 20 asymptomatic HBV carriers in Long An County were found to be genotype C viruses.

Characterization of HBV genome structure

The full-length HBV-DNA sequence of HBV isolated from sample No. 624 was determined by direct sequencing. This strain contained 3 215 bases. Its serotype is adw. There were 40 point mutations in polymerase gene resulting in changes of 11 amino acids. There were 11, 2, 3 point mutations in PreS1, PreS2 and S genes, leading to 3, 1, 1 amino acids changed in the respective regions. The amino acid mutation in PreS1 was TPP→PHQ at codes 68-70. Six point mutations including the double mutations were found in X gene causing changes of 4 amino acids. There were also 13 point mutations in C gene, leading to 2 amino acids changed. No mutation was found in "a" determinant and Pre C.

Phylogeny analysis

The homology with 23 HBV strains in GenBank was determined by using the programme TreePuzzle. The HBV strain isolated from sample No. 624 in Long An County was closer to the Vietnamese HBV of genotype C, with 97% homology between them, as compared to the isolates of the same genotype from Shanghai, Beijing and Tibet in evolution (Figure 1).

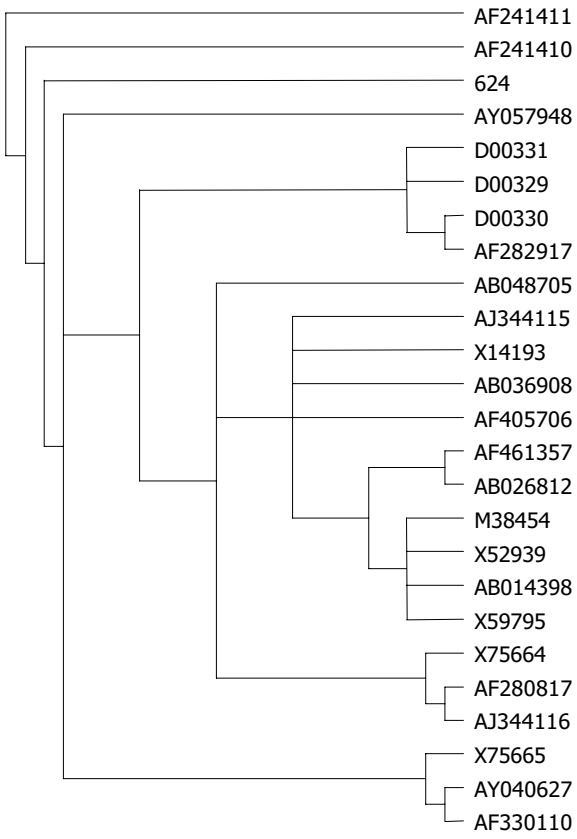

Figure 1 Phylogenetic trees based on comparison of the whole genome. The trees were created by maximum likelihood analysis using the TreePuzzle software with AF241411 as outgroup.

Prevalence of occult HBV infection

After nested PCR amplification, six samples of 52 family members of children without immunization of HBV vaccine were positive for HBV DNA, counting for 11.5% (6/52) (Table 2). The region of surface ORF of the samples with positive HBV DNA positive, including the "a" determinant of HBsAg, was sequenced. A point mutation from guanosine to adenosine at nucleotide position 587 resulted in an amino acid substitution from glycine to arginine in the highly antigenic "a" determinant of HbsAg, which was found in sample No. 37 only and was negative for both HBsAg and anti-HBs. The other samples with positive HBV DNA did not have unusual amino acid substitutions in or around the "a" determinant, and were attributed to the wild-type HBV of genotype C.

DISCUSSION

In 1988, Okamoto *et al*.[3] established a method to classify HBV, and analyzed the complete HBV nucleotide sequences and classified them into four different HBV genotypes designated from A to D, according to an intergroup divergence of >8%, and an intragroup divergence of <5.6%. Today, HBV has been classified into eight different genotypes designated from A to H[4,5,16,17] and HBV genotypes have a pattern of geographical distribution[18,19]. Genotype A is prevalent in Northern and Central Europe, but is also common in North America and sub-Saharan Africa. Genotypes B and C are confined to Asia, genotype D is widespread but is the predominant genotype in

the Mediterranean region, while genotype E is found mainly in West Africa. Genotype F shows the highest divergence among the genotypes and is indigenous to aboriginal populations of the Americas[20]. Genotype G was found in USA and France[4], genotype H in the Central America[5], and genotypes A, B, C and D in China. The predominant genotype in China is genotypes B and C[21,22].

The incidence of HCC in Long An County is about 49.9/100 000 and the prevalence of HBsAg in the county is 16%[13,23] and more than 90% of hepatocellular carcinoma (HCC) cases are individuals positive for HBsAg in serum[12]. In Japan, HBV genotype C was found to be closely associated with severe liver diseases and the development of HCC[7,24], although young HCC patients were found to be HBV genotype C in Taiwan[25].

HBV infection is usually diagnosed when the circulating HBsAg is detected. However, advances in molecular biology techniques revealed that a low level of HBV DNA could be detected in serum and liver tissue in some individuals who were negative for HBsAg[26,27]. Although there are some studies on occult HBV infection, the precise prevalence of this clinical entity is still unknown. Luo *et al*.[28] found that the prevalence rate of occult HBV infection in Guangdong and Hainan Provinces was 2.0% (6/294) and 3.4% (68/1 995), respectively in the general population. Bower *et al*.[29] reported that the prevalence was 4.3% (11/258) in subjects without liver disease in USA. In this study, we found that the prevalence of occult HBV infection in Long An County was higher (11.5%, 6/52). The mechanisms that HBV carriers have a low, but stable level of viral replication remain to be defined. HBV strains might have mutations in S region resulting in occult HBV infection[30,31]. This kind of mutations was found in one of our samples. In addition, this type of carriers should be added to the typical HBsAg-positive carriers constituting about 16% of the general population, to estimate more precisely the propotion of asymptomatic HBV carriers in Long An County. It is clear that the prevalence of HBV infection in Long An County is in correspondence with its high incidence of HCC.

To extend the knowledge of molecular features of natural HBV isolates, sample No. 624 in this study was selected for whole genome sequencing. This strain contained 3 215 bases. HBsAg region sequence showed that it belonged to serotype adw. No special mutation which could change the expression function of viral proteins was found in the sequence of this isolate. By homology analysis with 23 HBV strains in GenBank, this isolate was found to be closer to the Vietnamese HBV genotype C strain[32] than to the genotype C isolates from Shanghai in evolution[33], with 97% homology with the Vietnamese isolate. At present, the only explanation about this is that Long An County is geographically close to Vietnam.

In summary, HBV infections in Long An County are attributable to HBV genotypes C. The prevalence of occult HBV infection in Long An County is higher.

ACKNOWLEDGMENTS

We are very grateful to the Beijing Municipal Committee of Science and Technology for the financial support in part and the Center for Disease Prevention and Control of Long An County for their help in collecting samples.

REFERENCES

1 **Magnius LO,** Norder H. Subtypes, genotypes and molecular epidemiology of the hepatitis B virus as reacted by sequence variability of the S-gene. *Intervirology* 1995; **38:** 24-34
2 **Le Bouvier GL,** McCollum RW, Hierholzer WJ Jr, Irwin GR, Krug-man S, Giles JP. Subtypes of Australia antigen and hepatitis-B virus. *JAMA* 1972; **222**: 928-930
3 **Okamoto H,** Tsuda F, Sakugawa H, Sastrosoewignjo RI, Imai M, Miyakawa Y, Mayumi M. Typing hepatitis B virus by homology in nucleotide sequence: comparison of surface antigen subtypes. *J Gen Virol* 1988; **69**: 2575-2583
4 **Stuyver L,** DeGendt S, VanGeyt C, Zoulim F, Fried M, Schinazi RF, Rossau R. A new genotype of hepatitis B virus: complete genome and phylogenetic relatedness. *J Gen Virol* 2000; **81**: 67-74
5 **Arauz-Ruiz P,** Norder H, Robertson BH, Magnius LO. Genotype H: a new Amerindian genotype of hepatitis B virus revealed in Central America. *J Gen Virol* 2002; **83**: 2059-2073
6 **Ding X,** Mizokami M, Yao GB, Xu B, Orito E, Ueda R, Nakanishi M. Hepatitis B virus genotype distribution among chronic hepatitis B virus carriers in Shanghai, China. *Intervirology* 2001; **44**: 43–47
7 **Fujie H,** Moriya K, Shintani Y, Yotsuyanagi H, Iino S, Kimura S, Koike K. Hepatitis B virus genotypes and hepatocellular carcinoma in Japan. *Gastroenterology* 2001; **120**: 1564–1565
8 **Orito E,** Ichida T, Sakugawa H, Sata M, Horiike N, Hino K, Okita K, Okanoue T, Iino S, Tanaka E, Suzuki K, Watanabe H, Hige S, Mizokami M. Geographic distribution of hepatitis B virus (HBV) genotype in patients with chronic HBV infection in Japan. *Hepatology* 2001; **34**: 590–594
9 **Kao JH,** Chen PJ, Lai MY, Chen DS. Hepatitis B genotypes correlate with clinical outcomes in patients with chronic hepatitis B. *Gastroenterology* 2000; **118**: 554–559
10 **Paterlini P,** Gerken G, Nakajima E, Terre S, D'Errico A, Grigioni W. Polymerase chain reaction to detect hepatitis B virus DNA and RNA sequences in primary liver cancers from patients negative for hepatitis B surface antigen. *N Engl J Med* 1990; **323**: 80-85
11 **Paterlini P,** Poussin K, Kew M, Franco D, Brechot C. Selective accumulation of the X transcript of hepatitis B virus in patients negative for hepatitis B surface antigen with hepatocellular carcinoma. *Hepatology* 1995; **21**: 313-321
12 **Yeh FS,** Yu MC, Mo CC, Luo S, Tong MJ, Henderson BE. Hepatitis B virus, aflatoxins, and hepatocellular carcinoma in southern Guangxi, China. *Cancer Research* 1989; **49**: 2506–2509
13 **Ding ZG.** Epidemiological study on relationship between hepatitis B and liver cancer: a prospective study on development of liver cancer and distribution of HBsAg carriers and liver damage persons in Guangxi. *Zhonghua Liuxingbingxue Zazhi* 1988; **9**: 220–223
14 **Altschul SF,** Gish W, Miller W, Myers EW, Lipman DJ. Basic local alignment search tool. *J Mol Biol* 1990; **215**: 403–410
15 **Strimmer K,** Haeseler A. Quartet puzzling: a quartet maximum-likelihood method for reconstructing tree topologies. *Mol Biol Evolution* 1996; **13**: 964-969
16 **Norder H,** Hammas B, Logfdahl S, Courouce AM, Magnius LO. Comparison of the amino acid sequences of nine different serotypes of hepatitis B surface antigen and genomic classification of the corresponding hepatitis B virus strains. *J Gen Virol* 1992; **73**: 1201-1208
17 **Norder H,** Courouce AM, Magnius LO. Complete genomes, phylogenetic relatedness, and structural proteins of six strains of the hepatitis B virus, four of which represent two new genotypes. *Virology* 1994; **198**: 489-503
18 **Nakano T,** Lu L, Hu X, Mizokami M, Orito E, Shapiro C, Hadler S, Robertson B. Characterization of hepatitis B virus genotype among Yuipa Indians in Venezuela. *J Gen Virol* 2001; **82**: 359–365
19 **Naumann H,** Schaefer S, Yoshida CF, Gaspar AM, Repp R, Gerlich WH. Identification of a new hepatitis B virus genotype from Brazil that expresses HBV surface antigen subtype adw 4. *J Gen Virol* 1993; **74**: 1627-1632
20 **Norder H,** Hammas B, Lee SD, Bile K, Courouce AM, Mushahwar IK, Magnius LO. Genetic relatedness of hepatitis B viral strains of diverse geographical origin and natural variations in the primary structure of the surface antigen. *J Gen Virol* 1993; **74**: 1341-1348
21 **Ding X,** Mizokami M, Ge XM, Orito E, Iino S, Ueda R, Nakanishi M. Different hepatitis B virus genotype distributions among asymptomatic carriers and patients with liver diseases in Nanning, southern China. *Hepatology Research* 2002; **22**: 37-44
22 **Xia G,** Nainan OV, Jia Z. Characterization and distribution of hepatitis B virus genotypes and subtypes in 4 provinces of

China. *Zhonghua Liuxingbingxue Zazhi* 2001; **22**: 348-351

23 **Wang SS,** Xu ZY, Maynard JE, Prince AM, Beasley RP, Yang JY, Li YC, Nong YZ. Evaluation of the hepatitis B model immunization program in Long An county, China. *Guangxi Yufang Yixue Zazhi* 1995; **1**: 1-4

24 **Orito E,** Mizokami M, Sakugawa H, Michitaka K, Ishikawa K, Ichida T, Okanoue T, Yotsuyanagi H, Iino S. A case-control study for clinical and molecular biological differences between hepatitis B viruses of genotypes B and C. *Hepatology* 2001; **33**: 218–223

25 **Kao JH,** Chen DS. Hepatitis B virus genotypes and hepatocellular carcinoma in Japan: reply. *Gastroenterology* 2001; **120**: 1565

26 **Wang JT,** Wang TH, Sheu JC, Shih LN, Lin JT, Chen DS. Detection of hepatitis B virus DNA by polymerase chain reaction in plasma of volunteer blood donors negative for hepatitis B surface antigen. *J Infect Dis* 1991; **163**: 397-399

27 **Zhang YY,** Hansson BG, Kuo LS, Widell A, Nordenfelt E. Hepatitis B virus DNA in serum and liver is commonly found in Chinese patients with chronic liver disease despite the presence of antibodies to HBsAg. *Hepatology* 1993; **17**: 538-544

28 **Luo KX,** Zhou R, He C, Liang ZS, Jiang SB. Hepatitis B virus DNA in sera of virus carriers positive exclusively for antibodies to the hepatitis B core antigen. *J Med Virol* 1991; **35**: 55–59

29 **Bower WA,** Xia GL, Gao FX, Nainan OV, Kruszon-Moran D, Margolis HS. Isolated hepatitis B core antibody. *Antiviral Ther* 2000; **5**(Suppl 1): B22

30 **Blackberg J,** Kidd-Ljunggren K. Occult hepatitis B virus after acute self-limited infection persisting for 30 years without sequence variation. *J Hepatol* 2000; **33**: 992-997

31 **Yamamoto K,** Horikita M, Tsuda M, Itoh K, Akahane Y, Yotsumoto S, Okamoto H, Miyakawa Y, Mayumi M. Naturally occurring escape mutants of hepatitis B virus with various mutations in the S gene in carriers seropositive for antibodies to hepatitis B surface antigen. *J Virol* 1994; **68**: 2671-2676

32 **Hannoun C,** Norder H, Lindh M. An aberrant genotype revealed in recombinant hepatitis B virus strains from Vietnam. *J Gen Virol* 2000; **81**: 2267–2272

33 **Gan RB,** Chu MJ, Shen LP, Qian SW, Li ZP. The complete nucleotide sequence of the cloned DNA of hepatitis B virus subtype adr in pADR-1. *Sci Sin* 1987: 507-521

Edited by Ren SY and Wang XL **Proofread by** Xu FM

PO Box 2345, Beijing 100023, China
Fax: +86-10-85381893
E-mail: wjg@wjgnet.com www.wjgnet.com

World J Gastroenterol 2004;10(22):3269-3273
World Journal of Gastroenterology
 ISSN 1007-9327

• VIRAL HEPATITIS •

Capsule oxymatrine in treatment of hepatic fibrosis due to chronic viral hepatitis: A randomized, double blind, placebo-controlled, multicenter clinical study

Yi-Min Mao, Min-De Zeng, Lun-Gen Lu, Mo-Bin Wan, Cheng-Zhong Li, Cheng-Wei Chen, Qing-Chuen Fu, Ji-Yao Wang, Wei-Min She, Xiong Cai, Jun Ye, Xia-Qiu Zhou, Hui Wang, Shan-Ming Wu, Mei-Fang Tang, Jin-Shui Zhu, Wei-Xiong Chen, Hui-Quan Zhang

Yi-Min Mao, Min-De Zeng, Lun-Gen Lu, Shanghai Institute of Digestive Disease, Renji Hospital, Shanghai Second Medical University, Shanghai 200001, China
Mo-Bin Wan, Cheng-Zhong Li, Changhai Hospital, Second Military Medical University, Shanghai 200433, China
Cheng-Wei Chen, Qing-Chuen Fu, Nanjing Military Command Liver Disease Research Center, Shanghai 200233, China
Ji-Yao Wang, Wei-Min She, Zhongshan Hospital, Fudan University, Shanghai 200032, China
Xiong Cai, Changzheng Hospital, Second Military Medical University, Shanghai 200003, China
Jun Ye, Shanghai Putuo District Central Hospital, Shanghai 200333, China
Xia-Qiu Zhou, Hui Wang, Ruijin Hospital, Shanghai Second Medical University, Shanghai 200025, China
Shan-Ming Wu, Mei-Fang Tang, Shanghai General Hospital of Infectious Diseases, Shanghai 200083, China
Jin-Shui Zhu, Wei-Xiong Chen, Shanghai No.6 People's Hospital, Shanghai 200230, China
Hui-Quan Zhang, Shanghai Shibei Hospital, Shanghai 200073, China
Supported by Grants From the Key Project of Shanghai Medical Development Foundation, NO:99ZDI001 and Grants From 1999 Youth Liver Diseases Foundation of Chinese Liver Diseases Association
Correspondence to: Yi-Min Mao, M.D., Shanghai Institute of Digestive Disease, Renji Hospital, Shanghai Second Medical University, Shanghai 200001, China. maoyimin1@sina.com
Telephone: +86-21-33070834 **Fax:**+86-21-63364118
Received: 2003-12-17 **Accepted:** 2004-02-24

Abstract

AIM: To evaluate the efficacy and safety of oxymatrine capsule in treatment of hepatic fibrosis in patients with chronic viral hepatitis.

METHODS: It was a randomized, double blind, placebo-controlled, multicenter clinical study. One hundred and forty-four patients were divided into oxymatrine capsule group (group A) and placebo group (group B).The course was 52 wk. Patients were visited once every 12 wk and the last visit was at 12 wk after cessation of the treatment. All patients had liver biopsy before treatment. part of them had a second biopsy at the end of therapy. Clinical symptoms, liver function test, serum markers of hepatic fibrosis were tested. Ultrasound evaluation was performed before, during and at the end of therapy.

RESULTS: One hundred and forty-four patients enrolled in the study. Of them 132 patients completed the study according to the protocol,49 patients had liver biopsy twice (25 patients in group A and 24 in group B). At the end of therapy, significant improvements in hepatic fibrosis and inflammatory activity based on Semi-quantitative scoring system (SSS) were achieved in group A. The total effective rate of the treatment was 48.00%, much higher than that of 4.17% in group B (P<0.05). Significant improvement in serum markers of hepatic fibrosis such as hyaluronic acid (HA) and type III procollagenic peptide (P III P) in group A was seen (P<0.05). The total effective rate of serum markers at the end of therapy in group A was 68.19%, much higher than that of 34.85% in group B (P<0.05). The total effective rate of noninvasive markers at the end of therapy in group A was 66.67%, much higher than that of 30.30% in group B (P<0.05). The rate of adverse events was similar in two groups.

CONCLUSION: Oxymatrine capsule is effective and safe in treatment of hepatic fibrosis due to chronic viral hepatitis.

Mao YM, Zeng MD, Lu LG , Wan MB, Li CZ, Chen CW, Fu QC, Wang JY, She WM, Cai X, Ye J, Zhou XQ, Wang H, Wu SM, Tang MF, Zhu JS, Chen WX, Zhang HQ. Capsule oxymatrine in treatment of hepatic fibrosis due to chronic viral hepatitis: A randomized, double blind, placebo-controlled, multicenter clinical study. *World J Gastroenterol* 2004; 10(22): 3269-3273
http://www.wjgnet.com/1007-9327/10/3269.asp

INTRODUCTION

Hepatic fibrosis is a kind of compensating and healing response in the liver to liver injury induced by a variety of causes and also a common pathological process of many chronic liver diseases characterized by hyperplasia and deposition of fibro-connective tissues. It is essential to block the genesis and progress of hepatic fibrosis[1-5,30,31]. Oxymatrine is a kind of alkaloid extracted from a Chinese herb Sophora alopecuraides L. which has been proved to have antihepatic fibrosis effect[6,7,18-20]. In this paper, we reported the clinical study data of oxymatrine capsule in treatment of hepatic fibrosis in patients with chronic viral hepatitis.

MATERIALS AND METHODS

Resarch design

This study was a clinical trial characterized by multicentre, randomization, double blinding, and placebo-control. Enrolled patients were randomly assigned into oxymatrine capsule group (group A) or vacant placebo control group (group B), with 72 cases in each group and a treatment course of 52 wk. This study was conformed to the Good Clinical Practice (GCP) of China. The research protocol was discussed and approved by the Ethic Committee of National Clinical Research Base of Drugs in the Institute of Digestive Disease of Renji Hospital. Informed consent was obtained from each patient.

Selection of subjects

Enrolled criteria were age: 18-65 years regardless of sex; positive serum markers of hepatitis B virus (HBV) and hepatitis C virus (HCV) for at least 6 mo before enrollment; abnormal serum value of alanine transaminase (ALT) twice or more within 6 mo before enrollment; liver biopsy examination during 1 mo before enrollment indicating the stage of hepatic fibrosis from 1 to 4 according to National Criteria of Grading and Staging for chronic

viral hepatitis amended in 1995 and the scores of stage equal or more than 1 assessed by the semi-quantitative scoring system (SSS) of hepatic fibrosis; total serum bilirubin level less than or equal to 85.5 μmol/L; no history of administrating following drugs: antiviral drugs, immunoregulating drugs and other antifibrotic agents; promising not to receive other systemic antiviral agents, cytotoxic agents, immunoregulators, drugs capable of reducing serum enzyme activity and bilirubin level, and Chinese traditional medicines, *etc.* Following situations should be excluded: patients with positive laboratory test of HIV; uncompensable liver diseases; suggestive of autoimmune diseases with antinuclear antibody (ANA) titer greater than a 1:160 dilution; bone marrow inhibition; abnormality of serum creatinine with a value 1.5 times greater than normal; concurrence of other associated diseases which might affect the present treatment such as unstable diabetes, renal insufficiency, unstable angina pectoris, alcoholic liver disease, epilepsy, obvious manifestations of neurosis, drug abuser, psychosis, pancreatitis, disability of absorption and malignant disease, and so on; Having taken other drugs in clinical trial within 30 d before the first medication; hypersensitive to oxymatrine capsule; pregnancy and during breast-feeding period; female conceptive patients not adopting any contraceptives.

Treatment procedures and drugs

After completion of selection and assessment, qualified subjects were allocated into group A or B randomly. The patients in group A took 300 mg oxymatrine capsules orally 3 times a day, and 2 tablets of complex vitamins B and C at the same time for 52 wk. The patients in group B took 3 tablets of vacant capsules instead of oxymatrine capsules and complex vitamins B and C at the same frequency as described above for 52 wk. All patients received follow-up once every 12 wk during treatment and were followed up at out-patient department 12 wk after treatment. Oxymatrine capsule, vacant placebo capsule, complex vitamins B and C tablets were manufactured and provided by Ningxia Pharmaceutic Institute and Shanghai Green Valley Ecological Engineering Co.LTD.

Observation of indexes and assessment

Clinical manifestations Clinical symptoms and signs were divided into grades from 0 to 3 according to the symptomatic grading criteria , evaluated at each follow-up visit, and examined 24 and 52 wk after treatment and 12 wk after drug withdrawal.

Analysis of blood and urine routines and related liver function indexes These indexes were evaluated at each follow-up visit and examined 52 wk after treatment and 12 wk after drug withdrawal.

Analysis of serum markers of hepatic fibrosis Tests of serum hyaluronic acid (HA), laminin (LN), type III procollagenic peptide (p III p), type IV collagen-7S (IV-7S) were fulfilled by Military Clinical Immunologic Research Centre of Changzheng Hospital, Second Military Medical University. The above markers were evaluated before treatment, 24 and 52 wk after treatment, 12 wk after drug withdrawal respectively, and examined 24 and 52 wk after treatment,12 wk after drug withdrawal, respectively.

Imaging examination (type B ultrasound) The detection included 5 indexes: maximal oblique radius of right liver lobe, main trunk diameter of portal vein and its blood flow parameters per minute; width of spleen at the hilus and the diameter of spleenic vein. Ultrasound examination was performed on fixed machines and by fixed operators and the data were recorded and input in computers which were read by experts. All the indexes were evaluated before treatment and 52 wk after therapy, examined 52 wk after drug withdrawal.

Histopathological detection Histopathological specimens were independently observed and assessed based on National Criteria of Grading and Staging for chronic viral hepatitis amended in 1995 and SSS by 3 pathologists from Department of Pathology, Medical College, Fudan University. The observed results were checked by another 3 pathologists who did not anticipate in the study by Kappa test. The reciprocal consistence among the above pathologists was satisfactory. The observed results in all patients were evaluated before therapy and part of them were evaluated 52 wk after therapy. All data were examined 52 wk after therapy.

During treatment and after therapy was terminated, the following events were recorded: combined medication, adverse reactions and the compliance of patients.

Assessment of therapeutic effects

Indexes of histopathology The curative effect was evaluated based on SSS. Distinctly effective: the scores of hepatic fibrosis based on SSS from liver biopsy decreased at least 6 scores compared with that before treatment. Effective: the above scores decreased at least 2 scores. Ineffective: the effect did not meet the effective criteria.

Assessment of indexes of noninvasive tests These indexes were evaluated comprehensively in terms of clinical manifestations, serum liver fibrotic markers and ultrasound detection data. Distinctly effective: any two values among serum liver fibrotic indexes decreased by at least 80% compared with that before treatment, at least the main trunk diameter of portal vein and splenic width returned to normal after treatment, clinical symptoms and signs disappeared or their total scores decreased by at least 75% compared with that before treatment. Effective: any two values among serum liver fibrotic indexes decreased by at least 40% compared with that before treatment, the main trunk diameter of portal vein and splenic width reduced after treatment, clinical symptoms and signs disappeared basically or their total scores decreased by at least 25% compared with that before treatment. Ineffective: the effect did not meet the effective criteria.

Assessment of safety

Any abnormal clinical manifestations and laboratory tests occurred during treatment were recorded and divided into 4 grades according to the criteria published by WHO and the Ministry of Public Health of China in 1994.

Statistical analysis

Statistical analyses were performed by professor Su BH and He QB from Department of Statistics, Shanghai Second Medical University, and SAS 6.12 software kit was used.

RESULTS

Selected patients

A total of 144 patients satisfied the selection criteria. Of them, 12 cases withdrew or were excluded during treatment, 132 cases fulfilled the treatment course according to the required protocol (66 cases in group A and 66 cases in group B). Before treatment, the following general data between two groups were similar (P>0.05, respectively): sex, age, drinking history, duration of hepatitis, duration of abnormality of liver function and a more than 2-fold normal elevation of serum ALT, *etc*. Each qualified patient received liver biopsy before treatment. A total of 49 cases had a second liver biopsy (25 cases in group A and 24 cases in group B).

Analysis of observed indexes

Clinical symptoms and signs Clinical manifestations in group A were obviously improved 52 wk after therapy (P<0.05), except for epistaxis (P = 1.0000). Heptomegaly was also improved significantly after therapy (P = 0.0313), symptoms of gum bleeding

and epistaxis were not improved obviously in group B (P>0.05). Signs of hepatomegaly, splenomegaly and liver palm were significantly improved in group B (P<0.05), improvement of anorexia in group A was greater than that in group B (P = 0.0263).

Liver function Indexes of liver function in group A were significantly improved 52 wk after treatment (P<0.05) except for serum gamma glutamino transpeptidase (GGT) and TB (P>0.05). In group B, indexes such as serum ALT, AST, TB and alkaline phosphatase (ALP) had no obvious difference before and after therapy (P>0.05). Compared with group B, the improvement of ALT and AST in group A was much greater (P = 0.0007 and 0.0025). Fifty-two wk after therapy, the normalization rate of ALT in group A was 70.77%, much higher than 39.68% in group B (P = 0.0003). In groups A and B, 14 out of 46 cases (30.43%) and 12 out of 25 cases (48.00%) had their serum ALT levels returned to normal 52 wk after treatment ,and their serum ALT levels became abnormal again after drug withdrawal.

Liver histologic examination Evaluation of hepatic fibrosis based on SSS: In group A, the scores of hepatic fibrosis after therapy were 4.72±5.63, much smaller than 6.76±6.67 before therapy (P = 0.0001), while the scores in group B after therapy increased significantly (P = 0.0009). There was an obvious difference between two groups (P = 0) (Table 1). Evaluation of histolgic inflammatory activity based on SSS: In group A, the scores of histologic activity decreased from 46.08±3.84 before treatment to 4.00±2.97 after therapy (P = 0.0002), while the scores in group B after therapy did not decrease obviously (P = 0.2344). There was an obvious difference between two groups (P = 0008) (Table 2).

Evaluation of serum markers of hepatic fibrosis In group A, serum levels of HA, LN, p III p and IV-7S decreased significantly 24 and 52 wk after treatment (P<0.05). In group B, serum levels of LN, p III p and IV-7S also decreased obviously after treatment (P<0.05). However, degrees of improvement in HA and p III p between two groups were distinctly different (P<0.05). In group A, except for LN (P = 0.1493), the other 3 liver fibrotic markers increased significantly 12 wk after drug withdrawal compared with that 52 wk after treatment (P<0.05). In group B, except for HA (P = 0.4212), the other markers also increased obviously 12 wk after drug withdrawal compared with that 52 wk after treatment (P<0.05). The increase of HA in group A was more than that in group B (P = 0.0002) and the increase of IV-7S in group B was more than that in group A (P = 0.0048).

Imaging examination After treatment, the average values of main trunk diameters of portal vein and splenic width in group A obviously decreased (P<0.05). However, in group B, the above two parameters and the parameters of blood flow volume per minute of portal vein and diameters of splenic vein all increased significantly compared with those before therapy (P<0.05). The changes in main trunk diameters of portal vein and splenic width between two groups were statistically significant (P<0.05).

Analysis of therapeutic effect

Assessment of histopathology based on SSS After treatment, the rates of distinct effectiveness and effectiveness in group A were both 24.00%, and the total effective rate was 48.00%. In group B, none achieved distinct effectiveness and the effective rate was only 4.17%; Comparison of the rates of distinct effectiveness and effectiveness between two groups had a significant difference (P = 0.004) (Table 3).

Assessment of serum markers of hepatic fibrosis The total effective rate of group A 24 and 52 wk after therapy was 57.43% and 68.19%, more than 24.24% and 34.85% of group B (P = 0.0002 and 0.0004, respectively). Twelve weeks after treatment, the total effective rate of group A was 50.00%, more than 15.16% of group B (P=0.00).

Assessment of noninvasive indexes of hepatic fibrosis After treatment, the rates of distinct effectiveness and effectiveness

Table 1 Liver fibrotic scores before and after therapy based on Semi-quantitative Scoring System

Group	Before	After	Before-after	Comparison before therapy		Comparison within group		Comparison between groups	
				Statistics	*P*	Statistics	*P*	Statistics	*P*
A									
(n = 25)	6.76±6.67	4.72±5.63	2.04±2.59			96.0	0.0001		
B				1.4098	0.1586			4.8834	0
(n = 24)	4.13±2.82	6.33±4.04	-2.21±3.72			83.0	0.0009		

Table 2 Liver histologic activity scores before and after therapy based on Semi-quantitative Scoring System

Group	Before	After	Before-after	Comparison before therapy		Comparison within group		Comparison between groups	
				Statistics	*P*	Statistics	*P*	Statistics	*P*
A									
(n = 25)	6.08±3.84	4.00±2.97	2.08±2.71			69.5	0.0002		
B				0.0407	0.9675			3.3543	0.0008
(n = 24)	6.08±4.06	6.92±4.17	-0.83±3.38			21.5	0.2344		

Table 3 Comparison of histopathology of hepatic fibrosis

Group	Distinctly effective	Effective	Ineffect-ive	Comparison between 2 groups	
				Statitics χ^2	*P*
A	6	6	13		
(n = 25)	(24.00%)	(24.00%)	(52.00%)		
B	0	1	23	12.6970	0.0004
(n = 24)	(0.00%)	(4.17%)	(95.83%)		

Table 4 Comparison of noninvasive markers of hepatic fibrosis

Group	Distinctly effective	Effective	Ineffect-ive	Comparison between 2 groups	
				Statitics χ^2	*P*
A	2	42	22		
(*n* = 66)	(3.03%)	(63.64%)	(33.33%)		
B	0	20	46	16.2494	0.0001
(*n* = 66)	(0.00%)	(30.30%)	(69.70%)		

in group A were respectively 3.03% and 63.64%, and the total effective rate was 66.67%. In group B, the rates of distinct effectiveness and effectiveness were respectively 0% and 30.30%, and the total effective rate was 30.30%.The comparison of the above statistics between two groups had a significant difference ($P = 0.0001$) (Table 4).

Adverse effects

In group A, there were 5 patients who suffered from adverse drug reactions and the incidence was 6.94%. The adverse drug reactions mainly included nausea, rash, chest discomfort, fever, epigastric comfort, diarrhea and poor taste, and most of them were mild or moderate. None of the patients withdrew because of adverse drug reactions. In group B, adverse effects occurred in 7 patients and the incidence was 9.72%. The manifestations were similar to those in group A and 1 patient withdrew because of weakness, anorexia, epigastric discomfort after taking drugs.

DISCUSSION

Hepatic fibrosis, a precuror of cirrhosis, is a consequence of sever liver damage that occurred in many patients with chronic liver disease, and involves the abnormal accumulation of extracellular matrix[3,4,11,12]. Liver fibrosis represents a major worldwide healthcare burden. Current therapy is limited to removing the causal agent. This approach has been successful in some diseases, particularly in haemochromatosis and chronic viral hepatitis[9,10,17,28]. However, for many patients treatment was not possible, while other patients presenting to medical attention were at an advanced stage of fibrosis[8,9]. There is therefore a great need for novel therapies for liver fibrosis. Tremendous insights into the understanding of hepatic fibrosis have taken place over the past ten years. Foremost among these is the recognition that hepatic stellate cells (formerly known as lipocytes, Ito cells, or fat-storing cells) play a central role based on their ability to undergo activation following liver injury of any cause[11,15,16,29]. Hepatic stellate cells have been recognised to be responsible for most of the excess extracellular matrix observed in chronic liver fibrosis. The detailed understanding of hepatic stellate cell biology has allowed the rational design of novel antifibrotic therapies[29]. Effective therapy for hepatic fibrogenesis would probably also be multifactorial, based on the basic mechanisms underlying the fibrogenic process[13,14,21-23].

At present, it is considered that treatment of hepatic fibrosis and antihepatic fibrosis are two different concepts and antifibrotic drugs should act on various parts of the genesis and development of hepatic fibrosis. Firstly, as for etiological treatment, oxymatrine could effectively treat chronic viral hepatitis and promote the serum markers of hepatitis B virus (HBV) and hepatitis C virus (HCV) in chronic hepatitis B and C to convert to negative and reduce serum level of ALT[6,7]. Secondly, oxymatrine could inhibit the proliferation of hepatic stellate cells (HSC) at the concentrations of 0.5-16 μg/mL *in vitro*. In addition, oxygen stress and lipid peroxidation are important mechanisms responsible for hepatic injury and hepatic stellate cell activation. Therefore, inhibition of lipid peroxidation is an essential strategy of antihepatic fibrosis[12-16]. By establishing D-galactosamine-induced rat liver fibrosis model, we observed the effect of oxymatrine on serum and tissue biochemical indexes, content of liver hydroxyline, expression of TGFβ1 mRNA and changes of tissue pathology, the results showed oxymatrine had prophylactic and therapeutic effects on D-galactosamine induced rat liver fibrosis. This was partly by protecting hepatocytes and suppressing fibrosis accumulation through anti-lipoperoxidation[10]. In present study, We found that the scores of hepatic fibrosis after therapy in group A were 4.72±5.63, much smaller than 6.76±6.67 before therapy, and the scores in group B after therapy increased significantly. There was an obvious difference between two groups. The scores of histological inflammatory activity in group A decreased from 46.08±3.84 before treatment to 4.00±2.97 after therapy, and the scores in group B after therapy did not decrease obviously. There was an obvious difference between two groups both in improvement of histopathology and in improvement of noninvasive indexes such as clinical manifestations, serum markers of hepatic fibrosis[24-27]. Associated indexes of liver function and imaging detection indicated that oxymatrine was an ideal drug of antihepatic fibrosis. It is valuable to pay more attentions to the basic and clinical research of oxymatrine in order to explore the accurate mechanisms of its effect on antihepatic fibrosis.

REFERENCES

1 **Arthur MJ.** Pathogenesis, experimental manipulation and treatment of liver fibrosis. *Exp Nephrol* 1995; **3**: 90-95
2 **Brenner DA,** Waterboer T, Choi SK, Lindquist JN, Stefanovic B, Burchardt E, Yamauchi M, Gillan A, Rippe RA. New aspects of hepatic fibrosis. *J Hepatol* 2000; **32**(Suppl): 32-38
3 **Albanis E,** Friedman SL. Hepatic fibrosis. Pathogenesis and principles of therapy. *Clin Liver Dis* 2001; **5**: 315-334
4 **Friedman SL.** Molecular mechanisms of hepatic fibrosis and principles of therapy. *J Gastroenterol* 1997; **32**: 424-430
5 **Rockey DC.** The cell and molecular biology of hepatic fibrogenesis. Clinical and therapeutic implications. *Clin Liver Dis* 2000; **4**: 319-355
6 **Li J,** Li C, Zeng M. Preliminary study on therapeutic effect of oxymatrine in treating patients with chronic hepatitis C. *Zhongguo Zhongxiyi Jiehe Zazhi* 1998; **18**: 227-229
7 **Yu YY,** Wang QH, Zhu LM, Zhang QB, Xu DZ, Guo YB, Wang CQ, Guo SH, Zhou XQ, Zhang LX. A clinical research on oxymatrine for the treatment of chronic hepatitis B. *Zhonghua Ganzangbing Zazhi* 2002; **10**: 280-281
8 **Chen Y,** Li J, Zeng M, Lu L, Qu D, Mao Y, Fan Z, Hua J. The inhibitory effect of oxymatrine on hepatitis C virus *in vitro*. *Zhonghua Ganzangbing Zazhi* 2001; **9**(Suppl): 12-14
9 **Yang W,** Zeng M, Fan Z, Mao Y, Song Y, Jia Y, Lu L, Chen CW, Peng YS, Zhu HY. Prophylactic and therapeutic effect of oxymatrine on D-galactosamine-induced rat liver fibrosis. *Zhonghua Ganzangbing Zazhi* 2002; **10**: 193-196
10 **Schuppan D,** Porov Y. Hepatic fibrosis: From bench to bedside. *J Gastroenterol Hepatol* 2002; **17**(Suppl 3): S300-S305
11 **Li D,** Friedman SL. Liver fibrogenesis and the role of hepatic stellate cells: new insights and prospects for therapy. *J Gastroenterol Hepatol* 1999; **14**: 618-633
12 **Poli G.** Pathogenesis of liver fibrosis: role of oxidative stress. *Mol Aspects Med* 2000; **21**: 49-98

13 **Poli G,** Parola M. Oxidative damage and fibrogenesis. *Free Radic Biol Med* 1997; **22**: 287-305
14 **Bjorneboe A,** Bjorneboe GE. Antioxidant status and alcohol-related diseases. *Alcohol Alcohol* 1993; **28**: 111-116
15 **Tsukamoto H,** Rippe R, Niemela O, Lin M. Roles of oxidative stress in activation of Kupffer and Ito cells in liver fibrogenesis. *J Gastroenterol Hepatol* 1995; **10**(Suppl 1): S50-53
16 **Kim KY,** Choi I, Kim SS. Progression of hepatic stellate cell activation is associated with the level of oxidative stress rather than cytokines during CCl4-induced fibrogenesis. *Mol Cells* 2000; **10**: 289-300
17 **Dong Y,** Xi H, Yu Y, Wang Q, Jiang K, Li L. Effects of oxymatrine on the serum levels of T helper cell 1 and 2 cytokines and the expression of the S gene in hepatitis B virus S gene transgenic mice: a study on the anti-hepatitis B virus mechanism of oxymatrine. *J Gastroenterol Hepatol* 2002; **17**: 1299-1306
18 **Xiang X,** Wang G, Cai X, Li Y. Effect of oxymatrine on murine fulminant hepatitis and hepatocyte apoptosis. *Chin Med J* 2002; **115**: 593-596
19 **Song J,** Wang LL, Zhu L, Zhong HM, Yao P. Effects of oxymatrine on procollagen metabolism and its gene expression in experimental fibrotic rats. *Zhonghua Ganzangbing Zazhi* 2003; **11**: 697
20 **Liu J,** Manheimer E, Tsutani K, Gluud C. Medicinal herbs for hepatitis C virus infection: a Cochrane hepatobiliary systematic review of randomized trials. *Am J Gastroenterol* 2003; **98**: 538-544
21 **Coutinho EM,** Barros AF, Barbosa A Jr, Oliveira SA, Silva LM, Araujo RE, Andrade ZA. Host nutritional status as a contributory factor to the remodeling of schistosomal hepatic fibrosis. *Mem Inst Oswaldo Cruz* 2003; **98**: 919-925
22 **Hui JM,** Sud A, Farrell GC, Bandara P, Byth K, Kench JG, McCaughan GW, George J. Insulin resistance is associated with chronic hepatitis C and virus infection fibrosis progression. *Gastroenterology* 2003; **125**: 1695-1704
23 **Perrillo RP.** Management of the patient with hepatitis B virus-related cirrhosis. *J Hepatol* 2003; **39**(Suppl 1): S177-180
24 **Kim CW,** Yoon SK, Jo BS, Shin JY, Jang JW, Choi JY, Han NI, Lee CD, Chung KW, Sun HS. Prediction of hepatic fibrosis using serum hyaluronic acid in patients with chronic liver disease. *Korean J Gastroenterol* 2003; **42**: 510-518
25 **Tang M,** Potter JJ, Mezey E. Activation of the human alpha1 (I) collagen promoter by leptin is not mediated by transforming growth factor beta responsive elements. *Biochem Biophys Res Commun* 2003; **312**: 629-633
26 **Xu GG,** Luo CY, Wu SM, Wang CL. The relationship between staging of hepatic fibrosis and the levels of serum biochemistry. *Hepatobiliary Pancreat Dis Int* 2002; **1**: 246-248
27 **Xie SB,** Yao JL, Zheng SS, Yao CL, Zheng RQ. The levels of serum fibrosis marks and morphometric quantitative measurement of hepatic fibrosis. *Hepatobiliary Pancreat Dis Int* 2002; **1**: 202-206
28 **Xie Y,** Zhao H, Dai WS, Xu DZ. HBV DNA level and antigen concentration in evaluating liver damage of patients with chronic hepatitisB. *Hepatobiliary Pancreat Dis Int* 2003; **2**: 418-422
29 **Oakley F,** Trim N, Constandinou CM, Ye W, Gray AM, Frantz G, Hillan K, Kendall T, Benyon RC, Mann DA, Iredale JP. Hepatocytes express nerve growth factor during liver injury: evidence for paracrine regulation of hepatic stellate cell apoptosis. *Am J Pathol* 2003; **163**: 1849-1858
30 **Kondou H,** Mushiake S, Etani Y, Miyoshi Y, Michigami T, Ozono K. A blocking peptide for transforming growth factor-beta1 activation prevents hepatic fibrosis *in vivo*. *J Hepatol* 2003; **39**: 742-748
31 **Dodig M,** Mullen KD. New mechanism of selective killing of activated hepatic stellate cells. *Hepatology* 2003; **38**: 1051-1053

Edited by Wang XL and Xu FM

PO Box 2345, Beijing 100023, China
Fax: +86-10-85381893
E-mail: wjg@wjgnet.com www.wjgnet.com

World J Gastroenterol 2004;10(22):3274-3277
World Journal of Gastroenterology
 ISSN 1007-9327

Neither gastric topological distribution nor principle virulence genes of *Helicobacter pylori* contributes to clinical outcomes

Yan Wing Ho, Khek Yu Ho, Felipe Ascencio, Bow Ho

Yan Wing Ho, Bow Ho, Department of Microbiology, Faculty of Medicine, National University of Singapore, Singapore
Khek Yu Ho, Department of Medicine, Faculty of Medicine, National University of Singapore, Singapore
Felipe Ascencio, Departamento de Patologia Marina, Centro de Investigaciones Biologicas del Noroeste (CIBNOR), La Paz, Mexico
Yan Wing Ho, is a National University of Singapore Research Scholar
Supported by NMRC Grant , No. 0415/2000, R-182-000-037-213
Correspondence to: Bow Ho, Department of Microbiology, Faculty of Medicine, National University of Singapore, 5 Science Drive 2, Singapore 117597, Republic of Singapore. michob@nus.edu.sg
Telephone: +65-68743672 **Fax:** +65-67766872
Received: 2004-02-27 **Accepted:** 2004-04-29

Abstract

AIM: Studies on *Helicobacter pylori* (*H pylori*) and gastroduodenal diseases have focused mainly on the distal sites of the stomach, but relationship with the gastric cardia is lacking. The aim of this study is to determine if the gastric topology and genotypic distribution of *H pylori* were associated with different upper gastrointestinal pathologies in a multi-ethnic Asian population.

METHODS: Gastric biopsies from the cardia, body/corpus and antrum were endoscoped from a total of 155 patients with dyspepsia and/or reflux symptoms, with informed consent. *H pylori* isolates obtained were tested for the presence of *26kDa*, *ureC*, *cagA*, *vacA*, *iceA1*, *iceA2* and *babA2* genes using PCR while DNA fingerprints were generated using random amplification polymorphic DNA (RAPD).

RESULTS: *H pylori* was present in 51/155 (33%) of patients studied. Of these, 16, 15 and 20 were isolated from patients with peptic ulcer diseases, gastroesophageal reflux diseases and non-ulcer dyspepsia, respectively. Of the *H pylori* positive patients, 75% (38/51) had *H pylori* in all three gastric sites. The prevalence of various genes in the *H pylori* isolates was shown to be similar irrespective of their colonization sites as well as among the same site of different patients. The RAPD profiles of *H pylori* isolates from different gastric sites were highly similar among intra-patients but varied greatly between different patients.

CONCLUSION: Topographic colonization of *H pylori* and the virulence genes harboured by these isolates have no direct bearing to the clinical state of the patients. In multi-ethnic Singapore, the stomach of each patient is colonized by a predominant strain of *H pylori*, irrespective of the clinical diagnosis.

Ho YW, Ho KY, Ascencio F, Ho B. Neither gastric topological distribution nor principle virulence genes of *Helicobacter pylori* contributes to clinical outcomes. *World J Gastroenterol* 2004; 10(22): 3274-3277
http://www.wjgnet.com/1007-9327/10/3274.asp

INTRODUCTION

Helicobacter pylori (*H pylori*) is a common gastric pathogen that has infected more than 50% of the world's population[1]. It is the major aetiological agent of chronic active gastritis and is generally accepted as being the primary cause of peptic ulcer disease and a carcinogenic factor for gastric cancer (GC)[2]. However, only a minority of *H pylori* infected subjects develops these diseases. This has led to the suggestion that clinical sequelae that develop may be dependent upon differentially expressed bacterial determinants, e.g., bacterial virulence genes: *cagA*, *vacA*, *iceA1*, *iceA2*, *babA2*[3-5]. In many parts of Asia, the prevalence of *cagA* and *vacA* strains is high regardless of the presence or absence of disease states[6]. This limits the usefulness of using these genes as markers to predict clinical outcome. Instead, other factors like host susceptibility as well as specific interactions between a particular strain and its host that occur during decades of coexistence might have contributed to an increased risk of developing certain clinical manifestations[7].

Our current knowledge on the epidemiology of the organism is predominantly based on data obtained from serologic studies. It has also been reported that a single strain of *H pylori* predominates the gastric antrum and corpus of infected patients in Singapore[8]. However, there is a need to study whether the topographic distribution of *H pylori* genotypes in various gastric sites in patients of different ethnic origins affects the disease state. Being an Asian country with a multi-ethnic population, Singapore is suitable for this investigation.

MATERIALS AND METHODS

Patients

Consecutive patients with dyspepsia and/or reflux symptoms presenting for upper gastrointestinal endoscopic examination to one of the authors (KYH) and who have not been exposed to antibiotics, proton pump inhibitors (PPI) or bismuth compounds within the past four week were invited to participate in the study. Patients who previously had been treated for *H pylori* infection, patients who refused gastric biopsies, patients who were unable to give consent because of age or mental illness and patients in whom gastric and oesophageal biopsies were contraindicated (*e.g.*, coagulopathy, oesophageal varices and severe co-morbidity), subjects who were pregnant and those who were <18 years old, were excluded. Informed consent was obtained from each patient.

A total of 155 patients were included in the study. The patient population comprised 122 (79%) Chinese, 17 (11%) Indians, 8 (5%) Malays and 8 (5%) subjects of other ethnicities. Of these, 95 (61%) were males and 60 (39%) females. The mean age was 48.4±15.5 (range, 24-88) years. Based on clinical history and endoscopic examination, patients were classified into the following groups: gastroesophageal reflux disease (GERD) (n = 50), peptic ulcer disease (PUD) (n = 36) and non-ulcer dyspepsia (NUD) (n = 69). GERD was defined as the presence of predominant symptoms of reflux, e.g., heartburn, acid regurgitation and/or the presence of any length of mucosal break in the oesophagus due to gastroesophageal reflux. NUD was defined as patients with neither a history of GERD nor endoscopic evidence of organic pathologies. PUD refers to patients who were either

Table 1 Primer sequences of genes of interest

Region	Primer	Nucleotide sequence (5'→3')	PCR product (bp)	Reference
26kDa	26kDa-F	TGGCGTGTCTATTGACAGCGAGC	298	9
	26kDa-R	CCTGCTGGGCATACTTCACCAAG		
ureC	*ureC*-F	AAGCTTTTAGGGGTGTTAGGGGTTT	294	10
	ureC-R	AAGCTTACTTTCTAACACTAACGC		
cagA	*cagA*-F	AATACACCAACGCCTCCAAG	400	11
	cagA-R	TTGTTGCCGCTTTTGCTCTC		
vacA	*vacA*-F	GCTTCTCTTACCACCAATGC	1160	12
	vacA-R	TGTCAGGGTTGTTCACCATG		
	m2-R	CATAACTAGCGCCTTGCAC		
iceA1	*iceA1*-F	GTGTTTTTAACCAAAGTATC	246	5
	iceA1-R	CTATAGCCAGTCTCTTTGCA		5
iceA2	*iceA2*-F	GTTGGGTDTDTCACAATTTAT	229/334	5
	iceA2-R	TTGCCCTATTTTCTAGTAGGT		5
babA2	*babA2*-F	AATCCAAAAAGGAGAAAAAGTATGAAA	831	4
	babA2-R	TGTTAGTGATTTCGGTGTAGGACA		4

F: forward primer R: reverse primer.

diagnosed upon endoscopy as suffering from gastric ulcers (ulcers at the corpus) or duodenal ulcers (ulcers at the antrum). A total of 465 biopsy specimens were obtained from the 155 patients.

Endoscopy

After an overnight or six hour fast, upper gastrointestinal endoscopy was performed according to standard technique. From each patient, one biopsy specimens was obtained using sterilized standard biopsy forceps from each of the three sites of the stomach: the cardia just below the z-line, the middle gastric corpus and the antrum within 2 cm of the pylorus, in that order. The biopsy forceps were thoroughly cleaned with alcohol swaps between biopsies to avoid contamination between specimens. The biopsies were transported in 0.85% sterile saline to the microbiological laboratory for processing within 6 h.

H pylori culture

Each biopsy specimen was homogenised aseptically in 500 μL of Brain Heart Infusion Broth (BHI, Oxoid Ltd., Basingstoke, UK) enriched with 4 g/L yeast extract (Oxoid Ltd., Basingstoke, UK). Approximately 100 μL homogenised specimens in BHI broth were inoculated onto *H pylori* selective chocolate blood agar plates and non-selective chocolate blood agar plates respectively. The selective blood chocolate agar was supplemented with 3 mg/mL vancomycin, 5 mg/mL trimethoprim, 10 mg/mL nalidixic acid and 2 mg/mL amphotericin B. All the antibiotics were from Sigma-Aldrich Chemie, Steinheim, Germany. The plates were incubated at 37 ℃ for up to 14 d in an incubator (Forma Scientific, USA) containing 50 mL/L CO_2.

Aliquots of 50 μL of BHI-biospy suspension were each inoculated into catalase reagent, oxidase reagent and 20 g/L urea solution for their respective testing. An isolate was identified as *H pylori* if minute (-1 mm in diameter) rounded translucent colonies with gram-negative S-shaped motile cells that exhibited positive catalase, oxidase and urease activities. For this study, a patient was considered positive for *H pylori* if the organism was isolated from any of the three gastric sites.

Genotyping of H pylori

The DNA of each 3-d old *H pylori* culture was extracted according to the method as described by Hua *et al*.[8]. A 50 ng working stock of DNA was used to amplify 26*kDa*[9], *ureC*[10], *cagA*[11], *vacA*[12], *iceA1*[5], *iceA2*[5] and *babA2*[4] genes according to the protocol as described by Zheng *et al*.[6] using the specific forward and reverse primers for each of the corresponding genes (Table 1). The DNA fingerprint of the *H pylori* was obtained by PCR using the universal primer, 5'- AACGCGCAAC-3' and amplified according to protocol as described by Hua *et al*.[13]. The PCR products obtained were electrophoresed and the ethidium bromide stained gels[13] were then photographed with filtered UV illumination on Chemi Genius^2 (SynGene, Cambridge, UK).

Statistical Calculation

The significance of the results obtained was calculated using SPSS v.10 for Windows (SPSS, Chicago IL) to determine the Pearson chi-square whereby a P value <0.05 was considered to indicate statistical significance.

RESULTS

H pylori isolates in various clinical groups

Of the 155 patients studied, 51 (33%) were found to harbour *H pylori* in at least one of the 3 gastric biopsy sites. In all, 43, 47 and 44 isolates were obtained from gastric antrum, corpus and cardia respectively, giving a total of 134 isolates. *H pylori* was present in 16/36 (44%) PUD patients as compared with 15/50 (30%) GERD patients (P = 0.169) and 20/69 (29%) NUD patients (P = 0.113) (Table 2).

Table 2 Relationship between *H pylori* status and disease states

Groups	No. of patients	No. of biopsies	No. of *H pylori* (+)	*P*
PUD	36	108	16 (44%)	-
GERD	50	150	15 (30%)	0.169
NUD	69	207	20 (29%)	0.113

PUD, peptic ulcer disease; GERD, gastroesophageal reflux disease; NUD, non-ulcer dyspepsia. All test values were calculated with respect to PUD; P<0.05 indicates statistical significance.

Relationship between topographic distribution of H pylori isolates and clinical outcomes

Of the 51 *H pylori* positive patients, 38 (75%) showed the presence of *H pylori* in all the three gastric sites while 1 (1%), 2 (4%) and 4 (8%) had *H pylori* isolated from antrum & corpus, antrum & cardia, and corpus & cardia, respectively. *H pylori*

was isolated from a single site of the stomach in 6 (12%) patients, among which 2 isolates were from the antrum and 4 were from the corpus. This topographical pattern of *H pylori* colonization was observed in all the patients irrespective of the underlying clinical diagnosis.

Relationship between topographic distribution of H pylori genes of interest and clinical outcomes

All the *H pylori* isolates possessed the 26*kDa* gene and the *ureC* genes. The prevalence of virulence genes of interest were present in equal ratios in all the *H pylori* isolates obtained from all the 3 different gastric biopsy sites: 74-81% for *cagA* and 80-86% for *vacA*; 53-59% for *iceA*1 and 36-42% for *babA*2 regardless of the underlying clinical diagnosis. However, the *iceA*2 gene was present less frequently, at 20-26% of the *H pylori* isolates. It is noted that the difference in gene frequency between the various sites was also not statistically significant (Table 3).

Similar observation was noted with respect to the distribution of virulence genes of *H pylori* isolated from the same site among the different disease groups. The prevalence for each virulence gene within the same site was highly similar. No significant association of the virulence gene was found to be associated with a particular biopsied site, regardless of the disease state, with the exception of *cagA* in isolates from the corpus of the stomach of GERD patients (Table 4).

Table 3 Anatomical location of the 134 *H pylori* isolates and their virulence genes

	Antrum (%) *n* = 43	Body / Corpus (%) *n* = 47	Cardia(%) *n* = 44
Clinical Diagnosis			
PUD	12 (33)	15 (42)	12 (33)
GERD	13 (26)	15 (30)	14 (28)
NUD	18 (25)	17 (24)	18 (26)
Genotype			
26kDa	43 (100)	47 (100)	44 (100)
ureC	43 (100)	47 (100)	44 (100)
cagA	35 (81)	35 (74)	33 (75)
vacA	37 (86)	38 (81)	35 (80)
*iceA*1	25 (58)	25 (53)	26 (59)
*iceA*2	10 (23)	12 (26)	9 (20)
*babA*2	18 (42)	20 (38)	16 (36)

PUD, peptic ulcer disease; GERD, gastroesophageal reflux disease; NUD, non-ulcer dyspepsia. All test values were calculated with respect to gastric antrum and none were significant.

Relationship between topographic distribution of H pylori strain based on RAPD fingerprinting and clinical outcomes

For comparison, differences in 2 or more bands of the RAPD profile are considered different while variations in band intensity were not taken into account. On this basis, the RAPD profiles of all the *H pylori* strains isolated showed an overall similarity in profiles within individual patients, with minor differences such as the presence or absence of a single band. However, distinct differences in the DNA profiles were observed between patients (Figure 1). In this study, no comparison could be made in 6 patients since *H pylori* was isolated from only one site of the stomach in these patients.

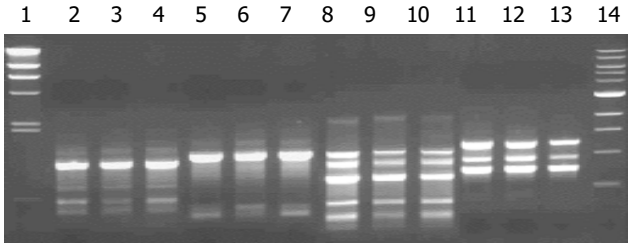

Figure 1 PCR-based RAPD patterns of *H pylori* isolated from 3 gastric sites of 4 individual patients. Lane1: λHindIII M marker, Lane 14: 1 kb M marker; Lane 2-4, 5-7, 8-10, 11-13 for patients 1, 2, 3 and 4 respectively. A: antrum; B: body; C: cardia.

DISCUSSION

It is noted that 50% of the world's population are infected with *H pylori* but only a small proportion manifest different gastroduodenal diseases[14]. One of the factors contributing to this phenomenon could be the patchy distribution of *H pylori* in different gastric sites of the stomach As most of the earlier studies focused on *H pylori* isolated from the distal sites of the stomach[8,15], the present study shows that *H pylori* isolates obtained from all the 3 gastric sites, namely cardia, corpus and antrum, in 38/51 (75%) *H pylori* patients were similar genotypically. Care was taken in cleaning and disinfecting the biopsy forceps between biopsies to avoid contamination between specimens. The results imply that *H pylori* colonises the entire stomach instead of a predominant site in three quarters of our *H pylori* positive patients, irrespective of the underlying clinical diagnosis. The finding suggests that the site of *H pylori* colonization or topographic distribution does not contribute significantly to the outcome of the infection.

Table 4 Distribution of virulence genes of 134 *H pylori* isolates from the same anatomical site of different patient groups

	Isolates	*26kDa* (%)	*ureC* (%)	*cagA* (%)	*vacA* (%)	*iceA1*(%)	*iceA2*(%)	*babA2*(%)
Antrum								
PUD	12	12 (100)	12 (100)	9 (75)	10 (83)	6 (50)	4 (33)	6 (50)
GERD	13	13 (100)	13 (100)	11 (85)	11 (85)	7 (54)	2 (15)	6 (46)
NUD	18	18 (100)	18 (100)	15 (83)	16 (89)	12 (67)	4 (22)	6 (33)
Body / Corpus								
PUD	15	15 (100)	15 (100)	9 (60)	10 (67)	6 (40)	5 (33)	7 (47)
GERD	15	15 (100)	15 (100)	14 (93)[1]	14 (93)	8 (53)	3 (20)	8 (53)
NUD	17	17 (100)	17 (100)	12 (71)	14 (82)	11 (65)	4 (24)	5 (29)
Cardia								
PUD	12	12 (100)	12 (100)	9 (75)	11 (92)	5 (42)	2 (17)	3 (25)
GERD	14	14 (100)	14 (100)	12 (86)	11 (79)	8 (57)	2 (14)	7 (50)
NUD	18	18 (100)	18 (100)	12 (67)	13 (72)	13 (72)	5 (28)	7 (39)

PUD, peptic ulcer disease; GERD, gastroesophageal reflux disease; NUD, non-ulcer dyspepsia. All test values were calculated with respect to PUD. [1]Indicates statistical significance ($P = 0.031$).

While studies in Europe suggested that virulence genes, e.g., *cagA* and *vacA* affect the clinical outcome of *H pylori* infection[3,5], the present study confirms previous studies carried out in Asian countries[6,15] that showed a high prevalence of *cagA* and *vacA* genes regardless of the clinical outcome. This study comprised Singapore patients of various ethnicities (Chinese, Malays, Indians and other races), also shows that each of the virulence genes, i.e., *cagA*, *vacA*, *iceA1*, *iceA2* and *babA2* were equally distributed in *H pylori* isolates obtained from all the three anatomical sites studied regardless of the disease states. Similarly, comparisons of these genes from the same anatomical site of different patients showed no significant presence, except for *cagA* in the corpus of GERD isolates. However, it is important to point out that the number of isolates obtained from each is relatively low ($n \leqslant 18$), regardless of the disease state. As such, the significant presence of *cagA* in the corpus of GERD patients needs further analysis with a larger pool of samples to confirm conclusively its contribution to the onset of GERD. The data therefore suggest that virulence genes and their topographic distribution do not contribute to the clinical status, at least in the Singapore population. This study supports the earlier reports[15-17] that identifying such virulence genes in order to predict clinical outcome may be of limited value in Asian *H pylori* isolates.

The finding that RAPD profiles of the *H pylori* isolates were similar from 3 different anatomical sites (antrum, corpus & cardia) of each patient further strengthens our earlier study[9] where isolates from 2 sites (antrum & corpus) were identical. This finding is complemented by the similar status of presence of various virulence genes in these isolates obtained from the respective patients. As such, the isolation of a strain from any gastric site in a single patient could be taken as representative of *H pylori* infection present in the *H pylori* infected gastric environment.

This study, which included consecutive patients with dyspepsia and/or reflux symptoms showed a lower frequency of PUD as compared with that of GERD. *H pylori* was found in only 44% of patients with PUD. This seems to run counter to the generally held view that *H pylori* occurs frequently in Asians patients with PUD[13]. However, this finding is supported by an earlier study from the same unit[18] showing the frequency of reflux oesophagitis was increasing while that of duodenal ulceration was decreasing in Singapore. The high frequency of patients with GERD in this study also relates to the fact that the endoscopist (KYH) sees most of the GERD patients in the hospital. The decreasing frequency of *H pylori* associated peptic ulcers was reported to be attributed to the increasing proportion of ulcers due to NSAID use[19].

In summary, the present study shows that in Singapore, the topographic colonization of *H pylori* and their virulence genes within the host stomach do not play a significant role in the clinical manifestations of *H pylori* infection. This study also demonstrates that in Singapore, which has a multiethnic Asian population, the stomach of each patient with dyspeptic and/or reflux symptoms is colonized by a single predominant strain of *H pylori*, irrespective of the site of isolation and the clinical diagnosis of the patient. We suggest that the pathogenesis of *H pylori* induced gastroduodenal diseases is due to a more complex mechanism possibly involving host-pathogen interaction, environmental and dietary factors.

REFERENCES

1 **Everhart JE.** Recent developments in the epidemiology of *Helicobacter pylori*. *Gastroenterol Clin North Am* 2000; **29**: 559-578
2 **Go MF**. Review article: natural history and epidemiology of *Helicobacter pylori* infection. *Aliment Pharmacol Ther* 2002; **16**(Suppl 1): 3-15
3 **Arents NLA,** Van Zwet AA, Thijs JC, Kooistra-Samid AMD, van Slochteren R, Degener JE, Kleibeuker JH, van Doorn LJ. The importance of *vac*A, *cag*A and *ice*A genotypes of *Helicobacter pylori* infection in peptic ulcer disease and gastro-esophageal reflux disease. *Am J Gastroenterol* 2001; **96**: 2603-2608
4 **Gerhard M,** Lehn N, Neumayer N, Boren T, Rad R, Schepp W, Miehlke S, Classen M, Prinz C. Clinical relevance of the *Helicobacter pylori* gene for blood-group antigen-binding adhesin. *Proc Natl Acad Sci U S A* 1999; **96**: 12778-12783
5 **van Doorn LJ,** Figueiredo C, Sanna R, Plaiser A, Schneeberger P, DeBoer W, Quint W. Clinical relevance of the *cag*A, *vac*A and *ice*A status of *Helicobacter pylori*. *Gastroenterology* 1998; **115**: 58-66
6 **Zheng PY,** Hua J, Yeoh KG, Ho B. Association of peptic ulcer with increased expression of Lewis antigen but not *cag*A, *ice*A and *vac*A in *Helicobacter pylori* isolates in an Asian population. *Gut* 2000; **47**: 18-22
7 **Peek RM Jr.** The biological impact of *Helicobacter pylori* colonization. *Semin Gastreointest Dis* 2001; **12**: 151-166
8 **Hua J,** Ling KL, Ng HS, Ho B. Isolation of a single strain of *Helicobacter pylori* from the antrum and body of individual patients. *Eur J Gastroenterol Hepatol* 2000; **12**: 1129-1134
9 **Hammar M,** Tyszkiewicz T, Wadstrom T, O'Toole PW. Rapid detection of *Helicobacter pylori* in gastric biopsy material by polymerase chain reaction. *J Clin Microbiol* 1992; **30**: 54-58
10 **Labigne A,** Cussac V, Courcoux P. Shuttle cloning and nucleotide sequence of *Helicobacter pylori* genes responsible for urease activity. *J Bacteriol* 1991; **173**: 1920-1931
11 **Lage AP,** Godfroid E, Fauconnier A, Burette A, Butzler JP, Bollen A, Glupczynski Y. Diagnosis of *Helicobacter pylori* infection by PCR: comparison with other invasive techniques and detection of *cag*A found in gastric biopsy specimens. *J Clin Microbiol* 1995; **33**: 2752-2756
12 **Xiang Z,** Censini S, Bayeli PF, Telford JL, Figura N, Rappuoli R, Covacci A. Analysis of expression of CagA and VacA virulence factors in 43 strains of *Helicobacter pylori* reveals that clinical isolates can be divided into 2 major types and that CagA is not necessary for expression of the vacuolating cytotoxin. *Infect Immun* 1995; **63**: 94-98
13 **Hua J,** Ho B. Is the coccoid form of *Helicobacter pylori* viable? *Microbios* 1996; **87**: 103-112
14 **Hocker M,** Hohenberger P. *Helicobacter pylori* virulence factors-1 part of a big picture. *Lancet* 2003; **362**: 1231-1233
15 **Kim SY,** Woo CW, Lee YM, Son BR, Kim JW, Chae HB, Youn SJ, Park SM. Genotyping *cagA*, *vacA* subtype, *iceA1*, *babA* of *Helicobacter pylori* isolates from Korean patients, and their association with gastroduodenal diseases. *J Korean Med Sci* 2001; **16**: 579-584
16 **Kim JM,** Kim JS, Jung HC, Song IS, Kim CY. Virulence factors of *Helicobacter pylori* in Korean isolates do not influence proinflammatory cytokine gene expression and apoptosis in human gastric epithelial cells, nor do these factors influence the clinical outcome. *J Gastroenterol* 2000; **35**: 898-906
17 **Park SM,** Park J, Kim JG, Cho HD, Cho JH, Lee DH, Cha YJ. Infection with *Helicobacter pylori* expressing the *cagA* gene is not assocatied with an increase risk of developing peptic ulcer disease in Korean patients. *Scand J Gastroenterol* 1998; **33**: 923-927
18 **Ho KY,** Gwee KA, Yeoh KG, Lim SG, Kang JY. Increasing frequency of reflux esophagitis in Asian patients. *Gastroenterology* 2000; **118**: A1246
19 **Ong TZ**, Ho KY. The increasing frequency of non-*Helicobacter pylori* peptic ulcer disease in an Asian country is related to NSAID use. *Gastrointestinal Endoscopy* 2003; **57**: AB153

Edited by Pan BR and Zhang JZ **Proofread by** Xu FM

PO Box 2345, Beijing 100023, China
Fax: +86-10-85381893
E-mail: wjg@wjgnet.com www.wjgnet.com

World J Gastroenterol 2004;10(22):3278-3283
World Journal of Gastroenterology
 ISSN 1007-9327

A novel genetic polymorphism of inducible nitric oxide synthase is associated with an increased risk of gastric cancer

Jing Shen, Run-Tian Wang, Li-Wei Wang, Yao-Chu Xu, Xin-Ru Wang

Jing Shen, Yao-Chu Xu, Xin-Ru Wang, Department of Epidemiology & Biostatistics, School of Public Health, Nanjing Medical University, Nanjing 210029, Jiangsu Province, China
Run-Tian Wang, Health Science Center, Peking University, Beijing 100083, China
Li-Wei Wang, Yangzhong Cancer Research Institute, Yangzhong 212200, Jiangsu Province, China
Supported by Grants From the National Natural Science Foundation of China (30170827 to Jing. Shen and 30070671 to Run-Tian Wang)
Correspondence to: Jing Shen, Department of Environmental Health Sciences, Mailman School of Public Health, Columbia University, 701 West 168th St (Room 505), New York, NY 10032, USA. js2182@columbia.edu
Telephone: +212-305-8158 **Fax:** +212-305-5328
Received: 2003-07-12 **Accepted:** 2003-10-12

Abstract

AIM: Inducible nitric oxide synthase (iNOS) plays a central role in the pathway of reactive oxygen and nitrogen species metabolism when *Helicobacter pylori* (*H pylori*) infection occurs in humans. iNOS Ser^{608}Leu allele, a novel genetic polymorphism (C/T) occurring within exon 16 of the iNOS reductase domain, may have a dramatic effect on the enzymatic activity. The aim of this study was to determine whether iNOS C/T polymorphism was associated with increased susceptibility to gastric cancer.

METHODS: We conducted a population based case-control study in a high gastric cancer incidence area, Yangzhong, China. Questionnaires from 93 patients with intestinal type gastric cancer (IGC), 50 with gastric cardia cancer (GCC) and 246 healthy controls were obtained between 1997 and 1998, and iNOS genotyping was carried out. Odds ratios (ORs), interaction index (γ), and 95% confidence intervals for the combined effects of iNOS genotype and *H pylori* infection, cigarette smoking or alcohol drinking were estimated.

RESULTS: The frequency of (CT+TT) genotypes was higher in cases than in control group (24.48% *vs* 23.17%), but the difference was not statistically significant. After adjusting for age and gender, past cigarette smokers with (CT+TT) genotypes had a significantly increased risk of IGC (OR = 3.62, 95% CI: 1.23-10.64), while past alcohol drinkers with (CT+TT) genotypes had a significantly increased risk of GCC (OR = 3.33, 95% CI: 1.14-9.67). *H pylori* CagA negative subjects with (CT+TT) genotypes had a significantly increased risk of both IGC and GCC (OR = 2.19 and 3.52, respectively).

CONCLUSION: iNOS Ser^{608}Leu allele may be a potential determinant of susceptibility to cigarette -alcohol induced gastric cancer, but larger studies are needed to confirm the observations.

Shen J, Wang RT, Wang LW, Xu YC, Wang XR. A novel genetic polymorphism of inducible nitric oxide synthase is associated with an increased risk of gastric cancer. *World J Gastroenterol* 2004; 10(22): 3278-3283
http://www.wjgnet.com/1007-9327/10/3278.asp

INTRODUCTION

On a global scale, gastric cancer remains the world's second most common malignancy. There is a substantial international variation in gastric cancer incidence with the highest rates reported from China, Japan and other Eastern Asian countries[1]. The discovery of *Helicobacter pylori* (*H pylori*) in the early 1980 s has been proven to be a turning point in understanding the pathogenesis of this malignancy. A major advance in this field came with the recognition that chronic *H pylori* infection could induce physiologic and morphologic changes within the gastric milieu, which increase the risk of neoplastic transformation[2]. It has been widely accepted that chronic *H pylori* infection induces hypochlorhydria and gastric atrophy, both of which are precursors of gastric cancer[2]. Epidemiological studies have also indicated that infection with *H pylori* is considered as a risk factor for gastric cancer[3,4] and the WHO IARC has classified this bacterium as a definite biological carcinogen[5]. However, while the majority of infected individuals develop no significant clinical disease, others develop two kinds of divergent clinical outcomes-peptic ulcer disease and gastric cancer[2]. The reasons for developing these two extreme phenotypes, especially important in gastric cancer, have remained poorly understood, and are not explained by bacterial virulence factors alone[2]. This highlights the need to explore potential candidate genes of the host in the pathways involved in the natural history of *H pylori* infection and its interactions with other risk factors in the development of gastric cancer in a high-risk population.

The inducible form of nitric oxide (NO) synthase (iNOS) is one of the most important enzymes involved in the pathway of reactive oxygen and nitrogen species metabolism in the presence of *H pylori* infection in humans. iNOS is a major source of NO production that is produced during inflammation by macrophages[6,7]. Expression of iNOS in response to cytokines is part of the inflammatory response and contributes to tissue damage, suggesting its possible role in the processing of carcinogens[7]. iNOS contains many sites for prosthetic groups and substrate binding[8], which are all potentially important for the function of the enzyme. Furthermore, studies have indicated that even single amino acid changes may have dramatic effects on enzymatic activity[8,9]. The human iNOS gene comprises 27 exons with the transcription start site in exon 2 (E2) and the stop codon in E27[10]. E1-13 code for the oxygenase domain, and E14–27 encode for the reductase domain of the protein. Both of the domains represent different functional parts of the enzyme[9]. Increased iNOS activities have been observed in patients with chronic gastritis caused by *H pylori* infection, and gastric cancer[11,12]. A 13-21 years follow-up study showed that among the *H pylori* positive group, the expression of iNOS and nitro-tyrosine was significantly higher in the group that developed gastric cancer than the one that showed no evidence of gastric cancer, suggesting that *H pylori* positive subjects with high levels of reactive nitrogen species in gastric mucosa may be a high-risk group for gastric cancer[13]. Furthermore, recent studies have revealed that *H pylori* infection may lead to a sustained production of reactive nitrogen species and the formation of nitro-tyrosine contributes to DNA damage and apoptosis in gastric mucosa[12]. Infection with *H pylori* strains

possessing cytotoxin-associated gene (Cag) A, a molecular marker of *H pylori* virulence[14,15], is particularly associated with an increased risk of developing adenocarcinoma of the stomach. It is suggested that iNOS may be a susceptible gene involved in the metabolic pathway of nitrogen and oxygen species of free radicals, and thus may be associated with both gastric cancer risk and *H pylori* infection.

Yangzhong city is one of the areas in China with the highest gastric cancer mortality and incidence rate. The crude mortality rate of gastric cancer was from 96.9 to 110.9/100 000 during 1991 and 1997, and the average adjusted incidence rate in the same period was over 115/100 000 (unadjusted rate was 155.46/100 000), which is over ten times higher than that in the United States[16]. Based on the understanding of the physiology and pathogenesis of gastric cancer, and the genetic pathway related to *H pylori* infection, we hypothesized that higher frequency of iNOS $Ser^{608}Leu$ allele (i.e. C/T polymorphism)[9,17] was responsible for the higher gastric cancer incidence in this area. We were especially interested in knowing whether the association between the polymorphism and gastric cancer was modified by infection with *H pylori* CagA strains and cigarette smoking reflecting high exposure to nitrogen and oxygen species of free radicals. Therefore, the aim of this study was to determine whether iNOS C/T polymorphism was associated with increased susceptibility to gastric cancer, and the effects of *H pylori* infection.

MATERIALS AND METHODS

Study subjects

All gastric cancer patients and "healthy" controls in this study were Han ethnic Chinese living in Yangzhong city for at least 25 years. Gastric cancer was diagnosed according to the International Classification of Diseases for Oncology IX, code = 151, and the criteria of Laurén[18]. Because most diagnosed gastric cancer cases in Yangzhong were intestinal type gastric cancer (IGC) and gastric cardia cancer (GCC), we focused on these two kinds of cancers in the present study. A population based case-control design was used, and 165 gastric cancer cases (108 IGC, 57 GCC) and 295 controls were enrolled. The finally analyzed cases and controls were 143 (93 IGC, 50 GCC) and 246 cases, respectively, because of missing genotype data for some subjects. There were no significant differences comparing the finally analyzed subjects and those with missing data by age and sex. All cases were identified by endoscopic and pathological diagnosis in Yangzhong City Municipal Hospital from January 1997 to December 1998. To reduce misclassification of the histological types, two pathologists reviewed and confirmed all diagnosed cases. Controls were selected from cancer-free subjects living in the same community, who were either cases' siblings or their non-blood relatives (spouses and spouses' siblings with the same gender as cases). Both types of controls differed slightly in demographic features[19]. Their results were combined to increase the sample size and to decrease type I error. This study was approved by the regional ethics committee, and all participants were given an explanation of the nature of the study, and informed consents both written and oral, were obtained. Study subjects completed a questionnaire administered by trained interviewers.

The questionnaire was designed to obtain detailed information on cigarette smoking, alcohol drinking, family history of cancers, and occupational and hazard exposures. Cigarette smokers were defined as subjects who reported ever smoking at least one cigarette per day for 12 mo or more, or whose accumulated cigarette consumption was over 18 packs per year. Past smokers were those who had stopped smoking 1 or more years before the interview. Alcohol drinkers were defined as subjects who reported to have an average of one drink or more per week for one or more yeaes. Past alcohol drinkers were also defined as those who had stopped drinking for 1 or more years before the interview.

Laboratory analysis

Blood was drawn from each participant by the designated coordinator according to the Guidelines of the National Heart, Lung, and Blood Institute Working Group on Blood Drawing, Processing, and Storage for Genetic Studies. Twenty milliliters of forearm venous blood was collected from each subject via venipuncture into two 10-mL vacutainer tubes containing EDTA. Puragene DNA isolation kits (Gentra Systems, Minneapolis MN) were used to isolate genomic DNA for genotyping. All blood samples were separated, and plasma was collected as soon as possible. The plasma was then stored at -20 ℃ in six 1.5-mL tubes for the detection of IgG antibody to *H pylori* CagA.

Denaturing high performance liquid chromatography (DHPLC) was used to scan the potential single nucleotide polymorphisms (SNPs) in all exons of iNOS, and then sequencing was performed to confirm the possible mutations. Finally, a new C/T polymorphism, which changes the coding amino acid from serine (TCG) to leucine (TTG), was identified[17]. PCR-RFLP was carried out to identify the genotype of iNOS according to the features of SNP, which created a restriction enzyme recognition site of *Tsp 509 I*. Genomic DNA was amplified with primers F: 5'-TGTAAACCAACTTCCGTGGTG-3' (Tm = 60.82 ℃) and R: 5'-GTCTCTGCGGGTCTGAGAAG-3' (Tm = 60.14 ℃). PCR was performed in a MJRESEARCH PCR system (PTC-225, USA), and in a 10 μL reaction volume containing 1μL 10×PCR buffer, 1.6 μL dNTPs (1.25 μmol/L), 0.2 μL $MgCl_2$ (25 mmol/L), primers (20 μmol/L, Resgen Corp.) at 0.15 μL each, DMSO 0.5 μL, 6.34 μL dH2O, 50 ng genomic DNA dried on the plate, and Hot Start Taq DNA polymerase 0.06 μL (5 U/μL, Promega Corp.). Touch down PCR procedure was used to amplify the target fragment. After an initial denaturation at 94 ℃ for 15 min, amplification was carried out for 10 cycles at 94 ℃ for 30 s, at 61 ℃ for 45 s, at 72 ℃ for 45 s and decreasing 0.5 ℃ per cycle. Then amplification was again carried out for 35 cycles at 94 ℃ for 30 s, at 56 ℃ for 45 s, and at 72 ℃ for 45 s, followed by a final elongation at 72 ℃ for 7 min. Then, 10 μL PCR products was digested with 0.2 μL *Tsp* 509 I (10 U/μL, NEB Corp.) in a 15 μL volume including 2 μL 10×buffer 1 (NEB Corp.), 0.15 μL BSA (100×) and 2.65 μL dH2O. Digestion was performed for 15 h at 65 ℃. The products were then electrophoresed on a 30 g/L agarose gel to allow unambiguous detection with ethidium bromide staining. Homozygous wide-type individuals (CC) showed 113 bp and 175 bp fragments, heterozygous individuals (CT) showed three bands: 113 bp, 142 bp and 175 bp, and homozygous rare allele individuals (TT) showed two bands: 113 bp and 142 bp[17].

H pylori CagA IgG antibody in plasma was measured by an enzyme-linked immunosorbent assay (ELISA) kit offered by Jingying Biotech Limited Company, Shanghai, China (batch number 0052). The Absorbency at 450 nm was determined after terminating the enzyme reaction. The cutoff value equaled to the average *A* of the negative controls provided by the manufacturer plus 0.3 *A* units. *A* values of samples equaled to or higher than the cutoff point were considered positive.

Statistical analysis

All data were input double blinded into EPI-6 program by two persons separately. After modifying all errors and non-logical data, the differences in the relative associations between cases and controls were assessed by calculating crude odds ratios (OR) from contingency tables. The corresponding chi-square test on the cancer patients and controls was carried out, and 95% confidence intervals (95% CI) were determined using the Fisher exact test. A P-value <0.05 was considered statistically significant. Unconditional logistic regression analysis was performed in both univariate and multivariate models to assess the association between iNOS functional polymorphism and

gastric cancer susceptibility after adjusting for important confounding factors such as age and sex. Test of trend and interaction index (γ) that was determined by coefficient (β) in a multiple logistic regression model were calculated through logistic models based on dummy variables to examine the potential gene-environment interaction[20]. All analyses were performed with the SAS package Genmod (SAS Institute, Cary, NC).

RESULTS

Table 1 compares the characteristics of study subjects. The mean age of cases was significantly greater than the controls (59.36 *vs* 51.89, $P<0.01$). There was no significant difference in the male/female ratio between cases and controls. The proportions of past smokers and alcohol drinkers was significantly greater in the cancer group (36.97% and 30.30%) than in the control group (12.54% and 14.92%). However, there were more current smokers and drinkers in the control (47.12% and 30.85%) than in the case group (26.67% and 10.91%). Compared with controls, cases were significantly less likely to be positive for *H pylori* CagA antibody.

The frequency of iNOS genotypes in gastric cancer and control subjects showed no significant difference, although the frequency of (CT+TT) genotypes was slightly higher in cases than in controls (24.48% versus 23.17%). A gene dose-response effect was not observed, i.e. the effect of heterozygote (CT) genotypes did not lie at or between the homozygotes (CC and TT).

For (CT+TT) the genotype frequency of iNOS in the past smoking subgroup, there were significant differences between the total cases and the controls and between GCC group and controls with an OR of 3.62 (95% CI: 1.23-10.64) and 4.63 (95% CI: 1.15-18.58), respectively. No significant difference was found between IGC cases and controls (Table 2). Although no gene dose-response effect was observed in heterozygote (CT) and homozygote (TT) individuals because of the small number in each cell, there was still a possible interaction between C/T polymorphism and past cigarette smoking in increasing the risk of GCC. In the past alcohol drinkers, there were significant differences in the C/T polymorphism between total cases and controls and between IGC group and controls with an OR of 3.33 (95% CI: 1.14-9.67) and 3.42 (95% CI: 1.03-11.35), respectively. No significant difference between GCC group and control group was found (Table 3). In *H pylori* CagA negative group, subjects with (CT+TT) genotypes had significantly increased risk of both IGC and GCC, with an OR of 2.19 (95% CI: 1.01-4.76) and 3.52 (95% CI: 1.44-8.61), respectively. *H pylori*

Table 1 Covariate distribution among study subjects and ORs for gastric cancer

Characteristics		No Cases (%) (n = 165)	No. Controls (%) (n = 295)	OR (95% CI)
Age (yr)				
	Mean (yr±SD)	59.36±9.29[a]	51.89±10.24	
	Min. (yr)	34.72	30.77	
	Max. (yr)	81.95	78.21	
Gender				
	Male (%)	110 (66.67)	190 (64.41)	
	Female (%)	55 (33.33)	105 (35.59)	
	Ratio	2.00:1	1.81:1	
Smoking habit				
	Never	60 (36.36)	119 (40.34)	1.00
	Current	44 (26.67)	139 (47.12)	0.26 (0.15–0.46)[b]
	Past	61 (36.97)	37 (12.54)	3.15 (1.77–5.61)[b]
Alcohol habits				
	Never	97 (58.79)	160 (54.24)	1.00
	Current	18 (10.91)	91 (30.85)	0.18 (0.10–0.35)[b]
	Past	50 (30.30)	44 (14.92)	1.80 (1.06–3.08)
Plasma *H Pylori* CagA antibody				
	Negative	136 (82.42)	107 (49.31)	1.00
	Positive	29 (17.58)	110 (50.69)	0.18 (0.11–0.31)[b]
iNOS genotyping				
	CC	108 (75.52)	189 (76.83)	1.00
	CT	33 (23.08)	49 (19.92)	1.15 (0.68–1.96)
	TT	2 (1.40)	8 (3.25)	0.42 (0.08–2.16)
	CT+TT	35 (24.48)	57 (23.17)	1.03 (0.59–1.79)

[a]$P<0.05$ *vs* control group after adjusted for age and gender, [b]$P<0.01$ *vs* control.

Table 2 Interaction between C/T polymorphism and past cigarette smoking for the risk of gastric cancer

C/T polymorphism	Past smoking	Total cases (n = 143)	Controls (n = 246)	OR[1]	95%CI	IGC (n = 93)	OR[2]	95%CI	GCC (n = 50)	OR[3]	95%CI
CC	No	67	162	1.00		46	1.00		21	1.00	
CT+TT	No	22	51	0.98	0.55-1.78	12	0.75	0.36-1.54	10	1.44	0.63-3.27
CC	Yes	41	27	2.92	1.53-5.57	27	2.47	1.19-5.09	14	3.65	1.42-9.38
CT+TT	Yes	13	6	3.62	1.23-10.64	8	3.06	0.91-10.35	5	4.63	1.15-18.58

[1]Adjusted for age and gender, $\chi^2_{trend} = 26.26$, df = 1, $P = 0.00$, $\gamma = 1.29/1.07 = 1.21$ [2]Adjusted for age and gender, $\chi^2_{trend} = 18.40$, df = 1, $P = 0.00$, $\gamma = 1.12/0.90 = 1.24$ [3]Adjusted for age and gender, $\chi^2_{trend} = 17.53$, df = 1, $P = 0.00$, $\gamma = 1.53/1.29 = 1.19$.

Table 3 Interaction between C/T polymorphism and past alcohol drinking for the risk of gastric cancer

C/T polymorphism	Past alcohol drinking	Total cases (n = 143)	Controls (n = 246)	OR[1]	95%CI	IGC (n = 93)	OR[2]	95%CI	GCC (n = 50)	OR[3]	95%CI
CC	No	76	157	1.00		53	1.00		23	1.00	
CT+TT	No	24	51	0.83	0.46-1.50	13	0.62	0.30-1.28	11	1.22	0.55-2.70
CC	Yes	32	32	1.34	0.72-2.52	20	1.36	0.67-2.75	12	1.27	0.50-3.19
CT+TT	Yes	11	6	3.33	1.14-9.67	7	3.42	1.03-11.35	4	3.25	0.80-13.13

[1]Adjusted for age and gender, χ^2_{trend} = 10.29, df = 1, P = 0.001, γ = 1.20/0.30 = 4.00 [2]Adjusted for age and gender, χ^2_{trend} = 5.65, df = 1, P = 0.017, γ = 1.23/0.31 = 3.97 [3]Adjusted for age and gender, χ^2_{trend} = 8.95, df = 1, P = 0.003, γ = 1.18/0.24 = 4.9.

Table 4 Interaction between C/T polymorphism and *H pylori* CagA status for the risk of gastric cancer

C/T polymorphism	CagA antibody	Total cases (n = 143)	Controls (n = 178)	OR[1]	95%CI	IGC (n = 93)	OR[2]	95%CI	GCC (n = 50)	OR[3]	95%CI
CC	No	87	64	1.00		61	1.00		26	1.00	
CT+TT	No	28	19	2.53	1.29-4.98	17	2.19	1.01-4.76	11	3.52	1.44–8.61
CC	Yes	21	73	0.45	0.25-0.81	12	0.34	0.17-0.70	9	0.76	0.33-1.73
CT+TT	Yes	7	22	0.43	0.17-1.10	3	0.24	0.07-0.89	4	0.86	0.27-2.79

[1]Adjusted for age and gender, χ^2_{trend} = 33.40, df = 1, P = 0.00, γ = -0.84/-0.79 = 1.06 [2]Adjusted for age and gender, χ^2_{trend} = 28.53, df = 1, P = 0.00, γ = -1.41/-1.08 = 1.31 [3]Adjusted for age and gender, χ^2_{trend} = 12.42, df = 1, P = 0.0004, γ = -0.15/-0.27 = 0.56.

CagA positivity showed significant protective effects in IGC group in both on CC and CT+TT iNOS genotypes, with an OR of 0.24 (95% CI: 0.07-0.89) and 0.34 (95% CI: 0.17-0.70), respectively. However, no significant association was observed between iNOS genotypes and GCC (Table 4).

DISCUSSION

H pylori infection could produce a state of chronic immuno-stimulation in gastric epithelium[21]. It could lead to changes in many factors that are important in the pathogenesis of gastric cancer, including reactive oxygen and nitrogen oxide species [22]. NO, a potentially toxic gas with free radical properties is one of the most important bio-regulatory and signaling molecules produced in the process. It has been recently reported that NO, acting as a messenger molecule mediating various physiological functions[23,24], may also play a role in the process of carcinogenesis.

It has been found that NO is synthesized enzymatically from L-arginine by NO synthase[23,25]. Chronic infection and immuno-stimulation elevate endogenous synthesis of NO. High concentration of NO generated by macrophages after iNOS induction contributed to their cytotoxic and carcinogenic activity[26]. There is now increasing evidence that NO produced by activated phagocytes may play a role in multistage carcinogenesis by mediating DNA damage[27,28]. A to T substitution in the iNOS gene, leads to more activated iNOS expression in the target cells, and finally elevates NO to a high level. Hence, it is reasonable to assume that human iNOS gene may be another important candidate gene for the development of gastric cancer by elevating NO production in target cells when functional polymorphisms occur. Nevertheless its genomic localization at chromosome 17q11.2[29] was not the same as other gastric cancer susceptible genes related to the inflammatory response pathway, such as interleukin 1β and interleukin 1RN, located at 2q14[30]. The key question for gastric cancer agents is how *H pylori* infection could be associated with such totally divergent clinical outcomes as gastric cancer and peptic ulcer disease. A large number of previous studies have focused on the role of the bacterial virulence factors that contribute to the degree of tissue damage in the pathogenesis of these diseases. But these results still could not explain the different outcomes[2,22,31]. With the development of a key concept about the interaction between acid secretion and *H pylori*-induced gastritis during 1990 s, El-Omar proposed the idea for the first time that host genetic factors relevant to pro-inflammatory responses might be relevant to the development of gastric cancer. They explored a candidate IL-1β gene in the context of *H pylori* related disease[32,33]. Because IL-1β can also induce the expression of many other genes, including pro-inflammatory mediator iNOS, by either regulating at the transcriptional level or initiating their mRNA[8,9,34], it is easy to consider that functional polymorphisms occurring in the iNOS gene might also contribute to the increased risk of *H pylori* related gastric cancer.

We have previously reported a newly discovered C/T polymorphism in a Chinese population[17] that had a high mutated allele frequency (24.4%). A report by Johannesen also showed that C/T polymorphism was one of the most frequent SNPs among 10 polymorphisms of human iNOS gene identified in a Danish population. They suggested that the amino acid change in exon 16 might be of functional interest[9]. Our results showed no significant difference in the frequency of (CT+TT) genotypes between cases and controls, and no apparent gene dose-response effect was found. However, in past cigarette smokers and past alcohol drinkers, C/T polymorphism significantly increased the risk of gastric cancer despite the histological subtypes differed, i.e. past cigarette smokers with (CT+TT) genotypes had an increased risk of IGC, while past alcohol drinkers with (CT+TT) genotypes had increased risk of GCC. These findings suggest that C/T polymorphism in iNOS gene alone is not sufficient to show the increasing risk of gastric cancer. The importance of the interaction between C/T polymorphism and cigarette smoking or alcohol drinking varied depending on different histological subtypes of gastric cancer. Similar results were found by Machado for IL-1 genetic markers[35]. Although these findings were not the major hypothesis we proposed, it is biologically plausible that oxidative stress due to carcinogenesis in cigarette might attribute to the increase of gastric cancer risk through interactions with iNOS C/T polymorphism. Larger and independent studies are needed to confirm these findings.

In the *H pylori* CagA positive group, regardless of whether subjects had CC or (CT+TT) genotypes, we always observed a significant protective effect when comparing IGC cases with controls. This suggests that plasma positive for *H pylori* CagA antibody in a highly infected area plays a protective role. This

is in concordance with the finding that *H pylori* density became progressively lower with progression from mild gastritis to severe gastritis, atrophy, intestinal metaplasia and finally gastric cancer[29]. In *H pylori* CagA negative subjects with (CT+TT) genotypes, a high risk was found for gastric cancer group (OR = 2.53, 95% CI: 1.29-4.98) and both subgroups (IGC and GCC). No interaction was found between iNOS genotype and infection with *H pylori* CagA strains.

iNOS protein is a catalytic enzyme with two domains. In terms of functional importance, the deletion mutants retained maximal NO activity at lower concentrations of free Ca^{2+} compared with the wild-type[36]. Identified C/T polymorphism in E16 of iNOS was located at the N-terminal of six amino acids from the deletion reported by Daff *et al*., and the amino acid change in E16 might be of functional interest[9]. To our knowledge, this study was the first one to examine the significance of iNOS polymorphism in gastric cancer. A research on other type of disease might support our observation[9]. Gastric cancer patients having allele T polymorphism could have an increased expression of iNOS, resulting in higher levels of NO in gastric mucosa, mediating many pathological changes and finally leading to carcinogenesis in these patients. But specific functional tests of C/T shift need to be performed to substantiate the putative importance of the $Ser^{608}Leu$ locus in gastric cancer development.

Potential weaknesses in our study include possible recruitment bias in the selection of controls including cases' siblings. This kind of selection might create overmatching. Siblings were more likely to have the same genotypes as the cases than the non-blood related controls, thereby leading to some loss of statistical efficiency, i.e., larger sample sizes were required to attain the same statistical precision[37]. Thus, our data may be more likely to underestimate the true effect of iNOS T alleles on the risk of gastric cancer. But others considered that the use of sibling controls could generally improve efficiency for gene-environment interactions[38,39]. We could not rule out the potential influence of systematic differences between participants and non-participants.

In conclusion, the risk of gastric cancer is increast among past cigarette smoking or alcohol drinking individuals with a C/T polymorphism in E16 of iNOS gene in a Chinese population. But the findings need to be confirmed in other ethnic populations.

ACKNOWLEDGEMENTS

We thank Zhao-Xi Wang for his excellent technical assistance; and Professor Regina M. Santella and Dr. Yu-Jing Zhang for editing the manuscript. We also thank all the doctors for their kind help in collecting the biological samples and epidemiological data. We thank all participatants for their co-operation.

REFERENCES

1 **Parkin DM,** Pisani P, Ferlay J. Estimates of the worldwide incidence of 25 major cancers in 1990. *Int J Cancer* 1999; **80**: 827-841

2 **El-Omar EM,** Chow WH, Rabkin CS. Gastric cancer and *H pylori*: Host genetics open the way. *Gastroenterology* 2001; **121**: 1002-1004

3 **Correa P.** Human gastric carcinogenesis: a multistep and multifactorial process-first american cancer society award lecture on cancer epidemiology and prevention. *Cancer Res* 1992; **52**: 6735-6740

4 **Komoto K,** Haruma K, Kamada T, Tanaka S, Yoshihara M, Sumii K, Kajiyama G, Talley NJ. *Helicobacter pylori* infection and gastric neoplasia: correlations with histological gastritis and tumor histology. *Am J Gastroenterol* 1998; **93**: 1271-1276

5 Schistosomes, liver flukes and *Helicobacter pylori*. IARC Working Group on the Evaluation of Carcinogenic Risks to Humans. Lyon, 7-14 June 1994. *IARC Monogr Eval Carcinog Risks Hum* 1994; **61**: 1-241

6 **Felley CP,** Pignatelli B, Van Melle GD, Crabtree JE, Stolte M, Diezi J, Corthesy-Theulaz I, Michetti P, Bancel B, Patricot LM, Ohshima H, Felley-Bosco E. Oxidative stress in gastric mucosa of asymptomatic humans infected with *Helicobacter pylori*: effect of bacterial eradication. *Helicobacter* 2002; **7**: 342-348

7 **Vallance P,** Collier J. Biology and clinical relevance of nitric oxide. *Br Med J* 1994; **309**: 453-457

8 **Stuehr DJ.** Mammalian nitric oxide synthases. *Biochim Biophys Acta* 1999; **1411**: 217-230

9 **Johannesen J,** Pie A, Paiot F, Kristiansen OP, Karlsen AE, Nerup J. Linkage of the human inducible nitric oxide synthase gene to type 1 diabetes. *J Clin Endocrinol Metab* 2001; **86**: 2792-2796

10 **Xu W,** Charles IG, Liu L, Moncada S, Emson P. Molecular cloning and structural organization of the human inducible nitric oxide synthase gene (NOS2). *Biochem Biophys Res Commun* 1996; **219**: 784-788

11 **Mannick EE,** Bravo LE, Zarama G, Realpe JL, Zhang XJ, Ruiz B, Fontham ET, Mera R, Miller MJ, Correa P. Inducible nitric oxide synthase, nitrotyrosine, and apoptosis in *Helicobacter pylori* gastritis: effect of antibiotics and antioxidants. *Cancer Res* 1996; **56**: 3238-3243

12 **Wee A,** Kang JY, Teh M. *Helicobacter pylori* and gastric cancer: correlation with gastritis, intestinal metaplasia, and tumour histology. *Gut* 1992; **33**: 1029-1032

13 **Rajnakova A,** Goh PM, Chan ST, Ngoi SS, Alponat A, Moochhala S. Expression of differential nitric oxide synthase isoforms in human normal gastric mucosa and gastric cancer tissue. *Carcinogenesis* 1997; **18**: 1841-1845

14 **Blaser MJ,** Perez-Perez GI, Kleanthous H, Cover TL, Peek RM, Chyou PH, Stemmermann GN, Nomura A. Infection with *Helicobacter pylori* strains possessing CagA is associated with an increased risk of developing adenocarcinoma of the stomach. *Cancer Res* 1995; **55**: 2111-2115

15 **Goto T,** Haruma K, Kitadai Y, Ito M, Yoshihara M, Sumii K, Hayakawa N, Kajiyama G. Enhanced expression of inducible nitric oxide synthase and nitrotyrosine in gastric mucosa of gastric cancer patients. *Clin Cancer Res* 1999; **5**: 1411-1415

16 **Stadtlander CT,** Waterbor JW. Molecular epidemiology, pathogenesis and prevention of gastric cancer. *Carcinogenesis* 1999; **20**: 2195-2208

17 **Shen J,** Wang RT, Wand LW, Wang ZX, Xing HX, Wang BY, Guo CH, Wang XR, Xu XP. Ser/Leu polymorphism of iNOS gene was found and identified in Chinese by denaturing high performance liquid chromatography. *Peking Daxue Xuebao* 2001; **33**: 486-492

18 **Laurén P.** The two histological main types of gastric carcinoma: diffuse and so-called intestinal-type carcinoma. An attempt at a histo-clinical classification. *Acta Pathol Microbiol Scand* 1965; **64**: 31-49

19 **Shen J,** Wang R, Wang Z, Xing H, Wang L, Wang B, Li M, Hua Z, Wang J, Guo C, Wang X, Xu X. The distributive features of three kinds of metabolic genes polymorphisms in population of Han nationality in south area of China. *Zhonghua Yixue Yichuanxue Zazhi* 2002; **19**: 302-307

20 **Taioli E,** Zocchetti C, Garte S. Models of interaction between metabolic genes and environmental exposure in cancer susceptibility. *Environ Health Perspect* 1998; **106**: 67-70

21 **Shapiro KB,** Hotchkiss JH. Induction of nitric oxide synthesis in murine macrophages by *Helicobacter pylori*. *Cancer Lett* 1996; **102**: 49-56

22 **El-Omar EM.** The importance of interleukin 1 beta in *Helicobacter pylori* associated disease. *Gut* 2001; **48**: 743-747

23 **Moncada S,** Palmer RM, Higgs EA. Nitric oxide: physiology, pathophysiology, and pharmacology. *Pharmacol Rev* 1991; **43**: 109-142

24 **Son HJ,** Rhee JC, Park DI, Kim YH, Rhee PL, Koh KC, Paik SW, Choi KW, Kim JJ. Inducible nitric oxide synthase expression in gastroduodenal diseases infected with *Helicobacter pylori*. *Helicobacter* 2001; **6**: 37-43

25 **Forstermann U,** Schmidt HH, Pollock JS, Sheng H, Mitchell JA, Warner TD, Nakane M, Murad F. Isoforms of nitric oxide synthase. Characterization and purification from different cell types. *Biochem Pharmacol* 1991; **42**: 1849-1857

26 **Grisham MB,** Ware K, Gilleland HE Jr, Gilleland LB, Abell CL, Yamada T. Neutrophil-mediated nitrosamine formation: role

of nitric oxide in rats. *Gastroenterology* 1992; **103**: 1260-1266
27 **Esumi H,** Tannenbaum SR. US-Japan Cooperative Cancer Research Program: seminar on nitric oxide synthase and carcinogenesis. *Cancer Res* 1994; **54**: 297-301
28 **Ohshima H,** Bartsch H. Chronic infections and inflammatory processes as cancer risk factors: possible role of nitric oxide in carcinogenesis. *Mutat Res* 1994; **305**: 253-264
29 **Marsden PA,** Heng HH, Duff CL, Shi XM, Tsui LC, Hall AV. Localization of the human gene for inducible nitric oxide synthase (NOS2) to chromosome 17q11.2-q12. *Genomics* 1994; **19**: 183-185
30 **Patterson D,** Jones C, Hart I, Bleskan J, Berger R, Geyer D, Eisenberg SP, Smith MF Jr, Arend WP. The human interleukin-1 receptor antagonist (IL1RN) gene is located in the chromosome 2q14 region. *Genomics* 1993; **15**: 173-176
31 **Graham DY,** Yamaoka Y. Disease-specific *Helicobacter pylori* virulence factors: the unfulfilled promise. *Helicobacter* 2000; **5** (Suppl 1): S3-S9
32 **El-Omar EM,** Carrington M, Chow WH, McColl KE, Bream JH, Young HA, Herrera J, Lissowska J, Yuan CC, Rothman N, Lanyon G, Martin M, Fraumeni JF Jr, Rabkin CS. Interleukin-1 polymorphisms associated with increased risk of gastric cancer. *Nature* 2000; **404**: 398-402
33 **El-Omar EM,** Carrington M, Chow WH, McColl KE, Bream JH, Young HA, Herrera J, Lissowska J, Yuan CC, Rothman N, Lanyon G, Martin M, Fraumeni JF Jr, Rabkin CS. The role of interleukin-1 polymorphisms in the pathogenesis of gastric cancer. *Nature* 2001; **412**: 99
34 **Cho HJ,** Xie QW, Calaycay J, Mumford RA, Swiderek KM, Lee TD, Nathan C. Calmodulin is a subunit of nitric oxide synthase from macrophages. *J Exp Med* 1992; **176**: 599-604
35 **Machado JC,** Pharoah P, Sousa S, Carvalho R, Oliveira C, Figueiredo C, Amorim A, Seruca R, Caldas C, Carneiro F, Sobrinho-Simoes M. Interleukin 1B and interleukin 1RN polymorphisms are associated with increased risk of gastric carcinoma. *Gastroenterology* 2001; **121**: 823-829
36 **Daff S,** Sagami I, Shimizu T. The 42-amino acid insert in the FMN domain of neuronal nitric-oxide synthase exerts control over Ca(2+)/calmodulin-dependent electron transfer. *J Biol Chem* 1999; **274**: 30589-30595
37 **Thomas DC,** Witte JS. Point: population stratification: a problem for case-control studies of candidate-gene associations? *Cancer Epidemiol Biomark Prev* 2002; **11**: 505-512
38 **Gauderman WJ,** Witte JS, Thomas DC. Family-based association studies. *J Natl Cancer Inst Monogr* 1999; **26**: 31-37
39 **Witte JS,** Gauderman WJ, Thomas DC. Asymptotic bias and efficiency in case-control studies of candidate genes and gene-environment interactions: basic family designs. *Am J Epidemiol* 1999; **149**: 693-705

Edited by Xia HHX and Wang XL **Proofread by** Xu FM

PO Box 2345, Beijing 100023, China
Fax: +86-10-85381893
E-mail: wjg@wjgnet.com www.wjgnet.com

World J Gastroenterol 2004;10(22):3284-3288
World Journal of Gastroenterology
 ISSN 1007-9327

A new subtype of 3′ region of *cagA* gene in *Helicobacter pylori* strains isolated from Zhejiang Province in China

Ran Tao, Ping-Chu Fang, Hai-Yan Liu, Yun-Shui Jiang, Jing Chen

Ran Tao, Ping-Chu Fang, Hai-Yan Liu, Yun-Shui Jiang, Jing Chen, Department of Medical Microbiology and Parasitology, Zhejiang University School of Medicine, Hangzhou 310006, Zhejiang Province, China
Supported by China Medical Board, No. 96-628, and Natural Science Fund of Zhejiang Province, No. 302023
Correspondence to: Professor Ping-Chu Fang, Department of Medical Microbiology and Parasitology, Zhejiang University School of Medicine, 353 Yan'an Road, Hangzhou 310006, Zhejiang Province, China. fangpc@zju.edu.cn
Telephone: +86-571-87217403
Received: 2004-04-15 **Accepted:** 2004-05-09

Abstract

AIM: To isolate the subtypes of 3′ region of *cagA* gene in *Helicobacter pylori* (*H pylori*) strains from Zhejiang Province in China and to investigate their relations to *H pylori*-associated gastroduodenal diseases.

METHODS: One hundred and thirty-seven *H pylori* clinical strains were isolated from the gastric mucosa specimens of 74 patients with chronic gastritis, 61 with peptic ulceration, and 2 with gastric cancer. Bacterial genomic DNA was extracted and 3′ region of *cagA* gene was amplified by polymerase chain reaction (PCR). Subtypes of 3′ region of *cagA* gene were determined by the size of PCR amplified segments. The sequences of the subtypes were analyzed by PCR-based sequencing.

RESULTS: Of the 137 *H pylori* isolates from Zhejiang Province, 132 (96.4%) yielded PCR products that could be classified into three groups of subtypes, named as subtypes I, II, and III according to their sizes. The sizes of subtypes I, II, and III were 648-650 bp, 705-707 bp, and 815 bp, respectively. Among the 132 *cagA*-positive *H pylori* strains, 123 (93.2%) belonged to the group of subtype I, 6 (4.5%) presented subtype II, 1 (0.8%) was subtype III, and 2 (1.5%) presented subtypes I and III both. The primary structure of subtype I was composed of 3 repeats of R1, 1 repeat of R2 and 1 repeat of R3. Subtype II possessing 4 repeats of R1, 2 repeats of R2 and 1 repeat of R3 was a newly found type of 3′ region of *cagA* gene which had not been reported before. The primary structure of subtype III consisted of 4 repeats of R1, 1 repeat of R2 and 2 repeats of R3. Comparison of the sequences of subtype I strains with the corresponding sequences deposited in GenBank, showed a similarity of 95.0% (94.0-96.1%) for nucleotide sequences and 95.9% (94.9-97.4%) for deduced amino acid sequences. Comparison of the sequences of subtype III strains with the corresponding sequences deposited in GenBank, showed a similarity of 93.9% (90.8-96.9%) for nucleotide sequences and 93.2% (90.2-96.2%) for deduced amino acid sequences. Among subtype II strains, the nucleotide and deduced amino acid sequences showed a similarity of 95.2% (94.1-96.5%) and 96.4% (93.8-97.9%), respectively. There were no statistical differences in the distribution of subtypes of 3′ region of *cagA* gene among different *H pylori*-associated gastroduodenal diseases ($\chi^2 = 11.544$, $P > 0.05$).

CONCLUSION: There are three subtypes (I, II, and III) of 3′ region of *cagA* gene in *H pylori* strains isolated from Zhejiang Province, and subtypeIis predominant. Subtype II is a newly found subtype of 3′ region of *cagA* gene. The result of this study does not support the view that the subtypes of 3′ region of *cagA* gene in *H pylori* isolated from Zhejiang Province are correlated with the clinical outcomes of *H pylori* infection.

Tao R, Fang PC, Liu HY, Jiang YS, Chen J. A new subtype of 3′ region of *cagA* gene in *Helicobacter pylori* strains isolated from Zhejiang Province in China. *World J Gastroenterol* 2004; 10(22): 3284-3288
http://www.wjgnet.com/1007-9327/10/3284.asp

INTRODUCTION

Although *Helicobacter pylori* (*H pylori*) is present in stomachs of at least half of the world's population[1], only a small proportion of the carriers develop symptomatic diseases[2]. The clinical spectrum of *H pylori* infection ranges from asymptomatic gastritis to peptic ulcer and gastric cancer[3]. The causes of different outcomes of *H pylori* infection may include the virulence of infectious strains, the susceptibility of hosts, and environmental cofactors[4-8]. The cytotoxin-associated gene A (*cagA*) is located at one end of a 40-kilobase DNA segment called *cag* pathogenicity island (*cag* PAI), which contains open reading frames encoding for a putative *H pylori* secretion system that may be associated with export of virulence factors to the extracellular compartment[9,10]. The presence of *cagA* gene can be considered as a marker for *cag* PAI and is associated with more virulent *H pylori* strains[11]. The structure of *cagA* gene contains a 5' highly conserved region and a variable 3' region, in which the presence of a variable number of repeat sequences results in a protein (CagA) with a molecular mass of 120 to 140 ku[12]. Yamaoka *et al*.[13] from Japan found that the structural organization of 3' region of *cagA* gene in Japanese *H pylori* isolates could be divided into four types (types A to D), and type C was associated with gastric atrophy and carcinoma. However, the genetic structure of 3' region of *cagA* gene in Chinese *H pylori* strains has been little exploited. In this study, we attempted to investigate the subtypes of 3' region of *cagA* gene in *H pylori* strains isolated from Zhejiang Province in China and their relations to *H pylori*-associated gastroduodenal diseases.

MATERIALS AND METHODS

H pylori isolates

A total of 137 *H pylori* isolates were obtained from *H pylori*-infected patients at the Second Affiliated Hospital of Zhejiang University and the Renmin Hospital of Daishan County in Zhejiang Province. The patients, consisting of 95 men and 42

women with a mean age of 42.6 years (ranging from 16 to 71 years), were classified into 3 groups including chronic gastritis ($n = 74$), peptic ulcer ($n = 61$), and gastric cancer ($n = 2$), according to the results of endoscopic and histological examination.

H pylori culture

Bacteria isolated from biopsy specimens were cultured on ECY selective solid medium[14] at 37 ℃ for 5 d, under 100% humidity and microaerophilic conditions (50 mL/L O_2, 100 mL/L CO_2, and 850 mL/L N_2). *H pylori* strains were identified by the following criteria: Gram staining, colony morphology, rapid urease test, and catalase test. The cultured bacteria were defined to be *H pylori* if they formed typical colonies on the medium, were negative Gram stain with curved or spiral shape, and positive for urease and catalase production[15].

Preparation of H pylori genomic DNA

The bacteria were harvested from the agar plates, then genomic DNA was extracted and purified from each *H pylori* isolate using cetyltrimethyl ammonium bromide (CTAB), phenol-chloroform-isoamyl alcohol, and ethanol precipitation[16].

Amplification of 3' region of cagA gene by PCR

The primers 5'-ACCCTAGTCGGTAATGGGTTA-3' (CAG1) and 5'-GTAATTGTCTAGTTTCGC -3' (CAG2) described by Yamaoka *et al*.[13] were used to amplify 3' region of *cagA* gene in this study. PCR was performed in a volume of 25 μL containing 2.5 μL of 10×PCR buffer, 2 μL of 25 mmol/L $MgCl_2$, 2.5 μL of 2 mmol/L dNTPs, 0.5 μL of 20 μmol/L primer sets, 0.2 μL of Taq DNA polymerase, 1 μL of bacterial genomic DNA, and 15.8 μL of H_2O. PCR amplification was performed as following: an initial denaturation at 95 ℃ for 3 min, followed by 30 cycles, each consisting of denaturation at 94 ℃ for 30 s, annealing at 56 ℃ for 30 s, and extension at 72 ℃ for 45 s. The final cycle included a further extension at 72 ℃ for 7 min to ensure the full extension of PCR products. PCR products were analyzed by 20 g/L agarose gel electrophoresis with ethidium bromide staining.

Sequences analysis

PCR products were purified with the DNA purification kit (Shanghai Shenyou Biotechnology Co., Ltd.) according to the manufacturer's instructions. Purified PCR products were consigned to Shanghai BioAsia Biotechnology Co., Ltd. for sequencing. Biological software DNAssist (version 1.0) was used to analyze the sequences of 3' region of *cagA* gene and to compare them with the corresponding sequences deposited in GenBank.

Statistical analysis

The categorical data were analyzed using Chi-square (χ^2) test, and $P<0.05$ was considered statistically significance.

RESULTS

PCR products of 3' region of cagA gene

PCR products of 3' region of *cagA* gene were electrophoresed on 20 g/L agarose gel (containing 0.5 μg/mL ethidium bromide). Of the 137 *H pylori* strains isolated from Zhejiang Province, 132 (96.4%) strains yielded PCR products of three different sizes. The three different-size PCR-amplified segments were respectively named as subtype I (648-650 bp), subtype II (705-707 bp), and subtype III (815 bp) (Figure 1). Among the 132 *cagA*-positive strains, 123 (93.2%) presented subtype I, 6 (4.5%) presented subtype II, 1 (0.8%) presented subtype III, and 2 (1.5%) presented both subtypes I and III.

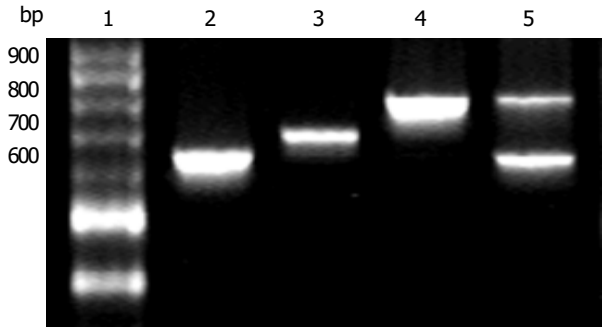

Figure 1 Amplified products of 3' region of *cagA* gene by PCR (20 g / L agarose gel electrophoresis) Lane 1: 100 bp DNA ladder; Lane 2: subtype I (648 bp); Lane 3: subtype II (705 bp); Lane 4: subtype III (815 bp); Lane 5: from a patient with both subtypes I and III.

Sequence analysis of subtypes of 3' region of cagA gene

The primary structure of 3' region of *cagA* gene was composed of a variable number of repeat regions, including R1 (15 bp), R2 (42 bp) and R3 (147 bp). The primary structures of the subtypes of 3' region of *cagA* gene in this study are illustrated in Figure 2. The primary structure of subtype I was composed of 3 repeats of R1, 1 repeat of R2 and 1 repeat of R3, so subtype I was equal to type A in Japanese *H pylori* strains reported by Yamaoka *et al*.[13]. The primary structure of subtype III consisting of 4 repeats of R1, 1 repeat of R2 and 2 repeats of R3 was similar to that of type C reported by Yamaoka *et al*.[13]. Subtype II possessing 4 repeats of R1, 2 repeats of R2 and 1 repeat of R3 had the primary structure not similar to any types reported by Yamaoka *et al*[13] and was regarded as a newly found subtype of 3' region of *cagA* gene in *H pylori*. Comparison of the sequences of 5 *H pylori* strains presented subtype I with the corresponding sequences of a Japanese type A strain JK25 deposited in GenBank (GenBank accession number AF043487), showed a similarity of 95.0% (94.0-96.1%) for nucleotide sequences and 95.9% (94.9-97.4%) for deduced amino acid sequences. Comparison of the sequences of 2 *H pylori* strains presented subtype III (including a strain presented both subtypes I and III) with the corresponding sequences of a Japanese type C strain Jk269 deposited in GenBank (GenBank accession number AF043489), showed a similarity of 93.9% (90.8-96.9%) for nucleotide sequences and 93.2% (90.2-96.2%) for deduced amino acid sequences. Among the 6 *H pylori* strains presented subtype II in this study, the nucleotide and deduced amino acid sequences showed a similarity of 95.2% (94.1-96.5%) and 96.4% (93.8-97.9%), respectively. Alignments of the deduced amino acid sequences of 5 strains presented subtype I and 2 strains presented subtype III with the corresponding sequences deposited in GenBank are illustrated in Figure 3 A, B. Alignments of the deduced amino acid sequences of 6 strains presented subtype II are also illustrated in Figure 3 C.

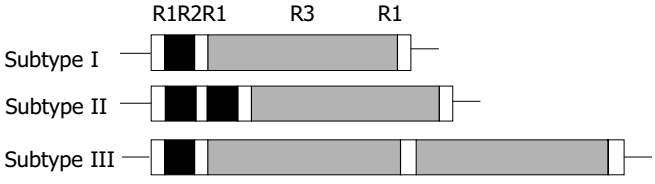

Figure 2 Primary structures of three subtypes of 3' region of *cagA* gene R1: 15 bp repeat region; R2: 42 bp repeat region; R3: 147 bp repeat region.

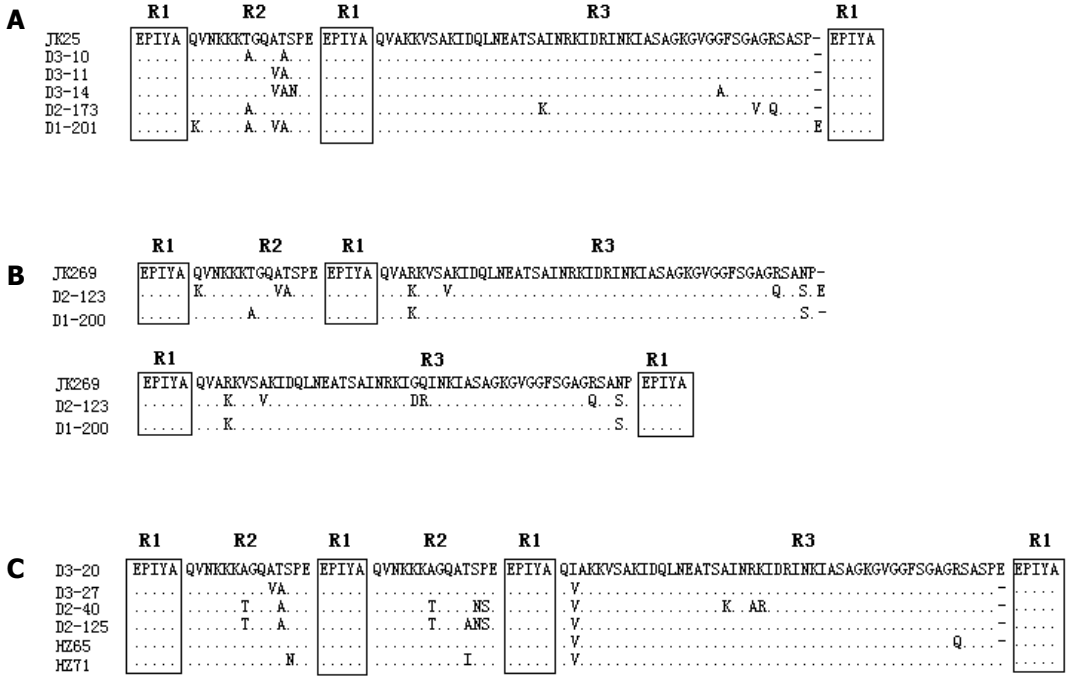

Figure 3 Alignment of amino acid sequences of subtypes of 3' region of *cagA* gene. A: Alignment of the deduced amino acid sequences of subtype I strains with the sequence of the corresponding region of a Japanese type A strain JK25 (GenBank accession number AF043487). Strain D2-173 was from a patient with chronic gastritis, and the remaining four strains were from patients with peptic ulcer. B: Alignment of the deduced amino acid sequences of subtype III strains with the sequence of the corresponding region of a Japanese type C strain JK269 (GenBank accession number AF043489). Strain D1-200 was from a patient with chronic gastritis, and strain D2-123 was from a patient with gastric ulcer. C: Alignment of the deduced amino acid sequences of six subtype II strains. Strain HZ65 and HZ71 were from patients with chronic gastritis, strain D2-40 was from a patient with gastric cancer, and the remaining three strains were from patients with peptic ulcer.

Relationship between subtypes of 3' region of cagA gene and gastroduodenal diseases

The distributions of the subtypes of 3' region of *cagA* gene in different groups of gastroduodenal diseases are demonstrated in Table 1. Statistical analysis showed that there were no significant differences among the subtypes of 3' region of *cagA* gene in different groups of gastroduodenal diseases ($\chi^2 = 11.544$).

Table 1 Relationship between subtypes of 3' region of *cagA* gene and different group of gastroduodenal diseases (*n*, %)

Group of diseases	Subtype I	Subtype II	Subtype III	Subtypes I and III	Total
Chronic gastritis	69 (95.8)	2 (2.8)	0 (0)	1 (1.4)	72
Peptic ulcer	53 (91.4)	3 (5.2)	1 (1.7)	1 (1.7)	58
Gastric cancer	1 (50.0)	1 (50.0)	0 (0)	0 (0)	2
Total	123 (93.2)	6 (4.5)	1 (0.8)	2 (1.5)	132

$\chi^2 = 11.544$, $P = 0.17 > 0.05$.

DISCUSSION

H pylori, a spiral shaped gastric organism, is the cause of chronic gastritis, and plays an important role in the pathogenesis of peptic ulceration, mucosa associated lymphoid tissue lymphoma, and gastric adenocarcinoma[17-20]. It has been reported that 50-60% of *H pylori* strains contain *cagA* gene and consequently produce CagA protein[21]. The CagA is a highly immunogenic outer membrane protein with a molecular weight of 120 to 140 ku. Variation in size of the protein has been correlated with the presence of a variable number of repeat sequences located in 3' region of the gene[22,23]. The biological importance of the repeat sequences in 3' region of *cagA* gene remains unknown. Because CagA is strongly immunogenic, these repeat sequences have been supposed to alter immunogenicity of the protein[24]. This alteration in the gene and its protein seems to correlate with clinical outcomes *in vivo*. The proportion of *cagA*-positive *H pylori* isolates varies from one geographic region to another. Studies from Japan, Korea, and China have shown that more than 90% of *H pylori* strains are *cagA*-positive[25-28], while in the United States of America, Canada, and Europe, these percentages are lower[24,29,30]. Therefore, *cagA* gene cannot be used as a marker for the presence of severe gastroduodenal diseases in those regions where the prevalence of *cagA*-positive *H pylori* strains is uniformly high. Since allelic variation in *cagA* exists and distinct *H pylori* subtypes may circulate in different regions, differences in *cagA* subtype might provide a marker for differences in virulence among *cagA*-positive *H pylori* strains[12].

Yamaoka *et al*.[13] reported that 3' region of *cagA* gene in *H pylori* isolated from Japanese patients could be classified into four types (types A, B, C, and D) depending on the types and number of repeat regions including R1 (15 bp), R2 (42 bp) and R3 (147 bp). The PCR products of type A ranged from 642 to 651 bp, and possessed 1 repeat of R2 and 1 repeat of R3. The PCR products of type B and type D were all 756 bp, but type B possessed 3 repeats of R2 and 1 repeat of R3, while type D had 2 repeats of R3 and no repeat of R2. Type C having 1 repeat of R2 and 2 repeats of R3 yielded PCR products of 813-815 bp and was associated with high levels of CagA antibody and severe degrees of atrophy. The same authors have also found that the sequences of the second repeat regions of 3' region of *cagA* gene in *H pylori* strains from East Asia are completely different from those in strains from non-Asian countries[31]. Non-Asian strains possess 102 bp second repeat regions, and East Asian strains possess 162 bp second repeat regions[31,32].

In the present study, we used the same PCR primers as those described by Yamaoka *et al*.[13] and found 132 (96.4%) of 137 strains yielded amplified products. The high prevalence of *cagA*-positive strains in Zhejiang Province was in accordance

with the result of our previous study[33] and the findings in other Chinese areas[11,27]. The PCR products could be classified into three subtypes according to their sizes and were named as subtype I, subtype II, and subtype III, respectively. The PCR products of subtype I ranged from 648 to 650 bp and possessed 1 repeat of R2 and 1 repeat of R3, so subtype I was equal to type A reported by Yamaoka *et al*.[13]. The predominance of subtype I strains (93.2%) in this study was in agreement with that of type A strains (93.5%) in Japanese patients[13]. The size and genetic structure of subtype III indicated that subtype III in this study was equal to type C in Japanese strains[13]. Three (including 2 multiple subtypes strains) of 132 *cagA*-positive strains presented subtype III, and the prevalence of this subtype (2.3%) was close to that of type C (4.5%). In contradiction to the two above-mentioned subtypes, subtype II having the size of PCR product of 705-707 bp and the structure of 2 repeats of R2 and 1 repeat of R3 has not been reported before. Because sequence analysis showed that the structure of subtype II still accorded with the characteristics of 3' region of *cagA* gene in Asian strains, subtype II in this study was regarded as a new subtype of 3' region of *cagA* gene in Asian *H pylori* strains. The fact that we did not find type B and type D reported by Yamaoka *et al*.[13], but discovered a new subtype revealed the diversity and randomicity of the assembling mode of repeat regions located at 3' region of *cagA* gene and the possibility that this assembling mode varied in *H pylori* strains isolated from different areas. In addition, 2 strains presenting more than one subtype were observed in this study and thought to be from the patients with multiple *H pylori* infection. Sequence analysis revealed high similarities between the sequences of 3' region of *cagA* gene in *H pylori* isolated from Zhejiang Province and those in *H pylori* strains from Japanese patients and high similarities among the 6 subtype II strains, so we could draw a conclusion that despite of the genetic diversity of 3' region of *cagA* gene in *H pylori* strains isolated from Zhejiang Province, the sequences of the same subtype were still conservative. There were no significant differences among the subtypes of 3' region of *cagA* gene in different groups of gastroduodenal diseases, so the subtypes of 3' region of *cagA* gene in *H pylori* isolated from Zhejiang Province seemed not to be correlated with the clinical outcomes of *H pylori* infection.

In conclusion, there are three subtypes of 3' region of *cagA* gene in *H pylori* strains isolated from Zhejiang Province. Subtype I is a predominant one and subtype II is a newly found subtype of Asian *H pylori* strains. The result of this study does not support the view that the subtypes of 3' region of *cagA* gene in *H pylori* isolated from Zhejiang Province are correlated with the clinical outcomes of *H pylori* infection.

REFERENCES

1 **Blaser MJ**. Ecology of *Helicobacter pylori* in the human stomach. *J Clin Invest* 1997; **100**: 759-762
2 **Perng CL**, Lin HJ, Lo WC, Tseng GY, Sun IC, Ou YH. Genotypes of *Helicobacter pylori* in patients with peptic ulcer bleeding. *World J Gastroenterol* 2004; **10**: 602-605
3 **Dunn BE**, Cohen H, Blaser MJ. *Helicobacter pylori*. *Clin Microbiol Rev* 1997; **10**: 720-741
4 **Kidd M**, Lastovica AJ, Atherton JC, Louw JA. Heterogeneity in the *Helicobacter pylori vacA* and *cagA* genes: association with gastroduodenal disease in South Africa? *Gut* 1999; **45**: 499-502
5 **Gunn MC**, Stephens JC, Stewart JA, Rathbone BJ, West KP. The significance of *cagA* and *vacA* subtypes of *Helicobacter pylori* in the pathogenesis of inflammation and peptic ulceration. *J Clin Pathol* 1998; **51**: 761-764
6 **Henriksson AE**, Edman AC, Nilsson I, Bergqvist D, Wadstrom T. *Helicobacter pylori* and the relation to other risk factors in patients with acute bleeding peptic ulcer. *Scand J Gastroenterol* 1998; **33**: 1030-1033
7 **Olbe L**, Fandriks L, Hamlet A, Svennerholm AM. Conceivable mechanisms by which *Helicobacter pylori* provokes duodenal ulcer disease. *Baillieres Best Pract Res Clin Gastroenterol* 2000; **14**: 1-12
8 **Dore MP**, Graham DY. Pathogenesis of duodenal ulcer disease: the rest of the story. *Baillieres Best Pract Res Clin Gastroenterol* 2000; **14**: 97-107
9 **Censini S**, Lange C, Xiang Z, Crabtree JE, Ghiara P, Borodovsky M, Rappuoli R, Covacci A. *Cag*, a pathogenicity island of *Helicobacter pylori*, encodes type I-specific and disease-associated virulence factors. *Proc Natl Acad Sci U S A* 1996; **93**: 14648-14653
10 **Akopyants NS**, Clifton SW, Kersulyte D, Crabtree JE, Youree BE, Reece CA, Bukanov NO, Drazek ES, Roe BA, Berg DE. Analyses of the *cag* pathogenicity island of *Helicobacter pylori*. *Mol Microbiol* 1998; **28**: 37-53
11 **Qiao W**, Hu JL, Xiao B, Wu KC, Peng DR, Atherton JC, Xue H. *cagA* and *vacA* genotype of *Helicobacter pylori* associated with gastric diseases in Xi'an area. *World J Gastroenterol* 2003; **9**: 1762-1766
12 **Rota CA**, Pereira-Lima JC, Blaya C, Nardi NB. Consensus and variable region PCR analysis of *Helicobacter pylori* 3' region of *cagA* gene in isolates from individuals with or without peptic ulcer. *J Clin Microbiol* 2001; **39**: 606-612
13 **Yamaoka Y**, Kodama T, Kashima K, Graham DY, Sepulveda AR. Variants of the 3' region of the *cagA* gene in *Helicobacter pylori* isolates from patients with different *H pylori*-associated diseases. *J Clin Microbiol* 1998; **36**: 2258-2263
14 **Fang PC**, Zhu YL, Yin X, Wu QD, Lan MG, Wu PJ. Study on ECY blood-free medium for the isolation of *Helicobacter pylori*. *Zhonghua Yixue Jianyan Zazhi* 1993; **16**: 131-133
15 **Dore MP**, Sepulveda AR, El-Zimaity H, Yamaoka Y, Osato MS, Mototsugu K, Nieddu AM, Realdi G, Graham DY. Isolation of *Helicobacter pylori* from sheep-implications for transmission to humans. *Am J Gastroenterol* 2001; **96**: 1396-1401
16 **Xu C**, Li ZS, Tu ZX, Xu GM, Gong YF, Man XH. Distribution of *cagG* gene in *Helicobacter pylori* isolates from Chinese patients with different gastroduodenal diseases and its clinical and pathological significance. *World J Gastroenterol* 2003; **9**: 2258-2260
17 **Danesh J**. *Helicobacter pylori* infection and gastric cancer: systematic review of the epidemiological studies. *Aliment Pharmacol Ther* 1999; **13**: 851-856
18 **Higashi H**, Tsutsumi R, Fujita A, Yamazaki S, Asaka M, Azuma T, Hatakeyama M. Biological activity of the *Helicobacter pylori* virulence factor *cagA* is determined by variation in the tyrosine phosphorylation sites. *Proc Natl Acad Sci U S A* 2002; **99**: 14428-14433
19 **Watanabe T**, Tada M, Nagai H, Sasaki S, Nakao M. *Helicobacter pylori* infection induces gastric cancer in mongolian gerbils. *Gastroenterology* 1998; **115**: 642-648
20 **Uemura N**, Okamoto S, Yamamoto S, Matsumura N, Yamaguchi S, Yamakido M, Taniyama K, Sasaki N, Schlemper RJ. *Helicobacter pylori* infection and the development of gastric cancer. *N Engl J Med* 2001; **345**: 784-789
21 **Abasiyanik MF**, Sander E, Salih BA. *Helicobacter pylori* anti-CagA antibodies: prevalence in symptomatic and asymptomatic subjects in Turkey. *Can J Gastroenterol* 2002; **16**: 527-532
22 **Covacci A**, Censini S, Bugnoli M, Petracca R, Burroni D, Macchia G, Massone A, Papini E, Xiang Z, Figura N, Rappuoli R. Molecular characterization of the 128-kDa immunodominant antigen of *Helicobacter pylori* associated with cytotoxicity and duodenal ulcer. *Proc Natl Acad Sci U S A* 1993; **90**: 5791-5795
23 **Tummuru MK**, Cover TL, Blaser MJ. Cloning and expression of a high-molecular-mass major antigen of *Helicobacter pylori*: evidence of linkage to cytotoxin production. *Infect Immun* 1993; **61**: 1799-1809
24 **Rudi J**, Kolb C, Maiwald M, Kuck D, Sieg A, Galle PR, Stremmel W. Diversity of *Helicobacter pylori vacA* and *cagA* genes and relationship to *VacA* and *cagA* protein expression, cytotoxin production, and associated diseases. *J Clin Microbiol* 1998; **36**: 944-948
25 **Maeda S**, Ogura K, Yoshida H, Kanai F, Ikenoue T, Kato N,

Shiratori Y, Omata M. Major virulence factors, *VacA* and *cagA*, are commonly positive in *Helicobacter pylori* isolates in Japan. *Gut* 1998; **42**: 338-343

26 **Miehlke S**, Kibler K, Kim JG, Figura N, Small SM, Graham DY, Go MF. Allelic variation in the *cagA* gene of *Helicobacter pylori* obtained from Korea compared to the United States. *Am J Gastroenterol* 1996; **91**: 1322-1325

27 **Pan ZJ**, van der Hulst RW, Feller M, Xiao SD, Tytgat GN, Dankert J, van der Ende A. Equally high prevalences of infection with *cagA*-positive *Helicobacter pylori* in Chinese patients with peptic ulcer disease and those with chronic gastritis-associated dyspepsia. *J Clin Microbiol* 1997; **35**: 1344-1347

28 **Shimoyama T**, Fukuda S, Tanaka M, Mikami T, Saito Y, Munakata A. High prevalence of the *cagA*-positive *Helicobacter pylori* strains in Japanese asymptomatic patients and gastric cancer patients. *Scand J Gastroenterol* 1997; **32**: 465-468

29 **Peek RM Jr**, Miller GG, Tham KT, Perez-Perez GI, Cover TL, Atherton JC, Dunn GD, Blaser MJ. Detection of *Helicobacter pylori* gene expression in human gastric mucosa. *J Clin Microbiol* 1995; **33**: 28-32

30 **Perez-Perez GI**, Bhat N, Gaensbauer J, Fraser A, Taylor DN, Kuipers EJ, Zhang L, You WC, Blaser MJ. Country-specific constancy by age in *cagA*+ proportion of *Helicobacter pylori* infections. *Int J Cancer* 1997; **72**: 453-456

31 **Yamaoka Y**, Osato MS, Sepulveda AR, Gutierrez O, Figura N, Kim JG, Kodama T, Kashima K, Graham DY. Molecular epidemiology of *Helicobacter pylori*: separation of *H pylori* from East Asian and non-Asian countries. *Epidemiol Infect* 2000; **124**: 91-96

32 **Yamaoka Y**, Graham DY. Clarifications regarding the 3' repeat region of the *cagA* gene in *Helicobacter pylori* and clinical outcome. *J Clin Microbiol* 2001; **39**: 2369-2370

33 **You JF**, Fang PC, Ye SJ, Mao HY, Zhou LF, Qiu X. *Helicobacter pylori cagA*, *vacA* and *iceA* status of Zhejiang province and relationship to clinical outcomes. *Zhonghua Weishengwuxue He Mianyixue Zazhi* 2003; **23**: 111-112

Edited by Kumar M and Wang XL **Proofread by** Xu FM

PO Box 2345, Beijing 100023, China
Fax: +86-10-85381893
E-mail: wjg@wjgnet.com www.wjgnet.com

World J Gastroenterol 2004;10(22):3289-3291
World Journal of Gastroenterology
 ISSN 1007-9327

Pathogenicty and immune prophylaxis of cag pathogenicity island gene knockout homogenic mutants

Huan-Jian Lin, Jing Xue, Yang Bai, Ji-De Wang, Ya-Li Zhang, Dian-Yuan Zhou

Huan-Jian Lin, Jing Xue, Yang Bai, Ji-De Wang, Ya-Li Zhang, Dian-Yuan Zhou, PLA Institute of Digestive Medicine, Nan Fang Hospital, the First Military Medical University, Guangzhou 510515, Guangdong Province, China
Correspondence to: Dr. Huan-Jian Lin, Institute for Digestive Medicine, Nan Fang Hospital, the First Military Medical University, Guangzhou 510515, Guangdong Province, China. xj0302@fimmun.com
Received: 2003-06-16 **Accepted:** 2003-08-25

Abstract

AIM: To clarify the role of cag pathogenicity island (cagPAI) of *Helicobacter pylori* (*H pylori*) in the pathogenicity and immune prophylaxis of *H pylori* infection.

METHODS: Three pairs of *H pylori* including 3 strains of cagPAI positive wildtype bacteria and their cagPAI knockout homogenic mutants were utilized. *H pylori* binding to the gastric epithelial cells was analyzed by flow cytometry assays. Apoptosis of gastric epithelial cells induced by *H pylori* was determined by ELISA assay. Prophylaxis effect of the wildtype and mutant strains was compared by immunization with the sonicate of the bacteria into mice model.

RESULTS: No difference was found in the apoptasis between cagPAI positive and knockout *H pylori* strains in respective of the ability in the binding to gastric epithelial cells as well as the induction of apoptosis. Both types of the bacteria were able to protect the mice from the infection of *H pylori* after immunization, with no difference between them regarding to the protection rate as well as the stimulation of the proliferation of splenocytes of the mice.

CONCLUSION: The role of cagPAI in the pathogenicity and prophylaxis of *H pylori* infection remains to be cleared.

Lin HJ, Xue J, Bai Y, Wang JD, Zhang YL, Zhou DY. Pathogenicty and immune prophylaxis of cag pathogenicity island gene knockout homogenic mutants. *World J Gastroenterol* 2004; 10(22): 3289-3291
http://www.wjgnet.com/1007-9327/10/3289.asp

INTRODUCTION

Helicobacter pylori (*H pylori*) infected over half of human adults in the world, especially in Asian-Pacific countries. Only a small portion of patients display clinical symptoms such as peptic ulcer and gastric cancer[1-14]. The difference between the infection and the outcomes is determined by both bacterial factors and host responses. Among the bacterial factors, cag pathogenicity island (PAI) had been studied widely, while the immune response to the infection is the overwhelming host factor that affects the outcome of infection. In respect of the bacterial factors, cytotoxin associated gene A (cag A) protein is usually considered as a toxic marker of the bacterium. A related gene cluster, PAI encodes several proteins with the similar biological activities. To define the relationship bwteen cagPAI and the pathogenicity of *H pylori*, three pairs of *H pylori* haboured cagPAI and their isogenic PAI knockout mutants were utilized. Their roles in the binding and apoptosis inducing activities as well as the immune protection were compared *in vivo* and *in vitro*.

MATERIALS AND METHODS

Materials

CT, PKH26, PMA and Ionomycin were obtained from Sigma Co. U.S.A; granulocyte-macrophage-colony-stimulating-faction (GM-CSF) enzyme linked immunosorbent assay (ELISA) kit was bought from Boehringer-Mannheim Co. German; Three pairs of *H pylori* habouring cagPAI and their isogenic PAI knockout mutants were provided kindly by Professor Peter B Ernst from DyKesas University USA; *H pylori* strains and gastric epithelial cells (Kato-III) were from the Research Institute of Digestive Disease, Nanfang Hospital, First Military Medical University in Guanzhou , China. *H pylori* strains are showed in Table 1.

Table 1 cagA positive wildtype bacteria and their cagA knockout homogenic mutants

H pylori	cagPAI
LC11	+ wildtype
AH244	knockou cagPAI knockout of LC11
84183	+ wildtype
2-1	knockou cagPAI knockout of 84183
26695	+ wildtype
8-1	knockou cagPAI knockout of 26695

Methods

***H pylori* culture and *H pylori* sonicate (SON) preparation were performed by standard procedures** There was no difference between the groups of wildtype and knockout bacteria in the rate of growing (Figure 1).

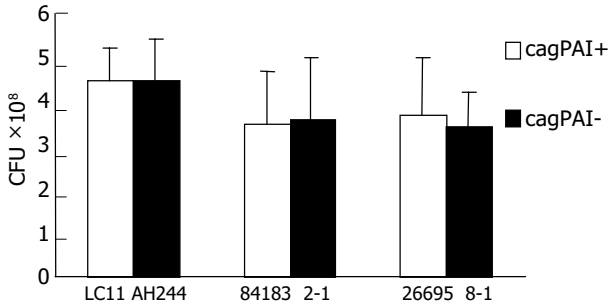

Figure 1 Eqivalent growth of wildtype and knockout strains after 2 d culture.

Flow cytometry was used to detect adhesion of *H pylori* binding to gastric epithelial cells *H pylori* strain (ATCC26695) was marked by 10 mL/L PKH-26 and washed three times. The liqiud after the third washing was used in the control groups, then bound to gastric epithelial cells (KatoIII) (bactria/cells = 300:1), and incubated at 37 ℃ for 60 min. After washed, the sample was detected by FACs.

ELISA was used to detect apoptosis of gastric epithelial cells induced by *H pylori* The basic mechanism was to detect the release of DNA combined histone. Accroding to the recommended procedures, cracked Kato-III cells with anti-histone monoclonal antibody were incubated and color was developed after adding substrate. Absorbency at the 405 nm level was measured in the enzyme-tagging instrument. Then, the apoptotic index (AI) was calculated in comparison with control group.

Mice were divided into 4 groups, five mice each group,except for the natural death. PBS Group: 200 μL PBS /one mouse was fed once via mouth as negative control; CT Group: CT (10 μg) 200 μL/per mouse was fed once via mouth as adjuvant control Group; CagPAI positive Group: ultrasonic smashed *H pylori* 26695 (100 μL)and CT (10 μg) was fed at a time via mouth; CagPAI negative Group: ultrasonic smashed *H pylori* 8-1 (100 μL) and CT (10 μg) were fed once via mouth.

Immunity procedures

Before immunization and inoculation of *H pylori*, the mice were prohibited from water and food for over 12 h. Thirty min before inoculation, the mouse was fed with 200 μL (0.01 mol/L) $NaHCO_3$ solution to neutralize gastric acid. The experimental group and the control group were inoculated with antigens and adjuvants, immunized on d 0, 7, and 14. They were allowed to drink water 1 h after immunization. Each group was attacked with *H pylori* 10^8CFU once every other day, 3 wk after the latest immunization. The mice were killed 8 wk after the latest attack.

Evaluation of bacterial implantation

The spleen and stomach were removed immediately after the mouse neck was broke. The spleen was kept in the axenic cell culture media temporarily and dealt with it for 4 h. The stomach was cut along the greater curvature, washed with axenic fluid, then some tissues were sampled for rapid urea enzyme test and histological examination. Histological examination was graded semi-quantitatively according to the standard as follows: 0 point: no *H pylori*; 1 point: 1-2 *H pylori* in some gastric pits; 2 points: 3-10 *H pylori* in majority of gastric pits and 3 points: over 10 *H pylori* in majority of gastric pits.

Spleen cell proliferation text

Spleen tissue was triturated into homogenates at asepsis environment. The spleen cells were counted and implanted in the 96 well plate (2×10^5 cells/well) containing 500 ng/mL PMA and 10 ng/mlionomycin RPMI1640 (including cow blood serum, mycillin, Hepes *ect*), *H pylori* ultrasonic smashed antigen was added into them in terms of 2.5, 5, 10 mg/mL, cultured for 24 h, then H^3-thymidine was added, and cultured for 8 h, then the celt were collected and degraded. Each control group was compared with the blank control group in the count, and the proliferation quotiety was calculated. Differential proliferation quotiety epuals each group's proliferation quotiety/PBS group's proliferation quotiety ×100%.

Statistical analysis

Data and their variance were analyzed using EXCEL software. $P<0.05$ was considered statistically significant.

RESULTS

Adherence of CagPAI and H pylori

CagPAI positive culture and mutant strains showed a different bacteria/cell ratio, and were, marked with PKH26, then they were incubated with stomach cell Kato-III, the adherence ability was measured with flow cytometry positive cells and mean fluorescence intensity (MFI) were calculated. No difference was found between wild strain and mutant strain. The result was displayed in Figure 2.

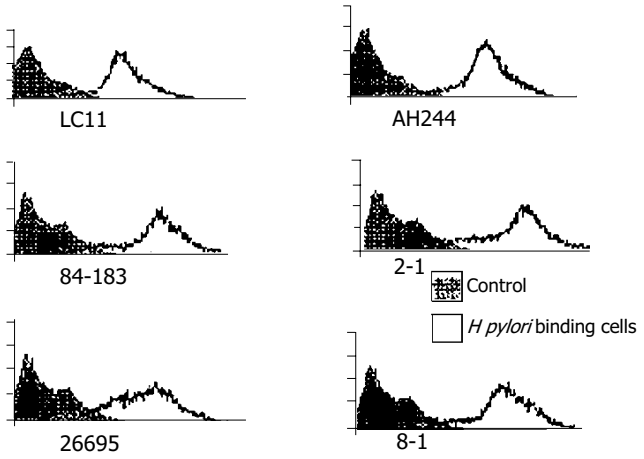

Figure 2 Binding of cag PAI wildtype *H pylori* and their mutant to gastric epithelial cell Kato-III.

Apoptosis-induced ability of cagPAI and H pylori

CagPAI and mutant strain were cultured with gastric epithelia cells at the ratio 300:1 for 24 h. The cells were degeaded, the cell apoptosis was detected by ELISA. We found that the apoptosis-induced ability of 26 695 was slighty higher than that of 8-1 strain, and no diffirence was found in other couples. The result is displayed in Figure 3.

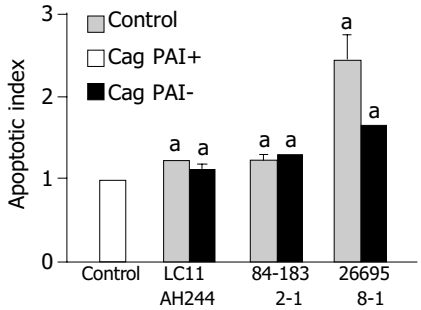

Figure 3 Apotosis of gastric epithelial cells induced by positive cagPAI and knockout *H pylori strains* (determined by ELISA $^aP<0.05$ *vs* the control).

Immune prevention to the cagPAI and H pylori

The protection rate of groups PBS ,CT, 26695 and 8-1 was 0%, 0%, 40%. 60% (Table 2). CagPAI positive strain ATCC26695 and mutant strain 8-1 companied with mucous membrane adjuvant choleratoxin prevented *H pylori* from growing in the stomach of mice. There was no difference between the CagPAI positive strain and CagPAI negative strain. We found that full-protect rate of the two *H pylori* immune group was only 20% or so. It was found that immune was apparently decrease in semi-quantitative counting. No obvious difference was found between groups, and CT grouphad no prevention effect. The result is displayed in Figure 4.

Table 2 Ultrasonic smashed substance's protection against mice *H pylori* (result of urease test)

Immune project	Urease test (+)/number of animals (piece)	Protecting ratio (%)
PBS	5/5	0
CT	5/5	0
26695 SON+CT	3/5	40[a]
8-1 SON+CT	2/5	60

$^aP<0.05$, *vs* control groups.

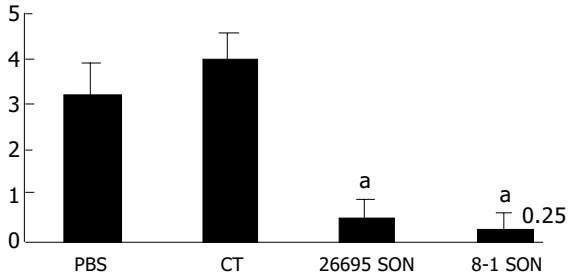

Figure 4 Semi-quantatative results of bacteria by histological examination. [a]$P<0.05$ *vs* PBS control.

cagPAI and cell Immune of mice H pylori

Comparing with PBS control, the CT control number of spleen cells was slightly increased, but that of two *H pylori* antigen-immune groups was greatly increased. The number of CagPAI mutant strains was more obvious. Compared with the two groups, no difference was found, ($P<0.05$, Figure 5).

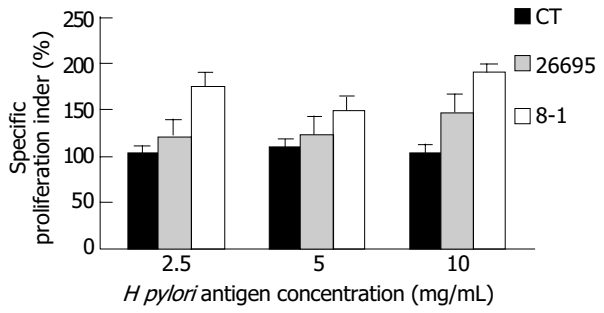

Figure 5 Specific proliferation index of immunized mice (compared to PBS group).

DISCUSSION

CagA is cytotoxin correlative protein, which is one of *H pylori* nosogenetic factors. The PAI is regarded as one of the signs of *H pylori* infection. Early researches found that this positive sign was higher in peptic ulcer and gastric carcinoma than in gastritis. For example, foreign reseachers found that anti-CagPAI in serum was positive in 93% of the gastric carcinoma patients[2], it is different in Asian-Pacitic area, the positive ratio of the bacterial strain was much higher. A large number of reports approved that the pathogenicity of CagA (+) was stronger than that of CagA (-), inducing the production of IL-8 and GRO-α, ENA78 could produce and activated related nucleic transcription factors[3]. Few reports about comparson of wildtype strain isogenic mutant strain *in vitro* were available. We studied three pairs of cagPAI wildtype strain and cagPAI gene-knockout mutant strain constructed by Dr. Bery. No difference was found between the growing speed and activity of the two strains.

Therer were many gene produces concerned with *H pylori* adherence, including NLBH, porins, BabA *etc*[4-9]. Our study showed that there was no difference in adherence to the epithelia of stomach between cagPAI (+) strain and cagPAI (-) strain.

CagPAI (+) strain could cause apoposis and proliferation in stomach epithelia[10]. However, it was proved by ELISA in our research that *in vitro* cagPAI was not concerned with apoptosis-induced ability, which did agree with the result of Le'Negrate. They found that cagE in cagPAI participated in the prosess of Fas-induced *H pylori* causing stomach epithelial apoptosis due to different the strain. we chose two stains in three pairs of strains, so the result was probably accurate.

In the immune prevention of *H pylori* infection, it was reported that cagA could prevent infection of the cagPAI (+). In our research, SS1 strain which was used to infect animals was cag (+) strain, but we found that there was no difference in preventive effect between cagPAI (+) strain and mutant strain. Although there was no statistical difference, mutant stain had a higher protective trend. It showed that the immune prevention was not caused by protein coded by cagPAI. We do not support regarding cagPAI gene product is immune antigen of *H pylori* bacterin.

Cellular immunity, especially $CD4^+$T cellular immunity is a very important mechanism , which can help B cells produce sIgA. We selected the spleen cell proliferation test as the target in immune. Because B cells could not live *in vitro*, the proliferation cells were mainly T cells. Both cagPAI (+) and cagPAI (-) strain were stimulated to proliferate T cells, indicating that some special T cells clones are existed in spleen cells. The number of cagPAI mutant strains is more than that of cagPAI (+) strains, agreeing with the histology.

The effect of cagPAI on *H pylori* immune and pathogenesis is very complex and needs further study.

REFERENCES

1 **Bai Y,** Zhang YL, Wang JD, Zhang ZS, Zhou DY. Construction of the non-resistant attenuated Salmonella typhimurium strain expressing *Helicobacter pylori* catalase. *Diyi Junyi Daxue Xuebao* 2003; **23**: 101-105
2 **Vandenplas Y.** *Helicobacter pylori* infection. *World J Gastroenterol* 2000; **6**: 20-31
3 **Blaser MJ.** Hypothesis: the changing relationships of *Helicobacter pylori* and humans: implications for health and disease. *J Infect Dis* 1999; **179**: 1523-1530
4 **Covacci A,** Censini S, Bugnoli M, Petracca R, Burroni D, Macchia G, Massone A, Papini E, Xiang Z, Figura N, Rappuoli R. Molecular characterization of the 128-kDa immunodominant antigen of *Helicobacter pylori* associated with cytotoxicity and duodenal ulcer. *Proc Natl Acad Sci U S A* 1993; **90**: 5791-5795
5 **Blaser MJ,** Perez-Perez GI, Kleanthous H, Cover TL, Peek RM, Chyou PH, Stemmermann GN, Nomura A. Infection with *Helicobacter pylori* strains possessing CagA is associated with an increased risk of developing adenocarcinoma of the stomach. *Cancer Res* 1995; **55**: 2111-2115
6 **Odenbreit S,** Puls J, Sedlmaier B, Gerland E, Fischer W, Haas R. Translocation of *Helicobacter pylori* CagA into gastric epithelial cells by type IV secretion. *Science* 2000; **287**: 1497-1500
7 **Bai Y,** Dan HL,Wang JD, Zhang ZS, Odenbreit S, Zhou DY, Zhang YL. Cloning, expression, purification and identification of conservative region of four *Helicobacter pylori* adhesin genes in AlpA gene. *Prog Biochem Biophys* 2002; **29**: 922-926
8 **Bai Y,** Zhany YL, Chen Y, Wang JD, Zhou DY. Study of Immunogenicity and safety and adherence of conservative region of four *Helicobacter pylori* adhesin *in vitro*. *Prog Biochem Biophys* 2003; **30**: 422-426
9 **Bai Y,** Zhang YL, Wang JD, Zhang ZS, Zhou DY. Cloning and immunogenicity of conservative region of adhesin gene of *Helicobacter pylori*. *Zhonghua Yixue Zazhi* 2003; **83**: 736-739
10 **Bai Y,** Wang JD, Zhang ZS, Zhang YL. Construction of the Attenuated Salmonella typhimurium strain expressing *Helicobacter pylori* conservative region of adhesin antigen. *Chin J Biotech* 2003; **19**: 77-82
11 **Bai Y,** Chang SH, Wang JD, Chen Y, Zhang ZS, Zhang YL. Construction of the *E.coli* clone expressing adhesin BabA of *Helicobacter pylori* and evaluation of the adherence activity of BabA. *Diyi Junyi Daxue Xuebao* 2003; **23**: 293-295
12 **Bai Y,** Zhang YL, Wang JD, Lin HJ, Zhang ZS, Zhou DY. Conservative region of the genes encoding four adhesins of *Helicobacter pylori*: cloning, sequence analysis and biological information analysis. *Diyi Junyi Daxue Xuebao* 2002; **22**: 869-871
13 **Rudnicka W,** Covacci A, Wadstrom T, Chmiela M. A recombinant fragment of *Helicobacter pylori* CagA affects proliferation of human cells. *J Physiol Pharmacol* 1998; **49**: 111-119
14 **Wang RX,** Zhang LY, Yin DL, Mufson RA, Shi Y. Protein kinase C regulates fas (CD95/APO-1) expression. *J Immunol* 1998; **161**: 2201-2207

Edited by Wang XL and Zhang JZ **Proofread by** Xu FM

PO Box 2345, Beijing 100023, China
Fax: +86-10-85381893
E-mail: wjg@wjgnet.com www.wjgnet.com

World J Gastroenterol 2004;10(22):3292-3298
World Journal of Gastroenterology
 ISSN 1007-9327

• BASIC RESEARCH •

Mechanisms mediating cholinergic antral circular smooth muscle contraction in rats

Helena F Wrzos, Tarun Tandon, Ann Ouyang

Helena F Wrzos, Tarun Tandon, Ann Ouyang, Division of Gastroenterology and Hepatology, Department of Medicine, College of Medicine, Pennsylvania State University, USA
Supported by NIH grant RO1-DK-34148
Correspondence to: Ann Ouyang, Division of Gastroenterology and Hepatology, Department of Medicine, College of Medicine, Pennsylvania State University, PO Box 850, Hershey, PA 17033, USA. aouyang@psu.edu
Telephone: +717-531-8741 **Fax:** +717-531-6770
Received: 2004-01-15 **Accepted:** 2004-02-13

Abstract

AIM: To investigate the pathway (s) mediating rat antral circular smooth muscle contractile responses to the cholinomimetic agent, bethanechol and the subtypes of muscarinic receptors mediating the cholinergic contraction.

METHODS: Circular smooth muscle strips from the antrum of Sprague-Dawley rats were mounted in muscle baths in Krebs buffer. Isometric tension was recorded. Cumulative concentration-response curves were obtained for (+)-cis-dioxolane (cD), a nonspecific muscarinic agonist, at 10^{-8}-10^{-4} mol/L, in the presence of tetrodotoxin (TTX, 10^{-7} mol/L). Results were normalized to cross sectional area. A repeat concentration-response curve was obtained after incubation of the muscle for 90 min with antagonists for M1 (pirenzepine), M2 (methoctramine) and M3 (darifenacin) muscarinic receptor subtypes. The sensitivity to PTX was tested by the ip injection of 100 mg/kg of PTX 5 d before the experiment. The antral circular smooth muscles were removed from PTX-treated and non-treated rats as strips and dispersed smooth muscle cells to identify whether PTX-linked pathway mediated the contractility to bethanechol.

RESULTS: A dose-dependent contractile response observed with bethanechol, was not affected by TTX. The pretreatment of rats with pertussis toxin decreased the contraction induced by bethanechol. Lack of calcium as well as the presence of the L-type calcium channel blocker, nifedipine, also inhibited the cholinergic contraction, with a reduction in response from 2.5±0.4 g/mm^2 to 1.2±0.4 g/mm^2 (P<0.05). The dose-response curves were shifted to the right by muscarinic antagonists in the following order of affinity: darifenacin (M_3)>methocramine (M_2)>pirenzepine (M_1).

CONCLUSION: The muscarinic receptors-dependent contraction of rat antral circular smooth muscles was linked to the signal transduction pathway(s) involving pertussis-toxin sensitive GTP-binding proteins and to extracellular calcium via L-type voltage gated calcium channels. The presence of the residual contractile response after the treatment with nifedipine, suggests that an additional pathway could mediate the cholinergic contraction. The involvement of more than one muscarinic receptor (functionally predominant type 3 over type 2) also suggests more than one pathway mediating the cholinergic contraction in rat antrum.

Wrzos HF, Tandon T, Ouyang A. Mechanisms mediating cholinergic antral circular smooth muscle contraction in rats. *World J Gastroenterol* 2004; 10(22): 3292-3298
http://www.wjgnet.com/1007-9327/10/3292.asp

INTRODUCTION

The mechanisms involved in the regulation of cholinergic contraction of intestinal smooth muscle are complex and not fully understood, despite the important role of the cholinergic system in the physiology of gastric emptying, and pathophysiology of several motility disorders. Cholinergic agonists activate muscarinic receptors which transduce cholinergic signals by activating G proteins[1,2]. Different signal transduction pathways in different species, as well as different pathways for the circular and longitudinal layers of intestinal smooth muscle have been reported[3-15].

Specific muscarinic receptors are abundantly present in the smooth muscles of gastrointestinal tract[16-22]. Muscarinic receptor subtypes have shown a G-protein coupling specificity, however the published data are inconsistent. In some studies M_1, M_3, M_5 receptor subtypes were preferentially coupled to the Gq/11 protein class, the M_2 and M_4 receptors were linked to the PTX-sensitive Gi/Go proteins[23-25], Whereas in other studies muscarinic M_2 receptors were insensitive to pertussis toxin[26].

Relatively few references are published characterizing rat stomach muscarinic receptor subtypes, again with conflicting results. Prevalence of M_3[13,22,27], or of M_1[28], or M_2 receptors[29-33] has been reported. Which muscarinic receptor is more functionally important in the cholinergic contraction of antral circular muscle has not been determined.

The aim of this study was to examine the signal transduction pathway (s) mediating rat antral smooth muscle cholinergic contraction to fill the existing knowledge gaps: (1) what type of calcium channel was involved and was there a dependence on extracellular Ca^{2+} influx; (2) whether PTX-sensitive- or PTX-insensitive-G proteins coupled to muscarinic receptors were involved; and (3) what subtypes of specific muscarinic receptors were functionally involved. Determining the physiology of the pathway (s) mediating cholinergic contraction of the antrum should be helpful in understanding the functional motility changes described in models of disease conditions, such as diabetes[34-36]. Preliminary accounts of some of these observations have been published in abstract form[37,38].

MATERIALS AND METHODS

Animals

Young adult male Sprague-Dawley rats (Charles River Breeding Laboratories), weighing 200-450 g were used. Animals were anesthetized by ip injection of sodium pentobarbital (30-65 mg/kg). Anesthesia was given immediately before the tissue removal to avoid the effect of anesthesia on the contractile properties of the tissue. The abdomen was explored through midline incision and the stomach was removed. After the tissue was removed, animals were euthanized by injection of an overdose of pentobarbital. All our studies were approved by the Institutional Animal Care and Use Committee of the PSU College of Medicine.

Smooth muscle strip bath preparation[39]

The antrum tissue was pinned in a dissecting dish in oxygenated Krebs solution, mucosa was gently removed by scraping, and strips were cut in the circular muscle orientation. The muscle was oxygenated in Krebs physiological buffer containing (in mmol/L) 130 Na, 4.7 K, 2.5 Ca, 1.0 Mg_2, 140.7 Cl, 19 HCO_3, 1.0 PO_4 and 10 glucose at 37 ℃. The strips were sutured at one end to a glass rod and at the other end to an inelastic wire. The tissue, the rod and a wire were placed in a 10-mL double walled glass chamber with a constant temperature 37 ℃. Glass surfaces were silicone coated with Sigmacote to prevent binding of the peptides. The chambers were filled with 5 mL of Krebs buffer and gassed with 95:5 mixture of O_2/CO_2. The free end of wire was attached to an isometric force transducer (Grass Instrument Co) and recordings were made on a multichannel rectilinear dynograph recorder (Beckman Instruments). The strips were allowed to equilibrate for 1 h. Tissues were stretched to an initial length (L_i) from which any additional stretch resulted in an increase in tension. The isometric tension response to bethanechol (10^{-4} mol/L) was noted. The strips were rinsed and the length increased by 1 mm increment until the maximum response to bethanechol (10^{-4} mol/L) was recorded. This length was labeled Lo. All subsequent studies were conducted at this length. Drugs were added to the tissue bath and the peak response within 8 min was compared with the maximum tension recorded during 5 min before addition of drugs. Antagonists were added 1 min before the addition of agonist. The peptidase inhibitors bestatin and phosphoramidon (both at 10^{-6} mol/L) were added at least 5 min before the agonist addition. The response was calculated as the change in the maximal force of contraction in g of tension normalized to the cross sectional area which was calculated as: cross section (mm^2) = weight (g)/specific density×length (mm), where the specific density of muscle tissue = 1.056 (g/mm^3).

Dispersed single muscle cell preparation[40,41]

Smooth muscle cells were isolated from the circular muscle layer of the antrum. The mucosa was removed by dissection and the longitudinal muscle layer (with enteric plexus ganglia) was removed in strips using a Stadie-Riggs tissue slicer (Thomas TM). The circular muscle layer was minced and incubated for 45 min twice in Hepes buffer containing collagenase (CLS type II, Worthington) and 0.1 g/L soybean trypsin inhibitor at 31 ℃. Partially digested strips were washed with enzyme-free Hanks' medium. Muscle cells were allowed to disperse spontaneously under the gentle force of bubbling 950 mL/L O_2+50 mL/L CO_2 for 30 min (no agitation), and then filtered through 500 μmol/L Nitinol mesh, to the culture media. Viability was checked by trypan blue exclusion test. Aliquots of cells were added to solutions containing the agonists at room temperature. The reaction was stopped after 30 min, by addition of acrolein to the final concentration of 1%. Aliquots were sealed under coverslips. Computerized image analysis (NIH Image 1.62) was used for quantification. A scale slide was used for reference. The length of single muscle cells was measured (at least 50 cells per concentration).

Contractile response of antrum smooth muscle strips to cholinergic agonist

To determine the effect of bethanechol on antrum circular smooth muscle contraction, muscle strips were exposed to the increasing doses of muscarinic agonist, bethanechol, at the concentrations of 10^{-4} to10^{-7} mol/L in an organ bath.

Characteristics of effect of extracellular Ca^{2+} and type of calcium channel involved

To determine whether cholinergic contraction depended on the influx of extracellular Ca^{2+}, the response to bethanechol chloride in the physiological Krebs buffer was tested, then the buffer was changed into Ca-free buffer (in mmol/L: NaCl 132.5; KCl 4.7; $MgCl_2$ 1.0; NaH_2PO_4 1.2; $NaHCO_3$ 20.0; D-glucose 10; EGTA (50 μmol/L), and contraction was subsequently recorded after 5 and 10 min.

To characterize the type of calcium channel involved in the cholinergic contraction, nifedipine (an L-type calcium channel antagonist) was used. Nifedipine was dissolved in ethanol and added to the physiological Krebs buffer at the concentration of 10^{-5} mol/L[42] and contraction was recorded. Statistical significance of the difference between contraction in the presence and absence of nifedipine was calculated by paired *t*-test, the results were considered statistically significant at $P \leqslant 0.05$.

Treatment with pertussis toxin (PTX)

In order to determine whether PTX-sensitive pathway was involved in cholinergic contraction, strips and dispersed muscle cells (myocytes) isolated from the antrum of PTX-pretreated and non-pretreated animals were compared.

Rats were injected with 100 mg/kg of PTX (dissolved in saline) intraperitoneally 5 d before the study[43]. Muscle strips from PTX-treated and control rats in the tissue bath were exposed to cholinergic agonist, bethanechol, at the concentration of 10^{-4} to 10^{-6} mol/L. Statistical significance of the difference between the contraction of the muscle from PTX-pretreated and non-treated rats was defined by non-paired *t*-test, the results were considered statistically significant at $P \leqslant 0.05$.

The changes in the pattern of contraction of muscle cells in dispersed cell suspension were also measured (detailed description in the "dispersed muscle cell preparation" section of Materials & Methods). Two concentrations of bethanechol (10^{-7} and 10^{-8} mol/L) were added to the cell suspensions in the tubes in the physiological buffer. Their contractions were measured as the percentage of the control cell diastolic length[44]. The mean lengths of cells from control rats were compared to those of the cells from PTX-treated animals. Results were presented as mean±SE. Statistical significance of the difference was calculated by the paired *t*-test, the results were considered statistically significant at $P \leqslant 0.05$.

Characterization of muscarinic receptor subtypes involved

For the characterization of muscarinic receptor subtypes involved in cholinergic contraction we used a non-selective muscarinic agonist, (+)-cis-Dioxolane[45,46] and relatively specific receptor subtype antagonists.

The conditions of organ bath were described above in the "Smooth muscle strip bath preparation" section of Materials and Methods. At the start of the experimental protocol, the viability of each tissue was assessed by determining the contractile response to bethanechol (10^{-4} mol/L). After washed, tissues were re-equilibrated for 10 min and allowed to regain baseline tension. Cumulative concentration-effect curves of (+)-cis-Dioxolane, (10^{-8} to 3×10^{-5} mol/L) were constructed for each tissue. Tissues were then equilibrated in either the absence (control) or presence of the antagonist for 90 min. Subsequently, a second concentration-effect curve to (+)-cis-Dioxolane was constructed. Smooth muscle strips were incubated with increasing concentrations of antagonists demonstrating a relative specificity for M_1, M_2 or M_3 muscarinic receptor subtypes (pirenzepine, methoctramine and darifenacin, respectively). Each antral smooth muscle strip was exposed to only one concentration of antagonists and incubated for 90 min at 37 ℃, with a fresh antagonist added to the medium every 30 min[47,48].

The EC_{50} values for muscarinic antagonists were obtained (i.e. antagonist concentration resulting in 50% of inhibition of the contraction induced by cholinergic agonist, (+)-cis-Dioxolane (10^{-6} mol/L).

Drugs

Tetrodotoxin (TTX), sigmacote, neurokinin A (NKA), nifedipine,

papain, peptidase inhibitors bestatin and phosphoramidon, soybean trypsin inhibitor, acrolein and pirenzepine (predominantly M_1 muscarinic receptor antagonist), were from Sigma, St. Louis, MO.

(+)-cis-dioxolane (cholinergic agonist) and methocramine (predominantly M_2 muscarinic receptor antagonist) were purchased from RBI Inc., Natick, MA. PTX was purchased from List Biological Labs, Inc., Campbell, CA. Bethanechol chloride was purchased from Merck, West Point, PA and collagenase (CLS type II) from Worthington, PA. Darifenacin (predominantly M_3 muscarinic receptor antagonist) was a generous gift from Pfizer Ltd, Sandwich, Kent, GB.

RESULTS

Dose-response curve to cholinergic agonist

A contractile dose-response was observed, when the antral circular smooth muscle strips were exposed to the increasing doses of muscarinic agonist, bethanechol, at the concentrations of 10^{-4} to 10^{-7} mol/L in an organ bath. A significant increase of the tension over the baseline was observed at the bethanechol concentrations of 10^{-4} to 10^{-6} mol/L (Figure 1, $n = 4$).

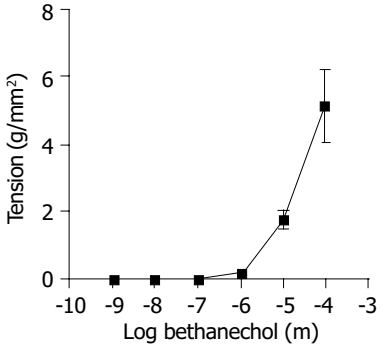

Figure 1 Effect of bethanechol on smooth muscle contraction. Antrum circular smooth muscle strips were incubated with increasing concentrations of bethanechol (10^{-4} mol/L to 10^{-7} mol/L). The vertical axis represents the developed tension (in grams per mm^2). Bethanechol significantly increased circular muscle tension ($P<0.05$; paired *t*- test). Each data point represents mean±SE, $n = 4$.

Effect of tetrodotoxin (TTX)

Antrum circular smooth muscle strips were exposed to bethanechol at the concentration of 10^{-5} mol/L, in a buffer containing tetrodotoxin (10^{-5} mol/L), added prior to bethanechol to the organ bath. The cholinergic contraction was not affected by tetrodotoxin, neuronal toxin, with the contraction at 94.9±3.2% of control.

The lack of inhibition of the contraction by TTX confirmed that a cholinergic agonist could induce contraction via muscarinic receptors present at the smooth *muscle*, without participation of neuronal factor.

Effect of calcium depletion on cholinergic contraction and characterization of a calcium channel subtype involved

Calcium-free buffer Incubation in calcium-free buffer diminished the antral contractile response to bethanechol (10^{-4} mol/L), with a reduction in response from 2.5±0.4 g/mm^2 to 1.2±0.4 g/mm^2 ($P<0.05$) after 5 min of incubation in calcium-free buffer. After 10 min of incubation in Ca^{2+} -free buffer contractile activity was almost abolished (Figure 2).

Full recovery of the contraction was seen after return of the Ca^{2+} to the tissue bath medium, indicating that there was no damage to the cell resulting in a decreased contraction. These results showed that cholinergic contraction was dependent on the presence of extracellular calcium, a receptor-operated Ca^{2+} or voltage-sensitive Ca^{2+} channels.

Effect of calcium channel blocker The L-type calcium channel blocker, nifedipine at a concentration of 10^{-5} mol/L inhibited the cholinergic contraction response of antrum to the bethanechol, at the concentration of 10^{-4} mol/L from 4.02±0.9 to 0.49±0.18 g/mm^2 ($P<0.05$), indicating that the L-calcium channel could mediate this contraction.

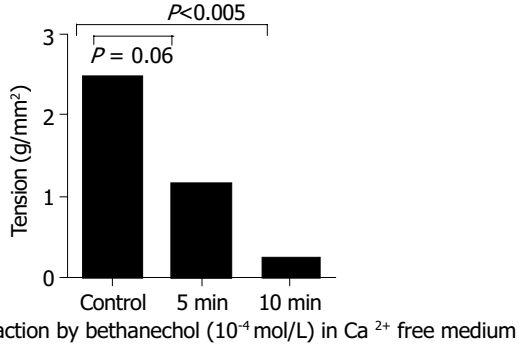

Figure 2 Effect of depletion of Ca^{2+} from medium on the contraction of antral circular smooth muscle strips to bethanechol (10^{-4} mol/L). Ca^{2+} depletion caused a significant decrease in the muscle tension; after 5 min incubation ($P<0.06$, paired *t*-test); and after 10 min incubation ($P<0.005$, paired *t*-test) compared to the base contraction induced by bethanechol before Ca^{2+} depletion. Each data point represents mean±SE, $n = 3$.

Identification of G-protein-linked signal transduction pathway by PTX

The response to bethanechol of antral circular muscle strips and dispersed smooth muscle cells from PTX-pretreated and control rats was compared (see Methods).

Smooth muscle strips The contractile response to bethanechol of the muscle strips from the PTX-pretreated animals was significantly lower than that of the muscle strip from the non-treated control rats at all concentrations, 10^{-6} to 10^{-4} mol/L (Figure 3, $P \leqslant 0.01$).

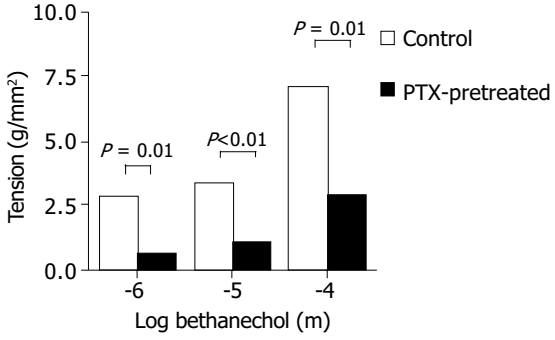

Figure 3 Effect of PTX on antrum circular smooth muscle strips contraction to bethanechol (10^{-4} mol/L to 10^{-6} mol/L). PTX significantly inhibited the contractile activity of the smooth muscle ($P \leqslant 0.01$; paired *t*-test) compared to control rats. Each point represents mean±SE, $n = 7$; dotted bars represent control animals; solid bars-PTX-pretreated animals.

The inhibiting effect of PTX on the contraction implied that cholinergic agonist was activating a PTX-sensitive pathway.

A low level of residual contractile activity was observed in the contraction of PTX-treated muscle strips suggesting either that there was a small *PTX-insensitive* fraction involved, or that the dose of PTX used was insufficient to completely inhibit PTX-sensitive pathways.

Dispersed antral smooth muscle cells When dispersed myocytes from PTX-treated rats and controls were compared, cells from PTX-pretreated rats showed significantly less contraction to

bethanechol than the cells isolated from the rats non-treated with PTX, at both bethanechol concentrations, 10^{-8} and 10^{-7} mol/L (Figure 4, $P \leqslant 0.005$). The inhibiting effect of PTX on the dispersed myocytes contraction, confirmed the smooth muscle strip data and suggested that the cholinergic agonist involved an occupation of specific muscarinic receptors coupled to PTX-sensitive mediated pathway.

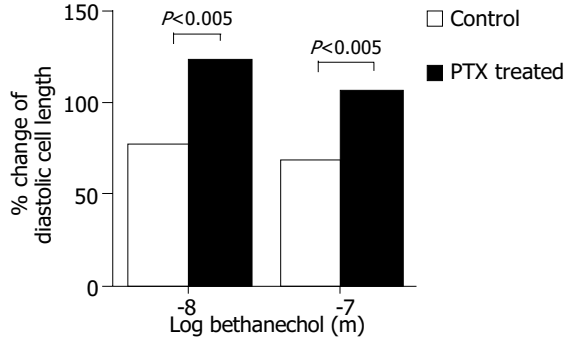

Figure 4 Effect of PTX on dispersed antral circular smooth muscle myocytes from PTX-pretreated rats contraction to bethanechol (10^{-7} mol/L and 10^{-8} mol/L). Myocytes from PTX-treated rats contracted less than myocytes from control rats. Each point represents mean±SE; of the percentage of the control cells diastolic length (no bethanechol). At least 50 myocytes per point were calculated, $P<0.005$; $n = 7$ and 11. Dotted bars represent control animals; solid bars PTX-pretreated animals.

Characterization of the type of muscarinic receptor subtypes involved in contraction to cholinergic agonist To define pharmacologically the muscarinic receptors involved in the cholinergic contraction, specific muscarinic receptor antagonists were used in the presence of tetrodotoxin (10^{-7} mol/L).

For this functional muscarinic receptor study we chose a non-selective cholinergic agonist, (+)-cis-Dioxolane (see Methods), instead of bethanechol, which has been reported to selectively stimulate M_3 receptor[45,46,49].

Pirenzepine, the M_1 muscarinic receptor antagonist, was used at the concentrations from 3×10^{-5} to 10^{-8} mol/L. Pirenzepine caused a significant inhibition of the of the contractile muscle response to the (+)-cis-dioxolane (Figure 5).

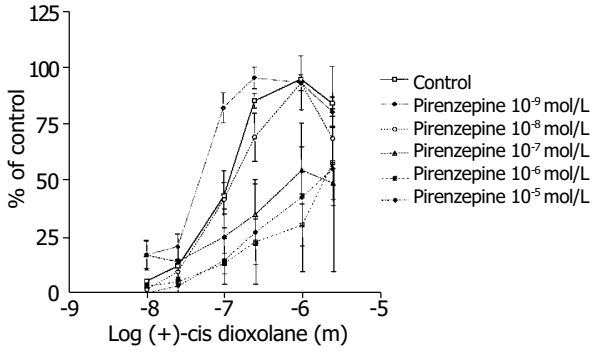

Figure 5 Concentration-response curves for the contractile effect of (+)-cis-Dioxolane alone and in combination with different concentrations of M_1 antagonist, pirenzepine (10^{-8} mol/L to 10^{-5} mol/L) on the rat antral circular smooth muscle strips. Each point represents the mean±SE, $n = 6$, 6, 7 and 8 strips. Cumulative concentration-effect curve was constructed for each strip for (+)-cis-Dioxolane, (10-^{8} to 3×10^{-5} mol/L). After washing, strips were equilibrated in either the absence (control) or presence of pirenzepine for 90 min. Subsequently, the second concentration-effect curve for (+)-cis-Dioxolane was constructed for each strip. Pirenzepine caused a significant inhibition of the contractile muscle response to (+)-cis-dioxolane.

Methocramine-M2 muscarinic receptor antagonist was used at the concentration range between 3×10^{-5} and 10^{-8} mol/L. Methocramine caused a significant inhibition of the of the contractile muscle response to the (+)-cis-dioxolane (Figure 6).

Darifenacin was used at the concentration range from 3×10^{-5} to 10^{-9} mol/L (Figure 7). Darifenacin caused a significant inhibition of the contractile muscle response to the (+)-cis-dioxolane.

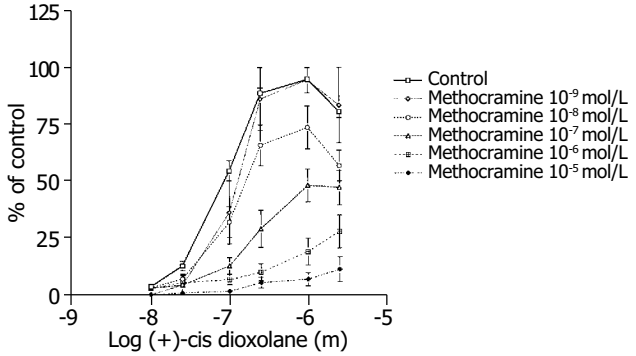

Figure 6 Concentration-response curves for the contractile effect of (+)-cis-Dioxolane alone and in combination with different concentrations of M_2 antagonist, methocramine (from 10^{-8} mol/L to 10^{-5} mol/L) on the rat antral circular smooth muscle strips. Each point represents the mean±SE; $n = 4$, 9, 10 and 11 strips. First, cumulative concentration-effect curve was constructed for each strip for (+)-cis-Dioxolane, (10^{-8} to 3×10^{-5} mol/L). After washing, tissues were equilibrated in either the absence (control) or presence of methocramine for a 90 min. Subsequently, the second concentration-effect curve for (+)-cis-Dioxolane was constructed for each strip. Methocramine caused a significant inhibition of the contractile muscle response to (+)-cis-Dioxolane.

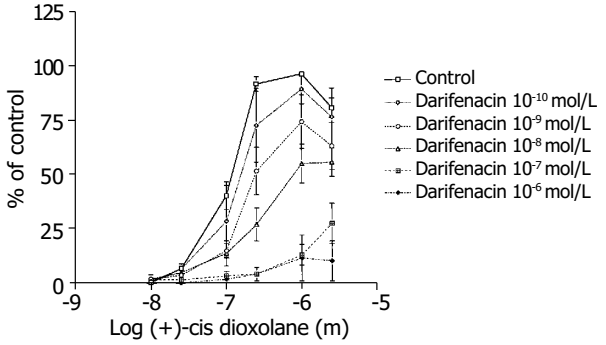

Figure 7 Concentration-response curves for the contractile effect of (+)-cis-Dioxolane alone and in combination with different concentrations of M_3 antagonist, darifenacin (from 10^{-10} mol/L to 10^{-6} mol/L) on the rat antral circular smooth muscle strips. Each point represents the mean±SE; $n = 4$, 7, 11, 10 strips. First, cumulative concentration-effect curve was constructed for each strip for (+)-cis-Dioxolane, (10^{-8} to 3×10^{-5} mol/L). After wash, tissues were equilibrated in either the absence (control) or presence of darifenacin for a 90 min. Subsequently, the second concentration-effect curve for (+)-cis-Dioxolane was constructed for each strip. Darifenacin caused a significant inhibition of the contractile muscle response to (+)-cis-Dioxolane.

Comparison the muscarinic M_1, M_2 and M_3 receptor antagonists mediating the rat antral circular smooth muscle contraction

All three receptors (M_1, M_2 and M_3) subtype antagonists inhibited the antral circular muscle contraction to cholinergic agonist (+)-cis-dioxolane. Darifenacin (M_3) was most potent in inhibiting rat antral smooth muscle cholinergic contraction. The dose-response curves were shifted to the right by muscarinic antagonists in the following order of affinity: darifenacin (M_3)

>methocramine (M_2) >pirenzepine (M_1). The EC_{50} for each antagonist was as follows: darifenacin 7.9, methacramine 7.2 and pirenzepine 6.8 (Figure 8).

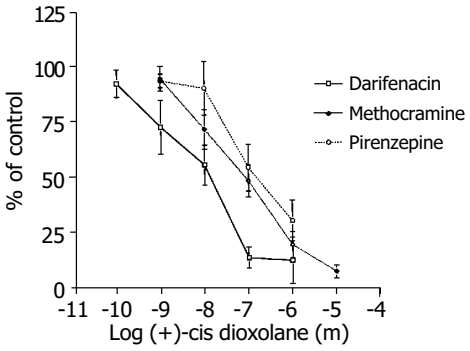

Figure 8 Comparison of the inhibition of the contractile response to cis-Dioxolane by 3 muscarinic receptor antagonists: M_3- darifenacin, M_2- methocramine, and M_1- pirenzepine. The M_3 antagonist, darifenacin, was the most potent inhibitor of the contraction induced by (+)-cis Dioxolane (10^{-6} mol/L). The EC_{50} values for each were: for darifenacin (M_3) -7.9; for methocramine (M_2) -7.2; and for pirenzepine (M_1) -6.8.

DISCUSSION

It is well established that cholinergic agonists are of major importance for the stimulation of antral smooth muscle contraction and that their effect is mediated by muscarinic receptors. In various smooth muscle cells, the action of cholinergic agonists involved the occupation of specific receptors, activation of receptor-coupled G-proteins and subsequent activation of the second messenger systems, which would lead to the mobilization of Ca^{2+} from intracellular storage pools[10]. Certain steps of the signaling pathway (s) for the cholinergic contraction of antral circular smooth muscle in rats are still not understood, for example, the second messenger system or the functional characteristics of the muscarinic receptor subtypes involved. In our study the cholinergic rat antral circular muscle contraction *in vitro* was sensitive to the depletion from the extracellular Ca^{2+} that significantly diminished the cholinergic contraction. This finding along with the inhibitory effect of nifedipine indicated a dependence on extracellular Ca^{2+} influx via L-type calcium channels[50].

It is still not clear whether cholinergic contractile pathways of antral circular smooth muscle are mediated by PTX-sensitive GTP-binding protein through an increased inflow of extracellular calcium, or mediated via PTX-insensitive, inositol triphosphate (IP_3)-dependent pathway. The circular muscle of cat esophagus and the lower esophageal sphincter (LES) were reported to be linked to different pathways. LES circular muscle cholinergic contraction was shown to be linked to the PTX-*insensitive* pathway, whereas esophageal circular muscle cholinergic contraction has been reported to be linked to the PTX-sensitive pathway[11-14].

In the present study, pretreatment with PTX significantly inhibited the contractile response to bethanechol of the antral smooth muscle strips in the organ bath and of the dissociated myocytes.

More than one muscarinic receptor may be responsible for cholinergically mediated contractility at a particular area[6,22,51-56]. A major role for M_3 and a minor role for M_2 receptors in cholinergic-induced smooth muscle contraction have been shown at the tissue of various species and organs[57-59], but it is still not clear how different receptors may interact to mediate a specific function. For example, M_2 receptor might serve as an inhibitory presynaptic autoreceptor[60], or M_2 receptor could act by gating cation channels that were subsequently modulated by M_3 receptors[61].

The functional characteristics of muscarinic receptor subtypes regulating antrum circular muscle cholinergic contraction have not been previously reported. In our functional studies, cholinergic contraction in response to cis-dioxolane in rat antral circular muscles was mediated mostly through M_3, less by M_2, and the least by M_1 muscarinic receptor subtypes.

The involvement of PTX-sensitive GTP-binding proteins in mediating the contractile response to muscarinic agonists has been reported to be linked to muscarinic M_2 receptor in many studies, such as in cat esophageal circular muscle[11,12]. In contrast, our experiments in rat antral circular muscles indicated that the M_3 muscarinic receptor was functionally prevalent, and yet, PTX-sensitive pathways were shown to be activated in the process of antral cholinergic contraction. A few published reports were in agreement with our results[13,22,26].

Possible explanations of the reported differences include: (1) Different experimental systems were used to compare the homogenous suspension of smooth muscle cells was compared with smooth muscle strips. (2) M_3 and M_2 receptors were expressed together at the shared site of the signaling pathways[22,54,57,60,62]. (3) The cholinergic agonist (+/- cis-Dioxolane) was used in our studies. Although, it has been reported to be non-selective[46,48,52], +/- cis-Dioxolane might be more selective for M3 muscarinic receptor than it was originally described[63]. (4) It has been suggested that seven transmembrane spanning receptors including muscarinic are promiscuous in that they could form interactions with multiple G-proteins[64] or activate many different transduction pathways at the same time[65]. (5) M_2 receptor might be masked by M_3 receptor, thus detectable when M3 receptor was inhibited. Separating out these possibilities would require more specific antagonists than the currently available.

In conclusion, the rat antral circular smooth muscle contracts to cholinergic agonists (bethanechol chloride and (+)-cis-Dioxolane) in a dose-dependent fashion through activation of muscarinic receptors at the smooth muscle. The contractile responses to cholinergic agonists are dependent on the increase in intracellular calcium induced by the influx of extracellular calcium via L-type voltage gated calcium channels. Bethanechol activates M_3 and M_2 muscarinic receptors coupled to pertussis-toxin sensitive GTP-binding protein (s). The presence of a residual contractile cholinergic response after 5 and 10 min in calcium-free buffer, as well as a residual contractile response after the treatment with nifedipine, suggests a role for an additional pathway (s). M_3 receptor is predominant out of three functionally tested M_1, M_2, and M_3 muscarinic receptors regulating cholinergic contraction. The involvement of more than one muscarinic receptor indicates more than one pathway (s) regulating the cholinergic contraction of rat antrum circular smooth muscle.

The results of these studies have important clinical implications for possible treatment of gastric dysfunction with muscarinic subtype-selective agents.

ACKNOWLEDGEMENTS

Authors would like to thank John Ellis, Ph.D, for helpful discussions. An excellent technical assistance of Rohini Polavarapu is acknowledged.

REFERENCES

1 **Berridge MJ**. Inositol trisphosphate and calcium signaling. *Nature* 1993; **361**: 315-325

2 **Bygrave FL,** Roberts HR. Regulation of cellular calcium through signaling cross talk involves an intricate interplay between the actions of receptors, G-proteins, and second messengers. *FASEB J* 1995; **9**: 1297-1303

3 **Akbulut H,** Goren Z, Iskender E, Eraslan A, Ozdemir O, Oktay S. Subtypes of muscarinic receptors in rat duodenum: a comparison with rabbit vas deferens, rat atria, guinea-pig ileum

and gallbladder by using imperialine. *Gen Pharmacol* 1999; **32**: 505-511

4 **Grider JR,** Makhlouf GM. Contraction mediated by Ca++ release in circular and Ca++ influx in longitudinal muscles cells. *J Pharmacol Exper Ther* 1988; **244**: 432-437

5 **Murthy KS,** Grider JR, Makhlouf GM. InsP3-dependent Ca2+ mobilization in circular but not longitudinal muscle cells of intestine. *Am J Physiol* 1991; **261**(6 Pt 1): G937-G944

6 **Li Z,** Ruan Y, Guo ZD, Cong H, Zhang KY, Takemura H. Function and localization of high and low affinity binding sites to muscarinic receptors in longitudinal and circular smooth muscles of human stomach. *Res Comm Chem Pathol Pharmacol* 1990; **67**: 31-42

7 **Kerr PM,** Hillier K, Wallis RM, Garland CJ. Characterization of muscarinic receptors mediating contractions of circular and longitudinal muscle of human isolated colon. *Br J Pharmacol* 1995; **115**: 1518-1524

8 **Lucchesi PA,** Romano FD, Scheid CR, Yamaguchi H, Honeyman TW. Interaction of agonists and selective antagonists with gastric smooth muscle muscarinic receptors. *Naunyn Schmiedebergs Arch Pharmacol* 1989; **339**: 145-151

9 **Miyazaki H,** Koyama I, Nakamura H, Taneike T, Ohga A. Regional differences in cholinergic innervation and drug sensitivity in the smooth muscles of pig stomach. *J Autonomic Pharmacol* 1991; **11**: 255-265

10 **Makhlouf GM,** Murthy KS. Signal transduction in gastrointestinal smooth muscle. *Cell Signal* 1997; **9**: 269-276

11 **Sohn UD,** Harnett KM, De Petris G, Behar J, Biancani P. Distinct muscarinic receptors G proteins, and phospholipases in esophageal and lower esophageal sphincter (LES) circular muscle. *J Pharmacol Exp Ther* 1993; **267**: 1205-1214

12 **Sohn UD,** Han B, Tashjian AH, Behar J, Biancani P. Agonist-dependent, muscle-type-specific signal transduction pathways in cat esophageal and lower esophageal sphincter circular smooth muscle. *J Pharmacol Exp Ther* 1995; **273**: 482-491

13 **Lin S,** Kajimura M, Takeuchi K, Kodaira M, Hanai H, Kaneko E. Expression of muscarinic receptor subtypes in rat gastric smooth muscle: effect of M_3 selective antagonist on gastric motility and emptying. *Dig Dis Sci* 1997; **42**: 907-914

14 **Cao W,** Chen Q, Sohn UD, Kim N, Kirber MT, Harnett KM, Behar J, Biancani P. Ca2+-induced contraction of cat esophageal circular smooth muscle cells. *Am J Physiol* 2001; **280**: C980-C992

15 **Bitar KN,** Saffouri B, Makhlouf GM. Cholinergic and peptidergic receptors on isolated human antral smooth muscle cells. *Gastroenterology* 1982; **82**: 832-837

16 **Konturek SJ,** Jaworek J, Tasler J, Cieszkowski M, Yanaihara N. Subtypes of muscarinic receptors in canine pancreatic secretion *in vivo* and *in vitro*. *Int J Pancreatol* 1987; **2**: 11-22

17 **Liebmann C,** Nawrath S, Schnittler M, Schubert H, Jakobs KH. Binding characteristics and functional G protein coupling of muscarinic acetylcholine receptors in rat duodenum smooth muscle membranes. *Naunyn Schmiedebergs Arch Pharmacol* 1992; **345**: 7-15

18 **Brann MR,** Ellis J, Jorgensen H, Hill-Eubanks H, Jones SVP. Muscarinic acetylcholine receptor subtypes: localization and structure/function. *Prog Brain Res* 1993; **98**: 121-127

19 **Preiksaitis HG,** Krysiak PS, Chrones T, Rajgopal V, Laurier LG. Pharmacological and molecular characterization of muscarinic receptor subtypes in human esophageal smooth muscle. *J Pharmacol Exp Ther* 2000; **295**: 879-888

20 **Eglen RM.** Muscarinic receptors and gastrointestinal tract smooth muscle function. *Life Sci* 2001; **68**: 2573-2578

21 **Li M,** Bullock CM, Knauer DJ, Ehlert FJ, Zhou QY. Identification of Two Prokineticin cDNAs: Recombinant Proteins Potently contract gastrointestinal smooth muscle. *Mol Pharmacol* 2001; **59**: 692-698

22 **Stengel PW,** Yamada M, Wess J, Cohen ML. $M_{(3)}$-receptor knockout mice: muscarinic receptor function in atria, stomach fundus, urinary bladder, and trachea. *Am J Physiol* 2002; **282**: R1443-R1449

23 **Migeon JC,** Thomas SL, Nathanson NM. Differential coupling of m_2 and m_4 muscarinic receptors to inhibition of adenylyl cyclase by Gi alpha and G (o) alpha subunits. *J Biol Chem* 1995; **270**: 16070-16074

24 **Murthy KS,** Makhlouf GM. Differential coupling of muscarinic m_2 and m_3 receptors to adenylyl cyclases V/VI in smooth muscle. Concurrent M_2 - mediated inhibition via Galphai3 and m_3-mediated stimulation via Gbetagammaq. *J Biol Chem* 1997; **272**: 21317-21324

25 **Kostenis E,** Zeng FY, Wess J. Structure-function analysis of muscarinic receptors and their associated G proteins. *Life Sci* 1999; **64**: 355-362

26 **Yokotani K,** Osumi Y. Cholinergic M_2 muscarinic receptor-mediated inhibition of endogenous noradrenaline release from the isolated vascularly perfused rat stomach. *J Pharmacol Exp Ther* 1993; **264**: 54-60

27 **Milovanovic DR,** Jankovic SM. Pharmacologic characterization of muscarine receptor subtypes in rat gastric fundus mediating contractile responses. *Indian J Med Res* 1997; **105**: 239-245

28 **Nelson DK,** Pieramico O, Dahmen G, Dominguez-Munoz JE, Malfertheiner P, Alder G. M_1-muscarinic mechanisms regulate interdigestive cycling of motor and secretory activity in human upper gut. *Dig Dis Sci* 1996; **41**: 206-215

29 **Hammer R.** Muscarinic receptors in the stomach. *Scandinavian J Gastroenterol Suppl* 1980; **66**: 5–11

30 **Herawi M,** Lambrecht G, Mutschler E, Moser U, Pfeiffer A. Different binding properties of muscarinic M_2-receptor subtypes for agonists and antagonists in porcine gastric smooth muscle and mucosa. *Gastroenterology* 1988; **94**: 630-637

31 **Moummi C,** Magous R, Strosberg D, Bali JP. Muscarinic receptors in isolated smooth muscle cells from gastric antrum. *Bioch Pharmacol* 1988; **37**: 1363-1369

32 **Hasler WL,** Heldsinger A, Owyang C. Cisapride acts on muscarinic (glandular M_2) receptors to induce contraction of isolated gastric myocytes: mediation via a calcium-phosphoinositide pathway. *J Pharmacol Exp Ther* 1991; **259**: 1294-1300

33 **Rhee JC,** Rhee PL, Park MK, So I, Uhm DY, Kim KW, Kang TM. Muscarinic receptors controlling the carbachol-activated nonselective cationic current in guinea pig gastric smooth muscle cells. *Jap J Pharmacol* 2000; **82**: 331-337

34 **Takahashi T,** Kojima Y, Tsunoda Y, Beyer LA, Kamijo M, Sima AA, Owyang C. Impaired intracellular signal transduction in gastric smooth muscle of diabetic BB/W rats. *Am J Physiol* 1996; **270**(3 Pt 1): G411-G417

35 **Xue L,** Suzuki H. Electrical responses of gastric smooth muscles in streptozotocin-induced diabetic rats. *Am J Physiol* 1997; **272** (1 Pt 1): G77-G83

36 **Maruyama Y,** Sakai Y, Nobe K, Momose K. Subcellular distribution of protein kinase C isoforms in gastric antrum smooth muscle of STZ-induced diabetic rats. *Life Sci* 1999; **64**: 1933-1940

37 **Wrzos HF,** Polavarapu R, Ouyang A. The signal transduction pathway involved in rat antral and colonic circular muscle response to muscarinic and neurokinin receptor agonists. Abstract. *Gastroenterology* 1997; **112**: A853

38 **Wrzos HF,** Tandon T, Ouyang A. Functional significance of muscarinic receptor subtypes on rat antral circular muscle. Abstract. *Neurogastroenterol Motil* 1998

39 **Bertiger G,** Reynolds JC, Ouyang A, Cohen S. Properties of the feline pyloric sphincter *in vitro*. *Gastroenterology* 1987; **92**: 1965-1972

40 **Bitar KN,** Makhlouf GM. Receptors on smooth muscle cells: characterization by contraction and specific antagonists. *Am J Physiol* 1982; **242**: G400-G407

41 **Biancani P,** Hillemeier C, Bitar KN, Makhlouf GM. Contraction mediated by Ca^{2+} influx in esophageal muscle and by Ca^{2+} release in LES. *Am J Physiol* 1987; **253**(6 Pt 1): G760-G766

42 **Maggi CA,** Zagorodnyuk V, Giuliani S. Specialization of tachykinin NK1 and NK2 receptors in producing fast and slow atropine resistant neurotransmission to the circular muscle of the guinea-pig colon. *Neuroscience* 1994; **63**: 1137-1152

43 **Thomas EA,** Ehlert FJ. Pertussis toxin blocks M_2 muscarinic receptor-mediated effects on contraction and cyclic AMP in the guinea pig ileum, but not M_3-mediated contractions and phosphoinositide hydrolysis. *J Pharmacol Exp Ther* 1994; **271**: 1042-1050

44 **von Schrenck T,** Mackensen B, Mende U, Schmitz W, Sievers J, Mirau S, Raedler A, Greten H. Signal transduction pathway of the muscarinic receptors mediating gallbladder contraction.

Naunyn Schmiedebergs Arch Pharmacol 1994; **349**: 346-354

45 **Choppin A,** Eglen RM. Pharmacological characterization of muscarinic receptors in dog isolated ciliary and urinary bladder smooth muscle. *Br J Pharmacol* 2001; **132**: 835-842

46 **Hegde SS,** Choppin A, Bonhaus D, Briaud S, Loeb M, Moy TM, Loury D, Eglen RM. Functional role of M_2 and M_3 muscarinic receptors in the urinary bladder of rats *in vitro* and *in vivo*. *Br J Pharmacol* 1997; **120**: 1409-1418

47 **Smith CM,** Wallis RM. Characterisation of [3H]-darifenacin as a novel radioligand for the study of muscarinic M_3 receptors. *J Rec Sign Transduction Res* 1997; **17**: 177-184

48 **Choppin A,** Eglen RM, Hegde SS. Pharmacological characterization of muscarinic receptors in rabbit isolated iris sphincter muscle and urinary bladder smooth muscle. *Br J Pharmacol* 1998; **124**: 883-888

49 **Barocelli E,** Morini G, Ballabeni V, Lavezzo A, Impicciatore M. Effects of two new pirenzepine analogs on the contractile response of the guinea-pig oesophageal muscularis mucosae to acetylcholine, bethanechol, histamine and high potassium. *European J Pharmacol* 1990; **179**: 89-96

50 **Okamoto H,** Inoue K, Kamisaki T, Takahashi K, Sato M. Regional differences in calcium sensitivity in the guinea-pig intestine. *J Pharm Pharmacol* 1997; **49**: 981-984

51 **Dietrich C,** Kilbinger H. Prejunctional M_1 and postjunctional M_3 muscarinic receptors in the circular muscle of the guinea-pig ileum. *Naunyn Schmiedebergs Arch Pharmacol* 1995; **351**: 237-243

52 **Eglen RM,** Harris GC. Selective inactivation of muscarinic M_2 and M_3 receptors in guinea-pig ileum and atria *in vitro*. *Br J Pharmacol* 1993; **109**: 946-952

53 **Ehlert FJ,** Sawyer GW, Esqueda EE. Contractile role of M_2 and M_3 muscarinic receptors in gastrointestinal smooth muscle. *Life Sci* 1999; **64**: 387-394

54 **Sawyer GW,** Ehlert FJ. Muscarinic M_3 Receptor inactivation reveals a pertussis toxin-sensitive contractile response in the guinea pig colon: evidence for M_2/M_3 receptor interactions. *J Pharmacol Exp Ther* 1999; **289**: 464-467

55 **Wang J,** Krysiak PS, Laurier LG, Sims SM, Preiksaitis HG. Human esophageal smooth muscle cells express muscarinic receptor subtypes M_1 through M_5. *Am J Physiol* 2000; **279**: G1059-G1069

56 **Ren J,** Harty RF. Presynaptic muscarinic receptors modulate acetylcholine release from rat antral mucosal/submucosal nerves. *Dig Dis Sci* 1994; **39**: 1099-1106

57 **Chen Q,** Yu P, de Petris G, Biancani P, Behar J. Distinct muscarinic receptors and signal transduction pathways in gallbladder muscle. *J Pharmacol Exp Ther* 1995; **273**: 650-655

58 **Bellido I,** Fernandez JL, Gomez A, Sanchez de la Cuesta F. Otenzepad shows two populations of binding sites in human gastric smooth muscle. *Can J Physiol Pharmacol* 1995; **73**: 124-129

59 **Hanack C,** Pfeiffer A. Upper gastrointestinal porcine smooth muscle expresses M_2- and M_3- receptors. *Digestion* 1990; **45**: 196-201

60 **Parkman HP,** Pagano AP, Ryan JP. Subtypes of muscarinic receptors regulating gallbladder cholinergic contractions. *Am J Physiol* 1999; **276**(5 Pt 1): G1243-G1250

61 **Bolton TB,** Zholos AV. Activation of M_2 muscarinic receptors in guinea-pig ileum opens cationic channels modulated by M_3 muscarinic receptors. *Life Sci* 1997; **60**: 1121-1128

62 **Braverman AS,** Tallarida RJ, Ruggieri MR Jr. Interaction between muscarinic receptor subtype signal transduction pathways mediating bladder contraction. *Am J Physiol Regul Integr Comp Physion* 2002; **283**: R663- R668

63 **Lanzafame A,** Christopoulos A, Mitchelson F. Interactions of agonists with an allosteric antagonist at muscarinic acetylcholine M_2 receptors. *Eur J Pharmacol* 1996; **316**: 27-32

64 **Nahorski SR,** Tobin AB, Willars GB. Muscarinic M_3 receptor coupling and regulation. *Life Sci* 1997; **60**: 1039-1045

65 **Parekh AB,** Brading AF. The M_3 muscarinic receptor links to three different transduction mechanisms with different efficacies in circular muscle of guinea-pig stomach. *Br J Pharmacol* 1992; **106**: 639-643

Edited by Chen WW and Wang XL **Proofread by** Xu FM

PO Box 2345, Beijing 100023, China
Fax: +86-10-85381893
E-mail: wjg@wjgnet.com www.wjgnet.com

World J Gastroenterol 2004;10(22):3299-3302
World Journal of Gastroenterology
 ISSN 1007-9327

• BASIC RESEARCH •

Coxsackievirus B_3 infection and its mutation in Keshan disease

Li-Qun Ren, Xiang-Jun Li, Guang-Sheng Li, Zhi-Tao Zhao, Bo Sun, Fei Sun

Li-Qun Ren, Xiang-Jun Li, Guang-Sheng Li, Zhi-Tao Zhao, Bo Sun, Department of Pathology, Institute of Frontier Medical Science, Jilin University, Changchun 130021, Jilin Province, China
Fei Sun, Department of Cellular Biology, Institute of Frontier Medical Science, Jilin University, Changchun 130021, Jilin Province, China
Supported by National Natural Science Foundation of China, No. 39870668
Correspondence to: to Professor Guang-Sheng Li, Department of Pathology, Institute of Frontier Medical Science, Jilin University, Changchun 130021, Jilin Province, China. ligs@public.cc.jl.cn
Telephone: +86-431-5619287
Received: 2003-12-28 **Accepted:** 2004-02-10

Abstract

AIM: To investigate coxsackievirus B_3 infection and its gene mutation in Keshan disease.

METHODS: The expression of Coxsackievirus B_3 RNA was detected in autopsy specimens of acute (12 cases), sub-acute (27 cases) and chronic (15 cases) Keshan disease by *in situ* hybridization. In sub-acute Keshan disease specimens, 3 cases with positive result by *in situ* hybridization were selected RT-PCR analysis. The DNA segments were then sequenced.

RESULTS: Coxsackievirus B_3 RNA was detected in the cytoplasm of myocardiocyte. The positive rate was 83% in acute, 67% in sub-acute and 80% in chronic Keshan disease. In the conservative region of Coxsackievirus B_3 genome, there was a mutation in 234 (C-T) compared to the non-cardiovirulent strain, $CVB_{3/0}$.

CONCLUSION: Coxsackievirus B_3 RNA can survive and replicate in heart muscle of Keshan disease, which may play an important role in the occurrence of Keshan disease. The possible mechanism of occurrence of Keshan disease is associated with point a mutation in Coxsackievirus B_3 genome.

Ren LQ, Li XJ, Li GS, Zhao ZT, Sun B, Sun F. Coxsackievirus B_3 infection and its mutation in Keshan disease. *World J Gastroenterol* 2004; 10(22): 3299-3302
http://www.wjgnet.com/1007-9327/10/3299.asp

INTRODUCTION

Enteroviruses, particularly Coxsackie B viruses (CVB), are the most common cause of human viral myocarditis and are associated with dilated cardiomyopathy (DCM)[1-3]. In general, neonates and children suffer more severe clinical syndromes due to CVB infection, often severe or life threatening, because of inflammation and necrosis of heart muscle[4]. Many diseases are considered to have relationship with CVB_3 infect, but the mechanism is still not well understood. Although the immune response of the host undoubtedly plays an important role in the pathogenesis of viral heart disease[5], direct viral cytotoxicity has been found to be crucial for organ pathology both during acute and persistent heart muscle infection. Coxsackievirus B_3 (CVB_3), one of six CVB serotypes, is a member of the genus *enterovirus* within the family *Picornaviridae* and its structure is well understood[6,7]. Some studies suggest that the 5'NTR of enteroviruses maybe play an important role in producing or sustaining the myocardial virulence[8-14].

Keshan disease is endemic exclusively in selenium-deficient rural areas of China, including 14 provinces and autonomous regions[15]. Its clinical features are low body selenium content and acute or chronic episodes of heart disorder characterized by cardiogenic shock, arrhythmia, ECG changes (for example, right branch block), and/or congestive heart failure, with an enlarged heart. Four types of the disease are seen: acute, subacute, chronic, and latent or compensated. The basic pathological change is multifocal myocardial necrosis and fibrous replacement throughout the myocardium, with various degrees of cellular infiltration and calcification, depending upon the type of disease[16,17]. Research suggests that not a single but several more factors may have a relationship with the occurrence of Keshan disease. The reasons are often considered as global, biological chemical factors (selenium deficiency), dietary nutritional factors (vitamin E deficiency) and infection (virus, especially enteroviruses). This hypothesis can explain both endemic and seasonal features of Keshan disease. Recent studies have also demonstrated a possible etiological role of enterovirus infection in a particular form of heart muscle disease, selenium deficiency-related endemic cardiomyopathy (Keshan disease), seen in China[18,19]. Presently, patients of Keshan disease are rare and there is no ideal animal model, research of viral etiology of Keshan disease is relatively few. In this study, we detected all the four types of Keshan disease using *in situ* hybridization and sequenced the 5'NTR of CVB3 from subacute Keshan disease in order to investigate the relationship between Keshan disease and CVB3 infection.

MATERIALS AND METHODS

Case selected

All the samples were cardiac tissue isolated at post mortem and fixed in formaldehyde and embedded in paraffin wax and preserved in Institute of Keshan Disease, Jilin University from 1959-1985. The samples included 12 acute patients (7 males, 5 females, average age 16.3 years), 27 subacute patients (12 males, 15 females, average age 4.3 years) and 15 chronic patients (9 males, 6 females, average age 23.8 years). We used three non-Keshan disease patients as controls, including two normal and one perinatal period cardiomyopathy. The cultured human amniotic cell containing a cardiovirulent strain of CVB_3 served as positive control and by RT-PCR.

In situ Hybridization

An obligonucleotide probe was purchased from Shanghai Sangon Biological Engineering Company. This probe, labeled with biotin, was designed to detect coxsackievirus B_3, whose sequence was 5'-GTC CGC AAT GGC GGG CGG TGG TGG TGT CTC-3'.

All slides were treated by APES solution (1:50 acetone) in order to prevent the section slipping from the slide. The 5 μm thick section was baked 3-4 h at 80 ℃ and overnight at 60 ℃.

The paraffin wax was removed by immersing the slide in xylene. The slides were then rehydrated, treated with 0.1 g/L Triton X-100 for 2 min, digested with proteinase K (0.25 mg/mL) in PBS for 5 min at room temperature, then sealed with histidine (2 mg/mL) for 2 min, and then dehydrated in graded concentrated

ethyl alcohol. The tissue sections were denatured on heating block for 2 min at 80 ℃ and then cooled on ice immediately. They were pre-hybridized for 3-4 h at 42 ℃ by covering them with pre-hybridization liquid (6×SSC, 5×Denhardt, 5 g/L SDS, 100 μg/mL herring sperm DNA, 500 g/L deionized formamide) in a wet chamber. After removal of the pre-hybridization liquid, the sections were allowed to hybridize overnight under the same conditions as described above.

Following the hybridization, the slides were rinsed twice with 2×SSC containing 500 g/L deionized formamide, twice with 2×SSC, treated with 1 g/L Triton X-100 for 2 min and washed twice with buffer I (1 mol/L NaCl, 0.1 mol/L Tris, pH 7.5). Buffer II (3 g bovine serum albumin dissolved in buffer I) was added to each section and incubated for 1 h. After pouring off buffer II, the SA-AP (streptavidin-alkaline phosphatase conjugation) was added onto the tissue sections, and allowed to react in this mixture for 20 min, rinsed with buffer I and then with buffer III (0.1 mol/L NaCl, 0.1 mol/L Tris-Cl, 50 mmol/L $MgCl_2$, pH 9.5). Finally, freshly prepared developer solution (BCIP/NBT) was applied to the slides and incubated for 30 min to 4 h. A brownish blue color reaction was produced. Following routine dehydration, the sections were cleared and mounted.

To assess the specificity of the hybridization signal, the culture cell infected by CVB3 were alternatively hybridized with the labeled obligonucleotide probe encoding CVB3 before and after digestion by Rnase, and hybridization solution without containing the labeled obligonucleotide probe encoding CVB3 was also used as negative control.

RT-PCR

Total RNA was extracted from paraffin-embedded heart tissue of patients with Keshan disease according to the following procedures. Several section slices (5-10 μm) were put into a 1.5 mL Eppendorf tube in which approximately 1 mL xylene was added in order to exclude paraffin. The xylene was changed every 2 h and the last time it was kept overnight at room temperature. After being centrifuged at 5 000 r/min for 5 min, the tissue was washed with non-water ethanol and then baked at 55 ℃. The total RNA from the dried tissue was then extracted using Trizol regent (GIBCO). Positive controls were the cultured human amniotic cells containing CVB_3. The RNA precipitate was dissolved in 10 μL of diethyl pyrocarbonate-treated H_2O.

The enterovirus specific primers used for RT-PCR and sequencing of the 5'NTR were purchased from Sigma Genosys Australia Pty. Ltd. The sequence of the primers was 3P: 5'-TCA ATT GTC ACC ATA AGC AGC AGC CA-3' and 5P: 5'-CGG TAC CTT TGT GCC CCT GTT TT-3'.

RT was carried out following the manufacturer's instructions. A 2 μL of specific primer 3P and 1 μL of 10 mmol/L dNTPs were mixed with 8 μL of RNA template. The mixture was immediately put on ice after incubated at 65 ℃ for 5 min. Then the mixture of 4 μL of 5×first strand buffer, 1 μL of Rnase inhibitor, 1 μL Superscript II Rnase H-free reverse transcriptase and 3 μL of diethyl pyrocarbonate-treated H_2O was added to the reaction tube, followed by incubation at 42 ℃ for 5 min, and at 70 ℃ for 15 min in order to inactivate the reverse transcriptase.

PCR was carried out with a 25 μL mixture containing 10 pmoL deoxynucleotide triphosphates, 15 pmoL forward primer (5P), 15 pmoL reverse primer (3P), 1×reaction buffer (Dingguo Biocompany), and 3 μL of the RT reaction product. The PCR reaction mixture was pre-denatured at 95 ℃ for 2 min, and then amplified through 30 cycles, each cycle consisting of denaturation at 95 ℃ for 45 s, annealing at 55 ℃ for 45 s, and extension at 72 ℃ for 45 s. Finally, an additional extension was carried out at 72 ℃ for 10 min. A negative control containing 22 μL of the reaction mixture plus 3 μL of autoclaved H_2O and a positive control containing 22 μL of the reaction mixture plus 3 μL of the RT reaction product from cells infected with the virulent laboratory strain of CVB_3 were included in each set of PCR.

The amplification products of PCR were analyzed on 17 g/L agarose gel by electrophoresis and stained with ethidium bromide. To assess the specificity of RT-PCR, the extracted total RNA were digested by Rnase then used for PCR as template. The distilled water was also used as template in PCR reaction as negative control.

DNA sequencing

The sequencing reaction cycle was carried out using 4 μL of DNA polymerase FS-terminator mix (PE-ABI), 3.2 mmol/L primer, and 5 ng of PCR product per 100 bp length of template DNA with the volume made up to 10 μL with H_2O. Reactions were run for 25 cycles as follows: 96 ℃ for 30 s, 50 ℃ for 15 s, and 60 ℃ for 4 min. DNA was precipitated, dissolved in loading buffer (167 g/L formamide, 733 g/L dextran), and separated on 41 g/L denaturing polyacrylamide gel on an ABI model 377 DNA sequencer. This procedure was performed by Shanghai Sangon Biological Engineering Company.

RESULTS

In situ Hybridization

According to the feature of positive signal of the culture cell, the positive hybridization signals of the Coxsackievirus RNA appeared as deep brownish blue mass or granules (Figure 1). This criterion was applied to the tissue sample. In longitudinal sections, they were seen to adhere to myofibrils in one or several strings of beads (Figure 2A). They varied in size and, in cross section, were usually localized in the sarcoplasm in proximity to myocyte nuclei, but no signals were found in the nuclei themselves. The color of signal was the darkest in the myocardium of papillary muscles, trabeculae carneae and subendocardial muscle. It was lighter and less intense in the cells of the outer layers than those in the middle layers of ventricular walls. The myocardial cells surviving in fresh lesions and surrounding old necrotic foci often showed the hybridization signal. No signal was found in necrotic foci, and there were slight differences in the distribution and manifestation of positive hybrid signals in several types of Keshan disease. In most acute and subacute

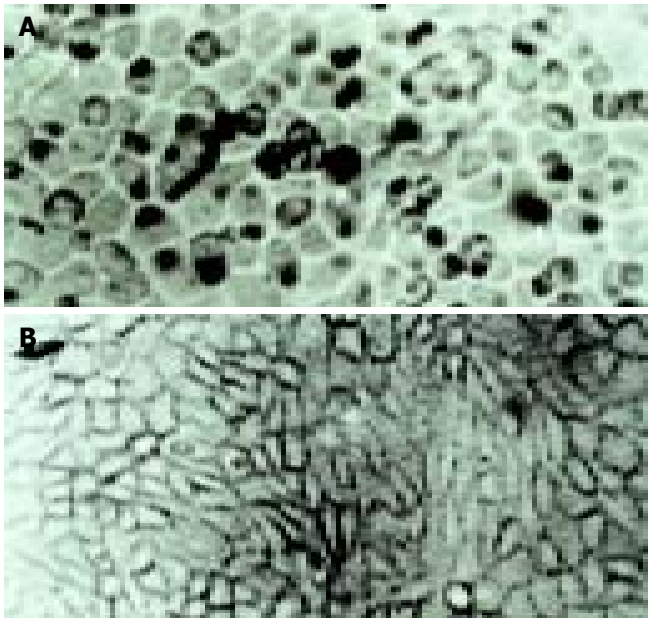

Figure 1 Positive signal in cultured cell A: the positive hybridization signals of the Coxsackievirus RNA appeared as deep brownish blue mass or granules (arrow) B: control, only hybridization solution was applied.

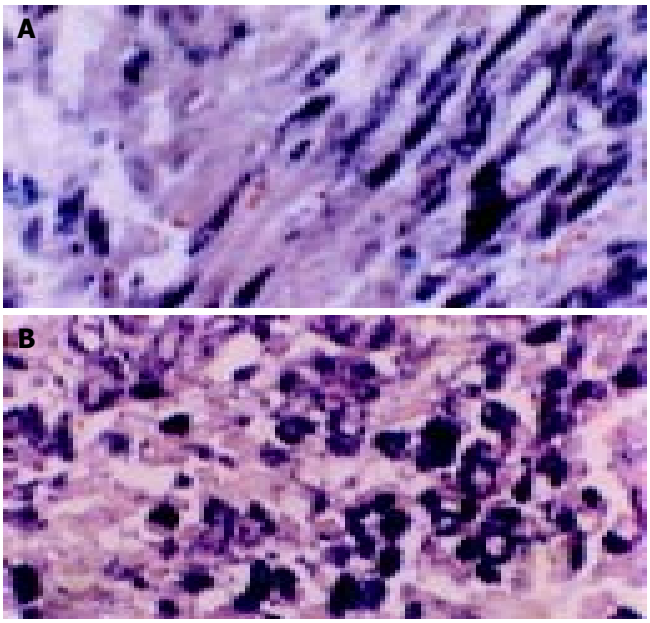

Figure 2 Positive signal of *in situ* hybridization in subacute myocardial tissue A: Feature positive signal of *in situ* hybridization with cardiac tissue is seen as deep brownish blue and seems to adhere onto myofibril, linked together in one or several strings of beads, when observed longitudinally (×400). B: The granules of positive signal were thick and with clear border in varying size and localized in the sarcoplasm.

cases, the signal appeared predominantly in the myocyte surrounding foci and surviving in fresh foci as well as cells beneath the endocardium and of papillary muscles. The hybridization-positive granules were thick, and had clear border. The sarcoplasm appeared dark, and sometimes, homogeneously blue (Figure 2B). In most of the chronic cases, the granules were usually distributed in all parts of the myocardium, and were small and without clear borders, like dirt. The detection rate in subacute specimens was the highest, and the rate in acute specimens was higher than that in chronic specimens, but there were no significant differences among the three types of Keshan disease.

The positive rate of hybridization in the three type of Keshan disease was 83% (10/12) in acute, 67% (18/27) in sub-acute and 80% (12/15) in chronic Keshan disease. No positive signals were found in any negative controls.

Results of 3 myocardial control specimens investigated with *in situ* hybridization were negative.

RT-PCR

RT-PCR revealed that the RNA extracted from the myocardial tissue with positive control of *in situ* hybridization amplified a DNA fragment about 541 bp, while the three negative controls did not amplify (Figure 3). The RNA extracted from cultured cell infected by CVB_3 were also amplified the DNA fragment about 541 bp.

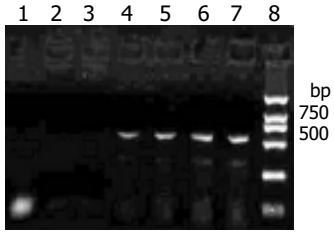

Figure 3 Agarose gel electrophoresis results Lanes 1, 2, 3: negative control; Lanes 4-6: subacute Keshan disease; Lanes 7: positive control; Lane 8: DL-2000 DNA Marker. A 541 bp DNA segment can be seen in lanes 4-7.

Sequence analysis

The DNA segments from RT-PCR were sequenced and compared to the non-cardiovirulent control, $CVB_{3/0}$, and the cardiovirulent strain, $CVB_{3/Nancy}$ and $CVB_{3/20}$. We found that the sequence of the amplified segment had one nucleotide different compared to that of $CVB_{3/0}$. The 234th nucleotide in the genome of $CVB_{3/0}$ was C while ours was T. But the sequence of our segment was similar that of $CVB_{3/Nancy}$, $CVB_{3/20}$ and the positive control (Figure 4).

DISCUSSION

Keshan disease has been studied for over 60 years in China. One of the key issues is the complex etiology of this endemic disease, with a focus on environmental nutritional factors and infectious agents. Selenium deficiency in the food chain has been recognized as a major but not exclusive environmental-nutritional factor, and increasing evidence supports an etiological role of enteroviruses in Keshan disease. Recently, Peng *et al*.[20] determined the sequences of the 5'NTR and the 3' end of the VP1 coding region from six enteroviruses isolate from cases of Keshan disease or outbreak myocarditis. From their results, they drew a conclusion that the sequence data confirm that coxsackievirus group B serotypes are predominant in the region where Keshan disease is endemic, and may be the etiological factors in outbreaks of myocarditis, and VP1 genotyping of enteroviruses is accurate and reliable. Animal experiments indicate that isolates may differ in pathogenicity. Virus infection combined with selenium deficiency in environments and vitamin E deficiency in dietary can illustrate both endemic and seasonal features of Keshan disease. The hypothesis of virus infection was accepted once it appeared, but the methods used in virology limited the development of a virus infection hypothesis of Keshan disease. The rapid development in molecular biology brings vitality to virology.

In situ hybridization is a method to detect the nucleic acids in a tissue or cell using a labeled obligonucleotide chain as probe. This technique has already been widely used in biology and medicine because of its high specificity, sensitivity and location precision. Using a cloned cDNA probe obtained from CVB_4 infected cells and labeled by biotin-11-dUTP, Easton *et al*.[21] found that 46% (6/13) patients who had been diagnosed coxsackievirus myocarditis can be found enterovirus infection in their myocardial tissue. Archard *et al*.[22] examined enteroviruses

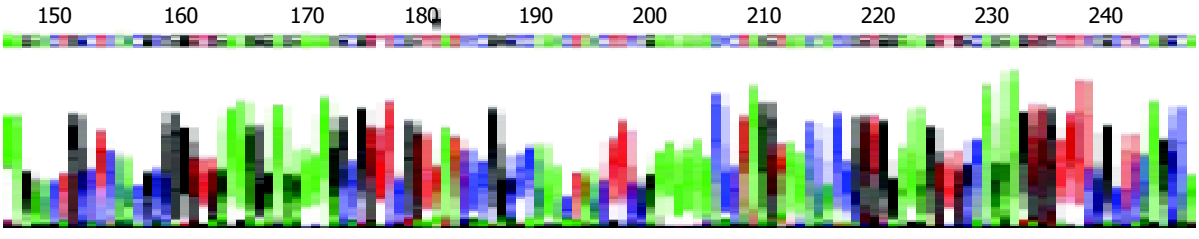

Figure 4 Sequence of segment of RT-PCR Compared to the nonvirulent strain of $CVB_{3/0}$, there was one nucleotide different (arrow). The nonvirulent strain of $CVB_{3/0}$ was C while ours was T.

infection in human myocardial tissue using an enterovirus specific probe, and found that the rate of enterovirus infection was 45% (21/47) in myocarditis patients and 43% (35/82) in cured myocarditis and DMC patients. In our research, the specific obligonucleotide probe of CVB_3 was labeled by biotin on 5' end, and the specimen was paraffin-embedded myocardial tissue from autopsy patients of Keshan disease. The object was to detect the coxsackievirus B_3 RNA by *in situ* hybridization. Among the three types of Keshan disease patients, we found the positive rate was 83%, 67%, and 80% in acute, sub-acute and chronic Keshan disease patients, respectively. Our results provide a new support to the hypothesis that enterovirus, especially CVB_3, might play an important role in pathogenesis of Keshan disease. Moreover, the area, range and the distribution of the positive signal of CVB_3 were associated with the development of Keshan disease. The positive signals in acute and sub-acute Keshan disease were located in the surviving myocardiocyte in or around the necrosis foci while they were dispersed in almost all the myocardiocyte in chronic Keshan disease. The results of *in situ* hybridization suggested that enterovirus could lead to heart muscle lesion when they involved in the myocardial tissue, and they can dispersed to the normal heart muscle with increase of time.

Though there was a high enterovirus infection rate in myocardial tissue of Keshan disease patients[23,24], it is well known that the enterovirus could also be detected in many patients who had no heart muscle lesion. The change of viral cardiovirulence can undoubtedly play an important role. Some research has demonstrated that under some conditions, such as selenium deficiency, vitamin deficiency, the phenotype of enterovirus can be changed, that is, a non-cardiovirulent strain can change into a cardiovirulent strain, or the cardiovirulence can be increased in these conditions[25-27]. Beck *et al.*[28] sequenced the mutated strain, $CVB_{3/0}$se_, which was extracted from the heart muscle of selenium deficient mice, and found that there were six mutation points in $CVB_{3/0}$se- and compared to the two-cardiovirulent strains, $CVB_{3/20}$, $CVB_{3/M1}$, all mutated points were turned into that of a cardiovirulent strain. Can the same episodes also happen in Keshan disease patients? In our research, we found an about 541 bp DNA segment by RT-PCR. Compared to CVB3/0, a non-cardiovirulent strain, the sequence of our segment had only one nucleotide different, which was 234 T. But the segment had the same sequence as that of CVB3/Nancy and CVB3/20, cardiovirulent strain. This result can give us some indications that the mutation of virus genome might play an important role in the pathogeny of Keshan disease. But this needs to further investigation.

As we know that RNA is degraded easily, so its detection is difficult, especially in paraffin-embedded tissue[29,30]. But the paraffin-embedded myocardial tissue we select have been kept in our institute for a long time (10-50 years), and are generally thought not to be optimal for RNA research, but our results displayed that results of both *in situ* hybridization and RT-PCR were satisfactory.

REFERENCES

1 **Woodruff JF**. Viral myocarditis. A review. *Am J Pathol* 1980; **101**: 425-484
2 **Bowles NE,** Richardson PJ, Olsen EG, Archard LC. Detection of Coxsackie-B-virus-specific RNA sequences in myocardial biopsy samples from patients with myocarditis and dilated cardiomyopathy. *Lancet* 1986; **1**: 1120-1123
3 **Martino TA,** Liu P, Sole MJ. Viral infection and the pathogenesis of dilated cardiomyopathy. *Circ Res* 1994; **74**: 182-188
4 **Kaplan MH,** Klein SW, McPhee J, Harper RG. Group B. coxsackievirus infections in infants younger than three months of age: a serious childhood illness. *Rev Infect Dis* 1983; **5**: 1019-1032
5 **Knowlton KU,** Badorff C. The immune system in viral myocarditis: maintaining the balance. *Circ Res* 1999; **85**: 559-561
6 **Muckelbauer JK,** Kremer M, Minor I, Diana G, Dutko FJ, Groarke J, Pevear DC, Rossmann MG. The structure of coxsackievirus B_3 at 3.5 A resolution. *Structure* 1995; **3**: 653-667
7 **Wimmer E,** Hellen CU, Cao X. Genetics of poliovirus. *Annu Rev Genet* 1993; **27**: 353-436
8 **Agol VI.** The 5'-untranslated region of picornaviral genomes. *Adv Virus Res* 1991; **40**: 103-180
9 **Minor PD.** The molecular biology of poliovaccines. *J Gen Virol* 1992; **73**(Pt 12): 3065-3077
10 **Rohll JB,** Percy N, Ley R, Evans DJ, Almond JW, Barclay WS. The 5'-untranslated regions of picornavirus RNAs contain independent functional domains essential for RNA replication and translation. *J Virol* 1994; **68**: 4384-4391
11 **Le SY,** Siddiqui A, Maizel JV Jr. A common structural core in the internal ribosome entry sites of picornavirus, hepatitis C virus, and pestivirus. *Virus Genes* 1996; **12**: 135-147
12 **Rinehart JE,** Gomez RM, Roos RP. Molecular determinants for virulence in coxsackievirus B1 infection. *J Virol* 1997; **71**: 3986-3991
13 **Dunn JJ,** Chapman NM, Tracy S, Romero JR. Genomic determinants of cardiovirulence in coxsackievirus B_3 clinical isolates: localization to the 5' non translated region. *J Virol* 2000; **74**: 4787-4794
14 **Tu Z,** Chapman NM, Hufnagel G, Tracy S, Romero JR, Barry WH, Zhao L, Currey K, Shapiro B. The cardiovirulent phenotype of coxsackievirus B_3 is determined at a single site in the genomic 5' non translated region. *J Virol* 1995; **69**: 4607-4618
15 **Ge K,** Yang G. The epidemiology of selenium deficiency in the etiological study of endemic diseases in China. *Am J Clin Nutr* 1993; **57**(2 Suppl): 259S–263S
16 **Li GS,** Wang F, Kang D, Li C. Keshan disease: an endemic cardiomyopathy in China. *Hum Pathol* 1985; **16**: 602-609
17 **Gu BQ.** Pathology of Keshan disease. A comprehensive review. *Chin Med J* 1983; **96**: 251-261
18 **Li Y,** Peng T, Yang Y, Niu C, Archard LC, Zhang H. High prevalence of enteroviral genomic sequences in myocardium from cases of endemic cardiomyopathy (Keshan disease) in China. *Heart* 2000; **83**: 696-701
19 **Li Y**, Yang Y**,** Chen H. Detection of enteroviral RNA in paraffin-embedded myocardial tissue from patients with Keshan by nested PCR. *Zhonghua Yixue Zazhi* 1995; **75**: 344-345
20 **Peng T,** Li Y, Yang Y, Niu C, Morgan-Capner P, Archard LC, Zhang H. Characterization of enterovirus isolates from patients with heart muscle disease in a selenium-deficient area of china. *J Clin Microbiol* 2000; **38**: 3538-3543
21 **Easton AJ,** Eglin RP. The detection of coxsackievirus RNA in cardiac tissue by *in situ* hybridization. *J Gen Virol* 1988; **69**(Pt 21): 285-291
22 **Archard LC,** Bowles NE, Cunningham L, Freeke CA, Olsen EG, Rose ML, Meany B, Why HJ, Richardson PJ. Molecular probes for detection of persisting enterovirus infection of human heart and their prognostic value. *Eur Heart J* 1991; **12**(Suppl D): 56-59
23 **Huang Z,** Xia Y, Jin Q, Wu H. Coxsackievirus B3 infection and Keshan disease. *Weisheng Yanjiu* 2002; **31**: 261-263
24 **Guanqing H.** On the etiology of Keshan disease: two hypotheses. *Chin Med J* 1979**; 92**: 416-422
25 **Levander OA,** Beck MA. Interacting nutritional and infectious etiologies of Keshan disease. Insights from coxsackie virus B-induced myocarditis in mice deficient in selenium or vitamin E. *Biol Trace Elem Res* 1997; **56**: 5-21
26 **Beck MA,** Kolbeck PC, Rohr LH, Shi Q, Morris VC, Levander OA. Benign human enterovirus becomes virulent in selenium-deficient mice. *J Med Virol* 1994; **43**: 166-170
27 **Beck MA,** Kolbeck PC, Rohr LH, Shi Q, Morris VC, Levander OA. Vitamin E deficiency intensifies the myocardial injury of coxsackievirus B_3 infection of mice. *J Nutr* 1994; **124**: 345-358
28 **Beck MA,** Shi Q, Morris VC, Levander OA. Rapid genomic evolution of a non-virulent coxsackievirus B3 in selenium-deficient mice results in selection of identical virulent isolates. *Nat Med* 1995; **1**: 433-436
29 **Jackson DP,** Quirke P, Lewis F, Boylston AW, Sloan JM, Robertson D, Taylor GR. Detection of measles virus RNA in paraffin-embedded tissue. *Lancet* 1989; **1**: 1391
30 **Sariol CA,** Pelegrino JL, Martinez A, Arteaga E, Kouri G, Guzman MG. Detection and genetic relationship of dengue virus sequences in seventeen-year-old paraffin-embedded samples from Cuba. *Am J Trop Med Hyg* 1999; **61**: 994-1000

Edited by Kumar M **Proofread by** Xu FM

PO Box 2345, Beijing 100023, China
Fax: +86-10-85381893
E-mail: wjg@wjgnet.com www.wjgnet.com

World J Gastroenterol 2004;10(22):3303-3307
World Journal of Gastroenterology
 ISSN 1007-9327

• BASIC RESEARCH •

Effect of actin microfilament on potassium current in guinea pig gastric myocytes

Xiang-Lan Li, Hai-Feng Zheng, Zheng-Yuan Jin, Meng Yang, Zai-Liu Li, Wen-Xie Xu

Xiang-Lan Li, Hai-Feng Zheng, Zheng-Yuan Jin, Meng Yang, Zai-Liu Li, Department of Physiology, Yanbian University College of Medicine, Yanji 133000, Jilin Province, China
Wen-Xie Xu, Department of Physiology, Shanghai Jiaotong University School of Medicine, 1954 Huashan Rd, Shanghai 200030, China
Supported by the National Natural Science Foundation of China, No. 30160028
Correspondence to: Professor Wen-Xie Xu, Department of Physiology, Shanghai Jiaotong University School of Medicine, 1954 Huashan Rd, Shanghai 200030, China. wenxiexu@sjtu.edu.cn
Telephone: +86-21-62932910 **Fax:** +86-21-62932528
Received: 2004-02-11 **Accepted:** 2004-03-18

Abstract

AIM: To investigate the effect of actin microfilament on potassium current and hyposmotic membrane stretch-induced increase of potassium current in gastric antral circular myocytes of guinea pig.

METHODS: Whole-cell patch clamp technique was used to record potassium current in isolated gastric myocyes.

RESULTS: When the membrane potential was clamped at -60 mV, an actin microfilament disruptor, cytochanlasin-B (Cyt-B, 20 μmol/L in pipette) increased calcium-activated potassium current ($I_{K(Ca)}$) and delayed rectifier potassium current ($I_{K(V)}$) to 138.4±14.3% and 142.1±13.1% respectively at +60 mV. In the same condition, an actin microfilament stabilizer phalloidin(20 μmol/L in pipette) inhibited $I_{K(Ca)}$ and $I_{K(V)}$ to 74.2±7.1% and 75.4±9.9% respectively. At the holding potential of -60 mV, hyposmotic membrane stretch increased $I_{K(Ca)}$ and $I_{K(V)}$ by 50.6±9.7% and 24.9±3.3% at +60 mV respectively. In the presence of cytochalasin-B and phalloidin (20 μmol/L, in the pipette) condition, hyposmotic membrane stretch also increased $I_{K(Ca)}$ by 44.5±7.9% and 55.7±9.8% at +60 mV respectively. In the same condition, cytochalasin-B and phalloidin also increased $I_{K(V)}$ by 23.0±5.5% and 30.3±4.5% respectively. However, Cyt-B and phalloidin did not affect the amplitude of hyposmotic membrane stretch-induced increase of $I_{K(Ca)}$ and $I_{K(V)}$.

CONCLUSION: Actin microfilaments regulate the activities of potassium channels, but they are not involved in the process of hyposmotic membrane stretch-induced increase of potassium currents in gastric antral circular myocytes of guinea pig.

Li XL, Zheng HF, Jin ZY, Yang M, Li ZL, Xu WX. Effect of actin microfilament on potassium current in guinea pig gastric myocytes. *World J Gastroenterol* 2004; 10(22): 3303-3307 http://www.wjgnet.com/1007-9327/10/3303.asp

INTRODUCTION

Cytoskeleton is an intracellular superstructure that consists of microfilaments of actin and associated proteins, microtubules, and intermediate filaments. Actin microfilaments of the cytoskeleton form a complex network, providing the structural basis for simultaneous interactions between multiple cellular structures. It is well established that many ion channels and transporters are anchored in the membrane by either direct or indirect association with the cytoskeleton. In addition, there is growing evidence that altering the integrity of cytoskeletal elements, in particular actin microfilaments, could modulate the activity of a variety of ion channels[1] and receptors[2]. Many previous studies have demonstrated that actin microfilament could mediate different types of potassium channels of a variety of cells such as those in rat collecting duct[3], smooth muscle cell line DDT1 MF-2[4], cardiac myocytes of guinea pig[5], human meningioma cells[6], rat hippocampal CA1 pyramidal neurons[7], rat ventricular myocytes[8] and xenopus oocytes[9]. Wang *et al*.[10] reported that neither the microfilaments nor the microtubules were involved in the enhancement of $I_{K(V)}$ induced by cell distension in ventricular muscle cells of guinea pig. However, Ribeiro *et al*.[11] showed that microtubule was involved in the cell volume-induced changes in K+ transport across the rat colon epithelial cells. Our previous study demonstrated that main outward current was carried by calcium-activated potassium channel and delayed rectifier potassium channel in gastric antral circular myocytes of guinea pig and hyposmotic cell swelling enhanced the activity of that two kinds of potassium channel[12,13]. In order to investigate the mechanism of hyposmotic membrane stretch-induced increase of potassium current, in the present study, the effect of actin microfilament on potassium currents was observed and the possibility whether acin microfilament was involved in the process of hyposmotic membrane stretch-induced increase of potassium currents was examined.

MATERIALS AND METHODS

Single cell preparation and electrophysiological recording

Fresh, single smooth muscle cells (SMCs) were isolated enzymatically from the circular layer of guinea pig antrum as previously described[14]. Isolated SMCs were stored at 4 ℃ KBS until the time of use. All experiments were performed within 12 h after cell dispersion. The isolated cells were transferred to a small chamber (0.1 mL) on the stage of an inverted microscope (IX-70 Olympus, Japan) for 10-15 min to settle down. Solution was perfused at a speed of 0.9-1.0 mL/min through the chamber by gravity from the 8-channel perfusion system (L/M-sps-8; list electronics, Germany). Glass pipette with a resistance of 3-5 M Ω was used to make a giga seal of 5-10 G Ω the whole-cell currents were recorded with an Axopatch 1-D patch-clamp amplifier (Axon Instrument, USA).

Drugs and solution

Tyrode solution containing (mmol /L) NaCl 147, KCl 4, $MgCl_2 \cdot 6H_2O$ 1.05, $CaCl_2 \cdot 2H_2O$ 0.42, $Na_2PO_4 \cdot 2H_2O$ 1.81, and 5.5 mmol/L glucose was used. Ca^{2+}-free PSS containing (mmol/L) NaCl 134.8, KCl 4.5, glucose 5, and N-[2-hydroxyethyl] piperazine- N-[2-ethanesulphonic acid] (HEPES) 10 was adjusted to pH 7.4 with Tris [hydroxymethyl] aminomethane (TRIZMA). Modified K-B solution containing (mmol/L) L-glutamate 50, KCl 50, taurine 20, KH_2PO_4 20, $MgCl_2 \cdot 6H_2O$ 3, glucose 10, HEPES 10 and egtazic

acid 0.5 was adjusted to pH 7.40 with KOH. Isosmotic solution (290 mOsmol/L) containing (mmol/L) NaCl 80, KCl 4.5, HEPES 10, $MgCl_2 \cdot 6H_2O$ 1, $CaCl_2 \cdot 2H_2O$ 2, Glucose 5, Sucrose 110, was adjusted to pH 7.4 with Tris. Hypoosmotic solution (200 mOsmol/L) contained (in mmol/L) sucrose 30, and other ingredients was the same as the isosmotic solution. Pipette solution recording $I_{K(ca)}$ contained (mmol/L) potassium-aspartic acid 110, Mg-ATP 5, HEPES 5, $MgCl_2 \cdot 6H_2O$ 1.0, KCl 20, egtazic acid 0.1, di-tris-creatine phoshate 2.5, disodium-creatine phosphate 2.5 and its pH was adjusted to 7.3 with KOH. Pipette solution recording $I_{K(V)}$ contained (mmol/L) EGTA 10, and other ingredients was the same as the pipette solution recording $I_{K(ca)}$. Cytochalasin-B was dissolved in dimethyl sulphoxide (DMSO, 20 mmol/L) and phalloidin was dissolved in alcohol (1 mmol/L). The same amount of DMSO or alcohol as the final experimental solution was added to the pipette solution. All the chemicals in this experiment were purchased from Sigma (USA).

Data analysis

All data were expressed as mean±SD. Statistical significance was evaluated by a *t*-test. Differences were considered to be significant when *P* value was less than 0.05.

RESULTS

Effect of Cyt-B and phalloidin on $I_{K(Ca)}$

Under the whole cell configuration, the membrane potential was clamped at -60 mV, $I_{K(ca)}$ was elicited by step voltage command pulse from -40 mV to +100 mV for 440 ms with a 20 mV increment at 10 s intervals. An actin microfilament disruptor, Cyt-B (20 μmol/L in pipette) markedly increased $I_{K(Ca)}$ to 138.4±14.3% at +60 mV (n = 15, Figures 1B, C). In the same condition, an actin microfilament stabilizer, phalloidin (20 μmol/L in pipette) inhibited $I_{K(Ca)}$ to 74.2±7.1% at +60 mV (n = 15, Figures 2B, C).

Effect of Cyt-B and phalloidin on $I_{K(V)}$

Under the whole cell configuration, the membrane potential was clamped at -60 mV, $I_{K(V)}$ was elicited by step voltage command pulse from -40 mV to +80 mV for 440 ms with a 20 mV increment at 10 s intervals. Cyt-B (20 μmol/L in pipette) markedly increased $I_{K(V)}$ to 142.1±13.1% at +60 mV (n = 12, Figures 3B, C). In the same condition, phalloidin (20 μmol/L in pipette) inhibited $I_{K(V)}$ to 75.4±9.9% at +60 mV (n = 12, Figures 4B, C).

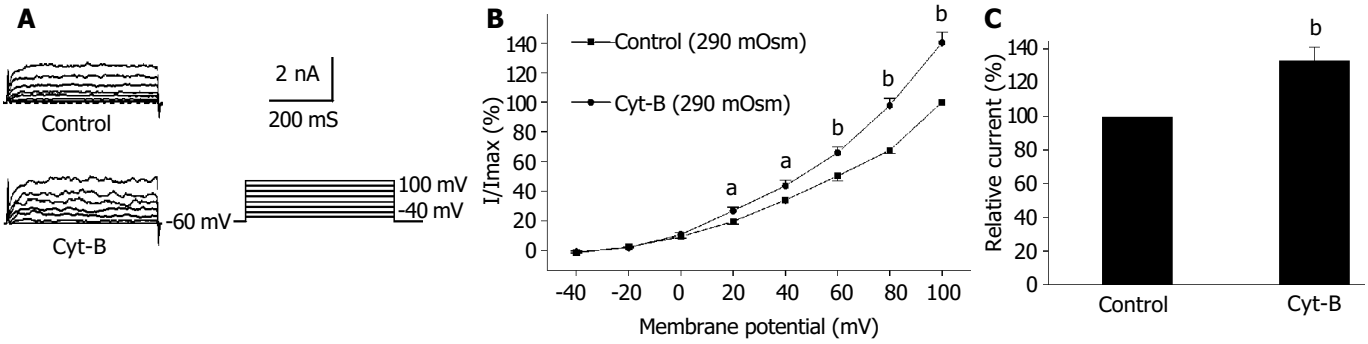

Figure 1 Effect of Cyt-B on $I_{K(Ca)}$. A: Representative current trace of $I_{K(Ca)}$. B: I/V relationship of $I_{K(Ca)}$. C: Cyt-B enhanced $I_{K(Ca)}$. In isosmotic condition. (n = 15, ^aP<0.05, ^bP<0.01 *vs* control).

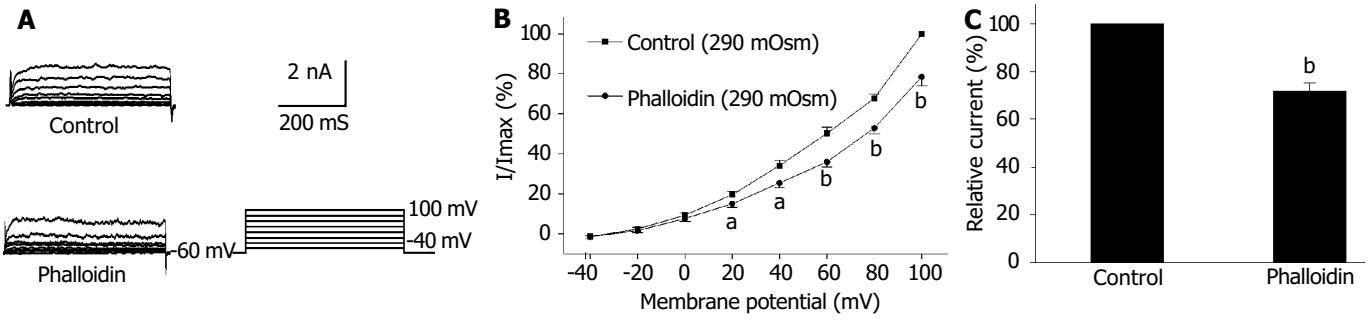

Figure 2 Effect of phalloidin on $I_{K(Ca)}$. A: Representative current trace of $I_{K(Ca)}$. B: I/V relationship of $I_{K(Ca)}$. C: Phalloidin inhibited $I_{K(Ca)}$ in isosmotic condition. (n = 15, ^aP<0.05, ^bP<0.01 *vs* control).

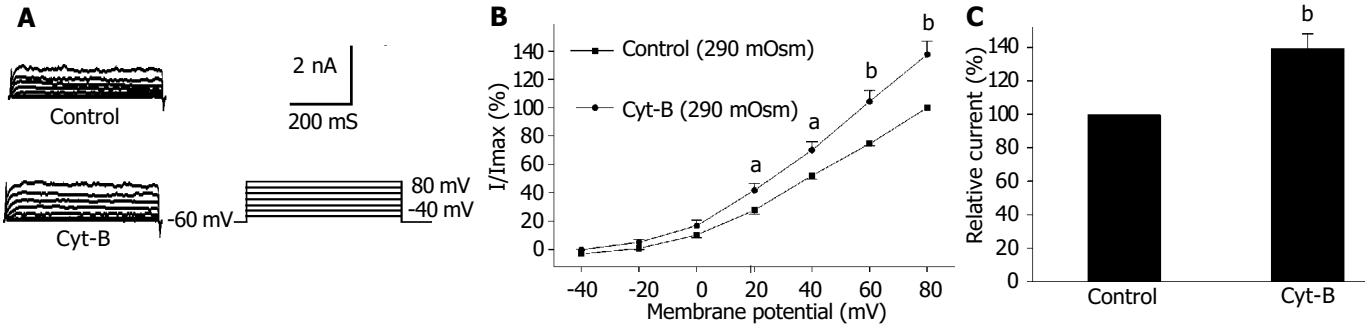

Figure 3 Effect of Cyt-B on $I_{K(V)}$. A: Representative current trace of $I_{K(V)}$. B: I/V relationship of $I_{K(V)}$. C: Cyt-B enhanced $I_{K(V)}$ inisosmotic condition.(n = 15, ^aP<0.05, ^bP<0.01 *vs* control).

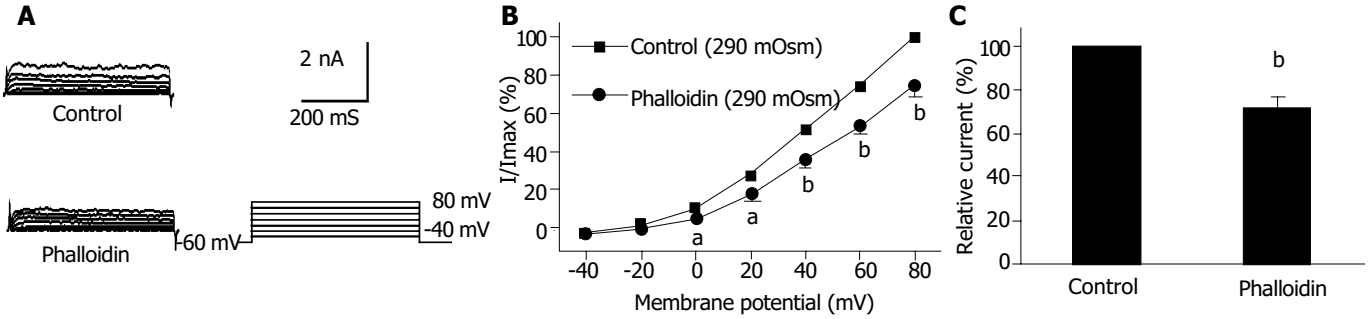

Figure 4 Effect of phalloidin on $I_{K(Ca)}$. A: Representative current trace of $I_{K(Ca)}$. B: I/V relationship of $I_{K(Ca)}$. C: Phalloidin inhibited $I_{K(Ca)}$ in isosmotic condition. (n = 15, ^aP<0.05, ^bP<0.01 *vs* control).

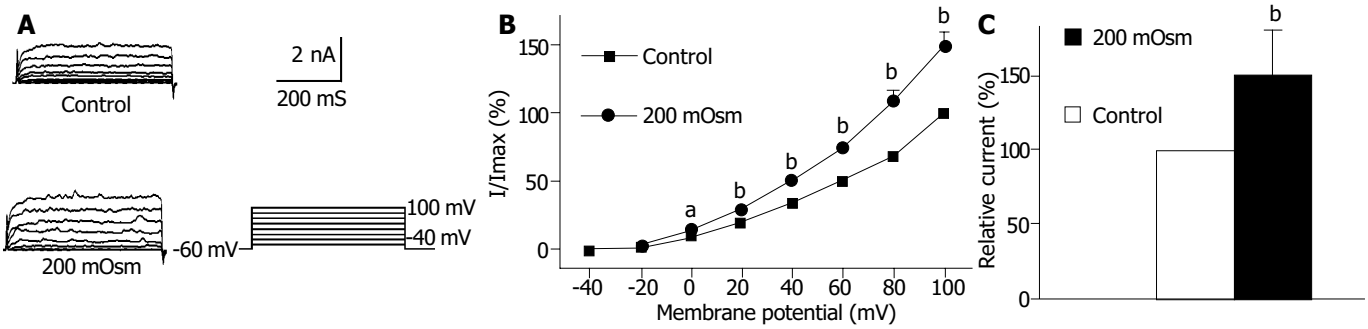

Figure 5 Effect of hyposmotic membrane stretch on $I_{K(Ca)}$. A: Representative current trace of $I_{K(Ca)}$. B: I/V relationship of $I_{K(Ca)}$. C: Hyposmotic membrane strech increased $I_{K(Ca)}$. (n = 15, ^aP<0.05, ^bP<0.01 *vs* control).

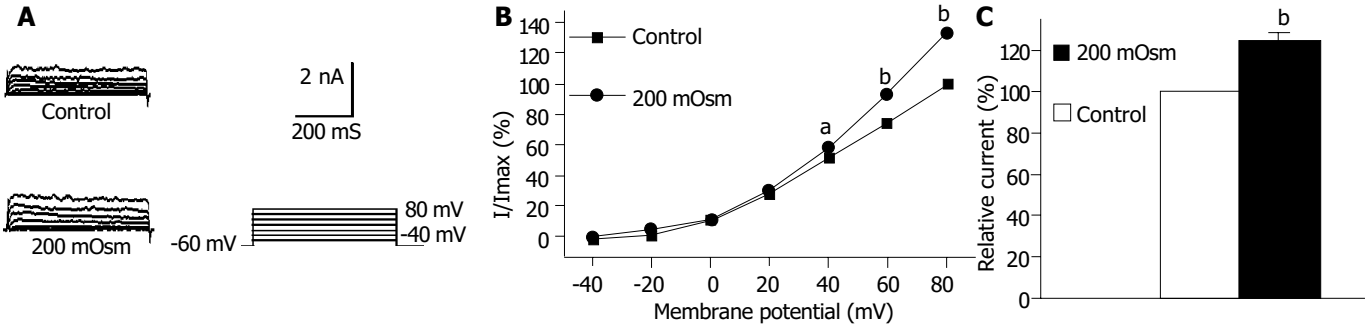

Figure 6 Effect of hyposmotic membrane stretch on $I_{K(V)}$. A: Representative current trace of $I_{K(V)}$. B: I/V relationship of $I_{K(V)}$. C: Hyposmotic membrane strech increased $I_{K(V)}$. (n = 15, ^aP<0.05, ^bP<0.01 *vs* control).

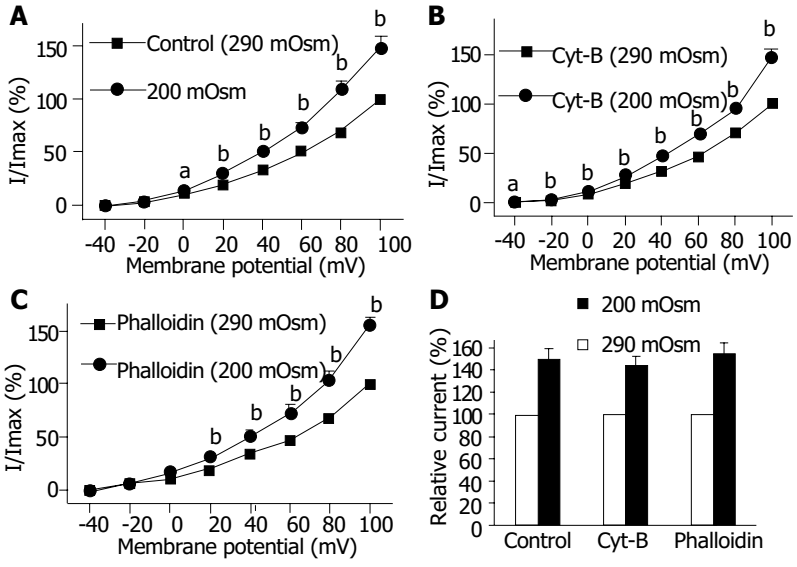

Figure 7 Effect of Cyt-B and phalloidin on hyposmotic membrane stretch-increase of $I_{(KCa)}$. A, B and C: I/V relationship of $I_{(KCa)}$. (n = 15, ^aP<0.05, ^bP<0.01 *vs* 290 mOsm). D: No effect of Cyt-B and phalloidin on the increased of $I_{K(Ca)}$ induced by hyposmotic membrane stretch (n = 15).

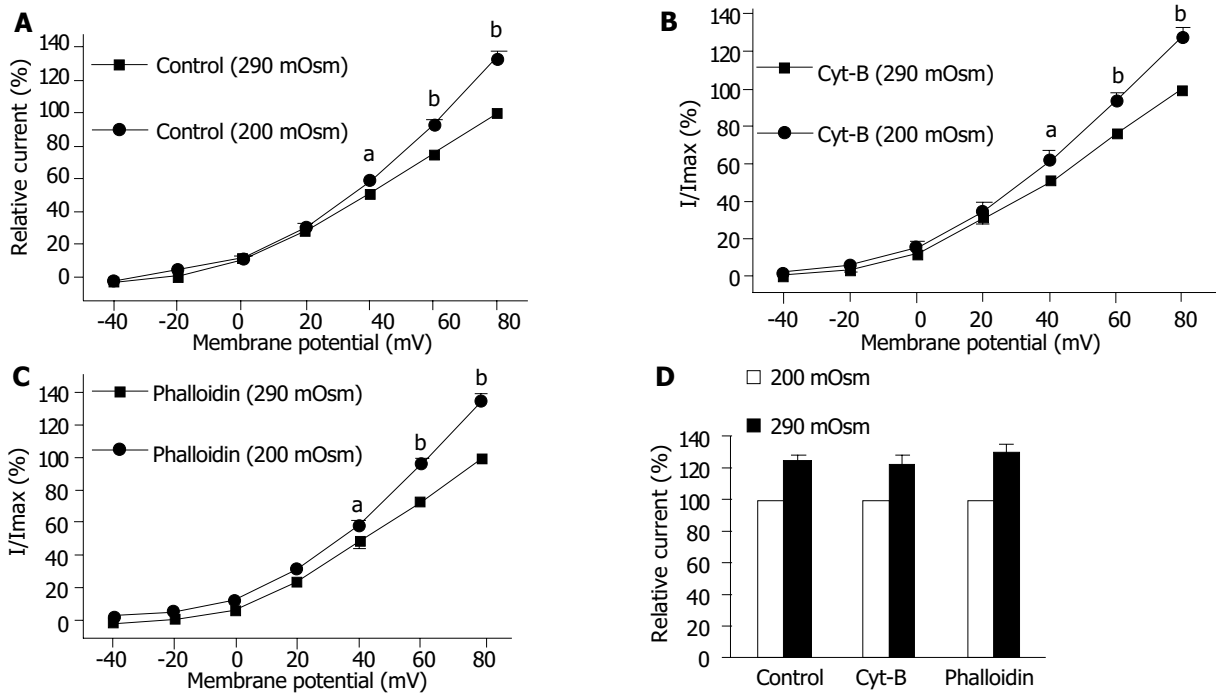

Figure 8 Effect of Cyt-B and phalloidin on hyposmotic membrane stretch-increase of $I_{K(V)}$. A, B and C: I/V relationship of $I_{K(V)}$. (n = 12, ^aP<0.05, ^bP<0.01 *vs* 290 mOsm). D: No effect of Cyt-B and phalloidin on the increased of $I_{K(V)}$ induced by hyposmotic membrane stretch (n = 12).

Effect of hyposmotic membrane stretch on $I_{K(Ca)}$ and $I_{K(V)}$

Using the same pulse protocol, the effect of hyposmotic membrane stretch on $I_{K(Ca)}$ and $I_{K(V)}$ was observed. When the cells were superfused with hyposmotic solution (200 mOsmol/L), step command pulse-induced $I_{K(Ca)}$ increased from 0mV (Figure 5B) and the increasing amplitude was 50.6±9.7% at +60 mV (n = 15, Figure 5C). In the same condition, hyposmotic superfusing increased step command pulse-induced $I_{K(V)}$ from +40 mV (Figure 6B) and the increasing amplitude was 24.9±3.3% at +60 mV (n = 12, Figure 6C).

Effect of Cyt-B and phalloidin on hyposmotic membrane stretch-induced increase of $I_{K(Ca)}$

To determine the possibility of actin microfilament involved in hyposmotic membrane stretch-induced increase of $I_{K(Ca)}$, the effects of Cyt-B and phalloidin on $I_{K(Ca)}$ in which cells were perfused with isosmotic and hypoosmotic solutions were observed respectively. Hyposmotic membrane stretch increased $I_{K(Ca)}$ from 0 mV (Figure 7A) and the increasing amplitude was 50.6±9.7% at 60 mV in the control group (n = 15, Figures 7A, 8D). In the presence of Cyt-B and phalloidin (20 μmol/L in pipette) hyposmotic membrane stretch also increased $I_{K(Ca)}$ by 44.5±7.9% (n = 15, Figures 7B, D) and 55.7±9.8% (n = 15, Figures 7C, D) at +60 mV respectively. There was no significant difference between control group and Cyt-B group or phalloidin group.

Effect of Cyt-B and phalloidin on hyposmotic membrane stretch-induced increase of $I_{K(V)}$

Hyposmotic membrane stretch increased $I_{K(V)}$ by 24.9±3.3% at +60 mV in the control group (n = 12, Figures 8A, D). In the presence of Cyt-B and phalloidin (20 μmol/L in pipette) hyposmotic membrane stretch also increased $I_{K(V)}$ by 22.9±5.5% (n = 12, Figures 8B, D) and 30.3±4.5% (n = 12, Figures 8C, D) at +60 mV respectively. There was no significant difference between control group and Cyt-B group or phalloidin group.

DISCUSSION

Cytoskeleton is an intracellular superstructure that consists of microfilaments of actin and associated proteins, microtubules, and intermediate filaments. Actin microfilament, in particular, are involved in structural support and a functional role in cell motility[15]. Recent evidence indicated, however, actin-based cytosleleton was involved in the control of ion channel activity across the plasma membranes of different cell types. For example, actin microfilaments were implicated in the regulation of soldium channels in human jejunal circular smooth muscle cells[16] and ATP-sensitive potassium channel in ventricular myocytes[5, 17]. Actin microfilaments could also regulate voltage-dependent channels, for example, actin microfilaments could mediate voltage-dependent epithelial soldium channels in neuron cells[18].

It was proposed that cell surface proteins and extra cellular matrix were linked to the cytoskeleton by transmembrane proteins and modulate ion channels and enzymes by mechanical deformation under physiological conditions. In the present study, we observed that an actin microfilament disruptor, Cyt-B increased $I_{K(Ca)}$ and $I_{K(V)}$ significantly (Figures 1B, C, Figures 3B, C). However, an actin microfilament stabilizer, phalloidin inhibited $I_{K(Ca)}$ and $I_{K(V)}$ markedly (Figures 2B, C, Figures 4B, C) in gastric myocytes. These results suggested that when actin microfilaments were disrupted, $I_{K(Ca)}$ or $I_{K(V)}$ could be activated; while, when actin microfilaments were stabilized, $I_{K(Ca)}$ or $I_{K(V)}$ could be inhibited in gastric myocytes. Many previous studies also supported our experiment. For example, Cyt-D activated calcium-activated potassium channel in human meningioma cells[6], Cyt-B activated K (ATP) channels in cardiac[5].

Stretch is a physiological stimulation in gut smooth mucles. There are two kinds of potassium current, calcium-activated potassium current and delayed rectifier potassium current. In the present study, the two kinds of potassium current were activated by hyposmotic swelling in gastric antral smooth muscle cells of guinea pigs (Figures 5-6). In order to investigate the mechanism of hyposmotic membrane stretch-induced increase of $I_{K(Ca)}$ and $I_{K(V)}$, the relationship between potassium channel activity and actin microfilaments was observed. When actin microfilaments were disrupted by Cyt-B or stabilized by phalloidin, hyposmotic membrane stretch-induced increase of

$I_{K(Ca)}$ and $I_{K(V)}$ was not affected (Figures 7-8). These results indicated that actin microfilaments were not involved in the increase of potassium current induced by hyposmotic cell swelling in gastric circular myocytes of guinea pig. Previous studies supported our results. For example, Wang *et al*.[10] observed that neither the microfilaments nor the microtubules were involved in the enhancement of $I_{K(V)}$ induced by cell distension in ventricular myocytes of guinea pig. We also observed that unsaturated fatty acids, exogenous and endogenous, were involved in the increase of calcium-activated potassium current induced by hyposmotic membrane stretch (data not shown). So that hyposmotic membrane stretch-induced increase of potassium currents may be related to unsaturated fatty acids in cell membranes.

Our previous study demonstrated that actin microfilaments played an important role in the modulation of membrane stretch-induced calcium influx and hyposmotic membrane stretch-induced increase of muscarinic current in guinea-pig gastric myocytes[19,20]. It is obvious that cytoskeleton plays a different role in different types of cells and different kinds of ion channels. In gastric smooth muscle actin microfilaments may be involved in the process of hyposmotic membrane stretch-induced depolarization of membrane potential. However, actin microfilaments would not be involved in the process of cell swelling-induced hyperpolarization of membrane potential.

In summary, actin microfilaments regulate potassium channel activities in normal condition. However, actin microfilaments are not involved in hyposmotic cell swelling-induced increase of potassium currents.

REFERENCES

1 **Janmey PA.** The cytoskeleton and cell signaling: component localization and mechanical coupling. *Physiol Rev* 1998; **78:** 763-781

2 **Wang H,** Bedford FK, Brandon NJ, Moss SJ, Olsen RW. $GABA_A$-receptor-associated proteins link $GABA_A$ receptors and the cytoskeleton. *Nature* 1999; **397:** 69-72

3 **Wang WH,** Cassola A, Giebisch G. Involvement of actin cytoskeleton in modulation of apical K channel activity in rat collecting duct. *Am J Physiol* 1994; **267**(4 Pt 2): F592-598

4 **Ehrhardt AG,** Frankish N, Isenberg G. A large-conductance K+ channel that is inhibited by the cytoskeleton in the smooth muscle cell line DDT1 MF-2. *J Physiol* 1996; **496**(Pt 3): 663-676

5 **Jovanovic S,** Jovanovic A. Diadenosine tetraphosphate-gating of cardiac K (ATP) channels requires intact actin cytoskeleton. *Naunyn Schmiedebergs Arch Pharmacol* 2001; **364:** 276-280

6 **Kraft R,** Benndorf K, Patt S. Large conductance Ca^{2+}-activated K^+ channels in human meningioma cells. *J Membr Biol* 2000; **175:** 25-33

7 **Huang H,** Rao Y, Sun P, Gong LW. Involvement of actin cytoskeleton in modulation of Ca (2+)-activated K (+) channels from rat hippocampal CA1 pyramidal neurons. *Neurosci Lett* 2002; **332:** 141-145

8 **Shimoni Y,** Ewart HS, Severson D. Insulin stimulation of rat ventricular K^+ currents depends on the integrity of the cytoskeleton. *J Physiol* 1999; **514**(Pt 3): 735-745

9 **Song DK,** Ashcroft FM. ATP modulation of ATP-sensitive potassium channel ATP sensitivity varies with the type of SUR subunit. *J Biol Chem* 2001; **276:** 7143-7149

10 **Wang Z,** Mitsuiye T, Noma A. Cell distension-induced increase of the delayed rectifier K^+ current in guinea pig ventricular myocytes. *Circ Res* 1996; **78:** 466-474

11 **Ribeiro R,** Heinke B, Diener M. Cell volume-induced changes in K+ transport across the rat colon. *Acta Physiol Scand* 2001; **171:** 445-458

12 **Li Y,** Xu WX, Li ZL. Effects of nitroprusside, 3-morpholino-sydnonimine, and spermine on calcium-sensitive potassium currents in gastric antral circular myocytes of guinea pig. *Acta Pharmacol Sin* 2000; **21:** 571-576

13 **Piao L,** Li Y, Li L, Xu WX. Increment of calcium-activated and delayed rectifier potassium current by hyposmotic swelling in gastric antral circular myocytes of guinea pig. *Acta Pharmacol Sin* 2001; **22:** 566-572

14 **Yu YC,** Guo HS, Li Y, Piao L, Li L, Li ZL, Xu WX. Role of calcium mobilization in sodium nitroprusside-induced increase of calcium-activated potassium currents in gastric antral circular myocytes of guinea pig. *Acta Pharmacol Sin* 2003; **24:** 819-825

15 **Stossel TP.** On the crawling of animal cells. *Science* 1993; **260:** 1086-1094

16 **Strege PR,** Holm AN, Rich A, Miller SM, Ou Y, Sarr MG, Farrugia G. Cytoskeletal modulation of sodium current in human jejunal circular smooth muscle cells. *Am J Physiol Cell Physiol* 2003; **284:** C60-66

17 **Terzic A,** Kurachi Y. Actin microfilament disrupters enhance K (ATP) channel opening in patches from guinea-pig cardiomyocytes. *J Physiol* 1996; **492**(Pt 2): 395-404

18 **Srinivasan Y,** Elmer L, Davis J, Bennett V, Angelides K. Ankyrin and spectrin associate with voltage-dependent sodium channels in brain. *Nature* 1988; **333:** 177-180

19 **Xu WX,** Kim SJ, So I, Kim KW. Role of actin microfilament in osmotic stretch-induced increase of voltage-operated calcium channel current in guinea-pig gastric myocytes. *Pflugers Arch* 1997; **434:** 502-504

20 **Wang ZY,** Yu YC, Cui YF, Li L, Guo HS, Li ZL, Xu WX. Role of actin microfilament in hyposmotic membrane stretch-induced increase in muscarinic current of guinea-pig gastric myocytes. *Shengli Xuebao* 2003; **55:** 77-182

Edited by Wang XL **Proofread by** Xu FM

PO Box 2345, Beijing 100023, China
Fax: +86-10-85381893
E-mail: wjg@wjgnet.com www.wjgnet.com

World J Gastroenterol 2004;10(22):3308-3312
World Journal of Gastroenterology
 ISSN 1007-9327

• BASIC RESEARCH •

Selection, proliferation and differentiation of bone marrow-derived liver stem cells with a culture system containing cholestatic serum *in vitro*

Yun-Feng Cai, Zuo-Jun Zhen, Jun Min, Tian-Ling Fang, Zhong-Hua Chu, Ji-Sheng Chen

Yun-Feng Cai, Department of Liver-biliary Surgery, the First Hospital of Foshan City, Foshan 528000, and Department of Hepatic-biliary Surgery, the 2nd Affiliated Hospital of Sun Yat-Sen University, Guangzhou 510120, Guangdong Province, China
Zuo-Jun Zhen, Department of Liver-biliary Surgery, the First Hospital of Foshan City, Foshan 528000, Guangdong Province, China
Jun Min, Department of Hepatic-biliary Surgery, Stem Cell Research Center, Research Center of Medicine, the 2nd Affiliated Hospital of Sun Yat-Sen University, Guangzhou 510120, Guangdong Province, China
Tian-Ling Fang, Zhong-Hua Chu, Ji-Sheng Chen, Department of Hepatic-biliary Surgery, the 2nd Affiliated Hospital of Sun Yat-Sen University, Guangzhou 510120, Guangdong Province, China
Supported by the National Natural Science Foundation of China, No. 30271277 and Natural Science Foundation of Guangdong Province, No.021851
Correspondence to: Dr. Yun-Feng Cai, Department of Liver-biliary Surgery, the First Hospital of Foshan City, 1 Dafu Nanlu, Foshan 528000, Guangdong Province, China. yfcai70@yahoo.com.cn
Telephone: +86-757-83833633-1119 **Fax:** +86-757-83835218
Received: 2003-10-20 **Accepted:** 2003-12-16

Abstract

AIM: To explore the feasibility of direct separation, selective proliferation and differentiation of the bone marrow-derived liver stem cells (BDLSC) from bone marrow cells with a culture system containing cholestatic serum *in vitro*.

METHODS: Whole bone marrow cells of rats cultured in routine medium were replaced with conditioning selection media containing 20 mL/L, 50 mL/L, 70 mL/L, and 100 mL/L cholestatic sera, respectively, after they attached to the plates. The optimal concentration of cholestatic serum was determined according to the outcome of the selected cultures. Then the selected BDLSC were induced to proliferate and differentiate with the addition of hepatocyte growth factor (HGF). The morphology and phenotypic markers of BDLSC were characterized using immunohistochemistry, RT-PCR and electron microscopy. The metabolic functions of differentiated cells were also determined by glycogen staining and urea assay.

RESULTS: Bone marrow cells formed fibroblast-like but not hepatocyte-like colonies in the presence of 20 mL/L cholestatic serum. In 70 mL/L cholestatic serum, BDLSC colonies could be selected but could not maintain good growth status. In 100 mL/L cholestatic serum, all of the bone marrow cells were unable to survive. A 50 mL/L cholestatic serum was the optimal concentration for the selection of BDLSC at which BDLSC could survive while the other populations of the bone marrow cells could not. The selected BDLSC proliferated and differentiated after HGF was added. Hepatocyte-like colony-forming units (H-CFU) then were formed. H-CFU expressed markers of embryonic hepatocytes (AFP, albumin and cytokeratin 8/18), biliary cells (cytokeratin 19), hepatocyte functional proteins (transthyretin and cytochrome P450-2b1), and hepatocyte nuclear factors (HNF-1α and HNF-3β). They also had glycogen storage and urea synthesis functions, two of the critical features of hepatocytes.

CONCLUSION: The selected medium containing cholestatic serum can select BDLSC from whole bone marrow cells. It will be a new way to provide a readily available alternate source of cells for clinical hepatocyte therapy.

Cai YF, Zhen ZJ, Min J, Fang TL, Chu ZH, Chen JS. Selection, proliferation and differentiation of bone marrow-derived liver stem cells with a culture system containing cholestatic serum *in vitro*. *World J Gastroenterol* 2004; 10(22): 3308-3312
http://www.wjgnet.com/1007-9327/10/3308.asp

INTRODUCTION

Several recent reports have highlighted the broad developmental potential of bone marrow-derived stem cells and the term "stem cell plasticity" has been coined[1]. Bone marrow-derived stem cells have been reported to produce not only all of the blood lineages, but also skeletal muscle[2,3], neurons[4,5], cardiac muscle[6,7], pulmonary epithelium[8], and liver epithelium[9]. The transdifferention of bone marrow-derived cells into hepatic cells was described in rats[9], mice[10] and humans[11,12]. This has brought a new hope for cell therapy using autologous bone marrow cells which have few ethical problems and applied to severe liver disease[13]. However, bone marrow contains hematopoietic[14,15], mesenchymal stem cells[16,17] and multipotent adult progenitor cells[18]. The characteristic surface markers of these specific bone marrow-derived liver stem cells (BDLSC) are still obscure. It is difficult to identify and sort these particular cells by immunological methods, such as fluorescent activated cell sorting (FACS)[14] and magnetic activated cell sorting (MACS)[19]. Although various bone marrow stem cells were found to proliferate injured liver cells, previous attempts at isolation of liver stem cells resulted in a mixture of hemotopoietic cells and potential hepatocyte progenitors because they all shared common cell surface receptors and antigens, including hematopoietic stem cell markers CD34, Thy-1, c-Kit, and flt-3[20-22]. It is necessary to find a new way to isolate and purify BDLSC. According to the principle that cells in culture can survive only when they accommodate to the existing environment, we assumed to develop a culture system that can select BDLSC from whole bone marrow cells directly. Within such a system, only BDLSC can survive while the other bone marrow cells cannot. This particular culture system must contain factors that can activate the proliferation of liver stem cells and ingredients inhibiting the growth of other cells. Studies of the relative mechanisms of liver regeneration and liver stem cells corresponding to liver injury[23-26] indicated that the pathological serum after severe liver injury might provide the above conditions. We developed the culture system using cholestatic serum obtained after ligation of common bile duct to induce liver lesions, to select and proliferate BDLSC from whole bone marrow cells *in vitro*. We named this medium system as "pathological microenvironment" selecting medium.

MATERIALS AND METHODS

Preparation of conditional selection medium

Preparation of cholestatic serum Sprague-Dawley (SD) rats weighing 200-250 g were performed common bile duct ligation and transection under general (ether) anesthesia to induce cholestasis. After 10 d, whole blood of each rat was collected and serum was separated. The serum was then subjected to liver function test, and inactivated and asepticized for culture use.

Ingredients of conditional selection medium Twenty mL/L, 50 mL/L, 70 mL/L, and 100 mL/L cholestatic serum were added into DMEM (Gibco) containing 20 mmol/L HEPES (Sigma), 10^{-7} mol/L dexamethasone (Sigma), and antibiotics to act as the conditional selection medium.

Selection, proliferation and differentiation of BDLSC

Culture of whole bone marrow cells Rat bone marrow cells were obtained by flushing femurs. The femurs were accessed through laparotomy to avoid contamination and to increase the cell yield. Bone marrow cells were suspended in DMEM and plated at the density of 1×10^9 cells/L onto culture dishes. DMEM enriched with 100 mL/L fetal bovine serum (FBS, Hyclone), 20 mmol/L HEPES, 10^{-7} mol/L dexamethasone, and antibiotics was used. Dishes were placed in a humidified incubator containing 50 mL/L CO_2-950 mL/L O_2 at 37 ℃.

Selection, proliferation and differentiation of liver stem cells Three days after the culture, the medium and suspended cells were discarded and replaced by conditional selection medium with various concentrations of cholestatic serum. Cells cultured in medium containing FBS were used as control. After 4 d, the media were enriched with 25 μg/L hepatocyte growth factor (HGF, Peprotech EC). Medium was replaced every 3 d and the cultures were maintained for about 2 wk.

Morphological and phenotypic markers of differentiated cells

Immunohistochemistry Bone marrow cells were cultured and selected with the conditional selection medium on 6-well dishes with cover glasses. Twelve days after replacement of the conditional selection medium, cover glasses and the above differentiated BDLSC were taken out and fixed with 40 g/L paraformaldehyde (Sigma) for 30 min at room temperature. The primary antibodies were goat anti-rat albumin, alpha-fetoprotein (AFP), and cytokeratin -8/18 (CK8/18) polyclonal antibodies. The slides were incubated with various primary antibodies at room temperature for 2 h in a humidified chamber. Blocking serum and biotinylated secondary antibody were matched with the primary antibody. Immunoperoxidase was stained and counterstained with DAB and Gill-I hematoxylin.

Electron microscopy Culture dishes were washed with PBS (pH 7.4), and fixed in cold 25 g/L glutaraldehyde in 0.1 mol/L sodium cacodylate buffer (pH 7.4) for 48 h. After fixation, cells were curetted and centrifuged to form aggregates. After postfixed in 10 g/L osmium tetroxide in 0.1 mol/L sodium cacodylate (pH7.4), cells were dehydrated in graded alcohols and embedded in low viscosity epoxy resin. Ultrathin sections were stained with uranyl acetate and lead citrate and viewed under electron microscope.

Total RNA isolation and reverse transcriptase-polymerase chain reaction (RT-PCR) Total RNA was extracted from 1×10^6 differentiated cells by using Trizol (Promega). cDNA was prepared from 2 μg of total RNA in a buffer containing MMLV reverse transcriptase (Promega) and 0.5 μg random primer (Takara). The RNA was incubated at 70 ℃ for 5 min, at 37 ℃ for 1 h, and at 95 ℃ for 5 min. Samples of cDNA corresponding to the input RNA were amplified in PCR reaction buffers containing primers and LA Taq DNA polymerase (Takara). Primers used for amplification were hepatocyte nuclear factor-1α (HNF-1α), hepatocyte nuclear factor-3β (HNF-3β), CK18, CK19, albumin, AFP, transthyretin (TTR), and cytochrome P450-2b1 (CYP2b1). The sequences are listed in Table 1. After initial denaturation (at 94 ℃ for 5 min), 30 cycles of PCR were performed (at 94 ℃ for 30 s, annealing at the optimal temperature for each pair of primers for 30 s, at 72 ℃ for 30 s), and extension at 72 ℃ for 7 min. Amplified products were subjected to electrophoresis in 20 g/L agarose gels and stained with ethidium bromide. All the procedures were performed according to the manufacturer's instructions.

Function tests of differentiated cells

Periodic acid-Schiff staining for glycogen Differentiated cells were fixed in 950 mL/L ethanol for 10min, rinsed in dH_2O. Afterwards, cells were oxidized in 10 g/L periodic acid for 15 min and rinsed three times in dH_2O, then treated with Schiff's reagent for 30 min and rinsed in dH_2O for 10 min, stained with Mayer's hematoxylin for 1 min and rinsed in dH_2O.

Urea assay Urea concentrations were determined by colorimetric assay (640-A, Sigma). Differentiated cells were plated on 6-well dishes. Each well contained 1×10^6 cells. Urea concentrations were detected every day for 4 d according to the manufacture's instructions. Culture medium and blank tube were used as negative controls.

Table 1 Sequence of primers and length of fragments

Gene	Primer	Fragment (bp)
HNF-1α	S:5'-AGCTGCTCCTCCATCATCAGA-3'	138
	A:5'-TGTTCCAAGCATTAAGTTTTCTATTCTAA-3'	
HNF-3β	S:5'-CCTACTCGTACATCTCGCTCATCA-3'	68
	A:5'-CGCTCAGCGTCAGCATCTT-3'	
CK-18	S:5'-GCCCTGGACTCCAGCAACT-3'	70
	A:5'-ACTTTGCCATCCACGACCTT-3'	
CK-19	S:5'-ACCATGCAGAACCTGAACGAT-3'	83
	A:5'-CACCTCCAGCTCGCCATTAG-3'	
Albumin	S:5'-CTGGGAGTGTGCAGATATCAGAGT-3'	141
	A:5'-GAGAAGGTCACCAAGTGCTGTAGT-3'	
AFP	S:5'-GTCCTTTCTTCCTCCTGGAGAT-3'	145
	A:5'-CTGTCACTGCTGATTTCTCTGG-3'	
TTR	S:5'-CAGCAGTGGTGCTGTAGGAGTA-3'	152
	A:5'-GGGTAGAACTGGACACCAAATC-3'	
CYP2b1	S:5'-ACTTTCCTGGTGCCCACA-3'	157
	A:5'-TCCTTCTCCATGCGCAGA-3'	

RESULTS

Preparation of the conditioning selection medium

Ten days after the ligation of common bile duct, TBIL of the cholestatic rats was 107±48.2 μmol/L. The conditional selection media containing 20 mL/L, 50 mL/L, 70 mL/L, and 10 mL/L cholestatic sera had TBIL concentrations of 2.1 μmol/L, 5.3 μmol/L, 7.4 μmol/L and 10.8 μmol/L accordingly.

Bone marrow cells cultured in different concentrations of cholestatic serum

In routine culture condition, part of the bone marrow cells attached to the plate in about 3 d, and then became elongated and fibroblast-like, conforming to the mesodermal characteristics of their origin. After replaced by the conditional selection medium containing 20 mL/L cholestatic serum, the attached cells still survived while the rapid growth was hindered. Seven days after cultured in the medium, colonies were mainly composed of fibroblast-like cells. Only a few colonies acquired hepatocyte-like morphology, although HGF was added. In the presence of 50 mL/L cholestatic serum, a large number of the attached cells exfoliated within 3 d, while many small colonies appeared (Figure 1). These colonies were composed of small, undifferentiated cells in the center, and epithelioid cells at the periphery. The cells enriched with HGF proliferated rapidly. In 70 mL/L cholestatic serum condition, most of the cells exfoliated, fewer colonies appeared, and HGF could not stimulate their proliferation. When the concentration increased to 100 mL/L, all of the cells exfoliated and became apoptosis.

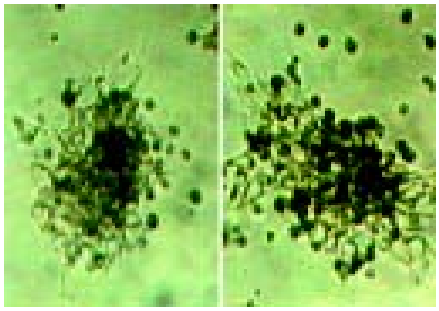

Figure 1 Cell colonies 3 d after selection. Polygonal surrounding cells could be seen.

Morphological evidence of BDLSC differentiation

During the first 3 d many colonies appeared in conditional selection culture containing 50 mL/L cholestatic serum. After enriched with HGF, the colonies enlarged, and the cells proliferated rapidly. Large hepatocyte-like colony-forming units (H-CFU) came into being in about 12 d. The H-CFU were composed of small, undifferentiated cells in the center, and large cells with regular multilateral contours, low nuclear-to-cytoplasmic ratio, and single round nuclei at the periphery. The differentiated cells formed cords or trabeculae resembling the hepatocyte cords in hepatic lobules (Figure 2). The largest colonies contained 1×10^6 cells and could be observed macroscopically, whereas the small colonies were about 30-50 cells. The central undifferentiated cells could still form H-CFU when they were picked out and cultured in the selection medium containing 50 mL/L cholestatic serum and HGF in about 1 wk.

Ultrastructurally, the differentiated cells were rich in endoplasmic reticulum and ribosomes and contained abundant ellipsoid mitochondria (Figure 3), which were different to the control cells. These ultrastructural features are typical of adult hepatocytes.

Phenotypic markers of differentiated cells

The identification of hepatocyte-like cells in 12-day-old selection medium cultures prompted us to analyze these cells for biochemical evidence of hepatocytic differentiation. Immunohistochemistry was performed in cells grew on the cover glasses for the existence of albumin (Figure 4), AFP and CK8/18, the characteristic proteins expressed during hepatocyte development. Immunoperoxidase staining for these proteins revealed diffuse cytoplasmic staining of hepatocte-like cells. In contrast, the fibroblast-like cells grew in the routine cultures did not express these proteins. RT-PCR further convinced the hepatocytic characteristics of differentiated cells as the results showed that there were mRNA transcripts of HNF-1α, HNF-3β, albumin, AFP, CK-18, CK-19, TTR, and CYP2b1, all of which were hepatic specific (Figure 5).

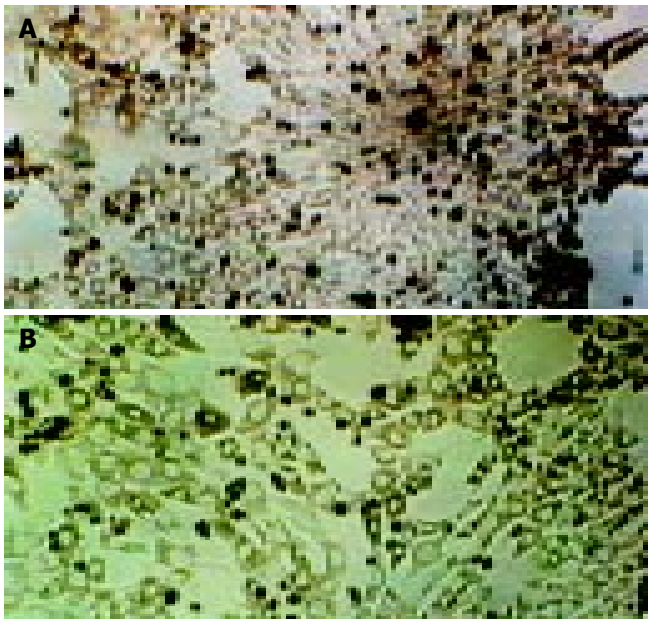

Figure 2 Appearance of hepatocyte-like colony forming units (H-CFU) 12 d after selection A: H-CFU, undifferentiated round cells in the center, surrounded by polygonal hepatocyte-like cells B: Regular arrangement of surrounding hepatocyte-like cells similar to the cords of hepatocytes.

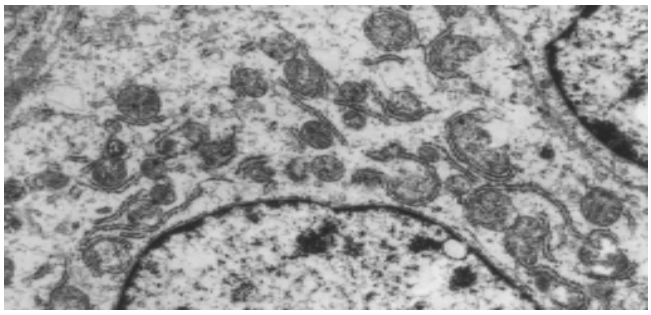

Figure 3 Ultrastructure of hepatocyte-like cells. 9 000×.

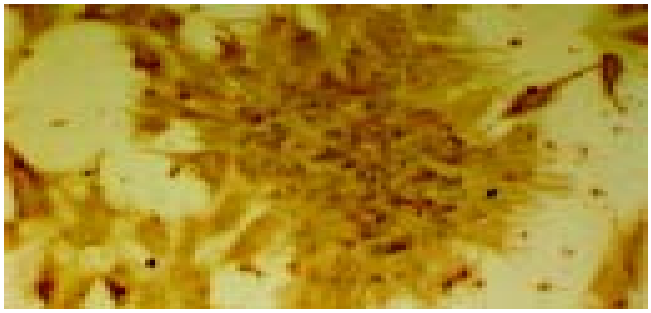

Figure 4 Positive staining of albumin immunohistochemistry 12 d after selection. ABC staining 200×.

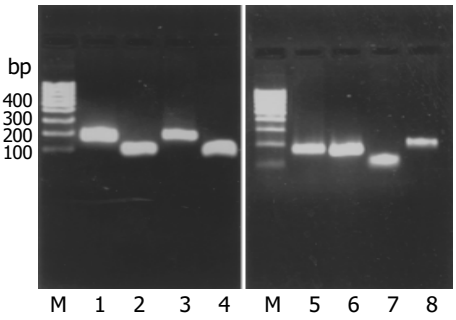

Figure 5 RT-PCR results M: marker, 1: AFP, 2: CK-18, 3: CYP2b1, 4: HNF-3β, 5: Albumin, 6: TTR, 7: CK-19, 8: HNF-1α.

Function tests of differentiated cells

We analyzed the levels of glycogen storage by periodic acid-Schiff (PAS) staining. Glycogen storage was seen as accumulation of magenta staining in the cytoplasms of hepatocyte-like differentiated cells (Figure 6). The control cells did not show similar staining. Urea production and secretion by hepatocyte-like cells were measured at various time points after the differentiated morphology appeared. Bone marrow cells and fibroblast-like cells did not produce urea. Urea assay revealed that urea concentration in the medium increased in a time-dependent manner (Figure 7).

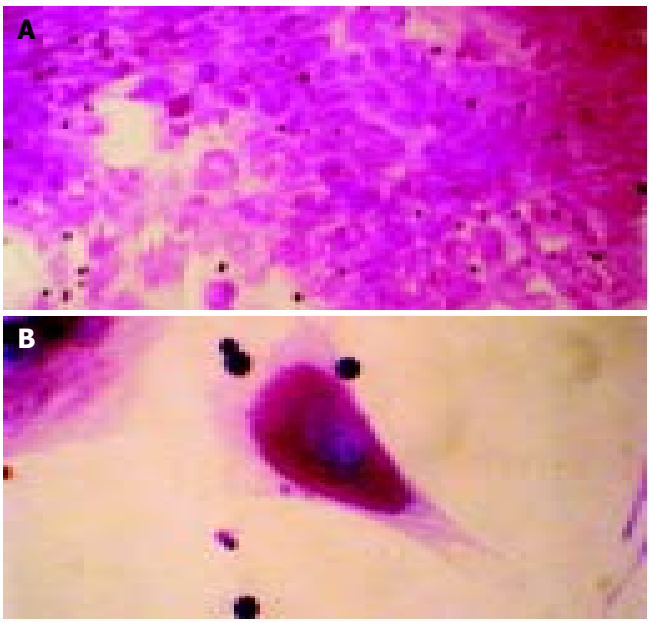

Figure 6 PAS staining of hepatocyte-like differentiated cells. The cells were positive in the cytoplasm (A) 200×, (B) 400×.

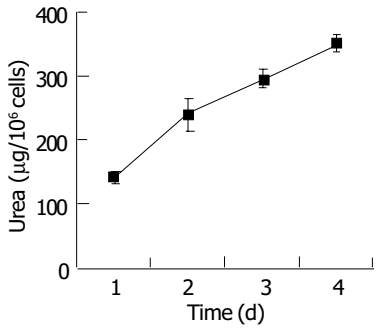

Figure 7 Urea synthetic function of bone marrow-derived liver stem cells (mean±SD, n = 4).

DISCUSSION

Since the results of cross-sex and cross-strain bone marrow and whole liver transplantation experiments indicated that the bone marrow might be a source of hepatocyte progenitors, great interests have been aroused in identification and isolation of liver stem cells from bone marrow cells. Until recently, several subsets of bone marrow cells have been found to have the potential to differentiate into hepatocytes, such as KTLS cells (c-kit^{high}Thy^{low}Lin$^-$Sca-1$^+$)[20], β_2-m$^-$Thy-1$^+$ cells[27,28], multipotent adult progenitor cells (MAPC, CD44$^-$CD45$^-$HLA$^-$c-kit$^-$)[18], and C1qR$_p^+$ Lin$^-$CD45$^+$CD38$^-$CD34$^{+/-}$ cells[29]. These stem cells could express different surface markers, and might represent different stages or different branches along the differentiation and developmental processes of bone marrow stem cells. So far, the characteristic surface markers of BDLSC and their pedigrees in the derivation of bone marrow stem cells remain obscure. Any subset sorting methods based on phenotypes would certainly lose other stem cells that have the ability to differentiate into hepatocytes. Furthermore, the sorting manipulations of the above stem cells with complicated surface markers are very difficult.

Studies on liver regeneration showed that liver stem cells could correspond to and repair liver injury only under certain severe pathological circumstances such as extensive liver necrosis due to chemical injury or hepatocytes treated with chemicals that could block their proliferation[24]. Based on this mechanism, we assumed to imitate the *in vivo* pathological microenvironment of liver injury in culture of whole bone marrow cells, in order to provide specific proliferation signals for BDLSC, and to avoid resource loss of liver stem cells and complicated manipulation due to subset sorting. The key of this method is to develop an optimal "pathological microenvironment". Olynyk *et al*. demonstrated that in the cholestatic model of common bile duct ligation, intrahepatic liver stem cells showed great proliferation[25]. Avital *et al*. recently reported that β_2-m$^-$Thy-1$^+$ cells in bone marrow could differentiate into cells with hepatocyte-like phenotypes when co-cultured with adult hepatocyes in a medium containing cholestatic serum[27], suggesting that there are stimulating factors in cholestatic serum. In our experiments, we used pathologically conditional selection medium containing cholestaic serum to culture whole bone marrow cells. Results showed that in the selection medium, a large number of the bone marrow cells exfoliated, only part of the remaining cells presented colonal growth during the first 3 d. When enriched with HGF on d 4, rapid proliferation and differentiation emerged, and H-CFU with various size appeared in 2 wk. The morphology and phenotypic markers manifested that the cells of H-CFU were similar to embryonic hepatoblasts. They expressed markers of embryonic hepatocytes (AFP, albumin and CK18), biliary cells (CK19), hepatocyte functional proteins (TTR and CYP2b1), and hepatocyte nuclear factors (HNF-1α and HNF-3β). HNF-1α is a transcription factor required for subsequent hepatocyte differentiation, and transcription factor HNF-3β was known to be important in endoderm specification. These results proved that H-CFU were colonies of liver stem cells.

In the culture system containing cholestatic serum, the concentration of "pathological microenvironment" needs to be considered. We found that 100 mL/L cholestatic serum was fatal to all of the bone marrow cells, 70 mL/L cholestatic serum prevented the colonies from growth and proliferation, 20 mL/L cholestatic serum could not inhibit the growth of other cells, while only 50 mL/L cholestatic serum acquired pure H-CFU. The differences can be explained by the toxic contents of cholestatic serum, which are the metabolic products cumulated under the circumstances of common bile duct obstruction and hepatic insufficiency, including bilirubin, bile acid, endotoxin, and ammonia, *etc*. When cholestatic serum was confined to the optimal concentration, BDLSC, possessing functions of bilirubin conjugation and detoxification[30], could metabolize these toxic

products and survive, and selectively proliferate responding to the signal of liver injury. On the other hand, non-BDLSC could not adapt to the environment and resulted in apoptosis. To confirm that if the H-CFU had functional characteristics of hepatocytes, we tested the glycogen and urea synthesis functions of the cells and proved that the selected cells possessed hepatocyte-like functions. Therefore, the "pathological microenvironment" selecting medium based on cholestatic serum can select BDLSC in two ways, providing selective proliferation signals for BDLSC and eliminating non-BDLSC, so as to purify BDLSC.

We demonstrated that a "pathological microenvironment" selecting medium could select, proliferate and differentiate BDLSC from whole bone marrow cells *in vitro*. This method can not only provide a new and effective way for the isolation and purification of extrahepatic liver stem cells, but also supply a clue to obtain a readily available alternate source of cells for clinical hepatocyte therapy.

ACKNOWLEDGEMENTS

The authors thank Xiao-Dong Zhou, Jing Wei, Yu-Ru Fu, and Yu-Shen Lin, Clinical Research Center of Medicine, the 2nd Affiliated Hospital and the Center of Electron Microscopy, Sun Yat-Sen University for their technical support.

REFERENCES

1 **Krause DS.** Plasticity of marrow-derived stem cells. *Gene Ther* 2002; **9**: 754-758
2 **Ferrari G,** Cusella-De Angelis G, Coletta M, Paolucci E, Stornaiuolo A, Cossu G, Mavilio F. Muscle regeneration by bone marrow-derived myogenic progenitors. *Science* 1998; **279**: 1528-1530
3 **Gussoni E,** Soneoka Y, Strickland CD, Buzney EA, Khan MK, Flint AF, Kunkel LM, Mulligan RC. Dystrophin expression in the mdx mouse restored by stem cell transplantation. *Nature* 1999; **401**: 390-394
4 **Brazelton TR,** Rossi FM, Keshet GI, Blau HM. From marrow to brain: expression of neuronal phenotypes in adult mice. *Science* 2000; **290**: 1775-1779
5 **Mezey E,** Chandross KJ, Harta G, Maki RA, McKercher SR. Turning blood into brain: cells bearing neuronal antigens generated *in vivo* from bone marrow. *Science* 2000; **290**: 1779-1782
6 **Orlic D,** Kajstura J, Chimenti S, Limana F, Jakoniuk I, Quaini F, Nadal-Ginard B, Bodine DM, Leri A, Anversa P. Mobilized bone marrow cells repair the infarcted heart, improving function and survival. *Proc Natl Acad Sci U S A* 2001; **98**: 10344-10349
7 **Orlic D,** Kajstura J, Chimenti S, Jakoniuk I, Anderson SM, Li B, Pickel J, McKay R, Nadal-Ginard B, Bodine DM, Leri A, Anversa P. Bone marrow cells regenerate infarcted myocardium. *Nature* 2001; **410**: 701-705
8 **Krause DS,** Theise ND, Collector MI, Henegariu O, Hwang S, Gardner R, Neutzel S, Sharkis SJ. Multi-organ, multi-lineage engraftment by a single bone marrow-derived stem cell. *Cell* 2001; **105**: 369-377
9 **Petersen BE,** Bowen WC, Patrene KD, Mars WM, Sullivan AK, Murase N, Boggs SS, Greenberger JS, Goff JP. Bone marrow as a potential source of hepatic oval cells. *Science* 1999; **284**: 1168-1170
10 **Theise ND,** Badve S, Saxena R, Henegariu O, Sell S, Crawford JM, Krause DS. Derivation of hepatocytes from bone marrow cells in mice after radiation-induced myeloablation. *Hepatology* 2000; **31**: 235-240
11 **Alison MR,** Poulsom R, Jeffery R, Dhillon AP, Quaglia A, Jacob J, Novelli M, Prentice G, Williamson J, Wright NA. Hepatocytes from non-hepatic adult stem cells. *Nature* 2000; **406**: 257
12 **Theise ND,** Nimmakayalu M, Gardner R, Illei PB, Morgan G, Teperman L, Henegariu O, Krause DS. Liver from bone marrow in humans. *Hepatology* 2000; **32**: 11-16
13 **Zhang Y,** Bai XF, Huang CX. Hepatic stem cells: Existence and origin. *World J Gastroenterol* 2003; **9**: 201-204
14 **Spangrude GJ,** Heimfeld S, Weissman IL. Purification and characterization of mouse hematopoietic stem cells. *Science* 1988; **241**: 58-62
15 **Baum CM,** Weissman IL, Tsukamoto AS, Buckle AM, Peault B. Isolation of a candidate human hematopoietic stem-cell population. *Proc Natl Acad Sci U S A* 1992; **89**: 2804-2808
16 **Pereira RF,** Halford KW, O'Hara MD, Leeper DB, Sokolov BP, Pollard MD, Bagasra O, Prockop DJ. Cultured adherent cells from marrow can serve as long-lasting precursor cells for bone, cartilage, and lung in irradiated mice. *Proc Natl Acad Sci U S A* 1995; **92**: 4857-4861
17 **Prockop DJ.** Marrow stromal cells as stem cells for nonhematopoietic tissues. *Science* 1997; **276**: 71-74
18 **Schwartz RE,** Reyes M, Koodie L, Jiang Y, Blackstad M, Lund T, Lenvik T, Johnson S, Hu WS, Verfaillie CM. Multipotent adult progenitor cells from bone marrow differentiate into functional hepatocyte-like cells. *J Clin Invest* 2002; **109**: 1291-1302
19 **Wong LS,** Bateman WJ, Morris AG, Fraser IA. Detection of circulating tumour cells with the magnetic activated cell sorter. *Br J Surg* 1995; **82**: 1333-1337
20 **Lagasse E,** Connors H, Al-Dhalimy M, Reitsma M, Dohse M, Osborne L, Wang X, Finegold M, Weissman IL, Grompe M. Purified hematopoietic stem cells can differentiate into hepatocytes *in vivo*. *Nat Med* 2000; **6**: 1229-1234
21 **Petersen BE,** Goff JP, Greenberger JS, Michalopoulos GK. Hepatic oval cells express the hematopoietic stem cell marker Thy-1 in the rat. *Hepatology* 1998; **27**: 433-445
22 **Omori M,** Omori N, Evarts RP, Teramoto T, Thorgeirsson SS. Coexpression of flt-3 ligand/flt-3 and SCF/c-kit signal transduction system in bile-duct-ligated SI and W mice. *Am J Pathol* 1997; **150**: 1179-1187
23 **Hoffman AL,** Rosen HR, Ljubimova JU, Sher L, Podesta LG, Demetriou AA, Makowka L. Hepatic regeneration: current concepts and clinical implication. *Semin Liver Dis* 1994; **14**: 190-210
24 **Sell S.** Heterogeneity and plasticity of hepatocyte lineage cells. *Hepatology* 2001; **33**: 738-750
25 **Olynyk JK,** Yeoh GC, Ramm GA, Clarke SL, Hall PM, Britton RS, Bacon BR, Tracy TF. Gadolinium chloride suppresses hepatic oval cell proliferation in rats with biliary obstruction. *Am J Pathol* 1998; **152**: 347-352
26 **Fausto N.** Liver regeneration: from laboratory to clinic. *Liver Transpl* 2001; **7**: 835-844
27 **Avital I,** Inderbitzin D, Aoki T, Tyan DB, Cohen AH, Ferraresso C, Rozga J, Arnaout WS, Demetriou AA. Isolation, characterization, and transplantation of bone marrow-derived hepatocyte stem cells. *Biochem Biophys Res Commun* 2001; **288**: 156-164
28 **Avital I,** Feraresso C, Aoki T, Hui T, Rozga J, Demetriou A, Muraca M. Bone marrow-derived liver stem cell and mature hepatocyte engraftment in livers undergoing rejection. *Surgery* 2002; **132**: 384-390
29 **Danet GH,** Luongo JL, Butler G, Lu MM, Tenner AJ, Simon MC, Bonnet DA. C1qRp defines a new human stem cell population with hematopoietic and hepatic potential. *Proc Natl Acad Sci U S A* 2002; **99**: 10441-10445
30 **Vilei MT,** Granato A, Ferraresso C, Neri D, Carraro P, Gerunda G, Muraca M. Comparison of pig, human and rat hepatocytes as a source of liver specific metabolic functions in culture systems-implications for use in bioartificial liver devices. *Int J Artif Organs* 2001; **24**: 392-396

Edited by Wang XL and Zhang JZ **Proofread by** Xu FM

PO Box 2345, Beijing 100023, China
Fax: +86-10-85381893
E-mail: wjg@wjgnet.com www.wjgnet.com

World J Gastroenterol 2004;10(22):3313-3317
World Journal of Gastroenterology
 ISSN 1007-9327

• CLINICAL RESEARCH •

Upper gastrointestinal endoscopy: Are preparatory interventions or conscious sedation effective? A randomized trial

Lucio Trevisani, Sergio Sartori, Piergiorgio Gaudenzi, Giuseppe Gilli, Giancarlo Matarese, Sergio Gullini, Vincenzo Abbasciano

Lucio Trevisani, Sergio Sartori, Piergiorgio Gaudenzi, Giancarlo Matarese, Sergio Gullini, Vincenzo Abbasciano, Digestive Endoscopy Service, Department of Internal Medicine, S. Anna Hospital, Ferrara, Italy
Giuseppe Gilli, Health Physics Department, S. Anna Hospital, Ferrara, Italy
Correspondence to: Dr. Lucio Trevisani, Centro di Endoscopia Digestiva, Azienda Ospedaliera "Arcispedale S. Anna", C.so Giovecca 203, 44100 Ferrara, Italy. tvl@unife.it
Telephone: +1139-532-237558 **Fax:** +1139-532-236932
Received: 2004-02-20 **Accepted:** 2004-04-09

Abstract

AIM: The fears and concerns are associated with gastroscopy (EGD) decrease patient compliance. Conscious sedation (CS) and non-pharmacological interventions have been proposed to reduce anxiety and allow better execution of EGD. The aim of this study was to assess whether CS, supplementary information with a videotape, or presence of a relative during the examination could improve the tolerance to EGD.

METHODS: Two hundred and twenty-six outpatients (pts), scheduled for a first-time non-emergency EGD were randomly assigned to 4 groups: Co-group (62 pts): throat anaesthesia only; Mi-group (52 pts): CS with i.v. midazolam; Re-group (58 pts): presence of a relative throughout the procedure; Vi-group (54 pts): additional information with a videotape. Anxiety was measured using the "Spielberger State and Trait Anxiety Scales". The patients assessed the overall discomfort during the procedure on an 100-mm visual analogue scale, and their tolerance to EGD answering a questionnaire. The endoscopist evaluated the technical difficulty of the examination and the tolerance of the patients on an 100-mm visual analogue scale and answering a questionnaire.

RESULTS: Pre-endoscopy anxiety levels were higher in the Mi-group than in the other groups ($P<0.001$). On the basis of the patients' evaluation, EGD was well tolerated by 80.7% of patients in Mi-group, 43.5% in Co-group, 58.6% in Re-group, and 50% in Vi-group ($P<0.01$). The discomfort caused by EGD, evaluated by either the endoscopist or the patients, was lower in Mi-group than in the other groups. The discomfort was correlated with "age" ($P<0.001$) and "groups of patients" ($P<0.05$) in the patients' evaluation, and with "gender" (females tolerated better than males, $P<0.001$) and "groups of patients" ($P<0.05$) in the endoscopist's evaluation.

CONCLUSION: Conscious sedation can improve the tolerance to EGD. Male gender and young age are predictive factors of bad tolerance to the procedure.

Trevisani L, Sartori S, Gaudenzi P, Gilli G, Matarese G, Gullini S, Abbasciano V. Upper gastrointestinal endoscopy: Are preparatory interventions or conscious sedation effective? A randomized trial. *World J Gastroenterol* 2004; 10(22): 3313-3317
http://www.wjgnet.com/1007-9327/10/3313.asp

INTRODUCTION

Esophagogastroduodenoscopy (EGD) is a safe and quick procedure, and can be carried out without sedation[1]. However, it can evoke anxiety, feelings of vulnerability, embarrassment and discomfort[2], and the fears and concerns associated with endoscopic procedure decrease patient compliance[2-4]. Indeed, anxiety, discomfort, and pain are interrelated, and each may increase the others[5], making EGD execution more difficult. Several methods can be used to reduce patient pre-procedural worries, such as psychological interventions using relaxation and coping techniques[6,7], hypnosis[8], relaxation music[9], acupuncture[10], educational materials including videotapes[11], and presence of a family member during EGD[12]. However, conscious sedation with benzodiazepines is the method most widely employed[5]. Although usually safe, such medications are not free of adverse effects[13-15], and the likelihood of sedative-related complications increases in the presence of high anxiety levels, requiring higher doses of drugs[2]. It follows that the role of conscious sedation is not well defined, and its use varies from country to country: up to 98% in USA, less frequently in European countries, and quite rarely in Asia and South America[16]. The use of conscious sedation is also declining in the United Kingdom[17], and many patients who receive detailed information about the advantages and risks of sedation choose to undergo EGD with pharyngeal anesthesia alone[18,19]. In our endoscopy service, a standardized information sheet about EGD is given to all patients, and the examination is routinely performed with pharyngeal anesthesia alone.

This randomized prospective study was to evaluate if conscious sedation, additional information with a videotape, or the presence of a family member during the procedure could improve the tolerance to EGD and make the execution of EGD easier. In addition, particular emphasis was put on psychologic and procedure-related factors having a potential impact on the patient perception of tolerance.

MATERIALS AND METHODS

Study population

For six consecutive months, the first two outpatients daily referred for diagnostic EGD, fulfilling the eligibility criteria, were asked to enter the study. Inclusion criteria were age between 18 and 65 years, no prior experience of endoscopic examinations, and capability (evaluated by the endoscopist) of fully understanding and filling up the questionnaires of the study. Exclusion criteria were prior gastrectomy, psychiatric diseases or long-term psychiatric drug addiction, presence of neoplastic or other serious concomitant diseases, history of intolerance to benzodiazepines. On the whole, two hundred and eighty patients were asked to enter the study, and 228 of them were accepted. The patients were randomly assigned to four groups by a computer procedure. In the control group (Co-group), EGD was performed with topical pharyngeal anesthesia alone (100 g/L lidocaine spray). In the other three groups the following methods were used in addition to pharyngeal anesthesia: conscious sedation with i.v. midazolam 35 μg/kg (Mi-group); presence of a relative in the endoscopy room throughout the procedure (Re-group); additional information about the procedure using a videotape lasting for

about 10 min (Vi-group).

The study protocol was approved by the ethical committee of our hospital, and all patients gave their written consent to participate in the study.

Patients' assessments

Anxiety Since the anxiety experienced by patients undergoing EGD was hypothesized to be a factor related to potential discomfort, anxiety was measured by the Spielberger State-Trait Anxiety Inventory (STAI)[20] in the validated Italian language version[21]. Patients were asked to complete STAI before EGD. STAI is a 40-item questionnaire designed to measure state anxiety and trait anxiety. State anxiety is a temporary and situational anxiety, and trait anxiety is the tendency to awaken state anxiety under stress. Both kinds of anxiety were scored in the range of 20 to 80 points, a higher score indicated a greater anxiety. Before EGD, the patients had also to specify what they dreaded more about endoscopic examination, choosing among five items: fear of pain, fear of stifling, fear of complications, fear of endoscopic findings, and other.

Tolerance

Patients' assessment of tolerance to EGD was carried out at least 2 h after the end of the procedure. This interval was chosen to minimize the risk of persisting anterograde amnesia, which could potentially influence patient judgment. Patients assessed their tolerance answering the question: "*how did you tolerate EGD?*" ("*well*", "*rather badly*", "*badly*"), and rated the overall discomfort during EGD on an 100-mm visual analogue scale (0: no discomfort; 100: unbearable).

Endoscopist's assessment

All EGDs were carried out by the same endoscopist, using video endoscopes with a diameter of 9.8 mm (Fujinon video endoscopic system-Fujinon, Tokyo, Japan). Immediately after endoscopy, the operator recorded if EGD was completed, or it had to be interrupted, or it could be completed only after administration of sedatives (for Mi-group, after further sedatives in addition to midazolam previously administered). Moreover, he evaluated the ease of introduction of the instrument ("*easy*": no failed attempt of introduction; or "*difficult*": one or more failed attempts of introduction). Finally, he rated the discomfort caused to patients during EGD on an 100-mm visual analogue scale (0: no discomfort; 100: unbearable), and assessed the tolerance of the patients grading it into three steps: *"good", "poor", "very bad"*.

Parameters monitored

Blood oxygen saturation (SaO2) and heart rate were continuously monitored during EGD. Desaturation was defined as a decrease in oxygen saturation below 90% for over 30 s. The occurrence of complications was recorded after each procedure. The duration of endoscopic examination was timed in all groups of patients. In Mi-group, the degree of sedation was evaluated using the Ramsay's scale[22].

Statistical analysis

Characteristics of patients in the four groups were analyzed using one-way ANOVA and chi-square test. Endoscopic findings, tachycardia, motives of fear, answers of patients to the questions about their tolerance to EGD, ease of introduction of the instrument, and endoscopist's evaluation of tolerance of patients to EGD were compared in the four groups by using chi-square-test.

State and trait pre-endoscopic anxiety levels, and the discomfort rated by the patients and endoscopist on the 100-mm visual analogue scale were analyzed using one-way and two-way ANOVA. Two-way ANOVA was also used to evaluate the influence of sex, age, and anxiety levels on the discomfort caused by EGD. Linear-regression analysis was used to assess the relationship between the state and trait anxiety scores, as well as the correlation between patients' and endoscopist's evaluation of the discomfort caused by EGD. A general linear model (GLM) procedure was used to analyze the influence of sex, age, groups of patients, state anxiety, duration of EGD, and endoscopic findings on the degree of discomfort caused by EGD, assessed by either the endoscopist or the patients.

Results were considered statistically significant if P values were <0.05 (two-tailed test).

RESULTS

Two patients (1 in Co-group and 1 in Mi-group) were excluded from the study, as EGD was not completed. Two hundred and twenty-six patients (90 males and 136 females, mean age 38±10.62 years, range 19-63 years) could be evaluated. The four groups did not differ in age, endoscopic findings, and duration of the examination. The male: female ratio was lower in Mi-group than in the other groups ($P<0.05$) (Table 1).

Fourteen point five percent of patients in Co-group (6/62), 21.1% in Mi-group (11/52), 20.6% in Re-group (12/58), 16.6% in

Table 1 Demographic and clinical data of the patients

	Co-group	Mi-group	Re-group	Vi-group
Patients (*n*)	62	52	58	54
Gender (m/f)	25/37	9/43[a]	28/30	28/26
Age (yr; mean±SD)	37.85±10.44	40.13±10.55	35.20±10.57	39.24±10.57
State anxiety (mean±SD)	46.66±10.73	54.19±10.89[b]	46.03±11.42	39.62±9.05
Trait anxiety (mean±SD)	38.30±7.16	44.26±9.43[b]	37.22±8.21	38.05±9.63
Duration of EGD (seconds; mean ± SD)	145.88±45.18	157.40±48.09	140.60±35.56	142.96±39.11
Endoscopic findings (No cases):				
Normal findings	30	25	26	22
Esophagitis	1	3	6	10
Hiatus Ernia	3	1	2	3
Gastritis or Duodenitis	24	19	19	14
Gastric or duodenal ulcer	2	2	3	3
Cancer	-	-	-	1
Other findings	2	2	2	1

[a]$P<0.05$, [b]$P<0.001$ *vs* the other three groups.

Table 2 Tolerance to EGD and patients' and endoscopist's assessment

	Patients' assesment[b]				Endoscopist's assessment			
	Co-G (*n*)	Mi-G (*n*)	Re-G (*n*)	Vi-G (*n*)	Co-G (*n*)	Mi-G (*n*)	Re-G (*n*)	Vi-G (*n*)
Good	27	42[b]	34	27	45	44[b]	54	42
Poor	31	10[b]	23	23	12	7[b]	4	7
Very bad	4	0[b]	1	4	5	1[b]	0	5

Mi-G: [b]$P<0.01$ *vs* the other three groups.

Table 3 Discomfort caused to patients during EGD and patients' and endoscopist's assessment (visual analogue scale)

	Co-G (mean±SD)	Mi-G (mean±SD)	Re-G (mean±SD)	Vi-G (mean±SD)
Patient evaluation	33.01±22.12	21.98±21.60	29.17±22.95	26.12±21.94
Endoscopist evaluation	23.51±22.99	14.17±18.07[a]	16.43±14.42	20.81±24.04

[a]$P<0.05$ *vs* Co-G.

Table 4 Influence of some parameters on degree of discomfort caused by EGD (GLM procedure)

	Patient's assessment			Endoscopist's assessment		
Parameter	Coefficient	SE	*P*	Coefficient	SE	*P*
Gender	-0.251	3.153	0.937	-10.094	2.901	0.001
Age (yr)	-0.621	0.140	0.000	-0.159	0.129	0.219
Groups of patients	-1.138	1.325	0.391	-1.012	1.219	0.407
State anxiety	0.104	0.136	0.445	0.237	0.126	0.060
Time for EGD	0.046	0.039	0.237	-0.057	0.036	0.112
Endoscopic findings	-0.813	1.774	0.647	3.158	1.632	0.054

Vi-group (9/54) had a heart rate higher than 100 beats/min before starting EGD. During EGD, the heart rate exceeded 130 beats/min for at least 30 seconds in 5, 2, 3, and 2 patients in the four groups, respectively. No complication occurred, and no case of oxygen desaturation was observed. According to Ramsay's scale, in Mi-group grade 2 sedation was reached in 50 patients, and grade 3 in 2 patients.

State anxiety scores before EGD were significantly higher in Mi-group than in the other groups ($P<0.001$), as well as trait anxiety scores ($P<0.001$) (Table 1). State and trait anxiety scores were strongly correlated ($P<0.001$).

In all groups the most frequent cause of fear before EGD was the fear of stifling (70 cases on the whole). The ease of introduction of gastroscope did not differ among the four groups, and the introduction resulted in difficulty just in one patient of Co-group and in 3 of Vi-group.

On the basis of patients' assessment, the tolerance to EGD was more frequently good when sedation was given: 80.7% of patients in Mi-group tolerated well gastroscopy, *vs* 43.5% in Co-group, 58.6% in Re-group, and 50% in Vi-group ($P<0.01$) (Table 2). Conversely, no significant difference among the four groups was observed in the evaluation of the endoscopist, who nevertheless found that the discomfort caused by EGD was lower in Mi-group than in Co-group ($P<0.05$) (Table 3). The degree of discomfort was lower in patients of Mi-group than in those of Co-group, but the difference was just close to threshold of significance, but did not reach it ($P = 0.059$) (Table 3). The other comparisons among the groups did not show any difference in the degree of discomfort caused by EGD. The evaluations of the patients and those of the endoscopist were strongly correlated ($P<0.001$, m = 0.45), even though the endoscopist underestimated the degree of discomfort (Figure 1).

Two-way ANOVA performed on the degree of discomfort assessed by the patients, evaluated for factors "gender" and "groups of patients" corrected for age, trait anxiety and state anxiety, showed an inverse influence of the age (i.e. better tolerance for older individuals, $P<0.001$) and the factor "groups of patients" ($P<0.05$). Conversely, the degree of discomfort assessed by the endoscopist was significantly influenced by the factors "gender" and "groups of patients" ($P<0.001$ and $P<0.05$, respectively). The factors "gender" and "groups of patients" showed a true and constant interaction (interaction factor $P<0.01$), reflecting behaviors significantly different between males and females within the four groups, in particular in Co-group (Figures 2A, B).

Also the GLM procedure showed that age exerted the greatest influence on the discomfort caused by EGD in opinion of the patients (inverse correlation, $P<0.001$), whereas in opinion of the endoscopist the discomfort was mainly influenced by the gender (females tolerated EGD better than males, $P<0.001$) (Table 4).

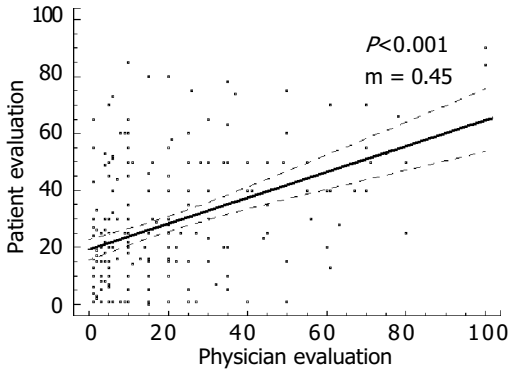

Figure 1 Linear regression of discomfort assessed by patients and endoscopist.

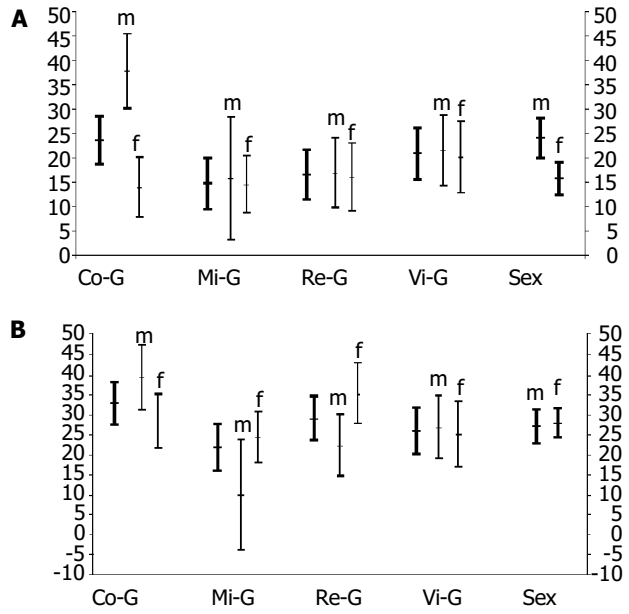

Figure 2 Discomfort assessed by patients and andoscopist, and mean values for factors "groups of patients" and "gender" with 95% c.l. Thick lines: m = males; f = females. Co-G: control group Mi-G: midazolam group Re-G: relatives group Vi-G: video group A: Discomfort assessed by patients B: Discomfort assessed by endoscopist.

DISCUSSION

Although conscious sedation is the method most widely used to reduce anxiety in patients undergoing EGD, its actual role is still an unresolved problem. Very large differences in sedation practice existed among different countries, and sometimes among different units within the same country[5]. To our knowledge, this is the first randomized trial comparing the efficacy in improving the tolerance to EGD of conscious sedation, the presence of a relative in the endoscopy room throughout the procedure, and additional information by using a videotape. Abuksis *et al*. demonstrated that previous endoscopy experience could reduce anxiety level and influence patients' compliance[23], and other authors identified endoscope size as a significant variable in determining tolerance to the procedure[24,25]. For these reasons, in our study all patients enrolled had no prior endoscopy experience, and all EGDs were carried out using gastroscopes with the same diameter.

Our results suggested that low-dose conscious sedation with midazolam could improve the tolerance to EGD, according to a previous trial reporting a lower discomfort in sedated patients than in controls[26]. Conversely, the presence of a relative attending the procedure and the use of informative videotape did not seem to give the patients significant advantages over the controls. However, better tolerance and lower discomfort were found in Re-group and Vi-group than in Co-group by either the patients or the endoscopist. Although these findings did not reach the significance level, in our opinion they suggested that the method used in controls (pharyngeal anesthesia only) was the worst approach to perform EGD. Indeed, the multivariate analysis showed constant differences among the groups of patients in concern of the discomfort caused by endoscopy, highlighting the usefulness of preparatory interventions in improving the tolerance to EGD.

The presence of relatives has been proved helpful in several medical fields, such as to children during hospitalization and to women during childbirth[27], but it is not a standard procedure in digestive endoscopy. At present, just one randomized study was published on this topic, and the results suggested that the presence of a family member throughout endoscopy could represent a promising approach[12]. Conversely, the usefulness of additional information to reduce the anxiety and to improve the compliance of patients has been widely investigated, but with conflicting results. Detailed information before endoscopy has been reported to reduce anxiety levels[11,28], but other studies failed in demonstrating any usefulness of this approach[29], and some authors found that the over-information about endoscopy could even increase anxiety levels[30,31].

The evaluation of the discomfort expressed by the patients and the endoscopist showed a strong correlation in our study (Figure 1). However, the endoscopist rated the patient degree of discomfort as lower than the patients themselves. According to the observation of Watson *et al*. that both endoscopists and nurses underestimated the discomfort felt by the patients [32]. Besides anxiety, in our experience age and gender also influenced significantly the tolerance to endoscopy. Indeed, high levels of discomfort during EGD have been recently reported to be associated with younger age and high levels of pre-endoscopic anxiety[24]. Older patients were likely to tolerate endoscopy better than their younger counterparts as they had a decreased pharyngeal sensitivity[33,34]. Unlike several studies reporting better tolerance in men[26,35], we found that female gender was associated with better tolerance. However, this gender-specific finding has been disputed by other authors[3, 24,33].

Despite the effectiveness of conscious sedation shown in our study, we think it should be avoided whenever possible in clinical practice. The extensive use of sedation would require several extra-charges, including the cost of drugs, prolongation of the procedure time, need of monitoring cardiopulmonary functions, need of recovery room for post-procedure observation, and the impossibility for patients to return to work immediately after endoscopic examination[36]. Furthermore, sedative drugs are not free of adverse effects. In our series, no complications and oxygen desaturation were observed, and low-dose midazolam induced just rarely significant alterations in cardiorespiratory parameters[26]. Nevertheless, conscious sedation could cause hypoxemia, which may induce cardiopulmonary complications, and most complications associated with endoscopy were attributable to the medications given for the procedure rather than the procedure itself[13-15]. For these reasons, we think that further studies incorporating cut-off points are necessary to identify the patients who are likely to tolerate diagnostic gastroscopy without sedation. Some other preparatory interventions might also be effective to reduce endoscopy-related anxiety[37]. The intervention techniques we used might be incorporated into our endoscopic practice, as they are simple, quick, easy to reproduce, and their extensive use doesa not require additional extra-charges, and expose the patients to the risk of complications.

REFERENCES

1 **Al-Atrakchi HA.** Upper gastrointestinal endoscopy without sedation: a prospective study of 2000 examinations. *Gastrointest Endosc* 1989; **35**: 79-81

2 **Brandt LJ.** Patients' attitudes and apprehensions about endoscopy: how to calm trobled waters. *Am J Gastroenterol* 2001; **96**: 280-284

3 **Campo R,** Brullet E, Montserrat A, Calvet X, Moix J, Rue M, Roque Donoso L, Bordas JM. Identification of factors that influence tolerance of upper gastrointestinal endoscopy. *Eur J Gastroenterol Hepatol* 1999; **11**: 201-204

4 **Dominitz JA,** Provenzale D. Patient preferences and quality of life associated with colorectal cancer screening. *Am J Gastroenterol* 1997; **92**: 2171-2178

5 **Bell GD.** Premedication, preparation, and surveillance. *Endoscopy* 2002; **34**: 2-12

6 **Gattuso SM,** Litt MD, Fitzgerald TE. Coping with gastrointestinal endoscopy: self-efficacy enhancement and coping style. *J*

Consult Clin Psychol 1992; **60**: 133-139
7 **Woloshynowych M,** Oakley DA, Saunders BP, Williams CB. Psychological aspects of gastrointestinal endoscopy: a review. *Endoscopy* 1996; **28**: 763-767
8 **Conlong P,** Rees W. The use of hypnosis in gastroscopy: a comparison with intravenous sedation. *Postgrad Med J* 1999; **75**: 223-225
9 **Bampton P,** Draper B. Effect of relaxation music on patient tolerance of gastrointestinal endoscopic procedures. *J Clin Gastroenterol* 1997; **25**: 343-345
10 **Li CK,** Nauck M, Loser C, Folsch UR, Creutzfeldt W. Acupuncture to alleviate pain during colonoscopy. *Dtsch Med Wochenschr* 1991; **116**: 367-370
11 **Luck A,** Pearson S, Maddem G, Hewett P. Effects of video information on precolonoscopy anxiety and knowledge: a randomised trial. *Lancet* 1999; **354**: 2032-2035
12 **Shapira M,** Tamir A. Presence of family member during upper endoscopy: what do patients and escorts think? *J Clin Gastroenterol* 1996; **22**: 272-274
13 **Herman LL,** Kurtz RC, McKee KJ, Sun M, Thaler HT, Winawer SJ. Risk factors associated with vasovagal reactions during colonoscopy. *Gastrointest Endosc* 1993; **39**: 388-391
14 **Iber FL,** Sutberry M, Gupta R, Kruss D. Evaluation of complications during and after conscious sedation for endoscopy using pulse oximetry. *Gastrointest Endosc* 1993; **39**: 620-625
15 **Mokhashi MS,** Hawes RH. Struggling toward easier endoscopy. *Gastrointest Endosc* 1998; **48**: 432-440
16 **Lazzaroni M,** Bianchi Porro G. Preparation, premedication and surveillance. *Endoscopy* 1998; **30**: 53-60
17 **Mulcahy HE,** Hennessy E, Connor P, Rhodes B, Patchett SE, Farthing MJ, Fairclough PD. Changing patterns of sedation use for routine out-patient diagnostic gastroscopy between 1989 and 1998. *Aliment Pharmacol Ther* 2001; **15**: 217-220
18 **Hedenbro JL,** Lindblom A. Patient attitudes to sedation for diagnostic upper endoscopy. *Scand J Gastroenterol* 1991; **26**: 1115-1120
19 **Pereira S,** Hussaini SH, Hanson PJ, Wilkinson ML, Sladen GE. Endoscopy: throat spray or sedation? *J R Coll Physicians Lond* 1994; **28**: 411-414
20 **Spielberger CD,** Gorsuch RL, Lushene RE. Manual for the State-Trait Anxiety Inventory. *Palo-Alto: Consulting Psychologists Press* 1970
21 **Spielberger CD,** Gorsuch RL, Lushene RE. Questionario di autovalutazione per l'ansia di stato e di tratto. Manuale di istruzioni. Traduzione di Lazzari R, Pancheri P. *Firenze: Organizzazioni Speciali* 1989
22 **Ramsay MA,** Savege TM, Simpson BR, Goodwin R. Controlled sedation with alphaxalone-alphadolone. *Br Med J* 1974; **2**: 656-659
23 **Abuksis G,** Mor M, Segal N, Shemesh I, Morad I, Plaut S, Weiss E, Sulkes J, Fraser G, Niv Y. A patient education program is cost-effective for preventing failure of endoscopic procedures in a gastroenterology department. *Am J Gastroenterol* 2001; **96**: 1786-1790
24 **Mulcahy HE,** Kelly P, Banks MR, Connor P, Patchet SE, Farthing MJ, Fairclough PD, Kumar PJ. Factors associated with tolerance to, and discomfort with, unsedated diagnostic gastroscopy. *Scand J Gastroenterol* 2001; **36**: 1352-1357
25 **Mulcahy HE,** Riches A, Kiely M, Farthing MJ, Fairclough PD. A Prospective controlled trial of an ultrathin versus a conventional endoscope in unsedated upper gastrointestinal endoscopy. *Endoscopy* 2001; **33**: 311-316
26 **Froehlich F,** Schwizer W, Thorens J, Kohler M, Gonvers JJ, Fried M. Conscious sedation for gastroscopy: patient tolerance and cardiorespiratory parameters. *Gastroenterology* 1995; **108**: 697-704
27 **Gjerdingen DK,** Froberg DG, Fontaine P. The effects of social support of women's health during pregnancy, labor and delivery, and the postpartum period. *Fam Med* 1991; **23**: 370-375
28 **Lembo T,** Fitzgerald L, Matin K, Woo K, Mayer EA, Nalidoff BD. Audio and visual stimulation reduces patient discomfort during screening flexible sigmoidoscopy. *Am J Gastroenterol* 1998; **93**: 1113-1116
29 **Levy N,** Landmann L, Stermer E, Erdreich M, Beny A, Meisels R. Does a detailed explanation prior to gastroscopy reduce the patient's anxiety? *Endoscopy* 1989; **21**: 263-265
30 **Dawes PJ,** Davison P. Informed consent: what do patients want to know? *J R Soc Med* 1994; **87**: 149-152
31 **Tobias JS,** Souhami RL. Fully informed consent can be needlessly cruel. *B M J* 1993; **307**: 1199-1201
32 **Watson JP,** Goss C, Phelps G. Audit of sedated versus unsedated gastroscopy: do patients notice a difference? *J Qual Clin Pract* 2001; **21**: 26-29
33 **Abraham N,** Barkun A, Larocque M, Fallone C, Mayrand S, Baffis V, Cohen A, Daly D, Daoud H, Joseph L. Predicting which patients can undergo upper endoscopy comfortably without consious sedation. *Gastrointest Endosc* 2002; **56**: 180-189
34 **Davies AE,** Kidd D, Stone SP, MacMahon J. Pharyngeal sensation and gag reflex in healthy subjects. *Lancet* 1995; **345**: 487-488
35 **Tan CC,** Freeman JG. Throat spray for upper gastrointestinal endoscopy is quite acceptable to patients. *Endoscopy* 1996; **28**: 277-282
36 **Schmitt CM.** Preparation for upper gastrointestinal endoscopy: opportunity or inconvenience? *Gastrointest Endosc* 1998; **48**: 430-432
37 **Hackett ML,** Lane MR, McCarthy DC. Upper gastrointestinal endoscopy: are preparatory interventions effective? *Gastrointest Endosc* 1998; **48**: 341-347

Edited by Wang XL **Proofread by** Xu FM

PO Box 2345, Beijing 100023, China
Fax: +86-10-85381893
E-mail: wjg@wjgnet.com www.wjgnet.com

World J Gastroenterol 2004;10(22):3318-3321
World Journal of Gastroenterology
 ISSN 1007-9327

• CLINICAL RESEARCH •

Opisthorchiasis-associated biliary stones: Light and scanning electron microscopic study

Banchob Sripa, Pipatphong Kanla, Poonsiri Sinawat, Melissa R. Haswell-Elkins

Banchob Sripa, Department of Pathology, Faculty of Medicine, Khon Kaen University, Khon Kaen 40002, Thailand
Pipatphong Kanla, Department of Anatomy, Faculty of Medicine, Khon Kaen University, Khon Kaen 40002, Thailand
Poonsiri Sinawat, Division of Anatomical Pathology, Khon Kaen Regional Hospital, Khon Kaen, Thailand and Department of Pathology, Faculty of Medicine, Khon Kaen University, Khon Kaen 40002, Thailand
Melissa R. Haswell-Elkins, Australia Centre for International and Tropical Health and Nutrition, University of Queensland, Brisbane, Australia
Supported by in part by the Tropical Health Program and NHMRC, Commonwealth Government, Australia
Correspondence to: Dr. Banchob Sripa, Department of Pathology, Faculty of Medicine, Khon Kaen University, Khon Kaen, 40002, Thailand. banchob@kku.ac.th
Telephone: +66-43-202024 **Fax:** +66-43-348375
Received: 2004-04-07 **Accepted:** 2004-05-25

Abstract

AIM: Biliary stones are frequently encountered in areas endemic for opisthorchiasis in Thailand. The present study was to describe the prevalence and pathogenesis of these stones.

METHODS: Gallstones and/or common bile duct stones and bile specimens from 113 consecutive cholecystectomies were included. Bile samples, including sludge and/or microcalculi, were examined for *Opisthorchis viverrini* eggs, calcium and bilirubin. The stones were also processed for scanning electron microscopic (SEM) study.

RESULTS: Of the 113 cases, 82 had pigment stones, while one had cholesterol stones. The other 30 cases had no stones. Most of the stone cases (76%, 63/83) had multiple stones, while the remainder had a single stone. Stones were more frequently observed in females. Bile examination was positive for *O. viverrini* eggs in 50% of the cases studied. Aggregates of calcium bilirubinate precipitates were observed in all cases with sludge. Deposition of calcium bilirubinate on the eggshell was visualized by special staining. A SEM study demonstrated the presence of the parasite eggs in the stones. Numerous crystals, morphologically consistent with calcium derivatives and cholesterol precipitates, were seen.

CONCLUSION: Northeast Thailand has a high prevalence of pigment stones, as observed at the cholecystectomy, and liver fluke infestation seems involved in the pathogenesis of stone formation.

Sripa B, Kanla P, Sinawat P, Haswell-Elkins MR. Opisthorchiasis-associated biliary stones: Light and scanning electron microscopic study. *World J Gastroenterol* 2004; 10(22): 3318-3321
http://www.wjgnet.com/1007-9327/10/3318.asp

INTRODUCTION

Liver fluke infestation caused by *Opisthorchis viverrini* remains a major public health concern in Southeast Asia[1], particularly in Thailand where an estimated 6 million people are infected[2]. This infection is associated with a number of benign hepatobiliary diseases, including cholangitis, obstructive jaundice, hepatomegaly, cholecystitis and biliary lithiasis[3]. Both experimental and epidemiological evidence implicate liver fluke infestation in the etiology of bile duct cancer, i.e. cholangiocarcinoma[1,4,5].

An association between liver fluke infection and biliary lithiasis is well-recognized. *Opisthorchis* worm and/or eggs have been observed in the stones of infected or previously treated individuals[6], just as *Clonorchis sinensis* eggs were found in the stones of those with Chinese liver fluke infection[7,8]. Several community-based studies in Northeast Thailand have shown a significant increase in the frequency of biliary sludge in people with a heavy infection[9-11]. Since biliary sludge is a precursor of stone formation[12-14], opisthorchiasis likely plays a role in the development of biliary stones in certain individuals. However, the mechanism of liver-fluke-associated stone development is unclear.

We report the incidence of stone types, its relationship with *O. viverrini* infection and bile/stone examinations. The potential pathogenesis of opisthorchiasis-associated stones, in patients from endemic areas of Thailand, is proposed.

MATERIALS AND METHODS

Patients

This study was carried out in Northeast Thailand, an area endemic for opisthorchiasis. The study population included 113 consecutive patients scheduled for cholecystectomy at Khon Kaen Regional Hospital from whom bile was obtained between 1990 and 1991. The gallbladder diseases associated with the cholecystectomies included cholelithiasis (n = 71), cholecystitis with cholangiocarcinoma (n = 29) and cholecystitis with other miscellaneous diseases (n = 13). None of the patients had any history of hemolytic anemia or severe thalassemia.

Patients ranged between 17 and 94 years of age (mean, 54.97±14.65) (45 females, 68 males). The study was carried out in accordance with the principles embodied in the 1975 Helsinki Declaration. A signed informed consent was obtained from each patient.

Specimen collection and laboratory investigations

Gallstones and/or common bile duct stones and bile specimens were collected from each individual. Bile samples aspirated from the gallbladder were centrifuged at 3 000 r/min for 10 min, then examined for the presence of *O. viverrini* eggs. At least four pellet-smears per individual were examined before the specimen was considered negative for eggs.

For a demonstration of calcium and bilirubin, the bile smears were air-dried and fixed in 40 g/L formaldehyde. Calcium and bilirubin staining were performed using histochemical methods[15]. Calcium was stained black, bilirubin deep green.

Five stones from each group with *Opisthorchis* egg-negative and -positive bile underwent scanning electron microscopic (SEM) study. Briefly, the stones were thoroughly washed in distilled water and dried. After mechanical breaking, the stones

were sputter-coated with gold (agar aids-PS3, UK) and observed under a Hitachi (Model S-3200N, Japan) scanning electron microscope and photographed.

Statistical analysis

The χ^2-test was used to analyze the association between the frequency of gallstones and sex, disease association, parasite egg status and age groups. A P value <0.05 was considered statistically significant.

RESULTS

Cholesterol or pigment stones were classified by visual inspection. Cholesterol stones were white or yellow and crystalline in composition, pigment stones were black or black-brown and amorphous.

Of the 113 cases, 83 had stones while 30 had none. Most of the stone cases (98.8%, 82/83) had pigment stones, while only one had cholesterol stone(s). In addition, 63 of the 83 cases (75.9%) contained multiple stones, while the remainder had a single stone. Of the 29 cases with cholangiocarcinoma, 9 (31.0%) contained stones while the others with miscellaneous diseases had stones in 3 out of 13 (23.1%) cases. The prevalence of stones in all of the sample groups was significantly higher in females (χ^2-test, P = 0.028). No association between stones and age groups (stratified as < 40, 40-49, 50-59 and > 60 years) was found (χ^2-test, P = >0.05).

Bile examination was positive for *O. viverrini* eggs in 57 of the 113 cases (49.6%) studied. The presence of parasite eggs was not associated with the frequency of stones or disease association (χ^2-test, P = >0.05). Most of the eggs were embedded in mucous gel. Aggregates of calcium bilirubinate precipitates were observed in all cases with sludge. Three cases had clear deposits of calcium bilirubinate on the eggshell, seen by special staining. Specifically, calcium was stained immediately adjacent to the eggshell, while bilirubin was observed in the outer layer (Figure 1 A, B). Examples of parasite egg-associated microcalculi aggregation and stone development are shown in Figures 2A-D.

A SEM study demonstrated the presence of parasite eggs in the center of stones from all of the *Opisthorchis* egg-positive cases. Interestingly, 3 of the 5 egg-negative cases contained the parasite eggs in the stones. Numerous crystals, morphologically consistent with calcium derivatives and cholesterol precipitates, were observed. Typical SEM pictures of the stones are shown in Figures 3A, B.

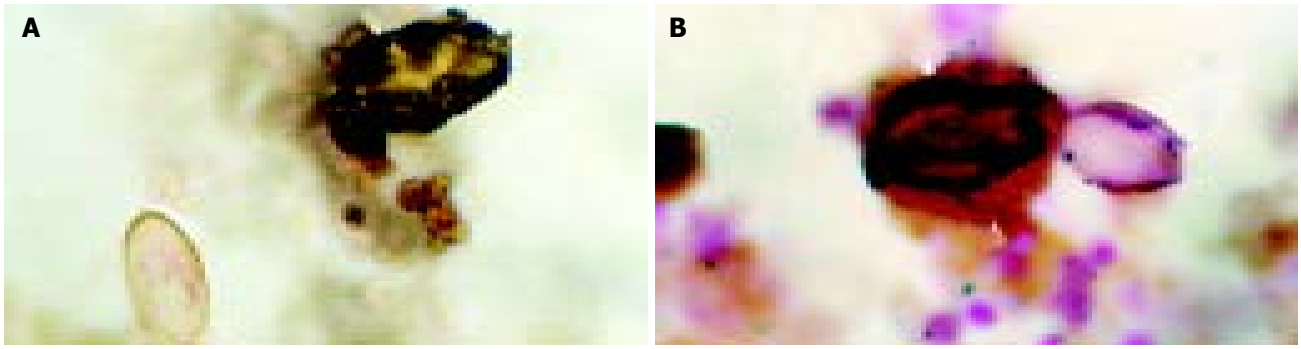

Figure 1 Histochemical staining of biliary sludge for bilirubin (A) and calcium (B). Calcium appears as dark deposits on the *Opisthorchis* eggshell (arrow) and bilirubin precipitates are demonstrated in the outer layer (arrowhead). Normal parasite eggs without deposition are shown in the same field. (A = Fouchet stain, B = von Kossa stain).

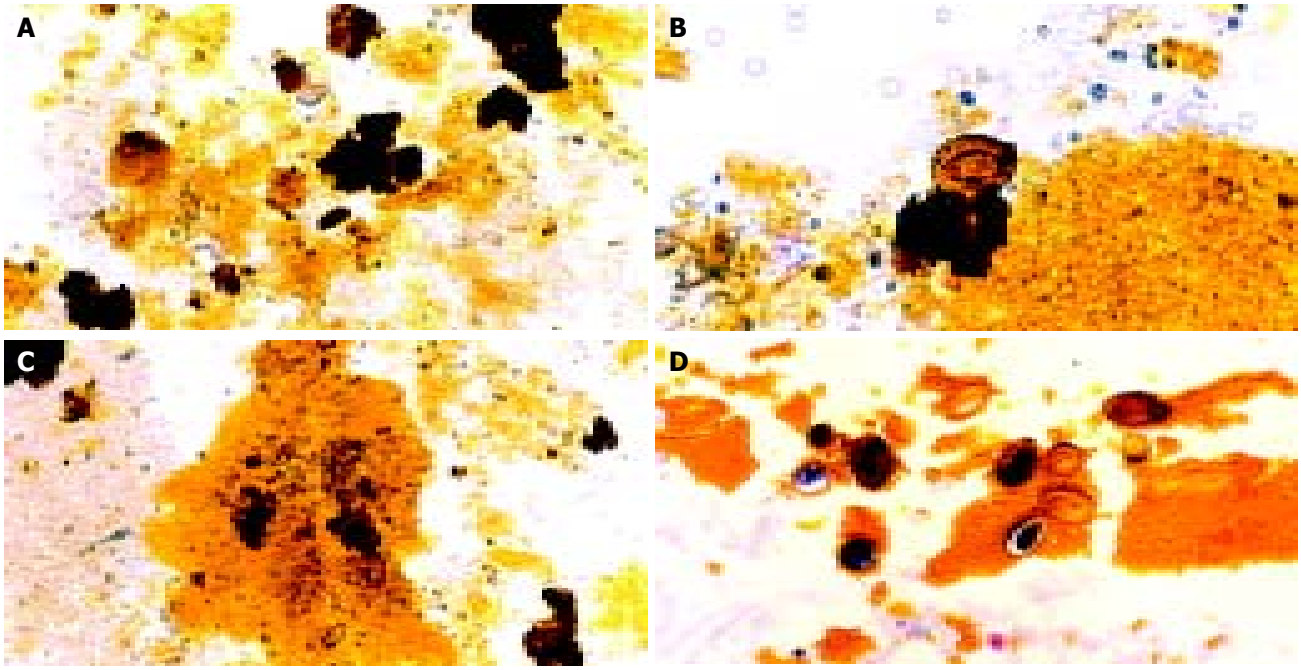

Figure 2 Typical pictures showing the cascades of *Opisthorchis* egg-associated stone formation starting from aggregation of the eggs admixed with mucin (A), deposition of calcium bilirubinate on the eggshells (B), and formation of tiny stones (C & D). Original magnification, x100 (A & C) and x200 (B & D).

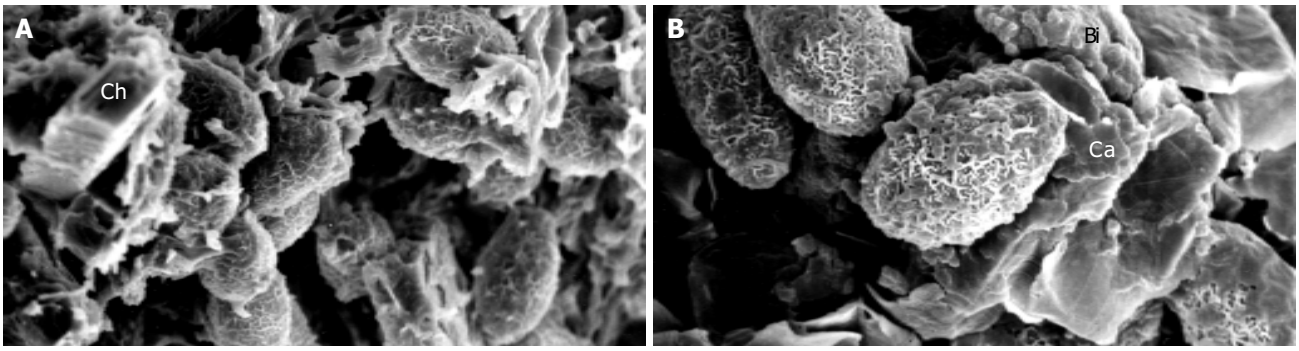

Figure 3 SEM micrographs of gallstones showing *Opisthorchis* eggs with typical musk-melon-eggshell surface in the nidi of the stones. Several crystalline structures consistent with calcium (Ca), bilirubin derivatives (Bi) and cholesterol (Ch) could be noted (AB). Higher magnification with highlighting calcium bilirubinate deposition on *Opisthorchis* eggshell and mucus is shown in Figure 3B.

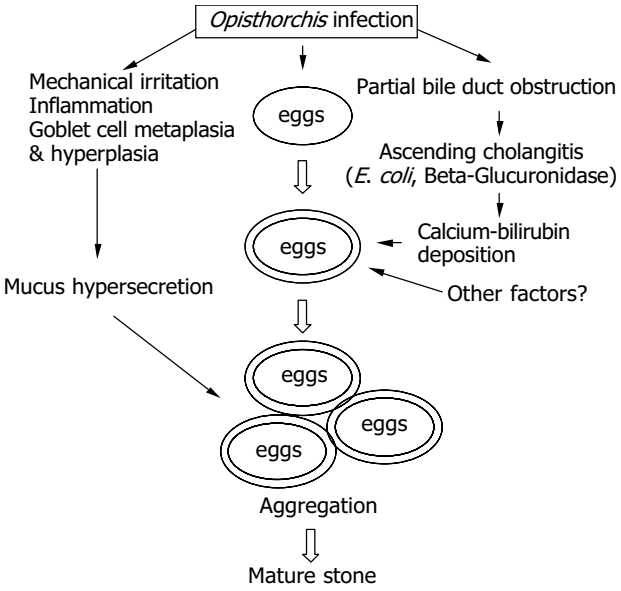

Figure 4 Diagram showing the proposed pathogenesis of *Opisthorchis*-associated biliary stone.

DISCUSSION

Biliary lithiasis is a common indication for cholecystectomy in most parts of the world. However, the prevalence and types of stones differ geographically[16-18]. Pigment stones, mostly containing calcium bilirubinate, generally constitute 10 to 27 percent of all gallstones in America and Europe, the predominant type was cholesterol stones[19-21]. In contrast, the prevalence of pigment stones is high in Asia, accounting for $\leqslant$90% of all stones in some parts of China[22]. In our study, almost all the cases (98.8%) of biliary lithiasis involved pigment stones. This is probably the highest reported relative frequency of pigment stones found during cholecystectomy. It exceeds a report from Bangkok, Central Thailand, where pure cholesterol stones represent $\leqslant$32% of stones[23]. Stones in our study of Northeast Thailand, however, occurred more frequently in females than in males as in other countries[19-20].

The association between certain parasitic infections and biliary stone formation is well documented[7,24-27]. Our study demonstrated *Opisthorchis* eggs in the sludge from the gallbladder bile confirmed the sludge seen in other ultrasound studies performed in Northeast Thailand[12-14]. However, our study failed to demonstrate the association between *O. viverrini* infection and the presence of stones, perhaps because of previous self-treatment with praziquatel, an anthelminthic widely used in Northeast Thailand[2]. We collected the treatment data, but they were not reliable as patients did not record when or how many times they took the medication before cholecystectomy. Moreover, re-infection is common in people in endemic areas.

SEM data from egg-negative patients revealed parasite eggs in the nidi of the stones, indicating these patients were previously infected. Budget constraints meant that only a limited number of cases were confirmed by SEM. More stones should be studied to test the validity of the findings.

The mechanism by which parasite infection enhances pigment stone formation is not clearly understood. The present study demonstrated *O. viverrini* eggs in the biliary sludge and gallstones in both bile smears and the SEM, while Riganti *et al*.[6] observed both adult worms and eggs in the nidi of gallstones from two patients. Riganti *et al.* also demonstrated calcium bilirubinate in pigment stones, as previously reported in stones associated with *C. sinensis*[7,8] and ascariasis[8,27,28]. These observations have led investigators to conclude that parasite eggs and/or worms may directly stimulate stone formation[6,8]. Our histochemical findings on the calcium and bilirubin coatings on the *O. viverrini* eggs support this hypothesis. The presence of calcium coating on the outer surface of the parasite eggshell suggests that the eggs may act as a nucleus for stone formation. This may be similar to peripheral calcification of existing cholesterol stones[29]. Since calcium is an active element, and can precipitate several bile constituents including bilirubin, carbonate and phosphate - major components of pigment stones[30]. The parasite eggs precipitated with calcium bilirubinate and admixed with mucin, which is abundant in a liver fluke infection[3,25]. Mucin secreted by biliary epithelial cells has been recognized as an important local factor in gallstone pathogenesis[31]. This orchestrated process can eventually produce mature pigment stones as generally described[32].

Additionally, liver flukes that inhabit the bile ducts can partially obstruct the lumen leading to bile stasis and ascending cholangitis[3]. *E. coli*, a common bacterial species infecting the biliary system[23,33], releases β-glucuronidases, which can hydrolyze the glucuronic acid from the conjugated bilirubin[34-36]. The resulting unconjugated bilirubin precipitates as calcium salts, which is the first step in pigment stone formation[32,34]. Bile stasis is not only a condition for ascending infection but also induces stagnation of the bile components leading to stone formation[37]. Heavy *Opisthorchis* infection can induce poor emptying of the gallbladder[9-11]. In addition, our recent report has shown that severe fibrosis of the gallbladder wall is the main histopathology of chronic opisthorchiasis[38]. These altogether support the role of this liver fluke in gallbladder stasis, ascending cholangitis and enhanced stone formation. From previous data and our own observations, a proposed pathogenesis of *Opisthorchis*-associated pigment stone formation

is presented in Figure 4.

In conclusion, Northeast Thailand has a high incidence of pigment stones compared to cholesterol stones at cholecystectomy. Our study clearly demonstrates that calcium bilirubinate precipitates on parasite eggshells both in light and SEM studies. This supports the role of *O. viverrini* infection in the pathogenesis of pigment stone formation.

ACKNOWLEDGMENTS

The authors thank Mr. Bryan Roderick Hamman for helping with the English-language presentation.

REFERENCES

1 Infection with liver flukes (*Opisthorchis viverrini*, *Opisthorchis felineus* and *Clonorchis sinensis*). *IARC Monogr Eval Carcinog Risks Hum* 1994; **61:** 121-175
2 **Jongsuksuntigul P**, Imsomboon T. Opisthorchiasis control in Thailand. *Acta Trop* 2003; **88**: 229-321
3 **Harinasuta T**, Riganti M, Bunnag D. *Opisthorchis viverrini* infection: pathogenesis and clinical features. *Arzneimittelforschung* 1984; **34**: 1167-1169
4 **Sithithaworn P**, Haswell-Elkins MR, Mairiang P, Satarug S, Mairiang E, Vatanasapt V, Elkins DB. Parasite-associated morbidity: liver fluke infection and bile duct cancer in north-east Thailand. *Int J Parasitol* 1994; **24**: 833-843
5 **Vatanasapt V**, Sripa B, Sithithaworn P, Mairiang P. Liver flukes and liver cancer. *Cancer Surv* 1999; **33**: 313-343
6 **Riganti M**, Pungpak S, Sachakul V, Bunnag D, Harinasuta T. *Opisthorchis viverrini* eggs and adult flukes as nidus and composition of gallstones. *Southeast Asian J Trop Med Public Health* 1988; **19**: 633-636
7 **Teoh TB**. A study of gall-stones and included worms in recurrent pyogenic cholangitis. *J Pathol Bacteriol* 1963; **86**: 123-129
8 **Ker CG**, Huang TJ, Sheen PC, Chen ER. A study of structure and pathogenesis of *Ascaris* and *Clonorchis* stones. *Kaohsiung J Med Sci* 1988; **4**: 231-237
9 **Elkins DB**, Haswell-Elkins MR, Mairiang E, Mairiang P, Sithithaworn P, Kaewkes S, Bhudhisawasdi V, Uttaravichien T. A high frequency of hepatobiliary disease and cholangiocarcinoma associated with heavy *Opisthorchis viverrini* infection in a small community in Northeast Thailand. *Trans R Soc Trop Med Hyg* 1990; **84**: 715-719
10 **Mairiang E**, Elkins DB, Mairiang P, Chaiyakum J, Chamadol N, Loapaiboon V, Posri S, Sithithaworn P, Haswell-Elkins MR. Relationship between intensity of *Opisthorchis viverrini* infection and hepatobiliary disease detected by ultrasonography. *J Gastroenterol Hepatol* 1992; **7**: 17-21
11 **Mairiang E**, Haswell-Elkins MR, Mairiang P, Sithithaworn P, Elkins DB. Reversal of biliary tract abnormalities associated with *Opisthorchis viverrini* infection following praziquantel treatment. *Trans R Soc Trop Med Hyg* 1993; **87**: 194-197
12 **Lee SP**, Nicholls JF. Nature and composition of biliary sludge. *Gastroenterology* 1986; **90**: 677-686
13 **Lee SP**, Maher K, Nicholls JF**.** Origin and fate of biliary sludge. *Gastroenterology* 1988; **94**: 170-176
14 **Terada T**, Nakanuma Y, Saito K, Kono N. Biliary sludge and microcalculi in intrahepatic bile ducts: Morphologic and X-ray microanalytical observations in 18 among 1 179 consecutively autopsied livers. *Acta Pathol Jpn* 1990; **40**: 894-901
15 **Luna LG**. Manual of histologic staining methods of the Armed Forces Institute of Pathology. 3rd ed. New York: *McGraw-Hill* 1968: 258
16 **Weedon D**. Pathology of the Gallbladder. New York: *Masson* 1984: 290
17 **Kim WR**, Brown RS Jr, Terrault NA, El-Serag H. Burden of liver disease in the United States: summary of a workshop. *Hepatology* 2002; **36**: 227-242
18 **Shi JS**, Ma JY, Zhu LH, Pan BR, Wang ZR, Ma LS. Studies on gallstone in China. *World J Gastroenterol* 2001; **7**: 593-596
19 **Friedman GD**, Kannel WB, Dawler TR. The epidemiology of gallstone disease: observation in the Framingham study. *J Chronic Dis* 1966; **19**: 273-292
20 **Trotman BW**, Soloway RD. Pigment *vs* cholesterol cholelithiasis: clinical and epidemiological aspects. *Am J Dig Dis* 1975; **20**: 735-740
21 **Johnston DE**, Kaplan MM. Pathogenesis and treatment of gallstones. *New Eng J Med* 1993; **11**: 411-421
22 **Crowther RS**, Soloway RD. Pigment gallstone pathogenesis: from man to molecules. *Semin Liver Dis* 1990; **10**: 171-180
23 **Teparut V**, Limsuvan B, Pitchayangura C, Vatanachote D, Banchuin C, Jenvatanavit T, Athiphanumpai A, Pokawatana C, Tancharoen S. Correlation among biliary stones, gallbladder pathology and aerobic biliary infections. *Bull Dept Med Serv* 1986; **11**: 523-532
24 **Cook J**, Hou PC, Ho HC, McFadzean AJS. Recurrent pyogenic cholangitis. *Br J Surg* 1954; **42**: 188-203
25 **Hou PC**. The pathology of *Clonorchis sinensis* infestation of the liver. *J Pathol Bacteriol* 1955; **70**: 53-64
26 **Cobo A**, Hall RC, Torres E, Cuello CJ. Intrahepatic calculi. *Arch Surg* 1964; **89**: 936-941
27 **Yellin AE**, Donovan AJ. Biliary lithiasis and helminthiasis. *Am J Surg* 1981; **142**: 128-136
28 **Maki T**. Cholelithiasis in Japanese. *Arch Surg* 1961; **82**: 599-612
29 **Moore EW**. Biliary calcium and gallstone formation. *Hepatology* 1990; **12**(3 Pt 2): 206S-214S
30 **Rege RV**. The role of biliary calcium in gallstone pathogenesis. *Front Biosci* 2002 **7**: E315-325
31 **Ko CW**, Lee SP. Gallstone formation. Local factors. *Gastroenterol Clin North Am* 1999; **28**: 99-115
32 **Cahalane MJ**, Neubrand MW, Carey MC. Physical-chemical pathogenesis of pigment gallstones. *Semin Liver Dis* 1988; **8**: 317-328
33 **Truedson H**, Elmros T, Holm S. The incidence of bacteria in gallbladder bile at acute and elective cholecystectomy. *Acta Chir Scand* 1983; **149**: 307-313
34 **Maki T**. Pathogenesis of calcium bilirubinate gallstone: Role of *E. coli*-β-glucuronidase and coagulation by inorganic ions, polyelectrolytes and agitation. *Ann Surg* 1966; **164**: 90-100
35 **Swidsinski A**, Lee SP. The role of bacteria in gallstone pathogenesis. *Front Biosci* 2001; **6**: E93-103
36 **Nakai K**, Tazuma S, Nishioka T, Chayama K. Inhibition of cholesterol crystallization under bilirubin deconjugation: partial characterization of mechanisms whereby infected bile accelerates pigment stone formation. *Biochim Biophys Acta* 2003; **1632**: 48-54
37 **Pauletzki J**, Paumgartner G. Review article: defects in gallbladder motor function-role in gallstone formation and recurrence. *Aliment Pharmacol Ther* 2000; **14**(Suppl 2): 32-34
38 **Sripa B**, Hawell-Elkins MR, Sinawat P. Histological analysis of cholecystitis in relation to opisthorchiasis in endemic areas of Thailand. *Acta Trop* 2003; **88**: 239-246

Edited by Wang XL **Proofread by** Zhu LH and Xu FM

PO Box 2345, Beijing 100023, China
Fax: +86-10-85381893
E-mail: wjg@wjgnet.com www.wjgnet.com

World J Gastroenterol 2004;10(22):3322-3327
World Journal of Gastroenterology
 ISSN 1007-9327

• CLINICAL RESEARCH •

Long-term results of graded pneumatic dilatation under endoscopic guidance in patients with primary esophageal achalasia

Ahmet Dobrucali, Yusuf Erzin, Murat Tuncer, Ahmet Dirican

Ahmet Dobrucali, Yusuf Erzin, Murat Tuncer, Department of Gastroenterology, Cerrahpasa Medical Faculty, Istanbul University, Istanbul, Turkey
Ahmet Dirican, Department of Bioistatistics, Cerrahpasa Medical Faculty, Istanbul University, Istanbul, Turkey
Correspondence to: Dr. Ahmet Dobrucali, Istanbul Universitesi, Cerrahpasa Tip Fakultesi, Ic Hastaliklari A.B.D., Gastroenteroloji B. D., Kocamustafapasa - Fatih, 34 300 Istanbul-Turkey. adobrucali@yahoo.com
Telephone: +90-532-4425551 **Fax:** +90-212-5307440
Received: 2004-02-27 **Accepted:** 2004-04-20

Abstract

AIM: Achalasia is the best known primary motor disorder of the esophagus in which the lower esophageal sphincter (LES) has abnormally high resting pressure and incomplete relaxation with swallowing. Pneumatic dilatation remains the first choice of treatment. The aims of this study were to determine the long term clinical outcome of treating achalasia initially with pneumatic dilatation and usefulness of pneumatic dilatation technique under endoscopic observation without fluoroscopy.

METHODS: A total of 65 dilatations were performed in 43 patients with achalasia [23 males and 20 females, the mean age was 43 years (range, 19-73)]. All patients underwent an initial dilatation by inflating a 30 mm balloon to 15 psi under endoscopic control. The need for subsequent dilatation was based on symptom assessment. A 3.5 cm balloon was used for repeat procedures.

RESULTS: The 30 mm balloon achieved a satisfactory result in 24 patients (54%) and the 35 mm ballon in 78% of the remainder (14/18). Esophageal perforation as a short-term complication was observed in one patient (2.3%). The only late complication encountered was gastroesophageal reflux in 2 (4%) patients with a good response to dilatation. The mean follow-up period was 2.4 years (6 mo - 5 years). Of the patients studied, 38 (88%) were relieved of their symptoms after only one or two sessions. Five patients were referred for surgery (one for esophageal perforation and four for persistent or recurrent symptoms). Among the patients whose follow up information was available, the percentage of patients in remission was 79% (19/24) at 1 year and 54% (7/13) at 5 years.

CONCLUSION: Performing balloon dilatation under endoscopic observation as an outpatient procedure is simple, safe and efficacious for treating patients with achalasia and referral of surgical myotomy should be considered for patients who do not respond to medical therapy or individuals that do not desire pneumatic dilatations.

Dobrucali A, Erzin Y, Tuncer M, Dirican A. Long-term results of graded pneumatic dilatation under endoscopic guidance in patients with primary esophageal achalasia. *World J Gastroenterol* 2004; 10(22): 3322-3327
http://www.wjgnet.com/1007-9327/10/3322.asp

INTRODUCTION

Achalasia is an uncommon disorder of the esophagus characterized by clinical, radiologic and manometric findings. Dysphagia, regurgitation, weight loss and chest pain are among the most recognized clinical features of the disease. Manometrically it is distinguished by esophageal aperistalsis and incomplete relaxation of the lower esophageal sphincter (LES). Esophageal dilatation and a tapered deformity of the distal esophagus are presumably late radiological manifestations of the disease[1,2]. The pathogenesis of achalasia remains unknown. Available data suggest hereditary, degenerative, autoimmune and infectious factors as possible causes for achalasia, the latter two are the most commonly accepted possible etiologies. The mean age of onset varies between 30 and 60 years with a peak incidence in the fifth decade. The incidence is 1.1 per 100 000 with a prevalence of 7.9 to 12.6 per 100 000[2,3].

Although there is no definite cure for achalasia, the goals of treatment should be: 1) relieving the patient's symptoms, 2) improving esophageal emptying and 3) preventing development of a megaesophagus. The optimal treatment of achalasia includes several options and presents a challenge for most gastroenterologists. It can be treated by botulinum toxin injection, pneumatic dilatation or esophagomyotomy, but the most effective treatment options are graded pneumatic dilatation and surgical myotomy. All of these therapeutic modalities are aimed at removing the functional barrier at the lower esophageal sphincter level. Although high success rates have been reported for these therapeutic modalities, the fact remains that the esophageal propulsive force is not usually restored and therefore it is conceivable that a normal esophageal function can never be expected among these patients[2,4,5].

The aim of our study was to evaluate the safety and efficacy of graded pneumatic dilation using two different size (3.0 and 3.5 cm) balloon dilators (Rigiflex) in patients with primary esophageal achalasia. We hereby report our experience, which indicates that pneumatic dilatation can be safely performed under direct endoscopic observation without fluoroscopic guidance and with only a short-term clinical monitoring in an outpatient setting prior to discharge.

MATERIALS AND METHODS

Patients

Forty-three consecutive patients (23 males and 20 females) were evaluated. The ages ranged from 19 to 73 years with a mean age of 43 years. All patients were referred because of typical symptoms of achalasia. All had dysphagia, but some also had regurgitation or pulmonary aspiration (Table 1). The diagnosis of achalasia was made on the basis of clinical, radiologic and manometric criteria. Barium esophagogram showed a distal narrowing of the esophagus (bird beak deformity) and variable degrees of dilation of the esophagus in most patients (93%). Mean esophagus diameter was 3.8 cm (range, 2-6.3 cm). Upper endoscopy was done in all patients to exclude secondary causes of achalasia. Computerized tomography of the chest was done in 12 patients over age 40 with significant weight loss over a short period (six months or less) to exclude mediastinal malignancy

causing pseudoachalasia.

Eligibility criteria for entry into the study required: a diagnosis of achalasia by manometry as defined above, absence of obstructive intrinsic or extrinsic esophageal lesions by X-ray and endoscopy, and Absence of esophageal or gastric carcinoma, a peptic stricture or a prior surgical fundoplication.

Symptoms of the patients were scored using a questionnaire requesting information regarding the presence and severity of their difficulty in swallowing solids and liquids on a 5 point subjective visual scale: 0 = no symptoms, 1 = mild, 2 = moderate, 3 = severe, 4 = very severe.

Table 1 Clinical characteristics and demographic data of patients [mean±SD, (min-max)]

Age (yr)	44±16 (19-73)
Gender (M/F)	23/20
Dysphagia	43 (100%)
Chest pain	5 (11%)
Regurgitation	34 (79%)
Pulmonary aspiration	9 (21%)
Mean duration of symptoms (mo)	35±21 (6-72)
Mean weight loss (kg)	7.7±2 (4-11)
LES pressure (mmHg)	
Before dilation	38.6±12 (19-66)
After dilation	11.8±8 (0-16)
Vigorous achalasia	1 (2.3%)
Esophagus diameter (cm)	3.8 (2-6.5)

Esophageal manometry

Esophageal manometry was performed in all patients with a four lumen polyvinyl catheter with Dent sleeve working with a pneumohydraulic capillary perfusion system (Synectic PC polygraph- Gastrosoft Inc.Upper GI edition, version 6.0). Manometric examinations were performed by the same author. LES was localised using the station pull-through technique. Other three orifices, located 5 cm apart and also oriented at 90º angles, for determination of the peristalsis and pressures, by placing the distal orifice 5 cm above the LES. The peristalsis was measured with 10 wet swallows of 5 mL of water, each at intervals of 60 s or more. Aperistalsis was the absolute manometric criteriron required for the diagnosis of achalasia with increased LES pressure and incomplete/absent relaxation were the complementary findings[7]. Incomplete relaxation was defined as the failure of LES pressure to drop to gastric baseline during a dry and /or wet swallow (Figure 1).

Technique of pneumatic dilation

All dilations were performed on outpatients. Dilations were done by the same authors using the Rigiflex achalasia balloon dilators (Microvasive) in a graded manner. A 3.0 cm dilator was always used first. If there was still no symptomatic response, a 3.5 cm dilator was used after 6-8 wk. After clear liquid diet for 24 h and an overnight fast, an endoscope (Pentax EG-2940) was passed after application of a local anesthetic to the pharynx under conscious sedation (Midazolam 0.04 mg/kg iv) to evacuate the residual liquid from the esophagus and to insert a guide wire. The guide wire was placed into the duodenum via stomach under endoscopic guidance and endoscope was removed. A Rigiflex balloon dilator, which was marked with a thick coloured marker at the mid section of the balloon was passed over the guidewire to stomach and slightly inflated (less than 5 psi) to get a soft tube shaped form. Endoscope was reinserted and positioned proximally to adjust and control the position of the balloon in the esophagus. Balloon was withdrawn to esophagus and marked part of the balloon was located within the gastroesophageal junction under endoscopic control (Figure 2). The balloon was then inflated until 15 psi. and inflation was maintained for 60 s. Ischemic ring at the lower esophageal sphincter level was seen during dilatation through the transparent balloon. After repeating of the same inflation procedure one more time at the same session endoscopic dilatation was terminated and endoscope, balloon and guidewire were removed. Balloon dilator surface was checked to see if there was blood on it. The procedure was well tolerated by all patients.

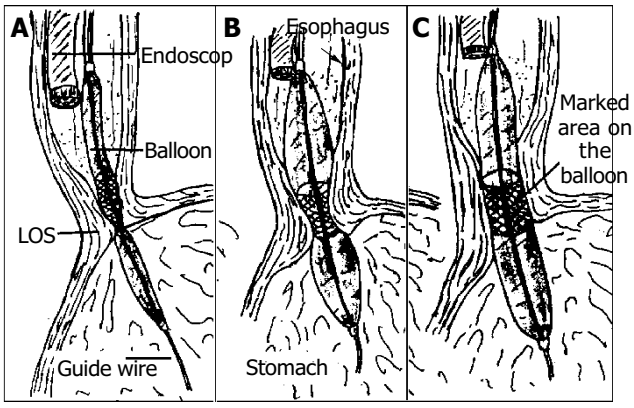

Figure 2 Technique for pneumatic dilatation under endoscopic control without fluoroscopy. The balloon was positioned so that its midsection was at the high pressure level (A). The balloon was inflated and the endoscopist observes with endoscope proximally to balloon (B). With successful dilatation the ischemic ring of dilated segment was diminished or disappeared (C).

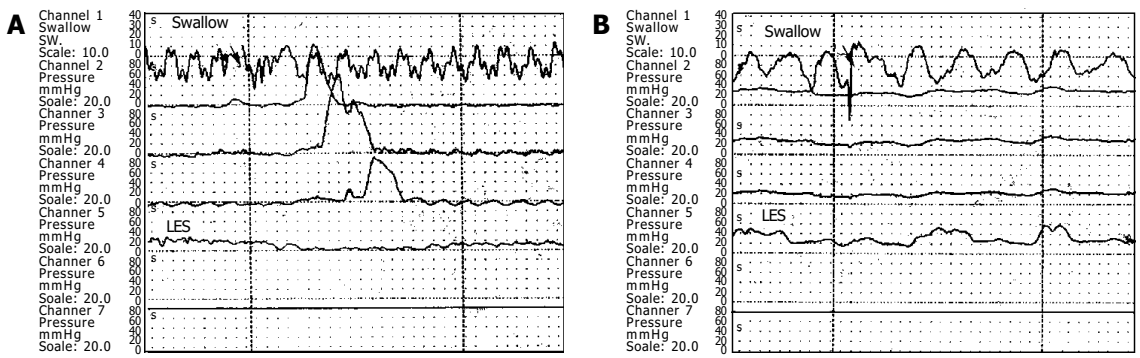

Figure 1 Manometric samples from a normal individual (A) and a patient with achalasia (B). Figure A illustrates the normal peristaltic activity forwarding at cranio-caudal direction whereas figure B shows typical manometric findings of achalasia. Note the aperistalsis, weak and simultaneous contractions (mirror sign), and incomplete LES relaxation after swallow. Basal LES pressure is high (40 mmHg).

The severity of chest pain in patients was scored after the balloon dilation on a scale of 0-10 (0, absence of pain; 10 severest pain). Gastrografin swallow was done few hours after dilation to exclude esophageal perforation. After an observation period of 6 h, patients were discharged and permitted to eat the next morning.

Second esophageal manometry and symptom scoring were performed in all patients with therapeutic response six weeks after pneumatic dilation to evaluate the efficacy of endoscopic balloon dilation.

The response to balloon dilation was considered excellent if there was no or very rare mild dysphagia, good if there was intermittent mild dysphagia, or poor if there was persistent daily mealtime dysphagia. The balloon therapy was considered successful if the patients had a good or excellent response.

Statistical analysis

Results were expressed as either percentages or mean±SD. Statistical analysis was performed using Chi-square test, Kendall's tau-b coefficient and Mann-Whitney U test as appropriate. $P<0.05$ was considered statistically significant. The cumulative remission rates of the patients treated with balloon dilation were estimated by the Kaplan-Meier method and the difference between treatment groups was tested by the log rank test.

RESULTS

The clinical characteristics and demographic data of patients are shown in Table 1. The mean LES pressure was 37.6±12 mmHg. Relaxation failure of LES and aperistalsis with low amplitude simultaneous uniformed waves were present in all patients. Only one of the 5 patients with retrosternal pain was diagnosed as a vigorous achalasia (2.3%) at esophageal manometry. The LES pressures and symptom scores of successfully dilated patients were decreased significantly one month after dilation, (37.6±12 *vs* 9.5±3) and (2.9±0.6 *vs* 0.8±0.6) respectively ($P<0.01$) (Figure 3). There was no significant correlation between the parameters of age, sex, initial LES pressure, symptom score and barium study findings.

Chest pain was reported by all patients during the initial dilation, with a mean pain score of 7.2±2.3 (range, 4-10). Chest pain score was 8.1±1.8 in patients who were successfully dilated at the first session although score was 4.8±2.1 in patients with a poor response to initial balloon dilation ($P<0.05$). Chest pain after the procedure usually lasted for 30-60 min and was substernal in nature, diminishing gradually over time and resolved completely within 2 to 6 h.

The results of balloon dilation are summarized in Table 2. A total of 65 dilatations were performed in 43 patients for an average of 1.7 dilations per patient. The 3 cm balloon was always used first. Twenty-four patients (56%) were successfully dilated with a 3 cm balloon only. Fourteen patients had an excellent response (32.5%) and 10 patients had a good response (23%) to 3.0 cm balloon dilation. Old age at the time of initial pneumatic dilatation was significantly associated with a better clinical response to treatment as assessed by the need for subsequent treatments (Kendall's tau-b = 0.414, $P = 0.016$) (Table 3).

Table 2 Results of rigiflex balloon dilation under endoscopic control

Inflation pressure (psi)	15
Dilation time per session (s)	2×60
Success with 3.0 cm balloon	24/42(56%)
Success with 3.5 cm balloon	14/18(78%)
Overall success rate at first year[1]	19/24(80%)
Overall success rate at 5 years[1]	7/13(54%)
Complications	
Perforation	1(2.3%)
Bleeding	-
Mortality	-

[1]Among the patients whose long term follow up information was available.

Table 3 Effect of age, LES pressure and esophageal diameter on the clinical benefit of the initial pneumatic dilation. [1]With 3 cm balloon

	Patients with successful initial pneumatic dilation (n = 24)	Patients with successful initial pneumatic dilation (%)	P
Age (yr)			
<35	4/14	28	<0.01
35-55	11/17	65	
>55	9/11	82	
LES pressure (mmHg)			
<30	6/12	50	
30-45	13/21	62	NS
>45	5/9	55	
Esophageal diameter (cm)			
<3	4/7	57	
3-4	11/21	52	NS
>4	9/14	64	

NS: Non significant.

Eighteen patients (42%) with a poor response to 3.0 cm balloon were dilated with a 3.5 cm balloon at intervals of 6-8 wk. Nine patients had excellent, five had good and four patients had poor response to the second dilation with a 3.5 cm balloon.

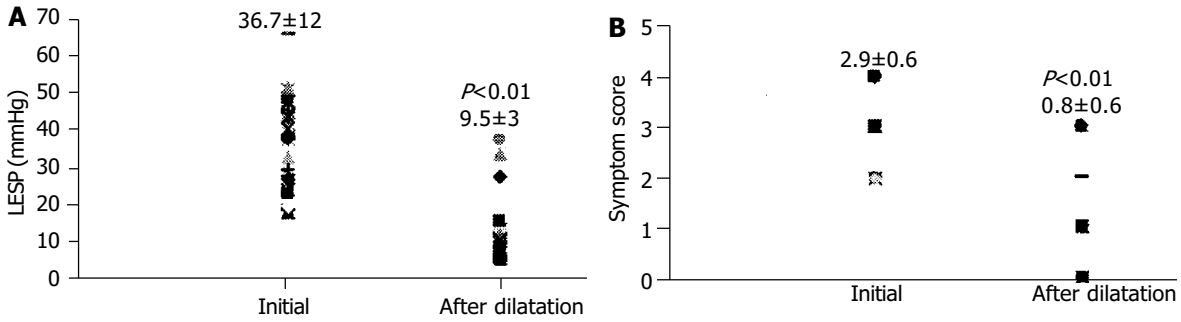

Figure 3 Lower esophageal sphincter pressures (LESP) (A) and symptom scores (B) of patients with therapeutic response initially and at one month after pneumatic dilatation.

Patients with a poor response to the second dilation with a 3.5 cm balloon were dilated with a 3.5 cm balloon at the third time but all of them were symptomatic after a while and these patients were no longer treated with a larger balloon (4 cm), instead, surgical treatment was suggested. One patient who refused surgery had repeated dilation every 6 to 12 mo with a 3.5 cm balloon due to symptom recurrence.

The mean follow-up period in the entire group was 2.4 years (range, 6 mo -5 years). Among the 38 patients whose long term follow up information was available, 33 (87%) at six months were asymptomatic [Among them 23 (70%) required once and 10 (30%) required twice dilation]. At the end of the first year, 16 of 24 patients (66%) whose follow up information was available were asymptomatic. Among the 24 patients, 3 (12.5%) complained of mild intermittent dysphagia and 5 (21%) had intermittent severe dysphagia. The total number of asymptomatic patients and patients with mild dysphagia was 19 (79%) at the end of the first year. Among these, 10 patients (52%) required a second dilation.

Among patients whose follow up information was available at 3 years the 19, 13 were in remission (68%) (5 asymptomatic and 8 with intermittent mild dysphagia). Among patients whose follow up information was available at 5 years the 13, 7 were in remission (54%) (3 were asymptomatic and 4 with mild intermittent dysphagia). Among the total, 3 patients (44%) required once and 4 (56%) required twice dilation (Figure 4). Figure 5 shows the Kaplan-Meier plot for the two treatment groups of patients who were dilated once or twice. The cumulative one, three and five year remission rates were higher in patients dilated twice but this difference was not statistically significant (Log rank χ^2 = 2.10, P = 0.1471).

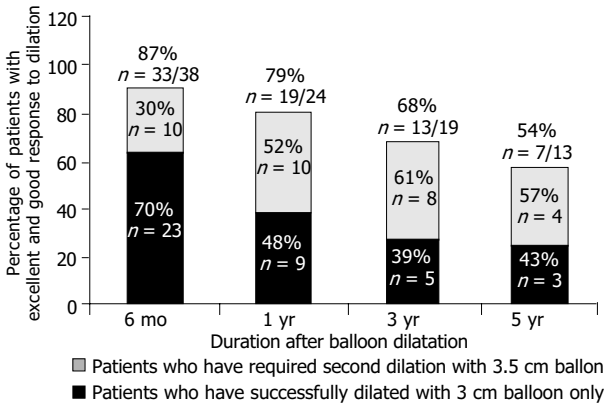

Figure 4 Percentage of patients with excellent and good response to dilatation at 6 mo, 1, 3 and 5 years.

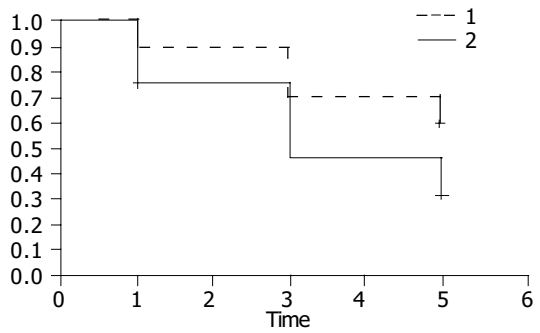

Figure 5 Kaplan-Meier plot for the two treatment groups of patients who were dilated once[2] or twice[1]. The cumulative one, three and five year remission rates were higher in patients dilated twice but this difference was not statistically significant (Log rank χ^2 = 2.10, P = 0.1471).

Gastrografin swallow done immediately after balloon dilation revealed esophageal perforation in one patient (2.3%) (a 60 years old female) with persistent chest pain and surgical therapy was required. There were no other immediate complications. Reflux esophagitis as a late complication was observed in two of the patients who had a good response to dilatation during the follow up period (4%).

Blood on the balloon after dilatation was a common finding. There was no statistically significant correlation between bloody dilator and dilatation success (P>0.05).

DISCUSSION

This study analysed the effectiveness of pneumatic balloon dilation and the clinical outcome in patients with achalasia. Our results showed that once or twice pneumatic dilatation provided good results in the majority of patients with achalasia and long term results were 79% at 1 year and 54% at 5 years. Of the patients studied, 38 (88%) were relieved of their symptoms after one or two sessions. An initial pneumatic dilation was an effective single treatment with no further treatment needed in 57% of patients in a short term period. The remaining 43% of patients treated initially with pneumatic dilation needed additional treatments due to persistent or recurrent symptoms and only 11% of patients failing pneumatic dilatation were referred for surgery (4 with poor response to repeated dilations and 1 with perforation due to dilation). Four patients with a poor response to the second dilation with a 3.5 cm balloon were dilated with a 3.5 cm balloon the third time but all of them were symptomatic after a while and these patients were not treated with a larger balloon. Some studies have reported using a 3.5 cm balloon instead of a 3 cm balloons one as the initial balloon but others have used 3 cm for the initial dilatation[8,9,11]. In our series application of the second pneumatic dilation increased the long term clinical benefit of pneumatic dilation from 30% at six months to 57% at 5 years, but this difference was not statistically significant (P>0.05) (Figure 4). To some extent, our results about the clinical benefit of a single pneumatic dilatation and the use of the second dilatation for patients with persistent symptoms are in agreement with other studies. It has been shown that the overall efficacy of endoscopic balloon dilation was approximately 85%, with an excellent to good response for 3, 3.5 and 4 cm dilators being 70%, 87% and 93% respectively (9 studies; four prospective, five retrospective, 261 patients, a mean follow up of 1.9 years (range; 0.3 to 6 years)[10-17] (Table 4). Approximately 50% (range, 17% to 75%) of all patients required repeat dilations, equaling to 1.2 to 2 dilations per patient. About one half of patients responded to a repeat dilation, with the remainder either proceeding to surgical management or deciding to live with their persistent symptoms. The reported overall long-term efficacy of pneumatic dilatation was 50-90% at 1 year and 60% at 5 years[1]. The major adverse event with pneumatic dilatation was esophageal perforation with a 2% cumulative rate. The American Society for Gastrointestinal Endoscopy has recommended that if a single dilation session (size of the balloon dilator unspecified) does not produce satisfactory relief, a second attempt may be warranted and if this fails, surgery usually is indicated[15].

The patient population undergoing initial dilation in this study was not large enough to compare the effect of age on the dilation success, but our results indicate that initial pneumatic dilation was more effective in older patients (χ^2 value: 8.215[a], P = 0.016, Kendall's tau-b 0.414, P = 0.001). This increased clinical benefit of pneumatic dilation in old patients has also been described by other investigators[19,21,22]. There was no significant difference between the mean ages of the patients with and without remission at the end of 1 and 5 years although

Table 4 Cumulative effectiveness of graded pneumatic dilators for achalasia

Author	Pt. #	Study design	Dilator % (size / cm)	Decrease of LESP	% Improvement Excellent / Good	Follow-up (yr) Mean (range)	Perforation (%)
Barkin[11]	50	Prospec.	3.5	-	90	1.3 (1–3.4)	0
Levine[12]	62	Retrosp.	3-3.5	-	85-88	-	0
Wehrmann[15]	40	Retrosp.	3–3.5	42	89	2–5	2.5
Lee[9]	28	Prospec.	3–3.5-4	-	-	-	7
Gelfand[10]	24	Prospec.	3–4	60-68	70–93	-	0
Kadakia[13]	29	Prospec.	3–3.5–4	67	62–79–93	4 (3–6)	0
Abid[14]	36	Retrosp.	3.5–4	-	88–89	2.3 (1–4)	6.6
Lambroza[16]	27	Retrosp.	3	-	67	1.8 (0.1–4.8)	0
Bhatnagar[17]	15	Prospec.	3–3.5	-	73-93	1.2 (0.3–3)	0

the patients in remission at 5 years were older, [43±16 (n = 19) *vs* 48±16 (n = 5) (P>0.05) at 1 year and 53±17 (n = 7) *vs* 37±14 (n = 6) (P>0.05), at 5 years respectively]. The efficacy of pneumatic dilatation was not influenced by initial LES pressure and esophageal diameter (Table 3).

After balloon dilation, the mean LES pressure was 11.8±4 mmHg (range, 0-16 mmHg) and it represented 75% decrease of basal LES pressure. It has been shown that basal LES pressure decreased from 39% to 68% after dilation but these changes did not allways indicate a dilation success. In general, a decrement in LES pressure of more than 50% or an absolute end-expiratory LES pressure of less than 10 mmHg were more indicative of clinical success[2]. Timed barium esophagogram or scintigraphy may correlate with symptomatic improvement in up to 72% of patients. In spite of this similarity, approximately one third of patients who noted complete relief showed less than 50% improvement in barium column height and esophageal diameter[21].

Only one of 43 patients in our series had an esophageal perforation during treatment with pneumatic dilatation (2.3%). This complication rate is similar to those reported by other experienced groups[9,19,20]. Gradual increase in dilator size based on symptomatic response and the use of inflation pressure between 10 to 15 psi can minimize the risk of perforation. Esophageal perforation may occur in up to 5% of all reported cases, with a possible increased risk if hiatal hernia is present. In our study gastrograffin swallow was performed in all patients. Using immediate contrast studies to exclude perforation became routine in the late 1970's, and using this approach has been recommended in several studies and text books. Some authors suggested that contrast studies were indicated only when there was clinical suspicion of perforation. It has been reported that an immediate contrast study may not always exclude a perforation which may become clinically evident several hours later[5].

Less commonly, intramural hematoma, diverticula at gastric cardia, mucosal tears, reflux esophagitis, prolonged post-procedure chest pain, fever, hematemesis without changes in hematocrit and angina may occur after pneumatic dilatation. Objective assessment of gastroesophageal reflux after pneumatic dilation rarely has been studied. Abnormal 24 h pH scores have been documented in approximately 20% to 33% of patients after dilation. In spite of these abnormal scores, very few of these patients were symptomatic or developed endoscopic or clinical evidence of GERD related complications. It has been shown that postdilatation LES pressures and gastric emptying were similar between reflux and non-reflux groups[2]. Since GERD related symptoms correlated poorly in achalasia patients, 24 h pH monitoring has been recommended for patients that developed frequent heartburn, reflux or chest pain in spite of an otherwise good clinical response to dilation. One of the important points of this study was the dilatation technique which did not require fluoroscopic control (see materials and methods). Our experience shows that Rigiflex balloon can be successfully positioned across the gastroesophageal junction and inflated under direct endoscopic observation. This technique is as effective as conventional fluoroscopic technique and has an advantage to prevent patients and endoscopists from an additional X-ray. Furthermore we have seen that patient tolerability was very good and success rates were reasonable and comparable with others. Safety and efficacy of pneumatic dilation for achalasia without fluoroscopic control also have been shown by Lambroza and Levine[16,18].

In a recently published interesting study, Cheng *et al*. evaluated the usefulness of temporariy placing of covered stents for 3-7 d versus pneumatic dilatation and found that the early and late (at one and three years respectively) relapse rates were quite low in the stent treated group versus the pneumatic dilatation treated one[23]. The success of this method was suggested to be due to chronic tearing of the cardia muscularis which resulted in a diminished amount of fibrosis and so restenosis after the stent was withdrawn.

The results of our study suggest that pneumatic dilatation for achalasia without fluoroscopic guidance is a safe and effective treatment modality. A graduatl increase in dilator size based on symptomatic response minimizes complications. Symptomatic patients with achalasia who are good surgical candidates should be given an option of graded pneumatic dilatation before surgery. Although surgical myotomy, once with a high mortality and long hospital stay, can now be performed laparoscopically with a similar efficacy to the open surgical approach, reduced morbidity and hospitalization time, referral of myotomy should be considered for patients who do not respond to medical therapy or individuals that do not desire pneumatic dilatations. The advantages of pneumatic dilatation over surgical myotomy are a brief period of discomfort, a very short hospital stay and consequently low exposure.

REFERENCES

1 **Clouse RE**, Diamant NE. Esophageal motor and sensory function and motor disorders of the esophagus. In: Sleisenger MH, Friedman LS, Feldman M. Eds: Gastrointestinal and Liver Disease. *Philadelphia Saunders* 2002: 561-598

2 **Dunaway PM,** Wong RK. Achalasia. *Curr Treat Opt Gastroenterol* 2001; **4:** 89-100

3 **Howard PJ,** Maher L, Pryde A, Cameron EW, Heading RC. Five year prospective study of the incidence, clinical features and diagnosis of achalasia in Edinburgh. *Gut* 1992; **33:** 1011-1015

4 **Csendes A,** Braghetto I, Henriquez A, Cortes C. Late results of a prospective randomised study comparing forceful dilatation and oesophagomyotomy in patients with achalasia. *Gut* 1989; **30:** 299-304

5 **Ciarolla DA,** Traube M. Achalasia. Short-term clinical monitoring after pneumatic dilation. *Dig Dis Sci* 1993; **38:** 1905-1908

6 **Prakash C,** Clouse RE. Esophageal motor disorders. *Curr Op Gastroenterol* 1999; **15:** 339-346

7 **Nair LA,** Reynolds JC, Parkman HP, Ouyang A, Strom BL,

Rosato I, Cohen S. Complications during pneumatic dilation for achalasia or diffuse esophageal spasm. Analysis of risk factors, early dinical characteristics, and outcome. *Dig Dis Sci* 1993; **38:** 1893-1904

8 **Stark GA,** Castell DO, Richter JE, Wu WC. Prospective randomized comparison of Brown-McHardy and microvasive balloon dilators in treatment of achalasia. *Am J Gastroenterol* 1990; **85:** 1322-1326

9 **Richter JE,** Lightdale CJ. Management of achalasia. AGA Postgraduate Course, May 19-20. 2001: 303-308

10 **Gelfand MD,** Kozarek RA. An experience with polyethylene balloons for pneumatic dilation in achalasia. *Am J Gastroenterol* 1989; **84:** 924-927

11 **Barkin JS,** Guelrud M, Reiner DK, Goldberg RI, Phillips RS. Forceful balloon dilation: an outpatient procedure for achalasia. *Gastrointest Endosc* 1990; **36:** 123-126

12 **Levine ML,** Moskowitz GW, Dorf BS, Bank S. Pneumatic dilation in patients with achalasia with a modified Gruntzing dilator (Levine) under direct endoscopic control: results after 5 years. *Am J Gastroenterol* 1991; **86:** 1581-1584

13 **Kadakia SC,** Wong RK. Graded pneumatic dilation using Rigiflex achalasia dilators in patients with primary esophageal achalasia. *Am J Gastroenterol* 1993; **88:** 34-38

14 **Abid S,** Champion G, Richter JE, McElvein R, Slaughter RL, Koehler RE. Treatment of achalasia: the best of both worlds. *Am J Gastroenterol* 1994; **89:** 979-985

15 **Wehrmann T,** Jacobi V, Jung M, Lembcke B, Caspary WF. Pneumatic dilation in achalasia with a low-compliance balloon: results of a 5-year prospective evaluation. *Gastrointest Endosc* 1995; **42:** 31-36

16 **Lambroza A,** Schuman RW. Pneumatic dilation for achalasia without fluoroscopic guidance: safety and efficacy. *Am J Gastroenterol* 1995; **90:** 1226-1229

17 **Bhatnagar MS,** Nanivadekar SA, Sawant P, Rathi PM. Achalasia cardia dilatation using polyethylene balloon (rigiflex) dilators. *Indian J Gastroenterol* 1996; **15:** 49-51

18 **Levine ML,** Dorf BS, Moskowitz G, Bank S. Pneumatic dilatation in achalasia under endoscopic guidence: correlation pre- and postdilatation by radionuclide scintiscan. *Am J Gastroenterol* 1987; **82:** 311-314

19 **Parkman HP,** Reynolds JC, Ouyang A, Rosato EF, Eisenberg JM, Cohen S. Pneumatic dilatation or esophagomyotomy treatment for idiopathic achalasia: clinical outcomes and cost analysis. *Dig Dis Sci* 1993; **38:** 75-85

20 **Robertson CS,** Fellows IW, Mayberry JF, Atkinson M. Choice of therapy for achalasia in relation to age. *Digestion* 1988; **40:** 244-250

21 **Vaezi MF,** Richter JE, Wilcox CM, Schroeder PL, Birgisson S, Slaug RL, Koehler RE, Baker ME. Botulinum toxin versus pneumatic dilatation in the treatment of achalasia: a randomised trial. *Gut* 1999; **44:** 231-239

22 **Fellows IW,** Ogilvie AL, Atkinson M. Pneumatic dilatation in achalasia. *Gut* 1983; **24:** 1020-1023

23 **Cheng YS,** Li MH, Chen WX, Chen NW, Zhuang QX, Shang KZ. Selection and evaluation of three interventional procedures for achalasia based on long-term follow-up. *World J Gastroenterol* 2003; **9:** 2370-2373

Edited by Zhu LH and Wang XL **Proofread by** Xu FM

PO Box 2345, Beijing 100023, China
Fax: +86-10-85381893
E-mail: wjg@wjgnet.com www.wjgnet.com

World J Gastroenterol 2004;10(22):3328-3331
World Journal of Gastroenterology
 ISSN 1007-9327

• CLINICAL RESEARCH •

Seasonal variation in the onset of acute pancreatitis

Massimo Gallerani, Benedetta Boari, Raffaella Salmi, Roberto Manfredini

Massimo Gallerani, Benedetta Boari, Roberto Manfredini, Section of Internal Medicine, Department of Clinical and Experimental Medicine, University of Ferrara, via Savonarola 9, I-44100 Ferrara, Italy
Raffaella Salmi, Department of Internal Medicine, St Anna Hospital, corso Giovecca 203, I-44100 Ferrara, Italy
Supported by a Research Grant "ex-60%" From the University of Ferrara
Correspondence to: Roberto Manfredini, Section of Internal Medicine, Department of Clinical and Experimental Medicine, University of Ferrara, via Savonarola 9, I-44100 Ferrara, Italy. mfr@unife.it
Telephone: +39-532-236817 **Fax:** +39-532-210884
Received: 2003-11-12 **Accepted:** 2004-02-24

Abstract

AIM: A circannual variation in the onset of several acute diseases, mostly dealing with cardiovascular system, has been reported. The present study was to verify the possible existence of a seasonal variability in the onset of acute pancreatitis.

METHODS: All patients consecutively admitted to the Hospital of Ferrara, Italy, between January 1998 to December 2002, whose discharge diagnosis was acute pancreatitis, were considered. According to the time of admission, cases were categorized into twelve 1-mo intervals and in four periods by season. χ^2 test for goodness of fit and partial Fourier series were used for statistical analysis.

RESULTS: During the study period, 549 cases of acute pancreatitis were observed. A significant peak of higher incidence was found in March-May, both for total population, males and subgroups with and without cholelithiasis or alcoholism. Fourier analysis showed the existence of a circannual rhythmic pattern with its main peak in March (95% C.L.: February-April, $P = 0.005$), and a secondary one in September. Death occurred more frequently in December-February, compared to the other periods ($P = 0.029$), and chronobiologic analysis yielded a seasonal peak in November-December ($P<0.001$).

CONCLUSION: This study shows the existence of a circannual variation in the onset of acute pancreatitis, with a significantly higher frequency of events in the spring, especially for patients with cholelithiasis or alcoholism. Moreover, events occurring during the colder months seem to be characterized by a higher mortality rate.

Gallerani M, Boari B, Salmi R, Manfredini R. Seasonal variation in the onset of acute pancreatitis. *World J Gastroenterol* 2004; 10(22): 3328-3331
http://www.wjgnet.com/1007-9327/10/3328.asp

INTRODUCTION

Many studies have shown a circannual variation in the onset of several diseases mostly dealing with cardiovascular system, characterized by an abrupt onset, e.g., fatal pulmonary embolism[1,2], ischemic and hemorrhagic stroke[3,4] and rupture of aortic aneurysms[5,6]. Seasonal specific patterns have also been reported for a series of miscellaneous diseases characterized by an acute onset, treated by the Emergency Department, including paralysis of cranial nerves[7], microcristalline arthritis[8], herpes zoster infection[9], epistaxis[10], urinary retention[11]. In the last few years several studies have investigated gastroenterologic diseases, and seasonal etiological patterns have been reported for the onset of peptic ulcer[12-15] and exhacerbation of inflammatory bowel diseases[16-18]. The aim of the present study was to determine by means of a validated chronobiological analysis, whether acute pancreatitis, a common but potentially harmful entity, might show a rhythmic seasonal variation as well.

MATERIALS AND METHODS

All cases of acute pancreatis (International Classification of Diseases, 9th Revision, Clinical Modification, ICD9-CM code: 577.0-8) consecutively observed from 1 January 1998 to 31 December 2002 at the St. Anna Hospital of Ferrara, Italy, were considered for the study. Ferrara is a small town in northern Italy particularly well suited for epidemiological studies. It has a stable population of approximately 150 000 inhabitants, almost exclusively white. The only available hospital in this community is St Anna Hospital, which also serves as the sole teaching center for the School of Medicine. The day and month of each event were categorized both into four 3-mo periods (according to seasons) and into twelve 1-mo intervals. Diagnosis was always made on the basis of clinical features, physical examination, laboratory data (serum amylase, isoamylase, lipase, and urinary amylase), and instrumental examinations, when necessary. For all subjects with acute pancreatitis the presence or absence of the two leading specific risk factors (alcoholism and biliary tract disease), was carefully investigated.

For statistical analysis, two different methods were used: χ^2 test for goodness of fit and partial Fourier series. To investigate possible differences in frequency peaks, χ^2 test for goodness of fit was applied to the total sample population and subgroups by gender, comparing observed against expected events during the four intervals season[19]. On the other hand, to verify the possible existence of a reproducible rhythmic pattern, cosinor analysis and partial Fourier series were applied to the time series, using specific commercially available software written for the Apple Macintosh computer[20]. The program allows, among all the possible combinations of the periods chosen by the user, the selection of the harmonic or the combination of harmonics that best explain the variance of data. The percentage of rhythms (PR: percentage of overall variability of data about the arithmetic mean attributable to the fitted rhythmic function) and the probability value resulting from the F statistic used to test the hypothesis of zero amplitude, were chosen to be reported in the results as representative parameters of goodness of fit and statistical significance of each fitted function, respectively. The program was used to calculate the midline estimating statistic of rhythm (MESOR: the rhythm-adjusted mean over the time period analyzed) and the amplitude (half the distance between the absolute maximum and minimum of the function) of the best-fitting-curve. The program was also used to calculate peak (ortophase) and trough (bathyphase) times of the fitted curves (times of occurrence of the absolute maximum and minimum) and the acrophase of each single harmonic change, together with the 95% confidence limits (CL). Significance

levels were always assumed for $P<0.05$. Conventional statistical analysis was performed using Student's *t* test for unpaired data. Significance levels were always set at $P<0.05$.

RESULTS

From January 1998 to December 2002, 549 consecutive cases of acute pancreatitis were observed, 285 cases were males (51.9%) and 264 were females (48.1%), their mean age was 65±17 years (difference between sexes $t = 2.7$, $P = 0.007$). Two hundred and eighty-six had cholelithiasis (52.1%) and 48 had chronic alcoholism (8.7%).

Deaths from acute pancreatitis were 18 (14 males and 5 females), accounting for 3.2%. Their mean age was 56±16 years,

Table 1 Monthly distribution of acute pancreatitis by gender and risk factors

Month	Total (*n* = 549)	Males (*n* = 285)	Females (*n* = 264)	Biliary tract disease (*n* = 286, 52.1%)	No bil. tract disease (*n* = 263, 48.9%)	Alcoholism (*n* = 48, 8.7%)	Fatal cases (*n* = 18, 3.2%)
January	34	18	16	17	17	1	3
February	46	19	27	22	24	2	2
March	62	35	27	28	34	8	1
April	61	33	28	31	30	7	0
May	56	32	24	35	21	5	0
June	44	23	21	19	25	3	0
July	40	20	20	23	17	2	1
August	45	25	20	30	15	4	1
September	39	20	19	22	17	4	1
October	40	20	20	19	21	2	2
November	46	25	21	22	24	6	3
December	36	15	21	17	19	3	4

Table 2 Seasonal distribution of acute pancreatitis (χ^2 test for goodness of fit)

	n (%)	December-February *n* (%)	March-May *n* (%)	June-August *n* (%)	September-November *n* (%)	χ^2	*P*
Total	549	116 (21.1)	179 (32.6)	129 (23.5)	125 (22.8)	17.5	0.001
Males	285 (51.9)	52 (18.2)	100 (35.1)	68 (23.9)	65 (22.8)	17.05	0.001
Females	264 (48.1)	64 (24.2)	79 (29.9)	61 (23.1)	60 (22.7)	3.55	0.316
Biliary tract disease	286 (52.1)	56 (19.5)	94 (32.8)	73 (25.4)	64 (22.3)	11.02	0.011
No bil. tract disease	263 (47.9)	60 (22.9)	85 (32.4)	56 (21.4)	61 (23.3)	7.93	0.049
Chronic alcoholism	48 (8.7)	6 (12.5)	20 (41.7)	10 (20.8)	12 (25)	8.67	0.035
Fatal cases	18 (3.2)	9 (50)	1 (5.6)	2 (11.1)	6 (33.3)	9.11	0.029

Table 3 Seasonal variation of acute pancreatitis (chronobiologic parameters by Fourier analysis)

	n	Period (h)	PR (%)	MESOR	Amplitude	Peak	95% CL	*P*
Total	549	8766	51.1			March	February-April	0.006
		4383	33.7			September	August-October	0.017
		Overall	84.8	45.68	3.28	March	February-April	0.005
Males	285	8766	42.6			March	February-April	0.030
		4383	32.7			September	NS	0.052
		Overall	75.4	23.71	9.06	March	February-April	0.027
Females	264	8766	50.9			March	February-April	0.024
		4383	22.3			September	NS	0.121
		Overall	73.3	21.97	4.52	March	February-April	0.035
Biliary tract disease	286	8766	42.2			March	NS	0.074
		4383	19.5			August	NS	0.234
		Overall	61.8	23.72	7.60	March	NS	0.108
No bil. tract disease	263	8766	44.8			March	February-April	0.041
		4383	25.1			October	NS	0.119
		Overall	69.9	21.96	7.66	March	NS	0.052
Chronic alcoholism	48	8766	13.2			March	NS	0.415
		4383	40.7			September	NS	0.109
		Overall	53.9	3.91	2.51	March	NS	0.192
Fatal cases	18	8766	86.2			November	November-December	<0.001
		4383	10.9			June	May-July	0.004
		Overall	97.1	1.50	1.90	November	November-December	<0.001

PR = percentage of rhythm (percentage of overall variability of data about arithmetic mean attributable to the rhythmic fitted function MESOR = midline estimated statistics of rhythm, the rhythm-adjusted mean over the time period analysed amplitude: half the distance between the absolute maximum and minimum of the function of the best-fitting curve 95% CL = 95% confidence limits NS = not significant, (when acrophase did not reach the significance level, 95% CL could not be given).

significantly lower than that of survived subjects (65±17 years, $t = 2.20$, $P = 0.028$). Among the subgroups of fatal events, 3 had gallstones (16.6%, $\chi^2 = 1.91$ $P = 0.178$), and 4 had chronic alcoholism (22.2%, $\chi^2 = 3.78$ $P = 0.075$). Table 1 shows the monthly distribution by gender, and subgroups by risk factors. A peak of higher frequency of events was found in the period March-May for the total samples and in particular for males and subgroups of subjects with and without gallstones and chronic alcoholism (Table 2). The percentage of fatal events was significantly higher in December-February ($n = 9$, 17.3% of acute pancreatitis observed in that period, 50% of total deaths, $\chi^2 = 9.11$, $P = 0.029$, compared to the other periods).

Chronobiologic analysis (Table 3) showed the existence of a circannual rhythmic variation characterized by a main peak in March (PR 84.8, 95% CL: February-April, $P = 0.005$), and a secondary peak in September. This pattern was confirmed also for subgroups by gender (men: PR 75.4, 95% CL: February-April, $P = 0.027$), and (women: PR 73.3, 95% CL: February-April, $P = 0.035$). Moreover, a highly significant peak was noticed for fatal cases in late November (PR 97.1, 95% CL: October-December, $P<0.001$). NO statistically significant trend for a peak in March was found for subgroups of subjects with or without cholelithiasis (respectively: PR 61.8, 95% CL: February-April, $P = 0.109$; and PR 69.9, 95% CL: February-April, $P = 0.052$).

DISCUSSION

Identification of patients with acute pancreatitis is important due to the increased risk of death.

To our knowledge, there was only one recent study in medical literature, which aimed to evaluate the seasonal variation in the onset of acute pancreatitis[20]. In a total of 263 cases observed for a period of 9 years in a German hospital, no correlation between admissions and a specific month or season was found, other earlier reports were mostly hypotheses[21,22]. Our study instead showed a clear seasonal variation in the onset of acute pancreatitis characterized by a higher frequency in the spring, with a maximum in March-May. This pattern was particularly evident for patients with cholelithiasis and chronic alcoholism. It is difficult to give an exhaustive explanation for such a temporal pattern. Seasonal and circannual patterns have been reported for the prevalence of *Helicobacter pylori* infection[14], or for relapses of inflammatory bowel disease for hospital admissions[15,23].

As for circadian aspects, some acute dramatic clinical events, e.g., variceal and gastrointestinal bleeding[24-26] showed obvious circadian patterns. Daily variations of some biologic functions have also been found as possible co-factors in several gastrointestinal diseases, e.g., fibrinolysis in liver cirrhosis and esophageal varices[27], electrical uncoupling and ectopic pacemaker activity in intestinal motor dysfunction[28], melatonin and duodenal ulcer[29,30], colonic motility in diverticular disease[31] and rectal motor activity in constipation[32].

At present we do not know enough about seasonal biological changes potentially affecting onset of acute pancreatitis, e.g., secretion of pancreatic enzymes, biliary acids. However, it is possible that variations in physiological functions with seasonal change may be associated with an increased risk of pancreatitis. Oxygen free radicals, for example, were known to be a meaningful index for the severity of pancreatitis[33], but possible variations in free radical generation have not been investigated yet. Our results seemed to be able to identify a higher mortality for colder months (November-December). This is particularly interesting when considering that both the mean age of subjects and the incidence of risk factors (gallstones, alcoholism) in the subgroup of fatal cases were significantly lower compared with those in the subgroup of non fatal events. Thus, it seems that acute events of pancreatitis occurring in the colder months may be more at risk in terms of severity and mortality. Further studies conducted on larger samples and addressed to other countries of different latitudes would be needed.

ACKNOWLEDGEMENTS

The authors thank Mr. Franco Guerzoni, from the Statistical Service of Ferrara St Anna Hospital, for his helpful assistance in collection of cases and analysis of data.

REFERENCES

1 **Gallerani M,** Manfredini R, Ricci L, Grandi E, Cappato R, Calo G, Pareschi PL, Fersini C. Sudden death from pulmonary thromboembolism: chronobiological aspects. *Eur Heart J* 1992; **13**: 661-665
2 **Manfredini R,** Gallerani M, Salmi R, Zamboni P, Fersini C. Fatal pulmonary embolism in hospitalized patien: evidence for a winter peak. *J Int Med Res* 1994; **22**: 85-89
3 **Gallerani M,** Trappella G, Manfredini R, Pasin M, Napolitano M, Migliore A. Acute intracerebral haemorrhage: circadian and circannual patterns of onset. *Acta Neurol Scand* 1994; **89**: 280-286
4 **Gallerani M,** Portaluppi F, Maida G, Chieregato A, Calzolari F, Trapella G, Manfredini R. Circadian and circannual rhythmicity in the occurrence of subarachnoid hemorrhage. *Stroke* 1996; **27**: 1793-1797
5 **Manfredini R,** Portaluppi F, Salmi R, Zamboni P, la Cecilia O, Kuwornu Afi H, Regoli F, Bigoni M, Gallerani M. Seasonal variation in the occurrence of nontraumatic rupture of thoracic aorta. *Am J Emerg Med* 1999; **17**: 672-674
6 **Mehta HR,** Manfredini R, Hassan F, Sechtem U, Bossone E, Oh JK, Cooper JV, Smith DE, Portaluppi F, Penn M, Hutchison S, Nienaber CA, Isselbacher EM, Eagle KA. Chronobiological patterns of acute aortic dissection. *Circulation* 2002; **106**: 1110-1115
7 **Gallerani M,** Delli Gatti C, Salmi R, Kuwornu Afi H, la Cecilia O, Manfredini R. Seasonal variations in the incidence of cranial nerve paralysis. *J Int Med Res* 1999; **27**: 130-133
8 **Gallerani M,** Govoni M, Mucinelli M, Bigoni M, Trotta F, Manfredini R. Seasonal variation in the onset of acute microcrystalline arthritis. *Rheumatology* 1999; **38**: 1003-1006
9 **Gallerani M,** Manfredini R. Seasonal variation in herpes zoster infection. *Br J Dermatol* 2000; **142**: 588-589
10 **Manfredini R,** Gallerani M, Portaluppi F. Seasonal variation in the occurrence of epistaxis. *Am J Med* 2000; **108**: 759-760
11 **Braverman DZ,** Morali GA, Patz JK, Jacobsohn WZ. Is duodenal ulcer a seasonal disease? A retrospective endoscopic study of 3105 patients. *Am J Gastroenterol* 1992; **87**: 1591-1593
12 **Tivon K,** Cohen P. Seasonality in duodenal ulcer disease: possible relationship with circannually cycling neurons enclosed in the biological clock. *Am J Gastroenterol* 1995; **90**: 1189-1190
13 **Thomopoulos KC,** Katsakoulis EC, Margaritis VG, Mimidis KP, Vagianos CE, Nikolopoulou VN. Seasonality in the prevalence of acute upper gastrointestinal bleeding. *J Clin Gastroenterol* 1997; **25**: 576-579
14 **Raschka C,** Schorr W, Koch HJ. Is there seasonal periodicity in the prevalence of *Helicobacter pylori*? *Chronobiol Int* 1999; **16**: 811-819
15 **Sonnenberg A,** Jacobsen SJ, Wasserman IH. Periodicity of hospital admissions for inflammatory bowel disease. *Am J Gastroenterol* 1994; **89**: 847-851
16 **Moum B,** Aadland E, Ekbom A, Vatn MH. Seasonal variations in the onset of ulcerative colitis. *Gut* 1996; **38**: 376-378
17 **Zeng L,** Anderson FH. Seasonal change in the exacerbations of Crohn's disease. *Scand J Gastroenterol* 1996; **31**: 79-82
18 **Ott L,** Memdenhall W, Larson R. Statistical test of hypotheses: the one sample case. In: Statistics. Boston , MA: *Duxbury Press* 1978: 242-246
19 **Mojon A,** Fernandez JR, Hermida RC. Chronolab: an interactive software package for chronobiologic time series analysis written for the Macintosh computer. *Chronobiol Int* 1992; **9**: 403-412
20 **Lankisch PG,** Assmus C, Pflichthofer D. The calendar and acute pancreatitis. *Pancreas* 1998; **16**: 465-467
21 **Poikolainen K.** Seasonality of alcohol-related hospital admis-

sions has implications for prevention. *Drug Alcohol Depend* 1982; **10**: 65-69
22 **Reimann HA.** Letter: Three periodic diseases as causes of recurrent abdominal pain in childhood. *Arch Dis Child* 1976; **51**: 244
23 **Minoli G,** Imperiali G, Colombo E, De Franchis R, Mortara G, Prada A, Rocca F. Biphasic annual periodicity in relapses of inflammatory bowel diseases. Gruppo di studio per le malattie infiammatorie intestinale. *J Clin Gastroenterol* 1995; **21**: 27-29
24 **Manfredini R**, Gallerani M, Salmi R, Calo G, Pasin M, Bigoni M, Fersini C. Circadian variation in the time of onset of acute gastrointestinal bleeding. *J Emerg Med* 1994; **12**: 5-9
25 **Siringo S,** Bolondi L, Sofia S, Hermida RC, Gramantieri L, Gaiani S, Piscaglia F, Carbone C, Misitano B, Corinaldesi R. Circadian occurrence of variceal bleeding in patients with liver cirrhosis. *J Gastroenterol Hepatol* 1996; **11**: 1115-1120
26 **Mann NS,** Hillis A, Mann SK, Buerk CA, Prasad VM. In cirrhotic patients variceal bleeding is more frequent in the evening and correlates with severity of liver disease. *Hepatogastroenterology* 1999; **46**: 391-394
27 **Piscaglia F,** Siringo S, Hermida RC, Legnani C, Valgimigli M, Donati G, Palareti G, Gramantieri L, Gaiani S, Burroughs AK, Bolondi L. Diurnal changes of fibrinolysis in patients with liver cirrhosis and esophageal varices. *Hepatology* 2000; **31**: 349-357
28 **Der T,** Bercik P, Donnelly G, Jackson T, Berezin I, Collins SM, Huizinga JD. Interstitial cells of cajal and inflammation-induced motor dysfunction in the mouse small intestine. *Gastroenterology* 2000; **119**: 1590-1599
29 **Malinovskaya N,** Komarov FI, Rapoport SI, Voznesenskaya LA, Wetterberg L. Melatonin production in patients with duodenal ulcer. *Neuroendocrinol Lett* 2001; **22**: 109-117
30 **Kato K,** Murai I, Asai S, Takahashi Y, Nagata T, Komuro S, Mizuno S, Iwasaki A, Ishikawa K, Arakawa Y. Circadian rhythm of melatonin and prostaglandin in modulation of stress-induced gastric mucosal lesions in rats. *Aliment Pharmacol Ther* 2002; **16**(Suppl 2): 29-34
31 **Bassotti G,** Battaglia E, Spinozzi F, Pelli MA, Tonini M. Twenty-four hour recordings of colonic motility in patients with diverticular disease: evidence for abnormal motility and propulsive activity. *Dis Colon Rectum* 2001; **44**: 1814-1820
32 **Rao SS,** Sadeghi P, Batterson K, Beaty J. Altered periodic rectal motor activity: a mechanism for slow transit constipation. *Neurogastroenterol Motil* 2001; **13**: 591-598
33 **Park BK,** Chung JB, Lee JH, Suh JH, Park SW, Song SY, Kim H, Kim KH, Kang JK. Role of oxygen free radicals in patients with acute pancreatitis. *World J Gastroenterol* 2003; **9**: 2266-2269

Edited by Wang XL **Proofread by** Xu FM

PO Box 2345, Beijing 100023, China
Fax: +86-10-85381893
E-mail: wjg@wjgnet.com www.wjgnet.com

World J Gastroenterol 2004;10(22):3332-3335
World Journal of Gastroenterology
 ISSN 1007-9327

• CLINICAL RESEARCH •

Composite score of reflux symptoms in diagnosis of gastroesophageal reflux disease

Jin-Hai Wang, Jin-Yan Luo, Lei Dong, Jun Gong, Ai-Li Zuo

Jin-Hai Wang, Jin-Yan Luo, Lei Dong, Jun Gong, Ai-Li Zuo, Department of Gastroenterology, Second Hospital of Xi'an Jiaotong University, Xi'an 710004, Shaanxi Province, China
Supported by Janssen Research Foundation of China (2001)
Correspondence to: Dr. Jin-Hai Wang, Department of Gastroenterology, Second Hospital of Xi'an Jiaotong University, 710004, Shaanxi Province, China. jinhaiwang@hotmail.com
Telephone: +86-29-7679290 **Fax:** +86-29-7231758
Received: 2003-12-19 **Accepted:** 2004-02-01

Abstract

AIM: To evaluate the significance of the composite score of reflux symptoms in the diagnosis of gastroesophageal reflux disease (GERD), and to determine the relationship of the composite score with reflux esophagitis (RE) and pathological gastroesophageal reflux (PGER).

METHODS: Upper digestive endoscopy and /or 24-h esophageal pH monitoring were performed in 244 subjects. Of these, 54 were consecutive patients attending our clinic with symptoms suggestive of GERD, and 190 were randomly selected from 2532 respondents who participated in our previous general population-based study on GERD. A standardized questionnaire was used to classify both the frequency and severity of typical symptoms of GERD (heartburn, acid and food regurgitation) using a 4-score scale, and the composite score of main reflux symptoms (score index: SI, range from 0 to 18) were calculated for every subject. RE was diagnosed according to the Savary-Miller criteria. Subjects with abnormal pH-metry (DeMeester score more than 14.7) were considered to have PGER. GERD patients were defined as the subjects with RE and/or PGER.

RESULTS: The sensitivity of SI in the diagnosis of GERD was inversely associated with SI, but the specificity tended to increase with increased SI. With the cut-off of 8, the SI achieved the highest accuracy of 70.0%, with a sensitivity of 78.6% and a specificity of 69.2% in diagnosing GERD, followed by the cut-off of 3, which had an accuracy of 62.1%, a sensitivity of 96.4% and a specificity of 34.6%. The prevalence of RE, PGER and GERD was strongly associated with increased SI ($P<0.01$), but there was no significant association between the severity of RE and SI ($P>0.05$). Among patients with RE, 69.2% had PGER, and 30.8% were confirmed to have negative findings of pH monitoring. Among patients with PGER, 52.9% were identified to have RE and 47.1% had negative endscopic findings in esophagus.

CONCLUSION: According to the composite score of main reflux symptoms, the diagnosis of GERD can be made without further tests in most cases. However, 24-h esophageal pH monitoring and upper digestive endoscopy are still indicated in patients with mild and atypical symptoms.

Wang JH, Luo JY, Dong L, Gong J, Zuo AL. Composite score of reflux symptoms in diagnosis of gastroesophageal reflux disease. *World J Gastroenterol* 2004; 10(22): 3332-3335
http://www.wjgnet.com/1007-9327/10/3332.asp

INTRODUCTION

Gastroesophageal reflux disease (GERD) is a very common disorder both in China[1-2] and Western countries[3-8]. The disease results from the abnormal reflux of gastric contents into the distal esophagus causing symptoms in most patients and subsequent mucosal damage in some patients. It has been proved that chronic GERD tends to develop to Barrett's esophagus associated with an increased risk of esophageal adenocarcinoma[9-13]. Heartburn and regurgitation are the typical symptoms of GERD, and 24-h esophagus pH monitoring and upper digestive endoscopy are the main methods to confirm the diagnosis. These examinations, however, are inconvenient and not universal in many hospitals of China, especially 24-h esophagus pH monitoring. Although the relationship between reflux symptoms and GRED were evaluated by some clinical studies, the results varied considerably because the symptoms were quantified by different criteria and methods[3,14-16]. As far as we know, data about the relationship between the combination of main reflux symptoms and proven GERD are lacking. The aim of this study was to establish a standard system to quantify the severity and frequency of typical reflux symptoms, and to evaluate the role of the composite score of main reflux symptoms in the diagnosis of GERD, and to determine the association between the composite score and reflux esophagitis (RE), pathological gastroesophageal reflux (PGER), and GERD.

MATERIALS AND METHODS

Subjects

Two hundred and forty-four subjects were included in this study. Among these, 54 were consecutive patients (32 men and 22 women; mean age, 45.3±13.2 years) who attended our clinic with symptoms suggestive of GERD and underwent both 24-h esophageal pH monitoring and upper digestive endoscopy. The remaining 190 subjects were randomly selected from 2532 respondents who were previously enrolled in our general population-based study on GERD, according to the composite score (score index, SI) of main reflux symptoms (Table 1), and who underwent 24-h esophageal pH monitoring (50 subjects) or/and upper digestive endoscopy (140 subjects). Patients with previous foregut surgery and other systemic disorders affecting the gastrointestinal motility were excluded. Five selected respondents (3 in the normal group and 1 in the mild symptom group) refused to participate in this study, 1 (normal group) had intolerance to pH monitoring, and 1(normal group) did not complete the evaluation. All of the 7 incomplete respondents were replaced by our clinic patients with same gender, SI, and similar age (±5 years). There were no appreciable differences in age or gender among these groups ($P>0.05$).

Questionnaire

A standardized questionnaire based on our previous work was

Table 1 Gender and age distribution of 190 subjects in symptom severity groups

Severity of symptoms	Responders	Upper digestive endoscopy			24-h pH monitoring		
		Subjects	Men/Women	Mean age (yr)	Subjects	Men/Women	Mean age (yr)
Normal	2 102	40	17/23	45.5±9.9	15	8/7	45.3±10.4
Mild	332	40	20/20	46.1±14.4	15	6/9	46.5±13.3
Moderate	74	40	18/22	47.4±9.6	10	5/5	47.4±10.6
Severe	24	20	11/9	49.1±10.2	10	4/6	49.7±11.5
Total	2 532	140	66/74	47.0±11.0	50	23 /27	47.2±11.5

Table 2 Relationship between SI and RE, PGER, GERD

Criteria of SI	Endoscopic examination		pH monitoring		Endoscopic or/and pH examination	
	Subjects	RE (%)	Subjects	PGER (%)	Subjects	GERD (%)
Normal (SI = 0-2)	40	0 (0.0)	15	0 (0.0)	55	0 (0.0)
Mild (SI = 3-7)	40	3 (7.5)	15	2 (13.3)	52	4 (7.69)
Moderate (SI = 8-12)	40	11 (27.5)[b]	10	4 (40.0)[a]	45	12 (26.7)[b]
Severe (SI≥13)	20	13 (66.5)[b]	10	6 (60.0)[b]	24	13 (54.2)[b]

[a]$P<0.05$ and [b]$P<0.01$ *vs* normal group.

used to classify both the frequency and severity of typical symptoms of GERD (heartburn, acid regurgitation and food regurgitation) for all subjects before pH monitoring and upper digestive endoscopy. Personal interviews were carried out in our clinic with patients and respondents.

Endoscopy

General upper digestive endoscopy was performed using a Pentax videoendoscope, and the same two gastrointestinal physicians made the diagnosis according to VHS videocassettes recorded.

Twenty-four hour esophageal pH monitoring

Twenty-four hour ambulatory esophageal pH monitoring was performed using a Synectic device. The pH electrode should be positioned 5 cm above the lower esophageal sphincter. Subjects were instructed to fill in diary cards regarding the time of meals, supine position and the time of symptoms experienced during the 24-h period. In addition, they were asked to press a button on the digital data logger at the beginning of each symptom episode. No restrictions were imposed on food and beverage intake or smoking.

Definitions

The following definitions for symptom categories and diseases were used. Only symptoms occurring in the past year before the interview were considered. Heartburn was defined as a burning pain or burning sensation behind the breastbone in the chest, acid regurgitation as a bitter or sour-tasting fluid coming into throat or mouth, food regurgitation as eaten foods coming into mouth. Heartburn, acid regurgitation and food regurgitation were considered to be the typical symptoms of GERD. Each of these symptoms was estimated according to its severity and frequency measured on a 4-score scale. Severity was assessed as follows: 0, none; 1, mild (could be ignored); 2, moderate (could not be ignored but did not affect lifestyle); 3, severe (affected lifestyle). The score of symptom frequency was estimated as follows: 0, none or less than one occasion per month on average; 1, several occasions (once to three times) a month; 2, several occasions (once to six times) a week; 3, one or more daily occasions. Based on the scores of severity and frequency of the main GERD symptoms, the composite score (SI: ranged from 0 to 18) of every subject was calculated. All subjects were grouped as follows: SI = 0-2, normal; SI = 3-7, mild; SI = 8-12, moderate; SI≥R13, severe. Patients with symptomatic gastroesophageal reflux disease(SGERD) were defined as subjects with SI≥R3. Those with RE were defined as subjects whose endoscopic findings met Savary-Miller criteria, those with PGER as subjects with abnormal pH-metry (DeMeester score more than 14.7), those with GERD as subjects with RE and/or PGER.

Statistical analysis

Data were analyzed with descriptive statistics and expressed as mean±SD. Median values and ranges were used for nonparametric variables. Relative proportions were calculated for the analysis of prevalence and relative frequencies. The comparison between groups was performed by means of parametric tests such as the Student's *t* test for dimensional variables and χ^2 test for non-dimensional variables. The critical two-tailed value of alpha was set at 0.05.

RESULTS

Relationship between SI and its diagnostic accuracy for GERD

Among the 54 outpatients with symptoms suggestive of GERD, 28 patients (51.9%) were identified as GERD (16 patients with RE, 12 patients with PGER, 10 patients with RE and PGER), and 26 patients (48.1%) were normal, based on the findings of upper digestive endoscopy and 24-h esophageal pH monitoring. Figure1 summarizes the relationship between criteria and its diagnostic accuracy for GERD compared with the diagnosis of endoscopy and pH monitoring. The sensitivity was inversely associated with increased SI, but the specificity tended to be higher with increased SI. The SI≥8 had the highest accuracy (70.0%) for diagnosing GERD with a sensitivity of 78.6% and a specificity of 69.2%, followed by SI≥3 with a accuracy of 62.1%, a sensitivity of 96.4% and a specificity of 34.6%.

Relationship between SI and RE, PGER, GERD

As shown in Table 2, the rate of RE was the highest in the severe group, followed by moderate, mild and normal groups, and the results were similar to both PGER and GERD. The rate of RE, PGER and GERD was strongly associated with increased SI. In the severe and moderate groups, the frequency of RE, PGER and GERD was significantly higher than that of the normal group ($P<0.05$ or $P<0.01$).

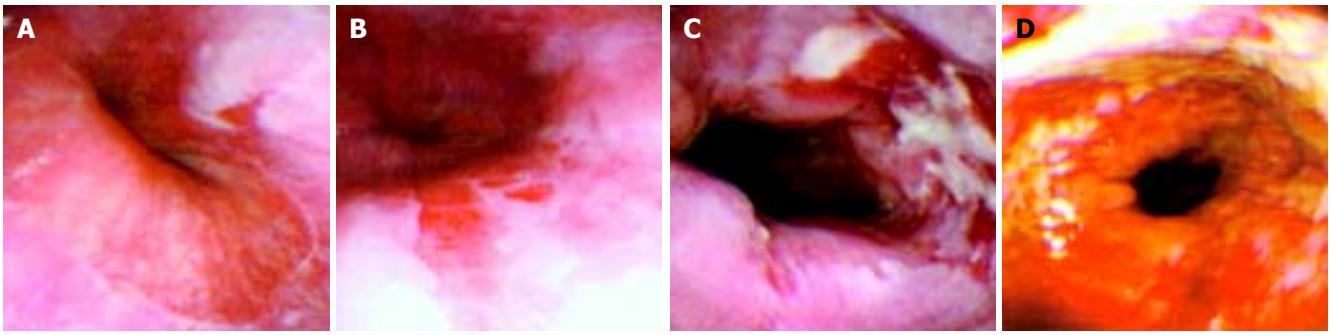

Figure 2 Endoscopic photographs of some patients with RE. A: Female, 46 years old, SI = 12, grade I RE; B: Male, 50 years old, SI = 16, grade II RE; C: Male, 42 years old, SI = 12, grade III RE; D: Male, 51 years old, SI = 13, grade IV RE.

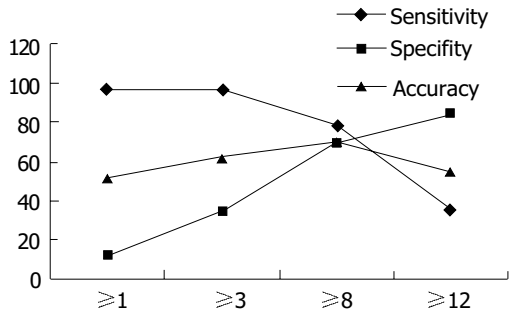

Figure 1 Relationship between SI and its diagnostic accuracy.

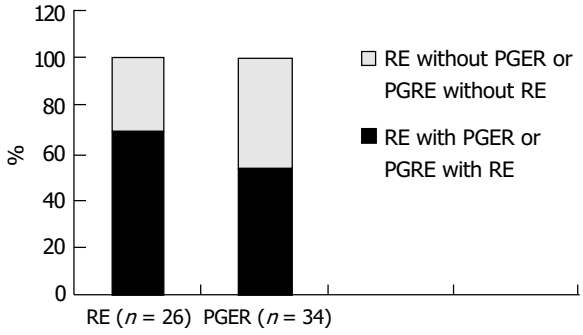

Figure 3 The relationship between RE and PGER.

Relationship between SI and degree of RE

RE was diagnosed in a total of 43 patients on the basis of endoscopic findings (16 cases were outpatients and 27 cases came from general subjects). Thirty patients were males and 13 were females. The mean age was 55.3±6.8 years. Table 3 shows the relationship between SI and the severity of RE. The SI was similar among all groups (from grade I to grade IV, $P>0.05$). Figure 2 illustrates endoscopic photographs of some patients with RE.

Table 3 Relationship between severity of symptoms and grade of RE

Severity of RE	Patients	SI (mean±SD)
Grade I	19	10.63±4.74
Grade II	13	11.32±5.26
Grade III	7	11.85±5.11
Grade IV	4	12.00±4.12

Relationship between RE and PGER

Of the 43 patients with RE, 26 patients underwent 24-h esophageal pH monitoring. Eighteen patients with RE (69.2%) complicated by PGER and 8 patients (30.8%) were confirmed to have negative pH monitoring. Upper gastrointestinal tract endoscopy was performed in 34 patients with PGER, of them, 18 (52.9%) were identified to have RE, but the remaining 16 (47.1%) patients were proven to have a negative endoscopic finding in the esophagus. The results are summarized in Figure 3.

DISCUSSION

Gastroesophageal reflux disease is a common disease with many typical and atypical symptoms. A low pressure exerted by the lower esophageal sphincter (LES) and an increased frequency of transient LES relaxation might contribute to the development of GERD[17-19]. Esophageal testing, particularly 24-h pH monitoring has become the key to make the diagnosis and to ensure adequate acid suppression or prior to surgical therapy[20]. Although the test could yield accurate and reliable information, it is inconvenient for patients. The problem is whether all patients require 24-h esophageal pH monitoring to establish the diagnosis of GERD. If so, its use, however, is not popular and many hospitals in China are unable to perform this special testing. For these reasons, we are trying to develop a standard system to quantify the symptoms and to evaluate the accuracy of the combination of typical reflux symptoms in the diagnosis of GERD with the hope of eliminating the need for the monitoring.

Laboratory studies have demonstrated that there is a close relationship between classic reflux symptoms and esophageal acid exposure, but some clinical studies revealed that these symptoms were neither specific nor sensitive to the diagnosis of GERD[15,21-23]. For example, Tefera and his colleagues[21] reported that moderate or severe heartburn could be used to diagnose GERD with a sensitivity of 68.42% and a specificity of 62.96%, and moderate or severe regurgitation with a sensitivity of 56.76% and a specificity of 65.08%. There were some common grounds in these clinical studies. These symptoms were evaluated separately. The frequency of each symptom was quantified but the severity was not considered. In our study, every typical symptom was estimated by quantifying both the frequency and the severity, and a combination score (SI) of all symptoms was calculated for every subject to exclude those subjects with trivial symptoms and to improve the accuracy of SI in the diagnosis of GERD.

We found that the sensitivity of the composite score of main reflux symptoms in the diagnosis of GERD was inversely associated with increased SI, but the specificity tended to be higher with increased SI. SI≥8 had the highest accuracy of 70.0% for diagnosing GERD with a sensitivity of 78.6% and a specificity of 69.2%, followed by SI≥3 with an accuracy of 62.1%, a sensitivity of 96.4%, and a specificity of 34.6%. Because SI≥3 had the highest sensitivity, this criterion is the common choice in epidemiological studies. With the highest accuracy, SI≥8 is very useful for diagnosing GERD in clinical work. We, therefore, prompted to develop a criterion based on the main reflux symptoms. The standardized symptom questionnaire and the scoring techniques (system) are important for

gastroenterological doctors to estimate the patients with typical reflux symptoms, especially in hospitals or clinics without objective tests. We suggest that patients with SI$\geqslant$8 may be treated pharmaceutically combined with life style counseling. If the symptoms have not improved after 6 to 12 wk, 24-h pH monitoring and/or endoscopical examination should be performed, and if necessary, barium radiographing and manometry should be done.

Our study showed that the prevalence of RE, PGER and GERD was strongly associated with increased SI, but no significant association was found between the severity of RE and SI, indicating that patients with more severe reflux symptoms tend to have GERD, but the grade of esophagitis could not be evaluated on the basis of the severity of typical symptoms.

The present study also revealed that almost one third of patients with RE (30.8%) were confirmed to have negative pH monitoring and half of patients with PGER (47.1%) had negative endoscopic findings in the esophagus, the results were similar to previous studies[24-26]. Excessive bile exposure of esophageal mucosa was the main cause of RE with normal acid exposure[27-29]. We suggest that endoscopy-negative reflux disease (ENRD) should be treated as endoscopy positive GERD because longterm acid exposure would rapidly damage esophageal mucosa.

Patients with atypical symptoms such as cough, asthma, hoarseness, chest pain, and ear, nose and throat symptoms were not included in this study because they always had their first visit at specialized services. According to some studies the prevalence of GERD in patients with atypical symptoms ranged from 25% to 80%. We suggest that diagnostic tests such as upper digestive endoscopy and 24-h pH monitoring are a necessity for patients with atypical symptoms.

In conclusion, developing a criterion based on the composite score of typical reflux symptoms is useful to the diagnosis of GERD. Symptom questionnaire and scoring techniques are an important step in this analysis. For patients with a moderate or severe composite score, the diagnosis of GERD can be made without further tests in most situations. However, 24-h esophageal pH monitoring is still needed in patients with mild and atypical symptoms.

REFERENCES

1 **Lim LG**, Ho KY. Gastroesophageal reflux disease at the turn of *millennium*. *World J Gastroenterol* 2003; **9**: 2135-2136
2 **Pan GZ**, Xu GM, Ke MY, Han SM, Guo HP, Li ZS, Fang XC, Zou DW, Lu SC, Liu J. Epidemiological study of symptomatic gastroesophageal reflux disease in China: Beijing and Shanghai. *Chin J Dig Dis* 2000; **1**: 2-8
3 **Kennedy T**, Jones R. The prevalence of gastro-oesophageal reflux symptoms in a UK population and the consultation behaviour of patients with these symptoms. *Aliment Pharmacol Ther* 2000; **14**: 1589-1594
4 **Locke GR III**, Talley NJ, Fett SL, Zinsmeister AR, Melton LJ III. Prevalence and clinical spectrum of gastroesophageal reflux: a population based study in Olmsted County. *Gastroenterology* 1997; **112**: 1448-1456
5 **Talley NJ**, Zinsmeister AR, Schleck CD, Melton LJ III. Dyspepsia and dyspepsia subgroups: a population-based study. *Gastroenterology* 1992; **102**: 1259-1268
6 **Talley NJ**, Boyce P, Jones M. Identification of distinct upper and lower gastrointestinal symptom groupings in an urban population. *Gut* 1998; **42**: 690-695
7 **Isolauri J**, Laippala P. Prevalence of symptoms suggestive of gastro-oesophageal reflux disease in an adult population. *Ann Med* 1995; **27**: 67-70
8 **Louis E**, DeLooze D, Deprez P, Hiele M, Urbain D, Pelckmans P, Deviere J, Deltenre M. Heartburn in Belgium: prevalence, impact on daily life, and utilization of medical resources. *Eur J Gastroenterol Hepatol* 2002; **14**: 279-284
9 **Bytzer P**, Christensen PB, Damkier P, Vinding K, Seersholm N. Adenocarcinoma of the esophagus and Barrett's esophagus: a population-based study. *Am J Gastroenterol* 1999; **94**: 86-91
10 **Falk GW**. Barrett's esophagus. *Gastroenterology* 2002; **122**: 1569-1591
11 **Buttar NS**, Wang KK, Leontovich O, Westcott JY, Pacifico RJ, Anderson MA, Krishnadath KK, Lutzke LS, Burgart LJ. Chemoprevention of esophageal adenocarcinoma by COX-2 inhibitors in an animal model of Barrett's esophagus. *Gastroenterology* 2002; **122**: 1101-1112
12 **Shirvani VN**, Ouatu-Lascar R, Kaur BS, Omary MB, Triadafilopoulos G. Cyclooxygenase 2 expression in Barrett's esophagus and adenocarcinoma: Ex vivo induction by bile salts and acid exposure. *Gastroenterology* 2000; **118**: 487-496
13 **Sampliner RE**. Practice guidelines on the diagnosis, surveillance, and therapy of Barrett's esophagus. *Am J Gastroenterol* 1998; **93**: 1028-1033
14 **Klauser AG,** Schindlbeck NE, Muller-Lissner SA. Symptoms in gastro-oesophageal reflux disease. *Lancet* 1990; **335**: 205-208
15 **Costantini M**, Crookes PF, Bremner RM, Hoeft SF, Ehsan A, Peters JH, Bremner CG, DeMeester TR, Calif LA. Value of physiologic assessment of foregut symptoms in a surgical practice. *Surgery* 1993; **114**: 780-787
16 **Ho KY**, Kang JY, Seow A. Prevalence of gastrointestinal symptoms in a multiracial Asian population, with particular reference to reflux-type symptoms. *Am J Gastroenterol* 1998; **93**: 1816-1822
17 **Grossi L**, Ciccaglione AF, Travaglini N, Marzio L. Transient lower esophageal sphincter relaxations and gastroesophageal reflux episodes in healthy subjects and GERD patients during 24 hours. *Dig Dis Sci* 2001; **46**: 815-821
18 **Kahrilas PJ**, Shi G, Manka M, Joehl RJ. Increased frequency of transient lower esophageal sphincter relaxation induced by gastric distention in reflux patients with hiatal hernia. *Gastroenterology* 2000; **118**: 688-695
19 **Cadiot G**, Bruhat A, Rigaud D, Coste T, Vuagnat A, Benyedder Y, Vallot T, Le Guludec D, Mignon M. Multivariate analysis of pathophysiological factors in reflux oesophagitis. *Gut* 1997; **40**: 167-174
20 **Ueno M**, Hongo M. Clinical significance of 24-hour intraesophageal pH monitoring in GERD patients. *Nippon Rinsho* 2000; **58**: 1818-1822
21 **Tefera L,** Fein M, Ritter MP, Bremner CG, Crookes PF, Peters JH, Hagen JA, DeMeester TR. Can the combination of symptoms and endoscopy confirm the presence of gastroesophageal reflux disease? *Am Surg* 1997; **63**: 933-936
22 **Colas-Atger E**, Bonaz B, Papillon E, Gueddah N, Rolachon A, Bost R, Fournet J. Relationship between acid reflux episodes and gastroesophageal reflux symptoms is very inconstant. *Dig Dis Sci* 2002; **47**: 645-651
23 **Ott DJ**, McManus CM, Ledbetter MS, Chen MY, Gelfand DW. Heartburn correlated to 24-hour pH monitoring and radiographic examination of the esophagus. *Am J Gastroenterol* 1997; **92**: 1827-1830
24 **Arango L**, Angel A, Molina RI, Marquez JR. Comparison between digestive endoscopy and 24-hour esophageal pH monitoring for the diagnosis of gastroesophageal reflux esophagitis: "presentation of 100 cases". *Hepatogastroenterology* 2000; **47:** 174-180
25 **Chan CC**, Lee CL, Wu CH. Twenty-four-hour ambulatory esophageal pH monitoring in patients with symptoms of gastroesophageal reflux. *J Formos Med Assoc* 1997; **96**: 874-878
26 **Quigley EM**. Non-erosive reflux disease: part of the spectrum of gastro-oesophageal reflux disease, a component of functional dyspepsia, or both? *Eur J Gastroenterol Hepatol* 2001; **13**(Suppl 1): S13-18
27 **Kauer WK**, Peters JH, DeMeester TR, Ireland AP, Bremner CG, Hagen JA. Mixed reflux of gastric and duodenal juices is more harmful to the esophagus than gastric juice alone. The need for surgical therapy re-emphasized. *Ann Surg* 1995; **222**: 525-531
28 **Lin KM,** Ueda RK, Hinder RA, Stein HJ, DeMeester TR. Etiology and importance of alkaline esophageal reflux. *Am J Surg* 1991; **162**: 553-557
29 **Vaezi MF**, Richter JE. Role of acid and duodenogastroesophageal reflux in gastroesophaeal reflux disease. *Gastroenterology* 1996; **111**: 1192-1199

Edited by Wang XL **Proofread by** Zhu LH and Xu FM

PO Box 2345, Beijing 100023, China
Fax: +86-10-85381893
E-mail: wjg@wjgnet.com www.wjgnet.com

World J Gastroenterol 2004;10(22):3336-3338
World Journal of Gastroenterology
 ISSN 1007-9327

• CLINICAL RESEARCH •

Clinical characteristics and prognostic factors of severe acute pancreatitis

Lei Kong, Nn Santiago, Tian-Quan Han, Sheng-Dao Zhang

Lei Kong, Nn Santiago, Tian-Quan Han, Sheng-Dao Zhang, Shanghai Institute of Digestive Surgery, Department of Surgery, Ruijin Hospital, Shanghai Second Medical University, Shanghai 200025, China
Correspondence to: Dr. Tian-Quan Han, Department of Surgery, Ruijin Hospital, Shanghai Second Medical University, Shanghai Institute of Digestive Surgery, 197 Ruijin II Road, Shanghai 200025, China. digsurgeryrj@yahoo.com.cn
Telephone: +86-21-64373909 **Fax:** +86-21-64373909
Received: 2004-04-22 **Accepted:** 2004-04-29

Abstract

AIM: To investigate the clinical characteristics and prognostic factors of a consecutive series of patients with severe acute pancreatitis (SAP).

METHODS: Clinical data of SAP patients admitted to our hospital from January 2003 to January 2004 were retrospectively reviewed. Collected data included the age, gender, etiology, length of hospitalization, APACHE II score at admission, local and organ/systemic complications of the patients.

RESULTS: Of the 268 acute pancreatitis patients, 94 developed SAP. The mean age of SAP patients was 52 years, the commonest etiology was cholelithiasis (45.7%), the mean length of hospitalization was 70 d, the mean score of APACHE II was 7.7. Fifty-four percent of the patients developed necrosis, 25% abscess, 58% organ/systemic failure. A total of 23.4% (22/94) of the SAP patients died. Respiratory failure was the most common organ dysfunction (90.9%) in deceased SAP patients, followed by cardiovascular failure (86.4%), renal failure (50.0%). In the SAP patients, 90.9% (20/22) developed multiple organ/systemic failures. There were significant differences in age, length of hospitalization, APACHE II score and incidences of respiratory failure, renal failure, cardiovascular failure and hematological failure between deceased SAP patients and survived SAP patients. By multivariate logistic regression analysis, independent prognostic factors for mortality were respiratory failure, cardiovascular failure and renal failure.

CONCLUSION: SAP patients are characterized by advanced age, high APACHE II score, organ failure and their death is mainly due to multiple organ/systemic failures. In patients with SAP, respiratory, cardiovascular and renal failures can predict the fatal outcome and more attention should be paid to their clinical evaluation.

Kong L, Santiago N, Han TQ, Zhang SD. Clinical characteristics and prognostic factors of severe acute pancreatitis. *World J Gastroenterol* 2004; 10(22): 3336-3338
http://www.wjgnet.com/1007-9327/10/3336.asp

INTRODUCTION

Acute pancreatitis, as a relatively common pancreatic disease, can be found in every part of the world with an incidence of 35-80 cases per 100 000 inhabitants per year[1,2]. According to Atlanta Classification, acute pancreatitis is clinically classified into a mild or severe type depending on the presence of local and systemic complications[3]. Severe acute pancreatitis (SAP) is characterized by high morbidity and mortality. The mortality of SAP patients varies from 7% to 47%[4]. The factors most closely linked to a poor prognosis are pancreatic necrosis, infection and multiple organ/systemic failures, which are associated with a mortality of 50%[4-7]; although in recent years this mortality rate has tended to decrease[8]. Many attempts have been made to achieve an early prognosis of SAP. However, none seems to be reliable enough to justify its routine use.

In view of the high mortality associated with SAP, it is important to identify the cases that require close monitoring and aggressive resuscitation. The aim of this study was therefore to investigate the clinical characteristics and factors which could predict the outcome of patients with organ/systemic failure admitted to our hospital.

MATERIALS AND METHODS

Clinical data

From January 2003 to January 2004, the clinical histories of patients with acute pancreatitis (AP), admitted to the Department of Surgery, Ruijin Hospital of Shanghai Second Medical University, were retrospectively reviewed. The diagnosis of AP was established in cases with clinical presentations and biochemical findings when other causes were excluded. The severities of AP were assessed according to the Atlanta classification system[3]. Etiology was divided into two groups: cholelithiasis and non-cholelithiasis. A biliary etiology was confirmed by ultrasonography, CT scan, ERCP, MRCP and operation. Pancreatic necrosis and abscess were defined by the findings on contrast-enhanced CT scan or in operation. The local and organ/systemic complications were defined according to the Atlanta classification system[3, 9].

The patients with SAP were divided according to their outcomes into two groups: deceased group and survived group. The data recorded for each patient included age, gender, etiology, length of hospitalization, APACHE II score at admission and the presence and type of local and organ/systemic complications. The relationship between clinical characteristics, specific single or multiple organ/systemic failures with mortality was evaluated in above-mentioned two groups.

Statistical analysis

Results were expressed as mean±SD. Statistical studies were made using SAS 6.12. Continuous data were evaluated by *t* rest, and categorized data were analyzed by Chi-square test or Fisher's exact test. To identify the risk factors for SAP, multiple logistic regression analysis with backward elimination was used. $P<0.05$ was considered statistically significant.

RESULTS

Of the 268 patients with AP, 35.1% (94/268) developed SAP. Of the 94 SAP patients, 23.4% (22/94) died. The patients in the deceased group were significantly older and had a higher

APACHE II score than those in the survived group. The length of hospitalization was significantly shorter in those with a fatal outcome. There was no difference in etiology or gender (Table 1).

Regarding the local complications, the incidences of necrosis and abscess were significantly higher in the survived group than those in the deceased group. No patient in the deceased group developed pseudocysts (Table 2).

Table 1 Comparison of clinical characteristics (mean±SD)

Characteristics	Survival (*n* = 72)	Deceased (*n* = 22)	Total (*n* = 94)
Mean age (yr)	49.7±14.9[b]	62.8±14.4	52.7±15.8
(range)	(15-82)	(42-83)	(15-83)
Gender			
(male / female)	45 / 27	10 / 12	55 / 39
Etiology			
(biliary / non-biliary)	31 / 41	12 / 10	43 / 51
Hospitalization (d)	84.4±65.3[b]	26.2±28.2	70.8±63.7
(range)	(8-253)	(1-94)	1-253)
APACHE II score	6.3±3.5[b]	12.5±6.8	7.72±5.2
(range)	(0-14)	(1-33)	(0-33)

[b]*P*<0.01 *vs* deceased group.

Table 2 Comparison of local complications

Local complications	Survival (*n*=72)	Deceased (*n*=22)	Total (*n*=94)
Necrosis, *n* (%)	47 (5.3)[b]	7 (31.8)	54 (57.4)
Abscess, *n* (%)	23 (31.4)[a]	2 (9.1)	25 (26.6)
Pseudocyst, *n* (%)	11 (15.3)	0 (0)	11 (11.7)

[a]*P*<0.05, [b]*P*<0.01 *vs* deceased group.

A total of 61.7% (58/94) patients with SAP developed organ/systemic failures. In the deceased group, 90.9% (20/22) patients showed multiple organ/systemic failures (maximum 5 organ/systemic failures), only 18.1% (13/94) patients showed multiple organ/systemic failures in the survived group (Tables 3, 4). With regard to the organ/systemic complications, we found that the deceased group experienced a significantly greater incidence of episodes of respiratory failure, acute renal failure, cardiovascular failure and hematological failure than the survived group (Table 4).

Table 3 Comparison of the number of organ / systemic failure

Number of organ / systemic failure	Survival (*n*=72)	Deceased (*n*=22)	Total (*n*=94)
1, *n* (%)	23 (31.9)[a]	2 (9.1)	25 (26.6)
2, *n* (%)	10 (13.9)	6 (4.5)	16 (17.0)
3, *n* (%)	3 (4.2)[a]	4 (18.2)	7 (7.4)
4, *n* (%)	0 (0)[b]	7 (31.8)	7 (7.4)
5, *n* (%)	0 (0)[a]	3 (13.6)	3 (3.2)
Total, *n* (%)	36 (50.0)[b]	22 (100.0)	58 (61.7)

[a]*P*<0.05, [b]*P*<0.01 *vs* deceased group.

As for the frequency of different specific single organ failures, pulmonary failure occurred in 35.1% (33/94) patients, cardiovascular failure in 22.3% (21/94) patients, gastrointestinal failure in 19.1% (18/94) patients, hepatic failure in 15.9% (15/94) and renal failure in 14.9% (14/94) patients. The incidences of neurologic and hematological failures were relatively lower, only in 8.5% (8/94) patients respectively (Table 5).

Logistic regression analysis was carried out for the independent prognostic factors including all the variables studied. Respiratory failure, cardiovascular failure and renal failure were found to be independent prognostic factors of the mortality in SAP patients (Table 6).

Table 4 Comparison of the features of organ / systemic failure

Organ / systemic failure	Survival (*n*=72)	Deceased (*n*=22)	Total (*n*=94)
Multiple organ / systemic failures *n* (%)	13 (18.1)[b]	20 (90.9)	33 (35.1)
Respiratory *n* (%)	13 (18.1)[b]	20 (90.9)	33 (35.1)
Renal *n* (%)	3 (4.2)[b]	11 (50.0)	14 (14.9)
Gastrointestinal *n* (%)	11 (15.3)	7 (31.8)	18 (19.1)
Hepatic *n* (%)	12 (16.7)	3 (13.6)	15 (15.9)
Neurologic *n* (%)	6 (8.3)	2 (9.1)	8 (8.5)
Cardiovascular *n* (%)	2 (2.8)[b]	19 (86.4)	21 (22.3)
Hematological *n* (%)	2 (2.8)[b]	6 (27.3)	8 (8.5)

[b]*P* <0.01 *vs* deceased group.

Table 5 Frequency of organ / systemic failure

Organ / systemic	Number of organ / systemic failure	Frequency (%)
Respiratory	33	35.1
Renal	14	14.9
Gastrointestinal	18	19.1
Hepatic	15	15.9
Neurologic	8	8.5
Cardiovascular	21	22.3
Hematological	8	8.5

Table 6 Independent factors of the logistic regression model

Variable	OR	OR 95% confidence interval	*P*
Respiratory failure	186.5	9.942-999.0	0.006
Cardiovascular failure	29.9	2.243-999.0	0.021
Renal failure	118.7	3.784-999.0	0.029
Hospitalization, days	0.957	0.908-0.989	0.037

DISCUSSION

Most deaths of SAP patients were mainly related to multiple organ/systemic failures[10]. Regarding the survival time, patients died more often of multiple organ/systemic failures in the first few days after admission[5,11]. In the early phase of SAP, multiple organ/systemic failures seemed to be caused by cytokine and inflammatory mediators released due to systemic inflammatory response syndrome, and sterile pancreatic necrosis might even occur[12]. Early deaths of SAP patients were commonly associated with multiple organ/systemic failure, accounting for 40-60% of mortality, and over the past decade this proportion has not declined[13]. The present study showed that in the deceased group 90.9% (20/22) patients developed multiple organ/systemic failure and 50% (11/22) patients died within 2 wk after admission.

Previous studies[14-16] showed that in SAP patients, organ/systemic failure occurred in 72-90.3%, single organ failure in 24.7-37%, multiple organ failure in 35-65.6%. Among the single organ failures, respiratory failure was the most common organ/systemic complications (39.1-63%), followed by cardiovascular failure (23-37.7%), hepatic failure (20.7%) and renal failure (8.5-13%). The present data showed that organ failure occurred in 61.7% (58/94) patients, single organ failure in 26.6% (25/94) patients, and multiple organ failure in 38.3% (36/94) patients. Respiratory failure was the most common single organ failure (35.1%, 33/94), followed by cardiovascular failure (22.3%, 21/94), gastrointestinal failure (19.1%, 18/94), hepatic failure (15.9%, 15/94) and renal failure (14.9%, 14/94). In a recent study, five independent prognostic factors for hospital mortality in SAP patients were the age and chronic health situation of the patients and organ failures (renal, respiratory and cardiovascular)[4]. In our study, respiratory failure, cardiovascular failure and renal failure were shown to be the independent prognostic factors of

mortality by multivariate logistic analysis, which are consistent with the reports by Fernandez-Cruz *et al*. and Halonen *et al*.[6, 17]. Apparently, the development of one of the above-mentioned complications is by far the worst prognostic factor in SAP, closely related to mortality.

Up to now, the development of pancreatic necrosis and infection has been considered as an important factor in the occurrence of multiple organ/systemic failure and subsequent death[6,18,19]. There are even studies relating the site and extent of necrosis to the outcome and development of multiple organ failures[18,20]. In other studies, infected pancreatic necrosis and combined of organ/systemic failures were the most significant causes for hospital mortality of SAP patients[1,21]. The mortality rate of SAP patients was 7-47% (that of sterile necrotizing pancreatitis patients was 6-13% and SAP patients with infected necrosis was 14-80%)[4,22-26]. Conversely, there was a higher proportion of patients with necrosis and abscess in the survived group in our study. Using logistic regression analysis failed to identify necrosis and abscess as independent prognostic factors for mortality, although statistically significant difference was found between survived and deceased groups. This suggested that, rather than the development of necrosis or abscess itself, necrosis and abscess were not correlated with an increased mortality. The main factor indicating a poor prognosis in SAP was the development of multiple organ/systemic failures[27,28].

Although there was a higher incidence of pseudocysts in the survived group, no statistically significant difference was found compared with the deceased group. This observation must be made cautiously, because 50% (11/22) of the patients in deceased group died within 2 wk, which might be too short to develop a pseudocyst. In addition, in many patients the only complication was a pseudocyst, so they were classified as having SAP according to the Atlanta Criteria, although their clinical recovery was excellent[3]. Patients with pseudocysts may develop complications, but since it takes at least 4 wk to develop a pseudocyst, it has no effect on early mortality.

Our results did not show that age was an independent poor prognosis factor in mortality, which was consistent with previous studies, but in contradiction to other investigators[4,6,]. When deaths due to complications of acute pancreatitis were analyzed, the mortality rate was not significantly different between the young and elderly groups. Moreover, the complication rate and the proportion of patients with SAP (judged by the number of prognostic signs) were not higher in the elderly. Thus the severity of acute pancreatitis was not intrinsically due to advanced age when the influence of other secondary factors was not taken into consideration.

In conclusion, SAP patients are characterized by advanced age, high APACHE II score at admission, development of organ/systemic failure, and their death is mainly due to multiple organ/systemic failures. In SAP patients, respiratory, cardiovascular and renal failures can predict their fatal outcome and more attention should be paid to their clinical evaluation.

REFERENCES

1 **Steinberg W,** Tenner S. Acute pancreatitis. *N Engl J Med* 1994; **330**: 1198-1210

2 **Company L,** Saez J, Martinez J, Aparicio JR, Laveda R, Grino P, Perez-Mateo M. Factors predicting mortality in severe acute pancreatitis. *Pancreatology* 2003; **3**: 144-148

3 **Bradley EL.** A clinically based classification system for acute pancreatitis, 3rd. Summary of the international symposium on acute pancreatitis, Atlanta, Ga, September 11 through 13, 1992. *Arch Surg* 1993; **128**: 586-590

4 **Halonen KI,** Leppaniemi AK, Puolakkainen PA, Lundin JE, Kemppainen EA, Hietaranta AJ, Haapiainen RK. Severe acute pancreatitis: prognostic factors in 270 consecutive patients. *Pancreas* 2000; **21**: 266-271

5 **Baron TH,** Morgan DE. Acute necrotizing pancreatitis. *N Engl J Med* 1999; **340**: 1412-1417

6 **Fernandez-Cruz L,** Navarro S, Valderrama R, Saenz A, Guarner L, Aparisi L, Espi A, Jaurietta E, Marruecos L, Gener J, De Las Heras G, Perez-Mateo M, Garcia Sabrido JL, Roig J, Carballo F. Acute necrotizing pancreatitis: a multicenter study. *Hepatogastroenterology* 1994; **41**: 185-189

7 **Banks PA.** Predictors of severity in acute pancreatitis. *Pancreas* 1991; **6**: S7-12

8 **Talamini G,** Bassi C, Falconi M, Sartori N, Frulloni L, Di Francesco V, Vesentini S, Pederzoli P, Cavallini G. Risk of death from acute pancreatitis. Role of early, simple "routine" data. *Int J Pancreatol* 1996; **19**: 15-24

9 **Gotzinger P,** Wamser P, Exner R, Schwanzer E, Jakesz R, Fugger R, Sautner T. Surgical treatment of severe acute pancreatitis: timing of operation is crucial for survival. *Surg Infect* 2003; **4**: 205-211

10 **Miskovitz P.** Acute pancreatitis: further insight into mechanisms. *Crit Care Med* 1998; **26**: 816-817

11 **Isenmann R,** Rau B, Beger HG. Early severe acute pancreatitis: characteristics of a new subgroup. *Pancreas* 2001; **22**: 274-278

12 **Wilson PG,** Manji M, Neoptolemos JP. Acute pancreatitis as a model of sepsis. *J Antimicrob Chemother* 1998; **41**: 51-63

13 **McKay CJ,** Evans S, Sinclair M, Carter CR, Imrie CW. High early mortality rate from acute pancreatitis in Scotland, 1984-1995. *Br J Surg* 1999; **86**: 1302-1305

14 **Buchler MW,** Gloor B, Muller CA, Friess H, Seiler CA, Uhl W. Acute necrotizing pancreatitis: treatment strategy according to the status of infection. *Ann Surg* 2000; **232**: 619-626

15 **Gotzinger P,** Sautner T, Kriwanek S, Beckerhinn P, Barlan M, Armbruster C, Wamser P, Fugger R. Surgical treatment for severe acute pancreatitis: extent and surgical control of necrosis determine outcome. *World J Surg* 2002; **26**: 474-478

16 **Zhu AJ,** Shi JS, Sun XJ. Organ failure associated with severe acute pancreatitis. *World J Gastroenterol* 2003; **9**: 2570-2573

17 **Halonen KI**, Pettila V, Leppaniemi AK, Kemppainen EA, Puolakkainen PA, Haapiainen RK. Multiple organ dysfunction associated with severe acute pancreatitis. *Crit Care Med* 2002; **30**: 1274-1279

18 **Isenmann R,** Rau B, Beger HG. Bacterial infection and extent of necrosis are determinants of organ failure in patients with acute necrotizing pancreatitis. *Br J Surg* 1999; **86**: 1020-1024

19 **Raty S,** Sand J, Nordback I. Difference in microbes contaminating pancreatic necrosis in biliary and alcoholic pancreatitis. *Int J Pancreatol* 1998; **24**: 187-191

20 **Kemppainen E,** Sainio V, Haapiainen R, Kivisaari L, Kivilaakso E, Puolakkainen P. Early localization of necrosis by contrast-enhanced computed tomography can predict outcome in severe acute pancreatitis. *Br J Surg* 1996; **83**: 924-929

21 **McFadden DW.** Organ failure and multiple organ system failure in pancreatitis. *Pancreas* 1991; **6**(Suppl 1): S37-43

22 **de Beaux AC,** Palmer KR, Carter DC. Factors influencing morbidity and mortality in acute pancreatitis; an analysis of 279 cases. *Gut* 1995; **37**: 121-126

23 **Karimgani I,** Porter KA, Langevin RE, Banks PA. Prognostic factors in sterile pancreatic necrosis. *Gastroenterology* 1992; **103**: 1636-1640

24 **Uomo G,** Visconti M, Manes G, Calise F, Laccetti M, Rabitti PG. Nonsurgical treatment of acute necrotizing pancreatitis. *Pancreas* 1996; **12**: 142-148

25 **de Beaux AC,** Goldie AS, Ross JA, Carter DC, Fearon KC. Serum concentrations of inflammatory mediators related to organ failure in patients with acute pancreatitis. *Br J Surg* 1996; **83**: 349-353

26 **Widdison AL,** Karanjia ND. Pancreatic infection complicating acute pancreatitis. *Br J Surg* 1993; **8**: 148-154

27 **Tenner S,** Sica G, Hughes M, Noordhoek E, Feng S, Zinner M, Banks PA. Relationship of necrosis to organ failure in severe acute pancreatitis. *Gastroenterology* 1997; **113**: 899-903

28 **Lankisch PG,** Pflichthofer D, Lehnick D. No strict correlation between necrosis and organ failure in acute pancreatitis. *Pancreas* 2000; **20**: 319-322

Edited by Wang XL and Chen WW **Proofread by** Xu FM

PO Box 2345, Beijing 100023, China
Fax: +86-10-85381893
E-mail: wjg@wjgnet.com www.wjgnet.com

World J Gastroenterol 2004;10(22):3339-3341
World Journal of Gastroenterology
 ISSN 1007-9327

• BRIEF REPORTS •

A double stapled technique for oesophago-enteric anastomosis

A Kotru, A K John, E P Dewar

A Kotru, A K John, E P Dewar, Department of Surgery, Airedale General Hospital, Keighly BD20 6TD, UK
Correspondence to: A Kotru, 273-Spen Lane, West Park, Leeds LS16 5EJ, UK. ajokjohn@yahoo.com
Telephone: +44-1132288911
Received: 2004-02-11 **Accepted:** 2004-04-07

Abstract

AIM: Leakage from oesophageal anastomosis is associated with substantial morbidity and mortality. This study presented a novel, safe and effective double stapled technique for oesophago-enteric anastomosis.

METHODS: The data were obtained prospectively from hospital held clinical database. Thirty nine patients (26 males, 13 females) underwent upper-gastrointestinal resection between 1996 and 2000 for carcinoma (n = 36), gastric lymphoma (n = 1), and benign pathology (n = 2). Double stapled oesophago-enteric anastomosis was performed in all cases.

RESULTS: No anastomotic leak was reported. In cases of malignancy, the resected margins were free of neoplasm. Three deaths occurred, which were not related to anastomotic complications.

CONCLUSION: Even though the reported study is an uncontrolled one, the technique described is reliable, and effective for oesophago-enteric anastomosis.

Kotru A, John AK, Dewar EP. A double stapled technique for oesophago-enteric anastomosis. *World J Gastroenterol* 2004; 10(22): 3339-3341
http://www.wjgnet.com/1007-9327/10/3339.asp

INTRODUCTION

Leakage is a major problem associated with oesophago-enteric anastomosis. The anastomosis may be hand sewn or stapled[1-4]. Even though there is no proven advantage between either techniques, basic principles of anastomosis surgery- tension free, good vascularity, and good mucosal apposition apply to both. A technique of double stapled anastomosis avoids stretch at oesophageal side of anastomosis and circumvents damage to vascularity.

MATERIALS AND METHODS

The double stapled oesophago-enteric reconstruction was performed as follows. The oesophagus was mobilized in the standard way to above the proposed level of division. A transverse incision was made in the anterior wall of the oesophagus at least 3 cm above the proximal extent of the tumour in those cases undergoing surgery for malignancy (Figure 1). An appropriately sized circular stapler (CA Ethicon) was selected based on the oesophageal diameter. A 2-0 polypropylene suture was placed through the 'eye-hole' situated in the plastic spike that fits the head of the circular stapler. The polypropylene suture should be tied such that around 5 cm of suture with the attached needle remained attached to the spike attached to the circular stapler head. The transverse anterior oesophagotomy should be of sufficient size to allow insertion of the stapler head with attached spike - see step 7 (Figure 2). The circular stapler head with spike and attached needle were placed through the oesophagotomy into the proximal oesophagus (Figure 3). The suture needle was brought out through the anterior oesophageal wall 2 cm proximal to the oesophagotomy. The oesophagus was then cross-stapled and divided transversely below the site of needle puncture but above the oesophagotomy. The suture attached to the spike was used to pull the spike and axis of the circular stapler head through the anterior wall of the oesophagus, around 2 cm proximal to the transverse staple line (Figure 4). The spike was then removed from the stapler head. Resection of the gastric or oesophago-gastric specimen was then completed. The distal conduit (either distal stomach or jejunal limb) was prepared and mobilized to allow a tension free anastomosis. The body of the circular stapler was introduced into the lumen of the efferent conduit through an appropriately placed enterotomy (Figure 5). The circular stapler head was engaged with the body of the circular stapler gun. The gun was closed and fired creating a double stapled oesophago-enteric anastomosis (Figure 5). A naso-gastric tube was fed across the oesophago-enterostomy after completion of the anastomosis.

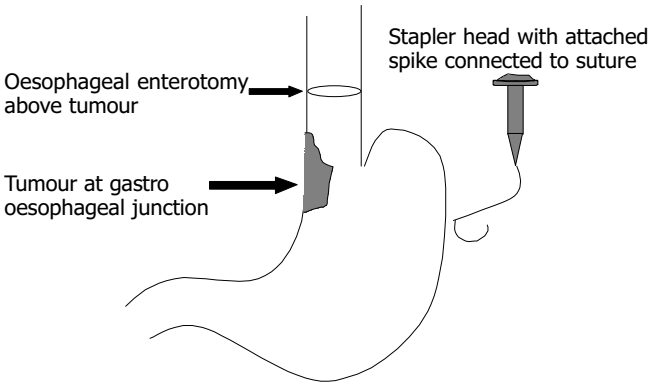

Figure 1 Transverse incision in anterior wall of oesophagus.

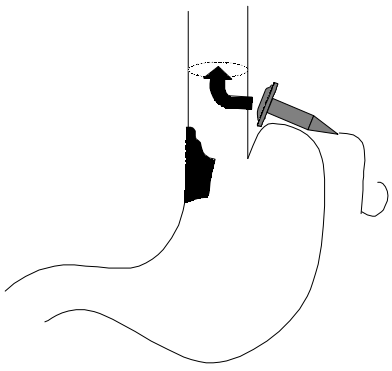

Figure 2 Transverse anterior oesophagotomy. Stapler head spike with attached needle inserted through oesophagotomy into proximal oesophagus.

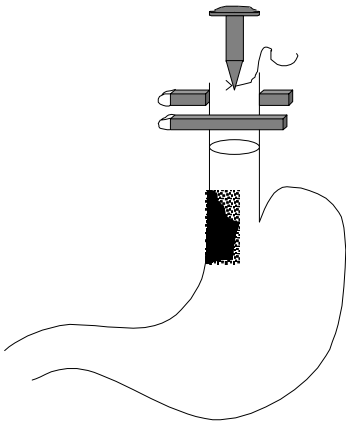

Figure 3 Placement of a circular stapler head with spike and attached needle. Needle was used to puncture anterior oesophagus -2 cm above the oesophagotomy. The oesophagus was then cross- stapled between the needle puncture site & the oesophagotomy.

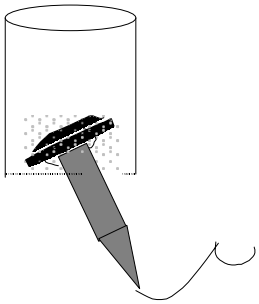

Figure 4 Suture used to drive head spike through oesophageal wall above transverse suture line.

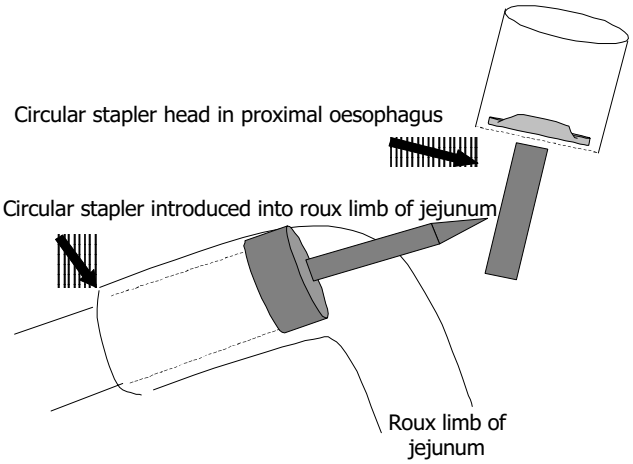

Figure 5 Introduction of the circular stapler body into the lumen of efferent conduit.

RESULTS

All patients were operated on by or under the direct supervision of a consultant surgeon with an upper gastrointestinal interest. Patients with malignancy underwent pre-operative staging with thoraco-abdominal computed tomography scan. Laparoscopy was used in selected instances. In elective cases, mechanical bowel preparation was employed. Thoracic epidural anaesthesia was employed for post-operative pain relief. Patients were kept nil by mouth for 5 d post-operatively. If the post-operative course was uneventful, fluids were introduced on d 5. Water soluble contrast studies were not routinely used to assess anastomotic integrity unless there was clinical indication.

Data were obtained prospectively from the hospital-held clinical database.

Thirty-nine patients (26 males, 13 females) underwent upper gastrointestinal resection (total gastrectomy $n = 24$, Ivor -Lewis oesophago-gastrectomy $n = 15$) between 1996 and 2000. Indication for surgery was carcinoma ($n = 36$), gastric non-Hodgkin's lymphoma ($n = 1$), revision of a neo-gastric jejunal pouch ($n = 1$), gastric infarction secondary to volvulus ($n = 1$). The median age was 67 (36-82) years. Patient ASA grades were: ASA-1 $n = 12$, ASA- 2 $n = 14$, ASA- 3 $n = 9$, ASA- 4 $n = 3$, ASA- 5 $n = 1$. The median operative time for total gastrectomy was 175 (120-240) min and was 240 (180-360) min for Ivor-Lewis oesophago-gastrectomy. The median transfusion requirements were 2 (0-7) units for both procedures. The resection margins were free of tumour on histopathological examination in all cases of malignancy.

Morbidity and mortality rates are shown below (Tables 1-3). Risk adjusted morbidity and mortality rates were calculated using the physiological and operative scoring system for enumeration of morbidity and mortality (POSSUM) and Portsmouth POSSUM (P-POSSUM) models[5,6].

Table 1 Morbidity and mortality of oesophago-gastrectomy (*n*, %)

	Total patients ($n = 15$)	POSSUM prediction	P-POSSUM prediction
Morbidity	5 (33)	63	-
Mortality	2 (14)	18	6

Table 2 Morbidity and mortality of total gastrectomy (*n*, %)

	Total patients ($n = 15$)	POSSUM prediction	P-POSSUM prediction
Morbidity	6 (25)	48	-
Mortality	1 (4)	16	9

Table 3 Analysis of morbidity

	Oesophagogastrectomy (*n*)	Total gastrectomy (*n*)
Chest infection	2	5
Chylothorax	1	-
DVT/PE	1	1
Anastomotic leak	-	-
Wound sepsis	1	-

Three deaths occurred, two post oesophago-gastrectomy and one post total gastrectomy. The deaths after oesophago-gastrectomy were shown at post-mortem to be due to left ventricular failure and myocardial infarction respectively. The patient who died after total gastrectomy deteriorated suddenly on the 10th post-operative day tolerated diet for three days. Symptoms, blood gases and electrocardiogram were compatible with a pulmonary embolus. Permission for a post-mortem was refused. No anastomotic leaks occurred on clinical grounds.

DISCUSSION

Anastomotic leakage following oesophago-enteric reconstruction may result in significant morbidity and mortality. The standard principles governing any gastro-intestinal anastomosis apply in dealing with the oesophagus. The anastomosis should be tension-free, well vascularized and there should be accurate mucosal apposition. Oesophageal anastomoses may be hand sewn (in one, two or even three layers) or stapled[1-4]. There is no proven advantage to either the hand sewn or stapled technique.

Stapled anastomoses might be associated with a higher rate of subsequent benign stricture formation[7]. The stapled technique that is commonly used requires a purse string suture in the cut end of the proximal oesophagus to retain the head of the circular stapler. The anastomosis is completed by a single firing of the circular stapler.

It is the authors' contention that the oesophageal purse string may be a contributory factor to subsequent anastomotic related complications (leak and stricture). This is based on the observation that the distal oesophagus is stretched over the head of the circular stapler, and therefore possibly devascularized by the purse string suture. To avoid the use of a purse string, a double stapled oesophago-enteric anastomotic technique has been devised.

This paper described a novel technique of oesophago-enteric anastomosis using a double stapled technique. Whilst this was an uncontrolled study, the technique has proved reliable and to date has not resulted in any anastomotic leaks. Whilst this study cannot implicate the use of a proximal oesophageal purse string suture as a factor in anastomotic leakage, it is interesting to speculate whether the double stapled anastomosis does allow improved anastomotic healing through omission of a purse string suture. The technique described merits further evaluation either in the setting of a larger uncontrolled study or more preferably in the context of a randomised trial.

REFERENCES

1 **Skinner DB**. Oesophageal reconstruction. *Am J Surg* 1980; **139**: 810-814
2 **Akiyama H**. Surgery for cancer of the oesophagus. Baltimore: *Williams Wilkins* 1990: 74-75
3 **Sweep RH**. Thoracic surgery. Philadelphia, London: *WB Saunders* 1950: 256-294
4 **Griffin SM**, Raimes SA. Upper gastrointestinal surgery. London, Philadelphia, Toronto, Sydney, Tokyo: *WB Saunders* 1997: 111-144
5 **Copeland GP**, Jones D, Walters M. POSSUM: A scoring system for surgical audit. *Br J Surg* 1991; **78**: 355- 360
6 **Prytherch DR**, Whiteley MS, Higgins B, Weaver PC, Prout WG, Powell SJ. POSSUM and Portsmouth POSSUM for predicitng mortality. Physiological and Operative Severity Score for the enUmeration of Mortality and Morbidity. *Br J Surg* 1998; **85**: 1217-1220
7 **Bardini R**, Asolati M, Ruol A, Bonavina L, Baseggio S, Peracchia A. Anastomosis. *World J Surg* 1994; **18**: 373- 378

Edited by Wang XL **Proofread by** Xu FM

PO Box 2345, Beijing 100023, China
Fax: +86-10-85381893
E-mail: wjg@wjgnet.com www.wjgnet.com

World J Gastroenterol 2004;10(22):3342-3344
World Journal of Gastroenterology
 ISSN 1007-9327

• BRIEF REPORTS •

Helicobacter pylori seroprevalence in patients with lung cancer

Nikiphoros Philippou, Panagiotis Koursarakos, Evgenia Anastasakou, Vasiliki Krietsepi, Stavroula Mavrea, Anastasios Roussos, Dionissia Alepopoulou, Irineos Iliopoulos

Nikiphoros Philippou, Panagiotis Koursarakos, Vasiliki Krietsepi, Anastasios Roussos, Irineos Iliopoulos, 9th Department of Pulmonary Medicine, "SOTIRIA" Chest Diseases Hospital, Athens, Greece
Evgenia Anastasakou, Stavroula Mavrea, Dionissia Alepopoulou, Section of Immunology and Infectious Diseases, "SOTIRIA" Chest Diseases Hospital, Athens, Greece
Correspondence to: Dr. Nikiphoros Philippou, 9th Department of Pulmonary Medicine, "SOTIRIA" Chest Diseases Hospital, 152 Mesogion Street, PO Box 11527, Athens, Greece. roumar26@yahoo.com
Telephone: +301-210-8646215 **Fax:** +301-210-8646215
Received: 2003-08-02 **Accepted:** 2003-09-12

Abstract

AIM: To assess *Helicobacter pylori* (*H pylori*) seroprevalence in a cohort of Greek patients with lung cancer.

METHODS: Seventy-two lung cancer patients (55 males and 17 females, aged 58.2±11.7 years) and 68, age and gender-matched, control subjects were enrolled. All subjects underwent an enzyme-linked immunosorbent assay IgG serologic test for *H pylori* diagnosis.

RESULTS: A correlation between age and *H pylori* IgG level was detected for both lung cancer patients ($r = 0.42$, $P = 0.004$) and controls ($r = 0.44$, $P = 0.004$). Seropositivity for *H pylori* did not differ significantly between patients with lung cancer and controls (61.1% *vs* 55.9%, $P>0.05$). Concerning the mean serum concentration of IgG antibodies against *H pylori*, no significant difference between the two groups was detected (32.6±19.1 *vs* 27.4±18.3 U/mL, $P>0.05$).

CONCLUSION: No significant association between *H pylori* infection and lung cancer was found.

Philippou N, Koursarakos P, Anastasakou E, Krietsepi V, Mavrea S, Roussos A, Alepopoulou D, Iliopoulos I. *Helicobacter pylori* seroprevalence in patients with lung cancer. *World J Gastroenterol* 2004; 10(22): 3342-3344
http://www.wjgnet.com/1007-9327/10/3342.asp

INTRODUCTION

Helicobacter pylori (*H pylori*) infection of the gastric mucosa affects approximately 50% of the world's population[1]. It seems to be the main cause of chronic antral gastritis[2] and is strongly associated with peptic ulcer disease[3], gastric cancer[4], and gastric MALT-lymphoma[5]. In the past few years, a variety of extradigestive disorders, including cardiovascular, skin, rheumatic and liver diseases, have also been associated with *H pylori* infection[6,7]. As regards respiratory diseases, an increased *H pylori* seroprevalence has been found in active bronchiectasis[8], chronic bronchitis[9,10] and active pulmonary tuberculosis[11]. The activation of inflammatory mediators by *H pylori* seems to be the common pathogenetic mechanism underlying the observed associations[12].

It is well known that the prevalence of lung cancer in peptic ulcer patients is increased 2 to 3 fold compared with findings in ulcer-free controls[13-18]. The major factor underlying this association seems to be the impact of cigarette smoking on both diseases. However, a recent pilot study, in a small number of patients, showed that *H pylori* infection, *per se*, might be implicated in lung cancerogenesis[19]. It suggested that the prolonged release of gastrin and cyclooxygenase (COX)-2 in *H pylori* infected patients might account for the stimulation of lung cancer growth and tumor neoangiogenesis[19]. However, insufficient information is available on the prevalence of *H pylori* infection in lung cancer patients.

Therefore, in order to further investigate the relationship between *H pylori* infection and lung cancer, we assessed *H pylori* seroprevalence in a cohort of Greek patients with lung cancer and control subjects.

MATERIALS AND METHODS

Study subjects

The present study was conducted at the 9th Department of Pulmonary Medicine, "Sotiria" Chest Diseases Hospital (Athens, Greece). The local ethics committee approved the study and written informed consent was obtained from each participant. Following a predefined protocol, between March 1, 2002 and April 30, 2001, 104 consecutive patients with, histologically verified, primary lung cancer were recruited from our department. Exclusion criteria were: (1) prior *Helicobacter* eradication therapy, (2) consumption of acid suppressive drugs or antibiotics in the preceding 6 mo and (3) a history of vagotomy or operations of the upper gastrointestinal tract. A total of 32 patients were excluded. Therefore, 72 patients were eligible for analysis.

Controls were selected randomly from subjects who attended courses designed for public health education during the period of the study. Exclusion criteria for controls were: (1) a known history of lung cancer and (2) a known history of gastrointestinal tract pathology. Finally, we selected 68 controls out of 99 healthy subjects and we matched them with the patients for sex, age (within 2 years) and socioeconomic status.

Methods

All subjects enrolled (lung cancer patients and controls) underwent an enzyme-linked immunosorbent assay (ELISA) IgG serologic test for *H pylori* diagnosis (HEL-P test, Park Co, Athens, Greece), in accordance with the manufacturer's guidelines. A positive, borderline or negative result was assigned when the concentration of IgG antibodies against *H pylori* was greater than 25, between 20 and 25 and less than 20 U/mL respectively. The specificity and sensitivity of the serology test, validated in our local population, were 95% and 85% respectively.

Statistical analysis

Results are expressed as mean±SD. Significance of difference between groups was assessed by unpaired Student's *t*-test for continuous variables and χ^2-test for proportions. Correlation coefficients between variables were determined using conventional

Pearson's correlation analysis. Statistical analysis was performed using SPSS program (SPSS Inc, IL, USA) and *P*-values were two-tailed analyzed. *P* less than 0.05 was considered statistically significant.

RESULTS

The demographic data of both patients and controls are shown in Table 1. There was no statistical difference in age or gender between the two groups. The majority of lung cancer patients were current cigarette smokers (60 patients, 83.3%) or ex-smokers (10 patients, 13.9%) and only 2 patients (2.8%) had never smoked. On the other hand, 40 out of 68 control subjects (58.8%) were never-smokers, 20 (29,4%) were current and 8 (11.8%) were previous smokers.

A correlation between age and *H pylori* IgG level was detected for both lung cancer patients ($r = 0.42$, $P = 0.004$) and controls ($r = 0.44$, $P = 0.004$). Among the lung cancer patients, 44 (61.1%) were anti-*H pylori* IgG positive, 2 (2.8%) had borderline values and 26 (36.1%) were seronegatives. Of the control subjects 38 (55.9%) were anti-*H pylori* IgG positive, 2 (2.9%) were borderline and 28 (41.2%) were seronegatives.

H pylori seropositivity did not differ significantly between patients with lung cancer and controls ($P>0.05$) (Table 1). Concerning the mean serum concentration of IgG antibodies against *H pylori* no significant difference between the two groups was detected ($P>0.05$).

Table 1 Demographic data and *H pylori* serologic parameters

Parameter	Control ($n = 68$)	Lung cancer ($n = 72$)	*P*
Age (yr)	54.8±12.1	58.2±11.7	0.79
Male gender (%)	73.5	76.3	0.88
H pylori IgG level (U / mL)	27.4±18.3	32.6±19.1	0.18
H pylori IgG seropositivity (%)	55.9	61.1	0.23

DISCUSSION

Data in literature on the relationship between *H pylori* infection and lung cancer are poor. Recently, Gocyk *et al*. carried out a pilot study in a sample of 50 Polish patients with lung cancer and showed an increased *H pylori* seroprevalence (89%). Moreover, they proposed that the seropositive patients might be considered for *H pylori* eradication in order to reduce the hypergastrinemia and COX-2 expression[19], provoked by this bacterium. As both overexpression of COX-2 in lung tissue[20-22] and increased serum levels of gastrin[23] have been reported in lung cancer patients, a pathogenetic link between *H pylori* infection and lung cancer seems to exist.

Our study is the first one focusing on seroprevalence of *H pylori*, in a relatively large population of Greek patients with lung cancer. According to our results, *H pylori* seroprevalence in lung cancer patients did not differ significantly from that of the control subjects. The age-related pattern of infection, which in our study was detected for both lung cancer patients and controls, was common in developed countries and explained by the cohort effect[24]. The socioeconomic status, which was related with both *H pylori* infection and risk of lung cancer, was similar between the two groups. Tobacco use could be another confounding factor. Cigarette smoking was the most important etiologic factor of lung cancer and seemed to fully account for the, observed in previous studies, association between peptic ulcer and lung cancer[13-18]. However, data on the relationship between *H pylori* infection and smoking habits are controversial. The prevalence of *H pylori* infection in smokers has been variously reported as low[25], normal[26], and high[27]. In the present study, we did not match patients with control subjects in smoking habits. As the relation between smoking and *H pylori* infection has not been clarified yet, the possible impact of cigarette smoking on both lung cancer and *H pylori* infection should be regarded as a potential study limitation.

The present study did not focus on the potential pathogenetic mechanisms underlying a possible association between *H pylori* infection and chronic bronchitis. This association might reflect either susceptibility induced by common factors or a kind of causal relationship between these diseases. As far as we know, there are no common factors implicated in the susceptibility to both lung cancer and *H pylori* infection. However, we can not rule out this possibility, as the predisposing conditions to *H pylori* infection have not been clarified yet. With regard to the aetio-pathogenetic role of *H pylori* infection in lung cancer development, it has been suggested that the prolonged release of gastrin and cyclooxygenase (COX)-2 in *H pylori* infected patients might stimulate lung cancer growth and lead to tumor neoangiogenesis[19]. The spilling or inhalation of *H pylori* or its exotoxins into the respiratory tract might also lead to their accumulation in lung tissue. However, as far as we know, neither identification of *H pylori* species in human bronchial tissue, nor isolation of *H pylori* from bronchoalveolar lavage (BAL) fluid has been achieved yet[24]. Studies estimating the relative risk of developing lung cancer for *H pylori* infected patients and the effect of *H pylori* eradication on the natural history of chronic bronchitis are also needed to further investigate these hypotheses.

In conclusion, the present study suggests that *H pylori* seroprevalence in lung cancer patients did not differ significantly from that of control subjects. Our results should be confirmed in a larger number of patients. Further studies are needed to clarify the pathogenetic mechanisms, if those exist, underlying a possible association between these two diseases.

REFERENCES

1 **Mitchell H,** Megraud F. Epidemiology and diagnosis of *Helicobacter pylori* infection. *Helicobacter* 2002; **7**(Suppl 1): 8-16
2 **Cave DR.** Chronic gastritis and *Helicobacter pylori*. *Semin Gastrointestinal Dis* 2001; **12:** 196-202
3 **Cohen H.** Peptic ulcer and *Helicobacter pylori*. *Gastroenterol Clin North Am* 2000; **29**: 775-789
4 **Eslick GD,** Lim LL, Byles JE, Xia HH, Taley NJ. Association of *Helicobacter pylori* infection with gastric carcinoma: a meta-analysis. *Am J Gastroenterol* 1999; **13:** 1295-1302
5 **Parsonnet J,** Hansen S, Rodriguez L, Gelb AB, Warnke RA, Jellum E, Orentreich N, Vogelman JH, Friedman GD. *Helicobacter pylori* and gastric lymphoma. *N Engl J Med* 1994; **330:** 1267–1271
6 **Realdi G,** Dore MP, Fastame L. Extradigestive manifestations of *Helicobacter pylori* infection. Fact and fiction. *Dig Dis Sci* 1999; **44:** 229-236
7 **Gasbarrini A,** Franceschi F, Armuzzi A, Ojetti V, Candelli M, Sanz Torre E, Lorenzo AD, Anti M, Pretolani S, Gasbarinni G. Extradigestive manifestations of *Helicobacter pylori* gastric infection. *Gut* 1999; **45**(Suppl 1): 9-12
8 **Tsang KW,** Lam SK, Lam WK, Karlberg J, Wong BC, Yew WW, Ip MS. High seroprevalence of *Helicobacter pylori* in active bronchiectasis. *Am J Resp Crit Care Med* 1998; **158:** 1047-1051
9 **Gaselli M,** Zaffoni E, Ruina M, Sartori S, Trevisani L, Ciaccia A, Alvisi V, Fabbri L, Papi A. *Helicobacter pylori* and chronic bronchitis. *Scand J Gastroenterol* 1999; **34:** 828-830
10 **Roussos A**, Tsimpoukas F, Anastasakou E, Alepopoulou D, Paizis I, Philippou N. *Helicobacter pylori* seroprevalence in patients with chronic bronchitis. *J Gastroenterol* 2002; **37:** 332-335
11 **Filippou N,** Roussos A, Tsimboukas F, Tsimogianni A, Anastasakou E, Mavrea S. *Helicobacter pylori* seroprevalence in patients with pulmonary tuberculosis. *J Clin Gastroenterol* 2002; **34:** 189

12 **Roussos A,** Philippou N, Gourgoulianis KI. *Helicobacter pylori* infection and respiratory diseases: a review. *World J Gastroenterol* 2003; **9:** 5-8
13 **Viskum K**. Peptic ulcer and pulmonary disease. *Scand J Respir Dis* 1974; **55:** 284-290
14 **Bonnevie O**. Causes of death in duodenal and gastric ulcer. *Gastroenterology* 1977; **73:** 1000-1004
15 **Hole DJ,** Quigley EM, Gillis CR, Watkinson G. Peptic ulcer and cancer. *Scand J Gastroenterol* 1987; **22:** 17-23
16 **Moller H,** Toftgaard C. Cancer occurrence in a cohort of patients surgically treated for peptic ulcer. *Gut* 1991; **32:** 740-744
17 **Caygill CP,** Knowles RL, Hall R. Increased risk of cancer mortality after vagotomy for peptic ulcer: a preliminary analysis. *Eur J Cancer Prev* 1991; **1:** 35-37
18 **Svanes C,** Lie SA, Lie RT, Soreide O, Svanes K. Causes of death in patients with peptic ulcer perforation: a long-term follow-up study. *Scand J Gastroenterol* 1999; **34:** 18-24
19 **Gocyk W,** Niklinski T, Olechnowicz H, Duda A, Bielanski W, Konturek PC, Konturek SJ. *Helicobacter pylori*, gastrin and cyclooxygenase-2 in lung cancer. *Med Sci Monit* 2000; **6:** 1085-1092
20 **Koki A,** Khan NK, Woerner BM. Cyclooxygenase-2 in human pathological disease. *Adv Exp Med Biol* 2002; **507:** 177-184
21 **Ermert L,** Dierkes C, Ermert M. Immunohistochemical expression of cyclooxygenase isoenzymes and downstream enzymes in human lung tumors. *Clin Cancer Res* 2003; **9:** 1604-1610
22 **Fang HY,** Lin TS, Lin JP, Wu YC, Chow KC, Wang LS. Cyclooxygenase-2 in human non-small cell lung cancer. *Eur J Surg Oncol* 2003; **29:** 171-177
23 **Zhou Q,** Zhang H, Pang X, Yang J, Tain Z, Wu Z, Yang Z. Pre- and postoperative sequential study on the serum gastrin level in patients with lung cancer. *J Surg Oncol* 1992; **51:** 22-25
24 **Peterson WL,** Graham DY. *Helicobacter pylori.* In: Feldman M, Scharschmidt BF, Sleisenger MH, eds. Gastrointestinal and liver Disease. Pathophysiology, Diagnosis, Management. 6th ed. Philadelphia: *WB Saunders* 1998: 604–619
25 **Ogihara A,** Kikuchi S, Hasegawa A, Kurosawa M, Miki K, Kaneko E. Relationship between *Helicobacter pylori* infection and smoking and drinking habits. *J Gastroenterol Hepatol* 2000; **15:** 271-276
26 **Brenner H,** Rothenbacher D, Bode G, Adler G. Relation of smoking and alcohol and coffee consumption to active *Helicobacter pylori* infection: cross sectional study. *BMJ* 1997; **315:** 1489-1492
27 **Parasher G,** Eastwood GL. Smoking and peptic ulcer in the *Helicobacter pylori* era. *Eur J Gastroenterol Hepatol* 2000; **12:** 843-853

Edited by Chen WW and Zhu LH **Proofread by** Xu FM

PO Box 2345, Beijing 100023, China
Fax: +86-10-85381893
E-mail: wjg@wjgnet.com www.wjgnet.com

World J Gastroenterol 2004;10(22):3345-3348
World Journal of Gastroenterology
 ISSN 1007-9327

• BRIEF REPORTS •

Patients with brain metastases from gastrointestinal tract cancer treated with whole brain radiation therapy: Prognostic factors and survival

Susanne Bartelt, Felix Momm, Christian Weissenberger, Johannes Lutterbach

Susanne Bartelt, Department of Radiation Oncology, University of Freiburg, Freiburg i. Br., Germany
Felix Momm, Department of Radiation Oncology, University of Freiburg, Freiburg i. Br., Germany
Christian Weissenberger, Department of Radiation Oncology, University of Freiburg, Freiburg i. Br., Germany
Johannes Lutterbach, Department of Radiation Oncology, University of Freiburg, Freiburg i. Br., Germany
Correspondence to: Susanne Bartelt, M.D., Radiologische Universitätsklinik, Abteilung Strahlenheilkunde, Robert-Koch Strasse 3, 79106 Freiburg, Germany. bartelt@mst1.ukl.uni-freiburg.de
Telephone: +49-761-270-9462 **Fax:** +49-761-270-9582
Received: 2004-02-27 **Accepted:** 2004-04-14

Abstract

AIM: To identify the prognostic factors with regard to survival for patients with brain metastasis from primary tumors of the gastrointestinal tract.

METHODS: Nine hundred and sixteen patients with brain metastases, treated with whole brain radiation therapy (WBRT) between January 1985 and December 2000 at the Department of Radiation Oncology, University Hospital Freiburg, were analyzed retrospectively.

RESULTS: Fifty-seven patients presented with a primary tumor of the gastrointestinal tract (esophagus: $n = 0$, stomach: $n = 10$, colorectal: $n = 47$). Twenty-six patients had a solitary brain metastasis, 31 patients presented with multiple brain metastases. Surgical resection was performed in 25 patients. WBRT was applied with daily fractions of 2 Gray (Gy) or 3 Gy to a total dose of 50 Gy or 30 Gy, respectively. The interval between diagnoses of the primary tumors and brain metastases was 22.6 mo *vs* 8.0 mo for patients with primary tumors of the colon/rectum *vs* other primary tumors, respectively ($P<0.01$, log-rank). Median overall survival for all patients with brain metastases ($n = 916$) was 3.4 mo and 3.2 mo for patients with gastrointestinal neoplasms. Patients with gastrointestinal primary tumors presented significantly more often with a solitary brain metastasis than patients with other primary tumors ($P<0.05$, log-rank). In patients with gastrointestinal neoplasms ($n = 57$), the median overall survival was 5.8 mo for patients with solitary brain metastasis *vs* 2.7 mo for patients with multiple brain metastases ($P<0.01$, log-rank). The median overall survival for patients with a Karnofsky performance status (KPS) $\geqslant 70$ was 5.5 mo *vs* 2.1 mo for patients with KPS <70 ($P<0.01$, log-rank). At multivariate analysis (Cox Model) the performance status and the number of brain metastases were identified as independent prognostic factors for overall survival.

CONCLUSION: Brain metastases occur late in the course of gastrointestinal tumors. Pretherapeutic variables like KPS and the number of brain metastases have a profound influence on treatment outcome.

Bartelt S, Momm F, Weissenberger C, Lutterbach J. Patients with brain metastases from gastrointestinal tract cancer treated with whole brain radiation therapy: Prognostic factors and survival. *World J Gastroenterol* 2004; 10(22): 3345-3348
http://www.wjgnet.com/1007-9327/10/3345.asp

INTRODUCTION

The metastatic dissemination of a solid tumor to the brain is generally associated with a poor prognosis[1]. The most common primary tumors metastasizing to the brain are breast and lung cancer, whereas patients with other primary tumors, e.g. tumors of the gastrointestinal tract, rarely present with brain metastases[2-4]. Furthermore, within the group of gastrointestinal tumors, the incidence of brain metastases shows notable differences. They are extremely rare in esophageal tumors[5,6], but more common in rectal cancer. Few literatures concerning this group of patients are available and therefore prognosis and hence treatment strategies remain controversial.

We retrospectively evaluated patient-, tumor- and treatment-related variables in patients with brain metastases of primary tumors of the gastrointestinal tract (i.e. epithelial tumors of the esophagus, stomach, colon, sigma, and rectum) who were treated with whole brain radiation therapy (WBRT) at our institution. The aim of the study was to identify the prognostic factors with regard to the endpoint survival.

MATERIALS AND METHODS

The records of all patients with brain metastases, who were treated with WBRT at our institution between January 1985 and December 2000, were analyzed retrospectively. Brain metastases were detected by contrast-enhanced cerebral computed tomography (CT) ($n = 43$) or magnetic resonance imaging (MRI) ($n = 14$).

WBRT was performed in 16 patients with cobalt^{60} gamma rays, and in 41 patients with 6 MV photons of a linear accelerator. During the study period two fractionation schemes were used: conventional fractionation with daily fractions of 2 Gray (Gy), five days per week to a planned total dose of 50 Gy ($n = 42$) and since 1997 hypofractionation with daily fractions of 3 Gy, five days per wk to a planned total dose of 30 Gy ($n = 15$). None of the patients underwent a chemotherapy during WBRT.

The recursive partitioning analysis (RPA) was used to classify the patients with brain metastases[7]. Class I contained all patients with a Karnofsky performance status (KPS $\geqslant 70$, age < 65 years, a controlled primary tumor and no extracerebral metastases), Class III contained all patients with a KPS <70, and Class II contained all other patients.

All patients alive at the time of analysis were censored with the date of last follow-up. The endpoint of the study was overall survival. Survival was calculated from the first day of radiotherapy using the method of Kaplan and Meier. Survival curves were compared using the log-rank test. All factors with a P-value $\leqslant 0.1$ at univariate analysis were entered into a multivariate analysis using the proportional hazards model.

RESULTS

Patient characteristics

Fifty-seven (6.2%) of the 916 patients presented with brain metastases from a cancer of the gastrointestinal tract. The exact localization of the primary tumor is shown in Table 1. None of the patients had an esophageal tumor, the most common primary site was rectum ($n = 24$) and colon/sigma ($n = 23$). In all patients, histology obtained either from the primary tumor, brain metastases or from extracerebral metastases, was adenocarcinoma.

Table 1 Site of primary tumor within gastrointestinal tract[1]

Site of primary tumor	*n* (%)
Esophagus	0 (0)
Stomach	10 (17.5)
Colon	17 (30)
Sigma	6 (10.5)
Rectum	24 (42)

[1]Esophagus, stomach, colon, sigma, rectum.

Thirty patients were males, 27 females. Their median age at diagnosis was 65 years (range: 30-80 years). Twenty-nine patients (51%) had a KPS $\geqslant$70. Twenty-six patients (46%) had a solitary brain metastasis, 31 (54%) had multiple lesions. Location of the metastases is shown in Table 2. Gross total resection was performed in 25 patients (19 patients with single metastasis, six patients with multiple metastases).

Table 2 Location of brain metastases

Location	*n* (%)
Single lesion	26 (100)
Frontal	4 (15)
Temporal	1 (4)
Parietal	6 (23)
Occipital	1 (4)
Cerebellum	14 (54)
Brainstem	0 (0)
Multiple lesions	31(100)
Supratentorial	20 (64)
Infratentorial	3 (10)
Both	5 (16)
Unknown	3 (10)

All patients presented with extracerebral metastases, mostly of the lung and/or the liver. Grouped according to the RPA classes, none of the patients met the criteria for class I. Twenty-nine patients (51%) met the criteria for class II. Twenty-eight patients (49%) presented with a KPS <70, and therefore belonged to RPA class III.

Patients with a primary tumor of the gastrointestinal tract presented with a solitary brain metastasis significantly more often (46%) than patients with other primary tumors (30%) ($P < 0.05$, χ^2). In patients with a primary tumor of the gastrointestinal tract, 25% (14 of 43 patients) had a solitary metastasis localized in the cerebellum, whereas the localization of solitary metastases in the cerebellum in patients with other primary tumors was 5% (42 of 805 patients). This difference was statistically significant (P<0.01). Other locations of brain metastases were not significantly different between these two groups.

The time from the diagnosis of primary tumors to the diagnosis of brain metastases was 16.3 mo, 27 mo, and 20 mo in patients with gastric carcinoma, colon carcinoma , and rectum carcinoma, respectively, and showed no statistically significant difference. Compared with patients with other primary tumors, patients with primary tumors of the colon/rectum had a significant longer interval between the diagnoses of primary tumors and brain metastases (22.6 mo *vs* 8.0 mo, respectively, P<0.01).

Survival data

The median overall survival (OS) time for patients with a primary tumor of the gastrointestinal system was 3.2 mo and showed no significant difference compared to the overall survival time of 3.5 mo for patients with brain metastases and other primary tumors (Figure 1). OS rate for patients with gastrointestinal tumors was 49%, 30%, and 7%, at 3, 6, and 12 mo, respectively. Within the group of gastrointestinal tumors, patients with a primary tumor of the stomach, colon/sigma, and rectum had a median OS time of 2.7, 5.2, and 3.2 mo, respectively. This was not a statistically significant difference.

Prognostic factors

The potential prognostic factors tested for significance in univariate analysis were sex, age ($\geqslant$/< 65 years), pretherapeutic performance status (KPS $\geqslant$/< 70), number (single *vs* multiple) and distribution of brain metastases (Table 2), extracerebral tumor activity (yes *vs* no), resection status (operation yes *vs* no), and fractionation scheme (conventional fractionation *vs* hypofractionation). The fractionation scheme (2 Gy daily, 50 Gy total dose *vs* 3 Gy daily, 30 Gy total dose) showed no statistical significance for OS.

Three factors had a P-value $\leqslant$0.1 in univariate analysis and were entered into multivariate analysis: pretherapeutic performance status, number of brain metastases, and resection status. Concerning the OS, patients with a KPS $\geqslant$70 had a median OS time of 5.5 mo *vs* 2.1 mo for patients with a KPS < 70 (P<0.01) (Figure 2). The same values were found by comparing the patients in RPA class II *vs* RPA class III. The median OS time for patients with a solitary metastasis was 5.8 mo and 2.7 mo for patients with multiple metastases (P<0.01) (Figure 3). The median OS time for patients with resection of brain metastasis was 6.6 mo and 2.7 mo for patients without resection (P<0.01).

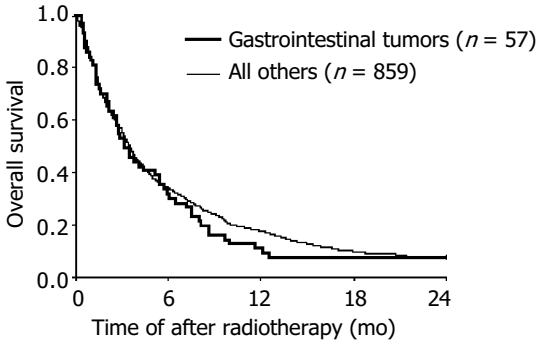

Figure 1 Overall survival according to primary tumor.

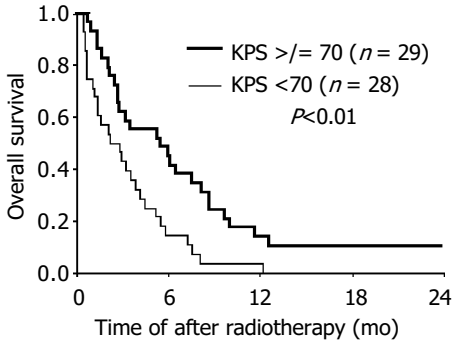

Figure 2 Overall survival according to KPS ($\geqslant$70 *vs* <70).

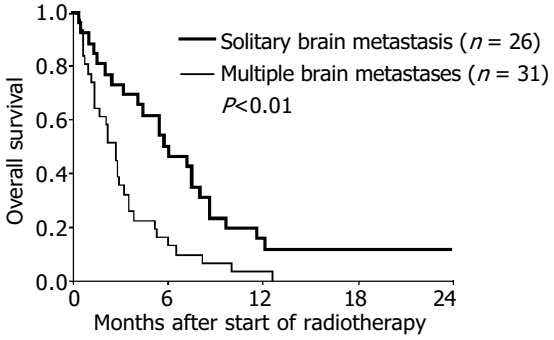

Figure 3 Overall survival according to the number of brain metastases (solitary *vs* multiple).

In the first multivariate model limited to pretherapeutic variables, the number of brain metastases (single *vs* multiple, relative risk [RR] 0.63, 95% confidence interval [KI] 0.45-0.88) and the KPS ($\geqslant$70 *vs* <70, RR 0.59, 95% KI 0.42-0.82) turned out to be independent prognostic factors. In the second multivariate analysis we added the therapeutic variable 'resection'. The KPS and the number of brain metastases were still independent prognostic factors (RR 0.59, 95% KI 0.43-0.79, P<0.01 and RR 0.65, 95% KI 0.45-0.90, P<0.05 respectively), whereas resection status was not a prognostic factor.

DISCUSSION

In our series, 6.2 % of the patients treated with WBRT presented with a primary tumor located in the gastrointestinal tract. None of the 916 patients had a primary esophageal carcinoma. Brain metastases from esophageal carcinoma were extremely rare, with a reported incidences of approximately 1-5% in autopsy series[8,9], and approximately 1-4% in clinical series[5,6,10,11].

In ten patients the primary tumor was a gastric carcinoma. The majority of publications on brain metastases from gastric carcinoma were case reports[12]. Two large studies found 0.7% of 3 320 patients, and 0.16% of 8 080 patients with gastric carcinoma to have brain metastases[13,14]. In an autopsy series by Poser and Chernik, 5 of 46 patients (10.8%) with gastric carcinoma had brain metastases[2]. The rarity of brain metastases both from esophageal and gastric cancer might result from the grim prognosis of these tumor entities[15]. In esophageal cancer, brain metastases tended to occur in patients with large primary tumors[5], usually implicating a short overall OS time. The low incidence in clinical trials might further result from an inadequate diagnostic evaluation, and symptoms indicating brain pressure like nausea and vomiting might be attributed to the primary tumor[14]. The reason for the relatively high incidence of brain metastases from gastric cancer in our group is not clear. Gastric carcinoma is rare in Europe compared to Asian countries. In half of our patients gastric carcinoma was a gastric cardia carcinoma, and recent studies suggested, that they were distinct from adenocarcinomas of the esophagus and stomach regarding epidemiological and biological factors[16-18]. These differences could possibly be associated with other pathways of metastatic spread, resulting in a relatively higher incidence of brain metastases.

Forty-seven patients had a primary colorectal carcinoma. The incidence of brain metastases in colorectal cancer ranged 2-10% in clinical studies[19-21]. As observed in other studies[14,21,22], the majority of primary tumors in our patients were located in the distal parts of the colon, i.e. sigma and rectum (64%). Significantly more patients with colorectal primary tumors presented with cerebellar metastases compared to patients with other primary tumors (25% *vs* 5%, respectively, P<0.01). Studies by Wronski and Alden confirmed this finding, with a frequency for infratentorial location of 35% and 55%, respectively[21,23]. The relative over-representation of cerebellar metastases in colorectal carcinoma might be due to tumor spread by way of the vertebral system (i.e. Batson's plexus), bypassing the lungs[24]. The two other possible routes of hematogeneous dissemination of colorectal cancer to the brain were via the rectal vein plexus to the inferior vena cava, bypassing the liver, or via the portal veins to the liver and lung and then to the brain[20,25]. The incidence of pulmonary metastases in our patients with colorectal cancer was 50% (23/46 patients), which was clearly higher than the approximatley 30% for patients with metastatic colorectal cancer[26], an observation also made in others[19-21]. Presumably the rectal plexus of veins, draining into the inferior vena cava and subsequently the lung are also an important route for tumor spread to the brain.

The interval between the diagnosis of primary tumor and brain metastases in our study group for patients with gastric and colorectal carcinoma was significantly longer (22.6 mo) than that for patients with other primary tumors (8.0 mo). Although only few larger studies on patients with colorectal carcinoma and brain metastases are available to date, all reported a late onset of brain metastases, with a period ranging 21-36 mo between detection of primary tumors and diagnosis of brain metastases[19-21,23,27-29] (the larger studies on gastric cancer did not give detailed information on this topic[13,14,30]). Corresponding to the late onset of brain metastases in the clinical course of gastric and colorectal tumors, all of our patients had further extracerebral metastases (consequently none of our patients was qualified for RPA-class I). The high rate of extracerebral metastases was confirmed by most authors[19-23,28,31,32] and even represented the most important prognostic factor in the study of Nieder *et al.*[31].

Although the onset of brain metastases in our patients with gastrointestinal tumors was late, and the systemic disease was advanced, its median OS time was not statistically different from the median OS time of patients with brain metastases of other primary tumors (3.2 *vs* 3.5 mo, respectively). It was comparable to the median OS time for patients with brain metastases and colorectal carcinoma or gastric carcinoma treated with WBRT seen by others, which ranged from 2.0 to 3.6 mo for colorectal carcinoma[20,22,23,32] and approximately 2 mo for gastric carcinoma[13,14]. Hasegawa, in contrary, found a shorter survival time in a radiosurgically treated series of patients with gastrointestinal tumors compared to patients with other primary tumors[27]. Several authors described a longer median OS time of approximately 9 mo for patients who underwent surgical resection of brain metastases as a sole treatment or followed by radiotherapy[21,22,27,32,33]. Whereas resection of brain metastases seemed to be a favorable prognostic factor in our patients in univariate analysis, it was not statistically significant in multivariate analysis.

The independent factors correlated with a better prognosis in our multivariate analysis were a KPS $\geqslant$70, and the presence of a solitary brain metastasis. It has been widely accepted that the pretherapeutic performance status is one of the most powerful predictive factors for the survival of patients with brain metastases[7,34-38] which could be validated for patients with brain metastases from gastrointestinal tumors in our study group. The more favourable prognosis for patients with primary tumors of the gastrointestinal system presenting with a solitary brain metastasis was also found by Farnell *et al.*[32], whereas others only found the surgical resection of brain metastases to be associated with a better survival[19,23,27]. In our second multivariate analysis, including the therapeutic variable 'resection' status could not be identified as an independent prognostic factor, as mentioned above. In order to diagnose brain metastases in an early phase, in which a resection could still be possible, discrete symptoms hinting cerebral tumor spread should be taken seriously.

A basic problem concerning treatment recommendations for patients with brain metastases of gastrointestinal tumors is that to date only few retrospective studies with a relatively small

number of patients are available. Therefore, the results concerning the prognostic factors should be regarded with caution. The different prognostic factors from each study should be kept in mind when considering a therapeutic concept for individual patients.

In conclusion, brain metastasis is a late event in the course of gastrointestinal tumors, and it occurs later as in patients with other primary tumors. However, the overall survival time is comparable to patients with brain metastases from other primary tumors. Independent prognostic factors in our group were KPS and the number of brain metastases.

REFERENCES

1 **Nussbaum E,** Djalilian H, Cho K, Hall W. Brain metastases. histology, multiplicity, surgery, and survival. *Cancer* 1996; **78**: 1781-1788
2 **Posner J,** Chernik N. Intracranial metastases from systemic cancer. *Adv Neurol* 1978; **19**: 579-592
3 **Sadahiro S,** Suzuki T, Ishikawa K, Nakamura T, Tanaka Y, Masuda T, Mukoyama S, Yasuda S, Tajima T, Makuuchi H, Murayama C. Recurrence patterns after curative resection of colorectal cancer in patients followed for a minimum of ten years. *Hepatogastroenterology* 2003; **50**: 1362-1366
4 **Weiss L,** Grundmann E, Torhorst J, Hartveit F, Moberg I, Eder M, Fenoglio-Preiser C, Napier J, Horne C, Lopez M. Hematogenous metastatic patterns in colonic carcinoma: an analysis of 1 541 necropsies. *J Pathol* 1986; **150**: 195-203
5 **Ogawa K,** Takafumi T, Sueyama H, Nobukazu F, Kakinohana Y, Kamata M, Adachi G, Saito A, Yoshii Y, Murayama S. Brain metastases from esophageal carcinoma. *Cancer* 2002; **94**: 759-764
6 **Quint L,** Hepburn L, Francis I, Whyte R, Orringer M. Incidence and distribution of distant metastases from newly diagnosed esophageal carcinoma. *Cancer* 1995; **76**: 1120-1125
7 **Gaspar L,** Scott C, Rotman M, Asbell S, Phillips T, Wasserman T, McKenna W, Byhardt R. Recursive partitioning analysis (RPA) of prognostic factors in three radiation therapy oncology group (RTOG) brain metastases trails. *Int J Radiat Oncol Biol Phys* 1997; **37**: 745-751
8 **Mandard A,** Chasle J, Marnay J, Villedieu B, Bianco C, Roussel A, Elie H, Vernhes J. Autopsy findings in 111 cases of esophageal cancer. *Cancer* 1981; **48**: 329-335
9 **Bosch A,** Frias Z, Caldwell W, Jaeschke W. Autopsy findings in carcinoma of the esophagus. *Acta Radiol Oncol Radiat Phys Biol* 1979; **18**: 103-112
10 **Gabrielsen T,** Eldevik O, Orringer M, Marshall B. Esophageal carcinoma metastatic to the brain: clinical value and cost-effectiveness of routine enhanced head CT before esophagectomy. *Am J Neuroradiol* 1995; **16**: 1915-1921
11 **Weinberg J,** Suki D, Hanbali F, Cohen Z, Lenzi R, Sawaya R. Metastasis of esophageal carcinoma to the brain. *Cancer* 2003; **98**: 1925-1933
12 **Perri F,** Bisceglia M, Giannatempo G, Andriulli A. Cerebellar Metastasis as a unique presenting feature of gastric cancer. *J Clin Gastroenterol* 2001; **33**: 80-81
13 **York J,** Stringer J, Ajani J, Wildrick D, Gokaslan Z. Gastric cancer and metastasis to the brain. *Ann Surg Oncol* 1999; **6**: 771-776
14 **Kim M.** Intracranial invol vement by metastatic advanced gastric carcinoma. *J Neuroncol* 1999; **43**: 59-62
15 **Brenner H.** Long-term survival rates of cancer patients achieved by the end of the 20th century: a period analysis. *Lancet* 2002; **360**: 1131-1135
16 **Wang LD,** Zheng S, Zheng ZY, Casson AG. Primary adenocarcinomas of lower esophagus, esophagogastric junction and gastric cardia: in special reference to China. *World J Gastroenterol* 2003; **9**: 1156-1164
17 **Powell J,** McConkey C. Increasing incidence of adenocarcinoma of the gastric cardia and adjacent sites. *Br J Cancer* 1990; **62**: 440-443
18 **Blot W,** Devesa S, Kneller R, Fraumeni F. Rising increase of adenocarcinoma of the esophagus and gastric cardia. *JAMA* 1991; **265**: 1287-1289
19 **Ko F,** Lui J, Chen W, Chiang J, Lin T, Lin J. Risk and patterns of brain metastases in colorectal cancer: 27-year experience. *Dis Colon Rectum* 1999; **42**: 1467-1471
20 **Cascino T,** Leavengood J, Kemeny N, Posner J. Brain metastases from colon cancer. *J Neuroncol* 1983; **1**: 203-209
21 **Wronski M,** Arbit E. Resection of brain metastases from colorectal carcinoma in 73 patients. *Cancer* 1999; **85**: 1677-1685
22 **Hammoud M,** McCutcheon I, Elsouki R, Schoppa D, Patt Y. Colorectal carcinoma and brain metastasis: distribution, treatment, and survival. *Ann Surg Oncol* 1996; **3**: 453-463
23 **Alden T,** Gianino J, Saclarides T. Brain Metastases from colorectal cancer. *Dis Colon Rectum* 1996; **39**: 541-545
24 **Batson O.** The role of the vertebral veins in metastatic processes. *Ann Intern Med* 1942; **16**: 38-45
25 **Burns F,** Pfaff JJ. Vascular invasion in carcinoma of the colon and rectum. *Am J Surg* 1956; **92**: 704-710
26 **Copeland E,** Miller L, Jones R. Prognostic factors in carcinoma of the rectum and colon. *Am J Surg* 1968; **116**: 875-881
27 **Hasegawa T,** Kondziolka D, Flickinger J, Lunsford L. Stereotactic Radiosurgery for brain metastases from gastrointestinal tract cancer. *Surg Neurol* 2003; **60**: 506-515
28 **Zorrilla M,** Alonso V, Herrero A, Corral M, Puertolas T, Trufero J, Artal A, Anton A. Brain metastases from colorectal carcinoma. *Tumori* 2001; **87**: 332-334
29 **Zulkowski K,** Kath R, Liesenfeld S, Patt S, Hochstetter A, Behrendt W, Höffken K. Zerebrale metastasen bei kolorektalen karzinomen. *Med Klin* 2002; **97**: 327-334
30 **Kasakura Y,** Fujii M, Mochizuki F, Suzuki T, Takahashi T. Clinicopathological study of brain metastasis in gastric cancer patients. *Surg Today* 2000; **30**: 485-490
31 **Nieder C,** Niewald M, Schnabel K. Brain metastases of colon and rectum carcinomas. *Wien Klin Wochenschr* 1997; **109**: 239-243
32 **Farnell G,** Buckner J, Cascino T, O'Connell M, Schomberg P, Suman V. Brain metastases from colorectal carcinoma. The long term survivors. *Cancer* 1996; **78**: 711-716
33 **D'Andrea G,** Isidori A, Caroli E, Orlando E, Salvati M. Single cerebral metastasis from colorectal adenocarcinoma. *Neurosurg Rev* 2004; **27**: 55-57
34 **Lutterbach J,** Bartelt S, Ostertag C. Long-term survival in patients with brain metastases. *J Cancer Res Clin Oncol* 2002; **128**: 417-425
35 **Lutterbach J,** Cyron D, Henne K, Ostertag C. Radiosurgery followed by planned observation in patients with one to three brain metastases. *Neurosurgery* 2003; **52**: 1066-1073
36 **Nieder C,** Nestle U, Motaref B, Walter K, Niewald M, Schnabel K. Prognostic factors in brain metastases: should patients be selected for aggressive treatment according to recursive partitioning analysis (RPA) classes ? *Int J Radiat Oncol Biol Phys* 2000; **46**: 297-302
37 **Lohr F,** Pirzkall A, Hof H, Fleckenstein K, Debus J. Adjuvant treatment of brain metastases. *Semin Surg Oncol* 2001; **20**: 50-56
38 **Schoeggl A,** Kitz K, Reddy M, Zauner C. Stereotactic radiosurgery for brain metastases from colorectal cancer. *Int J Colorectal Dis* 2002; **17**: 150-155

Edited by Wang XL and Xu FM

PO Box 2345, Beijing 100023, China
Fax: +86-10-85381893
E-mail: wjg@wjgnet.com www.wjgnet.com

World J Gastroenterol 2004;10(22):3349-3352
World Journal of Gastroenterology
 ISSN 1007-9327

• BRIEF REPORTS •

Development and distribution of mast cells and neuropeptides in human fetus duodenum

Xiao-Yu Chen, Xue-Mei Jia, You-Su Jia, Xiao-Rong Chen, Hui-Zhu Wang, Wei-Qin Qi

Xiao-Yu Chen, Xue-Mei Jia, You-Su Jia, Xiao-Rong Chen, Hui-Zhu Wang, Wei-Qin Qi, Department of Histology and Embryology, Anhui Medical University, Hefei 230032, Anhui Province, China
Supported by Youth Teacher Science and Technology Educational Foundation of Anhui Province, No. 2003jql24; National Natural Science Foundation of Anhui Province, No. 2003kj187
Correspondence to: Dr. Xiao-Yu Chen, Department of Histology and Embryology, Anhui Medical University, Hefei 230032, Anhui Province, China. chenxiaoyuzlx@163.com
Telephone: +86-551-5161135
Received: 2003-06-04 **Accepted:** 2003-11-06

Abstract

AIM: To study the developmental regularities and heterogeneity of mast cells (MC) in human fetus duodenum and the distribution and developmental regularities of substance P(SP), calcitonin gene-related peptide (CGRP)-immunoreactive (IR) peptidergic nerves in fetus duodenum, as well as the relationship between MC, SP and CGRP- IR peptidergic nerves.

METHODS: Duodena from 21 cases of human fetus and one term infant were stained by hematoxylin-eosin (HE), toluidine blue (TB) and immunohistochemical avidin-biotinylated peroxidase complex (ABC) method.

RESULTS: Lobe-shape intestinal villi in duodenum were already developed at the twelfth week. At the 21st wk, muscular mucosa appeared gradually, and four layers were observed in the wall of duodenum. TB staining showed that the granules in the immature MC were pale violet, while the mature MC were strong violet in color by TB staining. Connective tissue MC (CTMC) appeared occasionally in submucosa and muscular layer of duodenum at the 16th wk. While the mucosa MC (MMC) appeared at the 18th wk. At the 22nd wk, both CTMC and MMC were activated, and distributed in the surrounding blood vessels and ganglions. The verge of some MC were unclear, and showed degranular phenomena. At the 14th wk, SP and CGRP-IR nerve fibers and cells appeared in the myenteric and submucous plexuses in small intestine, and the responses were turn strongly. Neurons were light to deep brown, and nerve fibers were present as varicose and liner profiles. On the corresponding site of serial sections, SP and CGRP immunohistochemical reactions were coexisted in one nerve fiber or cell. Some of MC showed SP and CGRP-IR positive staining.

CONCLUSION: There are two heterogeneous kinds of MC in duodenum, MMC and CTMC. MC might play an important role in regulating blood circulation and sensation.

Chen XY, Jia XM, Jia YS, Chen XR, Wang HZ, Qi WQ. Development and distribution of mast cells and neuropeptides in human fetus duodenum. *World J Gastroenterol* 2004; 10 (22): 3349-3352
http://www.wjgnet.com/1007-9327/10/3349.asp

INTRODUCTION

Previous microscopic anatomy studies have shown that somatic and visceral nerves are both widely approached to MC. MC and nerve cells interact with each other by connecting with a lemma or degranular style, so that they could regulate microenvironments. As far as organizations are concerned, the anatomic relation means interaction with function, but no studies are available about the development and distribution of MC and developmental regularities of SP, CGRP-IR nerves and cells in human fetus duodenum. BY investigating the relationship between MC and nerve- endocrine- immunological network[1-3], we observed the histological changes in human fetus duodenum with HE staining, the developmental regularities and heterogeneity of MC with TB special staining, neuropeptide SP, CGRP by ABC methods, the relations between neuropeptide and MC. The study provided morphology data of the functional significance of mast cells in human fetus duodenum.

MATERIALS AND METHODS

Tissue specimens

Twenty-one fetuses of 3-9 mo old and one dead term infant were randomly collected within 1-5 h after birth, in which 10 were males and 11 were females. Duodena were taken out (near to bulbs), and fixed in 40 g/L formaldehyde for 12 h, cut into 10 mm×5 mm×3 mm, then embedded in paraffin and cut into 5μm thick serial section.

TB special staining

The paraffin embedded sections were deparaffined in serial xylene, dehydrated by alcohol solvents and mounted by xylene transparent neutral gum, then examined by microscopy and photographed.

Immunohistochemistry

The reactions were carried out according to the ABC method as previously reported[4]. Briefly, the paraffin sections were deparaffined in xylene and graded alcohol. Sections were incubated at room temperature for 10 min with 30 mL/L H_2O_2 solution to block endogenous peroxidase activity. After washed with phosphate buffered saline (PBS) 3 times for 5 min each, slides were digested with trypsin, treated with 3 g/L Triton X-100, followed by incubation with antibodies SP (1:2 000, Sigma) or CGRP (1:1 000, Sigma) at 37 ℃ for 2 h and at 4 ℃ for 24 h. The sections were then incubated with biotin-conjugated IgG (diluted in PBS, 1:100) for 2.5 h at room temperature and washed with PBS 3 times for 5 min each, followed by incubation with the streptavidin-peroxidase complex for 1 h. At last, chromogen 3,3'-diaminobenzidine tetrahydrochloride (DAB) (1:50, Wuhan Boster) was added to visualize the reaction products of peroxidase.

The specific neuropeptide antibodies were replaced by PBS or normal rabbit serum for the negative controls. Adult duodenum tissue sections were used as positive controls, which showed immunoreactivity for SP and CGRP.

The results were judged as follows. Pale-yellow was

negative (-), shallow brown was weak positive (+), brown was moderately positive (++), and deep brown was strongly positive (+++).

RESULTS

HE staining

The histological differentiations were found in lobe-shape intestinal villi in duodenum at the 12nd wk. At the 15th wk, duodenal glands of mucous cells were formed in the submucosa. At the 21st wk, muscular mucosa appeared with 4 layers in the wall of duodenum gradually.

TB special staining

The experiments showed that CTMC in submucosa and muscular layer appeared by staining with 5 g/L toluidine blue with 500 mL/L alcohol dyeing for 5 min, but MMC in mucous layer appeared by staining with 5 g/L toluidine blue with one equivalent hydrochloric acid for 5 d. At the 16th wk, CTMC appeared occasionally in submoucosa. But the time of MMC appearance was at the 18th wk. The granules in immature MC were pale violet, and strong violet in the mature MC as detected by TB special staining. CTMC in intermuscular appeared fusiform and cell bodies were small. MC in mucosa and submucosa layer were round or oval in shape and cell bodies were large (Figure 1A). With the increase of gestational age, the number of MC in duodenal wall increased gradually. At the 22nd wk, the two types of MC were activated and distributed in the surrounding blood vessels and ganglions. The verge of some MC was unclear, which might be a degranular phenomenon (Figure 1B). MC were closed together with connective tissue cells and there existed lemma connection in fetus duodenal mucous and submucous layer connective tissues.

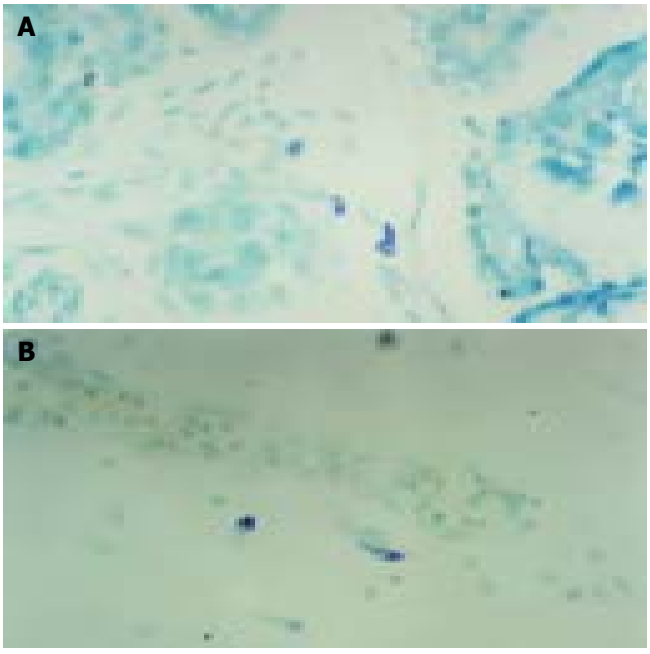

Figure 1 MC in submucous layer at the 21st wk (A) and in mucous layer at the 27th wk (B) of duodenum (TB×400).

Immune phenotype

The degree of positive SP-immunoreactivity (SP-IR) and CGRP-immunoreactivity (CGRP-IR) and their distribution in neurons and nerve fibers (NF) in fetus duodenum had no sex difference. At the 14th wk, SP-IR positive neurons appeared occasionally in the myenteric plexuses of duodenum and neuron cell bodies showed fusiform, few SP-IR-NF appeared in submucosal layer. But nerve plexuses of CGRP-IR appeared at the 16th wk. Diffused SP and CGRP-IR neurons were appeared in submucous at the 21st wk, pale-brown neuron cell bodies were round or oval in shape and nuclei were negative (Figure 2B). SP-IR-NF response to reinforcement (+ to ++) was found in myenteric connective tissue, showing string pearls in shape. A few CGRP-IR-NF appeared in submucous (+), were showing point line in shape. With the growth of gestational age, nerve fibers were mainly distributed in connective tissue of mucous, submucous and myenteric layers. Nerve plexus density increased, and staining turned deep gradually. The dark black positive nerve plexuses were identified (+++) in fetus duodenum after 34th wk, showing network structures and obvious varicosity (Figure 2B). On the corresponding site of serial sections, SP-IR and CGRP-IR materials were partially coexisted in nerve fibers and neurons. In serial sections of TB histochemistry and ABC immunohistochemistry staining, about 10% MC were SP-IR positive, and less MC were CGRP-IR positive. Some of SP, CGRP-IR-NF positive cells were coexisted with MC, while some were closely contacted.

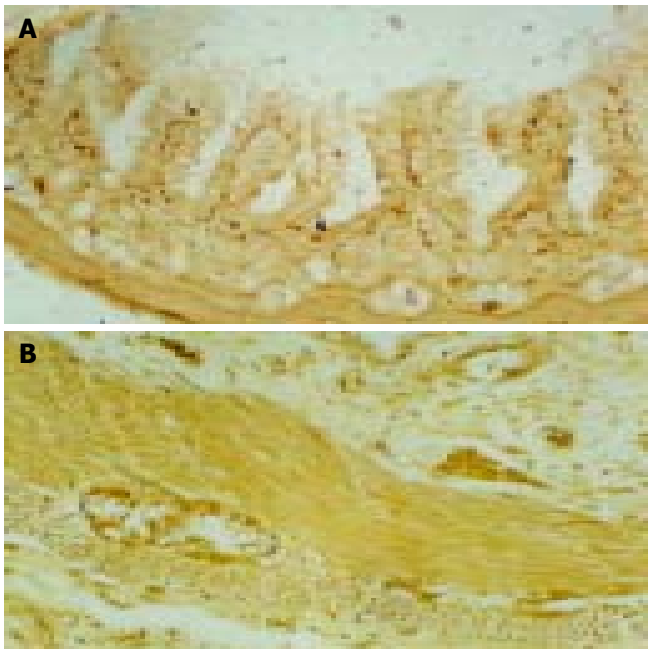

Figure 2 CGRP-IR (+) nerve fiber in duodenum submucous layer at the 21st wk (A) (ABC×100) and SP-IR (++) neuron in duodenum submucous layer and myenteric nerve plexuses at the 28th wk (B) (ABC×200).

DISCUSSION

The results of our experiment showed that there were two kinds of MC in connective tissue of fetus duodenum, namely MMC and CTMC, which possessed heterogeneity. our results are consistent with Wang *et al*.[5]. It might be related to many factors such as local microenvironment. The activated MC were localized around cells, small vessels and ganglions in submucosa, showing that MC were related with those cells and tissues. Surface of some MC boundary was not clear. MC showed degranulation, which means that the cells were releasing active media and affecting peripheral environments and cells, so we considered that MC might take part in allergic and other physiological activities during fetus development and maturation of its surrounding tissues and organs. With electron microscope, Li *et al*.[6] observed MC cytoplasm in intestinal mucosa lamina propria had electron dense round granules and electron-lucent inequality of size vesicles, which

were phenotype of activated MC. MC were important effector cells. It conducted the signal of inflammation cells, and induce the occurrence of mucosa correlated diseases[7-9]. Previous studies have shown the severity of gastrointestinal allergic diseases, such as *Hp* infection, stomach reflow in duodenum, neuro-psychical factor leading gastro-intestinal functional dyspepsia related with MC, and the more serious the disease, the more obviously increased the numbers of MC[10,11]. MC could release inflammatory medium, secretory cytokines (IL-2, TNF-α), biologically active molecules through phospholipase A_2 pathway in earlier period of various kinds of enteritis, which could evoke physiological injuries in the intestinal[12-14]. With the growth of gestational age, the number of MC in bowel wall connective tissue increases gradually, suggesting that MC play an important regulatory role in developing tissue cells in duodenum.

Our experiment showed that the SP-IR and CGRP-IR peptidergic nerves plexus appeared at different time. Owing to the difference of local microenvironments in gastrointestinal tract, various kinds of peptidergic nerves appeared in different time. This difference was decided by local microenvironments of neural crest cells on the way of migration or after its presence. The occurrence of peptidergic nerves was determined by interaction of microenvironmental factors and crest cells. Since different investigators used different specimen source, they adopted different methods and techniques, the detection rate of positive nerve fibers and neurons was different. for example, Larsson *et al*.[15] reported that CGRP-IR-NF was not observed in fetus duodenum mucosa membrane. But Yang *et al*.[16] reported that developing fetus from the 13th week showed mild CGRP-IR-NF in myenteric nerve plexus of duodenum. There were differences in the distribution of SP and CGRP peptidergic nerve plexus at the same gestational age. We found that the distribution and response of SP-IR-NF was slightly higher than those of CGRP-IR-NF in myenteric nerve plexus, but CGRP-IR-NF mainly existed in connective tissue of mucosa and submucosa layers, showing that there was a difference in distribution of peptidergic nerve fibers in the same individual organ. They were closely connected with the presence of digestive tract peptidergic nerve. SP peptidergic nerves exist mainly in duodenum myenteric connective tissue. It could activate cholinergic nerve of gastrointestinal tract, cause neurilemma depolarization in myentenic nerve plexus and increase the effect of acetylcholine, resulting in contraction of digestive tract smooth muscle and secretion of glands[17]. CGRP peptidergic nerves exit mainly in mucous and submucous layers. It is probably related to differentiation of duodenal epithelium and excretion of duodenal gland. CGRP could expand blood vessels of gastrointestinal tract and increase capillary permeability. CGRP could inhibit smooth muscles of gastrointestinal tract and cause relaxation of circular and longitudinal muscles and decrease duodenum vermiculation[18]. Previous studies have reported that decrease of the level of serum CGRP might be related to *Hp* infection, leading to occurrence of duodenal ampulla ulcer[19]. By observing adjacent sections, we found there was partial concordance in localization of SP-IR and CGRP-IR positive neurons. Therefore it is possible that SP and CGRP neurotransmitters coexist in peptidergic nerves. In previous studies, besides the coexistence of CGRP, cells of SP, somatostatin, vasoactive intestinal peptide (VIP) and neuropeptide Y were also coexisted in thymus, sensory ganglion and other organs[18,20,21]. Because SP, CGRP peptidergic nerve fibers project very extensive in central nervous system, it is possible that these neuropeptides together with nervous system produce an important effect on sensation, movement, endocrine and other aspects. Gastrointestine SP,CGRP could regulate stability of MC, which might play an important role in keeping homeostasis the occurrence and development of many pathologic alternations.

There are a lot of MC in connective tissue of human duodenum. Meanwhile, there also existed a huge nervous system, including rich peptidergic neurotransmitters[22,23]. Those made it possible to connect adequate information between MC and nervous system. Gastrointestinal mucous MC are next to gastrointestinal nervous system. It provides double directions of channel between center nervous system and intestinal tract. Thus nervous system can influence physiological functions of gastrointestinal tract. MC could also stimulate intestinal neurons and smooth muscle cells by releasing various kinds of media[24,25]. By electron microscopy some researchers found lemma connection was existed between MC plasmalemma and axon of nonmyelinated nerve fibers in enteron mucosa, form "plywood structure" and synaptic connection[6,26]. As far as organ is concerned, that MC closely contacted with nerves in anatomy means interaction of function by releasing certain active substances, such as histamine, nitrogen monoxide *etc*, as transmitters; On the other hand, nerves could affect MC growth and development. Animal experiments confirmed that the number of MMC and CTMC could be increased by nerve growth factor (NGF), moreover, NGF receptors have been discovered on the surface of MC in rat belly[27]. It has been confirmed that SP and VIP are coexisted in MC[28]. Jia *et al*.[29-31] observed MC in mouse submandibular glands or tongue, and found that most of the MC were SP-IR positive, and 14% MC were CGRP-IR positive. In our studies, we observed that about 10% MC in the wall of fetus duodenum were SP-IR positive, but fewer MC were CGRP-IR positive, indicating that MC in different species and organs contain different peptidergic activity substances. Thus, MC in fetus duodenum possess heterogeneity, whose physiological significance needs further research.

REFERENCES

1 **Delgado M,** Martinez C, Leceta J, Garrido E, Gomariz RP. Differential VIP and VIP1 receptor gene expression in rat thymocyte subsets. *Peptides* 1996; **17**: 803-807

2 **Wang ZH,** Chang XT, Fu XB. Relationship of small intestinal stem cells proliferation differentiation and development. *Shijie Huaren Xiaohua Zazhi* 2001; **9**: 1445-1448

3 **Ward SM**, Ordog T, Bayguinov JR, Horowitz B, Epperson A, Shen L, Westphal H, Sanders KM. Development of interstitial cells of Cajal and pacemaking in mice lacking enteric nerves. *Gastroenterology* 1999; **117**: 584-594

4 **Nakajima S**, Krishnan B, Ota H, Segura AM, Hattori T, Graham DY, Genta RM. Mast cell involvement in gastritis with or without *Helicobacter pylori* infection. *Gastroenterology* 1997; **113**: 746-754

5 **Wang JX,** Li JY, Zhang FJ, Zhang HW, Su JQ. Distribution of mast cells in adult porcine colon. *Zhongguo Shouyi Zazhi* 2001; **37**: 5-7

6 **Li ZS,** Dong WS, Zou DW, Zou XP, Zhang WJ. Enteromucosal mast cells in patients with irritable bowel syndrome. *Jiefangjun Yixue Zazhi* 2002**; 27**: 628-630

7 **Metcalfe DD,** Baram D, Mekori YA. Mast cells. *Physiol Rev* 1997; **77**: 1033-1079

8 **Drake-Lee AB**, Price J. Ultrastructure of nasal mast cells in normal subjects and patients with perennial allergic rhinitis. *J Laryngol Otol* 1991; **105**: 1006-1013

9 **Zhu LR**, Li QX, Hou XH. Increase in the number of gastric mucosal mast cells in patients with functional dyspepsia. *Weichangbingxue* 2002; **7**: 27-29

10 **Gu CM**, Ke MY, Zhang SQ, Jiang YX, Liu YP. An tropyloroduodenal dyscoordination in functional dyspepsia studied by color Doppler flow imaging. *Zhonghua Neike Zazhi* 1998; **37**: 511-514

11 **Li W,** Zheng TZ, Qu SY. Effect of cholecystokinin and secretin on contractile activity of isolated gastric muscle strips in guinea pigs. *World J Gastroenterol* 2000; **6**: 93-95

12 **Beil WJ**, Schulz M, McEuen AR, Buckley MG, Walls AF. Number, fixation properties, dye-binding and protease expression of duodenal mast cells: comparisons between healthy subjects and

patients with gastritis or Crohn's disease. *Histochem J* 1997; **29:** 759-773

13 **Pool V**, Braun MM, Kelso JM, Mootrey G, Chen RT, Yunginger JW, Jacobson RW, Gargiullo PM. Prevalence of anti-gelatin IgE antibodies in people with anaphylaxis after measles-mumps rubella vaccine in the United States. *Pediatrics* 2002; **110**: E71

14 **Gu CM**. Progress of study on gastrointestinal motility. *Shijie Yixue Zazhi* 1999; **3**: 82-85

15 **Larsson LT**, Helm G**,** Malmfors G, Sundler F. Ontogeny of peptide-containing neurons in human gut-an immunocytochemical study. *Regul Pept* 1987; **17**: 243-256

16 **Yang T**, Cai WQ. Ontogeny of 6 types of peptidergic nerves of small intestine in human fetuses. *Jiepou Xuebao* 1994; **25**: 84-87

17 **Lu CL**, Substance P. reference: Lu Changlin ed, Basic and clinical of neuropeptide. 1st ed. *Shanghai: Secondary Military Medicine University Press* 2000: 138-141

18 **Wang XQ**. Calcitonin gene related peptide. reference: Lu Changlin ed, Basic and clinical of neuropeptide. 1st ed. *Shanghai: Secondary Military Medicine University Press* 2000: 195-196

19 **Liu CQ**, Pu J, Li ZX. Changes of duodenal ulcer with peptide hormone in plasma. *Shijie Yixue Zazhi* 2000; **8**: 10-12

20 **Pan XF**, Sun PW, Zhu XH. An immunohistochemical study on neuropeptides in the thymus of adult BALB/c mice. *Beijing Yike Daxue Xuebao* 1998; **30**: 508-514

21 **Huang XQ**. Somatostatin—Probably the most widely effective gastrointestinal hormone in human body. *Huaren Xiaohua Zazhi* 1998; **6**: 93-96

22 **Ke MY.** Study on diseases of gastrointestinal motility. 1st ed. *Beijing: The Publishing Company of Science* 1996: 3-37

23 **Pan XZ,** Cai LM. Study on gastrointestinal hormones at the present stage. *Shijie Yixue Zazhi* 1999; **7**: 464-466

24 **Ruhl A**, Berezin I, Collins SM. Involvement of eicosanoids and macrophage-like cells in cytokine –mediated changes in rat myenteric nerves. *Gastroenterology* 1995; **109**: 1852-1862

25 **Suzuki R,** Furuno T, McKay DM, Wolvers D, Teshima R, Nakanishi M, Bienenstock J. Direct neurite-mast cell communication *in vitro* occurs via the neuropeptide substance P. *J Immunol* 1999; **163**: 2410-2415

26 **Zhai LP,** An W, Yan ML, Qiao CJ, Zhang Z. Ultrastructural features of human fetal mast cells in gastrointestinal tract. *Jiepouxue Zazhi* 1997; **20**: 57-60

27 **Lan W,** Tang CW. Effects of gut peptides on the activation of mast cells from rat intestinal mucosa *in vitro*. *Zhongguo Mingyixue Zazhi* 2002; **18**: 847-851

28 **Feng Y,** Wu JL, Wang YN. Histochemical and immunohistochemical observations on heterogeneity in mast cells of rat. *Jiepou Xuebao* 1999; **20**: 90-94

29 **Jia XM,** Jia YS, Qi WQ, Wang HZ. The heterogeneity Of mast cells in mouse submandibular gland. *Jiepouxue Zazhi* 1996; **19**: 344-347

30 **Jia XM,** Jia YS, Wang DB, Qi WQ. Localization study on substance P, vasoactive intestinal peptide and neuropeptide Y in rat tongue mast cells. *Jiepouxue Zazhi* 1998; **21**: 242-245

31 **Jia YS**, Jiang Y, Qi WQ, Wang HZ. Study on distribution ofF VIP- and SP- immunoreactive nerves in human duodenum. *Zhangguo Zuzhi Huaxue Yu Xibao Huaxue Zazhi* 1999; **8**: 282-285

Edited by Kumar M and Wang XL **Proofread by** Xu FM

PO Box 2345, Beijing 100023, China
Fax: +86-10-85381893
E-mail: wjg@wjgnet.com www.wjgnet.com

World J Gastroenterol 2004;10(22):3353-3355
World Journal of Gastroenterology
 ISSN 1007-9327

• BRIEF REPORTS •

Protective effect of rhIL-1β on pancreatic islets of alloxan-induced diabetic rats

Li-Ping Wu, Li-Hua Chen, Jin-Shan Zhang, Lan Sun, Yuan-Qiang Zhang

Li-Ping Wu, the Second Department of Geriatrics and Gerontology, Xijing Hospital, Fourth Military Medical University, Xi'an 710032, Shaanxi Province, China
Li-Hua Chen, Department of Immunology, the Fourth Military Medical University, Xi'an 710032, Shaanxi Province, China
Jin-Shan Zhang, Lan Sun, Yuan-Qiang Zhang, Department of Histology and Embryology, the Fourth Military Medical University, Xi'an 710032, Shaanxi Province, China
Supported by the National Natural Science Foundation of China, No. 39870109
Co-correspondents: Li-Hua Chen
Correspondence to: Professor Yuan-Qiang Zhang, Department of Histology and Embryology, the Fourth Military Medical University, 169 Changle West Road, Xi'an 710032, Shaanxi Province, China. zhangyq@fmmu.edu.cn
Telephone: +86-29-83374508 **Fax:** +86-29-83374508
Received: 2003-11-04 **Accepted:** 2003-12-08

Abstract

AIM: To observe the protective effect of rhIL-1β on pancreatic islets of alloxan-induced diabetic rats.

METHODS: Protection of rhIL-1β on pancreatic islets of alloxan-induced diabetic rats (n = 5) was demonstrated with methods of immunohistochemistry and stereology. The concentration of serum glucose was measured by GOD method and that of serum insulin by RIA.

RESULTS: The concentration of serum glucose increased but that of insulin decreased after administration of alloxan (150 mg/kg), and the volume density and numerical density of the islets were zero. In rhIL-1β pretreated rats, although the concentration of serum insulin decreased (from 11.9±3.0 mIU/L to 6.1±1.6 mIU/L, P<0.05), that of glucose was at normal level compared with the control group. As compared with alloxan group, the concentration of serum glucose in rhIL-1β pretreated rats decreased (from 19.4±8.9 mmol/L to 12.0±4.0 mmol/L, P<0.05) and the volume density increased(0/L to. 1/L, P<0.05).

CONCLUSION: rhIL-1β pretreatment may have protective effect on the islets of alloxan-induced diabetic rats.

Wu LP, Chen LH, Zhang JS, Sun L, Zhang YQ. Protective effect of rhIL-1β on pancreatic islets of alloxan-induced diabetic rats. *World J Gastroenterol* 2004; 10(22): 3353-3355
http://www.wjgnet.com/1007-9327/10/3353.asp

INTRODUCTION

The cytokine interleukin-1β (IL-1β) can not only promote immunological reaction but also regulate neuro-endocrine system[1]. Previous studies found that IL-1β could stimulate the central adrenalin system, promote production of PG, and downregulate glucose metabolism[2].

Diabetes mellitus implicates many organs and tissues. It has been found that IL-1β decreases serum glucose in experimental animals and may potentially be therapeutic for diabetes mellitus[3,4]. In this experiment, we observed changes in serum glucose and insulin in alloxan induced diabetic rats treated with IL-1β. In addition, we detected the variation of volume density and numerical density of insulin positive pancreatic islets by ABC immunohistochemistry and stereology.

MATERIALS AND METHODS

Animals

Twenty male Sprague-Dawley rats weighing 200 to 300 g were housed in a temperature-controlled room (24±1 ℃) with a 12-h light-dark cycle. The rats were provided with ordinary rat chow and water and divided into 4 groups (n = 5, every group): (1) Control group, each rat was injected with 2 mL saline every other day for 3 times, then injected with 2 mL saline on the 7th d; (2) rhIL-1β group, each rat was injected with 1×10^4 U rhIL-1β in 2 mL saline every other day for 3 times, then injected with 2 mL saline on the 7th d; (3) rhIL-1β pretreated group, each rat was injected with 1×10^4 U rhIL-1β in 2 mL saline every other day for 3 times, then was injected with 150 mg/kg alloxan in 2 mL saline on the 7th d; (4) Alloxan group, each rat was injected with 2 mL saline every other day for 3 times, then injected with 150 mg/kg alloxan in 2 mL saline on the 7th d.

Reagents

Guinea pig anti-rat insulin antibody and SPA-HRP were prepared by Professor Yun-Long Zhu (Department of Physiology) and Professor Cai-Fang Xue (Department of Parasitology) of our university respectively. DAB was purchased from Sigma.

Tissue preparation

Forty-eight hours after last injection of alloxan or saline, rats were anesthetized with ether and sacrificed by cervical dislocation. The blood was collected into heparinised tubes (50 kU/L) and centrifuged (3 000 g, 10 min, at room temperature). Plasma was aspirated and stored at -70 ℃ until assayed as described below. The pancreas was also removed and fixed in Bouin's solution overnight. Each piece was embedded in paraffin and 4-μm sections were prepared.

Immunohistochemistry

Four-micrometer sections from rat pancreas were employed for immunohistochemical analysis. Several dilutions of the antibody were tested to find the optimal staining concentration before the entire series was processed. The staining procedure was carried out as previously reported, but without protease treatment. Briefly, (1) the sections were deparaffinized in xylene, hydrated in ethanol, and blocked with 3 mL/L H_2O_2 in methanol for 30 min to remove endogenous peroxides, then treated with 30 mL/L normal goat serum for 40 min and rinsed in 0.01 mol/L PBS. (2) The sections were incubated at 4 ℃ for 24 h with primary antibody, guinea pig anti-rat insulin antibody (1:1 000 dilution, final concentration 5 mg/L); (3) then with secondary antibody, SPA-HRP (1:200 dilution), at room temperature for 1 h. (4) Peroxidative reaction was performed using DAB as chromogen. The sections were washed three times for 10 min after incubation.

All slides were stained at the same time and under identical conditions. Primary antibodies were replaced by irrelevant antibodies and normal guinea pig serum as specific antibody control. Primary antibody was replaced by PBS as negative control. Primary antibody was omitted as blank control.

Detection of serum glucose and insulin

The concentration of serum glucose was measured by routine GOD method[5] and the concentration of serum insulin was measured by RIA[6,7]. Every sample was measured three times and the results were displayed as mean±SD.

Morphometry

Five specimens from each group were used for morphometric analysis of slides processed for light microscopy. Two sections from each specimen were then selected and five different regions of each section were chosen for the measurement of volume density and number density by double blind method.

Statistical analysis

The results were calculated by the following formula; $Nv = 2/3\times\pi\times NA\times U (AT\times A)$; $Vv = A/AT$. Data were analyzed by χ^2 test. A *P* value of less than 0.05 was considered statistically significant.

RESULTS

Insulin expression in rat pancreas

There were more insulin immunoreactive cells in pancreas of control group and rhIL-1β group than in alloxan group. Immunoreactive cells were mainly located in the central region of the pancreas. Insulin immunopositive cells had dark-brown reaction products in the cytoplasm mostly and nuclei were not stained (Figure 1A, B). The number of insulin immunopositive cells in alloxan group decreased remarkably and there were only a few positive cells in each pancreatic islet (Figure 1C). The number of insulin immunopositive cells in rat pancreas of rhIL-1β pretreated group decreased slightly compared with that of control group and rhIL-1β group, whereas, the number of insulin immunopositive cells in rat pancreas of rhIL-1β pretreated group increased remarkably compared with that of alloxan group (Figure 1D).

Destructive effect of alloxan on rat pancreatic B cells

The concentration of serum glucose increased significantly but that of insulin decreased remarkably after administration of alloxan (150 mg/kg) for 48 h compared with those of control rats. At the same time, the volume density and numerical density of the islets were zero (Table 1).

Stimulatory effect of rhIL-1β on insulin secretion

Compared with control group rats, the concentration of serum insulin in rhIL-1β group rats increased significantly whereas that of glucose was at normal level. Immunohistochemistry and stereology data showed that there were no significant differences in the number density and volume density of the pancreatic islets between rhIL-1β group rats and control rats (Table 1).

Protective effect of rhIL-1β on pancreatic islets of alloxan-induced diabetic rats

In rhIL-1β pretreated group, when the rats were injected with

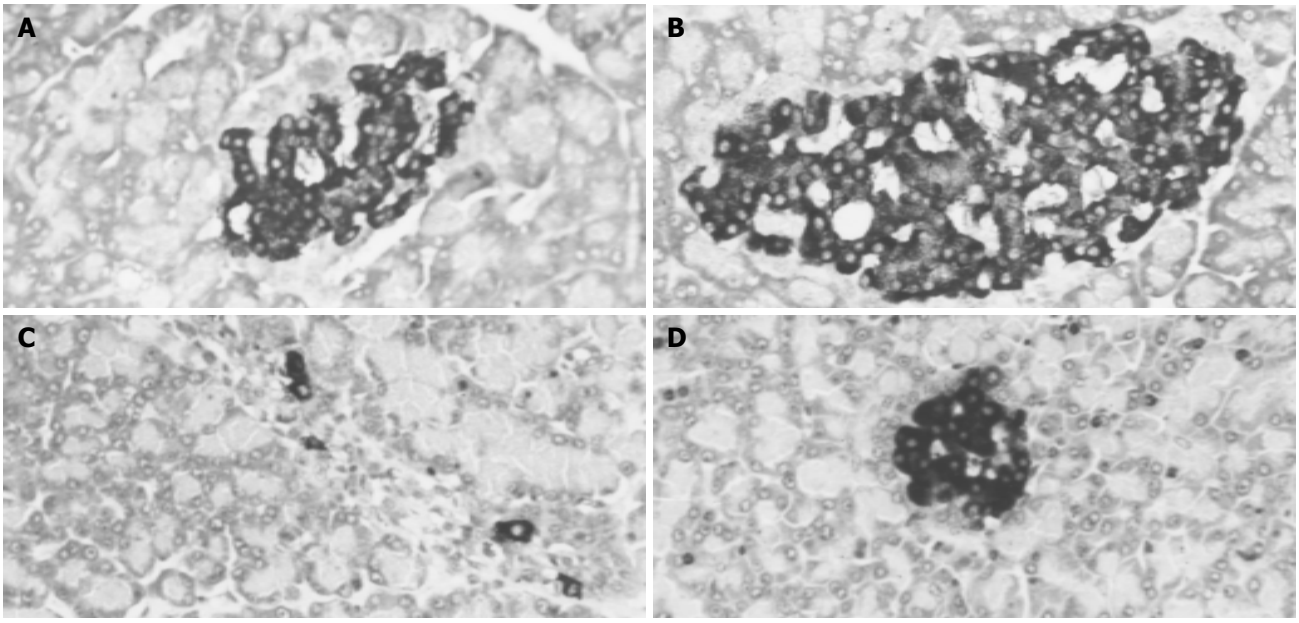

Figure 1 Insulin immunoreactive cells in pancreas. ABC method ×264 A: control group. B: rhIL-1β pretreated rat. C: alloxan-induced diabetic rat. D: rhIL-1β pretreated alloxan-induced diabetic rat.

Table 1 Protective effect of rhIL-1β on pancreatic islets of alloxan-induced diabetic rats

Group	Serum glucose (mmol/L, *n* = 5)	Serum insulin (mIU/L, *n* = 5)	Volume density (/L, *n* = 50)	Number density (/μm², *n* = 50)
Control	8.4±0.3	11.9±3.0	0.6±0.7	5.2±4.1
Alloxan	19.4±8.9[a]	4.7±1.0[a]	0[a]	0[a]
rhIL-1β	8.0±1.3	20.0±6.6[a]	0.6±0.5	5.6±5.3
rhIL-1β pretreated	12.0±4.0	6.1±1.6[a]	0.1±0.1[a]	5.0±5.7

[a]*P*<0.05 *vs* control.

alloxan for 48 h, although the concentration of serum insulin decreased significantly, that of glucose was at normal level compared with control group rats. Immunohistochemistry and stereology data showed that there were no significant differences in the number density of the pancreatic islets between rhIL-1β pretreated rats and control rats, whereas the volume density decreased markedly in rhIL-1β pretreated group (Table 1).

DISCUSSION

Interleukin 1β (IL-1β) is a multi-functional cytokine synthesized mainly by mononuclear/mo cells and is a key factor in the cytokine network[8,9]. IL-1β has many biological functions[9-21]. Previous study showed that IL-1β could decrease the serum glucose level and might be potentially a new drug for diabetes therapy[2-4]. In our experiment, when the rats were injected with alloxan (150 mg/kg) for 48 h, the concentration of serum glucose increased significantly, and that of insulin decreased remarkably. At the same time immunohistochemistry and stereology data showed that the value of number density and volume density of the pancreatic islets were zero. In rhIL-1β pretreated group, when the rats were injected with alloxan for 48 h, although the concentration of serum insulin decreased significantly, that of glucose was at normal level compared with control group rats. Immunohistochemistry and stereology data showed that there were no significant differences in the number density of the pancreatic islets between rhIL-1β pretreated rats and control rats, whereas the volume density decreased remarkably in rhIL-1β pretreated rats. Our results suggest that rhIL-1β has protective effect on pancreatic islets of alloxan-induced diabetic rats and provide the experimental evidence that rhIL-1β may be a new therapeutic drug for diabetes.

REFERENCES

1 **Song Y,** Shi Y, Ao LH, Harken AH, Meng XZ. TLR4 mediates LPS-induced HO-1 expression in mouse liver: Role of TNF-alpha and IL-1beta. *World J Gastroenterol* 2003; **9**: 1799-1803

2 **Lee SH,** Woo HG, Baik EJ, Moon CH**.** High glucose enhances IL-1beta-induced cyclooxygenase-2 expression in rat vascular smooth muscle cells. *Life Sci* 2000; **68**: 57-67

3 **Ikeda U,** Shimpo M, Murakami Y, Shimada K. Peroxisome proliferator-activated receptor-gamma ligands inhibit nitric oxide synthesis in vascular smooth muscle cells. *Hypertension* 2000; **35**: 1232-1236

4 **Doxey DL,** Cutler CW, Iacopino AM. Diabetes prevents periodontitis-induced increases in gingival platelet derived growth factor-B and interleukin 1-beta in a rat model. *J Periodontol* 1998; **69**: 113-119

5 **Nakashima E,** Nakamura J, Hamada Y, Koh N, Sakakibara F, Hotta N. Interference by gliclazide in the glucose oxidase/peroxidase method for glucose assay. *Diabetes Res Clin Pract* 1995; **30**: 149-152

6 **Li C,** Chen P, Vaughan J, Blount A, Chen A, Jamieson PM, Rivier J, Smith MS, Vale W. Urocortin III is expressed in pancreatic beta-cells and stimulates insulin and glucagon secretion. *Endocrinology* 2003; **144**: 3216-3224

7 **Durant S,** Alves V, Coulaud J, Homo-Delarche F. Nonobese diabetic (NOD) mouse dendritic cells stimulate insulin secretion by prediabetic islets. *Autoimmunity* 2002; **35**: 449-455

8 **Amel Kashipaz MR,** Swinden D, Todd I, Powell RJ. Normal production of inflammatory cytokines in chronic fatigue and fibromyalgia syndromes determined by intracellular cytokine staining in short-term cultured blood mononuclear cells. *Clin Exp Immunol* 2003; **132**: 360-365

9 **Musabak U,** Bolu E, Ozata M, Oktenli C, Sengul A, Inal A, Yesilova Z, Kilciler G, Ozdemir IC, Kocar IH. Gonadotropin treatment restores *in vitro* interleukin-1beta and tumour necrosis factor-alpha production by stimulated peripheral blood mononuclear cells from patients with idiopathic hypogonadotropic hypogonadism. *Clin Exp Immunol* 2003; **132**: 265-270

10 **Hasegawa K,** Ichiyama T, Isumi H, Nakata M, Sase M, Furukawa S. NF-kappaB activation in peripheral blood mononuclear cells in neonatal asphyxia. *Clin Exp Immunol* 2003; **132**: 261-264

11 **Tsirpanlis G,** Chatzipanagiotou S, Ioannidis A, Ifanti K, Bagos P, Lagouranis A, Poulopoulou C, Nicolaou C. The effect of viable Chlamydia pneumoniae on serum cytokines and adhesion molecules in hemodialysis patients. *Kidney Int Suppl* 2003; **84**: S72-75

12 **Li L,** Jacinto R, Yoza B, McCall CE**.** Distinct post-receptor alterations generate gene- and signal-selective adaptation and cross-adaptation of TLR4 and TLR2 in human leukocytes. *J Endotoxin Res* 2003; **9**: 39-44

13 **Allan SM,** Pinteaux E. The interleukin-1 system: an attractive and viable therapeutic target in neurodegenerative disease. *Curr Drug Target CNS Neurol Disord* 2003; **2**: 293-302

14 **Boche D,** Cunningham C, Gauldie J, Perry VH. Transforming growth factor-beta 1-mediated neuroprotection against excitotoxic injury *in vivo*. *J Cereb Blood Flow Metab* 2003; **23**: 1174-1182

15 **Abe T,** Sugano E, Saigo Y, Tamai M. Interleukin-1beta and barrier function of retinal pigment epithelial cells (ARPE-19): aberrant expression of junctional complex molecules. *Invest Ophthalmol Vis Sci* 2003; **44**: 4097-4104

16 **Molina-Holgado F,** Pinteaux E, Moore JD, Molina-Holgado E, Guaza C, Gibson RM, Rothwell NJ. Endogenous interleukin-1 receptor antagonist mediates anti-inflammatory and neuroprotective actions of cannabinoids in neurons and glia. *J Neurosci* 2003; **23**: 6470-6474

17 **Boutin H,** Kimber I, Rothwell NJ, Pinteaux E. The expanding interleukin-1 family and its receptors: do alternative IL-1 receptor/signaling pathways exist in the brain? *Mol Neurobiol* 2003; **27**: 239-248

18 **Jeremy AH,** Holland DB, Roberts SG, Thomson KF, Cunliffe WJ. Inflammatory events are involved in acne lesion initiation. *J Invest Dermatol* 2003; **121**: 20-27

19 **Xie Z,** Morgan TE, Rozovsky I, Finch CE. Aging and glial responses to lipopolysaccharide *in vitro*: greater induction of IL-1 and IL-6, but smaller induction of neurotoxicity. *Exp Neurol* 2003; **182**: 135-141

20 **Lu M,** Zhang M, Kitchens RL, Fosmire S, Takashima A, Munford RS. Stimulus-dependent deacylation of bacterial lipopolysaccharide by dendritic cells. *J Exp Med* 2003; **197**: 1745-1754

21 **Wheeler RD,** Brough D, Le Feuvre RA, Takeda K, Iwakura Y, Luheshi GN, Rothwell NJ. Interleukin-18 induces expression and release of cytokines from murine glial cells: interactions with interleukin-1 beta. *J Neurochem* 2003; **85**: 1412-1420

Edited by Zhu LH **Proofread by** Xu FM

PO Box 2345, Beijing 100023, China
Fax: +86-10-85381893
E-mail: wjg@wjgnet.com www.wjgnet.com

World J Gastroenterol 2004;10(22):3356-3360
World Journal of Gastroenterology
 ISSN 1007-9327

• BRIEF REPORTS •

Three new alternative splicing variants of human cytochrome P450 2D6 mRNA in human extratumoral liver tissue

Jian Zhuge, Ying-Nian Yu

Jian Zhuge, **Ying-Nian Yu**, Department of Pathophysiology, Environmental Genomics Center, School of Medicine, Zhejiang University, Hangzhou 310031, Zhejiang Province, China
Supported by the National Key Basic Research and Development Program of China, No. 2002CB512901, National Natural Science Foundation of China, No.39770868 and Natural Science Foundation of Zhejiang Province, No.397490
Correspondence to: Professor Ying-Nian Yu, Department of Pathophysiology, School of Medicine, Zhejiang University, Hangzhou 310031, Zhejiang Province, China. ynyu@hzcnc.com
Telephone: +86-571-87217149 **Fax:** +86-571-87217149
Received: 2004-01-10 **Accepted:** 2004-02-24

Abstract

AIM: To identify the new alternative splicing variants of human CYP2D6 in human extratumoral liver tissue with RT-PCR and sequencing.

METHODS: Full length of human *CYP2D6* cDNAs was amplificated by reverse transcription-polymerase chain reaction (RT-PCR) from a human extratumoral liver tissue and cloned into pGEM-T vector. The cDNA was sequenced. Exons from 1 to 4 of human *CYP2D6* cDNAs were also amplificated by RT-PCR from extratumoral liver tissues of 17 human hepatocellular carcinomas. Some RT-PCR products were sequenced. Exons 1 to 4 of *CYP2D6* gene were amplified by PCR from extratumoral liver tissue DNA. Two PCR products from extratumoral liver tissues expressing skipped mRNA were partially sequenced.

RESULTS: One of the *CYP2D6* cDNAs had 470 nucleotides from 79 to 548 (3' portion of exons 1 to 5' portion of exon 4), and was skipped. Exons 1 to 4 of CYP2D6 cDNA were assayed with RT-PCR in 17 extratumoral liver tissues. Both wild type and skipped mRNAs were expressed in 4 samples, only wild type mRNA was expressed in 5 samples, and only skipped mRNA was expressed in 8 samples. Two more variants were identified by sequencing the RT-PCR products of exons 1 to 4 of *CYP2D6* cDNA. The second variant skipped 411 nucleotides from 175 to 585. This variant was identified in 4 different liver tissues by sequencing the RT-PCR products. We sequenced partially 2 of the PCR products amplified of *CYP2D6* exon 1 to exon 4 from extratumoral liver tissue genomic DNA that only expressed skipped mRNA by RT-PCR. No point mutations around exon 1, intron 1, and exon 4, and no deletion in *CYP2D6* gene were detected. The third variant was the skipped exon 3 , and 153 bp was lost.

CONCLUSION: Three new alternative splicing variants of CYP2D6 mRNA have been identified. They may not be caused by gene mutation and may lose CYP2D6 activity and act as a down-regulator of CYP2D6.

Zhuge J, Yu YN. Three new alternative splicing variants of human cytochrome P450 2D6 mRNA in human extratumoral liver tissue. *World J Gastroenterol* 2004; 10(22): 3356-3360
http://www.wjgnet.com/1007-9327/10/3356.asp

INTRODUCTION

Over 90% medications are metabolized by cytochrome P450 (CYP) family of liver isoenzymes[1]. The most important enzymes are CYP1A2, 3A4, 2C9/19, 2D6 and 2E1. Although CYP2D6 accounts for <2% of the total CYP liver enzyme, nevertheless it mediates metabolism in 25% of drugs in clinical use such as antipsychotics, antidepressants, beta-blockers, antiarrhythmic agents and opiates[2]. CYP2D6 exhibits an extensive polymorphism[3]. Over 40 *CYP2D6* allelic variants have been reported[4].

Pre-mRNA splicing involves precise removal of introns from pre-mRNA, such that exons are spliced together to form mature RNAs with intact translation reading frames. Splicing requires exon recognition, followed by accurate cleavage and rejoining, which are determined by the invariant GU and AG intronic dinucleotides at the 5' (donor) and 3' (acceptor) exon-intron junctions, respectively[5]. Human genes typically contain multiple introns, and in many cases the exons can be joined in more than one way to generate multiple mRNAs, encoding distinct protein isoforms. This process named alternative splicing is a major mechanism for modulating the expression of cellular and viral genes and enables a single gene to increase its coding capacity, allowing synthesis of several structurally and functionally distinct protein isoforms[6-9].

CYP2D subfamily comprises *CYP2D6* gene and psudogenes, i.e. *CYP2D7P* and *CYP2D8BP*. Six mRNA splice variants of *CYP2D* have been identified in human liver[10], breast[11], lung[12], and brain tissues[13]. Variants a and b retain intron 5 and 6, respectively; variant b' has missed the 3' 91 bp portion of exon 6; variant c has missed exon 6; variant d retains 57 bp portion of intron 6; variant e retains the 3' portion of intron 6 and has missed the 61 bp fragment at the 3' end of exon 6. Forms b' and c are variants of *CYP2D6*, and forms d, c, b, b' are variants of *CYP2D7P*[10-13]. All of these CYP2D splice variant mRNAs disrupt open reading frames. If they are translated, they would not have CYP2D6 function.

Three new pre-mRNA alternative splicing variants of human *CYP2D6* in human extratumoral liver tissue were identified by RT-PCR and sequencing.

MATERIALS AND METHODS

Materials

Moloney murine leukemia virus (M-MuLV) reverse transcriptase was supplied by MBI Fermentas AB, Lithuania. Random hexamer primers, T4 DNA ligase and pGEM-T vector system were supplied by Promega Corp. PCR primers, DNA sequence primers, dNTPs and Taq DNA polymerase were synthesized or supplied by Shanghai Sangon Biotechnology Co. DNA sequencing kit was purchased from Perkin-Elmer Corp. Diethyl pyrocarbonate (DEPC) was from Sigma Chemical Co. DNA gel extraction kit was from Hangzhou V-gene Biotechnology Ltd. Other chemical reagents used were all of analytical purity from commercial sources. Extratumoral liver tissue samples were collected from patients undergoing hepatocellular carcinoma resection at affiliated hospitals of Zhejiang University School of Medicine and stored at -70 ℃.

Cloning and sequencing of human CYP2D6 cDNA from a human extratumoral liver tissue

Total RNA was extracted from a human extratumoral liver tissue from a Han nationality Chinese with AGPC method[14]. RT-PCR amplifications were described before[15,16]. Two specific 28 mer oligonucleotide PCR primers were designed according to cDNA sequence of *CYP2D6* reported by Gonzalez *et al*.[10] (GenBank accession no. NM_000106). The sequence of sense primer (CYP2D6 F) corresponds to base position of -39 to -12, i.e. 5'-AGGTGTGTCTCGAGGAGCCCATTTGGTA-3', with a restriction site of *Xho*I (underlined), and the antisense one (CYP2D6 R), corresponds to base position from 1 503 to 1 530, i.e. 5'-TGG CTAGGGATCCGGCTGGGGACTAGGT-3', with a restriction site of *Bam*H I (underlined). The anticipated PCR products were 1.569 kb in length. PCR was performed at 94 ℃ for 5 min, then 35 cycles, each at 94 ℃ for 60 s, at 62 ℃ for 60 s, at 72 ℃ for 2 min, and a final extension at 72 ℃ for 10 min. An aliquot (10 μL) from PCR was subjected to electrophoresis in a 10 g/L agarose gel. The PCR products were ligated with pGEM-T vector, and transformed into *E. coli* DH5α. The *CYP2D6* cDNA cloned in pGEM-T was sequenced by dideoxy chain-termination method marked with BigDye with primers of T7 and SP6 promoters and a specific primer of 5'-ACCTCATGAATCACGGCAGT-3' (nt 1 069 to 1 088) on Perkin-Elmer-ABI Prism 310 automated DNA sequencer.

RT-PCR and sequencing analysis of liver transcripts of CYP2D6 exons 1 to 4

Transcripts of *CYP2D6* exons 1 to 4 were assayed with RT-PCR using 17 extratumoral liver tissues from Han nationality Chinese, with CYP2D6 F and CYP2D6 4R primer: 5'-GCAGAAAGCCCG ACTCCTCCTTCA-3' (nt 638 to 661). Simultaneously the beta-actin (GenBank accession no. NM_001101) cDNA fragment was amplified in the same Eppendorf tube as an internal control[17]. The sequences of sense and antisense primers used for amplification of beta-actin cDNA fragment were 5'-TCCCTGGAGAAGAGCT ACGA-3' (nt 776 to 795) and 5'-CAAGAAAGGGTGTAACGCA AC-3' (nt 1 217 to 1 237) respectively. The anticipated PCR products of *CYP2D6* exons 1 to 4 were 700 bp in length, and those of beta-actin were 462 bp. PCR was performed at 94 ℃ for 3 min, then 35 cycles, each at 94 ℃ for 30 s, at 62 ℃ for 30 s, at 72 ℃ for 45 s, and a final extension at 72 ℃ for 7 min. An aliquot (10 μL) from PCR was subjected to electrophoresis in a 17 g/L agarose gel. Several RT-PCR products of *CYP2D6* exons 1 to exon 4 were shorter than the anticipated full length of 700 bp. The shorter RT-PCR products were separated by agarose gel electrophoresis and extracted using DNA gel extraction kit according to the manufacturer's instructions, and then sequenced by dideoxy chain-termination method marked with BigDye with primer of CYP2D6 F on Perkin-Elmer-ABI Prism 310 automated DNA sequencer.

Sequencing identification of exon 1 to exon 4 of CYP2D6 gene

Genomic DNA of human extratumoral liver tissues expressed full length of CYP2D6 exons 1 to 4 only (3 samples), or only exons skipped (2 samples) or both of full length and skipped ones (3 samples) were extracted according to the methods reported by Gross-Bellard *et al*[18]. The segment of *CYP2D6* gene from exons 1 to 4 was amplified with CYP2D6 F and CYP2D6 4R primers. The anticipated PCR products were 2043 bp (from 1581 to 3623) in length. Two PCR products from extratumoral liver tissues that only expressed skipped mRNA were partially sequenced by RT-PCR.

RESULTS

Identification of a new alternative splicing variant from a cDNA clone

During cloning of *CYP2D6* cDNA, a 1.1 kb RT-PCR product was obtained, which was much shorter than anticipated 1.57 kb (Figure 1).

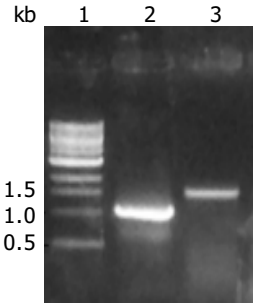

Figure 1 Electrophoresis of RT-PCR products of *CYP2D6* cDNA. Lane 1: 1 kb DNA marker, 2: Amplification of 1.1 kb in size, 3: Amplification of full length of 1.57 kb.

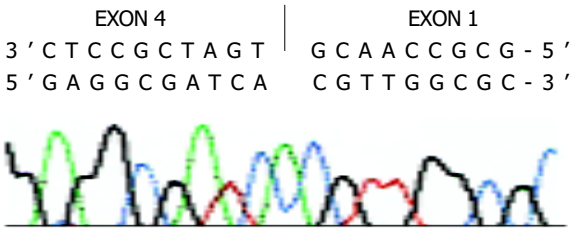

Figure 2 Partial sequences of the cloned human *CYP2D6* cDNA. The upper sequence represents the sense strand and the underside sequence represents the sequenced anti-sense strand.

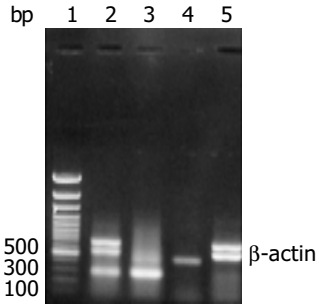

Figure 3 Representative electrophoresis of RT-PCR products of exons 1 to 4 of *CYP2D6* from human liver tissues and HepG2 cells with beta-actin as internal control (464 bp). Lane 1: 100 bp marker, lane 2: A sample having both full length of 700 bp and shorter 300 bp, lane 3: A sample having only shorter ones (300 bp), lane 4: HepG2 cells having no CYP2D6 expressed, Lane 5: A sample having only full length 700 bp of exons 1 to 4 of *CYP2D6*.

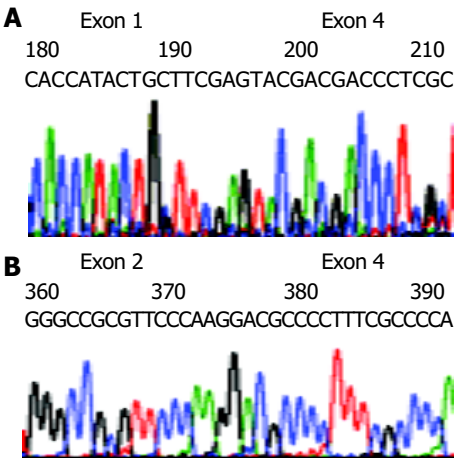

Figure 4 Partial sequences of two alternative splicing variants of *CYP2D6*. A: Part of skipped exon 1, exon 2, exon 3, and part of exon 4. B: Skipped exon 3.

Figure 5 Comparison of sequences of *CYP2D6* cDNA, *CYP2D7 BP* and 3 new *CYP2D6* alternative splicing variants, f, g, h. The different bases compared with wild type *CYP2D6* are indicated in boldface and "_", and the border of exons is indicated by '!'. The skipped parts are indicated by '-'.

The cDNA obtained was then inserted into pGEM-T vector and sequenced. Compared with human wild type *CYP2D6* cDNA sequence reported by Kimura *et al.*[19] (GenBank accession no.M33388), there were 470 nucleotides from 84 to 553, i.e., the 3' end portion 97 bp of exon 1 (180 bp), exon2, exon 3, and the 5' end portion 48 bp of exon 4 (161 bp) were skipped in the cDNA shorter in length (Figures 2, 5). Substitution, insertion and deletion occurred in 13 base pairs, i.e. 620A→G, 712G→T, 1196T→G,1401T→G,1405C→G,1408A→G,1410T→C,1432C →T, 1433A→C, 1435G→C, 1400 insG, 1442T→C, 1443T→A, 1449C del, 1457G→C. This cDNA had a premature stop codon at codon 96 and was named variant f.

RT-PCR analysis of transcripts of CYP2D6 exons 1 to 4 in 17 liver extratumoral tissues and HepG2 cells, two more new alternative splicing variants were identified by sequencing

In 17 liver tissues, 4 samples expressed both wild type and skipped mRNA, 5 samples expressed only wild-type mRNA, and 8 samples expressed only skipped mRNA. Representative electrophoresis of RT-PCR products of exons 1 to 4 of *CYP2D6* from human extratumoral liver tissues and HepG2 cells with beta-actin as internal control are shown in Figure 3.

The sequencing data of RT-PCR products demonstrated that the second variant lost 411 nucleotides (137 amino acid residues) from 177 to 587, i.e., the 3' end portion 4 bp of exon 1 (180 bp), exon 2, exon 3, and the 5' end portion 83 bp of exon 4 (161 bp) and gained a base substitution 100 C→T, resulting in one amino acid exchange P34S, as compared with the human wild type *CYP2D6* cDNA sequence reported by Kimura *et al*.[19] (GenBank accession no.M33388) (Figure 4A, 5). This variant was identified in 4 different extratumoral liver tissues by sequencing RT-PCR products and was named variant g.

The third variant had skipped exon 3, losing 153 bp from nucleotides 353 to 505 or 51 amino acid residues from 117 to 167, and had 2 base substitutions 100 C→T and 336 T→C, resulting in one changed amino acid P34S and a samesense mutation 112F, respectively. This variant was named variant h (Figure 4B, 5).

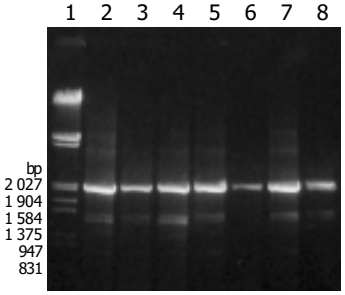

Figure 6 Electrophoresis of PCR products from genomic DNA amplified using CYP2D6 F and CYP2D6 4R primers. Lane 1: λ / *Eco*R I and *Hin*d III marker, lanes 2-4: PCR products from livers expressing full and short length RT-PCR products, Lanes 5, 6: PCR products from livers expressing full length RT-PCR products, Lanes 7, 8: PCR products from livers expressing only short length RT-PCR products.

No mutation events around splicing sites of exon 1 and exon 4 nor gene deletion from exon 1 to exon 4 of CYP2D6 gene

The segment of *CYP2D6* gene at exons 1 to 4 was amplified with CYP2D6 F and CYP2D6 4R primers by PCR. All amplified products from 8 samples gave anticipated 2.04 kb in length but no 0.3 kb PCR products as predicted from the possibility that the shorter cDNA was originated from deleted mutations in *CYP2D6* gene rather than due to alternative splicing (Figure 6). Two PCR products from extratumoral liver tissues expressed only skipped exon were purified and partially sequenced. One showed 3 mutations, i.e., 1719 (nt 100) C→T in exon 1, resulting in P34S, 3280 (nt 408) G→C in exon 3, and samesense mutations 136 V, 3056 G→C in intron 2. Another one showed 3 mutations, *i.e.*, 1719 (nt 100) C→T in exon 1, resulting in P34S, 1958 T→C in intron 1, and 3056 G→C in intron 2.

DISCUSSION

The mechanism of exon missed in cDNA may include gene deletion, alternative splicing, template sequence recombination present in PCR amplification[20-22], and retroviral recombination[23-25]. One or several exons missed entirely could ascribe to alternative splicing. The first mechanism of formation of recombinant molecules during PCR is mediated by premature termination of chain synthesis. Therefore, a short extension time or increased dissociation of polymerases from the template may promote recombination. The optimum values to minimize recombinant molecule formation could prolong the extension time and could be achieved using 30 or 34 amplification cycles respectively. The second mechanism is template switching, it implicates that a fragment elongating on one template, can continue this elongation on another homologous template. The high template concentrations could facilitate template switching and *de novo* synthesize recombinant molecules. We performed PCR with lower template concentrations, 1 min/kb extension, and 32 to 35 amplification cycles to minimize the PCR recombination. During synthesis of the first DNA strand, reverse transcriptase could switch templates from one to other copy of RNA, a phenomenon known as copy-choice. The term 'template switching' implies that the nascent DNA strand is transferred from one RNA (the 'donor') to the other (the 'acceptor'). This process depends on a ribonuclease (RNase H) activity, carried by reverse transcriptase, which could degrade the RNA template once it has been copied[26]. The RNA recombination is a very rare event. In this study, MMLV without RNase H activity was used and skipped mRNA was found in 12 out of 17 liver tissues by RT-PCR assay. Variant g was identified in 4 different extratumoral liver tissues by sequencing RT-PCR products. These facts indicated that the exon missed variant g did not come from PCR recombination or retroviral recombination. PCR amplification and sequencing identification of exon 1 to exon 4 of *CYP2D6* gene from genomic DNA indicated that the exon missed variant g came from neither gene mutation around splicing sites of exon 1 and exon 4 nor gene deletion.

Burset *et al*.[27] analyzed canonical and non-canonical splice sites in mammalian genomes, and found that 99.24% contained canonical dinucleotides GT and AG for donor and acceptor sites, respectively, 0.69% contained GC-AG, 0.05% contained AT-AC and only 0.02% contained other types of non-canonical splice sites. Some non-canonical splice sites seemed to be involved in immunoglobulin gene expression and the others in alternative splicing events.

CYP2D6 gene has 9 exons and 8 introns. All alternative splicing *CYP2D* reported are located in exon 6 to exon 7. No alternative splicing in exon 1 to exon 4 has been reported. We identified 3 new alternative splicing *CYP2D6* cDNA in exon 1 to exon 4 in human extratumoral liver tisssues. The skipped mRNA was not an unusually phenomenon, for 12 samples expressed skipped mRNA in 17 human liver tissue, whereas 9 samples expressed wild-type mRNA in this study.

We cloned a cDNA variant of human *CYP2D6*, the variant f with some exons skipped. The five nt 5'-CAACG-3', located at the boundary of partially skipped exons 1 and 4 (Figure 6). It looked as the 3' end portion of skipped exon 1 or the 5' end portion of exon 4. If we looked it as the 3' end portion of the skipped exon 1, then the splicing donor and acceptor sites would be CT-CG, which were not found as splice site pairs[27]. If we looked it as the 5' end portion of exon 4, then there would be 470 nucleotides from 79 to 548, i.e., the 3' end portion 102 bp of exon 1 (180 bp), exon 2, exon 3, and the 5' end portion 43 bp of exon 4 (161 bp) were skipped. The splicing donor and acceptor sites would be the non-canonical splice sites: CA-AG[27].

CYP2D gene exists in a number of structurally polymorphic haplotypes and also comprises several variants of *CYP2D7P* and *CYP2D8P* pseudogenes. *CYP2D6* is highly homologous to *CYP2D7* and *CYP2D8* pseudogenes. The characteristic base substitution, insertion and deletion of the variant f from 1401 to 1 457 in exon 9 indicated that this exon was derived from *CYP2D7BP*[28] (GenBank accession no.X58468). So this cDNA clone may be transcripted from *CYP2D6*36* (Trivial name: *CYP2D6Ch2 or CYP2D6*10C*) gene, which has gene conversion to *CYP2D7* in exon 9[29]. Johansson *et al*.[29] using allele-specific polymerase chain reaction analysis of genomic DNA from 90 Chinese individuals revealed that *CYP2D6*10* (*CYP2D6Ch1*)

allele was the most common one, *CYP2D6*36* was not a common allele[30] and so we got an alternative splicing variant from this allele only once.

Another alternative splicing *CYP2D6* cDNA, variant g, has 7 bp 5'-GCTTCGA-3', which locates at the boundary of partially skipped exons 1 and 4 (Figure 6). It can be regarded as the 3' end portion of skipped exon 1 or the 5' end portion of exon 4. The splicing donor and acceptor sites would be CC-GA or GC-CC which have not been found as splice site pairs[27]. If we regarded it as the skipped nucleotides from 175 to 585, then 411 nucleotides (137 amino acid residues), i.e., the 3' end portion 6 bp of exon 1 (180 bp), exon 2, exon 3, and the 5' end portion 81 bp of exon 4 (161 bp) were skipped. The splicing donor and acceptor sites would be the non-canonical splice sites: GA-TC[27]. As this variant has been identified in 4 different liver tissues by RT-PCR products sequencing, it could not be the RT-PCR artificial ones.

The third variant, variant h, having skipped the entire exon 3, would use the most common non-canonical GC-AG splice sites (Figure 6). It has an amino acid change of P34S which is a common polymorphism occurring in *CYP2D6*4*, *10*, *14*, *36*, *37*. This variant might come from *CYP2D6*10*, the most common allele in Chinese.

The cDNA sequence of *CYP2D6* is differed from that of *CYP2D7P* at nucleotides 629 to 639, *CYP2D6*[19] was AGG AGGGACTG whereas *CYP2D7P*[28] was AGGGAGGGATCG (Figure 6). All sequencing data of the alternative splicing cDNA and PCR products originated from related genomic DNA showed the characteristics of *CYP2D6*, so they were all derived from *CYP2D6* but not from *CYP2D7P*.

Variant f has premature stop codon at codon 96, which would cause loss of its enzyme activity. According to the homology modeling study of human CYP2 family enzyme reported by Lewis[31], the substrate could recognize site (SRS) 1 of human CYP2D6 located between amino acid residues 101 and 123 and the SRS2 located between amino acid residues 204 to 215. Variant g which lost 137 amino acid residues from 58 to 194, would lose SRS1, and might not have CYP2D6 activity. Variant h having skipped the entire exon 3, would lose 51 amino acid residues from 117 to 167, where part of SRS1 located. It might not have CYP2D6 activity.

All 3 CYP2D6 splice variants might not have CYP2D6 function. But the possibility of the expression of proteins with novel function(s) could not be excluded. The splice variants might have a role in the posttranscriptional down-regulation of the expression of CYP2D6. Formation of variant mRNAs at the expense of full-length mRNAs would ultimately result in a diminished expression of CYP2D6 protein.

Three new CYP2D6 pre-mRNA alternative splicing variants in human extratumoral liver tissues have been identified. Futher work is needed to clarify if they are commonly existed in liver tissue or only in extratumoral liver tissue, and their relation with hepatocellular carcinoma as well.

REFERENCES

1 **Danielson PB**. The cytochrome P450 superfamily: biochemistry, evolution and drug metabolism in humans. *Curr Drug Metab* 2002; **3**: 561-597

2 **Bertilsson L**, Dahl ML, Dalen P, Al-Shurbaji A. Molecular genetics of CYP2D6: clinical relevance with focus on psychotropic drugs. *Br J Clin Pharmacol* 2002; **53**: 111-122

3 **Cascorbi I**. Pharmacogenetics of cytochrome p4502D6: genetic background and clinical implication. *Eur J Clin Invest* 2003; **33**(Suppl 2): 17-22

4 **Bradford LD**. CYP2D6 allele frequency in European Caucasians, Asians, Africans and their descendants. *Pharmacogenomics* 2002; **3**: 229-243

5 **Nissim-Rafinia M**, Kerem B. Splicing regulation as a potential genetic modifier. *Trends Genet* 2002; **18**: 123-127

6 **Graveley BR**. Alternative splicing: increasing diversity in the proteomic world. *Trends Genet* 2001; **17**: 100-107

7 **Maniatis T**, Tasic B. Alternative pre-mRNA splicing and proteome expansion in metazoans. *Nature* 2002; **418**: 236-243

8 **Kriventseva EV**, Koch I, Apweiler R, Vingron M, Bork P, Gelfand MS, Sunyaev S. Increase of functional diversity by alternative splicing. *Trends Genet* 2003; **19**: 124-128

9 **Black DL**. Mechanisms of alternative pre-messenger RNA splicing. *Annu Rev Biochem* 2003; **72**: 291-336

10 **Gonzalez FJ**, Skoda RC, Kimura S, Umeno M, Zanger UM, Nebert DW, Gelboin HV, Hardwick JP, Meyer UA. Characterization of the common genetic defect in humans deficient in debrisoquine metabolism. *Nature* 1988; **331**: 442-446

11 **Huang Z**, Fasco MJ, Kaminsky LS. Alternative splicing of CYP2D mRNA in human breast tissue. *Arch Biochem Biophys* 1997; **343**: 101-108

12 **Huang Z**, Fasco MJ, Spivack S, Kaminsky LS. Comparisons of CYP2D messenger RNA splice variant profiles in human lung tumors and normal tissues. *Cancer Res* 1997; **57**: 2589-2592

13 **Woo SI**, Hansen LA, Yu X, Mallory M, Masliah E. Alternative splicing patterns of CYP2D genes in human brain and neurodegenerative disorders. *Neurology* 1999; **53**: 1570-1572

14 **Chomczynski P**, Sacchi N. Single-step method of RNA isolation by acid guanidinium thiocyanate-phenol-chloroform extraction. *Anal Biochem* 1987; **162**: 156-159

15 **Wu J**, Dong H, Cai Z, Yu Y. Stable expression of human cytochrome *CYP2B6* and *CYP1A1* in Chinese hamster CHL cells: their use in micronucleus assays. *Chin Med Sci J* 1997; **12**: 148-155

16 **Qian Y**, Yu Y, Cheng X, Luo J, Xie H, Shen B. Molecular events after antisense inhibition of *hMSH2* in a *Hela* cell line. *Mutat Res* 1998; **418**: 61-71

17 **Zhuge J**, Luo Y, Yu YN. Heterologous expression of human cytochrome P450 2E1 in HepG2 cell line. *World J Gastroenterol* 2003; **9**: 2732-2736

18 **Gross-Bellard M**, Oudet P, Chambon P. Isolation of high-molecular-weight DNA from mammalian cells. *Eur J Biochem* 1973; **36**: 32-38

19 **Kimura S**, Umeno M, Skoda RC, Meyer UA, Gonzalez FJ. The human debrisoquine 4-hydroxylase (CYP2D) locus: sequence and identification of the polymorphic CYP2D6 gene, a related gene, and a pseudogene. *Am J Hum Genet* 1989; **45**: 889-904

20 **Judo MS**, Wedel AB, Wilson C. Stimulation and suppression of PCR-mediated recombination. *Nucleic Acids Res* 1998; **26**: 1819-1825

21 **Zaphiropoulos PG**. Non-homologous recombination mediated by Thermus aquaticus DNA polymerase I. Evidence supporting a copy choice mechanism. *Nucleic Acids Res* 1998; **26**: 2843-2848

22 **Shammas FV**, Heikkila R, Osland A. Fluorescence-based method for measuring and determining the mechanisms of recombination in quantitative PCR. *Clin Chim Acta* 2001; **304**: 19-28

23 **Negroni M**, Buc H. Mechanisms of retroviral recombination. *Annu Rev Genet* 2001; **35**: 275-302

24 **Negroni M**, Buc H. Retroviral recombination: what drives the switch? *Nat Rev Mol Cell Biol* 2001; **2**: 151-155

25 **Chetverin AB**. The puzzle of RNA recombination. *FEBS Lett* 1999; **460**: 1-5

26 **Zhu S**, Li W, Cao ZJ. Does MMLV-RT lacking RNase H activity have the capability of switching templates during reverse transcription? *FEBS Lett* 2002; **520**: 185

27 **Burset M**, Seledtsov IA, Solovyev VV. Analysis of canonical and non-canonical splice sites in mammalian genomes. *Nucleic Acids Res* 2000; **28**: 4364-4375

28 **Heim MH**, Meyer UA. Evolution of a highly polymorphic human cytochrome P450 gene cluster: *CYP2D6*. *Genomics* 1992; **14**: 49-58

29 **Johansson I**, Oscarson M, Yue QY, Bertilsson L, Sjoqvist F, Ingelman-Sundberg M. Genetic analysis of the Chinese cytochrome P4502D locus: characterization of variant *CYP2D6* genes present in subjects with diminished capacity for debrisoquine hydroxylation. *Mol Pharmacol* 1994; **46**: 452-459

30 **Chida M**, Ariyoshi N, Yokoi T, Nemoto N, Inaba M, Kinoshita M, Kamataki T. New allelic arrangement *CYP2D6**36 x 2 found in a Japanese poor metabolizer of debrisoquine. *Pharmacogenetics* 2002; **12**: 659-662

Edited by Ren SY and Wang XL **Proofread by** Xu FM

PO Box 2345, Beijing 100023, China
Fax: +86-10-85381893
E-mail: wjg@wjgnet.com www.wjgnet.com

World J Gastroenterol 2004;10(22):3361-3364
World Journal of Gastroenterology
 ISSN 1007-9327

• BRIEF REPORTS •

Effects of endostatin on expression of vascular endothelial growth factor and its receptors and neovascularization in colonic carcinoma implanted in nude mice

Yun-He Jia, Xin-Shu Dong, Xi-Shan Wang

Yun-He Jia, Xin-Shu Dong, Xi-Shan Wang, Department of Abdominal Surgery, Tumor Hospital of Harbin Medical University, Harbin 150040, Heilongjiang Province, China
Supported by the Key Technologies Research and Development Program of Heilongjiang Province During the 9th Five-Year Plan Period, No. G99C19-5
Correspondence to: Dr. Yun-He Jia, Department of General Surgery of Nanjing Jinling Hospital, Nanjing 210002, Jiangsu Province, China. jyhcruse@0451.com
Telephone: +86-25-80860034
Received: 2003-12-23 **Accepted:** 2004-02-01

Abstract

AIM: To investigate the antiangiogenic effects of endostatin on colonic carcinoma cell line implanted in nude mice and its mechanism.

METHODS: Nude mice underwent subcutaneous injection with LS-174t colonic carcinoma cell line to generate carcinoma and were randomly separated into two groups. Mice received injection of vehicle or endostatin every day for two weeks. After the tumor was harvested, the tumor volumes were determined, and the expressions of CD34, VEGF and Flk-1 were examined by immunohistochemical method.

RESULTS: Tumor volume was significantly inhibited in the endostatin group (84.17%) and tumor weight was significantly inhibited in the endostatin group (0.197±0.049) compared to the control group (1.198±0.105) (F = 22.56, P = 0.001), microvessel density (MVD) was significantly decreased in the treated group (31.857±3.515) compared to the control group (100.143±4.290) (F = 151.62, P<0.001). Furthermore, the expression of Flk-1 was significantly inhibited in the treated group (34.29%) compared to the control group (8.57%) (χ^2 = 13.745, P = 0.001). However no significant decrease was observed in the expression of vascular endothelial growth factor (VEGF) between these two groups (χ^2 = 0.119,P = 0.730).

CONCLUSION: Endostatin can inhibit tumor growth and angiogenesis by blocking Vegf/Flk-1 pathway. This experiment provides the theory basis for developing a new anti-carcinoma drug through studying the properties of anti-angiogenesis inhibitors.

Jia YH, Dong XS, Wang XS. Effects of endostatin on expression of vascular endothelial growth factor and its receptors and neovascularization in colonic carcinoma implanted in nude mice. *World J Gastroenterol* 2004; 10(22): 3361-3364
http://www.wjgnet.com/1007-9327/10/3361.asp

INTRODUCTION

Angiogenesis is the process of sprouting of capillaries form preexisting blood vessels. The overall process is a complex one that involves many biological functions and cell types. Previous researches since 1970s have demonstrated that tumor angiogenesis is required for the growth and metastasis of primary solid tumor. Endothelial cell activation, migration, and proliferation are major cellular events in this process. All of these processes are under the tight regulation of factors that either "promote" or "inhibit" angiogenesis. When the balance of these factors is disturbed, angiogenic factors can be released from tumor cells, such as vascular endothelial growth factor (VEGF)[1] and basic fibroblast growth factor (bFGF), and migrate to the nearby blood vessel endothelia, signal the activation of the angiogenic response. Tumor cells also produce anti-angiogenic factors including angiostatin, endostatin. Administration of endostatin in tumor-bear mice has been shown to keep the primary tumor in a dormant state[2]. But the mechanisms are still unclear. One mechanism is that endostatin incombination with the endothelial cells to form a compound with tyrosine activity and thereby inducing apoptosis of endothelial cells. The other is that endostatin functions as a ligand for the integrin family of adhesion receptors on the surface of endothelial cells and is associated with MMP family[3]. So, in order to explore the mechanism of endostatin, we provided data that endostatin showed a broad antitumor effect, which might be a result of its inhibitory mechanism on tumor angiogenesis.

MATERIALS AND METHODS

Materials

Endostatin donated from Hefei Sunny Biology-technology Institute, was a 20 ku C-terminal fragment of collagen X VIII. Human endostatin was cloned and expressed in *Escherichia coli* and purified by gene cloning technology by Gene Med Ltd.

Colon cancer cell line HL-174T was purchased from Shanghai Cellular Research Institute. The cells were cultured in 1640 medium supplemented with 100 mL/L fetal bovine serum at 37 ℃ in 50 mL/L CO_2 and the culture media were changed twice a week and observed in the invert microscope to assay the reproduction situation. All reagents and media for cell culture were obtained from GIBCO.

Methods

Subcutaneous xenograft models Tumor cells were implanted (0.5×10^6 cells/animal) subcutaneously using a 27-gauge needle in the back region of BALB/C-nu/nu female mice of 6-8 wk old. Tumor volume was measured every 3 d using a slide gaug. Tumor volumes were measured as the product of (length×width) ×Π/6. Mice were fed with a standard rodent diet for two weeks, and 14 of 20 mice with a similar tumor volume were selected and divided into two groups randomly. Animals of each group were treated once daily with a 0.1mL (2 mg/mL) ip bolus injection of endostatin in saline or saline alone for 14 d. Upon termination of the efficacy portion of endostatin (3 d after drug withdrawal), the animals were euthanized, and the tumor was harvested from the animals and the volume was weighted. The tumors were submitted for immunohistochemical test.

Evaluation of MVD, VEGF and VEGFR/flk-1 expression in tumors Five-μm paraffin embedded sections of the tumors were evaluated by immunohistochemistry. The sections were stained with anti- CD34 antibody (DAKO, 1:2 000) and polyclonal anti-VEGF antibody and polyclonal anti-Flk-1 antibody that could recognize VEGF isoforms and their receptors, following avidin-biotin complex methods.

Microvessel density was assessed by light microscopy in areas of invasive tumors containing the highest number of capillaries and small venules per area (neovascular "hot point"). Areas of the highest neovascularization were found by scanning the tumor sections at a low magnification (×100) and identified with the greatest number of distinct CD34 stained (brown) microvessels per area. Necrotic areas within tumors, where microvessels were sparse, were not included in the vessel counts. After the area of the highest neovascularization was identified, individual microvessels were counted under ×400 field. A brown-stained endothelial cell or a endothelial cell cluster clearly separated from adjacent microvessels, tumor cells, and other connective-tissue elements, considered a single, countable microvessel. Vessel lumens were not necessary for a structure to be defined as a microvessel, and red cells were not used to define a vessel lumen. Results were expressed as the number of microvessels identified within 10 fields (×400).

VEGF was assessed by light microscopy (×100) in the areas of invasive tumor cells. VEGF expression was determined on adjacent serial visual fields and scored by a pathologic doctor. The number of positively and negatively stained cells was counted in 10 continuous visual fields. If more than 5% cells were brown stained, they were considered as positive, otherwise negative. The results were expressed as mean±SD.

Flk-1 was assessed by light microscopy (×400) in the areas of microvessel endothelial cells. The number of endothelial cells stained positively was counted in 10 continuous visual fields. Over 5% positively stained endothelial cells were determined as positive and else negative. The results were expressed as mean±SD.

Statistics

The analysis of variance test was used to compare the differences in tumor weight and MVD between the treated and control groups. The Chi-squared test was used to compare the differences in the expression of VEGF or VEGFR2/Flk-1 between the treated and control groups. The difference was considered statistically significant if the *P* value was less than 0.05. All the data were analyzed with SAS 6.22 by the statistical office of the Second Military Medical University.

RESULTS

Inhibition of tumor growth by endostatin

To determine the efficacy of endostatin on tumor growth, the volume of tumors were measured every three days after endostatin was used and tumors were weighed immediately after they were harvested. The tumor growth in the mice treated with endostatin was inhibited by 84.17% in volume. The growth of the tumors was stopped 3-5 d after using endostatin except two of them. The growth of primary colon tumor was significantly inhibited by endostatin (Figure 1). The tumor weight of the treated group was significantly less than that of the control group ($F = 22.56$; $P = 0.0005$) (Table 1).

Effects of endostatin on angiogenesis in primary tumors

Immunohistochemical analysis showed a significant inhibition of angiogenesis in the tumors treated with endostatin ($P<0.05$) (Table 1). The MVD of tumors was significantly different ($F = 151.62$, $P = 0.001$) between the two groups, the treated group had a significant lower MVD.

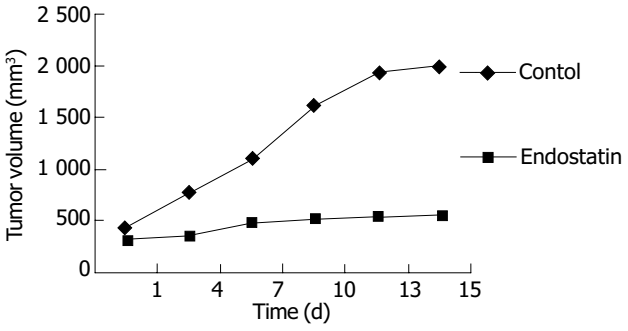

Figure 1 Changes in volume of tumors transplanted in dorsal skinfold chambers in nude mice.

Table 1 Reduction in tumor mass and MVD after endostatin treatment (mean±SD)

	Control	Endostatin	*F*	*P*
Mass	1.198±0.105	0.197±0.049	22.56	[a]*P* = 0.0005
MVD	100.143±4.290	31.857±3.515	151.62	[b]*P* = 0.0001

[a]*P* = Mass difference between Control group and Endostatin group, [b]*P* = MVD difference between Control group and Endostatin group.

Table 2 Expression of VEGF and VEGFR2/Flk-1 in tumor after Endostatin treatment

	Positive	Negative		χ^2	*P*
Control-VEGF (1)	65	5	(1) *vs* (2)	0.119	0.730
Endostatin-VEGF (2)	66	4			
Control-Flk-1 (3)	64	6	(3) *vs* (4)	13.745	[a]*P* = 0.001
Endostatin- Flk-1 (4)	46	24			

[a]*P* = Flk-1 difference between Control group and Endostatin group.

Selectivity and potency of endostatin on VEGF and Flk-1

Immunohistochemical analysis showed that endostatin had a potent inhibition on Flk-1 expression ($\chi^2 = 13.745$, $P = 0.001$) but no inhibition on VEGF expression in tumor cells (Table 2). There was a significant difference in the tumors of treated mice and control mice after staining of endothelial cells with Flk-1 monoclonal antibody (Table 2) but no difference in the tumor tissue stained with VEGF between the two groups (Table 2).

DISCUSSION

Angiogenesis is a fundamental process by which new blood vessels are formed. It is essential in reproduction, development, and wound repair. Under these conditions, angiogenesis is highly regulated, turned on for brief periods and then completely inhibited. However some diseases are driven by persistently unregulated angiogenesis. Tumor growth is one of these kinds of diseases. Tumor growth and metastasis are angiogenesis-dependent. A tumor must continuously stimulate the growth of new capillary blood vessels for the tumor itself to grow. MVD was significantly high in colon cancer tissues compared with normal colon tissues[4]. Tumor cells get oxygen and nutrition through angiogenesis. The Phenomena were also observed in other cancers, for example, breast carcinoma[5] lung cancer[6] prostate cancer[7] and pancreatic tumor[8], *etc*.

Endostatin, a 20-kD C-terminal cleavage product of collagen XVIII, was originally identified by O'Reilly *et al.*[2] as a tumor-derived, highly active, and endothelial specific angiogenic inhibitor[9]. Recombinant endostatin has been shown to inhibit

the growth of a wide variety of tumors in mice, with no toxic side effects observed. Importantly, tumors treated with several cycles of endostatin did not develop drug resistance and become dormant, which persisted even when the endostatin therapy was discontinued[10]. In our experiment, we found that the tumor growth slowed down or even stopped three days after usage of endostatin, but when the treatment was stopped the tumor began to grow rapidly. So endostatin must be used continuously to prevent tumor growth. It is difficult for the patients to accept the treatment in their whole lifetime, so further research is necessary for the usage of endostatin. At present, the molecular mechanism of endostatin action remains unknown. There are some theories which are supported by various studies.

Our results showed that endostatin blocked the VEGF-VEGFR/Flk-1 pathway to inhibit the angiogenesis of colon tumor in nude mice. VEGF pathway is the only well-defined signaling pathway known to be required for the normal development of vasculature as well as for the pathologic angiogenesis that accompanies cancer and other disease states[1,11,12]. The VEGF family of growth factors comprises at least five members, i.e., VEGF, placenta growth factor (PGF) , VEGF-B , VEGF-C[13], and VEGF-D. The VEGF pathway is initiated when VEGF binds to its receptors in endothelial cells. The three best characterized VEGF receptors are termed VEGF receptor 1 (VEGFR1/Flt-1) and VEGF receptor 2 (VEGFR2/Flk-1/KDR) and VEGF receptor 3 (VEGFR3/Flk-4). VEGFR1 and VEGFR2 are highly related transmembrane tyrosine kinases that use their ectodomains to bind to VEGF[14,15]. These binding in turn, activate the intrinsic tyrosine kinase activity of their cytodomains, initiating intracellular signaling. VEGFR3 is expressed almost exclusively by the lymphatic endothelium, thus being considered as a major regulator of lymphangiogenesis[16]. The blockade of VEGF by using a soluble VEGFR-3 extracellular domain could inhibit tumor lymphangiogenesis[17]. While PIGF could bind selectively to VEGFR1, VEGF-C and VEGF-D could bind to both VEGFR3[18,19] and VEGFR2. The corresponding receptor(s) for VEGF-B is VEGFR1. VEGF/VEGFR2 pathway is the most important for tumor angiogenesis, growth and metastasis. In our studies, we found VEGFR2 was obviously down-regulated in the endostatin group compared to the control group, but the expression of VEGF was not changed in both groups. So we think that endostatin can block the VEGF/VEGFR2 pathway by binding to VEGFR2, thus inhibiting the neovascularization.

Endostatin could function as a ligand for the integrin family of adhesion receptors on the surface of endothelial cells[20]. Integrins are potential targets for endostatin function and they are important in endothelial cell biology and angiogenesis. The endostatin-integrin interaction is of functional significance *in vitro*, and the immobilized endostatin supports endothelial cell survival and migration in an integrin-dependent manner. Soluble endostatin in turn could inhibit integrin-dependent endothelial cell functions, such as cell migration[20].

Matrix metalloproteinases (MMPs), a family of extracellular and membrane-associated endopeptidases, collectively digest almost all extracellular matrix and basement membrane components, thus playing an important role in tumor progression. Endostatin could prevent the fragmentation of pro-MMP-2 that is associated with reduction of catalytic activity. Endostatin had no effect on MMP-8 as shown by collagenase activity assays[3]. Endostatin could block the activation and activities of certain tumor-associated pro-MMPs, such as pro-MMP-2, -9, and -13, which may explain at least in part, the antitumor effect of endostatin[3,21].

Inhibition of angiogenesis has been shown to be an effective strategy in cancer therapy in mice. However, its widespread application has been hampered by difficulties in the large-scale production of antiangiogenic proteins. This limitation may be resolved by *in vivo* delivery and expression of antiangiogenic genes. A recombinant adenovirus that could expresses murine endostatin that was biologically active *in vitro* as determined in endothelial cell proliferation assays, and *in vivo* by suppression of angiogenesis induced by VEGF has been constructed[22]. Persistent high serum levels of endostatin were achieved after systemic administration of the vector to nude mice, which resulted in a significant reduction of the growth rates and the volumes of metastatic brain tumor[23]. If the method can be used safely in clinic, it can effectively resolve the recurrence and overgrowth of tumors during the rest periods. Different targets have been found and effective results were achieved in gene therapy. An adenoviral vector carrying Tie2 gene, an endostatin-specific receptor tyrosine kinase, was constructed and tested in established primary tumor, a murine mammary carcinoma or a murine melanoma, which could significantly inhibit the growth rate of both murine mammary carcinoma and melanoma by 64% and 47%, respectively. So the potential of vector-mediated antiangiogenic gene therapy as a component is a very novel and effective strategy in cancer therapy[24,25].

Synergy between endostatin and chemotherapy[26] can be used to eradicate spontaneous tumor and metastases of colon cancer or other angiogenesis dependent diseases. Tumor necrosis was demonstrated only in animals receiving the combination therapy, but not when each agent was applied as monotherapy. The results suggested that these synergistic treatment modalities might provide a novel and effective tool for future therapies of metastatic cancer. Synergy between endostatin and interventional therapy is another way to inhibit the neovascularization. Endostatin can be sent directly to the microvessels around the tumor and destroy the tunica intima of vessels to starve the tumor to death. Other strategies also were used to block the VEGF/VEGFR pathway to inhibit the tumor growth. VEGF-trap is a potent blocker against the angiogenesis of the tumor and could result in stunted and almost completely avascular tumors. VEGF-Trap-mediated blockade may be a hopeful way for tumor treatment[27]. More and more attention has been paid to the effectiveness and carrier and medication methods are paid more and more attention throughout the world. Endostatin may provide a novel and effective tool for future therapies of cancer[28,29].

REFERENCES

1 **Potti A**, Moazzam N, Tendulkar K, Javed NA, Koch M, Kargas S. Immunohistochemical determination of vascular endothelial growth factor (VEGF) overexpression in malignant melanoma. *Anticancer Res* 2003; **23**: 4023-4026

2 **O'Reilly MS**, Boehm T, Shing Y, Fukai N, Vasios G, Lane WS, Flynn E, Birkhead JR, Olsen BR, Folkman J. Endostatin: an endogenous inhibitor of angiogenesis and tumor growth. *Cell* 1997; **24:** 277-285

3 **Nyberg P**, Heikkila P, Sorsa T, Luostarinen J, Heljasvaara R, Stenman UH, Pihlajaniemi T, Salo T. Endostatin inhibits human tongue carcinoma cell invasion and intravasation and blocks the activation of matrix metalloprotease-2, -9, and -13. *J Biol Chem* 2003; **278**: 22404-22411

4 **Dkhissi F**, Lu H, Soria C, Opolon P, Griscelli F, Liu H, Khattar P, Mishal Z, Perricaudet M, Li H. Endostatin exhibits a direct antitumor effect in addition to its antiangiogenic activity in colon cancer cells. *Hum Gene Ther* 2003; **14**: 997-1008

5 **Atiqur Rahman M**, Toi M. Anti-angiogenic therapy in breast cancer. *Biomed Pharmacother* 2003; **57**: 463-470

6 **Sridhar SS**, Shepherd FA. Targeting angiogenesis: a review of angiogenesis inhibitors in the treatment of lung cancer. *Lung Cancer* 2003; **42**(2 Suppl): S81-S91

7 **Uehara H.** Angiogenesis of prostate cancer and antiangiogenic therapy. *J Med Invest* 2003; **50**: 146-153

8 **Schuch G**, Kisker O, Atala A, Soker S. Pancreatic tumor growth is regulated by the balance between positive and negative modulators of angiogenesis. *Angiogenesis* 2002; **5**: 181-190

9 **Sim BK**. Angiostatin and endostatin: endothelial cell-specific

endogenous inhibitors of angiogenesis and tumor growth. *Angiogenesis* 1998; **2**: 37-48

10 **Kuroiwa M**, Takeuchi T, Lee JH, Yoshizawa J, Hirato J, Kaneko S, Choi SH, Suzuki N, Ikeda H, Tsuchida Y. Continuous versus intermittent administration of human endostatin in xenografted human neuroblastoma. *J Pediatr Surg* 2003; **38**: 1499-1505

11 **Zachary I**. VEGF signalling: integration and multi-tasking in endothelial cell biology. *Biochem Soc Trans* 2003; **31**(Pt 6): 1171-1177

12 **Qi L**, Robinson WA, Brady BM, Glode LM. Migration and invasion of human prostate cancer cells is related to expression of VEGF and its receptors. *Anticancer Res* 2003; **23**: 3917-3922

13 **Karkkainen MJ**, Haiko P, Sainio K, Partanen J, Taipale J, Petrova TV, Jeltsch M, Jackson DG, Talikka M, Rauvala H, Betsholtz C, Alitalo K. Vascular endothelial growth factor C is required for sprouting of the first lymphatic vessels from embryonic veins. *Nat Immunol* 2004; **5**: 74-80

14 **Dales JP**, Garcia S, Bonnier P, Duffaud F, Carpentier S, Djemli A, Ramuz O, Andrac L, Lavaut M, Allasia C, Charpin C. Prognostic significance of VEGF receptors, VEGFR-1 (Flt-1) and VEGFR-2 (KDR/Flk-1) in breast carcinoma. *Ann Pathol* 2003; **23**: 297-305

15 **Endo A**, Fukuhara S, Masuda M, Ohmori T, Mochizuki N. Selective inhibition of vascular endothelial growth factor receptor-2 (VEGFR-2) identifies a central role for VEGFR-2 in human aortic endothelial cell responses to VEGF. *J Recept Signal Transduct Res* 2003; **23**: 239-254

16 **Pimenta FJ**, Sa AR, Gomez RS. Lymphangiogenesis in human dental pulp. *Int Endod J* 2003; **36**: 853-856

17 **Kaipainen A**, Korhonen J, Mustonen T, van Hinsbergh VW, Fang GH, Dumont D, Breitman M, Alitalo K. Expression of the fms-like tyrosine kinase 4 gene becomes restricted to lymphatic endothelium during development PNAS. *Proc Natl Acad Sci U S A* 1995; **92**: 3566–3570

18 **Nakamura Y**, Yasuoka H, Tsujimoto M, Yang Q, Imabun S, Nakahara M, Nakao K, Nakamura M, Mori I, Kakudo K. Flt-4-positive vessel density correlates with vascular endothelial growth factor-d expression, nodal status, and prognosis in breast cancer. *Clin Cancer Res* 2003; **9**: 5313-5317

19 **Van Trappen PO**, Steele D, Lowe DG, Baithun S, Beasley N, Thiele W, Weich H, Krishnan J, Shepherd JH, Pepper MS, Jackson DG, Sleeman JP, Jacobs IJ. Expression of vascular endothelial growth factor (VEGF)-C and VEGF-D, and their receptor VEGFR-3, during different stages of cervical carcinogenesis. *J Pathol* 2003; **201**: 544-554

20 **Rehn M,** Veikkola T, Kukk-Valdre E, Nakamura H, Ilmonen M, Lombardo CR, Pihlajaniemi T, Alitalo K, Vuori K. Interaction of endostatin with integrins implicated in angiogenesis. *Proc Natl Acad Sai U S A* 2001; **98**: 1024-1029

21 **Guan KP**, Ye HY, Yan Z, Wang Y, Hou SK. Serum levels of endostatin and matrix metalloproteinase-9 associated with high stage and grade primary transitional cell carcinoma of the bladder. *Urology* 2003; **61**: 719-723

22 **Sauter BV**, Martinet O, Zhang WJ, Mandeli J, Woo SLC. Adenovirus-mediated gene transfer of endostatin *in vivo* results in high level of transgene expression and inhibition of tumor growth and metastases PNAS. *Proc Natl Acad Sci U S A* 2000; **97**: 4802–4807

23 **Oga M**, Takenaga K, Sato Y, Nakajima H, Koshikawa N, Osato K, Sakiyama S. Inhibition of metastatic brain tumor growth by intramuscular administration of the endostatin gene. *Int J Oncol* 2003; **23**: 73-79

24 **Chen W**, Fu J, Liu Q, Ruan C, Xiao S. Retroviral endostatin gene transfer inhibits human colon cancer cell growth *in vivo. Chin Med J* 2003; **116**: 1582-1584

25 **Sridhar SS**, Shepherd FA. Targeting angiogenesis: a review of angiogenesis inhibitors in the treatment of lung cancer. *Lung Cancer* 2003; **42**(2 Suppl): S81-S91

26 **Plum SM**, Hanson AD, Volker KM, Vu HA, Sim BK, Fogler WE, Fortier AH. Synergistic activity of recombinant human endostatin in combination with adriamycin: analysis of *in vitro* activity on endothelial cells and *in vivo* tumor progression in an orthotopic murine mammary carcinoma model. *Clin Cancer Res* 2003; **9**: 4619-4626

27 **Byrne AT**, Ross L, Holash J, Nakanishi M, Hu L, Hofmann JI, Yancopoulos GD, Jaffe RB. Vascular endothelial growth factor-trap decreases tumor burden, inhibits ascites, and causes dramatic vascular remodeling in an ovarian cancer model. *Clin Cancer Res* 2003; **9**: 5721-5728

28 **Shibuya M**. VEGF-receptor inhibitors for anti-angiogenesis. *Nippon Yakurigaku Zasshi* 2003; **122**: 498-503

29 **Tee D**, DiStefano J 3rd. Simulation of tumor-induced angiogenesis and its response to anti-angiogenic drug treatment: mode of drug delivery and clearance rate dependencies. *J Cancer Res Clin Oncol* 2004; **130**: 15-24

Edited by Kumar M and Wang XL **Proofread by** Xu FM

PO Box 2345, Beijing 100023, China
Fax: +86-10-85381893
E-mail: wjg@wjgnet.com www.wjgnet.com

World J Gastroenterol 2004;10(22):3365-3368
World Journal of Gastroenterology
 ISSN 1007-9327

• BRIEF REPORTS •

Proteomic analysis of blood level of proteins before and after operation in patients with esophageal squamous cell carcinoma at high-incidence area in Henan Province

Ji-Ye An, Zong-Min Fan, Ze-Hao Zhuang, Yan-Ru Qin, Shan-Shan Gao, Ji-Lin Li, Li-Dong Wang

Ji-Ye An, Laboratory for Cancer Research and the Third Teaching Hospital, College of Medicine, Zhengzhou University, Zhengzhou 450052, Henan Province, China
Zong-Min Fan, Ze-Hao Zhuang, Yan-Ru Qin, Shan-Shan Gao, Li-Dong Wang, Laboratory for Cancer Research, College of Medicine, Zhengzhou University, Zhengzhou 450052, Henan Province, China
Ji-Lin Li, Department of Pathology, Yaocun Esophageal Cancer Hospital, Linzhou 456592, Henan Province, China
Supported by National Science Fund for Outstanding Young Scholars of China, No.30025016; State Basic Research Development Program of China, No.G1998051206; Foundation of Henan Education Committee, No.1999125 and the US NIH Grant, No.CA65871
Correspondence to: Professor Li-Dong Wang, Laboratory for Cancer Research, College of Medicine, Zhengzhou University, Zhengzhou 450052, Henan Province, China. lidong0823@sina.com
Telephone: +86-11-371-6970165 **Fax:** +86-11-371-6970165
Received: 2004-02-02 **Accepted:** 2004-02-18

Abstract

AIM: To characterize the protein files in blood from same patients with esophageal squamous cell carcinoma (ESCC) before and after operation at the high-incidence area for ESCC in Henan Province, China.

METHODS: Two-dimensional electrophoresis, silver staining and ImageMaster 2-DE analysis software were applied to the determination of protein files in the blood obtained from normal controls and ESCC patients before and after operation.

RESULTS: A total of 655, 662 and 677 protein spots were identified, respectively, from the normal controls and ESCC patients before and after operation. No significant difference in the number of protein spots was observed between the normal group and ESCC patients. A total of seven protein spots were identified with a dramatic difference among the samples before and after operation. Six protein spots were up-regulated and one protein spot was down-regulated in the group after operation compared with those in normal and before operation. Three protein spots were further characterized by matrix-assisted laser desorption/ionization time of flying mass spectrometry (MALDI-TOF-MS). The proteins from these three spots were identified as serum amyloid A (SAA), amyloid related serum protein and haptoglobin.

CONCLUSION: Serum amyloid A, amyloid related serum protein and haptoglobin may be related with ESCC and/or surgery. The significance of these proteins needs to be further characterized. The present study provides informative data for the establishment of serum protein profiles related with ESCC.

An JY, Fan ZM, Zhuang ZH, Qin YR, Gao SS, Li JL, Wang LD. Proteomic analysis of blood level of proteins before and after operation in patients with esophageal squamous cell carcinoma at high-incidence area in Henan Province. *World J Gastroenterol* 2004; 10(22): 3365-3368
http://www.wjgnet.com/1007-9327/10/3365.asp

INTRODUCTION

Esophageal squamous cell carcinoma (ESCC) is one of the six most common malignant diseases in the world with a remarkable geographical distribution. The ratio between the high- and low-incidence areas could be as high as 500:1. The prognosis of ESCC is very poor, the five-year survival rate is only about 10% for the patients at late or advanced stage. China is a country with the highest incidence and mortality rate of ESCC in the world. There are about 300 000 new ESCC patients identified all over the world each year, half of them occur in China. Linzhou City (formerly Linxian County) and its neighbouring counties in Henan Province have been well-recognized as the highest incidence area in the world, the average incidence ratio of males and females is 161 and 103 per 100 000, respectively[1]. ESCC remains the leading cause of cancer related-deaths in these areas. Unclear molecular mechanism, and lacking of sensitive and specific biomarkers for early diagnosis may be the reasons for the unchanged ESCC incidence pattern[2].

Many studies have been focused on gene level for early diagnosis of ESCC. However, because alterations in DNA and RNA may or may not induce similar protein changes, genetic changes could not reflect the stage and progression of the disease directly and objectively[3]. Proteomics based on two-dimensional electrophoresis and mass spectrometry is a new method for identification of cancer-specific protein markers[4]. In this study, we analyzed the serum protein changes in ESCC patients before and after operation and compared them with normal controls by proteomic methods to find the specific ESCC-related proteins.

MATERIALS AND METHODS

Blood samples

Blood samples were collected from ESCC patients in Yaocun Esophageal Cancer Hospital of Linzhou, Henan Province. Of the ESCC patients, there were 4 males and 2 females with an average age of 63 years (range, 52-74 years). All the blood samples were collected two times from each patient, just before and one week after the operation. The control blood samples (10 mL/subject) were collected in our laboratory from the normal people with matched ages as the patients. There were not any abnormalities identified by physical and biochemical examinations in volunteers of the control group.

Reagents

Electrophoresis reagents, including 400 g/L acrylamide solution, *N*, *N*-methylenebisacryl amide, *N*, *N*, *N'*, *N'*-tetramethylethylenediamine, urea, tris-base, glycine, glycerol, 3-[(3-cholannidopropyl)-dimethylammonio]-1-propanesulfonate (CHAPS), sodium dodecyl sulfate (SDS), dithiothreitol (DTT), ammonium persulfate, bromophenol blue, immobiline drystrips, immobilized pH gradient buffer and silver nitrate were from Amersham Pharmacia Biotechnology Inc. (Uppsala, Sweden). Iodoacetamide was from Acros (New Jersey, USA), sequence grade trypsin was from Washington Biochemical Corporation and trifluoroacetic acid (TFA) was from Fluka (Switzerland). All other reagents were of analytical grade.

Serum concentration detection

Serum samples were thawed and diluted by dH_2O as 1:5 (2 μL serum was added to 8 μL dH_2O), 1:10 (2 μL diluent was added to 18 μL dH_2O), 1:200 (4 μL diluent was added to 796 μL dH_2O) respectively, up to 1:10 000 dilution and then 800 μL 1:10 000 diluent was added to 200 μL protein assay reagent and absorbance was measured at 595 nm, finally the concentration of protein in serum was calculated.

First dimensional electrophoresis (Isoelectric focusing, IEF)

Precast IPG strips (pH 3-10 linear, 18 cm, Amersham Pharmacia Biotechnology Inc.) was used in the first dimension. A total amount of 250 μg proteins was diluted to a total volume of 350 μL with the buffer (8 mol/L urea, 20 g/L CHAPS, 5 g/L IPG buffer 3-10, 20 mol/L DTT and a trace of bromophenol blue). After being loaded on IPG strips, IEF was carried out according to the following protocol: rehydration for 6 h at 0 *V*, 10 h at 30 *V*, 1 h at 500 *V*, 1 h at 1 000 *V* and 7 h at 8 000 *V*. The current was limited to 50 μ *A* per gel.

Second dimensional electrophoresis (SDS-polyacrylamide gel electrophoresis, SDS-PAGE)

After IEF separation, the strips were immediately equilibrated for 2×15 min with equilibration solution (50 mmol/L Tris-HCl, pH 6.8, 6 mol/L urea, 300 g/L glycerol and 20 g/L SDS). Then 20 mmol/L DTT was included in the first equilibration solution, and 20 g/L iodoacetamide was added in the second equilibration step to alkylate thiols. Thirteen percent SDS-PAGE gels were handled to become 1 mm thick. The strips were held in place with 5 g/L agarose dissolved in SDS/Tris running buffer and electrophoresis was carried out at constant power (2.5 *W*/gel for 40 min and 15 *W*/gel for 6 h) and temperature (20 ℃) using Ettan Dalt II system (Amersham Pharmacia Biotechnology Inc.).

Silver staining

Gels were stained with silver nitrate according to the instructions of the silverstaining kit[5] (Amersham Pharmacia Biotechnology Inc.).

Gel scanning and image analysis

Protein profiles were obtained in normal controls and ESCC patients before and after operation through correcting the background to detect, match and quantify the spots by ImageMaster™ two-dimensional Elite analysis software (Amersham Biosciences).

In-gel protein digestion

Individual protein spots were excised from the gel by Ettan spot picker (Amersham Pharmacia Biotechnology Inc.), destained with the solution (15 mmol/L potassium ferricyanide, 50 mmol/L sodium thiosulfate) and washed till opaque and colorless with 25 mmol/L ammonium bicarbonate/500 g/L acetonitrile. After being dried with vacuum concentrator (SpeedVac Plus, USA), the gel was rehydrated with 3-10 μL of trypsin solution (10 ng/μL) at 4 ℃ for 30 min, followed by incubation at 37 ℃ overnight. Tryptic peptides were eluted and dried on SpeedVac vacuum concentrator.

Protein identification by MALDI mass spectrometry

The protein spots were analyzed by matrix-assisted laser desorption/ionization time of flying mass spectrometry (MALDI-TOF-MS) and SWISS-PROT database[6].

RESULTS

A total of 655, 662 and 677 protein spots were identified, respectively, from the normal control and ESCC patients before and after operation. No significant difference in number of protein spots was observed between normal group and ESCC patients. A total of seven protein spots were identified with a dramatic difference among the samples before and after operation. Six protein spots were up-regulated and one protein spot was down-regulated in the group after operation compared with those in normal and before operation. Of these six protein spots, three spots were further characterized by MALDI-TOF-MS. The proteins from these three spots were identified as serum amyloid A (SAA), amyloid related serum protein and haptoglobin (Figures 1, 2).

DISCUSSION

In the present study, we found that serum amyloid A (SAA) and its isoform amyloid related serum protein, and haptoglobin were significantly increased after operation in ESCC patients compared with those in normal and pre-operation by mass spectrum. It indicated that these proteins might be related with ESCC and/or surgery. Although the literatures have reported that these acute-phase proteins are associated with tumors, such as colon cancer, the changes of these proteins may be more concerned with stress response, for example, the trauma by operation. The significance for these proteins needs to be further characterized. Although two-dimensional electrophoresis coupled with mass spectrometry is a powerful tool for screening and identification of cancer-specific protein markers, it costs time and money. The present study provided informative data for the establishment of serum protein profiles related with ESCC.

SAA is an acute-phase protein existing as various isoforms in a molecular mass range of 11-14. It is derived mainly from two genes, SAA1 and SAA2[7], mapped at chromosome 11p15.4-15.1[8]. In normal individuals, SAA is produced by hepatocytes in the liver. After its production, it is secreted into serum and rapidly binds to high-density lipoproteins, 90% of the protein particles are bound to high-density lipoprotein. A review of the literature showed that only a low level of SAA could be found in the sera of healthy individuals[9], but during the acute-phase response, its level in the blood could elevate 1 000-fold after various injuries, including trauma, infection, inflammation and neoplasia[10,11].

Recently, many studies have shown that high SAA protein level is present in the serum of patients with disseminated cancer, reflecting the extent of malignant diseases, and inversely correlated with patient survival[12]. The mechanism is not clear. The mode of involvement of SAA in metastatic processes has not been elucidated. Several proposed functions for SAA proteins are compatible with the mechanism of tumor cell invasion and metastasis. These include inhibition of malignant cell attachment to extracellular matrix (ECM) proteins[13,14], induction of the expression of enzymes degrading the ECM[15] and induction of adhesion, migration, and tissue infiltration of cells[16-18]. Moreover, SAA contains functional arginine-glycine-aspartic acid (RGD) -like and tyrosine-isoleucine-glycine-serine-arginine (YIGSR) -like adhesion motifs[19], and the peptides containing these motifs could inhibit tumor cell invasion, metastasis, and angiogenesis[20,21]. Cumulatively, these findings, together with our observation of SAA alterations in blood after operation, imply that SAA may play a role in one or more steps of tumor progression or regression.

Glojnaric *et al*.[22] indicated that although the presence of colorectal carcinoma caused an increase in serum levels of all the acute phase reactants studied, SAA protein showed the most powerful reaction in pre-operative disease stage, with the mean value of 330 mg/L as compared to the normal values of <1.2 mg/L obtained in 30 healthy adults. SAA protein concentration increased to 487 mg/L after surgery and declined during the post-operative clinical course until the sixth chemotherapy cycle, but never returned to the normal range. In the later chemotherapy cycles, the mean SAA protein increased to 163 mg/L, probably as a result of the disease relapse. According to the statistical relations among exact confidence intervals for proportions, SAA protein showed the best specificity for colorectal carcinoma of all the acute phase proteins studied (83-100%) and also a sensitivity of 100%. They concluded that SAA protein seems to be a

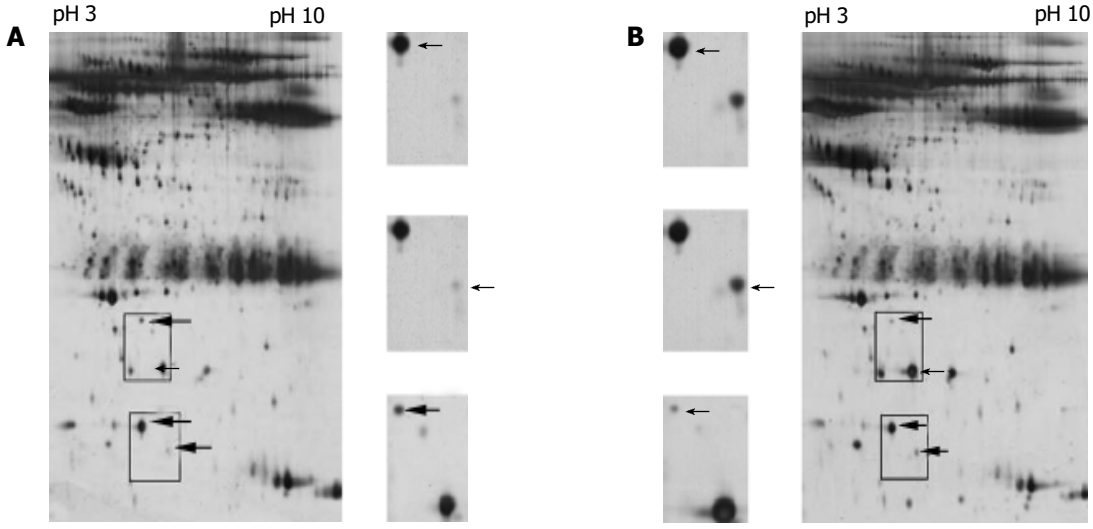

	Spot	Volume	Norm. Vol.	Vol+BkGnd	Peak Height	Area: Pixels	Background	Eq. Radius Pixels	Circularity
Pre-operation	218	2 411.42	0.635	2 411.42	1.816	2 830	0	30.01	0.78
Post-operation	218	1 946.84	0.698	1 946.84	1.746	2 381	0	27.53	0.84
Pre-operation	184	24.89	0.010	27.44	0.110	681	0	14.72	0.37
Post-operation	184	462.77	0.127	478.60	0.593	1 810	0	24.00	0.84
Pre-operation	172	86.42	0.024	86.42	0.359	954	0	17.43	0.74
Post-operation	172	27.71	0.012	39.30	0.134	540	0	13.11	0.57

Figure 1 Representative of two-dimensional electrophoresis profiles and three-matched protein spots (arrows) analysis of the sera from esophageal squamous cell carcinoma patients before (A) and after (B) operation with different acidity from pH 3 to pH 10. Norm: normalization, Vol: volume, BkGnd: background, Eq: equality.

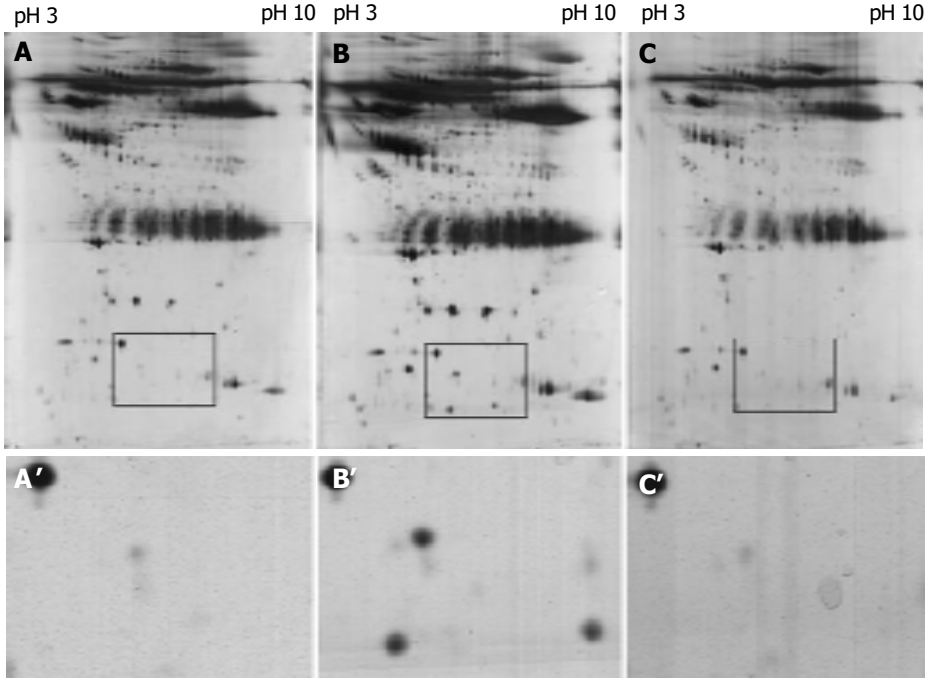

Figure 2 Representative of two-dimensional electrophoresis patterns of sera protein from the same esophageal squamous cell carcinoma patient before (A) and after (B) operation and the normal subject (C) with different acidity from pH 3 to pH 10. A', B' and C' are the magnification of A, B and C, respectively, for the sera protein with marked difference.

reliable parameter, which could be recommended for clinical routine as a non-specific tumor marker for colorectal carcinoma.

Haptoglobin is an acute phase protein capable of binding haemoglobin and may play a role in modulating many aspects of the acute phase response[23]. The complex of haptoglobin with haemoglobin is metabolized in the heptic reticuloendothelial system[24]. Biosynthesis of haptoglobin occurs not only in the liver, but also in adipose tissue and in lung, providing antioxidant and antimicrobial activity[25]. Changes in the measured concentrations of haptoglobin in serum may help to assess the disease status of patients with inflammations, infections, malignancy, *etc*[26]. Dynamic detection of haptoglobin in leukemia patient plasmas showed that haptoglobin level increased obviously in leukemia patients than that in normal persons and

dropped gradually with the improvement of diseases.

In conclusion, serum amyloid A, amyloid related serum protein and haptoglobin may be related with ESCC. The significance of these proteins needs to be further characterized. The present study provides informative data for the establishment of serum protein profiles related with ESCC.

REFERENCES

1 **Wang LD,** Zheng S. The mechanism of esophageal and gastric cardia carcinogenesis from the subjects at high-incidence area for esophageal cancer in henan. *Zhengzhou Daxue Xuebao* 2002; **37**: 717-729

2 **Wang LD,** Zhou Q, Feng CW, Liu B, Qi YJ, Zhang YR, Gao SS, Fan ZM, Zhou Y, Yang CS, Wei JP, Zheng S. Intervention and follow-up on human esophageal precancerous lesions in Henan, northern China, a high-incidence area for esophageal cancer. *Gan To Kagaku Ryoho* 2002; **29**(Suppl 1): 159-172

3 **Hanash SM,** Bobek MP, Rickman DS, Williams T, Rouillard JM, Kuick R, Puravs E. Integrating cancer genomics and proteomics in the post-genome era. *Proteomics* 2002; **2**: 69-75

4 **Anderson NL,** Anderson NG. The human plasma proteome: history, character, and diagnostic prospects. *Mol Cell Proteomics* 2002; **1**: 845-867

5 **Simpson RJ.** Proteins and Proteomics. A Laboratory Manual. 1st. *New York Cold Spring Harbor Laboratory Press* 2003: 75-76

6 **Bini L,** Magi B, Marzocchi B, Arcuri F, Tripodi S, Cintorino M, Sanchez JC, Frutiger S, Hughes G, Pallini V, Hochstrasser DF, Tosi P. Protein expression profiles in human breast ductal carcinoma and histologically normal tissue. *Electrophoresis* 1997; **18**: 2832-2841

7 **Yamada T.** Serum amyloid A (SAA): a concise review of biology, assay methods and clinical usefulness. *Clin Chem Lab Med* 1999; **37**: 381–388

8 **Watson G,** See CG, Woo P. Use of somatic cell hybrids and fluorescence in situ hybridization to localize the functional serum amyloid A (SAA) genes to chromosome 11p15.4-p15.1 and the entire SAA superfamily to chromosome 11p15. *Genomics* 1994; **23**: 694–696

9 **d'Eril GM,** Anesi A, Maggiore M, Leoni V. Biological variation of serum amyloid A in healthy subjects. *Clin Chem* 2001; **47**: 1498–1499

10 **Cho WC,** Yip TT, Yip C, Yip V, Thulasiraman V, Ngan RK, Yip TT, Lau WH, Au JS, Law SC, Cheng WW, Ma VW, Lim CK. Identification of serum amyloid a protein as a potentially useful biomarker to monitor relapse of nasopharyngeal cancer by serum proteomic profiling. *Clin Cancer Res* 2004; **10**(1 Pt 1): 43-52

11 **Urieli-Shoval S,** Linke RP, Matzner Y. Expression and function of serum amyloid A, a major acute-phase protein, in normal and disease states. *Curr Opin Hematol* 2000; **7**: 64-69

12 **Kimura M,** Tomita Y, Imai T, Saito T, Katagiri A, Ohara-Mikami Y, Matsudo T, Takahashi K. Significance of serum amyloid A on the prognosis in patients with renal cell carcinoma. *Cancer* 2001; **92**: 2072–2075

13 **Jensen LE,** Whitehead AS. Regulation of serum amyloid A protein expression during the acute-phase response. *Biochem J* 1998; **334**(Pt 3): 489-503

14 **Hershkoviz R,** Preciado-Patt L, Lider O, Fridkin M, Dastych J, Metcalfe DD, Mekori YA. Extracellular matrix-anchored serum amyloid A preferentially induces mast cell adhesion. *Am J Physiol* 1997; **273**(1 Pt 1): C179-187

15 **Preciado-Patt L,** Levartowsky D, Prass M, Hershkoviz R, Lider O, Fridkin M. Inhibition of cell adhesion to glycoproteins of the extracellular matrix by peptides corresponding to serum amyloid A. Toward understanding the physiological role of an enigmatic protein. *Eur J Biochem* 1994; **223**: 35-42

16 **Migita K,** Kawabe Y, Tominaga M, Origuchi T, Aoyagi T, Eguchi K. Serum amyloid A protein induces production of matrix metalloproteinases by human synovial fibroblasts. *Lab Invest* 1998; **78**: 535–539

17 **Urieli-Shoval S,** Shubinsky G, Linke RP, Fridkin M, Tabi I, Matzner Y. Adhesion of human platelets to serum amyloid A. *Blood* 2002; **99**: 1224-1229

18 **Badolato R,** Wang JM, Murphy WJ, Lloyd AR, Michiel DF, Bausserman LL, Kelvin DJ, Oppenheim JJ. Serum amyloid A is a chemoattractant: induction of migration, adhesion, and tissue infiltration of monocytes and polymorphonuclear leukocytes. *J Exp Med* 1994; **180**: 203-209

19 **Iwamoto Y,** Nomizu M, Yamada Y, Ito Y, Tanaka K, Sugioka Y. Inhibition of angiogenesis, tumour growth and experimental metastasis of human fibrosarcoma cells HT1080 by a multimeric form of the laminin sequence Tyr-Iie-Gly-Ser-Arg (YIGSR). *Br J Cancer* 1996; **73**: 589-595

20 **Ruoslahti E,** Pierschbacher MD. New perspectives in cell adhesion: RGD and integrins. *Science* 1987; **238**: 491-497

21 **Thorn CF,** Lu ZY, Whitehead AS. Regulation of the human acute phase serum amyloid A genes by tumour necrosis factor-alpha, interleukin-6 and glucocorticoids in hepatic and epithelial cell lines. *Scand J Immunol* 2004; **59**: 152-158

22 **Glojnaric I,** Casl MT, Simic D, Lukac J. Serum amyloid A protein (SAA) in colorectal carcinoma. *Clin Chem Lab Med* 2001; **39**: 129-133

23 **Wassell J.** Haptoglobin: function and polymorphism. *Clin Lab* 2000; **46**: 547-552

24 **Kurash JK,** Shen CN, Tosh D. Induction and regulation of acute phase proteins in transdifferentiated hepatocytes. *Exp Cell Res* 2004; **292**: 342-358

25 **Bernard D,** Christophe A, Delanghe J, Langlois M, De Buyzere M, Comhaire F. The effect of supplementation with an antioxidant preparation on LDL-oxidation is determined by haptoglobin polymorphism. *Redox Rep* 2003; **8**: 41-46

26 **Dobryszycka W.** Biological functions of haptoglobin-new pieces to an old puzzle. *Eur J Clin Chem Clin Biochem* 1997; **35**: 647-654

Edited by Kumar M and Wang XL **Proofread by** Xu FM

PO Box 2345, Beijing 100023, China
Fax: +86-10-85381893
E-mail: wjg@wjgnet.com www.wjgnet.com

World J Gastroenterol 2004;10(22):3369-3373
World Journal of Gastroenterology
 ISSN 1007-9327

• BRIEF REPORTS •

Tumor micrometastases in mesorectal lymph nodes and their clinical significance in patients with rectal caner

Yang-Chun Zheng, Yu-Ying Tang, Zong-Guang Zhou, Li Li, Tian-Cai Wang, Yi-Ling Deng, Dai-Yun Chen, Wei-Ping Liu

Yang-Chun Zheng, Zong-Guang Zhou, Li Li, Tian-Cai Wang, Department of Gastroenterological Surgery, West China Hospital, Sichuan University, Chengdu 610041, Sichuan Province, China
Yu-Ying Tang, Department of Anesthesiology, West China Hospital, Sichuan University, Chengdu 610041, Sichuan Province, China
Yi-Ling Deng, Dai-Yun Chen, Wei-Ping Liu, Department of Pathology, West China Hospital, Sichuan University, Chengdu 610041, Sichuan Province, China
Supported by the National Natural Science Foundation of China, No. 39925032
Correspondence to: Dr. Zong-Guang Zhou, Department of Gastroenterological Surgery, West China Hospital, Sichuan University, 37 Guo Xue Xiang, Chengdu 610041, Sichuan Province, China. zhou767@21cn.com
Telephone: +86-28-85422484 **Fax:** +86-28-85422484
Received: 2004-03-09 **Accepted:** 2004-04-05

Abstract

AIM: To investigate the number, size, and status of lymph nodes within the mesorectum and to explore the prognostic significance of lymph node micrometastases in patients with rectal cancer.

METHODS: Thirty-one patients with rectal cancer undergone total mesorectal excision between October 2001 and October 2002 were included. Mesorectal nodes retrieved from the resected specimens were detected with a combination of haematoxylin and eosin (HE) staining and immunohistochemistry (IHC). The relations between lymph node metastases, micrometastases and postoperative recurrence were analyzed.

RESULTS: A total of 548 lymph nodes were harvested, with 17.7±8.2 nodes per case. The average number of metastatic nodes in HE-positive patients and micrometastatic nodes in IHC-positive patients was 5.2±5.1 per case and 2.2±1.3 per case, respectively. The mean size of all nodes and metastatic nodes was 4.1±1.8 mm and 5.2±1.7 mm in diameter, respectively. The mean size of micrometastatic nodes was 3.9±1.4 mm in diameter. The size of the majority of mesorectal nodes (66.8%), metastatic nodes (52.6%), and micrometastatic nodes (79.5%) was less than 5 mm in diameter. During a median follow-up period of 24.6±4.7 mo, 5 patients (16.7%) had recurrence, of them 2 died and 3 survived. Another case died of tumor unrelated cause and was excluded. All 5 recurrent cases had 3 or more nodes involved, and one of them developed only lymph node micrometastases. The mean number of both metastatic and micrometastatic nodes per case differed significantly between the recurrent and non-recurrent groups ($P<0.01$ and $P = 0.01$, respectively).

CONCLUSION: The majority of lymph nodes, metastatic, and micrometastatic lymph nodes within the mesorectum are smaller than 5 mm in diameter. The nodal status and the number of lymph nodes involved with tumor metastases and micrometastases are related to the rapid postoperative recurrence.

Zheng YC, Tang YY, Zhou ZG, Li L, Wang TC, Deng YL, Chen DY, Liu WP. Tumor micrometastases in mesorectal lymph nodes and their clinical significance in patients with rectal caner. *World J Gastroenterol* 2004; 10(22): 3369-3373
http://www.wjgnet.com/1007-9327/10/3369.asp

INTRODUCTION

Lymph node involvement is one of the most important factors in determining the prognosis of patients with rectal cancer[1-6]. Patients with lymph node involvement were found to suffer from more advanced diseases according to the tumor-node-metastasis (TNM) classification system[6], and up to 30% of them eventually developed recurrences after a potentially curative resection[7,8]. In contrast, some patients without positive lymph nodes also had postoperative recurrences or developed metastatic diseases, which were reported to be associated with lymph node micrometastases missed by conventional pathological examination[9-13].

Lymph node spread of rectal cancer generally follows an anatomical route from the proximity to distance along the main supplying vessels of the rectum[14,15]. Lymph nodes contained in the mesorectum are thereby the earliest and most frequent ones that might be involved when tumor spread occurs[14-16]. Although reports have emphasized the importance of regional lymph nodes in the prognosis of rectal cancer[1,2,17-21], few studies available have investigated the number and size of lymph nodes within the rectal mesentery[22,23]. The clinical significance of mesorectal lymph node metastases and micrometastases remains to be fully acknowledged[22,23]. This study was conducted to examine the number, size, and status of lymph nodes within the mesorectum, and to investigate the prognostic value of lymph node metastases, especially lymph node micrometastases, in patients with rectal cancer.

MATERIALS AND METHODS

Patients

From October 2001 to October 2002, 31 patients with rectal cancer undergone total mesorectal excision (TME) at the Department of Gastroenterological Surgery of West China Hospital were included. There were 18 males and 13 females, with an average age of 55 (32-72) years. Of them, 7 cases were patients with high rectal cancer (above the peritoneal reflection) and 24 cases were patients with lower rectal cancer (below the peritoneal reflection). Three tumors were highly differentiated, 20 moderately differentiated, and 8 poorly differentiated. All patients received standard preoperative examination and the diagnosis of rectal adenocarcinoma was made by fibrocolonoscopy and confirmed by pathological biopsy before surgery. All operations were carefully performed by skillful surgeons following the principle of TME[24], and the rectal specimens resected were collected prospectively.

Specimen processing

After removal, the specimens were routinely processed with neutral buffered 100 mL/L formalin solution for 24 h, and immersed in lymph node revealing solution (LNRS) for 6 h or more[25]. Later, they were washed thoroughly with running

water. Fat tissues in the specimens were dissected carefully at intervals of 2-3 mm from upward down to the level of distant transaction along the runway of the superior rectal artery (SRA). Lymph nodes stood out as white, and chalky nodules against the background of yellow fat were harvested and recorded.

Pathological examination

After retrieval, each lymph node was embedded separately in paraffin. The block was then sectioned serially at intervals of 20-40 μm, with each section of 4 μm in thickness. Two sections sampled randomly from 10 representative levels were subjected to haematoxylin and eosin (HE) staining. For nodes diagnosed negatively by HE staining, another 3 sections were further singled out, one for HE re-examination, the other two for immunohistochemistry (IHC).

Immunohistochemistry was performed using labelled streptavidin biotin method (LsAB). Briefly, all sections were deparaffinized and rehydrated. Then, they were immersed in 30 mL/L H_2O_2 for 20 min to block the endogenous peroxidase activity. Sections were then incubated with 100 mL/L normal goat serum for 20 min, followed by incubation with mouse monoclonal anti-human cytokeratin (CK) 20 antibody (Neomarkers, Lab Vision Corporation, CA, USA) (1:50) at 4 ℃ overnight. After that, the sections were washed with phosphate buffered solution (PBS) (0.01 mol/L, pH 7.2) and sequentially incubated with biotinylated goat anti-mouse IgG, and streptavidin biotin horseradish peroxidase complex following the manufacturer's instructions (Histostain™-SP Kits, Zymed laboratories Inc., San Francisco, CA, USA). Staining was developed by immersing slides in 0.5 g/L 3,3'-diaminobenziding tetrahydrochloride (DAB) with 3.3 mol/L H_2O_2. All slides were counterstained with haematoxylin, dehydrated and mounted. Yellowish staining of the tumor cell cytoplasm was taken as positive. Previously confirmed rectal adenocarcinoma tissue served as positive control, and substitution of the primary monoclonal antibody with PBS was used as negative control. Tumor micrometastases were occult diseases generally missed by HE staining while detected by IHC, and were characterized as single cell or small cluster of cells showing malignant morphology.

Follow-up

All patients were regularly followed up to now. The follow-up interval was every 3 mo after surgery during the first year and every 6 mo thereafter. The time of recurrence and the cause of death were inquired and recorded.

Statistical analysis

The *t* test for difference in mean values and χ^2 test for difference in frequencies were performed using SPSS 10.0 software package. $P<0.05$ was considered statistically significant.

RESULTS

Micrometastases and number of lymph nodes

A total of 548 mesorectal lymph nodes were retrieved from the 31 specimens, with 17.7±8.2 lymph nodes per case. HE staining detected 114 lymph nodes positive in 22 patients (71.0%). The average number of metastatic lymph nodes in HE-positive patients was 5.2±5.1 per case. IHC re-examination of the remaining negative nodes revealed 39 lymph nodes (9.0%) positive with tumor micrometastases from 18 cases (58.1%). Among them, 5 cases (16.1%) with 10 nodes positive with IHC staining were previously assumed free of metastatic diseases. The average number of micrometastatic lymph nodes in IHC-positive patients was 2.2±1.3 per case.

Micrometastases and size of lymph nodes

The average diameter of all the 548 lymph nodes was 4.1±1.8 mm. The mean size of 114 metastatic lymph nodes (5.2±1.7 mm in diameter) was significantly larger than that of 39 micrometastatic lymph nodes (3.9±1.4 mm in diameter) ($P<0.01$). Of all the lymph nodes, 92 (16.8%) were ≤2 mm in diameter, with 4 metastatic and 3 micrometastatic lymph nodes; 182 (33.2%) ≥5 mm, with 54 metastatic and 8 micrometastatic lymph nodes; and 274 (50.0%) with a size between 2 mm and 5 mm in diameter, with 56 metastatic and 28 micrometastatic lymph nodes (Table 1). It was noted that the majority of lymph nodes (66.8%) were <5 mm in diameter, and 52.6% of the metastatic nodes and a higher proportion of the micrometastatic nodes (79.5%) were <5 mm in diameter also.

Lymph node metastases and micrometastases and prognosis

All the 31 patients were successfully followed-up. Patients with lymph node metastases received regular chemotherapy after surgery. However, during a median follow-up period of 24.6±4.7 mo, one

Table 1 Size of lymph nodes (LNs) and status of tumor metastases and micrometastases

Size of LNs (mm)	No. of LNs				Positive ratio (%)
	Total	HE-positive	IHC-positive	Sum of positive	
≤2	92	4	3	7	7.6[b]
2-5	274	56	28	84	30.7
≥5	182	54	8	62	34.1[d]
Total	548	114	39	153	27.9

[b]$P<0.01$, *vs* 2-5; [d]$P<0.01$, *vs* ≤ 2.

Table 2 Clinicopathological features of five recurrent patients with lower rectal cancer

Case No.	Sex	Age (yr)	Characteristics of tumor		No. of LNs			Site of recurrence	Outcome
			Differentiation	Invasion	Total	M	MM		
1	Female	35	Well	Muscle	15	3	2	Lung	Surviving
2	Female	65	Poor	Serosa	22	22	0	Pelvis+liver	Dead
3	Male	50	Moderate	Muscle	27	0	3	Pelvis	Surviving
4	Male	45	Poor	Serosa	30	17	4	Pelvis	Dead
5	Male	32	Poor	Muscle	21	5	5	Pelvis	Surviving

LNs: lymph nodes; M: metastatic; MM: micrometastatic.

Table 3 Comparison of recurrence between patients with different nodal status

Variables	HE-positive		HE-negative		Total
	IHC-positive	IHC-negative	IHC-positive	IHC-negative	
No. of case	13	8	5	4	30
Recurrence	3	1	1	0	5
Recurrence rate (%)	23.1	12.5	20	0	16.7

Table 4 Comparison of nodal status between recurrent and non-recurrent group

Grouping	LNs (mean±SD)				Positive ratio (%)
	Total	HE-positive	IHC-positive	Sum of positive	
Recurrent group	23.0±5.8	9.4±9.6	2.8±1.9	12.2±8.9	53.0
Non-recurrent group	17.0±8.2	2.6±2.5	1.0±1.2	3.6±3.0	21.4
P	0.135	0.003	0.01	0.000	0.000

patient died of tumor unrelated cardiovascular disturbance 24 mo post operation and was excluded from the analysis. Among the five cases (16.7%) with lower tumor recurrences, 3 cases were localized in the pelvic floor, one case spread to the lung, and one case with both pelvic and liver involvements. Two of them died and the other three remained alive. All the recurrent patients shared the characteristics of having 3 or more lymph nodes involved with tumor metastases and/or micrometastases. Of them, one case with mere lymph node micrometastases also developed local recurrence 17 mo after operation (Tables 2, 3). Comparison analysis showed that both the number of metastatic and micrometastatic lymph nodes between the recurrent and non-recurrent groups differed significantly ($P<0.01$ and $P = 0.01$, respectively), although such a statistical difference was not found between them in reference to the total number identified per case (Table 4).

DISCUSSION

The nodal status is the single powerful predictor of survival in rectal cancer[1,2,20,21]. Both the number and location of lymph nodes involved have significant impacts on the outcome of patients with rectal cancer[6,15,21,26]. However, the nodal staging accuracy is not easy to make[27-29]. Factors contributing to this dilemma include the mount of mesentery resected, diligence for search of nodes paid, number of histological slices investigated, and methods of pathological examination employed[30-33]. There are still wide variations regarding the minimum number of lymph nodes to be examined for a reliable node-negative diagnosis, the reported recommendations were 6 to 17 lymph nodes[34-36]. The non-uniform extent of lymph nodes collected for investigation made the results incomparable between authors, and the absence of consensus on the number of lymph nodes contained in the mesentery worsened the situation further[36,37].

It was established that the lymphatic spread of rectal cancer followed an anatomical way along which the normal lymphatic fluid drains[14,15]. As a consequence, lymph nodes contained in the mesorectum are the earliest and the most frequent ones that might be involved when the dissemination of tumor cells takes place[14-16]. Focused examination of the mesorectal lymph nodes, thereby, could identify most metastases and micrometastases in the first place[15], though skip metastases might exist in a few cases[38,39]. However, available data have provided little information on the lymph nodes enveloped within the mesorectum[22,23]. The number and size of lymph nodes, and their tumor status remain to be defined.

Recently, Canessa *et al*.[22] recovered 168 mesorectal lymph nodes from 20 cadavers and found that the mean number was 8.4 per specimen. They searched the lymph nodes from the division of the superior rectal artery which excluded the lymph nodes that lie above it, i.e., the lymph nodes along the main trunk of it, that should otherwise be referred to 'mesorectal' nodes by strict definition[40]. Also in an another study on cadavers, an average of 24.9 pelvic lymph nodes were identified from 7 fresh specimens, which included 13.6 mesorectal lymph nodes per case[23]. Their study employed modified LNRS to facilitate the identification of lymph nodes in the mesorectum. Therefore, the lymph nodes they retrieved outnumbered those in previous study markedly[23]. In the current study, the LNRS was also used to help identify lymph nodes embedded in the mesorectal fat. A mean number of 17.7 lymph nodes per case were dissected. The majority of them (82.2%) were located along the superior rectal artery. The sizes of 66.8% of the total lymph nodes, 59.8% of the metastatic lymph nodes and 79.5% of the micrometastatic lymph nodes were <5 mm in diameter. The minimal size of lymph nodes found was 0.7 mm in diameter. These lymph nodes, especially those with a diameter $\leqslant$2 mm, were at great risk of being missed in routine pathological sampling with only naked speculation and manual palpitation[41-43]. By further examining the HE-negative nodes with IHC staining, we identified 39 nodes positive with tumor micrometastases from 18 cases (58.1%). Of interest, 10 nodes with micrometastatic diseases in 5 cases (16.1%) were previously assumed free of tumor spread by routine pathological examination. Thus this group of patients was upstaged.

The superior sensitivity of IHC to HE staining in detecting micrometastases in colorectal cancer has been well recognized[44-47]. Although its sensitivity remained ten times lower compared to reverse transcriptase polymerase chain reaction (RT-PCR) techniques, IHC is probably more specific and reliable, in that it allows examining the morphology of stained cells and differentiating from that of non-specific background staining[44-46]. There are still many controversies regarding the prognostic significance of micrometastases in colorectal cancer[10,11,47-54]. It was argued that although the application of IHC technique had the added ability to identify overt diseases missed by HE staining, it offered little prognostic information on the postoperative recurrence and long year survival[10,49-52]. On the contrary, authors favoring the detection of lymph node micrometastases stated that it was not only one of the major concerns for the proper staging of diseases, but also of prognostic relevance to the outcome of patients with rectal cancer, thus suggesting helpful in the early planning of a multimodality treatment protocol for indicated patients[11,53,54].

Choi *et al*.[50] retrospectively reviewed 1 808 lymph nodes from 93 Dukes' B colorectal tumors with IHC staining and found that 54 lymph nodes (3.0%) from 29 cases (31.2%) harbored micrometastatic diseases. However, the five-year survival analysis showed no significant difference between the micrometastatic group and non-micrometastatic group. Yasuda *et al*.[11] employed

IHC method and examined a total of 1 013 lymph nodes from 12 recurrent and 30 non-recurrent patients with histologically determined Dukes' B colorectal cancer. Micrometastases were confirmed in 59 lymph nodes (16%) from 11 cases (92%) in the recurrent group, and 77 lymph nodes (12%) from 21 cases (70%) in the non-recurrent group. They further demonstrated that micrometastases in four or more lymph nodes occurred more frequently in the recurrent group than in the non-recurrent group (58% *vs* 20%, $P<0.05$), and micrometastases to N2 or higher nodes occurred more frequently in the recurrent group also (92% *vs* 47%, $P<0.01$). Afterwards they concluded that the number and level of positive micrometastatic lymph nodes were both significantly correlated with postoperative recurrence of histologically determined Dukes' B colorectal cancer[11].

In the present study, 5 patients with rectal cancer developed recurrences. The rate of recurrence was 16.7% within two years after curative operation. All patients suffering from recurrent diseases had three or more mesorectal nodes involved with tumor metastases and/or micrometastases, one patient with lymph node micrometastases developed recurrence also. It was noted that both the number of metastatic and micrometastatic lymph nodes differed significantly between the recurrent and non-recurrent groups ($P<0.01$ and $P = 0.01$, respectively), implying that lymph node micrometastases and the number of lymph nodes involved might also correlate with the outcome of patients with rectal cancer, while the prognostic value of lymph node metastases was confirmed.

In summary, by using the LNRS to facilitate identifying lymph nodes, and with a combination of HE and IHC to detect tumor metastases and micrometastases, we have provided a detailed description of both the number and size of lymph nodes enveloped in the mesorectum, as well as their tumor status with metastases and micrometastases in rectal cancer. The rapid recurrence of tumor after a cure-intended surgery is related to the tumor status of mesorectal lymph nodes. The presence of lymph node micrometastases and the number of lymph nodes involved might have some value for the prediction of tumor recurrence in rectal cancer[11,47,48,53,54], now that the importance of lymph node metastases has been widely acknowledged[1-6,19,21]. However, it is too cursory to draw a convincing conclusion, concerning the small samples included and only short-term outcome investigated in the current study. Future multi-central large-sample controlled studies are needed to clearly define the role of lymph node micrometastases in the prognosis of patients with rectal cancer.

REFERENCES

1 **Fujita S,** Shimoda T, Yoshimura K, Yamamoto S, Akasu T, Moriya Y. Prospective evaluation of prognostic factors in patients with colorectal cancer undergoing curative resection. *J Surg Oncol* 2003; **84**: 127-131

2 **Bannura G,** Cumsille MA, Contreras J, Melo C, Barrera A, Reinero M, Pardo L. Prognostic factors in colorectal neoplasm. Multivariate analysis in 224 patients. *Rev Med Chil* 2001; **129**: 237-246

3 **Bernick PE,** Wong WD. Staging: what makes sense? Can the pathologist help? *Surg Oncol Clin N Am* 2000; **9**: 703-720

4 **Gennari L,** Doci R, Rossetti C. Prognostic factors in colorectal cancer. *Hepatogastroenterology* 2000; **47**: 310-314

5 **Sobin LH.** TNM: evolution and relation to other prognostic factors. *Semin Surg Oncol* 2003; **21**: 3-7

6 **Compton C,** Fenoglio-Preiser CM, Pettigrew N, Fielding LP. American joint committee on cancer prognostic factors consensus conference: Colorectal working group. *Cancer* 2000; **88**: 1739-1757

7 **Demols A,** Van Laethem JL. Adjuvant chemotherapy for colorectal cancer. *Curr Gastroenterol Rep* 2002; **4**: 420-426

8 **Frizelle FA,** Emanuel JC, Keating JP, Dobbs BR. A multicentre retrospective audit of outcome of patients undergoing curative resection for rectal cancer. *N Z Med J* 2002; **115**: 284-286

9 **Shimoyama M,** Yamazaki T, Suda T, Hatakeyama K. Prognostic significance of lateral lymph node micrometastases in lower rectal cancer: an immunohistochemical study with CAM5.2. *Dis Colon Rectum* 2003; **46**: 333-339

10 **Noura S,** Yamamoto H, Ohnishi T, Masuda N, Matsumoto T, Takayama O, Fukunaga H, Miyake Y, Ikenaga M, Ikeda M, Sekimoto M, Matsuura N, Monden M. Comparative detection of lymph node micrometastases of stage II colorectal cancer by reverse transcriptase polymerase chain reaction and immunohistochemistry. *J Clin Oncol* 2002; **20**: 4232-4241

11 **Yasuda K,** Adachi Y, Shiraishi N, Yamaguchi K, Hirabayashi Y, Kitano S. Pattern of lymph node micrometastasis and prognosis of patients with colorectal cancer. *Ann Surg Oncol* 2001; **8**: 300-304

12 **Liefers GJ,** Cleton-Jansen AM, van de Velde CJ, Hermans J, van Krieken JH, Cornelisse CJ, Tollenaar RA. Micrometastases and survival in stage II colorectal cancer. *N Engl J Med* 1998; **339**: 223-228

13 **Isaka N,** Nozue M, Doy M, Fukao K. Prognostic significance of perirectal lymph node micrometastases in Dukes' B rectal carcinoma: an immunohistochemical study by CAM5.2. *Clin Cancer Res* 1999; **5**: 2065-2068

14 **Bartholdson L,** Hultborn A, Hulten L, Roos B, Rosencrantz M, Ahren C. Lymph drainage from the upper and middle third of the rectum as demonstrated by 198 Au. *Acta Radiol Ther Phys Biol* 1977; **16**: 352-360

15 **Cserni G,** Tarjan M, Bori R. Distance of lymph nodes from the tumor: an important feature in colorectal cancer specimens. *Arch Pathol Lab Med* 2001; **125**: 246-249

16 **Yamada H,** Katoh H, Kondo S, Okushiba S, Morikawa T. Mesenteric lymph nodes status influencing survival and recurrence pattern after hepatectomy for colorectal liver metastases. *Hepatogastroenterology* 2002; **49**: 1265-1268

17 **Mukai M,** Ito I, Mukoyama S, Tajima T, Saito Y, Nakasaki H, Sato S, Makuuchi H. Improvement of 10-year survival by Japanese radical lymph node dissection in patients with Dukes' B and C colorectal cancer: a 17-year retrospective study. *Oncol Rep* 2003; **10**: 927-934

18 **Cserni G.** Nodal staging of colorectal carcinomas and sentinel nodes. *J Clin Pathol* 2003; **56**: 327-335

19 **Ueno H,** Mochizuki H, Hashiguchi Y, Hase K. Prognostic determinants of patients with lateral nodal involvement by rectal cancer. *Ann Surg* 2001; **234**: 190-197

20 **Gervasoni JE Jr,** Taneja C, Chung MA, Cady B. Biologic and clinical significance of lymphadenectomy. *Surg Clin North Am* 2000; **80**: 1631-1673

21 **Takahashi K,** Mori T, Yasuno M. Histologic grade of metastatic lymph node and prognosis of rectal cancer. *Dis Colon Rectum* 2000; **43**(10 Suppl): S40-S46

22 **Canessa CE,** Badia F, Fierro S, Fiol V, Hayek G. Anatomic study of the lymph nodes of the mesorectum. *Dis Colon Rectum* 2001; **44**: 1333-1336

23 **Topor B,** Acland R, Kolodko V, Galandiuk S. Mesorectal lymph nodes: their location and distribution within the mesorectum. *Dis Colon Rectum* 2003; **46**: 779-785

24 **Heald RJ,** Husband EM, Ryall RD. The mesorectum in rectal cancer surgery-the clue to pelvic recurrence? *Br J Surg* 1982; **69**: 613-616

25 **Koren R,** Siegal A, Klein B, Halpern M, Kyzer S, Veltman V, Gal R. Lymph node-revealing solution: simple new method for detecting minute lymph nodes in colon carcinoma. *Dis Colon Rectum* 1997; **40**: 407-410

26 **Luna-Perez P,** Rodriguez-Ramirez S, Alvarado I, Gutierrez de la Barrera M, Labastida S. Prognostic significance of retrieved lymph nodes per specimen in resected rectal adenocarcinoma after preoperative chemoradiation therapy. *Arch Med Res* 2003; **34**: 281-286

27 **Turner RR,** Nora DT, Trocha SD, Bilchik AJ. Colorectal carcinoma nodal staging. Frequency and nature of cytokeratin-positive cells in sentinel and nonsentinel lymph nodes. *Arch Pathol Lab Med* 2003; **127**: 673-679

28 **Miyake Y,** Yamamoto H, Fujiwara Y, Ohue M, Sugita Y, Tomita N, Sekimoto M, Matsuura N, Shiozaki H, Monden M. Extensive micrometastases to lymph nodes as a marker for rapid recurrence of colorectal cancer: a study of lymphatic mapping.

Clin Cancer Res 2001; **7**: 1350-1357
29 **Joseph NE,** Sigurdson ER, Hanlon AL, Wang H, Mayer RJ, MacDonald JS, Catalano PJ, Haller DG. Accuracy of determining nodal negativity in colorectal cancer on the basis of the number of nodes retrieved on resection. *Ann Surg Oncol* 2003; **10**: 213-218
30 **Poller DN.** Method of specimen fixation and pathological dissection of colorectal cancer influences retrieval of lymph nodes and tumour nodal stage. *Eur J Surg Oncol* 2000; **26**: 758-762
31 **Rosenberg R,** Friederichs J, Gertler R, Hoos A, Mueller J, Nahrig J, Nekarda H, Siewert JR. Prognostic evaluation and review of immunohistochemically detected disseminated tumor cells in peritumoral lymph nodes of patients with pN0 colorectal cancer. *Int J Colorectal Dis* 2004; **19**: 430-437
32 **Johnson PM,** Malatjalian D, Porter GA. Adequacy of nodal harvest in colorectal cancer: a consecutive cohort study. *J Gastrointest Surg* 2002; **6**: 883-888
33 **Wong JH,** Steinemann S, Tom P, Morita S, Tauchi-Nishi P. Volume of lymphatic metastases does not independently influence prognosis in colorectal cancer. *J Clin Oncol* 2002; **20**: 1506-1511
34 **Cserni G,** Vinh-Hung V, Burzykowski T. Is there a minimum number of lymph nodes that should be histologically assessed for a reliable nodal staging of T3N0M0 colorectal carcinomas? *J Surg Oncol* 2002; **81**: 63-69
35 **Leibl S,** Tsybrovskyy O, Denk H. How many lymph nodes are necessary to stage early and advanced adenocarcinoma of the sigmoid colon and upper rectum? *Virchows Arch* 2003; **443**: 133-138
36 **Cianchi F,** Palomba A, Boddi V, Messerini L, Pucciani F, Perigli G, Bechi P, Cortesini C. Lymph node recovery from colorectal tumor specimens: recommendation for a minimum number of lymph nodes to be examined. *World J Surg* 2002; **26**: 384-389
37 **Ratto C,** Sofo L, Ippoliti M, Merico M, Bossola M, Vecchio FM, Doglietto GB, Crucitti F. Accurate lymph-node detection in colorectal specimens resected for cancer is of prognostic significance. *Dis Colon Rectum* 1999; **42**: 143-154
38 **Prabhudesai AG,** Kumar D. The sentinel lymph node in colorectal cancer - of clinical value? *Colorectal Dis* 2002; **4**: 162-166
39 **Vekic B,** Radovanovic D, Cvetanovic M, Zivanovic J, Pavlovic I. Skip metastases in rectosigmoid carcinoma. *Srp Arh Celok Lek* 2003; **131**: 48-51
40 **Shafik A.** Mesorectal lymph nodes and their relation to the superior rectal artery: do they exist below or above the superior rectal artery division? *Dis Colon Rectum* 2002; **45**: 1122
41 **Andreola S,** Leo E, Belli F, Gallino G, Sirizzotti G, Sampietro G. Adenocarcinoma of the lower third of the rectum: metastases in lymph nodes smaller than 5 mm and occult micrometastases; preliminary results on early tumor recurrence. *Ann Surg Oncol* 2001; **8**: 413-417
42 **Cserni G.** The influence of nodal size on the staging of colorectal carcinomas. *J Clin Pathol* 2002; **55**: 386-390
43 **Nagtegaal ID,** van Krieken JH. The role of pathologists in the quality control of diagnosis and treatment of rectal cancer-an overview. *Eur J Cancer* 2002; **38**: 964-972
44 **Nordgard O,** Aloysius TA, Todnem K, Heikkila R, Ogreid D. Detection of lymph node micrometastases in colorectal cancer. *Scand J Gastroenterol* 2003; **38**: 125-132
45 **O'Dwyer ST,** Haboubi NY, Johnson JS, Gardy R. Detection of lymph node metastases in colorectal carcinoma. *Colorectal Dis* 2001; **3**: 288-294
46 **van Wyk Q**, Hosie KB, Balsitis M. Histopathological detection of lymph node metastases from colorectal carcinoma. *J Clin Pathol* 2000; **53**: 685-687
47 **Tsavellas G,** Patel H, Allen-Mersh TG. Detection and clinical significance of occult tumour cells in colorectal cancer. *Br J Surg* 2001; **88**: 1307-1320
48 **Feezor RJ,** Copeland EM 3rd, Hochwald SN. Significance of micrometastases in colorectal cancer. *Ann Surg Oncol* 2002; **9**: 944-953
49 **Fisher ER,** Colangelo L, Wieand S, Fisher B, Wolmark N. Lack of influence of cytokeratin-positive mini micrometastases in "Negative Node" patients with colorectal cancer: findings from the national surgical adjuvant breast and bowel projects protocols R-01 and C-01. *Dis Colon Rectum* 2003; **46**: 1021-1025
50 **Choi HJ,** Choi YY, Hong SH. Incidence and prognostic implications of isolated tumor cells in lymph nodes from patients with Dukes B colorectal carcinoma. *Dis Colon Rectum* 2002; **45**: 750-755
51 **Noura S,** Yamamoto H, Miyake Y, Kim B, Takayama O, Seshimo I, Ikenaga M, Ikeda M, Sekimoto M, Matsuura N, Monden M. Immunohistochemical assessment of localization and frequency of micrometastases in lymph nodes of colorectal cancer. *Clin Cancer Res* 2002; **8**: 759-767
52 **Tschmelitsch J,** Klimstra DS, Cohen AM. Lymph node micrometastases do not predict relapse in stage II colon cancer. *Ann Surg Oncol* 2000; **7**: 601-608
53 **Deng H,** Shu XJ, Zhen HY, Deng L, Chen Y, Liu LJ. Prognostic significance of lymph node micrometastasis in colorectal cancer. *Aizheng* 2003; **22**: 762-766
54 **Clarke G,** Ryan E, O'Keane JC, Crowe J, MacMathuna P. The detection of cytokeratins in lymph nodes of Duke's B colorectal cancer subjects predicts a poor outcome. *Eur J Gastroenterol Hepatol* 2000; **12**: 549-552

Edited by Kumar M and Wang XL **Proofread by** Xu FM

PO Box 2345, Beijing 100023, China
Fax: +86-10-85381893
E-mail: wjg@wjgnet.com www.wjgnet.com

World J Gastroenterol 2004;10(22):3374-3376
World Journal of Gastroenterology
 ISSN 1007-9327

• BRIEF REPORTS •

Possible stem cell origin of human cholangiocarcinoma

Chao Liu, Jie Wang, Qing-Jia Ou

Chao Liu, Jie Wang, Qing-Jia Ou, Department of General Surgery, Sun Yat-Sen Memorial Hospital, Sun Yat-Sen University, Guangzhou 510120, Guangdong Province, China
Correspondence to: Dr. Chao Liu, Department of General Surgery and Transplantation, University Hospital Essen, Hufelandstr. 55, Essen D-45122, Germany. mdliuchao@hotmail.com
Telephone: +49-201-7231104 **Fax:** +49-201-7235946
Received: 2004-02-28 **Accepted:** 2004-04-29

Abstract

AIM: To investigate the expression of CD34 and c-kit (receptor of stem cell factor) in cholangiocarcinoma.

METHODS: Fifteen cases of intrahepatic cholangiocarcinoma and 17 cases of extrahepatic cholangiocarcinoma were studied in this experiment. Using Envision detection system, paraffin-embedded sections of the resected cholangiocarcinoma tissue were stained with antibodies against CD34 and c-kit, respectively. The sections were counterstained with hematoxylin, and the results were examined under light microscope. Normal tonsil and mammary tissues were used as positive controls for CD34 and c-kit, respectively.

RESULTS: CD34 was positive in all sections, but only in capillary endothelial cells of tumor tissue. No cholangiocarcinoma cells were positive for CD34. In one case of extrahepatic cholangiocarcinoma, a few tumor cells (about 5%) were immunoreactive with c-kit.

CONCLUSION: CD34 or c-kit positive cells in liver tissue may represent liver stem cells, as they can differentiate into mature biliary cells *in vitro*. The expression of c-kit by some cholangiocarcinoma cells suggests that cholangiocarcinoma might originate from liver stem cells. However, other mechanisms of hepatocarcinogenesis, such as de-differentiation of mature cholangiocytes, may also exist.

Liu C, Wang J, Ou QJ. Possible stem cell origin of human cholangiocarcinoma. *World J Gastroenterol* 2004; 10(22): 3374-3376
http://www.wjgnet.com/1007-9327/10/3374.asp

INTRODUCTION

Two theories are available to explain the process of hepatocarcinogenesis, one is de-differentiation of mature liver cells (hepatocytes and cholangiocytes), the other is maturation arrest of liver stem cells[1]. In normal liver, putative liver stem cells may exist at terminal bile ductules (canal of Hering) and periductular area[2,3]. In rodent animals, when damage and loss of hepatocytes and/or cholangiocytes are combined with impaired regeneration of the mature cells, liver stem cells may be activated. They proliferate and differentiate towards both hepatic and biliary lineages[2,4-7]. Activation of liver stem cells has been observed in various human liver diseases, such as acute liver necrosis[8], hemochromatosis[9], chronic cholestatic diseases[10], alcoholic liver diseases[9] and chronic viral hepatitis[9,11,12]. In human liver focal nodular hyperplasia[13], hepatic adenoma[14], hepatocellular carcinoma[15] and hepatoblastoma[16], some tumor cells have also been detected to express the specific markers of liver stem cells, indicating their possible stem cell origin. In animals, cholangiocarcinoma can also originate from liver stem cells[17].

CD34 and c-kit are two hemapoietic markers, but in periductular area and occasionally within bile ducts, CD34 and c-kit positive cells were also found[18]. CD34 or c-kit positive cells in human liver can be isolated with immunomagnetic separation techniques, and these isolated cells are able to differentiate into biliary epithelial cells *in vitro*[18]. Thus, CD34 and c-kit positive cells in human liver may represent liver stem cells. In this study, the expression of CD34 and c-kit in human cholangiocarcinoma was investigated.

MATERIALS AND METHODS

Specimens

Paraffin-embedded specimens from 32 cases of resected cholangiocarcinoma at Sun Yat-Sen Memorial Hospital were studied in this experiment. They included 18 male and 14 female patients, ranging from 24 to 80 years old (mean and medium 64 years old). Fifteen cases had the tumor located in intrahepatic bile duct (IBD), 4 cases in common hepatic bile duct (CHBD) and 13 cases in common bile duct (CBD). Some clinical characteristics of the patients are summarized in Table 1.

Immunohistochemistry

Each paraffin-embedded specimen was cut consecutively into 6 sections. Three sections of CD34 and 3 sections of c-kit were stained with Envision detection system (DAKO, Denmark). CD34 retrieval was performed by heating the sections in 10 mmol/L citrate buffer (pH 6.0). In brief, the tissue sections were incubated with peroxidase blocking reagent (DAKO) for 5 min, incubated with CD34 (monoclonal mouse anti-human, IgG_1, kappa, ready to use; DAKO) for 10 min or c-kit (polyclonal rabbit anti-human, 1:50; DAKO) for 30 min at room temperature. Then, the sections were incubated with peroxidase labelled polymer conjugated to goat anti-rabbit or goat anti-mouse immunoglobulin for 30 min at room temperature, incubated with diaminobezidine (DAB) chromogen for 5 min, counterstained with hematoxylin and mounted with coverslip. Between each of these steps, the sections were rinsed gently with Tris-HCl buffer. Normal human tonsil and mammary tissues were used as positive controls for CD34 and c-kit, respectively. Negative control was performed at the same conditions by omitting incubation with the first antibody. The stained tissue sections were examined under light microscope.

RESULTS

CD34 and c-kit were positive in the staining of capillary endothelial cells in tonsil and ductal cells in normal mammary tissues, respectively. Negative controls were all negative. Among the specimens of 32 cases of cholangiocarcinoma, CD34 was strongly positive in the staining of all capillary endothelial cells and negative in tumor cells (Figure 1). However, c-kit was positive in the staining of tumor cells in 1 case of cholangiocarcinoma originating from common bile duct (case 32, Table 1). This was an 80 years old patient with moderately differentiated cholangiocarcinoma, and about 5% of the tumor cells were positively stained at cell

membrane and cytoplasm (Figure 2). The positive result was repeatedly identified in several sections from the same specimen.

Table 1 Clinical characteristic of the patients with cholangiocarcinoma

No.	Sex	Age (yr)	Location of adenocarcinoma	Differentiation
1	F	78	CBD	moderately
2	F	68	CBD	moderately
3	M	63	CBD	moderately
4	M	67	IHBC	moderately
5	M	58	IHBC	well
6	M	49	CBD	poorly
7	M	80	IHBC	well
8	M	75	CBD	poorly
9	M	77	IHBC	well
10	F	74	CBD	well
11	M	50	CHBD	well
12	F	68	CBD	well
13	M	62	IHBC	well
14	F	69	IHBC	well
15	F	67	IHBC	well
16	M	52	IHBC	moderately
17	M	59	IHBC	moderately
18	F	74	CBD	poorly
19	M	64	CHBD	well
20	F	62	IHBC	moderately
21	F	68	IHBC	poorly
22	M	61	CHBD	poorly
23	F	46	CBD	moderately
24	F	73	CBD	moderately
25	F	62	IHBC	well
26	M	59	CHBD	well
27	M	64	CBD	poorly
28	M	76	IHBC	moderately
29	M	24	IHBC	well
30	M	56	IHBC	moderately
31	F	60	CBD	moderately
32	F	80	CBD	moderately

F: Female; M: Male; CBD: Common bile duct; CHBD: Common hepatic bile duct; IHBC: Intrahepatic bile duct.

Liver stem-like cells are small and oval in shape with relatively large oval nuclei. They are immunoreactive for OV-6 (rat oval cell marker), cytokeratin (CK) 8 and CK 18 (both are epithelial cell markers), CK 7 and CK 19 (both are biliary cell markers), CK 14, and chromogranin-A[15,19]. Liver stem-like cells are heterogeneous, and could be classified into 3 types based on their differentiation characteristics. Type I represents the most undifferentiated cells, type II the progenitor cells differentiating towards biliary lineage, and type III the progenitor cells differentiating towards hepatic lineage[19]. In human liver, these liver stem-like cells have been found in focal nodular hyperplasia, hepatic adenoma, hepatocellular carcinoma and hepatoblastoma[13-16].

CD34 and c-kit are two markers of hemapoietic stem cells. However, recently in normal human liver, c-kit was detected in canal of Hering where the putative liver stem cells may exist[3]. In patients with fulminant hepatic failure, over expression of c-kit was detected in activated liver stem-like cells[20]. CD34 was also identified in rat liver stem-like cells[21]. Using immunomagnetic separation method, CD34 and c-kit positive cells were isolated from human liver. These cells were able to proliferate and differentiate into both biliary epithelial and endothelial cells *in vitro*[18]. This suggested that CD34 and c-kit positive cells in liver might represent biliary progenitor cells, biliary and endothelial cells might share the same progenitor cells. Among the 12 cases of hepatoblastoma, Ruck *et al*. reported that CD34 was found to be immunoreactive with both tumor cells and endothelial cells in 1 case of small cell hepatoblastoma, and this indicated the possible stem cell origin of hepatoblastoma[22].

In this study, a few tumor cells in 1 of 32 cases of cholangiocarcinoma were immunoreactive with c-kit, and this suggested their possible origin of biliary stem cells.

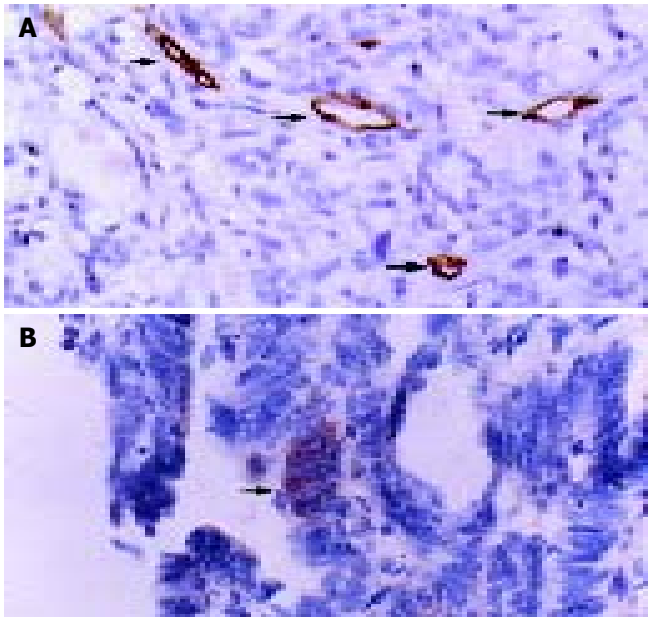

Figure 1 A: Immunohistochemical staining of cholangiocarcinoma with antibody against CD34. Arrowhead indicates strongly positive capillary endothelial cells. B: Immunohistochemical staining of cholangiocarcinoma with antibody against c-kit (Envision, original magnification: ×400). Arrowhead indicates positive tumor cells.

As putative liver stem cells possibly exist in terminal bile ductules (canal of Hering), intrahepatic cholangiocarcinoma is supposed to originate from liver stem cells more likely than extrahepatic cholangiocarcinoma. However, the cells with stem cell characteristics may not only exist in intrahepatic bile ducts, but also in extrahepatic bile ducts. In embryonic development of rat liver, both intra- and extrahepatic bile ducts originated from AFP- and albumin-containing hepatoblasts[23]. The remnant of embryo liver stem cells may also exist in extrahepatic bile ducts. In human, it was observed that hepatocellular carcinoma could also develop from extrahepatic bile ducts[24-26]. These tumors might originate from liver stem cells in extrahepatic bile ducts by maturation arrest. Thus, extrahepatic cholangiocarcinoma that was immunoreactive with c-kit in this experiment might also originate from putative liver stem cells.

Based on animal experiments, different carcinogenic regiments might act on different level of cells in hepatic lineage and produce hepatic carcinoma by different mechanisms[27]. Diethylnitrosamine acted on mature hepatocytes and induced hepatocellular carcinoma by de-differentiation. Furan injured bile duct progenitor cells and induced cholangiocarcinoma by maturation arrest. 2-acetylaminofluorene acted on ductular bipolar progenitor cells and induced hepatocellular carcinoma by maturation arrest. In choline deficiency models, the periductular stem cells could be activated to induce hepatocellular carcinoma by maturation arrest. The exact causes of human cholangiocarcinoma are still unclear, and there may be more than one mechanism of its carcinogenesis. In this study, only a few tumor cells in 1 case of cholangiocarcinoma were c-kit immunoreactive, and we could

not draw a sound conclusion. Tumor cells may lose their markers of stem cells during maturation arrest. Thus, further researches, such as increasing the number of cases and discovering new biliary progenitor cell markers, are needed to answer if human cholangiocarcinoma originates from stem cells.

ACKNOWLEDGEMENTS

The authors thank Professor Andrea Frilling at Department of General Surgery and Transplantation, University Hospital Essen, Germany, for the revision of the manuscript.

REFERENCES

1 **Sell S.** Cellular origin of cancer: dedifferentiation or stem cell maturation arrest? *Environ Health Perspect* 1993; **101**(Suppl 5): 15-26
2 **Sell S.** Is there a liver stem cell? *Cancer Res* 1990; **50**: 3811-3815
3 **Theise ND,** Saxena R, Portmann BC, Thung SN, Yee H, Chiriboga L, Kumar A, Crawfold JM. The canals of hering and hepatic stem cells in humans. *Hepatology* 1999; **30**: 1425-1433
4 **Zhang Y,** Bai XF, Huang CX. Hepatic stem cells: existence and origin. *World J Gastroenterol* 2003; **9**: 201-204
5 **Thorgeirsson SS.** Hepatic stem cells. *Am J Pathol* 1993; **142**: 1331-1333
6 **Sigal SH,** Brill S, Fiorino AS, Reid LM. The liver as a stem cell and lineage system. *Am J Physiol* 1992; **263**(2 Pt 1): G139-G148
7 **Alison M,** Sarraf C. Hepatic stem cells. *J Hepatol* 1998; **29**: 676-682
8 **Haque S,** Haruna Y, Saito K, Nalesnik MA, Atillasoy E, Thung SN, Gerber MA. Identification of bipotential progenitor cells in human liver regeneration. *Lab Invest* 1996; **75**: 699-705
9 **Lowes KN,** Brennan BA, Yeoh GC, Olynyk JK. Oval cell numbers in human chronic liver diseases are directly related to disease severity. *Am J Pathol* 1999; **154**: 537-541
10 **Crosby HA,** Hubscher S, Fabris L, Joplin R, Sell S, Kelly D, Strain AJ. Immunolocalization of putative human liver progenitor cells in livers from patients with end-stage primary biliary cirrhosis and sclerosing cholangitis using the monoclonal antibody OV-6. *Am J Pathol* 1998; **152**: 771-779
11 **Hsia CC,** Evarts RP, Nakatsukasa H, Marsden ER, Thorgeirsson SS. Occurrence of oval-type cells in hepatitis B virus-associated human hepatocarcinogenesis. *Hepatology* 1992; **16**: 1327-1333
12 **Ma X,** Qiu DK, Peng YS. Immunohistochemical study of hepatic oval cells in human chronic viral hepatitis. *World J Gastroenterol* 2001; **7**: 238-242
13 **Roskams T,** De Vos R, Desmet V. 'Undifferentiated progenitor cells' in focal nodular hyperplasia of the liver. *Histopathology* 1996; **28**: 291-299
14 **Libbrecht L,** De Vos R, Cassiman D, Desmet V, Aerts R, Roskams T. Hepatic progenitor cells in hepatocellular adenomas. *Am J Surg Pathol* 2001; **25**: 1388-1396
15 **Wu PC,** Lai VC, Fang JW, Gerber MA, Lai CL, Lau JY. Hepatocellular carcinoma expressing both hepatocellular and biliary markers also expresses cytokeratin 14, a marker of bipotential progenitor cells. *J Hepatol* 1999; **31**: 965-966
16 **Ruck P,** Xiao JC, Pietsch T, Von Schweinitz D, Kaiserling E. Hepatic stem-like cells in hepatoblastoma: expression of cytokeratin 7, albumin and oval cell associated antigens detected by OV-1 and OV-6. *Histopathology* 1997; **31**: 324-329
17 **Lee JH,** Rim HJ, Sell S. Heterogeneity of the "oval-cell" response in the hamster liver during cholangiocarcinogenesis following clonorchis sinensis infection and dimethylnitrosamine treatment. *J Hepatol* 1997; **26**: 1313-1323
18 **Crosby HA,** Kelly DA, Strain AJ. Human hepatic stem-like cells isolated using c-kit or CD34 can differentiate into biliary epithelium. *Gastroenterology* 2001; **120**: 534-544
19 **Roskams T,** De Vos R, Van Eyken P, Myazaki H, Van Damme B, Desmet V. Hepatic OV-6 expression in human liver disease and rat experiments: evidence for hepatic progenitor cells in man. *J Hepatol* 1998; **29**: 455-463
20 **Baumann U,** Crosby HA, Ramani P, Kelly DA, Strain AJ. Expression of the stem cell factor receptor c-kit in normal and diseased pediatric liver: identification of a human hepatic progenitor cell? *Hepatology* 1999; **30**: 112-117
21 **Omori N,** Omori M, Evarts RP, Teramoto T, Miller MJ, Hoang TN, Thorgeirsson SS. Partial cloning of rat CD34 cDNA and expression during stem cell- dependent liver regeneration in the adult rat. *Hepatology* 1997; **26**: 720-727
22 **Ruck P,** Xiao JC, Kaiserling E. Immunoreactivity of sinusoids in hepatoblastoma: an immunohistochemical study using lectin UEA-1 and antibodies against endothelium-associated antigens, including CD34. *Histopathology* 1995; **26**: 451-455
23 **Shiojiri N,** Lemire JM, Fausto N. Cell lineages and oval cell progenitors in rat liver development. *Cancer Res* 1991; **51**: 2611-2620
24 **Thomsen GH,** Kruse A, Petersen A. Hepatocellular carcinoma presenting as a tumour of the hilar and extrahepatic bile ducts. *Eur J Gastroenterol Hepatol* 1998; **10**: 803-804
25 **Cho HG,** Chung JP, Lee KS, Chon CY, Kang JK, Park IS, Kim KW, Chi HS, Kim H. Extrahepatic bile duct hepatocellular carcinoma without primary hepatic parenchymal lesions-a case report. *Korean J Intern Med* 1996; **11**: 169-174
26 **Park CM,** Cha IH, Chung KB, Suh WH, Lee CH, Choi SY, Chae YS. Hepatocellular carcinoma in extrahepatic bile ducts. *Acta Radiol* 1991; **32**: 34-36
27 **Sell S.** Cellular origin of hepatocellular carcinomas. *Semin Cell Dev Biol* 2002; **13**: 419-424

Edited by Wang XL and Chen WW **Proofread by** Xu FM

PO Box 2345, Beijing 100023, China
Fax: +86-10-85381893
E-mail: wjg@wjgnet.com www.wjgnet.com

World J Gastroenterol 2004;10(22):3377-3379
World Journal of Gastroenterology
 ISSN 1007-9327

• BRIEF REPORTS •

Epidemiology of peptic ulcer disease in Wuhan area of China from 1997 to 2002

Wei-Guo Dong, Chun-Sheng Cheng, Shao-Ping Liu, Jie-Ping Yu

Wei-Guo Dong, Chun-Sheng Cheng, Jie-Ping Yu, Department of Gastroenterology, Renmin Hospital of Wuhan University, Wuhan 430060, Hubei Province, China
Shao-Ping Liu, Department of Gastroenterology, Huangshi Central Hospital, Huangshi 435000, Hubei Province, China
Co-first-authors: Wei-Guo Dong and Chun-Sheng Cheng
Correspondence to: Professor Wei-Guo Dong, Renmin Hospital of Wuhan University, 238 Jiefang Road, Wuhan 430060, Hubei Province, China. dongwg@public.wh.hb.cn
Telephone: +86-27-88041919 Ext. 6448
Received: 2004-01-15 **Accepted:** 2004-03-12

Abstract

AIM: To describe the epidemiological features of peptic ulcer disease in Wuhan area during 1997-2002, to analyze the sex, age and occupation characteristics, as well as the geographic distribution of peptic ulcer disease, and to determine the effective methods of preventing and controlling peptic ulcer disease.

METHODS: In the early 1980s, the peptic ulcer disease registry system was established to collect the data of peptic ulcer disease in Wuhan area. Here we performed a statistically detailed analysis of 4876 cases of peptic ulcer disease during 1997-2002.

RESULTS: The morbidity of peptic ulcer disease between males and females was significantly different (χ^2 = 337.9, P<0.001). The majority of peptic ulcer diseases were found at the age of 20 to 50 years. Because of different occupations, the incidence of peptic ulcer disease was different in different areas.

CONCLUSION: The incidence of peptic ulcer disease is highly associated with sex, age, occupation and geographic environmental factors. By analyzing the epidemiological features of peptic ulcer disease, we can provide the scientific data for prevention and control of peptic ulcer disease.

Dong WG, Cheng CS, Liu SP, Yu JP. Epidemiology of peptic ulcer disease in Wuhan area of China from 1997 to 2002. *World J Gastroenterol* 2004; 10(22): 3377-3379
http://www.wjgnet.com/1007-9327/10/3377.asp

INTRODUCTION

During 1997 to 2002, 21693 patients had a gastroscopy in Outpatient Department of the Renmin Hospital in Wuhan University, of them, 4876 were diagnosed as peptic ulcer disease. Factors that increased the risk of serious peptic ulcer disease included older age, history of peptic ulcer disease, gastrointestinal hemorrhage, dyspepsia and previous non-steroidal anti-inflammatory drug-associated (NSAID) intolerance, as well as poor living conditions[1]. Furthermore, the epidemiological factors were important reasons leading to peptic ulcer disease. To explore the epidemiological features of peptic ulcer disease in Wuhan area, we performed a statistical analysis of the data about sex, age, occupation and geographic environmental distribution.

MATERIALS AND METHODS

A total of 21 693 patients with gastrointestinal symptoms received a gastroscopy in Outpatient Department of the Renmin Hospital of Wuhan University, of them, 4 876 were diagnosed as peptic ulcer disease. The patients were classified according to gastric ulcer (GU), duodenal ulcer (DU), complex ulcer (CU), sex, age, occupation and geographic environment and a database was set up. All the data were checked and analyzed using the SPSS statistical software.

RESULTS AND DISCUSSION

Peptic ulcer disease mainly refers to the chronic ulcer which occurs in stomach and duodenum, because the formation of ulcer is linked to the digestive function of gastric acid-pepsin[2]. Peptic ulcer disease is a worldwide common disease, but the incidence of peptic ulcer disease in different countries and regions is obviously different. The incidence of peptic ulcer disease has not been exactly investigated in China. Therefore, we performed a statistically detailed analysis of the data in Wuhan area from 1997 to 2002.

There were 4 876 cases of peptic ulcer disease out of 21 693 patients, and the incidence was 22.5%. Among the 4 876 cases diagnosed as peptic ulcer disease by gastroscope, 3 899 males (79.9%) and 977 females (20.1%) had peptic ulcer disease. The sex ratio (males to females) was 3.95:1. Among the patients with peptic ulcer disease, 3 397 had duodenal ulcer disease, 1066 had gastric ulcer disease and 413 had complex ulcer disease. Duodenal ulcer diseases accounted for 69.6%, gastric ulcer diseases accounted for 21.9% and complex ulcer diseases accounted for 8.5%. The ratio of the three was 8.2:2.6:1. The data of the sex, age, occupation characteristics and geographic distribution of peptic ulcer disease are shown in Tables 1-4.

Table 1 Sex ratio of six different age groups in 4 876 cases of peptic ulcer disease

Age (yr) group	Duodenal ulcer	Gastric ulcer	Complex ulcer	Peptic ulcer
10-	3.66	5.00	10.00	3.96
20-	5.13	4.03	6.13	4.93
30-	4.12	4.63	7.53	4.39
40-	2.65	5.82	3.04	3.26
50-	2.53	5.56	2.86	3.37
60-	3.43	5.70	6.75	4.39
Mean	3.59	5.12	6.05	4.05

Sex difference

The incidence of peptic ulcer disease in males was always higher than that in females in different age groups. From Table 1, we could see that the sex ratio in duodenal ulcer disease was 2.53-5.13:1, the maximum ratio was 5.13, and the average ratio was 3.59. The sex ratio in gastric ulcer disease was 4.03-5.82:1, the maximum ratio was 2.53, and the average ratio was 5.12. The cases of complex ulcer disease were so few that they had no

statistic significance. After analyzing the trend of the mortality of peptic ulcer disease from 1952 to 1980 in Western Germany, we found that the general trend of mortality of males was descending but there was a fluctuating ascending, and the general trend of mortality of females was steadily ascending[3]. Since the early 1960s in America, the incidence of the peptic ulcer disease in males has slightly decreased, but that of females has shown the increasing trend, and the difference of sex has gradually lessened[4]. Mortality from non- perforated ulcer decreased markedly, while that from perforated ulcer decreased slightly, similar trends were observed in men and women[5]. We carried out a statistical analysis of the data according to the different age groups (χ^2 = 337.9, P<0.001). From Table 2 and Figure 1, we could see that the incidence of peptic ulcer disease between males and females was significantly different.

Table 2 Comparison of sex among six different age groups in 4 876 cases of peptic ulcer disease

Gender	Age(yr) group					
	10-	20-	30-	40-	50-	60-
Male	190	858	1 340	880	576	282
Female	48	174	305	270	171	65

χ^2 = 337.9, P<0.001.

Table 3 Age distribution in 4 876 cases of peptic ulcer disease

Age (yr) group	Duodenal ulcer		Gastric ulcer		Complex ulcer	
	Male	Female	Male	Female	Male	Female
10-	150	41	30	6	10	1
20-	656	128	153	38	49	8
30-	932	226	295	64	113	15
40-	519	196	285	49	76	25
50-	263	104	250	45	63	22
60-	141	41	114	20	27	4
Total	2 661	736	1 127	222	338	75

Table 4 Occupation distribution in six different age groups in 1 068 cases of peptic ulcer

Age (yr) group	Worker			Farmer			Cadre			Student		
	DU	GU	CU	DU	GU	CU	DU	GU	CU	DU	GU	CU
10-	2	1	0	0	1	0	2	0	0	24	6	6
20-	86	18	6	36	12	4	6	2	0	10	0	0
30-	168	22	8	96	44	8	32	20	2			
40-	26	6	6	66	38	14	34	14	4			
50-	28	10	2	32	26	8	16	16	2			
60-	18	8	2	14	28	2	12	12	2			
Total	328	65	24	244	149	36	102	64	10	34	6	6

Age distribution

People who suffered from peptic ulcer disease could be found out at whatsoever ages, but the majority of patients with peptic ulcer disease were adults. Our data indicated that the youngest patient was 9 years old, the oldest was 73 years old, 78.7% of the patients were between 20 and 50 years old, the peak age of incidence was between 30 and 40 years old in duodenal ulcer disease patients. In gastric ulcer disease patients, the youngest was 11 years old, and the oldest was 75 years old, 82.9% of the patients were between 20 and 50 years old, 92.2% of the patients were between 30 and 60 years old, and the peak age of incidence was between 30 and 40 years old. People with gastric ulcer disease were older than those suffering from duodenal ulcer disease. The incidence of peptic ulcer disease in patients between 40 and 60 years old was obviously higher than that in patients between 10 and 30 years old. The actual number of peptic ulcers in the elderly decreased, however the percentage of elderly with peptic ulcer against total population increased[6]. The age distribution of complicated ulcer disease was basically similar to that of gastric ulcer disease. The incidence of peptic ulcer disease was 22.5% in Wuhan area, the ratio of duodenal ulcer to gastric ulcer was 3.2:1, and the ratio of different age groups was 1.24-5.1:1. From Figure 2, we could see that the incidences of duodenal ulcer disease and gastric ulcer disease were not significantly different after 50 years old. Huang *et al*.[7] found that peptic ulcer disease in children over 6 years old was mainly primary ulcer, the majority of them were duodenal ulcer, and the clinical symptoms of the peptic ulcer were similar to those in the adults. It was reported that 72-80% of peptic ulcer disease in Hunan and Guangdong provinces in China occurred in patients between 20 and 50 years old, which was similar to the results of the reports from India[8]. The location of duodenal ulcer disease was on anterior wall and greater curvature of bulb, but in gastric ulcer disease was on gastric angle and antrum, and the peak age of incidence was 21 to 50 years[9]. The results of our investigations were basically similar to them.

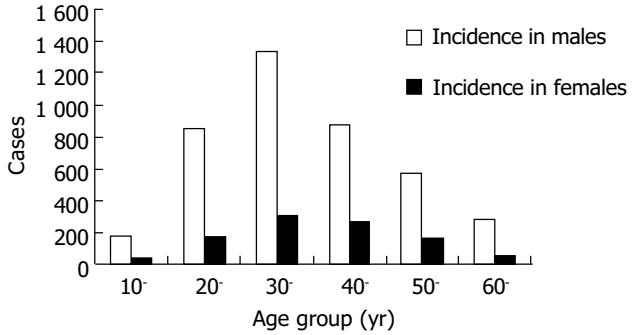

Figure 1 Age and sex distribution of peptic ulcer disease in Wuhan area, China.

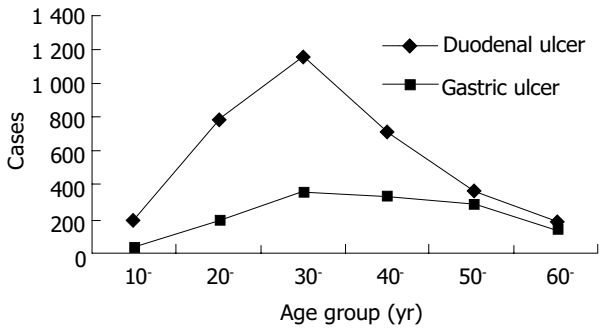

Figure 2 Age distribution of 4 876 cases of peptic ulcer disease in Wuhan area.

Social occupation factors

The sex difference and age distribution of peptic ulcer disease in different occupations were basically the same. The data of our study were divided into four parts, each from the workers, farmers, students and cadres, respectively, From Table 4, we know that the incidence of peptic ulcer disease among farmers was the highest, moderate in workers and the lowest in students. The incidence of duodenal ulcer disease was also very high among these special occupations such as drivers, firefighters and so on, which was similar to the report of Sonnenbeg *et al.*, who found the incidence of duodenal ulcer disease was very high among the firefighters, pilots and shift workers[10,11]. The

study results from Western Germany indicated that the consumption of body's energy was a dangerous factor for the development of peptic ulcer disease[11]. This may be related to social factors such as busy working, heavy mental stress and so on. It was reported that the occurrence, recurrence of peptic ulcer disease were closely associated with psychological contradiction, emotional-hindering and defective character. Depress, anxiety, fear, emotional irritability and cognitive disorganization were significantly increased in the integrated stress management program (ISMP) group in comparison with the progressive muscle relaxation (PMR) group, and the incidence of peptic ulcer disease was higher in the ISMP group than in the PMR group[12]. In addition, irregular meal, over-eating, and fast-eating might cause injures to the digestive tract mucosa, leading to the occurrence of peptic ulcer disease[13]. Peptic ulcer disease was more common in the working age groups. To any kind of occupation, age between 20 and 50 years was a period in which people were widely connected with society and participation in assorted social activities more frequently than ever. Heavy social psychological stress, frequent mobility and irregular working were extremely important factors in the formation of peptic ulcer disease. The increasing incidence of peptic ulcer disease in females was related to more and more social activities that females participated in gradually[14].

Geographic and environment factors

Environmental factors played a role in peptic ulcer disease[15]. The positive detectable rate of peptic ulcer disease in Han nationality was higher than that in Korea nationality at Yanbian area[16]. Thors *et al*.[17] demonstrated that peptic ulcer mortality and disease risk were particularly high in subjects born after the turn of the century and subsequent generations. Since 1945, a very rapid economic development has been achieved with the advent of electricity and refrigeration, clean water and food; The condition in Iceland changed from being anti-hygienic and poor to being rich and clean, the morbidity of peptic ulcer disease has decreased. The rise and fall in peptic ulcer during the 20th century might be caused by factors early in life in the generations born during these years with crowding and poor hygiene before living conditions and socio-economic status were improved. The incidence of peptic ulcer disease as reported was between 16% and 33% from different regions in China. The results from Hunan and Gansu Provinces indicated that the ratio of duodenal ulcer disease to peptic ulcer disease was 2.7-6.2:1 in the inpatient department during the same period. The peptic ulcer disease is very prevailing in all over China, but there is an increasing trend from the north to the south in region distribution. Furthermore, the morbidity of peptic ulcer disease is also different in different countries, and duodenal ulcer disease turns up more frequently than gastric ulcer disease in the majority of Western countries. The study report in Japan indicated that the incidence of gastric ulcer disease was higher than that of duodenal ulcer disease. The incidence of duodenal ulcer disease and gastric ulcer disease was almost equal to that in Norwegian. In respect to ethnicity, Bengali speaking Hindus showed high probability for gastric ulcers in both sexes[18]. The detecting rates of peptic ulcer disease in Han and Hui nationalities were 13.42% and 10.66% respectively. Among peptic ulcer diseases 44.4% were duodenal ulcer disease, and 50.63% were gastric ulcer disease, the ratio being 0.88:1. The detecting rate of peptic ulcer in Han nationality was higher than that in Hui nationality, and gastric ulcer disease occurred more often than duodenal ulcer disease in china. The regional difference in the type and level of peptic ulcer disease revealed that geographic and environmental factors probably played an important role in the development of peptic ulcer disease. Additionally, the incidence of peptic ulcer disease in the transition period between autumn and winter or between winter and spring was higher than that in other periods. The change of climate factors was also associated with occurrence of peptic ulcer disease; with the change of temperature and atmosphere, patients with peptic ulcer disease would appear gastroperiodynia.

In conclusion, the occurrence of peptic ulcer disease is highly associated with sex, age, occupation, geographic and environmental factors. By analyzing the epidemiological characteristics of peptic ulcer disease, we can provide the scientific data for prevention and control of peptic ulcer disease.

REFERENCES

1 **Griffin MR.** Epidemiology of Nonsteroidal Anti-inflammatory Drug-Associated Gastrointestinal Injury. *Am J Med* 1998; **104**: 23S-29S
2 **Xiao SD.** Peptic ulcer disease In: Ye RG eds. *MEDICINE fifth edition*. Beijing: *People Health Publishing House* 2002: 398
3 **Sonnenberg A**, Fritsch A. Changing mortality of peptic ulcer disease in Germany. *Gastroenterology* 1983; **84**: 1553-1557
4 **Wang YH,** Wang HZ. Epidemiology In: Wang HZ, Cao SZ, eds. *Xiandai Xiaohuaxing Kuiyangbingxue 1st ed.* Beijing: *People's Military Medical Pub* 1999: 64-65
5 **Thors H,** Svanes C, Thjodleifsson B. Trends in peptic ulcer morbidity and mortality in Iceland. *J Clin Epidemiol* 2002; **55**: 681-686
6 **Kawano S**, Fu HY. Epidemiology of peptic ulcer disease in the aged in Japan. *Nippon Rinsho* 2002; **60**: 1490-1498
7 **Huang QY**, Cao SZ, Wang HZ. Peptic ulcer disease in children In: Wang HZ, Cao SZ, eds. *Xiandai Xiaohuaxing Kuiyangbingxue 1st ed.* Beijing: *People's Military Medical Pub* 1999: 182-183
8 **Khuroo MS,** Mahajan R, Zargar SA, Javid G, Munshi S. Prevalence of peptic ulcer in India: an endoscopic and epidemiological study in urban Kashmir. *Gut* 1989; **30**: 930-934
9 **Huang BX,** Wang GZ. Clinical study of 2473 cases with peptic ulcer. *Zhonghua Xiaohua Neijing Zazhi* 2001; **18**: 27-29
10 **Segawa K,** Nakazawa S, Tsukamoto Y, Kurita Y, Goto H, Fukui A, Takano K. Peptic ulcer is prevalent among shift workers. *Dig Dis Sci* 1987; **32**: 449-453
11 **Sonnenberg A,** Sonnenberg GS, Wirths W. Historic changes of occupational work load and mortality from peptic ulcer in Germany. *J Occup Med* 1987; **29**: 756-761
12 **Han KS**. The effect of an integrated stress management program on the psychologic and physiologic stress reactions of peptic ulcer in Korea. *Int J Nurs Stud* 2002; **39**: 539-548
13 **Cai L**, Zheng ZL, Zhang ZF. Risk factors for the gastric cardia cancer: a case-control study in Fujian Province. *World J Gastroenterol* 2003; **9**: 214-218
14 **Chen SP.** Peptic ulcer disease In: Pan GZ, Cao SZ, eds. *Xiandai Weichangbingxue* Beijing: *Sic Pub* 1998: 899-900
15 **Chan FKL**, Leung WK. Peptic-ulcer disease. *Lancet* 2002; **360**: 933-941
16 **Pu FS,** Cai HF, Jin HY, Gen M, Liang H. Gastroscopic analysis of 4348 cases of peptic ulcer disease in Yanbian area. *Zhonghua Xiaohua Neijing Zazhi* 2001; **18**: 25-26
17 **Thors H,** Svanes C, Thjodleifsson B. Trends in peptic ulcer morbidity and mortality in Iceland. *J Clin Epidemiol* 2002; **55**: 681-686
18 **Hazra B**, Hazra J. Epidemiology of peptic ulcer in north Bengal, India. *Indian J Public health* 1998; **42**: 100-102

Edited by Wang XL and Zhang JZ **Proofread by** Xu FM

PO Box 2345, Beijing 100023, China
Fax: +86-10-85381893
E-mail: wjg@wjgnet.com www.wjgnet.com

World J Gastroenterol 2004;10(22):3380-3381
World Journal of Gastroenterology
 ISSN 1007-9327

• BRIEF REPORTS •

Effect of 2-(3-carboxy-1-oxopropyl) amino-2-deoxy-D-glucose on human esophageal cancer cell line

Jing Wu, Hong Lu, Yun Zhou, Liang Qiao, Rui Ji, Ai-Qing Wang, Wei-Min Liu, Qun-Ji Xue

Jing Wu, Ai-Qing Wang, Wei-Min Liu, Qun-Ji Xue, Lanzhou Institute of Chemical Physics, Chinese Academy of Sciences, Lanzhou 730000, Gansu Province, China
Jing Wu, Hong Lu, Yun Zhou, Rui Ji, Department of Gastroenterology and Hepatology, First Teaching Hospital of Lanzhou Medical College, Lanzhou 730000, Gansu Province, China
Liang Qiao, Storr Liver Unit, Westmead Millennium Institute, Department of Gastroenterology and Hepatology, Westmead Hospital, University of Sydney Westmead, NSW 2145, Australia
Correspondence to: Dr. Jing Wu, Department of Gastroenterology and Hepatology, First Teaching Hospital of Lanzhou Medical College, Lanzhou 730000, Gansu Province, China. wujing36@163.com
Telephone: +86-931-8619605
Received: 2004-04-22 **Accepted:** 2004-04-29

Abstract

AIM: To determine whether 2-(3-carboxy-1-oxopropy1) amino-2-deoxy-D-glucose (COPADG), a derivative of D-amino-glucose, inhibited the growth of human esophageal cancer cell line Eca-109.

METHODS: Effects of COPADG on Eca-109 cells cultured in RPMI 1640 medium were examined by a tetrazolium-based colorimetric assay (MTT assay).

RESULTS: COPADG inhibited the growth of Eca-109 cells in a dose- and time-dependent manner; the maximum inhibition rate was 83.75%.

CONCLUSION: COPADG can directly inhibit the proliferation of Eca-109 cells, which may serve as the experimental evidence for development of new drugs for esophageal cancer therapy.

Wu J, Lu H, Zhou Y, Qiao L, Ji R, Wang AQ, Liu WM, Xue QJ. Effect of 2-(3-carboxy-1-oxopropyl) amino-2-deoxy-D-glucose on human esophageal cancer cell line. *World J Gastroenterol* 2004; 10(22): 3380-3381
http://www.wjgnet.com/1007-9327/10/3380.asp

INTRODUCTION

2-(3-carboxy-1-oxopropy1) amino-2-deoxy-D-glucose (COPADG, structure is shown in Figure 1) is a derivative of D-glucose, a monose derivative of degraded chitosan. Previous researches have discovered that some amino-D-glucose derivatives are capable of inducing leukemia K562 cells to differentiate into macrophages[1], but their efficacy in inducing apoptosis of tumor cells remains unclear. We conducted this study to determine whether COPADG could inhibit the proliferation of human esophageal cancer cell line Eca-109, to provide experimental evidence for new drug development for esophageal cancer therapy.

MATERIALS AND METHODS

Materials

COPADG, synthesized by the Lanzhou Institute of Chemical Physics of Chinese Academy of Sciences, was dissolved in distilled water, filter-sterilized with 0.22 μm filter disc, and stored at 4 ℃ until use. Eca-109 cells were purchased from Shanghai Institute of Cell Biology of Chinese Academy of Sciences. RPMI 1640 medium, agarose, trypsin and fetal bovine serum (FBS) were obtained from Gibco BRL Company, and the reagents for MTT assay were purchased from Sigma Chemical Co. Ltd.

Cell culture

Eca-109 cells growing in logarithmic phase were cultured in RPMI 1640 medium supplemented with 100 mL/L heat-inactivated FBS, 100 μg/mL penicillin and 100 μg/mL streptomycin. The cells were maintained in a humidified atmosphere containing 50 mL/L CO_2 at 37 ℃. The medium was replaced every 48 h.

MTT colorimetric assay

MTT assay[2] was based on the enzymatic reduction of the tetrazolium salt MTT in viable and metabolically active cells. Cells at 85% to 100% confluency were harvested with the mixture of 2.5 g/L trypsin and 0.2 g/L EDTA solution and seeded into a 96-well plate at a density of 4×10^3 /well, followed by incubation of the cells with COPADG at varied concentrations (0.01-0.09 mol/L) for different lengths of time (24-96 h, Table 1). The control cells were treated in the same way except that incubation was performed with sterile PBS instead of COPADG. After treatment, the medium was replaced by fresh medium and the cells were incubated for 4 h with 5 mg/mL MTT, which was dissolved in 150 μL of 100 g/L DMSO and kept for 1 h. The optical densities at 490 nm (A_{490nm}) in the 96-well plates were determined using a microplate reader. Cell growth inhibition was estimated with the following formula: Growth inhibition (%) =1-A_{490nm} (treated cells)/A_{490nm} (control cells) ×100%.

Statistical analysis

Results were expressed as mean±SD. Each experiment was repeated at least three times. Statistical differences between each group were determined by single-factor analysis of variance and correlation analysis using SPSS 11.0 statistical software.

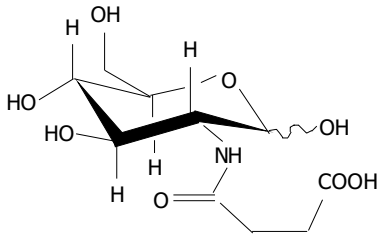

Figure 1 Chemical structure of 2-(3-carboxy-1-oxoprogy1) amino-2-deoxy-D-glucose.

RESULTS

COPADG could effectively inhibit the growth of Eca-109 cells, the maximum inhibition rate was 83.75%. The inhibition exhibited

Table 1 Inhibitory effect of COPADG on the proliferation of esophageal cancer cell line Eca-109 (mean±SD)

Concentra-tion (mol/L)	A_{490nm}			Inhibitory rate (%)		
	24 h	48 h	72 h	24 h	48 h	72 h
0 (Control)	1.505±0.090	1.686±0.067	1.745±0.077	12.76	20.81	31.29
0.01	1.313±0.053[b]	1.336±0.057[b]	1.199±0.083[b]	12.76	20.81	31.29
0.03	0.958±0.028	0.966±0.086	0.900±0.056	36.35	42.68	48.42
0.05	0.400±0.064[b,c]	0.429±0.065[b,a]	0.384±0.050[b,c]	73.42	74.57	77.99
0.07	0.383±0.045	0.360±0.039	0.342±0.037	74.55	78.66	80.44
0.09	0.355±0.046[c]	0.362±0.053 [c]	0.280±0.039[a]	76.41	78.54	83.75

At the same time point, $P<0.01$ *vs* the control group; [b]$P<0.01$ *vs* 0.03 mol/L; [a]$P<0.05$, [c]$P>0.05$ *vs* 0.07 mol/L.

an obvious time-and dose-dependent manner when the COPADG concentrations were below 0.05 mol/L, and higher concentrations tended to induce gradually stabilized inhibition, suggesting a saturation of the effects of COPADG (Table 1, Figure 2).

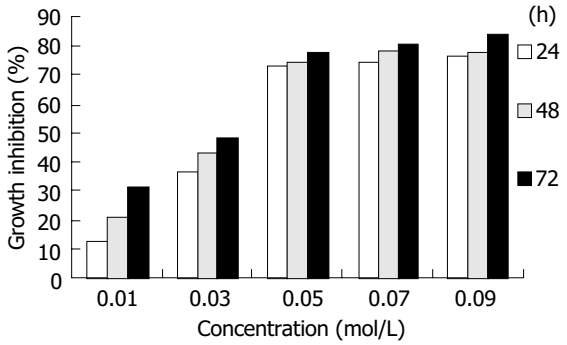

Figure 2 Inhibition of Eca-109 cell growth by COPADG.

DISCUSSION

COPADG is a derivative of D-glucose, which is a low-molecular-weight compound with multiple biological activities and a monosaccharide derived from chitosan through release of an acetyl group followed by degradation of the residual group. D-glucose is the intermediate during the synthesis of protein-polysaccharide macromolecules, and distributed in almost every human tissue as a part of the structural components of cell membrane and tissues. From the biological standpoint, D-glucose not only is involved in hepatic and renal detoxification against toxic agents, but also acts to stimulate the anti-inflammatory response and enhance the synthesis of protein-polysaccharides. Studies[3,4] have also shown that D-glucose could inhibit tumor cell growth, and partial derivatives of D-glucose could potently induce differentiation of tumor cells. Some D-amine-glucose derivatives were able to induce leukemia K562 cells to differentiate into macrophages[5], but this effect failed to be observed in human hepatocellular carcinoma cell line[1]. Currently, COPADG has become a new focus of interest in cancer therapy.

By conducting this study, we aimed to test whether COPADG, the newest derivative of D-glucose, had any effect on the proliferation of human esophageal cancer cells. MTT assay showed that COPADG could effectively inhibit Eca-109 cell proliferation, in a marked time- and dose-dependent manner below the concentration of 0.05 mol/L; the maximum inhibition rate was 83.75%. The inhibition, however, became stable when the concentrations were higher than 0.05 mol/L, indicating that the effects of the drug might be saturated at this concentration.

The development of cancer has been considered to be the combined results of unrestricted cell proliferation and impairment of normal cell apoptosis[6]. These concepts provide a basis for the development of new strategies for cancer treatment. Agents with antiproliferative properties and proapoptotic effects have been widely investigated as potential chemotherapeutic options[7,8].

Conclusion, COPADG has obvious time- and concentration-dependent inhibitory effects against the proliferation of human esophageal cancer cell line Eca-109 *in vitro*, but whether this effect can be achieved in other cell lines still awaits further examination, which may also be necessary to clarify the mechanism underlying this effect.

REFERENCES

1 **Wang Z,** Qiao Y, Huang GS, Wang AQ, Zhang YQ, Feng JL, Yang GR, Guo Y, Liang R. Glucosamine and glucosamine hydrochloride induced leukemia cell line K562 differention into macrophage. *Chin Pharmacological Bulletin* 2003; **19**: 290-293

2 **Mosmann T.** Rapid colorimetric assay for cellular growth and survival: application to proliferation and cytotoxicity assays. *J Immunol Methods* 1983; **65**: 55-63

3 **McDonnell TJ,** Meyn RE, Robertson LE. Implications of apoptotic cell death regulation in cancer therapy. *Semin Cancer Biol* 1995; **6**: 53-60

4 **Xie QL,** Dai Y, Sun FY, Lin J, Chen XY, Zhang MY, Chen XJ. The morphology of melanoma induced by glucosamine hydrochloride. *Anhui Zhongyixueyuan Xuebao* 2002; **21**: 42-44

5 **Wang Z,** Qiao Y, Huang GS, Wang AQ, Zhang YQ, Feng JL, Yang GR, Guo Y, Liang R. Induction of macrophagic differentiation of leukemia cell line K562 by N-acetyl-D glucosamine. *Disi Junyi Daxue Xuebao* 2003; **24**: 46-48

6 **Oka Y,** Naomoto Y, Yasuoka Y, Hatano H, Haisa M, Tanaka N, Orita K. Apoptosis in cultured human colon cancer cells indued by combined treatments with 5-fluorouracil tumor necrosis factor-alpha and interferon-alpha. *Jpn J Clin Oncol* 1997; **27**: 231-235

7 **Kerr JF,** Wyllie AH, Currie AR. Apoptosis: a basic biological phenomenon with wide-ranging implications in tissue Kinetics. *Br J Cancer* 1972; **26**: 239-257

8 **Kerr JF,** Winterford CM, Harmon BV. Apoptosis. Its significance in cancer and cancer therapy. *Cancer* 1994; **73**: 2013-2026

Edited by Chen WW and Wang XL **Proofread by** Xu FM

PO Box 2345, Beijing 100023, China
Fax: +86-10-85381893
E-mail: wjg@wjgnet.com www.wjgnet.com

World J Gastroenterol 2004;10(22):3382-3384
World Journal of Gastroenterology
 ISSN 1007-9327

• CASE REPORT •

A case of atypical caudate lobe hemangioma mimicking hepatocellular carcinoma: CT and angiographic manifestations

Hsin-Chi Chen, Chi-Ming Lee, Ching-Shyang Chen, Chih-Hsiung Wu

Hsin-Chi Chen, Chi-Ming Lee, Department of Radiology, Taipei Medical University Hospital, Taipei, Taiwan
Ching-Shyang Chen, Chih-Hsiung Wu, Department of Surgery, Taipei Medical University Hospital, Taipei, Taiwan
Correspondence to: Dr. Chi-Ming Lee, Department of Radiology, Taipei Medical University Hospital, No. 252 Wu-Hsing Street, Taipei 110, Taiwan. yayen0220@yahoo.com.tw
Telephone: +886-2-27372181 Ext. 1131 **Fax:** +886-2-23780943
Received: 2004-04-10 **Accepted:** 2003-05-13

Abstract

We report a case of caudate lobe hemangioma with an atypical CT enhancement pattern. In the present case, hemangioma exhibited a very subtle discontinuous peripheral rim enhancement at the post-enhanced arterial phase, and the peripheral enhanced zone had a moderately increased enhancement degree and with widened enhancement thickness during the portal-phase and delayed-phase. The slow enhancement rate for this caudate lobe hemangioma was due to sluggish perfusion by the small feeding arteries of caudate lobe branches as demonstrated by angiography.

Chen HC, Lee CM, Chen CS, Wu CH. A case of atypical caudate lobe hemangioma mimicking hepatocellular carcinoma: CT and angiographic manifestations. *World J Gastroenterol* 2004; 10 (22): 3382-3384
http://www.wjgnet.com/1007-9327/10/3382.asp

INTRODUCTION

Cavernous hemangioma is the most common benign hepatic tumor and usually presents with a typical enhancement pattern when studied by dynamic spiral computed tomography (CT). However, there are a small number of hemangiomas that exhibit atypical enhancement patterns due to the presence of intralesional non-enhanced or less-enhanced components[1-4]. Herein, we report a case of hepatitis B and C with an atypical caudate lobe hemangioma that preoperatively was misdiagnosed as a hepatocellular carcinoma because the caudate lobe mass was supplied by small caudate lobe arteries with very sluggish perfusion, resulting in a slow enhancement rate and atypical enhancement patterns when studied by dynamic CT. CT imaging features and corresponding angiographic findings of the atypical caudate lobe hemangioma were provided.

CASE REPORT

An asymptomatic 58-year-old woman was found incidentally to have a hepatic mass in the caudate lobe by ultrasound study during a health examination. She was a known hepatitis B carrier (serum positive HBsAg) for 10 years and also known as a hepatitis C carrier (positive IgG anti-HCV) for 1 year. Laboratory evaluation demonstrated normal liver and renal function. The counts of red blood cells, white blood cells, and platelets, coagulation function test, urinalysis, and serum biochemistry profile analysis were normal. The serum alpha-fetoprotein level was not elevated. Abdominal ultrasound detected a 4.0 cm×4.6 cm inhomogeneous hyperechoic mass situated at the caudate lobe.

Pre- and post-contrast triphasic spiral CT scans were subsequently performed with intravenous administration of a total of 100 mL of contrast material at an injection rate of 2 ml/s via a power injector. Hepatic arterial-phase, portal-phase and delayed-phase were obtained 35, 75 and 180 seconds, respectively, after the injection of contrast material. Pre-contrast CT revealed a well-circumscribed, low attenuation (attenuation value of 40 HU) ovoid mass (measuring approximately 4.0 cm×4.6 cm in dimension) occupying the caudate lobe. The mass exhibited a very faint discontinuous peripheral rim enhancement (attenuation value of 76 HU) at the arterial-phase (Figure 1A), with a moderately increased enhancement degree (attenuation value of 110 to 114 HU) and widened enhancement thickness for the enhanced peripheral zone during the portal-phase and delayed-phase (Figures 1B, C). Minimal enhancement (attenuation value of 61 HU) was also noted in the central portion of the mass during the delayed-phase.

The patient also received a conventional angiographic examination for further evaluation of the caudate lobe mass. Selective proper hepatic angiography showed two small, slightly tortuous, but not enlarged caudate lobe arteries deriving from the right and left hepatic arteries and supplying the caudate lobe mass. Very faint peripheral tumor stains were detected during the late arterial phase (Figure 2A) and parenchymal phase. However, there were no persistent, dense tumor stains at the late venous phase. During the angiographic study, 4 mL of lipiodol (iodized oil) was also slowly injected into the proper hepatic artery and showed several foci of spotty lipiodol retention in the peripheral and central portions of the caudate lobe mass (Figure 2B).

The patient underwent caudate lobe excision under the presumptive diagnosis of hepatocellular carcinoma based on the imaging findings. Pathological examination revealed a cavernous hemangioma occupying the caudate lobe. Only several small foci of organizing thrombi within the hemangioma were discovered.

DISCUSSION

Cavernous hemangioma is the most common benign hepatic tumor. The vast majority of hepatic hemangiomas present with a typically initial intense peripheral nodular enhancement with gradual central fill-in enhancement when studied by dynamic CT study, and it is easy to differentiate from other hepatic tumors. However a small number of hemangiomas could exhibit atypical enhancement patterns due to the presence of intralesional non-enhanced thrombosis, fibrotic, degenerated or calcified components[1,4]. In addition, variable vascularity of hemangiomas could also influence the lesion's enhancement rate and result in atypical enhancement patterns[2-4]. An atypical hemangioma may mimic a malignant hepatic tumor, causing diagnostic confusion, especially in patients at risk of malignancy.

Previous investigators[2-4] have observed that atypical enhancing hemangiomas were more common for smaller lesions than for larger lesions. Approximately 15.6% to 22.2% of

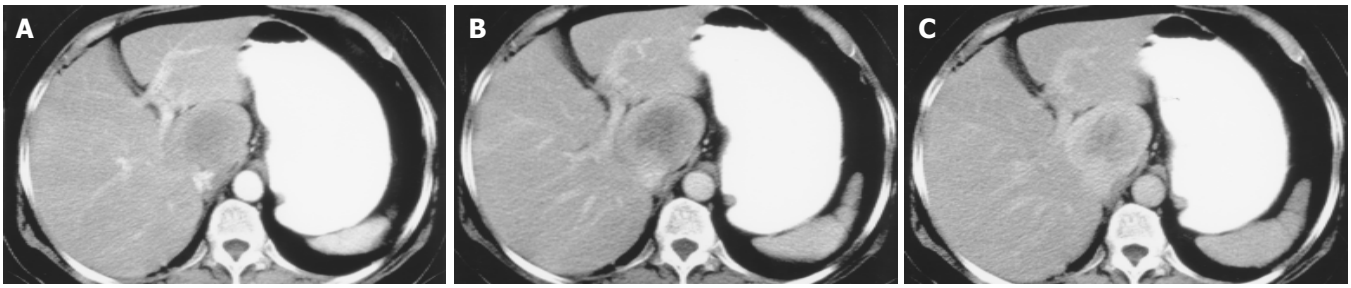

Figure 1 CT images were obtained from an asymptomatic 58-year-old woman with an atypical hepatic hemangioma. A: A 4.0 cm×4.6 cm caudate lobe mass, which exhibits a subtle, discontinuous peripheral thin-rim enhancement (attenuation value of 76 HU) shown by post-contrast triphasic CT scan at the arterial-phase. B and C: A moderately increased enhancement degree and a widened enhancement thickness for the enhanced peripheral zone (attenuation value of 110 to 114 HU) in the caudate lobe mass shown by post-contrast triphasic CT scans at the portal-phase and delayed-phase.

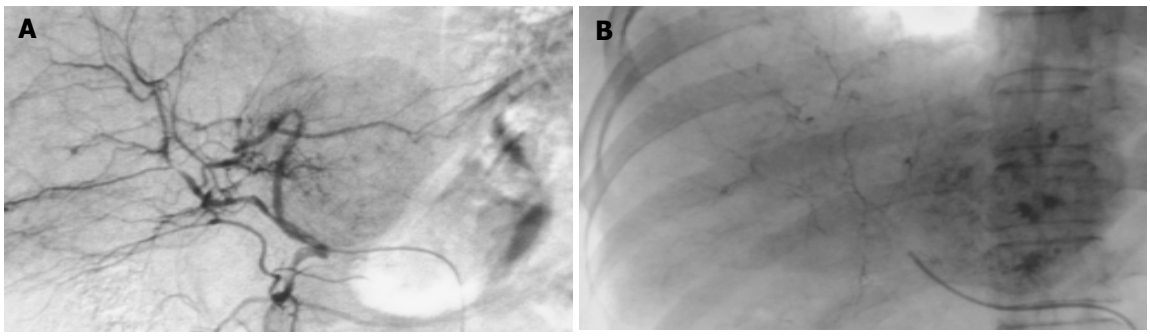

Figure 2 Peripheral tumor stains during the late arterial phase and foci of spotty lipiodol retention in the peripheral and central portions of the caudate lobe mass. A: Peripheral tumor stains during the late arterial phase. B: Foci of spotty lipiodol retention in the peripheral and central portions of the caudate lobe mass.

hemangiomas smaller than 2 cm in diameter might have an atypical enhancement pattern of low or iso-attenuation during the post-enhanced arterial and portal venous phases by dynamic CT[2-4]. However, atypical enhancement patterns of large hemangiomas were very rare. Yun *et al*.[2] reported that only 2.2% of hemangiomas larger than 2 cm in diameter presented with atypical enhancement patterns. These reports were correlated with the concept that the presence of typical peripheral nodular enhancement required larger blood supply vessels for hemangiomas and this was associated more with a larger lesion size. Thus, a hemangioma fed by small, not-enlarged supply arteries may fail to exhibit a typical enhancement pattern.

In this present case, although the caudate lobe hemangioma was larger than 4 cm in diameter, the angiograms showed that it was supplied by slightly tortuous, but un-enlarged feeding arteries due to its unique location on an independent hepatic segment of the caudate lobe that only receives the small diameter caudate arterial branches derived from the proximal portion of right and left hepatic arteries. So, this caudate lobe hemangioma failed to exhibit a typical initial peripheral nodular enhancement due to the absence of large feeding arteries. Moreover, the small caudate arteries with their sluggish perfusion also resulted in a slow enhancement rate for the caudate lobe hemangioma. On the post-enhanced arterial-phase, a very faint discontinuous peripheral rim enhancement was noted. During the portal-phase, there was a moderately increased enhancement degree for the enhanced peripheral zone, but the degree of enhancement was not as high as intra-hepatic vessels. At the delayed-phase, complete centripedal fill-in enhancement was not present in the hemangioma, but only a subtle enhancement of the intralesional central portion was noted. The enhancement pattern in the caudate lobe hemangioma thus simulated a well-differentiated hepatocellular carcinoma with delayed pseudocapsule enhancement, because a well-differentiated hepatocellular carcinoma might usually only possess a slightly increased arterial supplement and is not fed by markedly enlarged vessels[5]. Therefore, both a well-differentiated hepatocellular carcinoma and a hemangioma with small feeding arteries may exhibit a similar enhancement pattern on dynamic CT study. However, the thickness of pseudocapsules in a hepatocellular carcinoma was thinner than that of the enhanced peripheral rim in a hemangioma. Furthermore, the increased enhancement degree and the increased enhancement thickness of the intra-lesional peripheral rim also provided a diagnostic clue for the hemangioma with a slow progressive central fill-in enhancement. In contrast, a hepatocellular carcinoma usually exhibited contrast medium washout during the delayed-phase.

MR imaging is superior to CT study to improve diagnostic confidence for hepatic hemangiomas. CT has a sensitivity of 62-88% and a specificity of 84-100% (100% when enhancement is isoattenuating to the aorta) for detection of the typical globular enhancement in hemangiomas[6]. However, MR imaging has a higher sensitivity of 98% and a specificity of 98% for detection of the hemangiomas[7]. Some atypical hemangiomas can be diagnosed by MR imaging study. Nevertheless, some atypical hemangiomas will still remain uncertain at MR study due to the presence of intralesional thrombosis, calcified, hyalinized or cystic components that results in the loss of its characteristic appearance of markedly high signal intensity on heavy T2-weighted imaging and present with atypical enhancement patterns on post-enhanced study[8]; and these cases will require biopsy and histopathologic examination.

Except that hemangiomas can exhibit peripheral rim enhancement, the presence of peripheral rim enhancement could also be observed in hepatic metastatic lesions[9].

However, the peripheral rim enhancement in a metastatic lesion often has a serrated margin and not a lobular margin as seen in a hemangioma. Thus, in the present case, the caudate

lobe hemangioma had an enhanced peripheral rim with a lobular margin and not a serrated margin allowing it to be differentiated from a metastatic lesion.

As in the present case of a hepatitis carrier at risk for malignancy, CT and MR imaging were considered as complementary imaging study for detection of the malignant hepatic masses. Kang *et al*.[10] reported that although MR imaging study had a higher sensitivity of 95% than that of CT study with a sensitivity of 88% for detection of the hepatocellular carcinomas, However, there was no significant difference in the diagnostic specificity between MR study (97%) and the CT study (98%).

Intra-arterial lipiodol injection has also been used to increase detection of small hepatic neoplasms. Lipiodol retention with a spotty and/or nodular type distribution in the peripheral or central portions of hepatic hemangiomas has been described by Moon *et al*.[11]. However, the presence of spotty lipiodol retention has also been observed in other hepatic tumors, such as focal nodular hyperplasia, metastases and hepatocellular carcinoma. Hepatocellular carcinomas tended to exhibit a peripheral distribution of lipiodol accumulation, rather than a central distribution of lipiodol deposition as seen in hemangiomas. In this present case, conventional angiography failed to demonstrate the typical "cotton-wool" appearance of puddling of contrast material within the large vascular spaces and persisting into the venous phase of a caudate lobe hemangioma. The absence of persistent tumor stains in the hemangioma may be due to its unique location in the hepatic caudate lobe where there is a rapid venous drainage to the adjacent portal vein and inferior vena cava. In such a situation, it is difficult to distinguish a hemangioma from a hepatocellular carcinoma based only on conventional angiographic imaging findings. Whereas, intra-arterial lipiodol injection demonstrated spotty lipiodol retention at the intralesional peripheral and central portions, with a "cotton wool" appearance, and suggested a diagnosis of hemangioma. In addition, the number of lipiodol retention foci was also more pronounced than the number of contrast material stains as seen on conventional angiograms, because the lipiodol materials could be retained in the ectatic and tortuous vascular channels of the hemangioma, thus decreasing its venous washout degree via the portal vein and inferior vena cava. Therefore, intra-arterial lipiodol injection is able to help in the diagnosis of a hemangioma with a rapid venous drainage.

In conclusion, the presence of slow progressive peripheral rim enhancement persisting to the delayed phase, associated with the presence of central distributed spotty lipiodol retention in a caudate lobe mass should give rise to a suspicion of the possibility of hepatic hemangioma. This report emphasizes that a hepatic hemangioma in this unique caudate lobe location can present with an atypical enhancement pattern and resembles a hepatocellular carcinoma. Thus, we recommend that when studying a caudate lobe lesion, a longer post-enhanced delayed time (more than 3 min) is required on CT, in order to reflect its actual vascularity characteristics. In addition, further evaluation by MR study with a long echo time of 150 to 180 ms is also necessary to confirm the diagnosis of a cavernous hemangioma in order to prevent inappropriate therapeutic decision making.

REFERENCES

1 **Mitsudo K**, Watanabe Y, Saga T, Dohke M, Sato N, Minani K, Shigeyasu M. Nonenhanced hepatic cavernous hemangioma with multiple calcifications: CT and pathologic correlation. *Abdom Imaging* 1995; **20**: 459-461

2 **Yun EJ**, Choi BI, Han JK, Jang HJ, Kim TK, Yeon KM, Han MC. Hepatic hemangioma: contrast-enhancement pattern during the arterial and portal venous phases of spiral CT. *Abdom Imaging* 1999; **24**: 262-266

3 **Hanafusa K**, Ohashi I, Himeno Y, Suzuki S, Shibuya H. Hepatic hemangioma: findings with two-phase CT. *Radiology* 1995; **196**: 465-469

4 **Leeuwen MS**, Noordzij J, Feldberg MAM, Hennipman AH, Doornewaard H. Focal liver lesions: characterization with triphasic spiral CT. *Radiology* 1996; **201**: 327-336

5 **Hwang GJ**, Kim MJ, Yoo HS, Lee JT. Nodular hepatocellular carcinomas: detection with arterial-, portal-, and delayed-phase images at spiral CT. *Radiology* 1997; **202**: 383-388

6 **Leslie DF**, Johnson CD, Johnson CM, Ilstrup DM, Harmsen WS. Distinction between cavernous hemangiomas of the liver and hepatic metastases on CT: value of contrast enhancement patterns. *Am J Roentgenol* 1995; **164**: 625-629

7 **Soyer P**, Gueye C, Somveille E, Laissy JP, Scherrer A. MR diagnosis of hepatic metastases from neuroendocrine tumors verus hemangiomas: relative merits of dynamic gadolinium chelate-enhanced gradient-recalled echo and unenhanced spin-echo images. *Am J Roentgenol* 1995; **165**: 1407-1413

8 **Vilgrain V**, Boulos L, Vullierme MP, Denys A, Terris B, Menu Y. Imaging of atypical hemangiomas of the liver with pathologic correlation. *Radiographics* 2000; **20**: 379-397

9 **Mitchell DG**, Saini S, Weinreb JW, De Lange EE, Runge VM, Kuhlman JE, Parisky Y, Johnson D, Brown JJ, Schnall M, Herfkeas R, Davis PL, Gorczyca D, Sica G, Foster GS, Bernardino ME. Hepatic metastases and cavernous hemangiomas: distinction with standard- and triple-dose gadoteridol-enhanced MR imaging. *Radiology* 1994; **193**: 49-57

10 **Kang BK**, Lim JH, Kim SH, Choi D, Lim HK, Lee WJ, Lee SJ. Preoperative depiction of hepatocellular carcinoma: Ferumoxides-enhanced MR imaging versus triple-phase helical CT. *Radiology* 2003; **226**: 79-85

11 **Moon WK**, Han JK, Choi BI, Kim SH, Chung JW, Park JH, Han MC. Iodized-oil retention within hepatic hemangioma: characteristics on iodized-oil CT. *Abdom Imaging* 1996; **21**: 420-426

Edited by Wang XL **Proofread by** Zhu LH and Xu FM

PO Box 2345, Beijing 100023, China
Fax: +86-10-85381893
E-mail: wjg@wjgnet.com www.wjgnet.com

World J Gastroenterol 2004;10(22):3385-3387
World Journal of Gastroenterology
 ISSN 1007-9327

• CASE REPORT •

Recurrence of hepatocellular carcinoma with rapid growth after spontaneous regression

Tomoki Nakajima, Michihisa Moriguchi, Tadashi Watanabe, Masao Noda, Nobuaki Fuji, Masahito Minami, Yoshito Itoh, Takeshi Okanoue

Tomoki Nakajima, Michihisa Moriguchi, Tadashi Watanabe, Masao Noda, Masahito Minami, Yoshito Itoh, Takeshi Okanoue, Molecular Gastroenterology and Hepatology, Kyoto Prefectural University of Medicine Graduate School of Medical Science, Kyoto, Japan
Nobuaki Fuji, Department of Surgery, Kyoto Prefectural Yosanoumi Hospital, Kyoto, Japan
Correspondence to: Tomoki Nakajima M.D., Molecular Gastroenterology and Hepatology, Kyoto Prefectural University of Medicine Graduate School of Medical Science, Kawaramachi-Hirokoji, Kamigyo-ku, Kyoto 602-8566, Japan. tomnaka@silver.ocn.ne.jp
Telephone: +81-75-251-5519 **Fax:** +81-75-251-0710
Received: 2004-03-09 **Accepted:** 2004-04-16

Abstract

We report an 80-year-old man who presented with spontaneous regression of hepatocellular carcinoma (HCC). He complained of sudden right flank pain and low-grade fever. The level of protein induced by vitamin K antagonist (PIVKA)-II was 1 137 mAU/mL. A computed tomography scan in November 2000 demonstrated a low-density mass located in liver S4 with marginal enhancement and a cystic mass of 68 mm×55 mm in liver S6, with slightly high density content and without marginal enhancement. Angiography revealed that the tumor in S4 with a size of 25 mm×20 mm was a typical hypervascular HCC, and transarterial chemoembolization was performed. However, the tumor in S6 was hypovascular and atypical of HCC, and thus no therapy was given. In December 2000, the cystic mass regressed spontaneously to 57 mm×44 mm, and aspiration cytology revealed bloody fluid, and the mass was diagnosed cytologically as class I. The tumor in S4 was treated successfully with a 5 mm margin of safety around it. The PIVKA-II level normalized in February 2001. In July 2001, the tumor regressed further but presented with an enhanced area at the posterior margin. In November 2001, the enhanced area extended, and a biopsy revealed well-differentiated HCC, although the previous tumor in S4 disappeared. Angiography demonstrated two tumor stains, one was in S6, which was previously hypovascular, and the other was in S8. Subsequently, the PIVKA-II level started to rise with the doubling time of 2-3 wk, and the tumor grew rapidly despite repeated transarterial embolization with gel foam. In February 2003, the patient died of bleeding into the peritoneal cavity from the tumor that occupied almost the entire right lobe. Considering the acute onset of the symptoms, we speculate that local ischemia possibly due to rapid tumor growth, resulted in intratumoral bleeding and/or hemorrhagic necrosis, and finally spontaneous regression of the initial tumor in S6.

Nakajima T, Moriguchi M, Watanabe T, Noda M, Fuji N, Minami M, Itoh Y, Okanoue T. Recurrence of hepatocellular carcinoma with rapid growth after spontaneous regression. *World J Gastroenterol* 2004; 10(22): 3385-3387
http://www.wjgnet.com/1007-9327/10/3385.asp

INTRODUCTION

According to previous reports, spontaneous regression (SR) of malignant tumors is estimated to occur once in 60 000-100 000 cancer patients[1]. Neuroblastomas and urinary bladder cancers are well-known to regress spontaneously. However, in hepatocellular carcinoma (HCC) only 30 cases of SR have been reported in the English-language literature[2-7]. Among them, there has been only 1 report of 2 cases of recurrent HCC after SR[4]. In both cases, however, the new lesion developed at a different site in the liver while the preexisting HCC was regressing, suggesting that multicentric hepatocarcinogenesis was involved in the recurrence. In this paper, we present a case of spontaneously regressing HCC, which recurred locally during the course of 8 mo. Four months later, a new lesion developed at a different site in the liver, possibly through intrahepatic metastasis from the original tumor, and progressed rapidly. We discussed the possible mechanisms of SR in HCC.

CASE REPORT

An 80-year-old man was admitted to our hospital on November 14, 2000 due to right flank pain and low-grade fever, which continued for a day and worsened gradually. He drank 350 mL of beer every day but had no history of the use of herbal medicines.

His blood pressure was 170/104 mmHg and body temperature was 37.2 ℃. There was no remarkable physical finding. The laboratory data on admission revealed that his white blood cell count and C-reactive protein (CRP) were elevated to 10 600/mm^3 and 6.2 mg/dL, respectively. Aspartate aminotransferase (AST) and alanine aminotransferase (ALT) also were elevated to 201 IU/L and 234 IU/L, respectively. The level of alfa-fetoprotein (AFP) was within the normal limit, but protein induced by vitamin K antagonist (PIVKA)-II was 1 137 mAU/mL. His serum was negative for hepatitis B surface antigen and positive for hepatitis C antibody.

Enhanced computed tomography (CT) on admission demonstrated 2 hepatic tumors (Figure 1A). One was a low-density mass located in liver S4 with marginal enhancement. The other was a cystic mass of 68 mm×55 mm in S6 with slightly high density content but without marginal enhancement. Angiography demonstrated that the right hepatic lobe was supplied by the replaced right hepatic artery. A celiac arteriogram showed tumor stain in S4 with a size of 25 mm×20 mm, which was diagnosed as typical HCC (Figure 2A). Transarterial chemoembolization was performed using an emulsion of 3.2 mL Lipiodol (iodized oil manufactured by Andre Guerbert, Aulnay-sous-Bois, France) and 32 mg epirubicin[8]. The super mesenteric arteriogram, on the other hand, demonstrated that the tumor in S6 was hypovascular (Figure 2B). Because this image was atypical of HCC, no therapy was given.

Low-grade fever disappeared on the second day of admission and the white blood cell count, CRP and transaminases became almost normal on the eighth day. Because the patient wanted to undergo an operation for gallbladder stones, preoperative evaluation for cholecystectomy was carried out. In December 2000, just before the operation, a CT scan showed that Lipiodol was accumulated in the tumor in S4 and that the cystic mass in S6 was decreased in size spontaneously, down to 57 mm×44 mm (Figure 1B). During the operation in December 2000, microwave coagulation was performed for HCC in S4. The surface of the cystic tumor in S6 was dark red and needle aspiration revealed bloody fluid, which was diagnosed cytologically as class I. Because there was no evidence of malignancy, we did not give any treatment for this lesion.

After the operation, the tumor in S6 continued to decrease in size (Figure 1C), whereas the tumor in S4 was treated successfully with a 5 mm margin of safety around it. The PIVKA-II level fell to the normal limit in February 2001. A CT scan in July 2001 revealed that the tumor was decreased further in size but demonstrated an enhanced area at the posterior margin of the tumor (Figure 1D). Furthermore, the PIVKA-II level increased slightly. In November 2001, a CT scan demonstrated that the enhanced area extended to the surrounding area of the cystic tumor (Figure 1E). Histological evaluation by tumor biopsy from the lesion in S6 revealed a well-differentiated HCC (Figure 1F). The celiac arteriogram in November 2001 showed that the previous tumor stain in S4 disappeared. The super mesenteric arteriogram demonstrated 2 tumor stains; one was in S6, which was previously hypovascular, and the other was in S8 (Figure 2D).

Subsequently, transarterial embolization with gel foam (TAE) was repeated but the tumor resisted therapy, with rapid invasion and intrahepatic metastasis. In February 2003, the patient died of bleeding into the peritoneal cavity from the tumor that occupied almost the entire right lobe (Figure 3).

DISCUSSION

To our knowledge, there has been only 1 report of 2 cases of recurrence of HCCs after SR[4]. In both cases, the recurrent HCCs developed at different sites in the liver before the preexisting HCC regressed completely, suggesting that multicentric hepatocarcinogenesis, rather than intrahepatic metastasis, was likely to have been involved in the recurrence. However, in our case, evidence of local recurrence in the regressing tumor was observed by CT scan before the newly developed lesion in S8 was found by angiography. In addition, when local recurrence was detected by CT scan, the serum PIVKA-II level started to rise again. This clinical course suggests that the new lesion in S8 might be due to intrahepatic metastasis from the locally recurrent tumor in S6, rather than multicentric hepatocarcinogenesis.

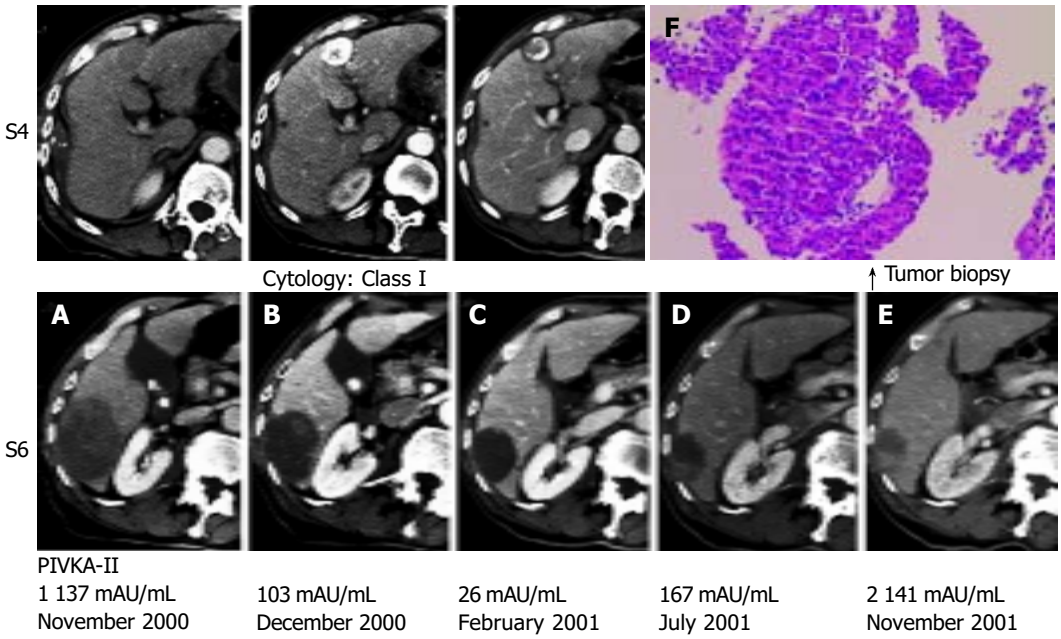

Figure 1 Enhanced computed tomography (CT). A: A low-density mass located in liver S4, with marginal enhancement and a cystic mass of 68 mm×55 mm in S6. B: Lipiodol accumulation in the tumor in S4 and the cystic mass in S6. C: Microwave coagulation performed for HCC in S4 during cholecystectomy. D: Further decrease in tumor size and enhanced area at the posterior cystic lumen of the tumor. E: Extension of the enhanced area to the surrounding area of cystic tumor. F: A well-differentiated HCC shown by histological evaluation.

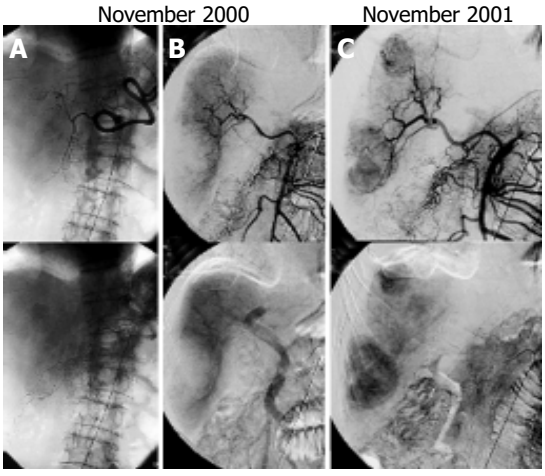

Figure 2 A: Celiac arteriogram showing tumor stain with a size of 25 mm×20 mm in S4. B: Blood supply of right hepatic lobe by the replaced right hepatic artery. C: Super mesenteric arteriogram demonstrating two tumor stains.

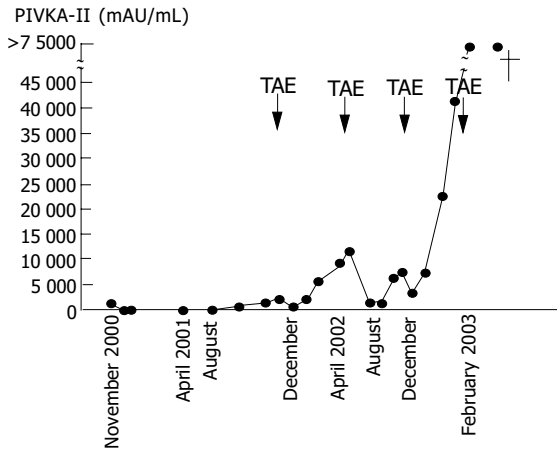

Figure 3 Clinical course of the patient. TAE: transarterial embolization with gel foam.

In previous reports, some authors made a definitive diagnosis by histological study after tumor resection but others suspected SR based on the following up radiological findings and the tumor markers[2-7]. In this case, the PIVKA-II level was 1 137 mAU/mL on the first admission and decreased dramatically to 103 in 1 mo. However, at that point we were not certain whether this was due to SR of the HCC in S6 or to transarterial chemoembolization for a typical HCC in S4. In addition, a diagnosis of class I by tumor aspiration cytology in S6 prevented us from performing S6 segmentectomy, in view of evidence-based medicine. We could not make a definitive diagnosis of the tumor in S6 until it showed radiological signs of recurrence and was proven histologically to be HCC.

The precise mechanism of SR of HCC remains unclear, but various factors have been speculated to play a role, such as alcohol withdrawal[9], androgen withdrawal[10], and intake of herbal medicine[2,11,12]. Secondary bacterial infection in the tumor has also been supposed to cause SR through the stimulation of cytokine production[13,14] and fever[15]. Because of the hypervascular nature of HCC, another important factor might be an insufficient blood supply to the tumor, possibly due to rapid natural tumor growth[16,17], spontaneous arterial thrombosis[18], or gastrointestinal bleeding[19,20]. In our case, there was no history of alcohol or androgen withdrawal or the use of herbal medicines. The initial symptoms of right flank pain and fever suddenly appeared and lasted for only a day. Laboratory data showed that the levels of transaminases were elevated on admission but almost normalized in about a week. In addition, angiography clarified that the tumor in S6 was hypovascular. Furthermore, this tumor was cystic with slightly high density content, from which bloody fluid was obtained. These clinical manifestations suggest that the acute onset of the symptoms was due to local ischemia, leading to intratumoral bleeding or hemorrhagic necrosis, and as a result, causing SR.

In this case, the PIVKA-II level after recurrence showed a logarithmic increase throughout the entire clinical course, except that it stabilized for one month after each TAE. The doubling time of the PIVKA-II level, which is thought to reflect the tumor doubling time, was calculated to be 2-3 wk. This indicates that the recurrent tumor grew very rapidly, compared with the average natural growth rate of HCC reported previously[21,22]. The PIVKA-II level was elevated to 1 137 mAU/mL on the first admission, decreased along with SR of the tumor in S6, and rose again after recurrence. It has been reported that HCCs with high PIVKA-II levels during the initial stage show aggressive behaviors and a poor prognosis. Therefore, we speculate that the initial tumor in S6 grew as fast as the recurrent tumor and this rapid growth itself might be the cause of insufficient blood supply to the tumor, finally inducing SR, as suggested in previous reports[16,17].

REFERENCES

1 **Cole WH.** Efforts to explain spontaneous regression of cancer. *J Surg Oncol* 1981; **17:** 201-209

2 **Takeda Y,** Togashi H, Shinzawa H, Miyano S, Ishii R, Karasawa T, Takeda Y, Saito T, Saito K, Haga H, Matsuo T, Aoki M, Mitsuhashi H, Watanabe H, Takahashi T. Spontaneous regression of hepatocellular carcinoma and review of literature. *J Gastroenterol Hepatol* 2000; **15:** 1079-1086

3 **Izuishi K,** Ryu M, Hasebe T, Kinoshita T, Konishi M, Inoue K. Spontaneous total necrosis of hepatocellular carcinoma: report of a case. *Hepatogastroenterology* 2000; **47:** 1122-1124

4 **Lee HS,** Lee JS, Woo GW, Yoon JH, Kim CY. Recurrent hepatocellular carcinoma after spontaneous regression. *J Gastroenterol* 2000; **35:** 552-556

5 **Matsuo R,** Ogata H, Tsuji H, Kitazono T, Shimada M, Taguchi K, Fujishima M. Spontaneous regression of hepatocellular carcinoma -a case report. *Hepatogastroenterology* 2001; **48:** 1740-1742

6 **Ikeda M,** Okada S, Ueno H, Okusawa T, Kuriyama H. Spontaneous regression of hepatocellular carcinoma with multiple lung metastases: a case report. *Jpn J Clin Oncol* 2001; **31:** 454-458

7 **Morimoto Y,** Tanaka Y, Itoh T, Yamamoto S, Mizuno H, Fushimi H. Spontaneous necrosis of hepatocellular carcinoma: a case report. *Dig Surg* 2002; **19:** 413-418

8 **Fan J,** Ten GJ, He SC, Guo JH, Yang DP, Wang GY. Arterial chemoembolization for hepatocellular carcinoma. *World J Gastroenterol* 1998; **4:** 33-37

9 **Gottfried EB,** Steller R, Paronetto F, Lieber CS. Spontaneous regression of hepatocellular carcinoma. *Gastroenterology* 1982; **82:** 770–774

10 **McCaughan GW,** Bilous MJ, Gallagher ND. Long-term survival with tumor regression in androgen-induced liver tumors. *Cancer* 1985; **56:** 2622-2626

11 **Chien RN,** Chen TJ, Liaw YF. Spontaneous regression of hepatocellular carcinoma. *Am J Gastroenterol* 1992; **87:** 903-905

12 **Lam KC,** Ho JC, Yeung RT. Spontaneous regression of hepatocellular carcinoma: a case study. *Cancer* 1982; **50:** 332-336

13 **Watanabe N,** Yamauchi N, Maeda M, Neda H, Tsuji Y, Okamoto T, Tsuji N, Akiyama S, Sasaki H, Niitsu Y. Recombinant human tumor necrosis factor causes regression in patients with advanced malignancies. *Oncology* 1994; **51:** 360-365

14 **Nishimura T,** Watanabe K, Yahata T, Ushaku L, Ando K, Kimura M, Saiki I, Uede T, Habu S. Application of interleukin 12 to antitumor cytokine and gene therapy. *Cancer Chemother Pharmacol* 1996; **38:** S27-34

15 **Jansen PM,** van der Pouw Kraan TC, de Jong IW, van Mierlo G, Wijdenes J, Chang AA, Aarden LA, Taylor FB Jr, Hack CE. Release of interleukin-12 in experimental Escherichia coli septic shock in baboons: relation to plasma levels of interleukin-10 and interferon-gamma. *Blood* 1996; **87:** 5144-5151

16 **Suzuki M,** Okazaki N, Yoshino M, Yoshida T. Spontaneous regression of a hepatocellular carcinoma: a case report. *Hepatogastroenterology* 1989; **36:** 160-163

17 **Iwasaki M,** Furuse J, Yoshino M, Moriyama N, Kanemoto H, Okumura H. Spontaneous regression of hepatocellular carcinoma: a case report. *Jpn J Clin Oncol* 1997; **27:** 278-281

18 **Imaoka S,** Sasaki Y, Masutani S, Ishikawa O, Furukawa H, Kabuto T, Kameyama M, Ishiguro S, Hasegawa Y, Koyama H. Necrosis of hepatocellular carcinoma caused by spontaneously arising arterial thrombus. *Hepatogastroenterology* 1994; **41:** 359-362

19 **Gaffey MJ,** Joyce JP, Carlson GS, Esteban JM. Spontaneous regression of hepatocellular carcinoma. *Cancer* 1990; **65:** 2779-2783

20 **Tocci G,** Conte A, Guarascio P, Visco G. Spontaneous remission of hepatocellular carcinoma after massive gastrointestinal haemorrhage. *BMJ* 1990; **300:** 641-642

21 **Ebara M,** Ohto M, Shinagawa T, Sugiura N, Kimura K, Matsutani S, Morita M, Saisho H, Tsuchiya Y, Okuda K. Natural history of minute hepatocellular carcinoma smaller than three centimeters complicating cirrhosis. A study in 22 patients. *Gastroenterology* 1986; **90:** 289-298

22 **Nakajima T,** Moriguchi M, Mitsumoto Y, Katagishi T, Kimura H, Shintani H, Deguchi T, Okanoue T, Kagawa K, Ashihara T. Simple tumor profile chart based on cell kinetic parameters and histological grade is helpful for estimating the natural growth rate of hepatocellular carcinoma. *Hum Pathol* 2002; **33:** 92-99

Edited by Wang XL **Proofread by** Zhu LH and Xu FM